Final
Report

December 1971

Preliminary Design of a Shuttle Docking and Cargo Handling System

MARTIN MARIETTA CORPORATION

MSC 05218

Final Report December 1971

PRELIMINARY DESIGN OF A SHUTTLE DOCKING AND CARGO HANDLING SYSTEM

Shepard B. Brodie
Program Manager

MARTIN MARIETTA CORPORATION
P.O. Box 179
Denver, Colorado 80201

FOREWORD

This document presents the results of work performed by the Martin Marietta Corporation's Denver Division while under contract to NASA Manned Spacecraft Center. This final report was prepared as partial fulfillment of Contract NAS9-11932, *Preliminary Design of a Shuttle Docking and Cargo Handling System*. The NASA Technical Monitor for the Contract was Mr. Richard B. Davidson, of the Spacecraft Design Office, Engineering Technology Branch.

CONTENTS

Figure

I. INTRODUCTION

The objective of this study is the preliminary design of a Shuttle docking and cargo handling remote manipulator system (RMS). This final report describes the work conducted during the study program. The first three chapters of the report following the Introduction and Summary represent the work performed prior to concept selection, and include (1) the requirements and guidelines used to formulate concepts, (2) analysis performed to determine detail requirements for reach, velocity, torque, etc., (3) the formulation of the alternative concepts, (4) the evaluation and ranking of these concepts, and (5) the selection of a concept. Chapter VI describes man-in-the-loop simulations performed with a six degree of freedom moving base simulator and a three degree of freedom manipulator arm. In Chapter VII, we present the analysis and tradeoffs of those design parameters which are the key to the preliminary design of an RMS, described in Chapter VIII. Chapter VIII is divided into subsystem sections following the system description. Chapter IX presents our estimates for a future development program and includes a schedule and manpower breakdown and cost estimate. A summary of the system design parameters including a weight and power breakdown and estimate is included in Chapter X. In addition, this Chapter enumerates those areas that required further analysis and tradeoffs. Lastly, references, and simulation data are included in Chapters XI and Appendix A, respectively. Appendix B presents a reference to the SOW tasks as they are discussed in the report.

II. SUMMARY

Requirements - The preliminary design of a Shuttle remote manipulator system (RMS) is based on an arm that is articulated at shoulder, elbow, and wrist. This arm enables the RMS to perform the following tasks: (1) "capturing" orbital payloads such as the Space Station, satellites, or a disabled Shuttle; (2) docking the Shuttle to orbital payloads, such as the Space Station, manned module, or a disabled Shuttle; (3) unload and deploy cargo from the Shuttle cargo bay; (4) unloading Space Station module from Shuttle, transfer and dock module to Space Station; and (5) assembling orbital payloads. Mission derivable requirements and design guidelines were established. These include operational time lines, minimum and maximum payloads, minimum arm reach, precontact and postcontact velocities, arm tip velocities and accelerations, etc.

A preliminary requirement analysis was conducted, and the significant results of this work were parametric design sensitivity curves relating arm reach, torque required, Shuttle attachment point, joint weight, and beam weight. From these curves penalties in arm weight were determined as other parameters were varied. Significantly, there was very little or no weight difference for arms between 9.1 m (30 ft) and 18.3 m (60 ft) long. Typically, torque requirements were 3400 N-m (2500 ft-lb) for docking the Shuttle to the Space Station in 10 minutes and 176.8 N-m (130 ft-lb) for transferrring a cargo module in 10 minutes.

Concept evaluation and Selection - Forty-two alternative concepts were formulated and screened to provide ten concepts. These were conceptually designed, evaluated, and ranked. The evaluation considered 20 comparative parameters, including development risk, Shuttle interface, crew work load, mechanical complexity, fail-operational capability, etc. A two-arm 15.3 m (50 ft) fixed length, fixed base concept was selected.

Simulations - Man-in-the-loop simulations were performed with 2.1-m (7-ft) manipulator arms and a TV system. The simulation investigated the controllability of manipulator arms. Both rotational hand controllers (joy stick) and a geometrically similar master were used for slave control. The simulations verified the feasibility of a Shuttle RMS for capturing moving targets.

Requirements Analysis - Detailed requirements analysis was carried out on the selected concept with emphasis on specific requirements for 14 system parameters: arm length, joint positional accuracy, joint rate accuracy, degrees of freedom, gimbal ordering, joint angular velocity, joint torques, reach envelope, joint angular travel, command and data link, tracking and ranging, arm deployment, control methods, and ground testing. The system characteristics analysis formed the basis for the RMS configuration.

System Description - A preliminary design of the RMS was established with emphasis on six subsystem areas: mechanical, structural, control, dynamics, crew systems and man/machine interface, and telecommunications. The system is described in the following paragraphs.

The RMS consists of two identical manipulator arms mounted near the forward bulkhead of the Shuttle Orbiter cargo bay as illustrated in Fig. II-1. The arms are designed so that only one arm is required to accomplish all tasks associated with capture, docking, and cargo handling operations. Thus, the RMS is redundant, in that if either arm fails, the other arm can be used to perform all required tasks except orbital assembly where two arms are needed.

The total arm length is 15.3 m (50 ft) long. The shoulder-to-elbow segment is 7.15 m (23.5 ft) and is equal to the elbow-to-wrist segment. The wrist extension makes the terminal device 0.9 m (3.0 ft) from the wrist. The arm diameter is such that each can be stowed in an envelope approximately 20.3 cm (8 in.) diameter by 15.3 m (50 ft) long. The deployment device places the shoulders 6.1 m (20 ft) apart for improved reach envelope. The weight of one arm and deployment mechanism is about 544.8 kg (1200 lb). Total RMS weight including aluminum arms, terminal device, four TV cameras, lights, deployment devices, complete control console, and control and data electronics is estimated at 1264 kg (2783 lb). This weight reduces to 619 kg (1364 lb) if Lockalloy replaces aluminum for the arm. The arm is designed for a maximum tip force of 44.5 N (10 lb) and for a maximum tip deflection of 2.54 cm (1.0 in.).

Each arm has a total of eight degrees of freedom: shoulder, two (pitch and yaw); elbow, two (roll and yaw); wrist, three (yaw, pitch, and roll); and terminal device, one. Joint accuracy provides for a tip positional error accuracy of ±5.1 cm (2 in.) and a tip velocity error of ±1.5 cm/sec (0.05 ft/sec).

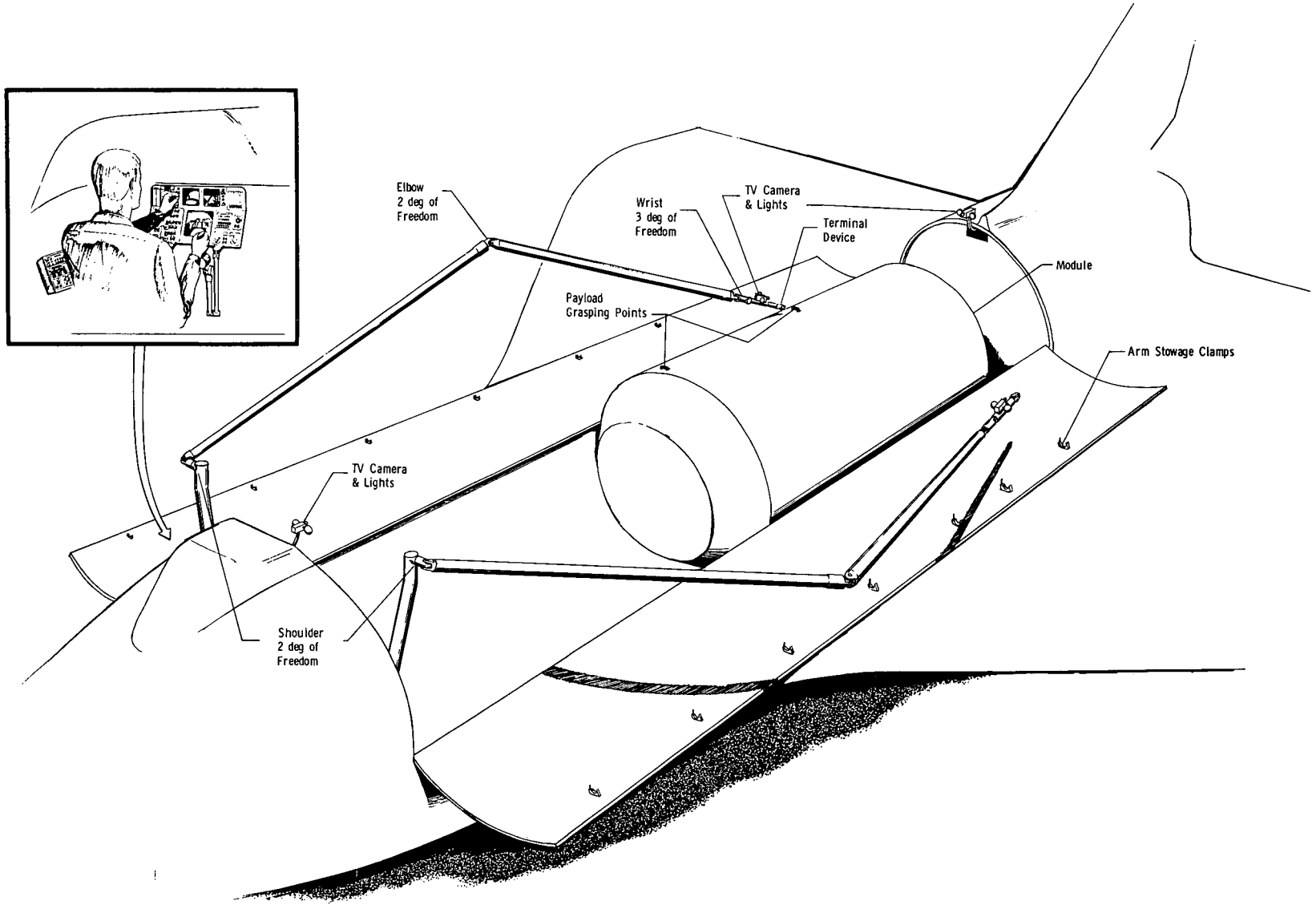

Fig. II-1 Shuttle Remote Manipulator System

Viewing for RMS operations is provided by direct viewing capability from the Shuttle cockpit, supplemented by four monoscopic TV cameras, each with two attached floodlights. The base-mounted TV camera automatically follows the terminal device.

The RMS control system incorporates force feedback to allow the operator to feel the contact forces and moments. The input controller consists of either a geometrically similar master controller, a six-degree-of-freedom handcontroller, or two three-degree-of-freedom hand controllers. For analysis purposes, the master arm controller was assumed, since it presents somewhat higher requirements from the standpoint of crew cabin volume and control logic. The control system has four basic modes of operation: (1) manual control with low sensitivity for positioning the arm in the general vicinity of the desired area; (2) manual control with high sensitivity for five manipulations; (3) computer augmentation for indexing and coordinate transformation requirements; and (4) computer programmed automatic control for predetermined tasks such as arm deployment and cargo transfer. The RMS is designed to be controlled by a single crewman.

The RMS is designed for maximum cargo payload of 29,400 kg (65,000 lb) and designed for docking with a Space Station or another 145,280 kg (320,000 lb) orbiter. For the docking operation, the arm, after capturing the payload, is used as a sensor to provide accurate position and velocity information to the Shuttle RCS thrusters. After the initial relative velocity between the Shuttle and Space Station is reduced to 0.03 m/sec (0.1 ft/sec), the arm can be used to supply the forces to reduce relative velocities to zero and bring the two spacecraft together for mechanical locking. The latter two operations can also be done using the arm as a sensor to provide precise information for controlling the Shuttle RCS for docking operations. Figure II-2 is a block diagram representation of the RMS system.

Many tasks other than those presently required can be accomplished with the RMS. The Large Space Telescope (LST) is an example of where capture and then holding of the LST can be done with one arm while performing maintenance and module replacement tasks with the other arm. Other satellite retrieval tasks with specially designed terminal devices also become feasible RMS tasks.

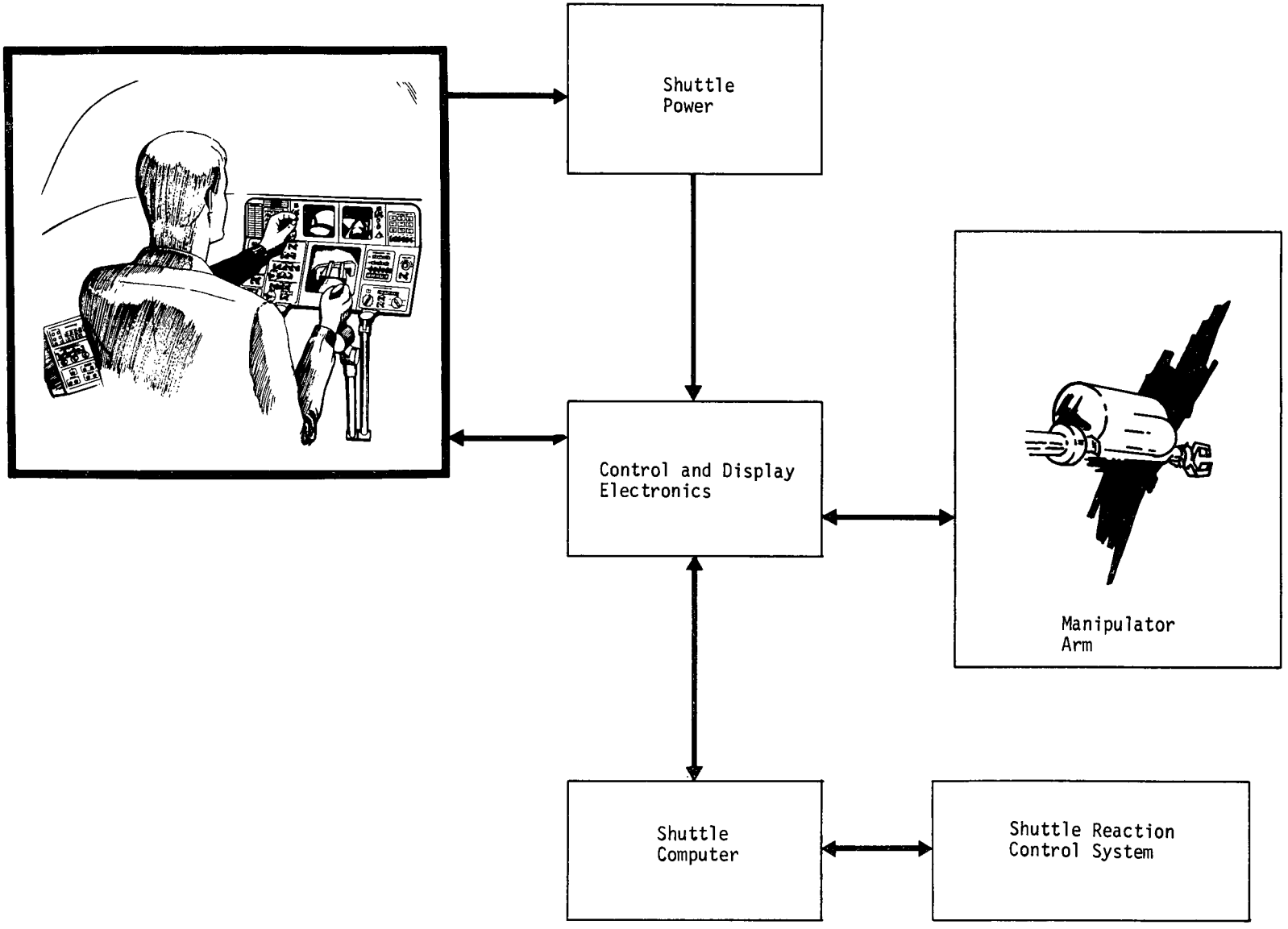

Fig. II-2 Remote Manipulator System Block Diagram

III. RMS REQUIREMENTS

The Shuttle Remote Manipulator System (RMS) requirements are based on manipulator arm(s) attached to the Shuttle Orbiter. For analysis purposes, the baseline Orbiter is the McDonnell Douglas design* with cargo erection device removed and with docking port placed forward of the cockpit, as illustrated in Fig. III-I. The primary requirements are performance characteristics and physical characteristics. The requirements are categorized as Mission Derivable Requirements and Design Guidelines. These requirements were modified later in the study to reflect updated Shuttle characteristics. These modifications are discussed in Section D of Chapter V.

A. MISSION DERIVABLE REQUIREMENTS

1. Operational Requirements

The matrix shown in Table III-1 lists the primary tasks to be performed by the manipulator system.† In addition, all inverse tasks (such as capture and load cargo) are also to be performed. For all tasks, the manipulator system provides all force and control for task accomplishment. These tasks are described in the following paragraphs.

Task A: PRE-CAPTURE. This task applies to all RMS operations and consists of deploying the manipulator from a ready position to a location such that the tip is near the point of first contact with the object to be captured.

Task B: CAPTURE. This task applies to all RMS operations and consists of alignment and mechanically coupling the RMS terminal device (hand) to the cargo. A typical captured arrangement is illustrated in Fig. III-2 for a single arm capturing the Space Station.

Task C: DOCK SHUTTLE TO ORBITING OBJECT. This task consists of arresting the relative velocities between the Shuttle and orbiting object, and maneuvering the object to the Shuttle docking port, so that mechanical coupling of the payload to the Shuttle can be made. This task is illustrated in Fig. III-3 for Shuttle-to-Space-Station docking.

---

*Phase B Final Report, June 30, 1971.

†Assembly of orbital payloads, not shown as task in Table I, was added before concept selection phase.

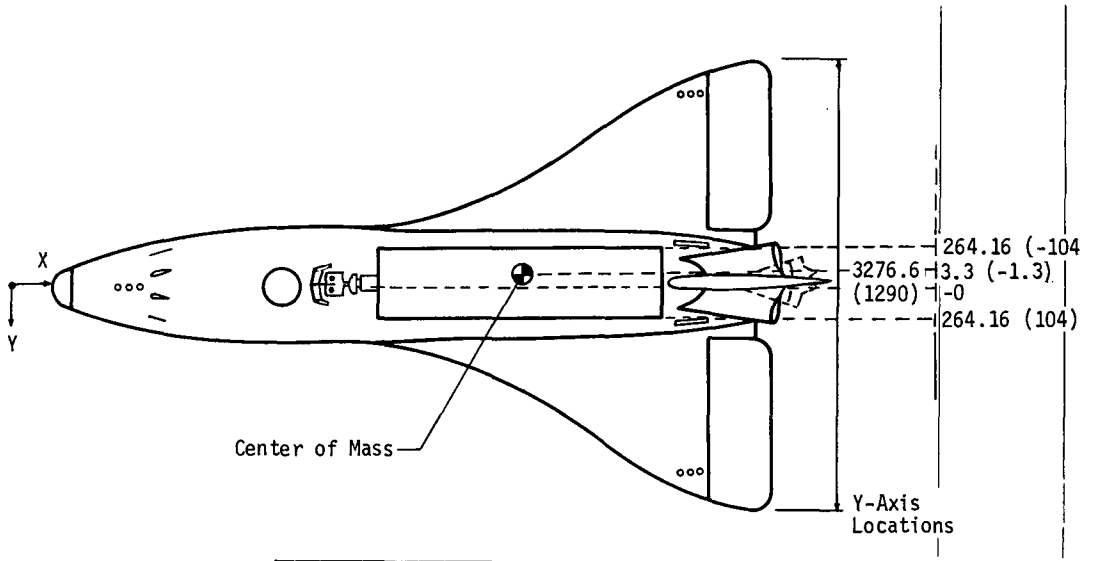

Note: All dimensions in centimeters (inches)

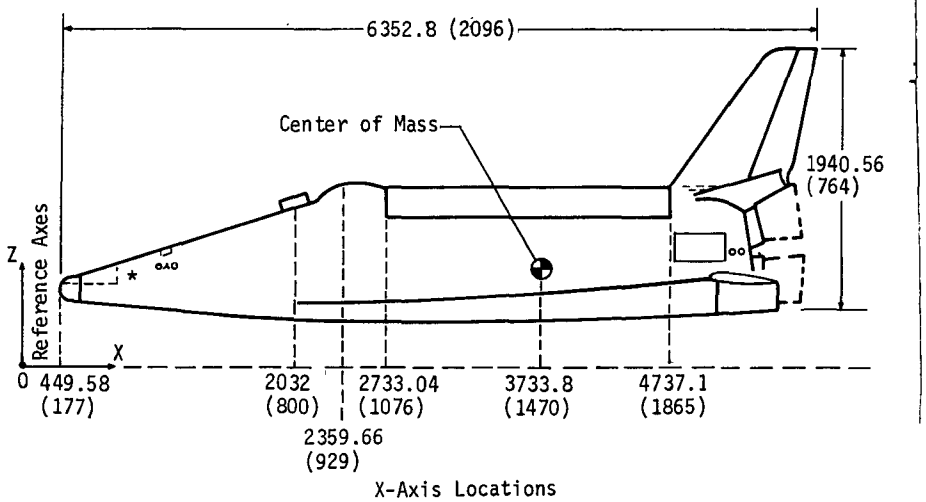

*See dimension on Z-axis figure

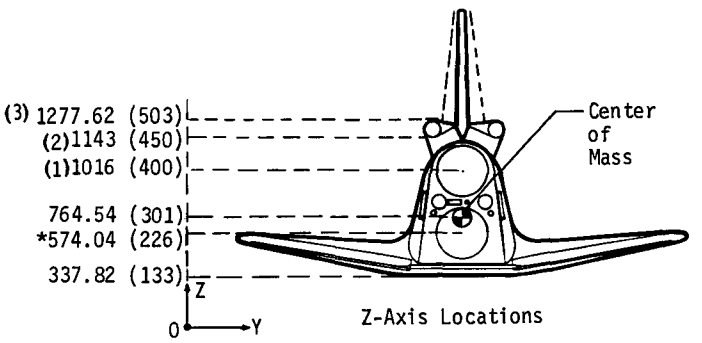

Legend:
(1) = Center of Cargo Bay
(2) = Base of Docking Port
(3) = Top of Cargo Bay Door
* See location on X-axis figure

Fig. III-1 Shuttle Orbiter Dimensions

Table III-1 RMS Operational Requirements

RMS FUNCTION	1. SPACE STATION	2. SPACE STATION MODULE (20,000 LB)	3. MAXIMUM ORBITER PAYLOAD (65,000 LB)	4. 2270 kg (5000 lb) SATELLITE	5. 182 kg (400 lb) SATELLITE	6. DISABLED SHUTTLE ORBITER
A. PRE-CAPTURE (Deploy Arms to Ready Position)	▲	▲	▲	▲	▲	▲
B. CAPTURE (Mechanically Couple Terminal Device & Object)	▲	▲	▲	▲	▲	▲
C. DOCK SHUTTLE TO ORBITING OBJECT.	▲	▲				▲
D. UNLOAD AND DEPLOY CARGO FROM SHUTTLE CARGO BAY.		▲	▲	▲	▲	
E. MODULE UNLOAD, TRANSFER, AND DOCK TO SPACE STATION.		▲				

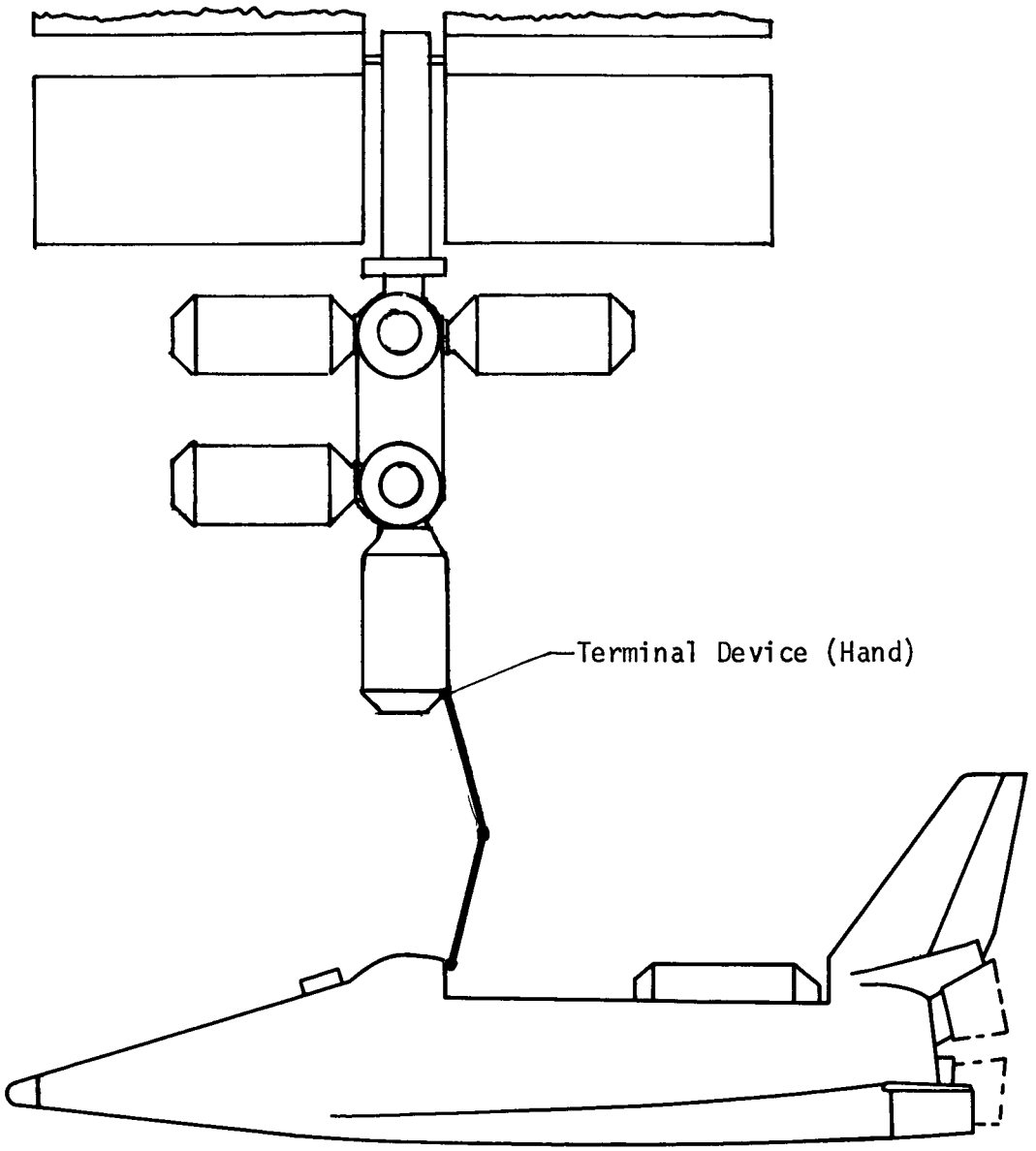

Fig. III-2 Task B: Capture

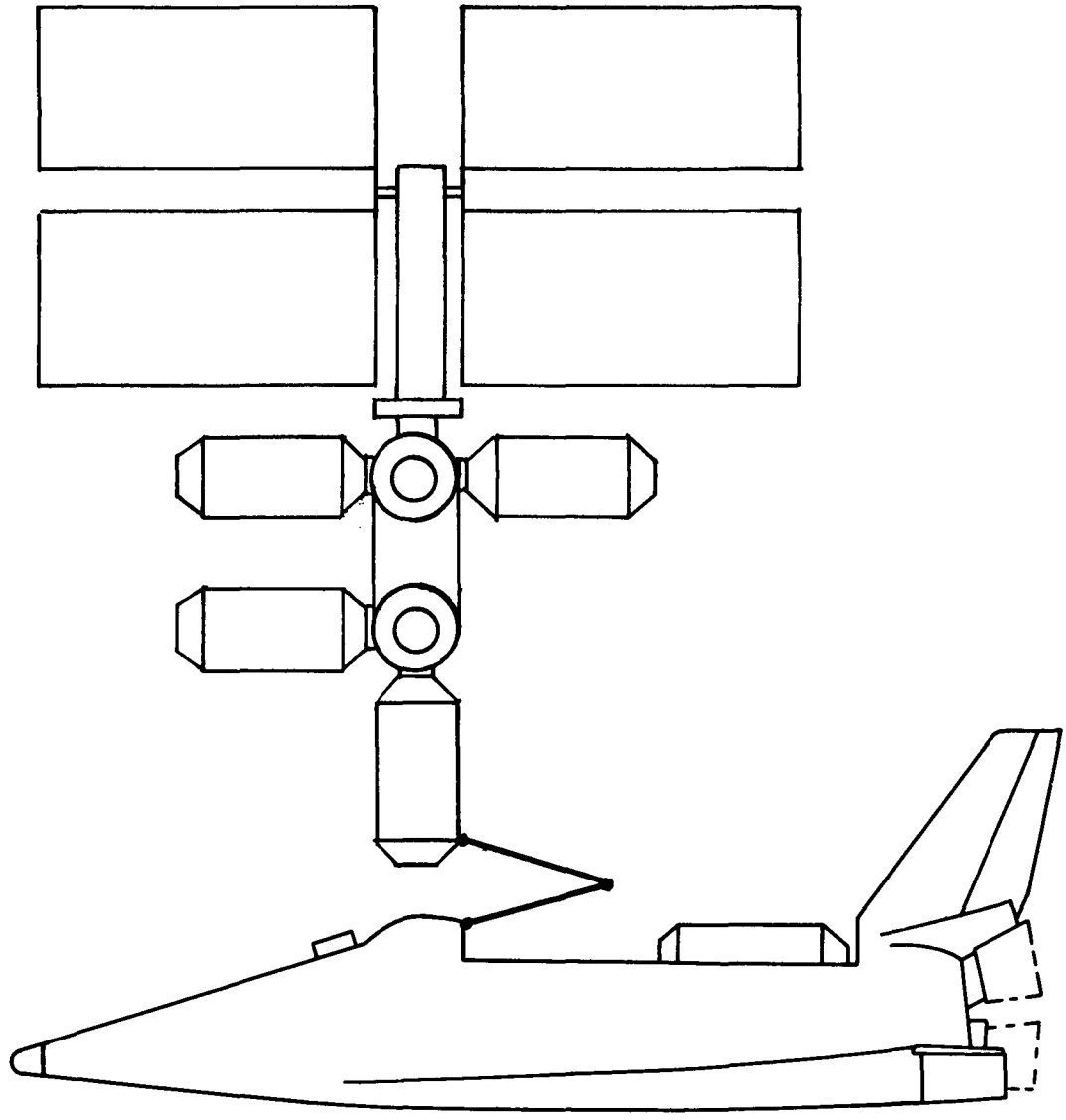

Fig. III-3 Task C: Dock Shuttle to Orbital Payload

Task D: UNLOAD AND DEPLOY CARGO. This task consists of moving a payload out of the cargo bay, deploying it above the Shuttle, and orientation and release of the cargo. A typical task is illustrated in Fig. III-4.

Task E: MODULE UNLOAD, TRANSFER, AND DOCK. This task consists of lifting cargo out of the cargo bay, transferring it to the vicinity of the Space Station, and docking it to the Space Station. This task is illustrated in Fig. III-5, for one typical mode of operation.

2. Payload Characteristics

The physical characteristics of the payloads to be handled by the manipulator system are given in Table III-2. The table lists only the extreme ranges of payloads and is not intended to exclude those payloads that fall within the upper and lower limits specified.

Table III-2 Payload Characteristics

PAYLOAD	LENGTH, m (ft)	DIAMETER, m (ft)	WEIGHT, kg (lb)	MOMENT OF INERTIA NEWTON METERS^2 (slug ft^2)		
				I_{xx}	I_{yy}	I_{zz}
Space Station (6-man)	35.7 (117)	22.8* (75)	76,000 (168,400)	4.6×10^6 (3.4×10^6)	4.6×10^6 (3.5×10^6)	4.7×10^6 (3.5×10^6)
Space Station Module	9.8 (32)	4.3 (14)	9,050 (20,000)	1.9×10^4 (1.4×10^4)	2.3×10^5 (1.7×10^5)	2.3×10^5 (1.7×10^5)
Maximum Orbiter Payload	18.3 (60)	4.6 (15)	29,400 (65,000)	7.7×10^4 (5.7×10^4)	8.7×10^4 (6.4×10^4)	8.7×10^4 (6.4×10^4)
5000-lb Satellite	6.1 (20)	4.3 (14)	2,270 (5,000)	5.1×10^3 (3.8×10^3)	9.2×10^3 (6.8×10^3)	9.2×10^3 (6.8×10^3)
400-lb Satellite	1.2 (4)	0.6 (2)	182 (400)	8.4 (6.2)	26.5 (19.6)	26.5 (19.6)
Disabled Shuttle Orbiter	53.2 (174.7)	32.8* (107.5)	145,000 (320,500)	3.1×10^6 (2.3×10^6)	20.4×10^6 (15.1×10^6)	20.4×10^6 (15.6×10^6)

*Maximum Width

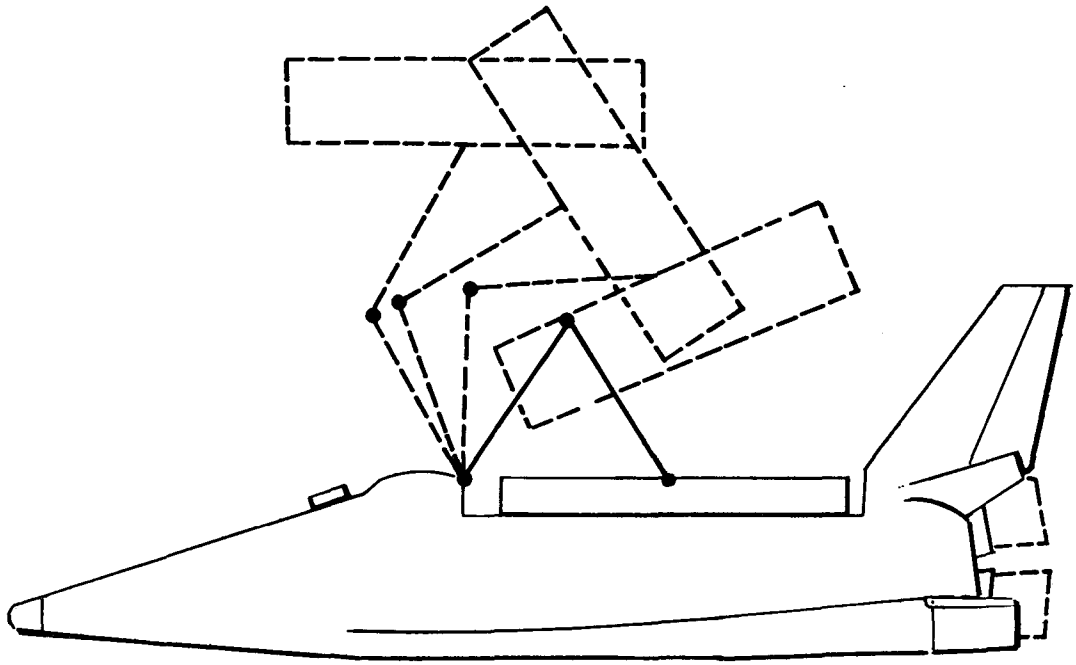

Fig. III-4 Task D: Payload Unload and Deploy

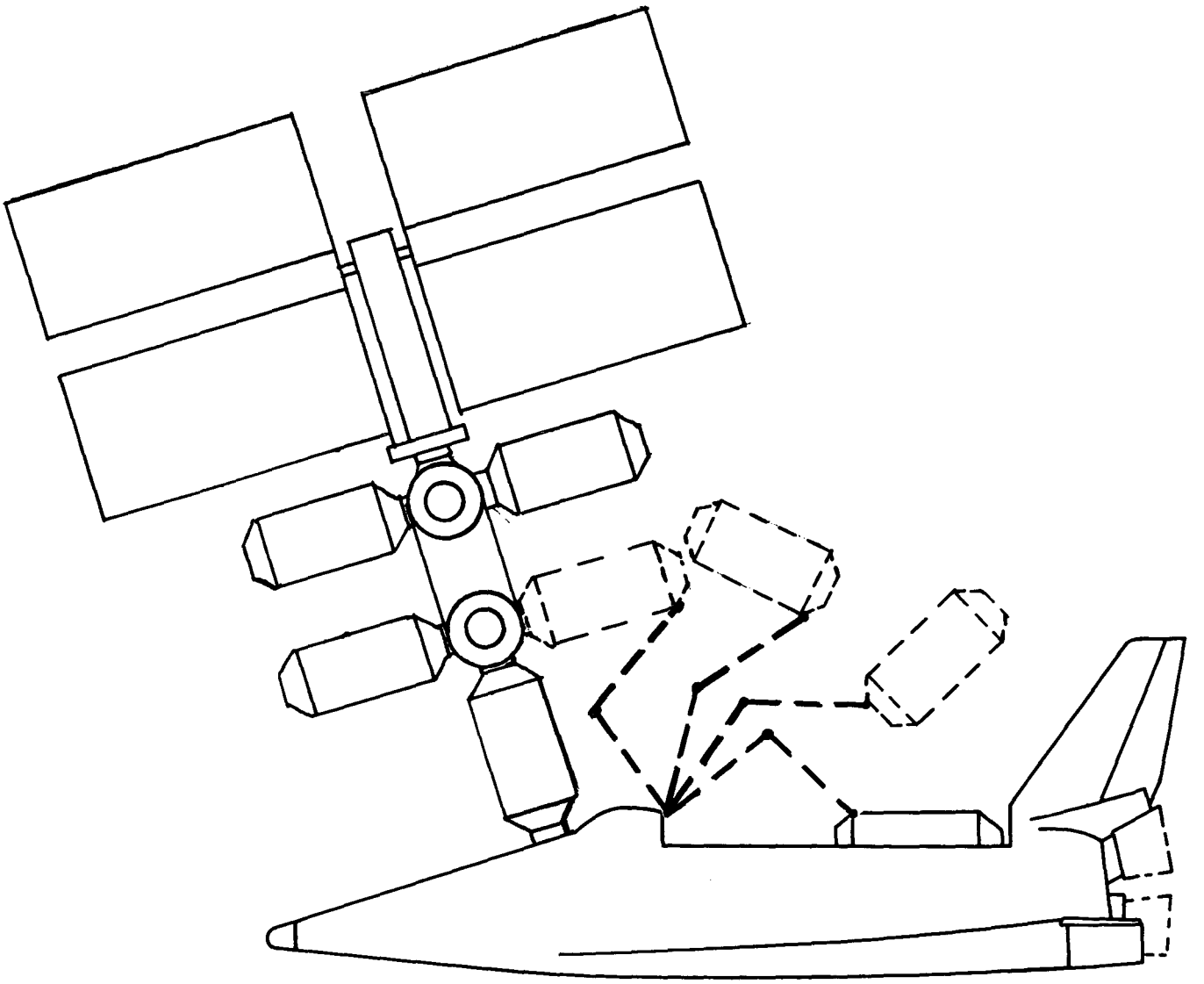

Fig. III-5 Task E: Station Module Unload, Transfer and Dock

3. Reach Envelope

The manipulator extension shall be adequate to reach any cargo in any location in the Shuttle cargo bay payload envelope. The reach distance shall be considered unobstructed from the manipulator base to the terminal device and shall be adequate to accomplish the docking and module transfer tasks.

4. Stowage

The manipulator system shall be stowed in a manner acceptable for launch, orbit, and reentry of the Shuttle Orbiter. The stowage technique shall not significantly affect the Shuttle thermal protection system.

5. Deployment

The system shall be deployed from its stowed position by remote control from the manipulator control station.

6. Safety

The system performance shall allow safe "redesignate and fly-around" during any phase of the deployment or operational maneuvers. No single mode failure or credible combination of failures shall prevent safe reentry of the Shuttle Orbiter. Caution and warning indications will be provided to the crew to indicate potentially hazardous conditions.

7. Operations and Monitoring

The manipulator system shall be operated and monitored by the Shuttle crew from a control and display station to be located in the Shuttle Orbiter. All computational requirements associated with normal operation shall be performed onboard the Shuttle. The system shall include illumination for the tasks to be performed.

8. Precontact Dynamics

The system design shall consider the following Shuttle docking closure rates and misalignments: forward velocity 0.1219 m/sec (0.4 ft/sec); lateral velocity 0.0475 m/sec (0.15 ft/sec); centerline miss distance ±0.1524 m (6 in.); angular rate 0.1 deg/sec; angular error ±3.0 deg.

B. DESIGN GUIDELINES

1. Operation

The manipulator system shall be operated by a single crewman in a shirtsleeve environment.

2. System Characteristics

The manipulator system shall consist of boom sections articulated at shoulder, elbow, and wrist joints.

3. Payload Characteristics

The baseline Space Station shall be the 6-man modular concept (North American Rockwell, Report MSC-02464, 1/71).

4. Power

The manipulator system shall be electrically actuated, using power sources onboard the Shuttle Orbiter.

5. Viewing

Baseline viewing shall be accomplished by means of direct viewing from the Shuttle cockpit with supplemental viewing provided by remote controlled television cameras.

6. Operations

Cargo transfer and docking to the Space Station shall be accomplished with the Shuttle Orbiter docked to the Space Station. Cargo transfer and docking from a stationkeeping Shuttle Orbiter shall be considered a possible alternative backup mode of operation.

7. Docking Port Contact Dynamics

The system shall control the Shuttle docking such that the following maximum docking port contact conditions shall be met:

Lateral alignment	±0.051 m (±2 in.)
Angular alignment	±1 deg
Closing velocity	±0.0305 m/sec (±0.1 ft/sec)

Lateral velocity	±0.0152 m/sec (0.05 ft/sec)
Angular velocity	0.05 deg/sec

8. Response Characteristics

The speed, acceleration, and accuracy characteristics of the system shall be such that the RMS tasks can be performed in the maximum times shown in the tabulation.

		Time (min)
Task A.	Precapture	3
Task B.	Capture	2
Task C.	Dock Shuttle	10
Task D.	Unload and Deploy Cargo	10
Task E.	Module Unload, Transfer and Dock to Station	10

9. Stowage

The manipulator arm(s) (exclusive of the deployment mechanism) shall be stowed in the Orbiter cargo bay in two volumes, each approximately 0.305 m (12 in.) in diameter by 18.4 m (60 ft) long.

10. Ground Operation

The manipulator arm(s) is not required to operate in a 1g environment. However, capability for limited ground checkout is required.

11. Acceleration Levels

The maximum no-load translational acceleration (with arm extended with 120 deg at elbow) will be such that from maximum velocity it can stop in 0.61 m (2 ft), or less.

The maximum translational acceleration while loaded (with arm extended 120 deg at elbow) shall be such that it can stop in 4.56 m (15 ft) or less from maximum velocity.

The maximum no-load angular acceleration of the terminal device (relative to the forearm) shall be such that it can stop in 10 deg or less from maximum angular velocity.

The maximum angular acceleration of the terminal device (relative to forearm) while loaded shall be such that it can be stopped in 15 deg or less.

12. Tip Deflection

The maximum manipulator tip deflection under full-load conditions shall be no greater than 0.025 m (1.0 in.).

13. Weight

The total weight of the manipulator arm(s) and deployment mechanism shall not exceed 264 kg (1200 lb).

IV. PRELIMINARY REQUIREMENTS ANALYSIS

In this chapter the RMS requirements of Chapter III are translated into meaningful manipulator design parameters. The objective is twofold: (1) provide a logical basis for formulating the alternative manipulator concepts, and (2) provide the data for evaluating the concepts. The requirements for the task* operations, their timelines, the precontact and postcontact velocity and misalignments, and the masses, inertias and dimensions of the principals are given. From these the design criteria for arm tip velocities and accelerations, arm lengths, docking and cargo handling torques, arm joint parameters, docking and cargo handling beam parameters, and electrical power are derived.

This chapter is divided into five sections: A. Reach Requirements, B. Velocity and Acceleration Requirements, C. Torque Requirements, D. Joint Weight and Beam Weight, and E. Electrical Power.

A. REACH REQUIREMENTS

This requirement is dictated by the geometry of the tasks to be performed and the arm attachment point on the Shuttle. As shown in Fig. IV-1, five reach points were considered: (A) Shuttle docking port; (B) Space Station module (near-side) docking port; (C) Space Station module (far-side) docking port; (D) Shuttle cargo bay, forward lower point; and (E) Shuttle cargo bay, rear lower point. The requirement to reach point C could be eliminated because it becomes identical to the point B requirement when the Shuttle docking direction is reversed. To reach other module docking ports on the Station, the Shuttle would dock at ports other than that shown in the figure.

*The assembly of orbital payloads was not a requirement at this phase of the work.

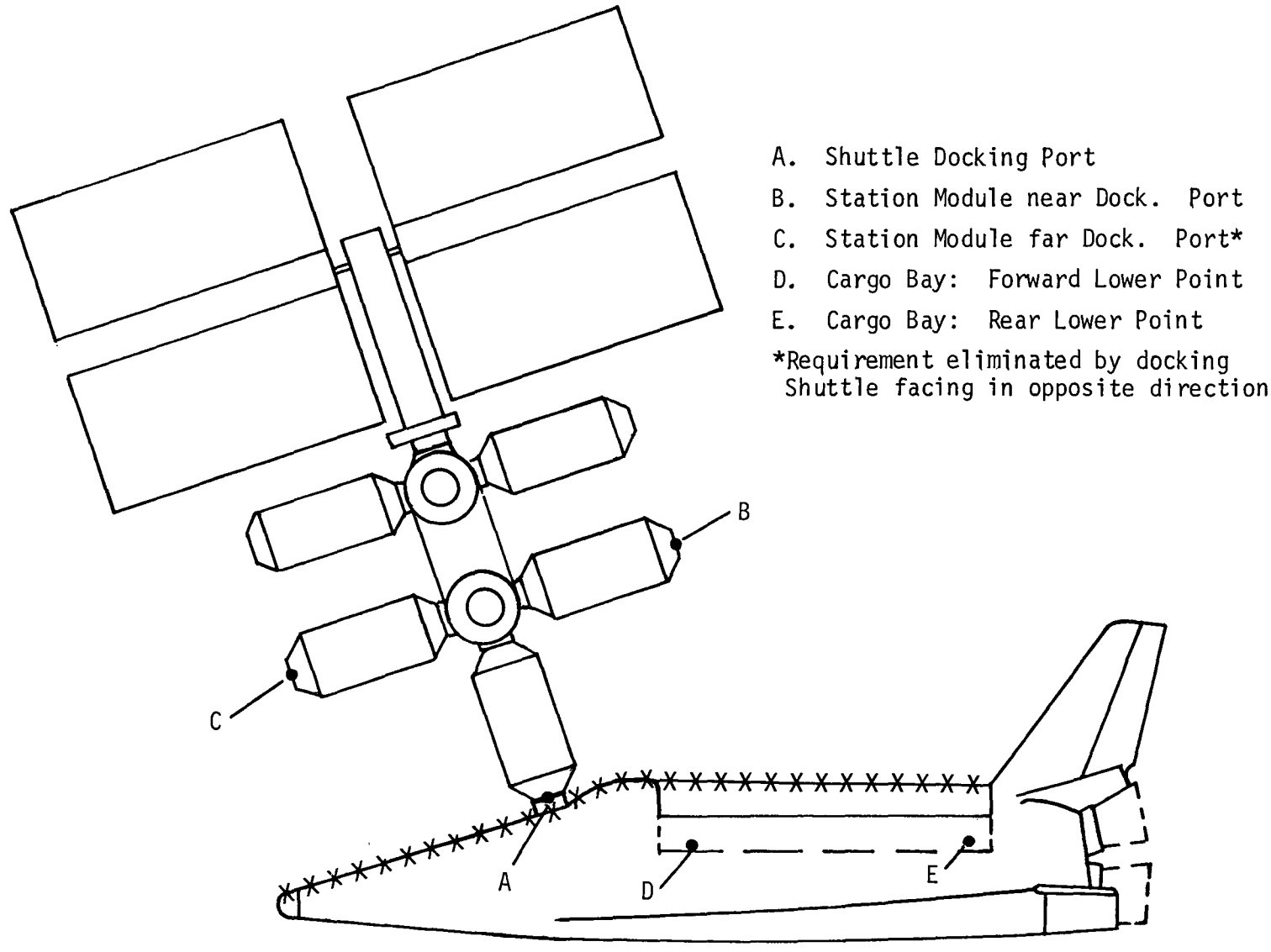

Fig. IV-1 Minimum Reach Requirements

Points* D [x = 2900 cm (1146 in.), y = 851 cm (335 in.)] and E [x = 4602 cm (1812 in.), y = 851 cm (335 in.)] are derived from the minimum sized cargo; namely a 181.6 kg (400 lb) satellite 0.61 m (2 ft) in diameter and 1.22 m (4 ft) long. For reach criteria it was assumed that this 181.6-kg (400 lb) payload could be stowed anywhere (and in any orientation) in the Shuttle cargo bay payload envelope (see Fig. III-1).

Next it was assumed that the RMS arms would be attached to the Shuttle in its symmetry plane somewhere between the nose and the tail on or near the top surface as shown in Fig. IV-1 by the "x" line. A simple digital computer program was written to calculate the distance from points along the attachment line to each of the reach points (A, B, C, D, E). To obtain arm lengths it was assumed that the reach was accomplished with an arm elbow angle of 150° for points A, B, and C and 180° for D and E. The complete extention of the arm in the latter was considered justifiable on the basis that the payload at points D or E was small 181.6 kg (400 lb) compared to the 29,516 kg (65,000 lb) payloads. The resulting data with corresponding letters have been plotted and are shown in Fig. IV-2. A matching Shuttle silhouette is shown above the curves.

Examining the curves in this figure it can be seen that from an x-station of 508 cm (200 in.) to an x-station of 2540 cm (1000 in.) (nose to approximately cargo bay forward bulkhead). Curve E dictates the minimum arm length; and from x-station 2540 cm (1000 in.) to the end of the cargo bay curve C dictates the minimum arm length. The C reach requirement is eliminated with the operational solution of Shuttle docking direction. Now curve E dominates until x-station 3226 cm (1270 in.) where B and A intercept with it. Curve B and then shortly curve A forms the envelope to station x 4737 cm (1865 in.) near the tail. It can readily be seen that the minimum length for a single fixed base arm is one mounted at x-station 3226 cm (1270 in.) and has a length of approximately 14.6 m (48 ft). From these curves one also concludes that there is no arm length reduction by mounting the arm(s) forward of the docking port [x-station 2032 cm (800 in.)].

If the requirement to reach a 181.6-kg (400 lb) satellite at point E could be relaxed (see Selected Concept, Section E, Chapter V), then the minimum length arm becomes 13.71 in. (45ft) with an attachment point at x-station 2743 cm (1080 in.), which is conveniently at the cargo bay forward bulkhead, a good attachment interface.

---

*MDAC Phase B, June 30, 1971 Orbiter reference coordinate system in inches.

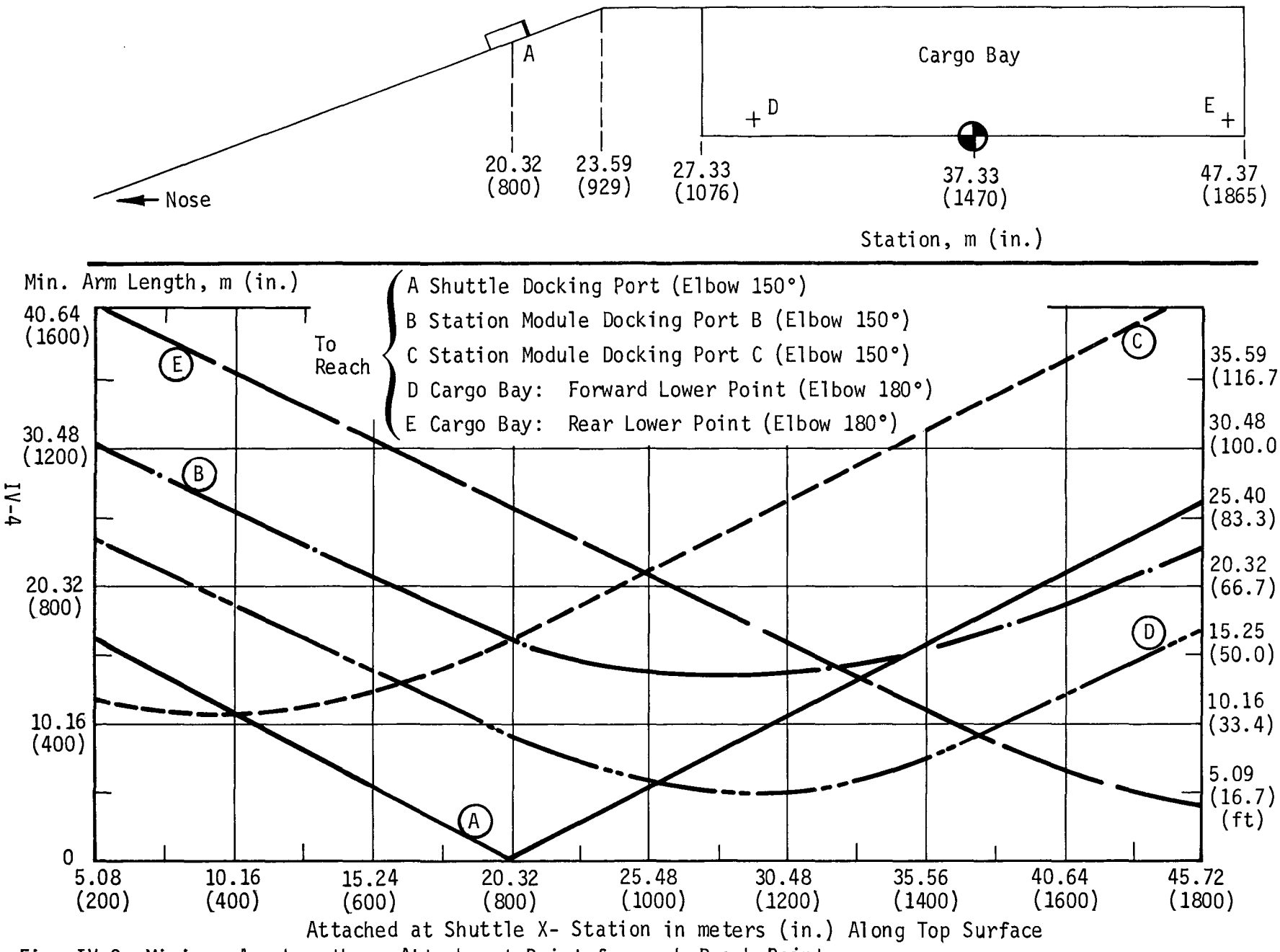

Fig. IV-2 Minimum Arm Length vs Attachment Point for each Reach Point

To examine the penalty for increased arm length we look at the torque requirements as a function of both arm length and attachment point. Before torque requirements can be established, the arm tip velocity and acceleration must first be established.

B. VELOCITY AND ACCELERATION REQUIREMENTS

The requirements for accelerating or decelerating a load attached to the arm(s) is one of the most significant design parameters of the RMS. It determines the forces produced on the arm(s), and consequently the actuator torque and arm structure.

Four RMS tasks were individually analyzed and an approximate timeline established for each. The total time allowed for each task (given in Chapter III) was divided between the functions of that task. The maximum velocity and acceleration (or deceleration) was calculated where applicable for each function. These data are shown in Table IV-1. For Task C (Docking Shuttle) a typical stopping distance of 12.2 m (40 ft) was selected with an initial (required) velocity of 0.12 m/sec (0.4 ft/sec) at capture. For the cargo handling tasks the requirement to bring the cargo to a stop from maximum velocity in a distance of 4.58 m (15 ft) was imposed, as shown in the following example calculation of the acceleration and velocity required for Task D, Function 4 (Table IV-1). As shown in the table, the cargo must move a total distance, d, of 4.88 m (16 ft) in time, t, of 3 minutes or 180 sec. Let d_1 and d_2 be the distances traveled during times t_1 and t_2, respectively. Then

$$d = d_1 + d_2 = \frac{1}{2} a t_1^2 + V_{max}\, t_2$$

$$16 = \frac{1}{2} a t_1^2 + a t_1\, t_2 \qquad \text{[IV-1]}$$

$$d_1 = 15 = \frac{1}{2} a t_1^2 \text{ or } a = \frac{30}{t_1^2} \qquad \text{[IV-2]}$$

$$t_2 = 180 - t_1 \qquad \text{[IV-3]}$$

Table IV-1 Manipulator Arm Velocity and Acceleration Requirements

RMS Tasks and Functions	Distance or Angle to Travel or Rate to Achieve	Estimated Time	V_{MAX} (tangential velocity at tip or angular rate of tip) m/sec (ft/sec)	A_{MAX} (tangential acceleration at tip) m/sec^2 (ft/sec^2)
A. PRECAPTURE (Cargo doors open) Translate tip to "ready" position	16.47 m (54 ft)	1.5 min	0.18 (0.60)	0.11 (0.36)
	Total Time	1.5 min		
B. CAPTURE				
1. Translate tip to compensate for lateral misalignments between Shuttle and object	0.3 m (1 ft)	5 sec	0.08 (0.27)	0.11 (0.36)
2. Achieve and maintain constant lateral velocity to compensate for lateral velocity between Shuttle and object	0.05 m/sec (0.15 ft/sec)	5 sec	0.04 (0.15)	0.009 (0.03)
3. Achieve and maintain constant (negative) radial velocity to compensate for closing velocity between Shuttle and object	0.12 m/sec (0.4 ft/sec)	5 sec	0.13 (0.43)	0.2 (0.08)
4. Decrease radial velocity of tip so that tip-to-receptacle relative velocity is 0.03 m/sec (0.1 ft/sec)	0.09 m/sec (0.3 ft/sec)	5 sec	0.1 (0.34)	0.006 (0.02)
5. Mechanically couple terminal device to receptacle on object	0.3 m (1 ft)	10 sec	0.13 (0.43)	0.003 (0.01)
	Total Time	30 sec		
C. DOCK SHUTTLE to (or undock Shuttle from) orbiting object				
1. Reduce (a) closing velocity, (b) relative lateral velocity, and (c) relative angular velocities to zero before the closing distance is less than 3.3 m (10 ft)	a. 0 ft/sec b. 0 ft/sec c. 0 deg/sec 12.20 m (40 ft) (typical)	3.5 min	a. 0.12 (0.4) b. 0.046 (0.15) c. 0.1 deg/sec	0.00061 (0.002) 0.0002287 (0.00075)
2. Bring the object and the vehicle together so that their docking ports are 0.61 m (2 ft) apart and all relative velocities are zero	7.32 (24 ft)	3.5 min	0.043 (0.132)	0.00036* (0.0012)
3. Position the two so that the docking ports are aligned to within maximum allowed values		2 min		
4. Bring the two together so that at contact the relative velocities and alignment are within the maximum allowed values		1 min	0.021 (0.066)	0.00034† (0.00111)
	Total Time	10 min		
D. UNLOAD AND DEPLOY (or Retrieve and Load) Cargo from (or into Shuttle Cargo Bay				
1. Translate tip so that tip to receptacle distance (on cargo) is 0.3 m (1 ft)	2.44 m (8 ft)	30 sec	0.08 (0.27)	0.11 (0.36)
2. Orient tip to match receptacle on cargo within maximum allowed misalignments		20 sec		
3. Translate tip so that mechanical coupling is achieved between tip and receptacle on cargo	0.305 m (1 ft)	10 sec	0.03 (0.10)	0.11 (0.36)
4. Move cargo upward out of bay until lowest point of cargo is above highest point of bay	4.88 m (16 ft)	3 min	0.053 (0.174)	0.000305 (0.001)
5. Move cargo away from Shuttle and stop	7.93 m (26 ft)	4 min	0.053 (0.174)	0.000305 (0.001)
6. Orient cargo in desired attitude		100 sec		
7. Release cargo		20 sec		
	Total Time	10 min		
E. MODULE UNLOAD, TRANSFER AND DOCK TO SPACE STATION (or undock module, transfer, and load into Shuttle)				
1. Translate tip so that tip to receptacle distance (on cargo) is 0.3 m (1 ft)	2.44 m (8 ft)	30 sec	0.08 (0.27)	0.109 (0.36)
2. Orient tip to match receptacle on cargo within maximum allowed misalighments		20 sec		
3. Translate tip so that mechanical coupling is achieved between tip and receptacle	0.3 m (1 ft)	10 sec	0.03 (0.10)	0.1098 (0.36)
4. Move cargo upward out of bay until lowest point of cargo is above highest point of bay	4.88 m (16 ft)	2.5 min	0.064 (0.21)	0.000436 (0.00143)
5. Move cargo from shuttle and stop when cargo docking port is 4 feet from docking port on space station	15.25 m (50 ft)	4 min	0.086 (0.28)	0.000793 (0.0026)
6. Align cargo so that lateral errors are within maximum limits		45 sec		
7. Orient cargo so that attitude errors are within maximum allowable limits		45 sec		
8. Dock cargo to Space Station with contact conditions within the maximum allowed values	1.22 m (4 ft)	40 sec	0.03 (0.10)	0.000762 (0.0025)
9. Release cargo		20 sec		
	Total Time	10 min		

*Minimum acceleration for this task. Full acceleration for 1.75 min and full deceleration for 1.75 min. Velocity is maximum attained.

†Minimum acceleration to move 0.61 m (2 ft) in 1 minute. Full acceleration total time. Velocity is maximum achieved at contact.

Substituting Eq [IV-2] and [IV-3] into Eq [IV-1]

$$16 = \frac{1}{2}\left(\frac{30}{t_1^2}\right)t_1^2 + \left(\frac{30}{t_1^2}\right)t_1\ (180 - t_1)$$

Solving for t_1

$$t_1 = 174 \text{ sec}$$

Substituting into Eq [IV-2]

$$a = \frac{30}{(174)^2} = 0.0003 \text{ m/sec}^2\ (0.001 \text{ ft/sec}^2)$$

Solving for V_{max}

$$V_{max} = at_1 = (0.001)\ (174) = 0.053 \text{ m/sec } (0.174 \text{ ft/sec})$$

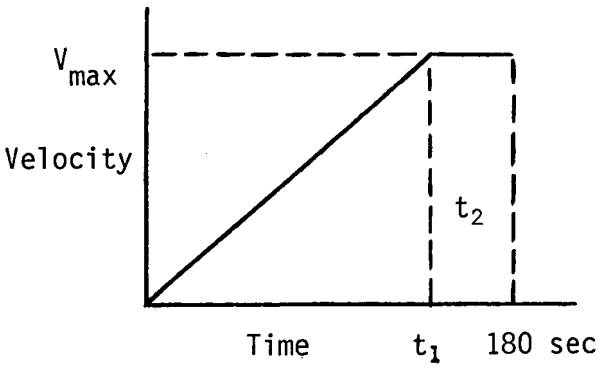

The functions of Tasks B, C, D and E are shown in the form of velocity curves in Fig. IV-3, IV-4, IV-5, and IV-6. A composite of events, capture Space Station, Dock Shuttle to Space Station and transfer module from Shuttle to Station (Tasks B, C, E) is shown in Fig. IV-7.

From the data presented above, it can be seen that the largest docking deceleration is 0.00061 m/sec^2 (0.002 ft/sec^2). This value can increase or decrease depending on the arm length, since a larger arm allows increased time to slow the Shuttle, i.e., reduce its relative velocity after capture and vice versa. In the next section we calculate the torque requirements of the RMS for varying arm lengths and for several Shuttle attachment points.

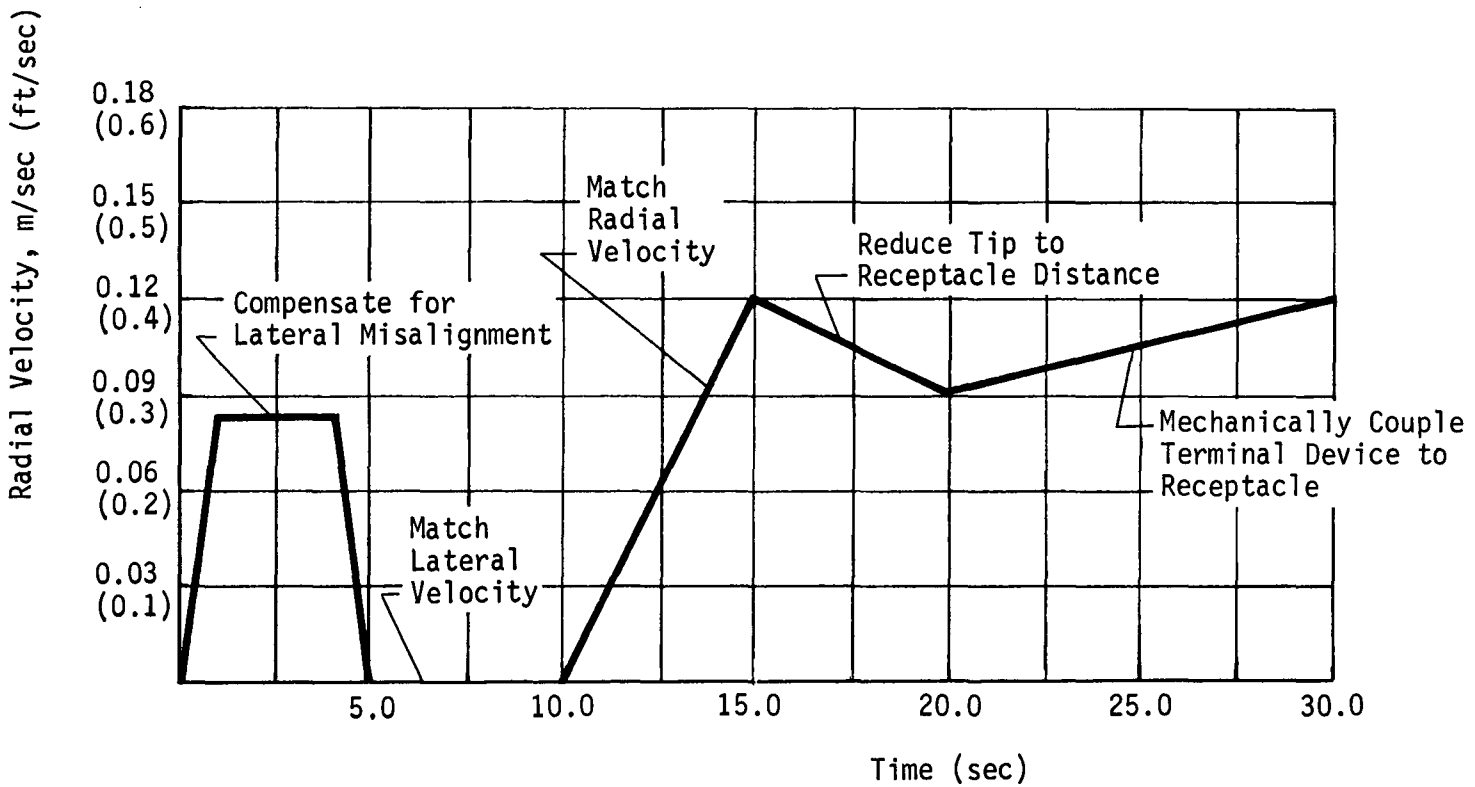

Fig. IV-3 RMS Tip Velocity Timeline: Task B - Capture

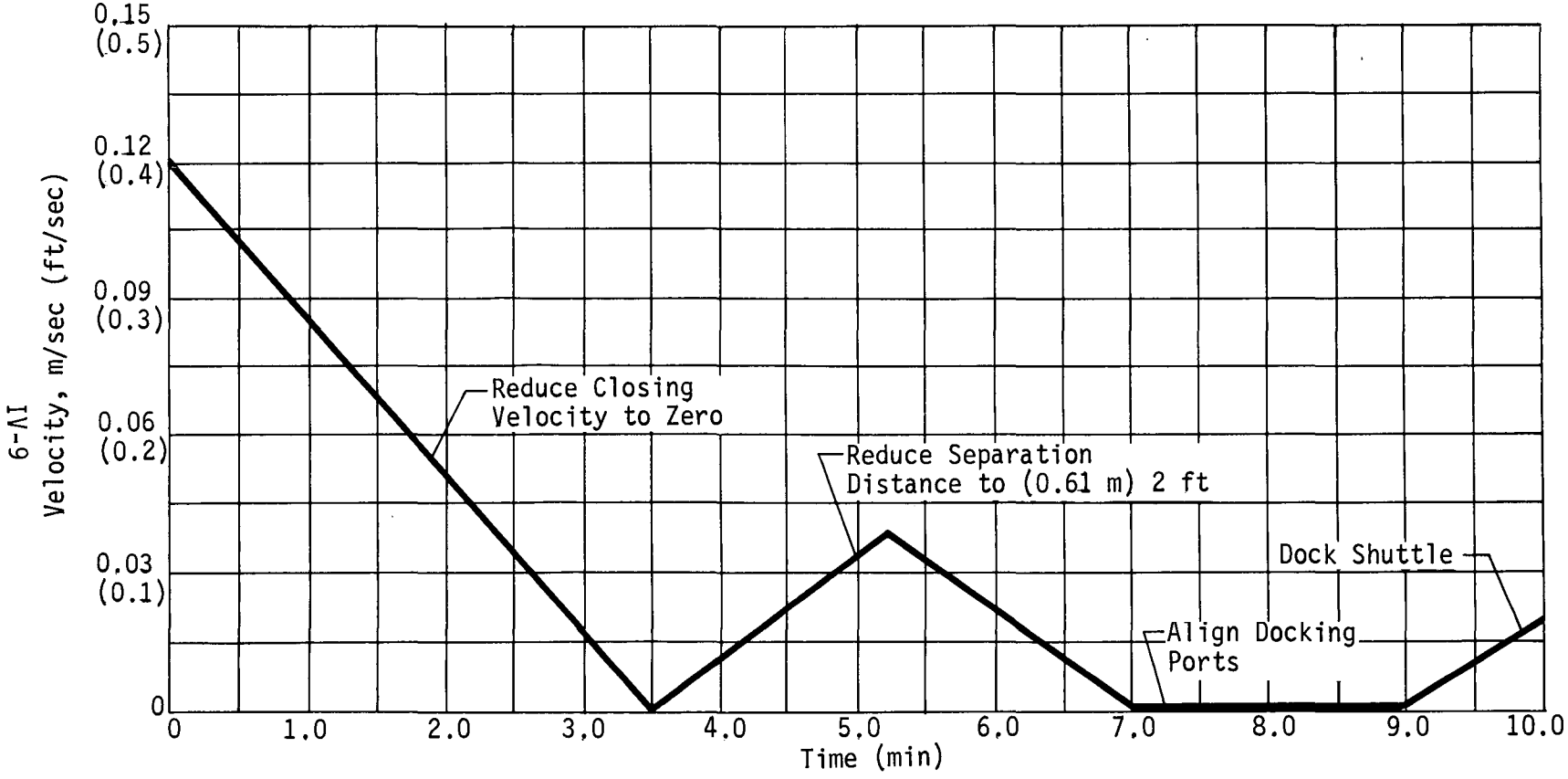

Fig. IV-4 RMS Tip Velocity Timeline: Task C - Dock Shuttle

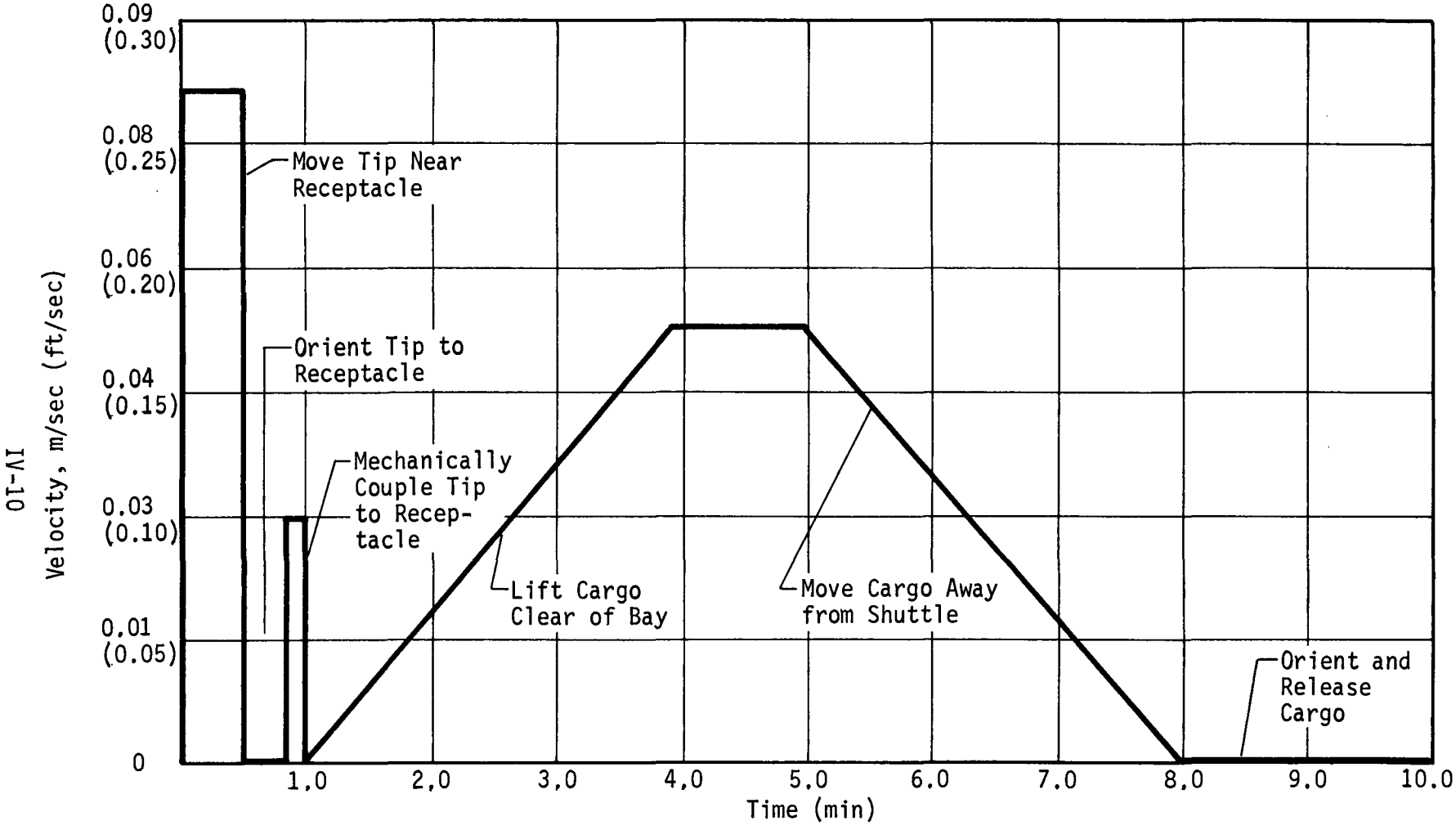

Fig. IV-5 RMS Tip Velocity Timeline: Task D - Unload and Deploy

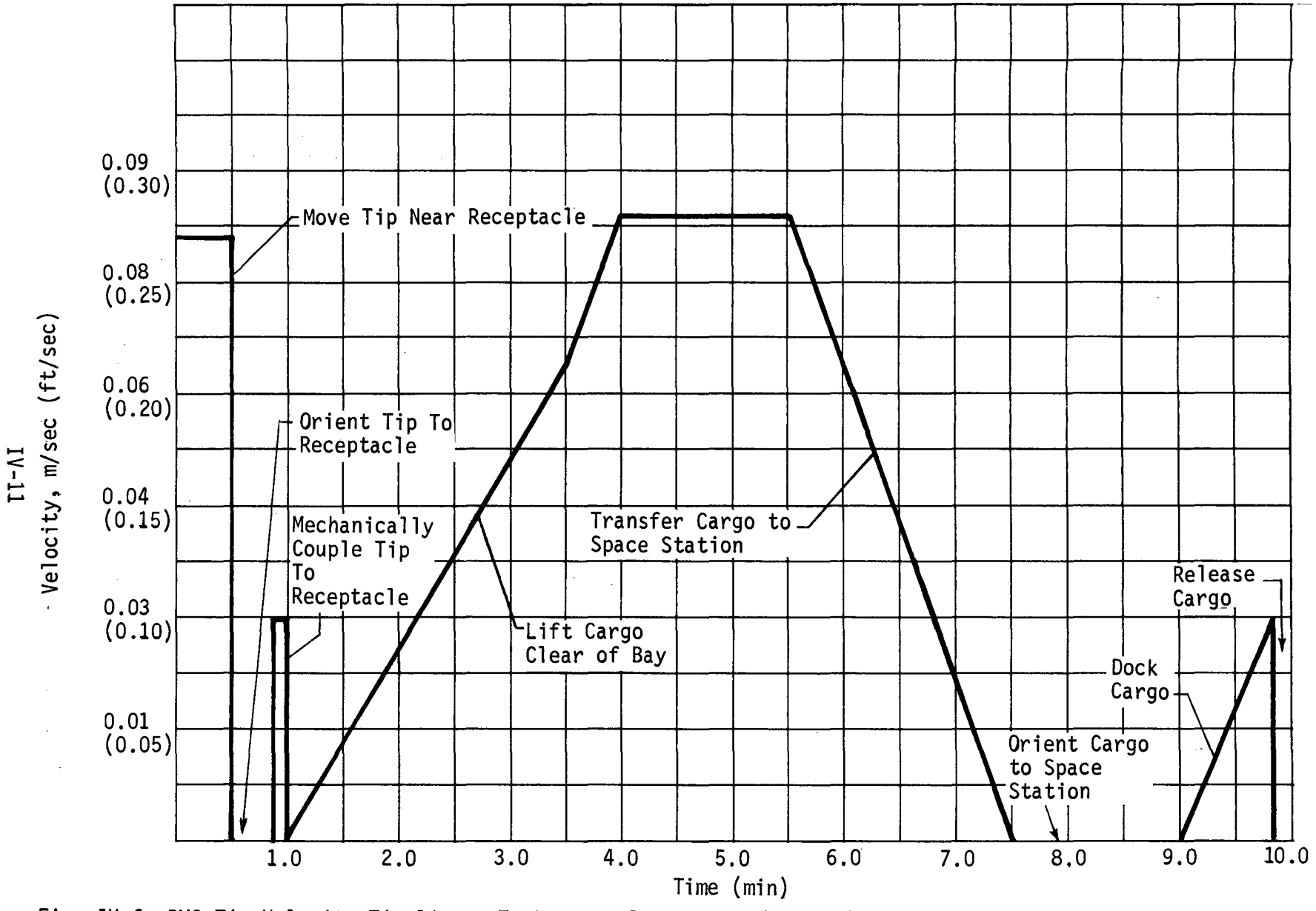

Fig. IV-6 RMS Tip Velocity Timeline: Task E - Unload, Transfer, and Dock Module

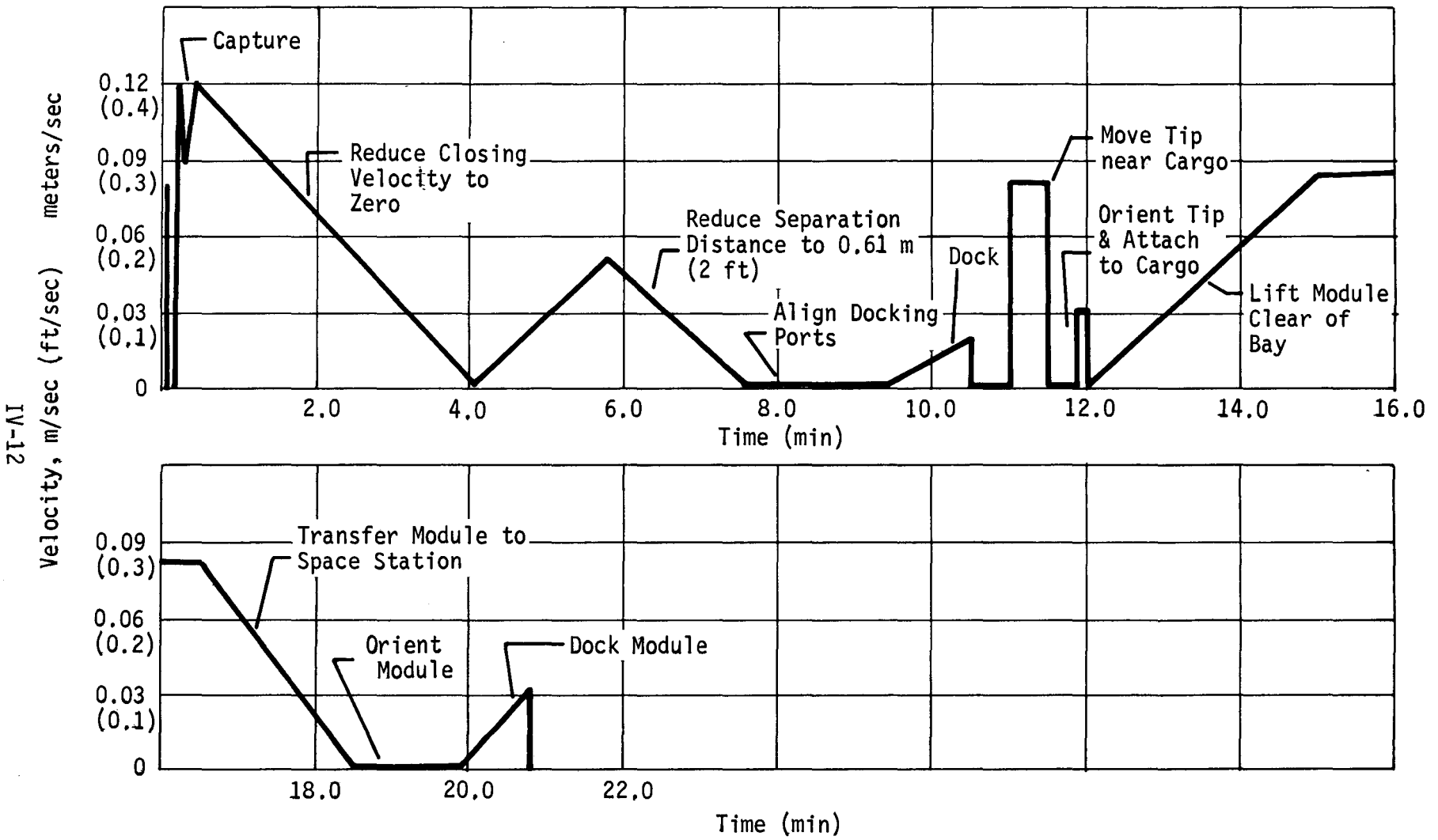

Fig. IV-7 RMS Tip Velocity Timeline: Capture, Dock, and Module Transfer (Tasks B, C, E)

C. TORQUE REQUIREMENTS

This section delves into the heart of the RMS requirements and sheds light on the nature of the problem. First, an initial force analysis is carried out. A Shuttle is moving with a velocity of 0.122 m/sec (0.4 ft/sec) relative to another body. The object is to apply an external restraining force, F, bringing the Shuttle to rest relative to the other body.

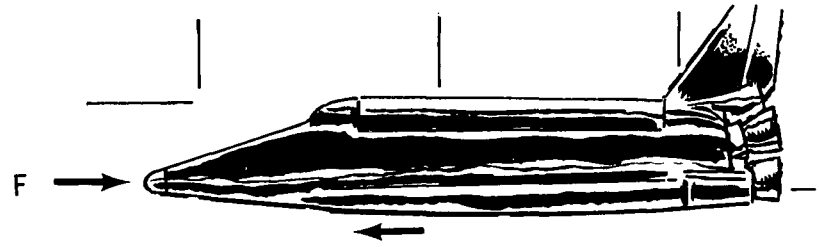

v = 0.122 m/sec (0.4 ft/sec)

Looking at Newton's first law, where m is the mass of the Shuttle

$$F = m\frac{dv}{dt} = m\frac{\Delta V}{\Delta t}$$

with a constant applied force, and incremental changes in velocity ΔV, and time, Δt. Rearranging, $F\Delta t = m\Delta V$ = constant. Figure IV-8 represents the above equation for a Shuttle mass of 10,000 slugs and a ΔV of 0.122 m/sec (0.4 ft/sec). Now, the fundamental tradeoff is apparent. We may reduce the applied force if we are willing to increase the time of application. In the cargo handling tasks, this time tradeoff is easy to comprehend. Merely maintain low acceleration and deceleration of the payloads to keep the required RMS applied forces low. For the docking task, increasing time means increasing stopping distance which means increasing arm length.

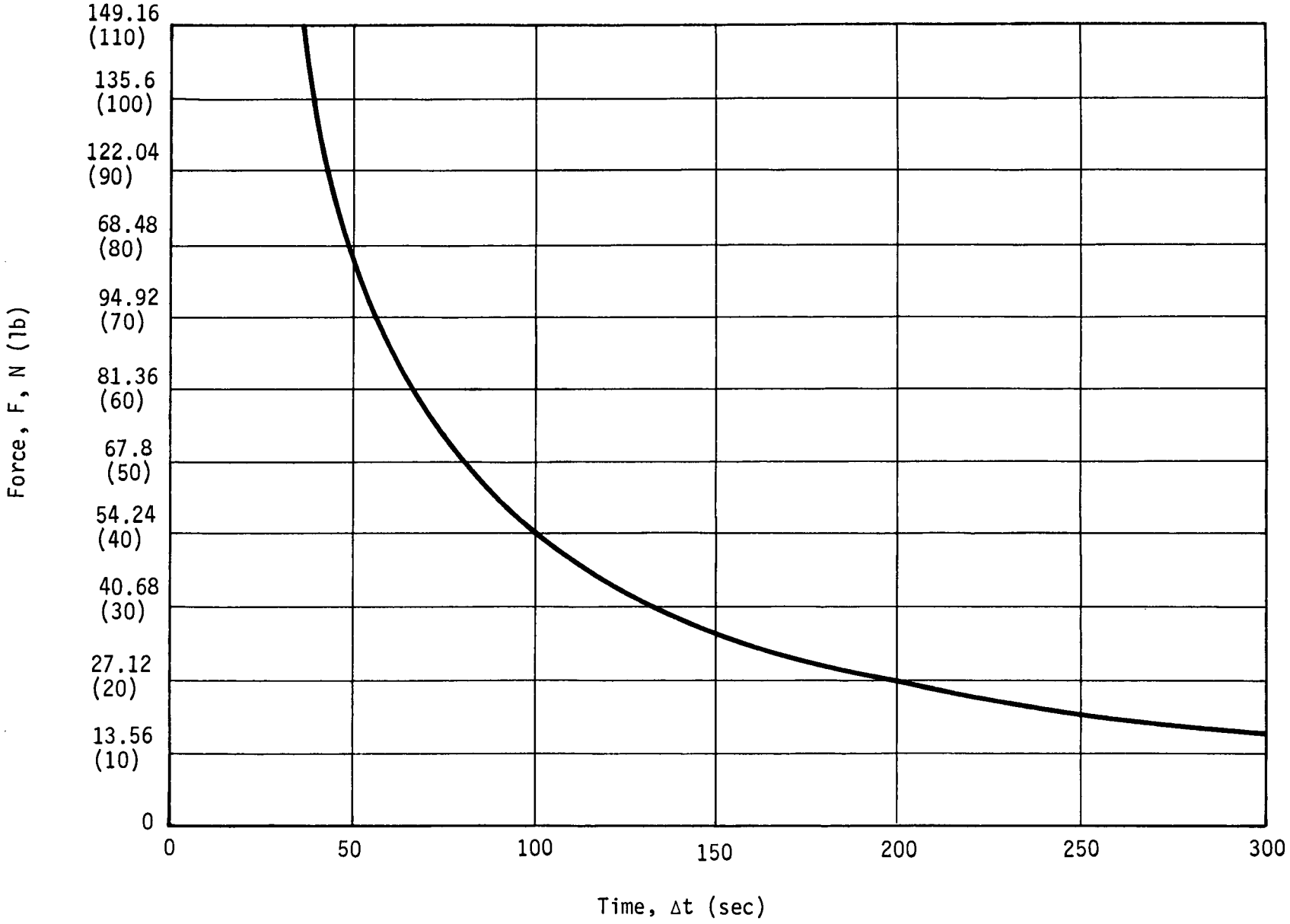

Fig. IV-8 Reducing Shuttle Velocity: Force vs Time Applied

Figure IV-9 is a plot of the distance to bring the ΔV to zero vs applied force. Two head-on cases are shown, the Shuttle approaching another Shuttle and the Shuttle approaching an infinitely massive Space Station. The applied force, F, is that which would be applied by the RMS arm(s) after capture. The stopping distance translates into a minimum arm length for the corresponding force.

For the arm to apply a tip force, torques must be applied at the joints. A comparison of the required torque in the head-on case with that required in the swingby case showed a somewhat increased value for the latter. Therefore, the swingby case was used for a conservative approach. Also the safety aspects were improved with the swingby method. For analysis purposes only one arm was used in the torque analysis. For worst-case conditions the arm terminal device (hand) was attached to an infinitely large mass. The Shuttle was allowed to swing through an arc of 1 radian (57°) during which a constant torque was applied at the wrist joint. In this planar case, the Shuttle velocity was taken to be perpendicular to the radius vector from the wrist to the shoulder joint, as shown in Fig. IV-10.

The swing angle, θ, began [with ΔV = 0.12 m/sec (0.4 ft/sec)] at θ = 0.5 radian and ended (with ΔV = zero) at θ = -0.5 radians. The elbow joint was held fixed at a 120° angle, and the shoulder joint was fixed at 60°. The torque, applied totally at the wrist joint, was calculated vs arm length for various Shuttle attachment points, A through H, where A is directly over the center of mass of the Shuttle. The equations developed for this case are derived below. The values calculated with the resulting equations are shown in Fig. IV-11.

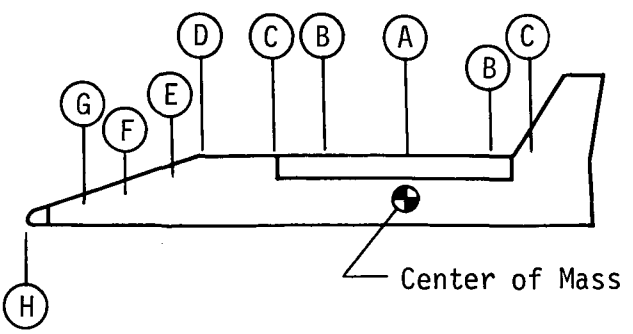

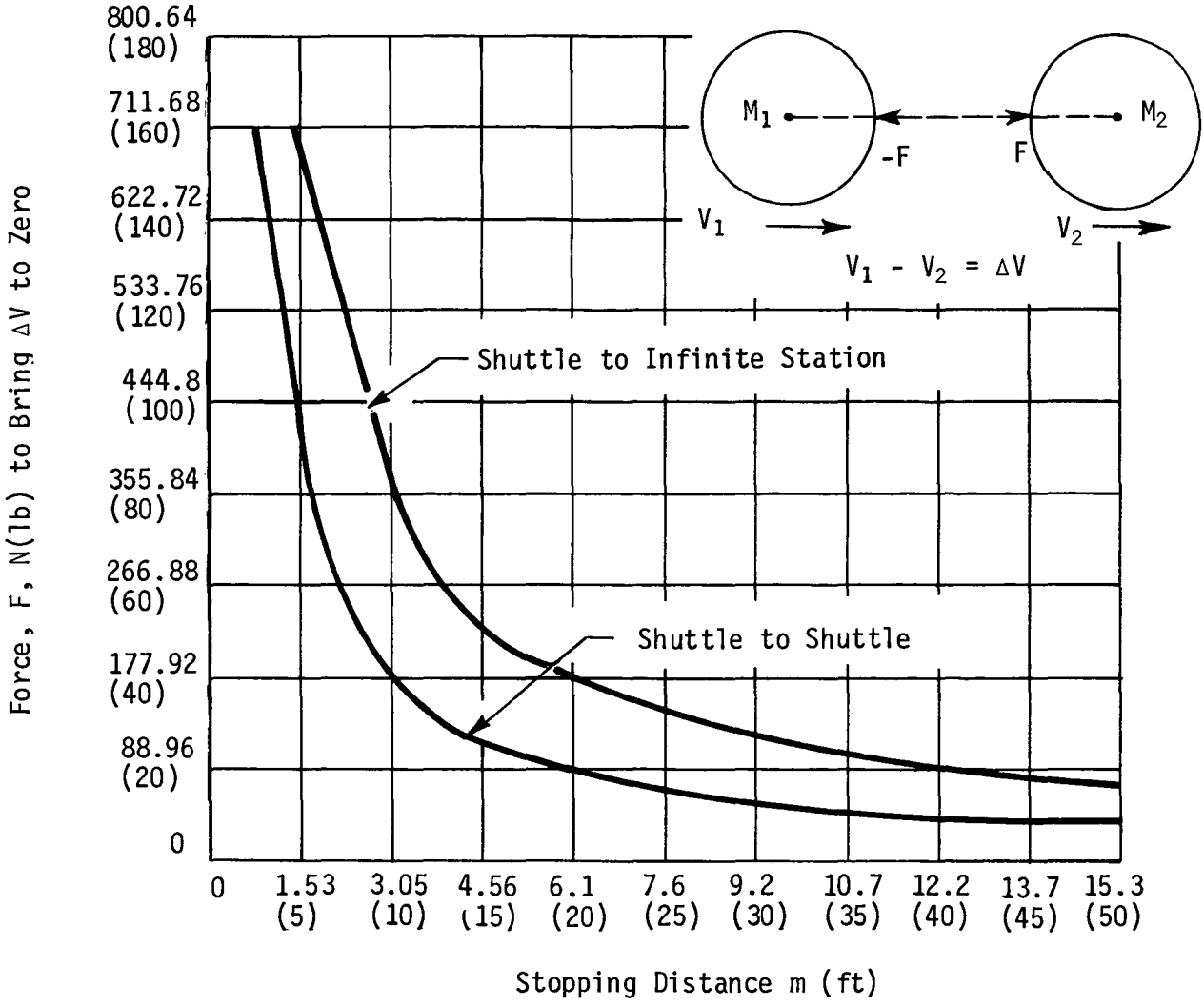

Fig. IV-9 Stopping Distance vs Applied Force: Head-On Case

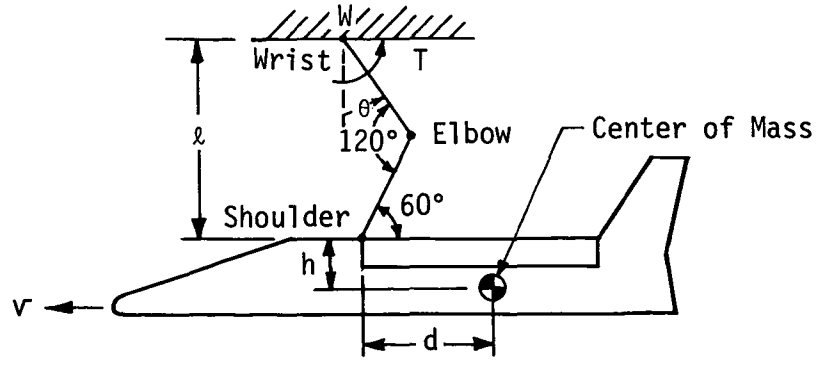

Fig. IV-10 Swingby Docking

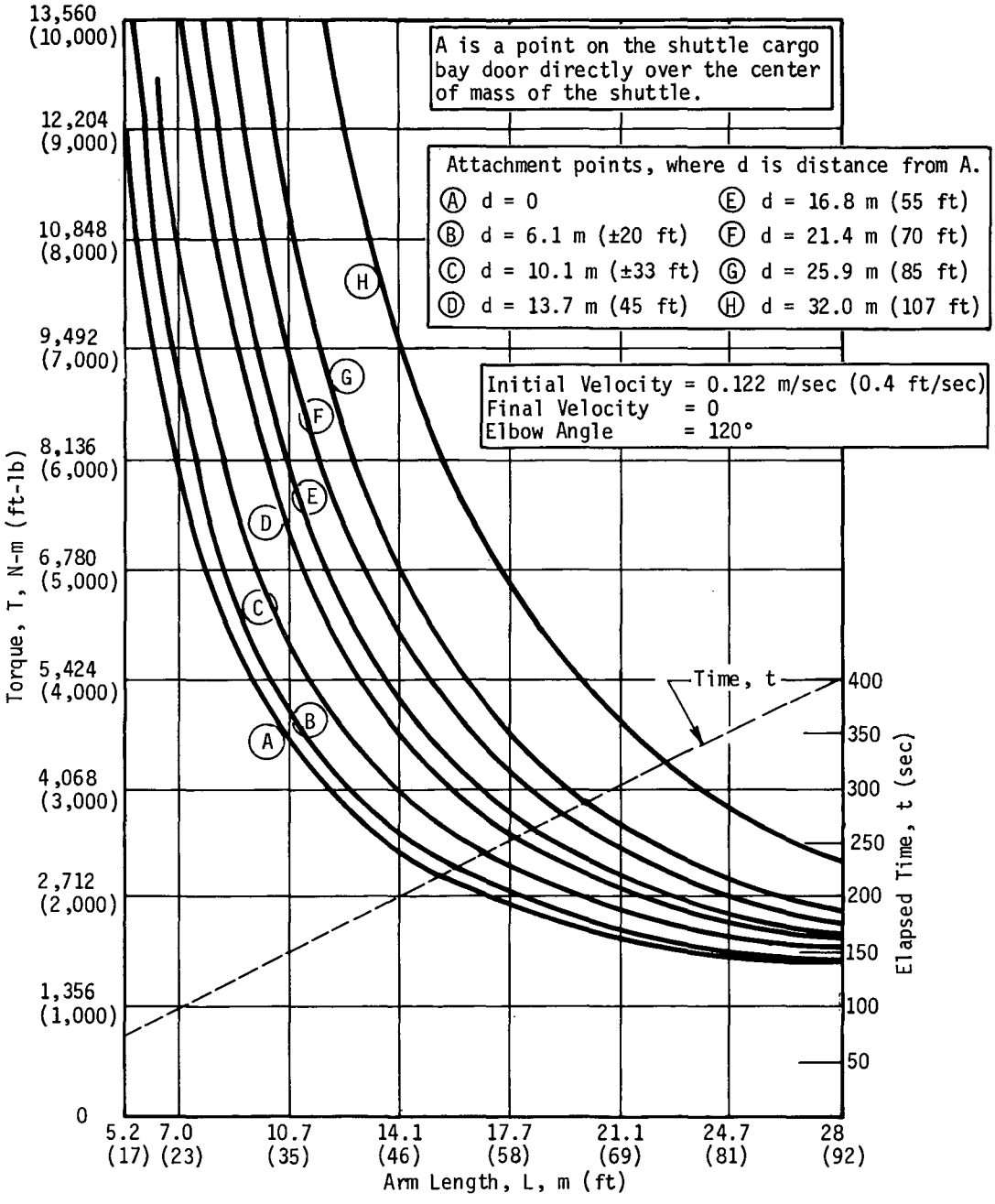

Fig. IV-11 Applied Torque and Elapsed Time vs Arm Length for Various Attachment Points: Swingby Case

Assuming the wrist is fixed in inertial space, one can write

$$T = I^{S/W} \ddot{\theta} \qquad \text{[IV-4]}$$

where dots denote differentiation with respect to time, t, and $I^{S/W}$ is the moment of inertia of the shuttle about W in the direction perpendicular to the plane of motion (see Fig. IV-10). Since the elbow and shoulder joints are fixed, it follows that

$$I^{S/W} = I^{S/CM} + M_S [(\ell + h)^2 + d^2] \qquad \text{[IV-5]}$$

where $I^{S/CM}$ is the moment of inertia of the Shuttle about its mass center and M_S is the mass of the Shuttle.

It follows from Eq [IV-5] that $I^{S/W}$ is constant and, therefore, one can integrate Eq [IV-4] twice to obtain

$$\dot{\theta} = \frac{T}{I^{S/W}} t + \dot{\theta}_o \qquad \text{[IV-6]}$$

and

$$\theta = \frac{T}{I^{S/W}} \frac{t^2}{2} + \dot{\theta}_o t + \dot{\theta}_o \qquad \text{[IV-7]}$$

where $\dot{\theta}_o$ and θ_o are the initial values of $\dot{\theta}$ and θ, respectively.

If t_f denotes the time required to stop the motion, it follows from Eq [IV-6] that (noting that $\dot{\theta}_o$ is negative)

$$t_f = - \frac{I^{S/W} \dot{\theta}_o}{T} \qquad \text{[IV-8]}$$

The angle through which the arm rotates during this time is obtained by substituting Eq [IV-8] into [IV-7]:

$$\Delta\theta = \theta - \theta_o = -\frac{1}{2}\frac{I^{S/W}\dot{\theta}_o^{\,2}}{T}$$

or, solving for T

$$T = -\frac{1}{2}\frac{I^{S/W}\dot{\theta}_o^{\,2}}{\Delta\theta} \qquad [IV-9]$$

Now, assuming the initial tangential velocity of the shoulder is v, it follows that

$$\dot{\theta}_o = -\frac{v}{\ell} \qquad [IV-10]$$

and recalling that $\Delta\theta = -1$ rad, one can write

$$T = \frac{1}{2}\frac{I^{S/W}v^2}{\ell^2} \qquad [IV-11]$$

and substitution from Eq [IV-10] and [IV-11] into [IV-8] yields:

$$t_f = \frac{2\ell}{v} \qquad [IV-12]$$

Now, if each arm segment is of length L/2 with a constant 120° angle at the elbow, it follows that

$$\ell = 0.866L \qquad [IV-13]$$

Finally, substitution from Eq [IV-5] and [IV-13] into [IV-11] gives

$$T = \frac{4v^2}{3L^2}\left\{I^{S/CM} + M_S\left[(0.866L + h)^2 + d^2\right]\right\} \qquad [IV-14]$$

and from Eq [IV-12] and [IV-13]

$$t_f = \frac{1.732L}{v} \qquad [IV-15]$$

Results obtained with Eq [IV-14] and [IV-15] are plotted in Fig. IV-11 for the following data:

$v = 0.122$ m/sec (0.4 ft/sec)

$I^{S/CM} = 20.5 \times 10^6$ kg-m^2 (15.124×10^6 slug-ft^2)

$M_S = 14.59 \times 10^4$ kg (10^4 slugs)

$h = 5.19$ m (17 ft) for $d \leq 13.85$ m (45.4 ft)

$h = 5.19 - 0.368\ (d - 13.85)$ for $d > 13.85$ m

The torque vs arm length curves show the increasingly high penalty paid in torque required for reducing the arm length. Increased torque (short arm length) means increased joint actuator weight and increased electrical power. The longer arm length that comes with decreased torque produces arm structural weight penalties and stowage problems. The variation in torque as a function of the attachment point shown in the curves was expected. As we move away from the center of mass the torque needed increases.

Next, the cargo handling torque requirements are examined. Four payloads are considered: (1) 181.6 kg (400 lb) satellite, (2) 2270 kg (5000 lb) satellite, (3) 9080 kg (20,000 lb) module, and (4) 29,510 kg (65,000 lb) module. Payloads (1), (2), and (4) are analyzed using the unload and deploy task while (3) is analyzed for both the unload and deploy (Task D) and the unload, transfer, and dock (Task E).

The basic requirement for cargo handling is the need to stop a cargo while being translated at maximum velocity in a stopping distance of 4.6 m (15 ft) or less. The maximum velocities while loaded, derived in Section B, for Task D is 0.053 m/sec (0.174 ft/sec) and for Task E is 0.085 m/sec (0.28 ft/sec). With these values of velocity and stopping distance as a basis, the torques required to stop the above cargoes have been calculated as a function of arm length. The resulting data are shown in Fig. IV-12. Each case is taken with two different payload attachment points. The equations used to develop these torques are derived here.

In this case, the Shuttle is assumed fixed inertially and the cargo is moved by applying a constant torque, T, at the shoulder joint S. The elbow and wrist angles are assumed fixed in such a way that the wrist to shoulder separation distance is ℓ. The center of mass of the cargo, C, is denoted by C* and is located by distances d and W from the attachment point (see Fig. IV-13).

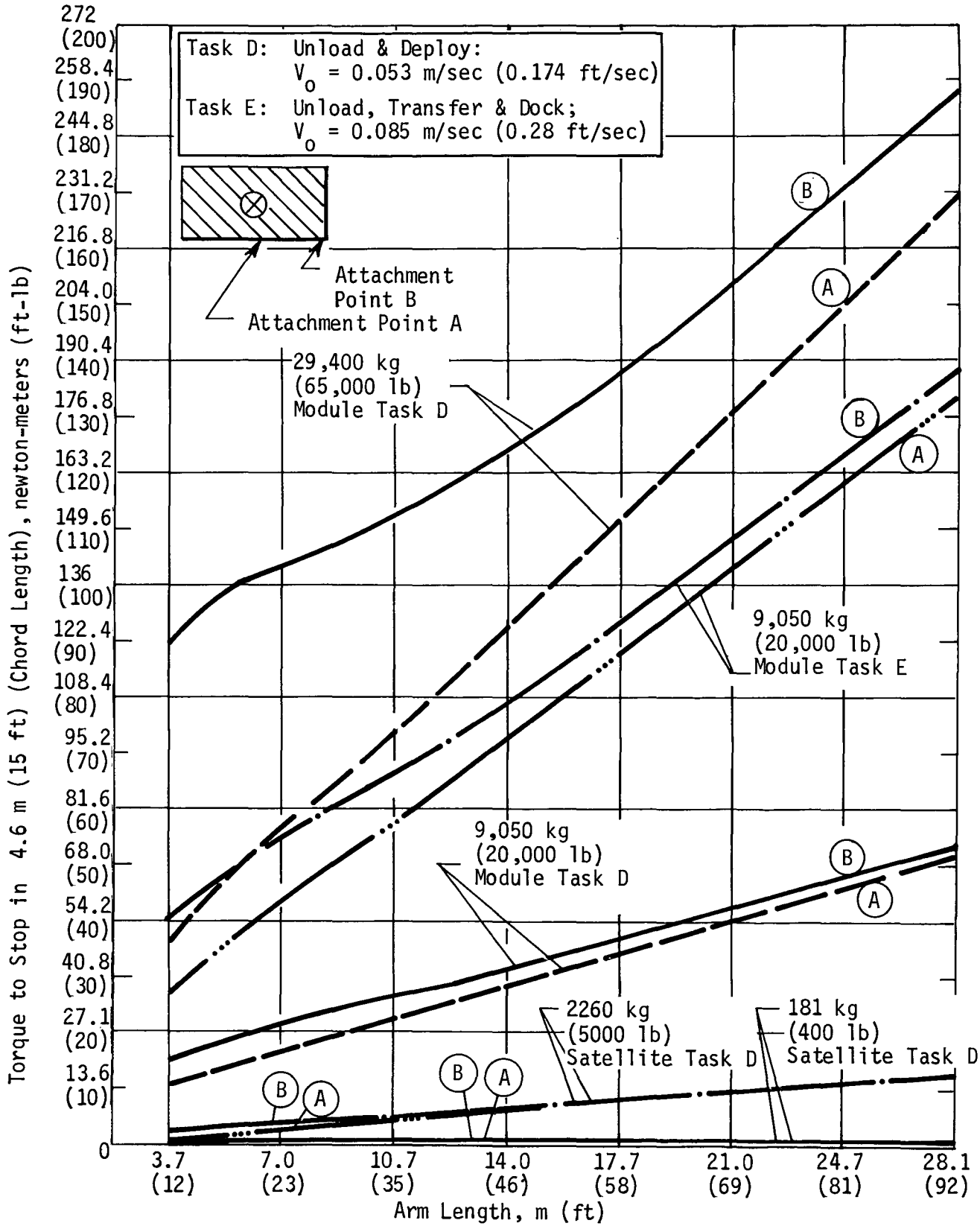

Fig. IV-12 Torque vs Arm Length to Stop Moving Cargo

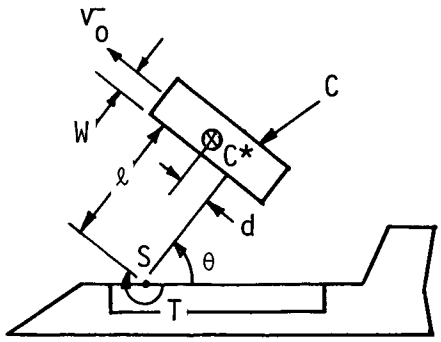

Fig. IV-13 Cargo Handling

Because the point S is fixed in inertial space one can write

$$T = -I^{C/S}\ddot{\theta} \qquad [IV\text{-}16]$$

where

$$I^{C/S} = I^{C/C^*} + M_C\,[(\ell + W)^2 + d^2] \qquad [IV\text{-}17]$$

and I^{C/C^*} is the moment of inertia of C about C*, perpendicular to the plane of motion, M_C is the mass of the cargo, and ℓ, W and d are indicated in Fig. IV-13.

Following the same procedure as in the swing-by docking case, one arrives at

$$T = -\frac{1}{2}\frac{I^{C/S}\dot{\theta}_o^{\,2}}{\Delta\theta} \qquad [IV\text{-}18]$$

for the torque required to stop the cargo in an angle, $\Delta\theta$, for an initial angular velocity of $\dot{\theta}_o$. Assuming the initial velocity of C* is v_o, it follows that

$$\dot{\theta}_o = \frac{v_o}{\ell + W} \qquad [IV\text{-}19]$$

and if $\Delta\theta$ is taken to be the angle necessary to translate the wrist through a chord length of ℓ_C, the following relationship exists:

$$\ell_C = 2\ell\ \mathrm{Sin}\left(\frac{\Delta\theta}{2}\right) \qquad [IV\text{-}20]$$

Thus, solving Eq [IV-20] for $\Delta\theta$ and substituting the result along with $\dot{\theta}_o$ from [IV-19] into [IV-18], one is left with

$$T = \frac{I^{C/S} v_o^2}{4(\ell + W)^2 \sin^{-1}\left(\frac{\ell_c}{2\ell}\right)} \qquad [IV-21]$$

where $I^{C/S}$ is given by Eq [IV-17].

As in the flyby case, if the wrist to shoulder separation, ℓ, is the result of two arm segments of length L/2 with a constant 120° angle at the elbow, one has

$$\ell = 0.866L \qquad [IV-22]$$

Assuming this to be the case, the graphs of T vs L for the two cargo handling tasks and the four payloads mentioned above are plotted in Fig. IV-12.

The next section examines the relationships between arm length and joint weight for docking and beam structural weight for both docking and for cargo handling.

D. JOINT WEIGHT AND BEAM WEIGHT

The torque requirements for docking, calculated in the preceding section and the velocity requirement established in Section B, were used to determine the motor and speed reducers necessary at each joint.

For purposes of analysis a DC torque motor, a harmonic drive, and spur gears as required, were used as the basis for the joint actuation. Also for the purpose of alternative concept comparison it was assumed that only one arm was used.

Figure IV-14 shows the penalty paid in the weight of the major components as the arm length is reduced (or docking torque required increased as shown in Fig. IV-11). The data for the curve were based on Inland Motor Company DC Torque Motors and on United Shoe Machinery Corporation harmonic drives. Adjustments were made for expected reduction in weight due to the use of lighter construction materials in these components.

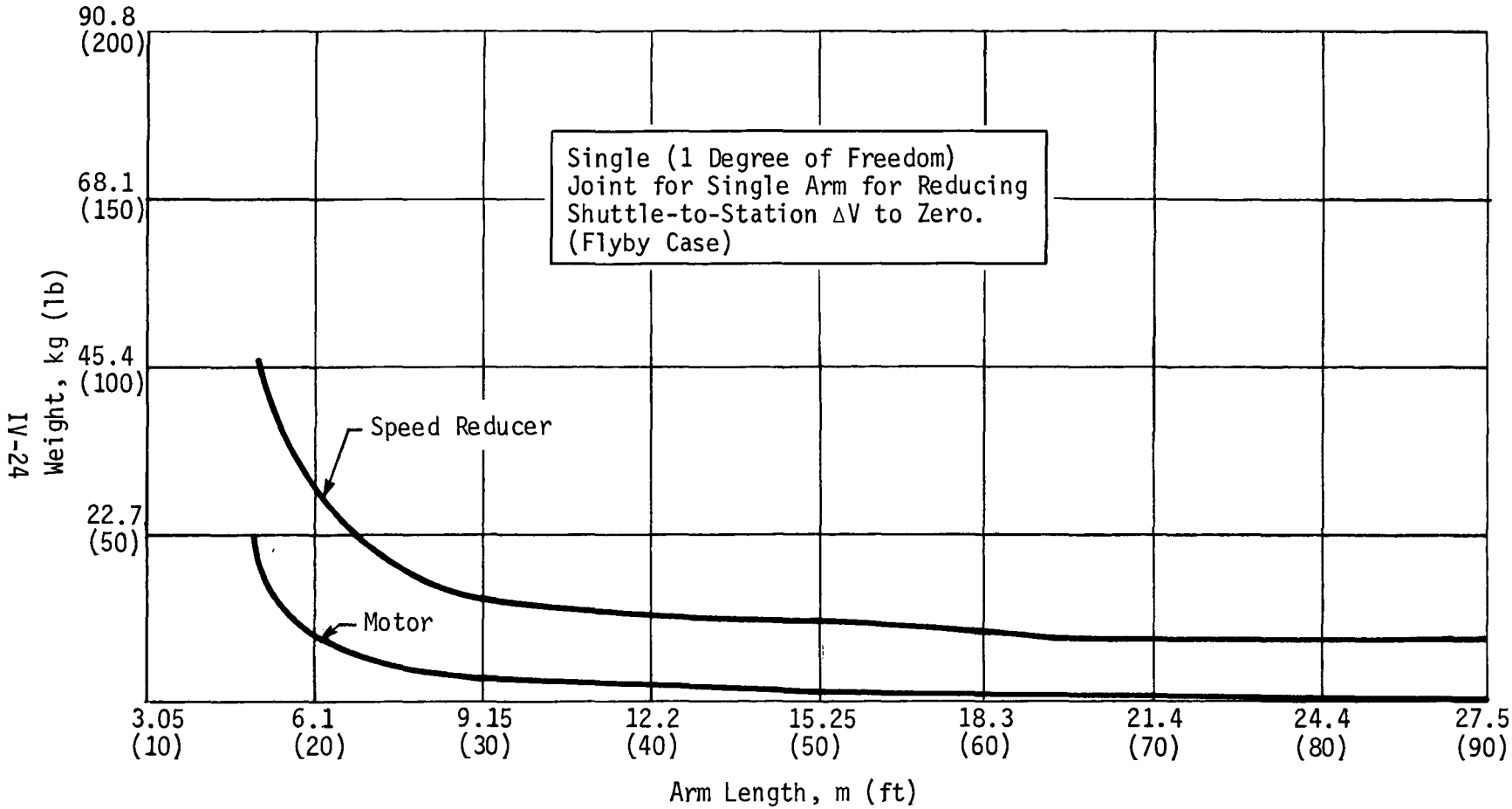

Fig. IV-14 Major Components of Joint Weight vs Arm Length

To obtain a more complete joint weight penalty picture, the weight of other components were added to that of the motor and speed reducer; namely, a potentiometer, tachometer, bearings, housing, and wiring. The weight for all joint components in a six-joint arm is shown vs arm length in Fig. IV-15.

Next, the beam structure between the joints is examined. Two structural materials are considered: aluminum alloy and boron-epoxy. The structural problem was first analyzed as a cantilever beam problem as shown in Fig. IV-16. The constraints were: (1) beam maximum diameter of 30.5 cm (12 in.) and (2) beam minimum wall thickness of 0.159 cm (1/16 in.). The elbow was taken to be locked in position at a 120° included angle. A maximum tip deflection of 2.54 cm (1 in.) at maximum load was taken as per the requirements in Chapter III. The resulting structural analysis is shown in Fig. IV-17 where beam weight is plotted vs arm length. Here the weight picture has changed. The weight penalty now increases for longer arms.

The curve for total joint weight is added to that for beam weight (boron-epoxy) and the resulting total arm weight vs arm length is shown in Fig. IV-18.

The structures problem was considered next with torques applied at both wrist and shoulder joints. This results in an S-shape deflection as shown in Fig. IV-19. This results in beams of one-fourth the weight, as shown in Fig. IV-20.

The total joint weight for the two-applied moments case was calculated for each arm length and the results added to the (boron epoxy) beam weight curve for the same case. The resulting curve of arm weight vs arm length is shown in Fig. IV-21. This curve reveals unexpected results; namely, that for a large spectrum of arm lengths the total arm weight is constant. And for lengths from 7.02 m (23 ft) to 25.01 m (82 ft) the weight for all is between 136.2 kg (300 lb) and 181.6 kg (400 lb).

Last in this section, the beam weights for handling the torques required for cargo handling are calculated vs arm length. Figure IV-22 displays the results. The curves are labeled as per the task and payload considered. The discontinuity in the curves is due to a change from 0.08 cm (1/32 in.) wall thickness (for diameters less than 12.7 cm (5 in.) to 0.16 cm (1/16 in.) wall.

The calculations were based on torques applied only at the shoulder joint and on boron-epoxy structural material.

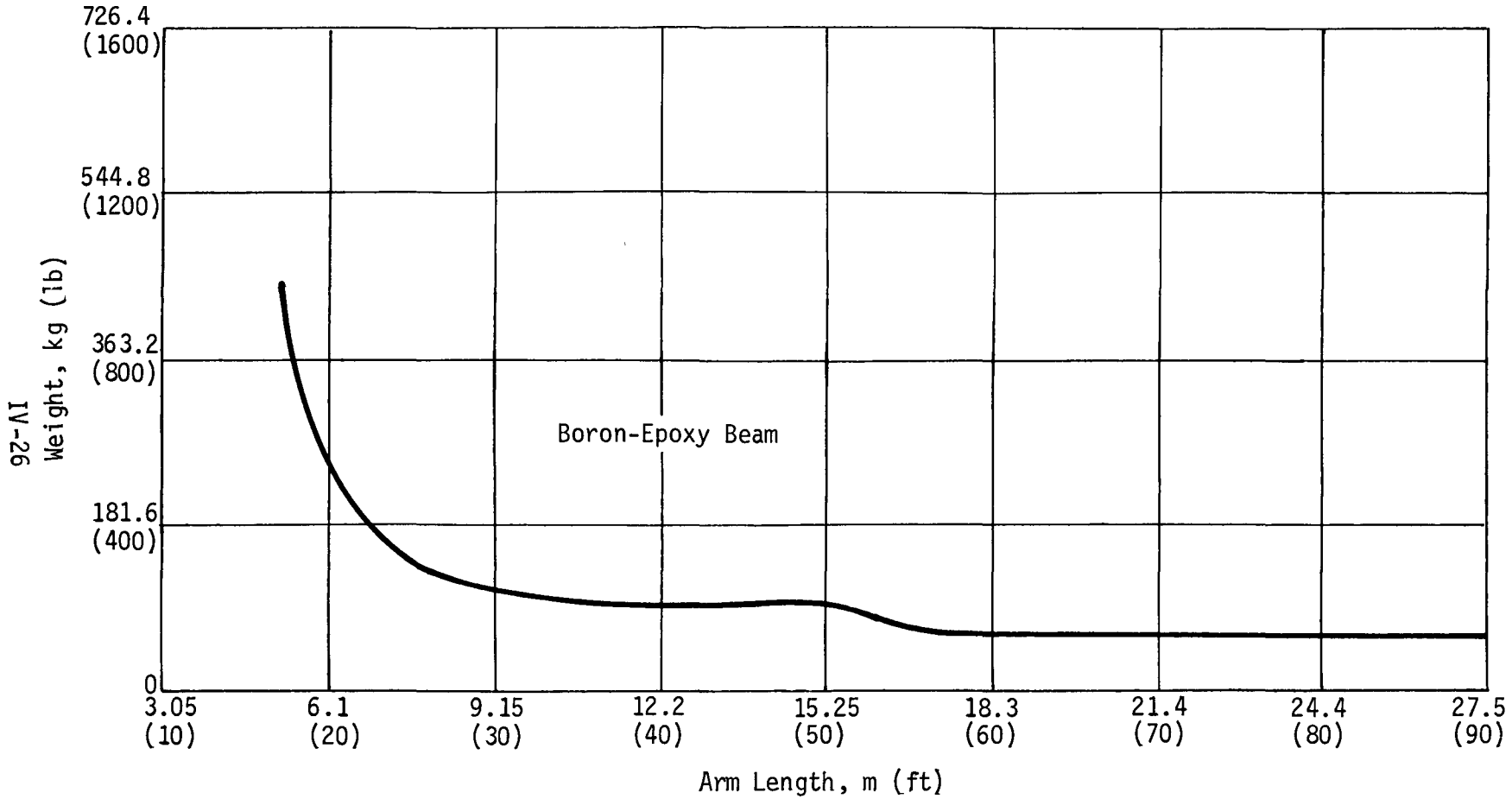

Fig. IV-15 Total Weight of Joints vs Arm Length - Single Docking Arm

CASE 1. ONE TORQUE MOTOR, M

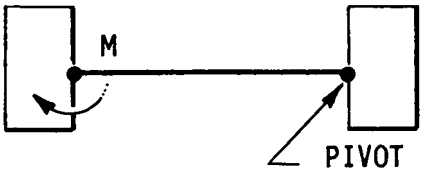

CANTILEVER DEFLECTION:

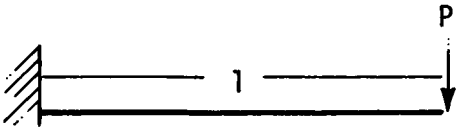

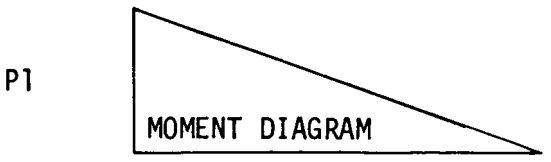

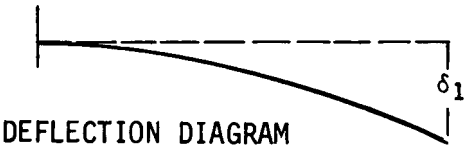

$$\delta_1 = \frac{Pl^3}{3EI}$$

Fig. IV-16 Torque Applied at One End of Arm: Cantilever Deflection

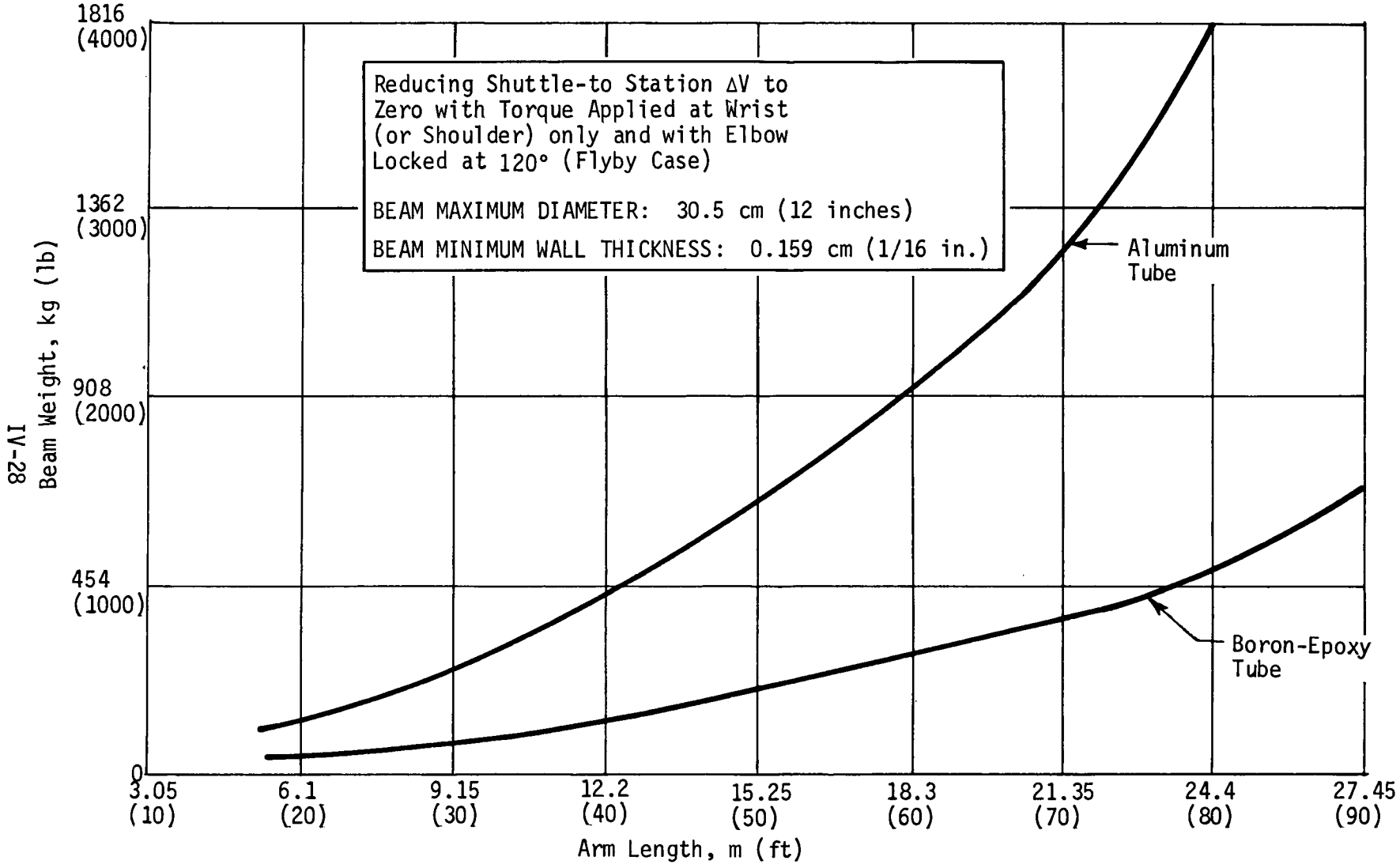

Fig. IV-17 Beam Weight vs Arm Length - One Applied Moment

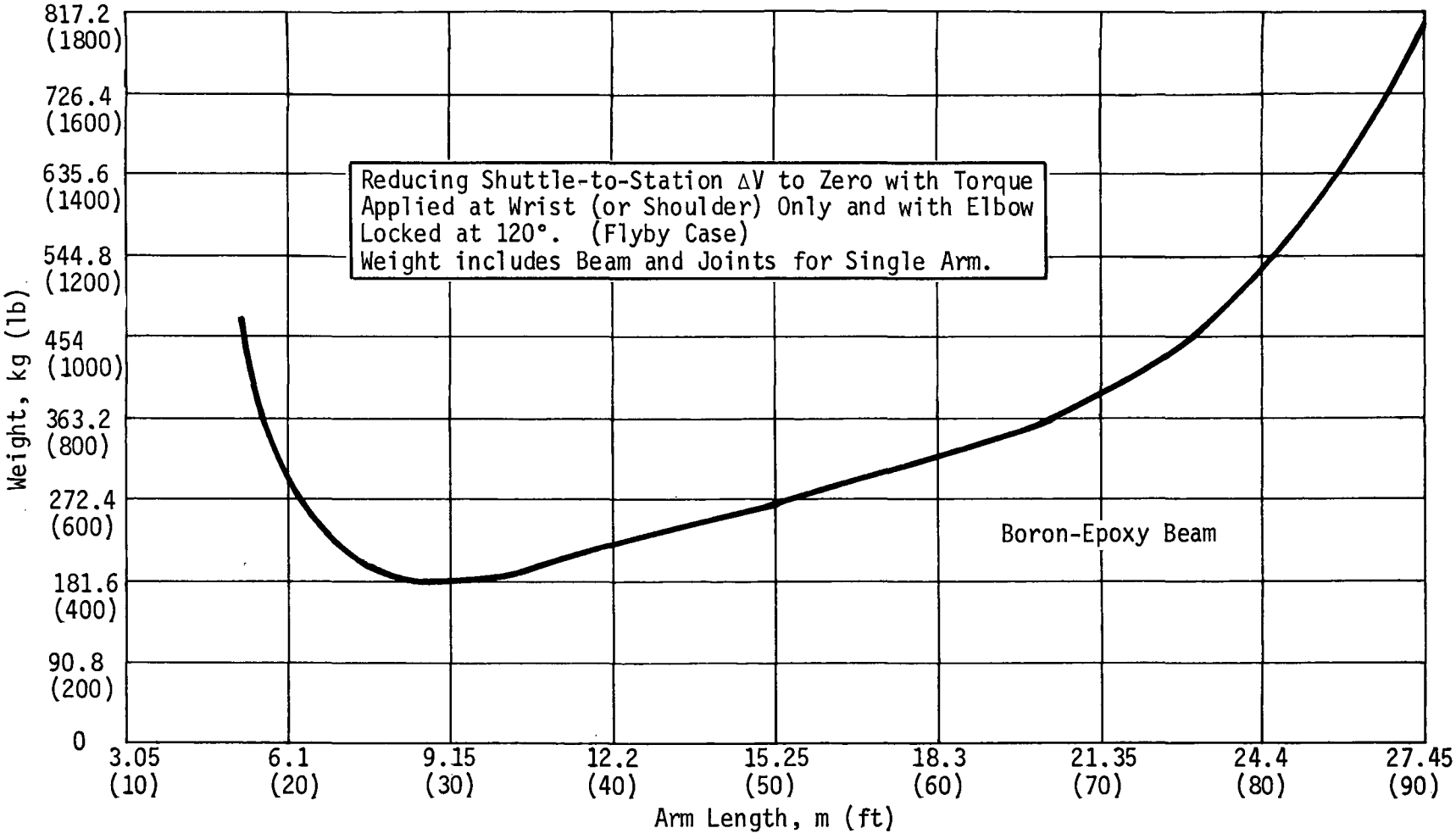

Fig. IV-18 Total Arm Weight vs Arm Length - One Applied Moment

CASE 2. TWO TORQUE MOTORS, M_1 and M_2:

S-SHAPE DEFLECTION:

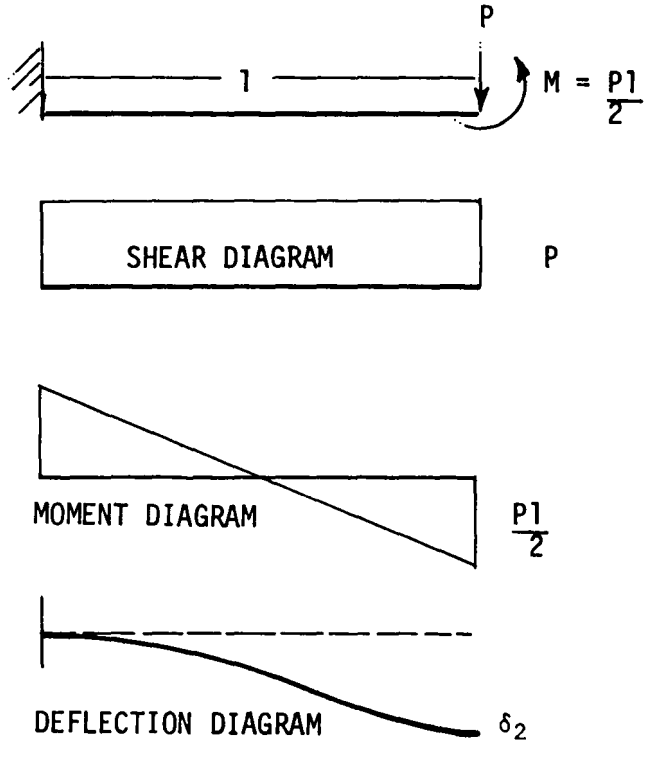

$$\delta_2 = \frac{Pl^3}{12EI}$$

Fig. IV-19 Torque Applied at Both Ends of Arm: S-Deflection

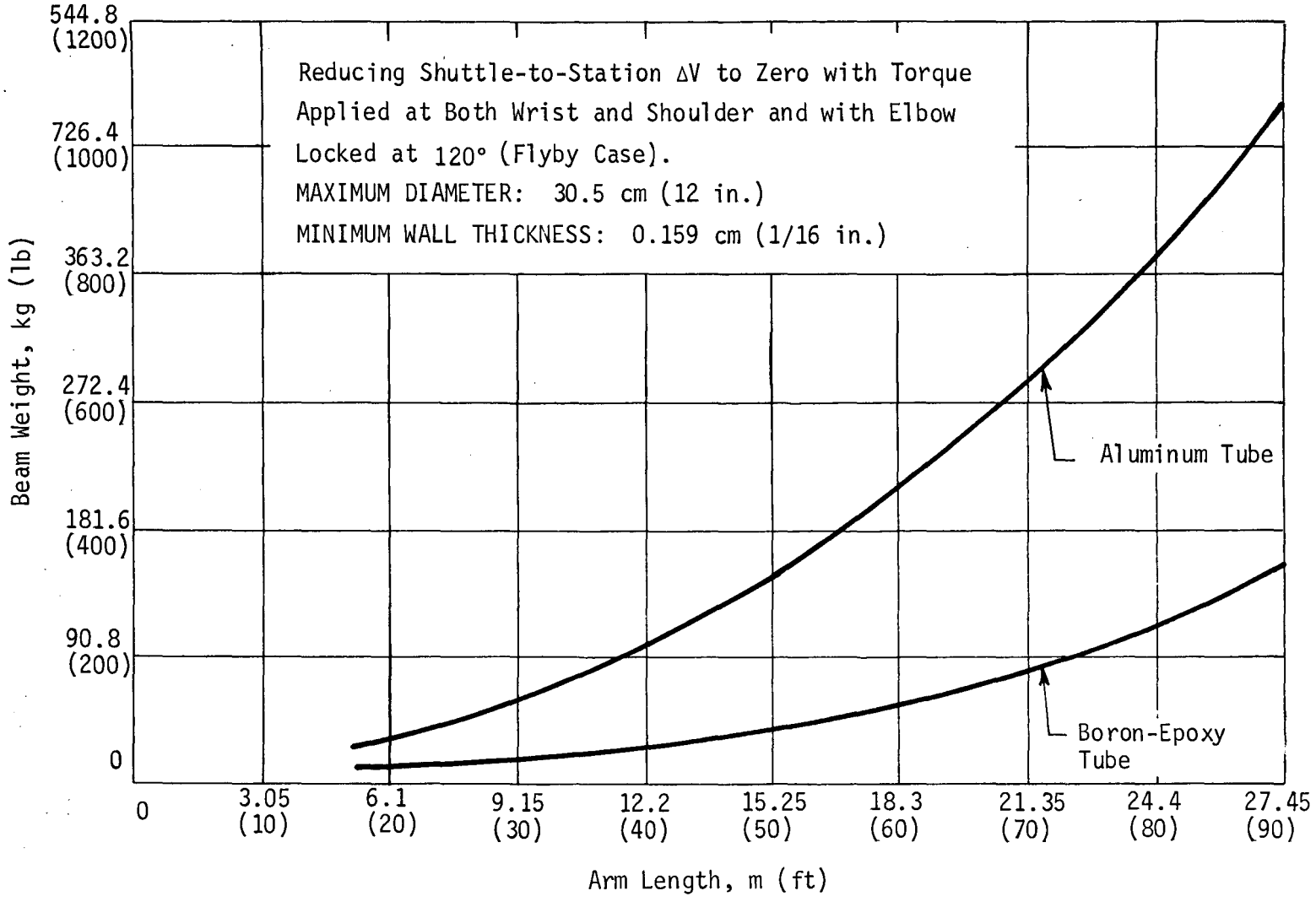

Fig. IV-20 Beam Weight vs Arm Length - Two Applied Moments

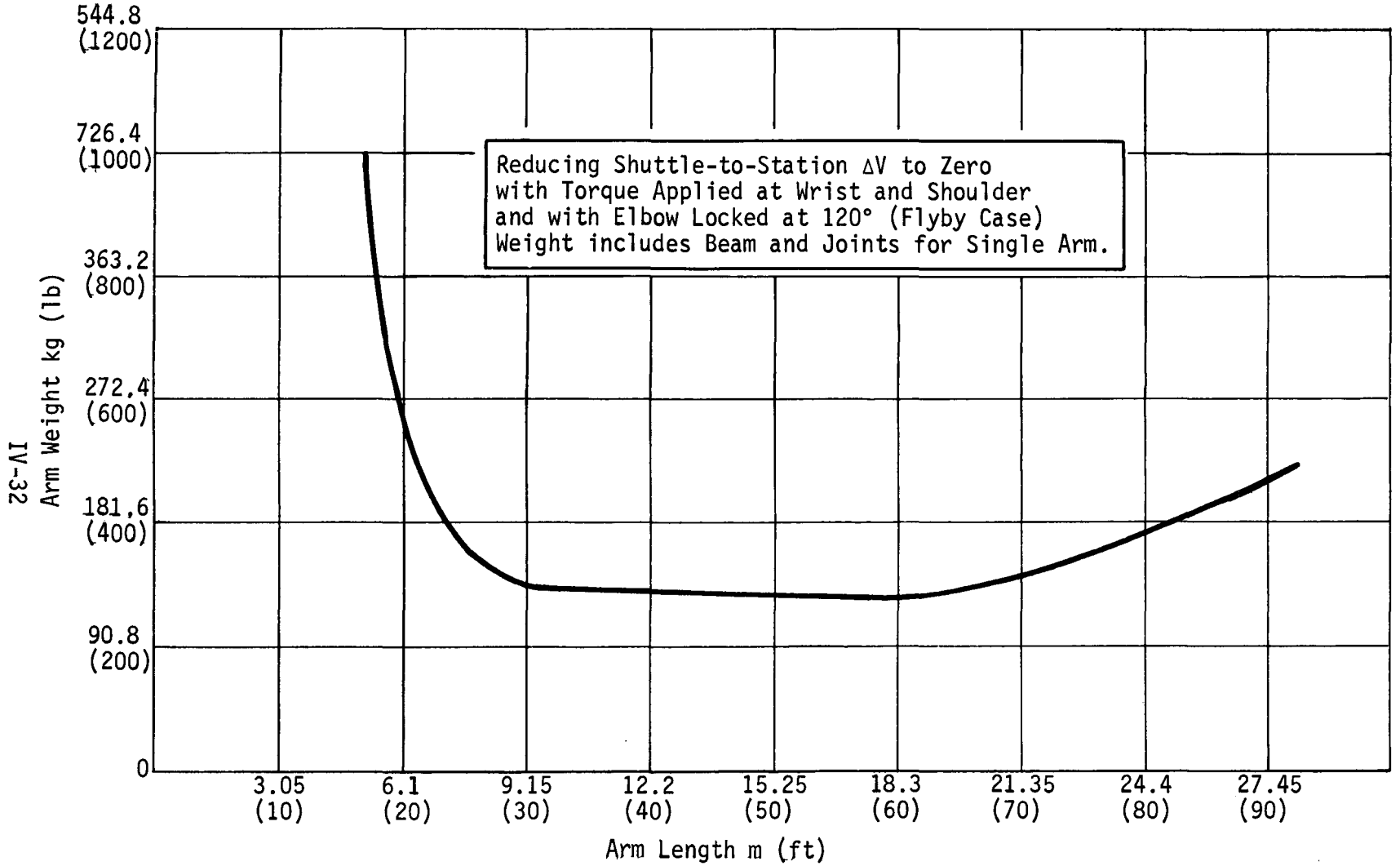

Fig. IV-21 Total Arm Weight vs Arm Length - Two Applied Moments

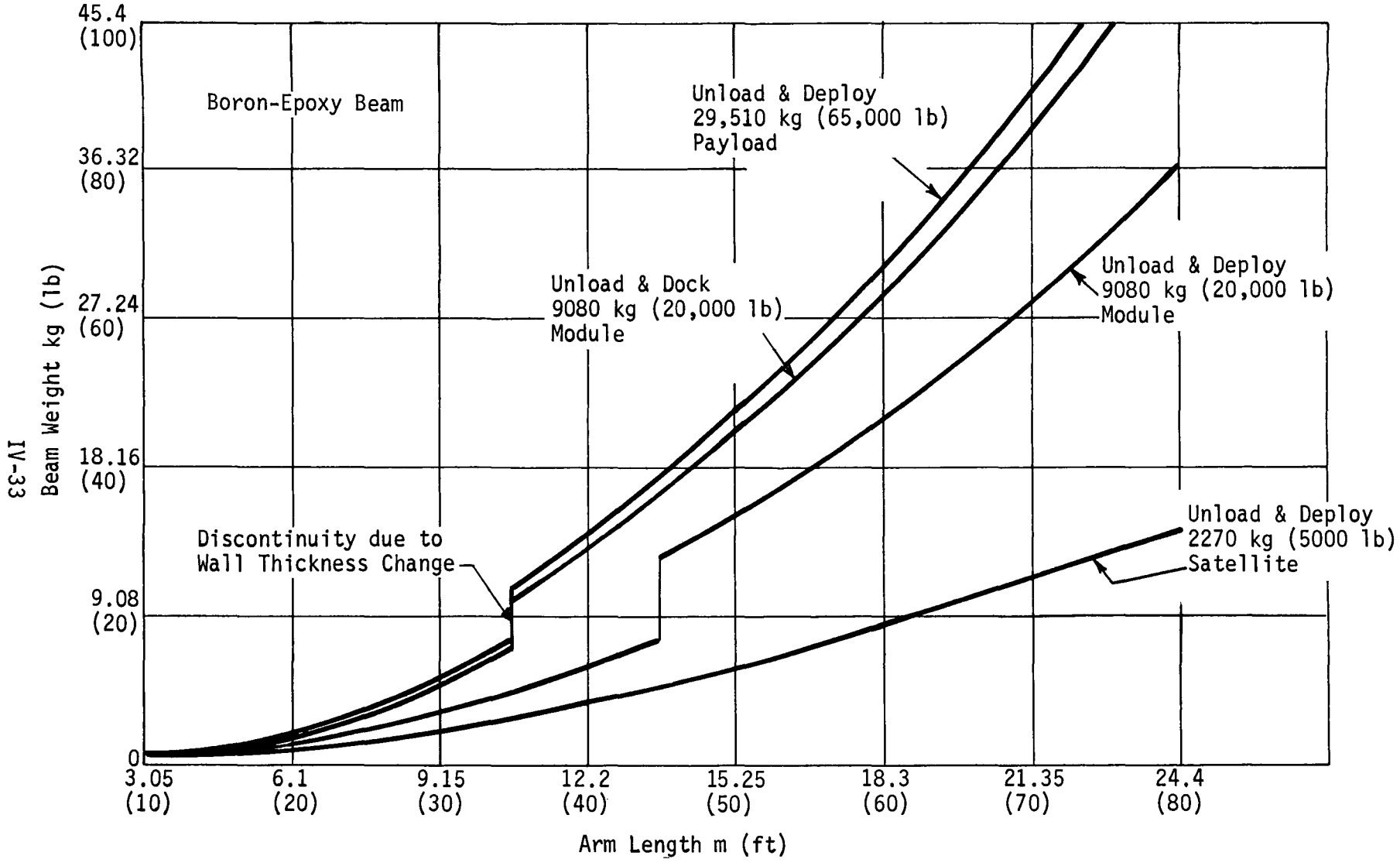

Fig. IV-22 Beam Weight for Cargo Handling

E. ELECTRICAL POWER

1. Estimate of RMS Power Requirements

The electrical power requirement was considered a parameter useful in evaluating alternative concepts. The shorter arms required higher torques and therefore higher power. The power required by the torque motor for the 7.63 m (25 ft) arm under maximum load is 500 watts. Assuming two motors operating simultaneously, 1000 watts power is required. A typical mission would include functions, times, and power as shown in the following tabulation.

Function	Time (min)	Power (W)
Docking	10	1000
Cargo Handling	10	1000
Undocking	5	1000
Television	25	10

	kw-hr
Docking	= 0.166
Cargo Handling	= 0.166
Undocking	= 0.083
Television	= 0.004
	0.419 KW-hr

To be conservative we assume total RMS power required to be approximately 1 kw-hr.

2. Shuttle Orbiter Electrical Power System

Two types of power sources are used in the baseline Orbiter; H_2/O_2 fuel cell modules, having an output of 120 vdc, and AC generators (120/208 V three phase, 400 Hz) driven by the auxiliary power units that also provide hydraulic power. These two source groups are connected to specific vehicle load groups, and are not redundant for each other. The fuel cell modules provide the electrical power required by the vehicle, except the AC required by the main propulsion engines.

Four fuel cell modules are used to meet the fail operational/fail operational/fail safe (FO/FO/FS) criteria. The AC generators provide the AC power required by the main propulsion engines, and three generators are used to provide a fail operational/fail safe power source for the engines, which are fail safe. One AC generator is gear driven by each auxiliary power unit.

Fuel Cell Subsystem - Four hydrogen-oxygen fuel cell modules are installed in the Orbiter. Each unit is capable of producing 7 kw continuous and peaks of 14 kw. Inherent fuel cell voltage regulation is used, thereby minimizing electronic regulation of the fuel cell output. Regulation is 120 ± 6 volts for 0.5 to 7 kw, and 117 ± 7 volts for 0.5 to 14 kw.

The total energy required from the DC system for a 7-day rendezvous mission is 667 kw-hr. The operational profile is shown for this system in Fig. IV-23. This represents approximately 0.15% of the total 7-day orbiter mission requirements.

3. Estimate of Shuttle Power Requirements for 37-hr Mission

(Steady-State Load)

	Time (hr)	kw	kw-hr		Time (hr)	kw	kw-hr
(Lift-Off)	1	9.5	9.5		4.5	4.1	18.45
	3	4.6	13.8		4	4.8	19.2
	1	4.8	4.8		1	7.8	7.4
	5	4.25	21.25	Reentry	0.5	9.1	4.55
	1	4.8	4.8				
	2.5	4.25	10.63		10		49.60
(Rest)	8.5	3.5	29.75				
	1	4.8	4.8				
	2	4.25	8.5		Total kw-hr = 171		
(Rendezvous)	2	6.25	12.5				
	27		120.33				

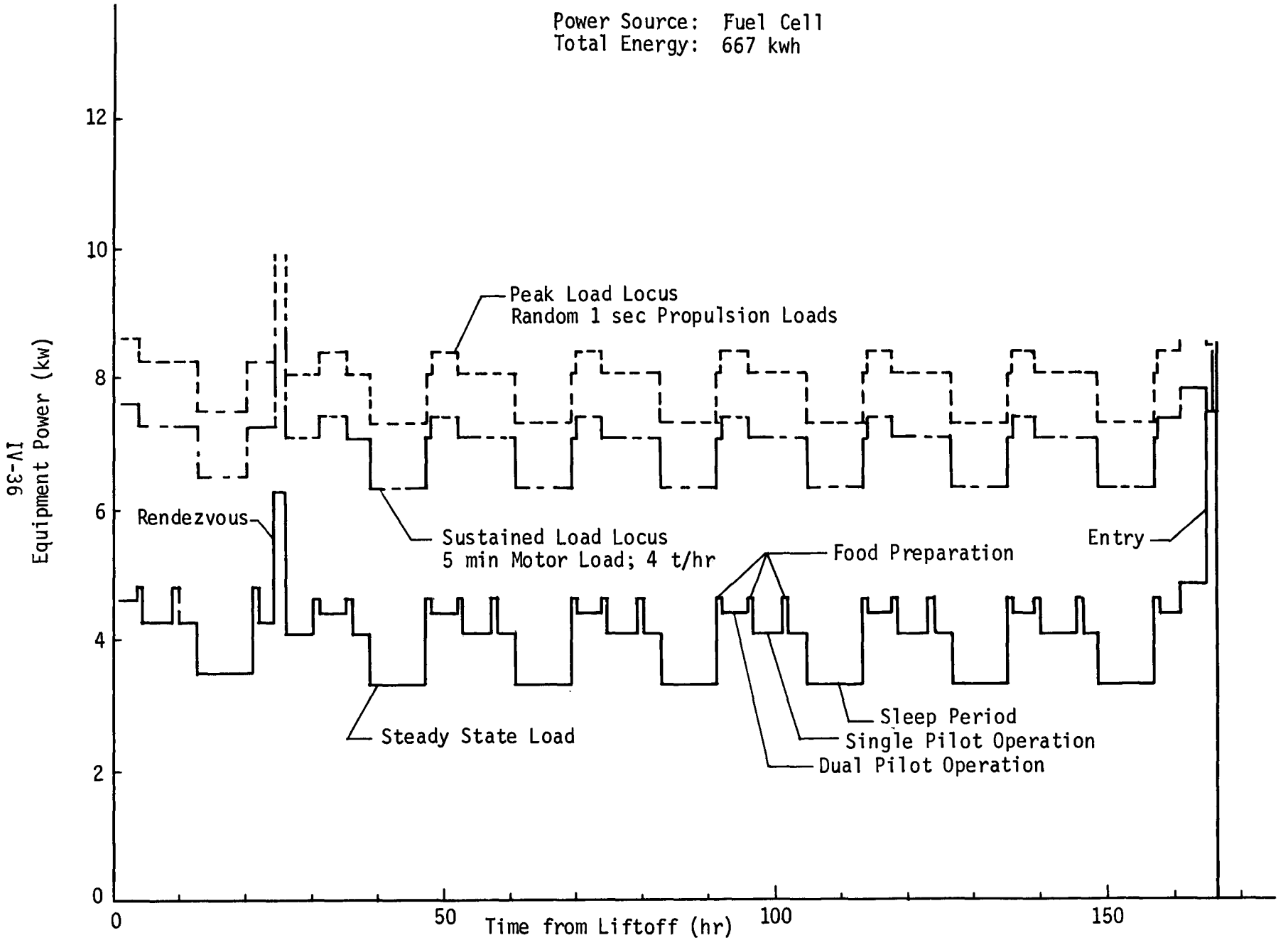

Fig. IV-23 Orbiter Operational Power Profile (120 vdc)

For a 37 hr Shuttle mission, the total T/O Power Requirements represents 1/171 or 0.64% of the total Shuttle requirements (steady-state load).

At any one time maximum peak load (at rendezvous) could go to 10.25 kw. Assuming an additional peak of 1 kw due to T/O requirements superimposed on this load, the resultant is still under the 14 kw peak capability of each Orbiter fuel cell.

Thus the difference in electrical power requirement of the motors of one length arm vs another cannot be considered a significant factor in alternative concepts evaluation.

V. ALTERNATIVE CONCEPTS, EVALUATION AND SELECTION

This chapter is the focal point for the study and analyses described in Chapters III and IV. The method of using the requirements to formulate and evaluate manipulator concepts is described in this chapter. The chapter concludes with newly introducted requirements that affect the selection of a manipulator concept. The chapter is divided in five sections: A. Alternative Concepts Formulation, B. Telecommunications Subsystem Conceptual Design, C. Concept Evaluation, D. Concept Ranking, and E. Selected Concept.

A. ALTERNATIVE CONCEPTS FORMULATION

Upon first examination, the variety of possible manipulator concepts seemed endless but engineering judgment was used to reduce the size of the problem. First, the possible Shuttle attachment points where narrowed down to include only the region from the forward cargo bay bulkhead to the rear bulkhead. The minimum reach requirements analysis and the stowage requirement helped substantiate this decision. Next, the multiplicity of arms was examined, and it was concluded that there was no justification for providing more than two manipulator arms. Thus, the number of alternative configurations was reduced significantly.

The parameters used to formulate possible concepts are tabulated.

1) Number of Arms;
   a) One arm,
   b) Two identical arms,
   c) Two arms, not identical;
2) Arm Length:
   a) Fixed length,
   b) Variable length;
3) Operating Locations:
   a) Fixed location,
   b) Several variable locations,

c) Several fixed locations;

4) Number of Bases:

a) One base,

b) Two separate bases.

These parameters were used to construct a comprehensive matrix as shown in Fig. V-1. Each of the 42 concepts shown in matrix were examined individually. For attachment points near the forward cargo bay bulkhead, the need for increased reach capability was identified (See Fig. IV-2.) with the small lightweight payload located at the extreme end of the payload envelope. Other than providing a fixed length arm to reach this payload, increased length capability could be provided by an additional arm at a different base, a variable length arm, or a moving base. The ground rules used were (1) only one means of increasing reach capability would be provided; e.g., if the concept included a telescoping (variable length) arm, it would not also be provided with a moving base to accomplish the same objective, and (2) only one arm (for 2-arm concepts) will have increased reach capability by one of the methods described above. The matrix shows a geometric symbol coded entry for those concepts eliminated as possible candidates. The ten remaining candidates, coded A through J, are the concept types upon which the alternative configurations, shown in Fig. V-2 through V-11 are based. Each illustration includes a side view (lower part of figure) with the arm or arms deployed, a top view (upper part of figure) with the arm or arms shown in both a deployed and stowed position. Included are two candidate deployment methods for each concept. Each concept was based on a manipulator with six degrees of freedom. A typical configuration meeting these minimum requirements is shown in Fig. V-12.

SELECTION FROM 42 POSSIBLE CONCEPTS							
Type of Operating Locations →		One Fixed Operating Location		Several Variable Operating Locations		Several Fixed Operating Locations	
Number of Arms ↓	Bases / Arm Length	One Base	Two Separate Bases	One Base	Two Separ. Bases (One Fixed)	One Base	Two Separ. Bases (One Fixed)
1 Arm	Fixed	A, I	●	C	●	F	●
	Variable	B	●	▲	●	▲	●
2 Ident. Arms (Size, Wt, Base, etc.)	Fixed	D	⬢	⬢	⬢	⬢	⬢
	Variable	⬢	⬢	▲	▲	▲	▲
2 Non-Ident. Arms	Both Fixed	■	E	⬢	H	⬢	J
	Both Variable	⬢	⬢	▲	▲	▲	▲
	One Fixed, One Variab.	G	▲	▲	▲	▲	▲

A, B, C, D, E, F, G, H, I, J = Selected Alternative Concepts

● Not Applicable

■ No Advantage to Keep Both Arms at One Operating Location

▲ Redundant Means of Increasing Reach Capability

⬢ Since need for increased reach capability is caused by the requirement to reach small (light) cargo, only one arm need have this capability. Also no need to have 2 identical arms if on separate bases.

Fig. V-1 Selection from 42 Possible Concepts

CONCEPT A

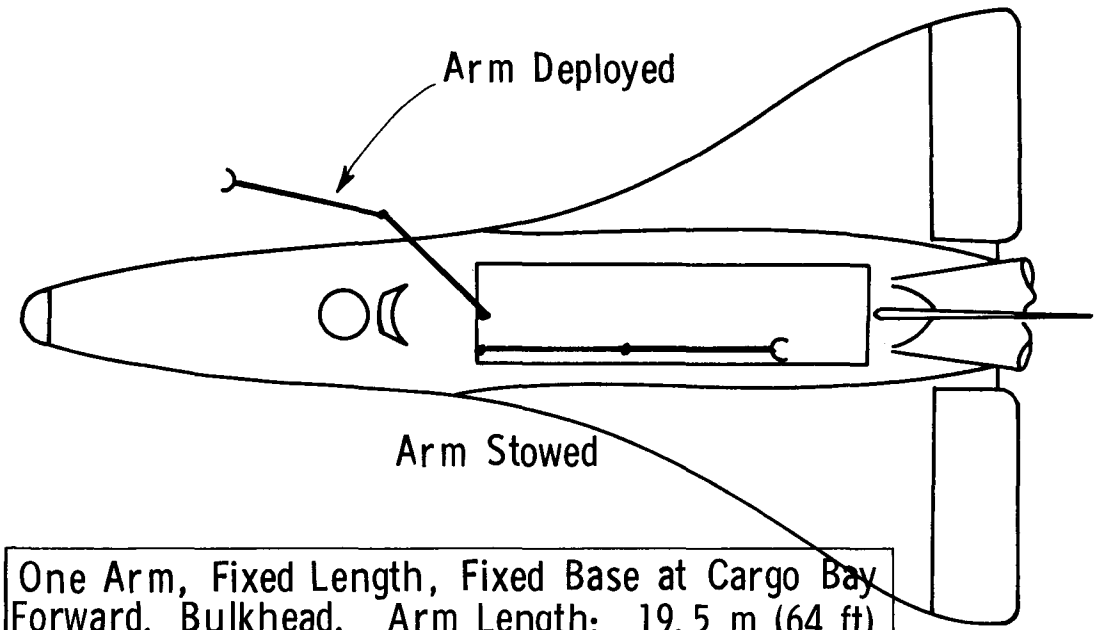

One Arm, Fixed Length, Fixed Base at Cargo Bay Forward, Bulkhead. Arm Length: 19.5 m (64 ft) Total Weight: 222 kg (489 lb)

DEPLOYMENT METHOD 1

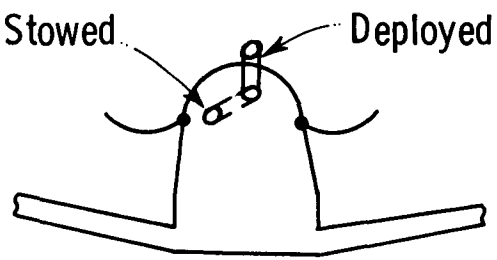

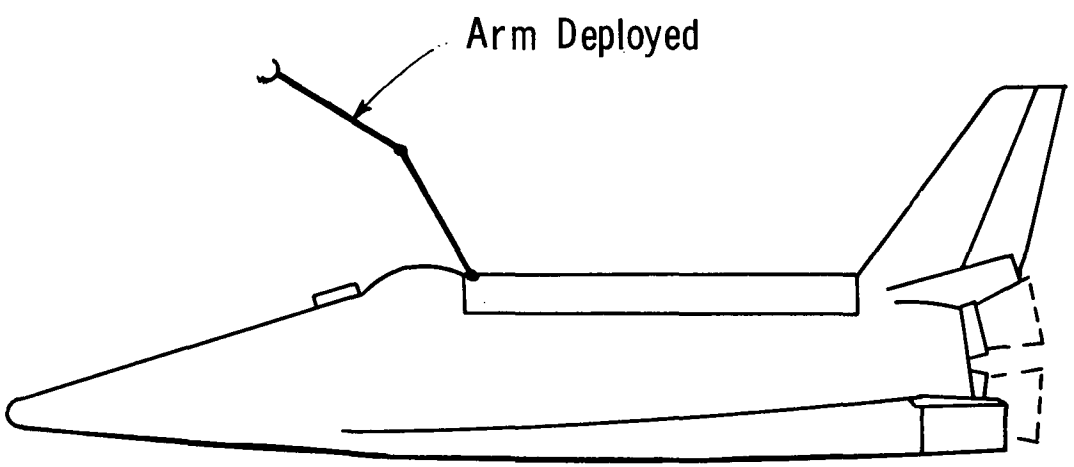

DEPLOYMENT METHOD 2

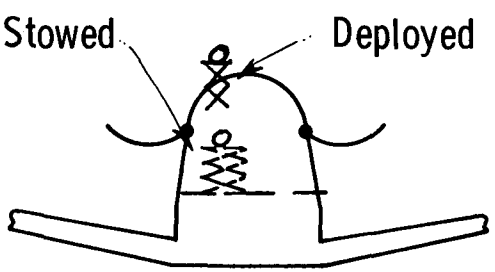

Fig. V-2 Concept A

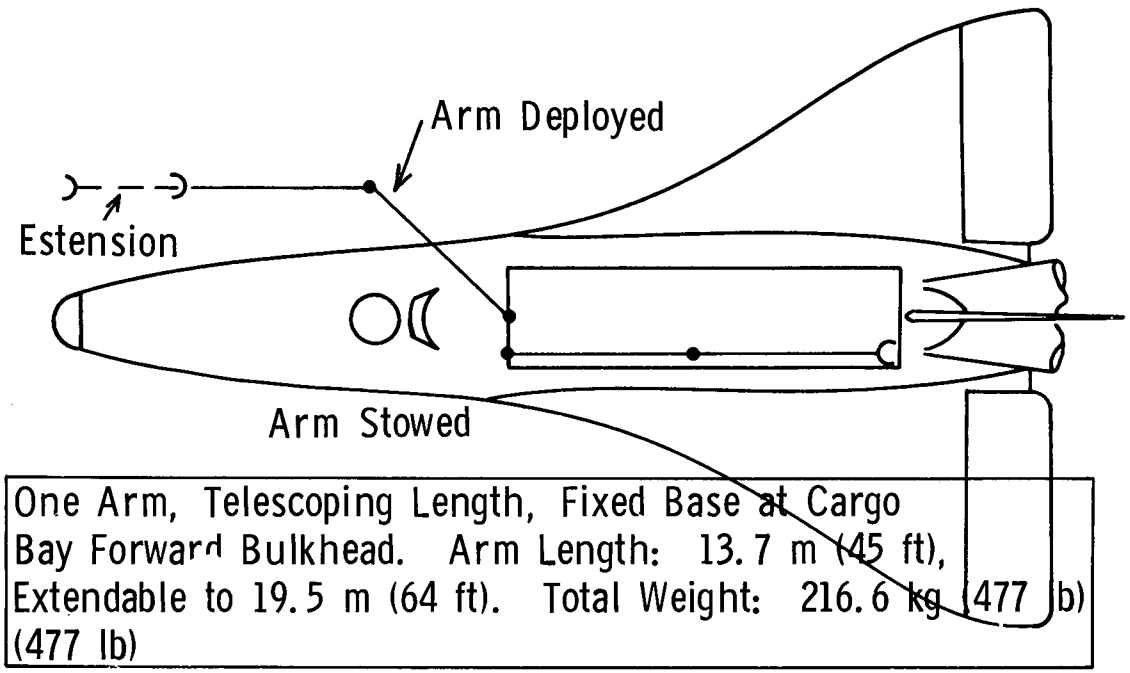

One Arm, Telescoping Length, Fixed Base at Cargo Bay Forward Bulkhead. Arm Length: 13.7 m (45 ft), Extendable to 19.5 m (64 ft). Total Weight: 216.6 kg (477 lb) (477 lb)

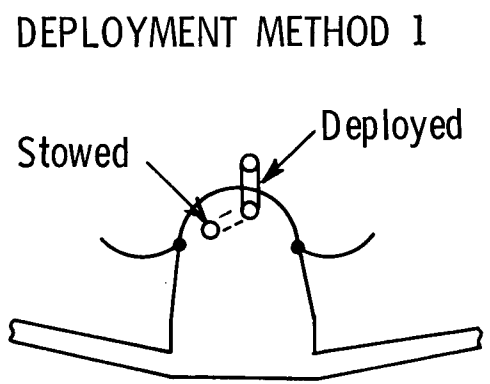

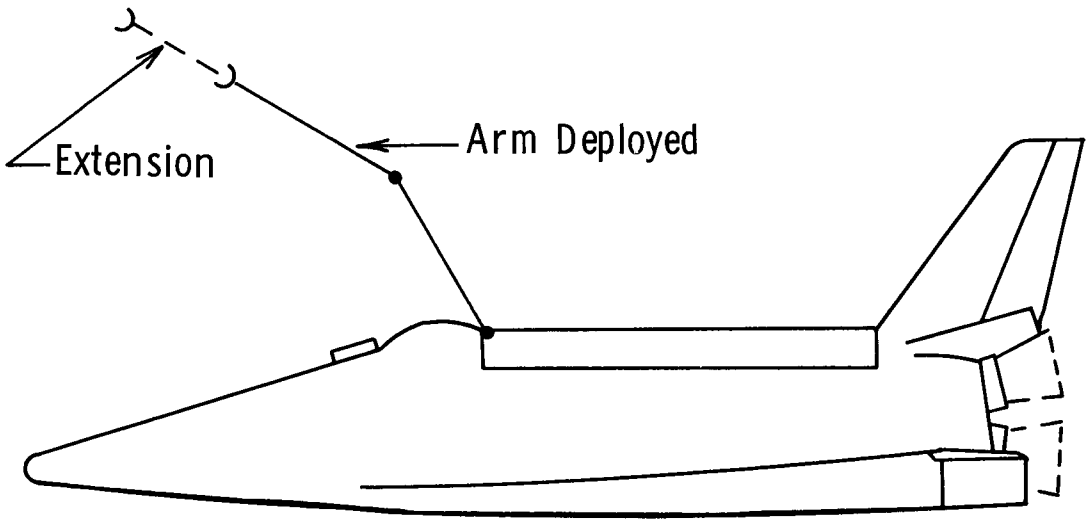

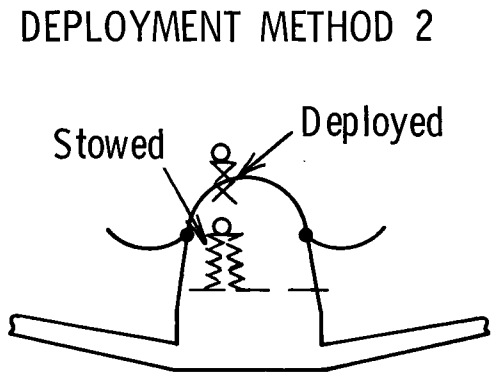

Fig. V-3 Concept B

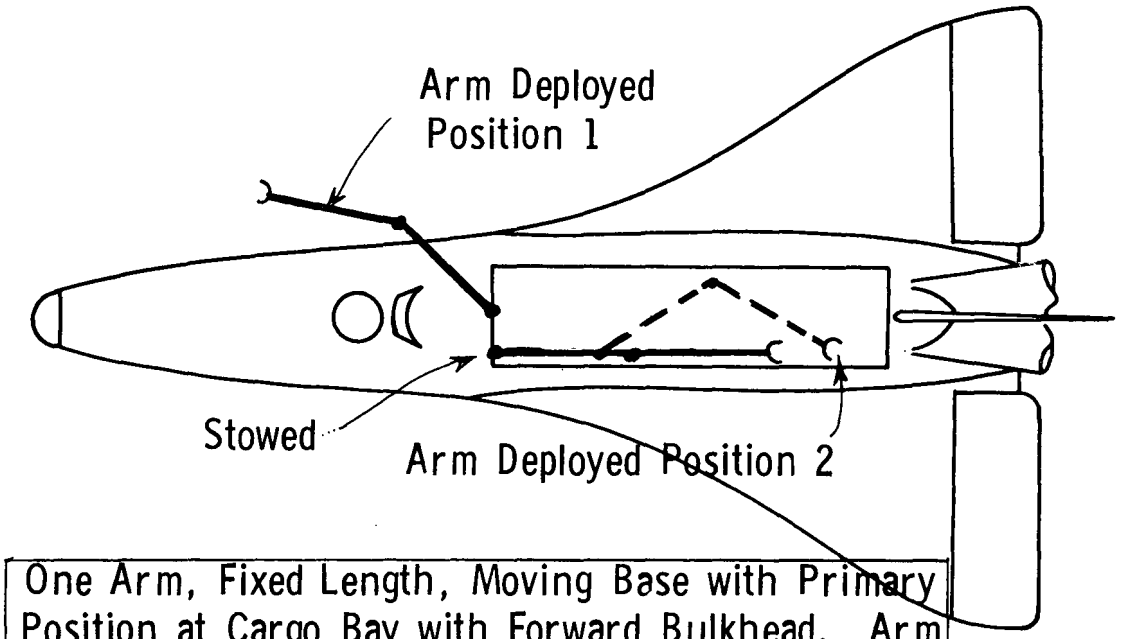

One Arm, Fixed Length, Moving Base with Primary Position at Cargo Bay with Forward Bulkhead. Arm Length 13.7 m (45 ft) Total Weight: 242.9 kg (535 lb)

DEPLOYMENT METHOD 1

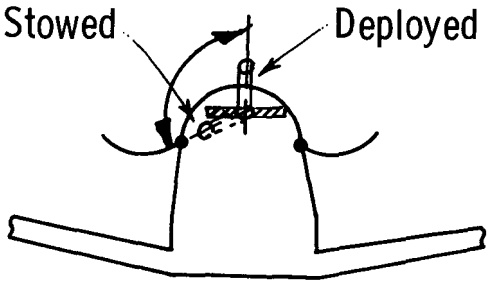

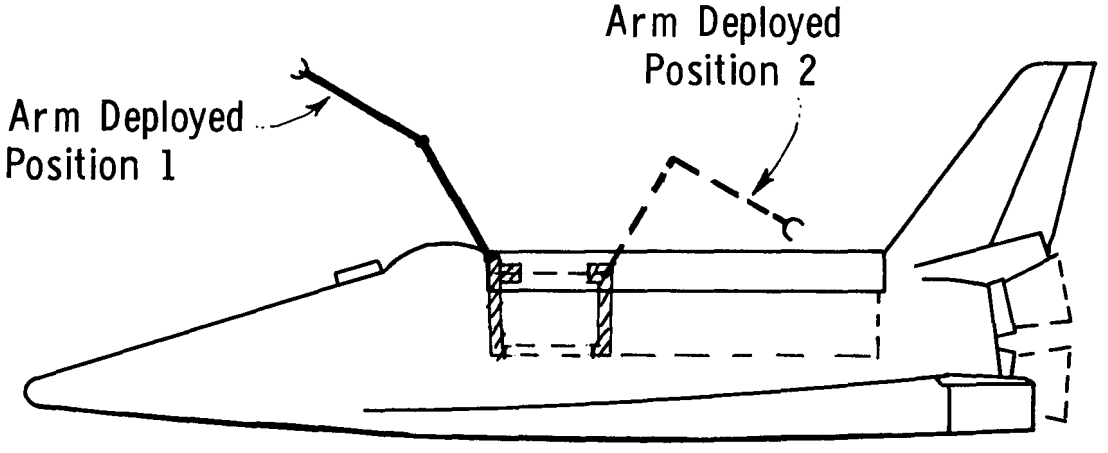

DEPLOYMENT METHOD 2

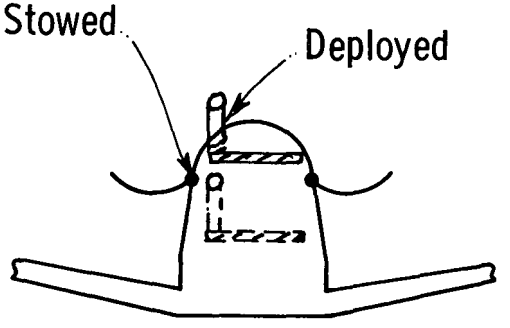

Fig. V-4 Concept C

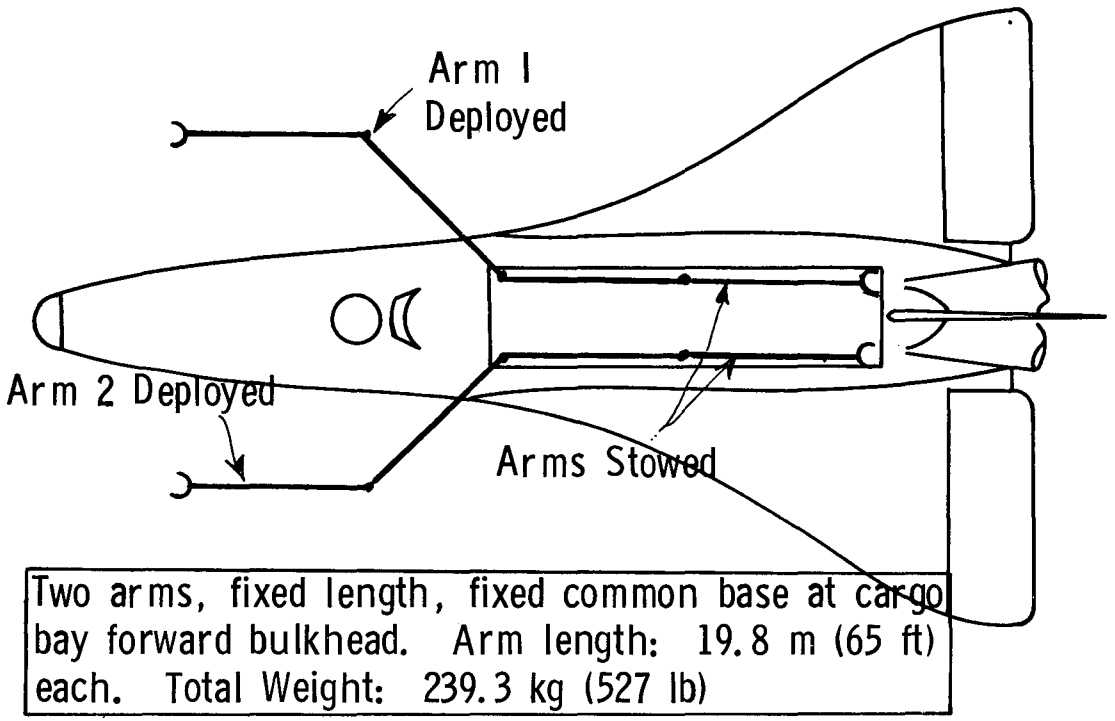

Two arms, fixed length, fixed common base at cargo bay forward bulkhead. Arm length: 19.8 m (65 ft) each. Total Weight: 239.3 kg (527 lb)

DEPLOYMENT METHOD 1

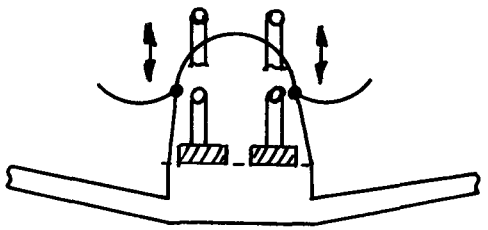

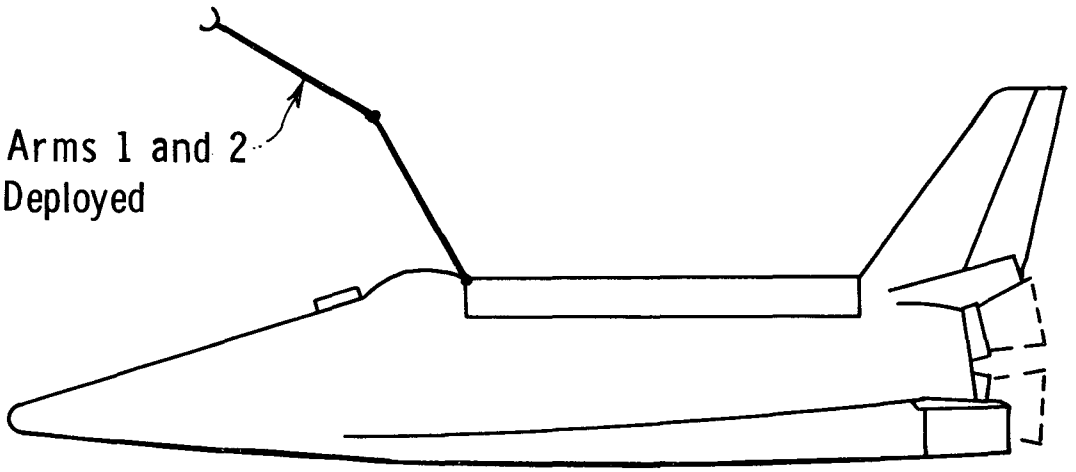

DEPLOYMENT METHOD 2

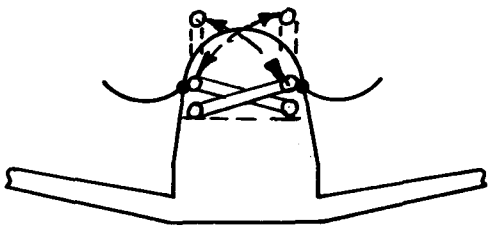

Fig. V-5 Concept D

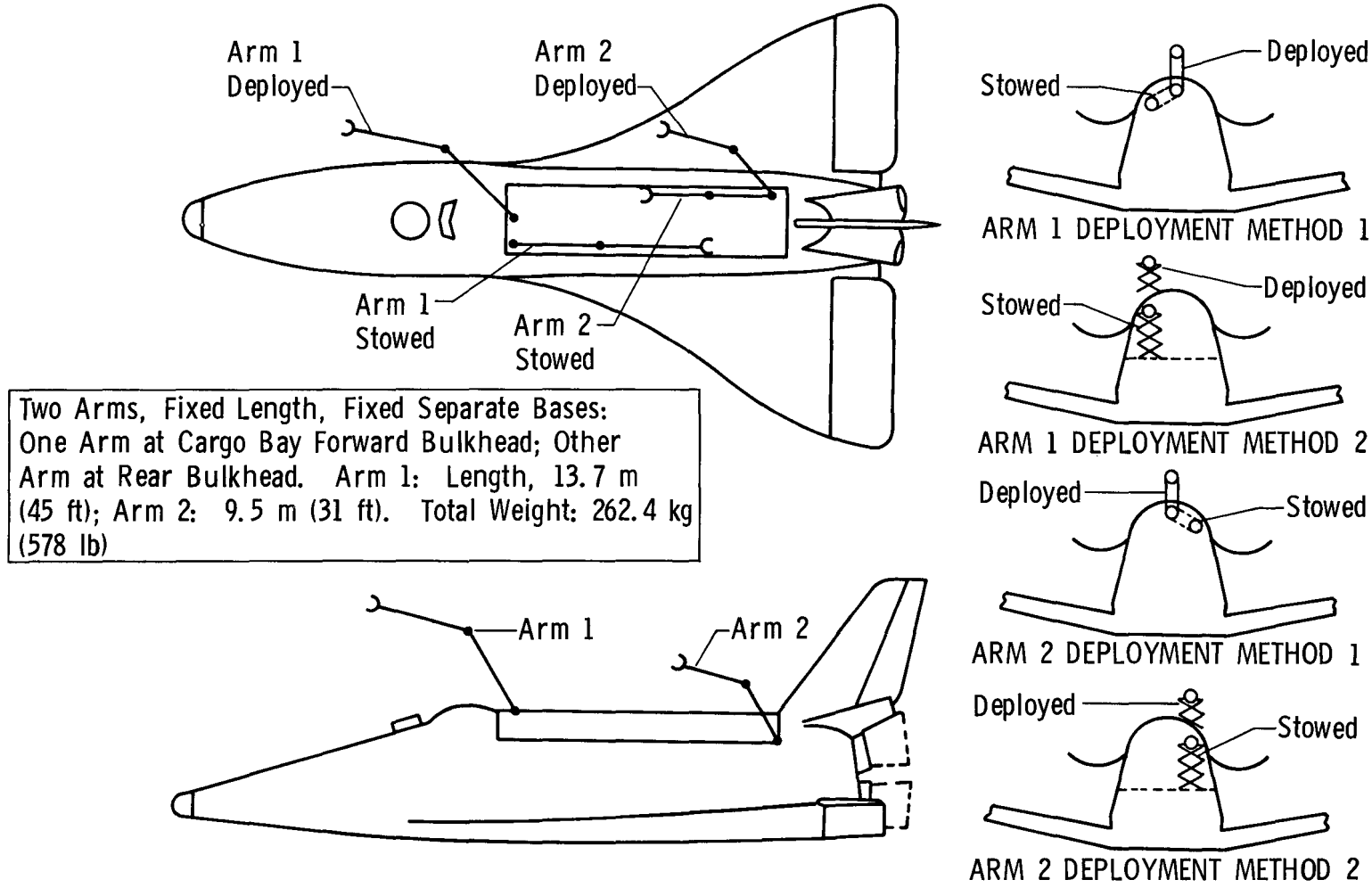

Fig. V-6 Concept E

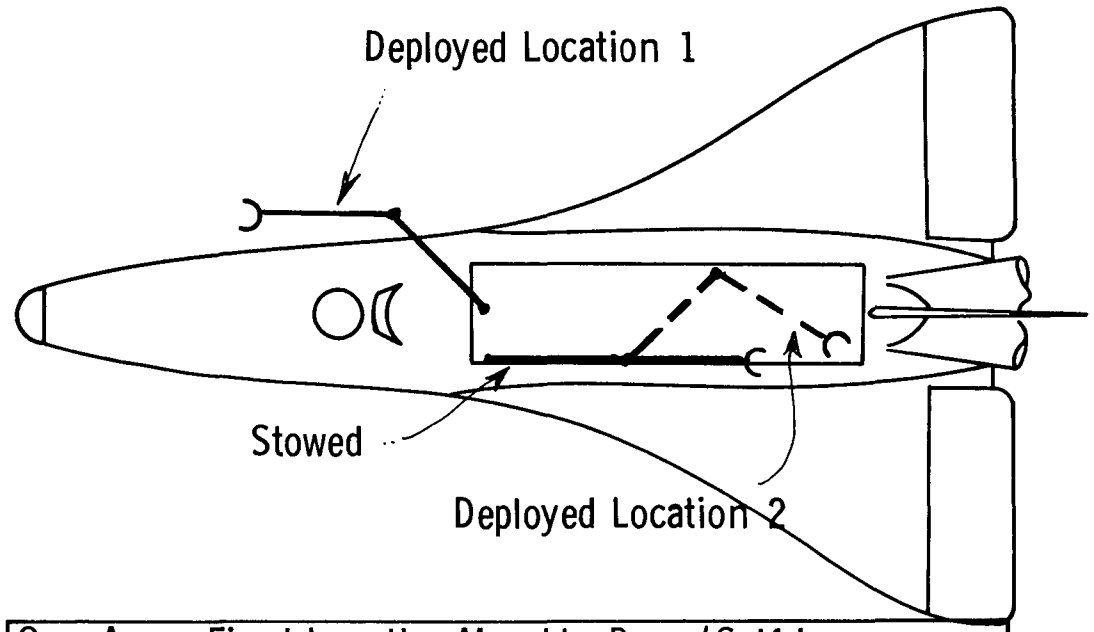

One Arm, Fixed Length, Movable Base (Self-Locomotion) with Primary Base at Cargo Bay Forward Bulkhead. Arm Length: 13.7 m (45 ft); Total Weight: 233.8 kg (515 lb)

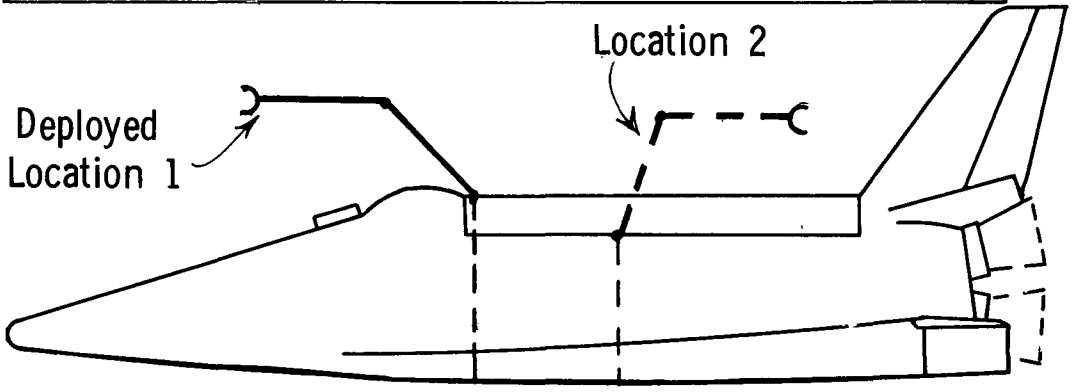

DEPLOYMENT METHOD 1

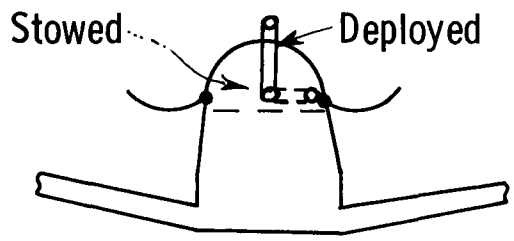

DEPLOYMENT METHOD 2

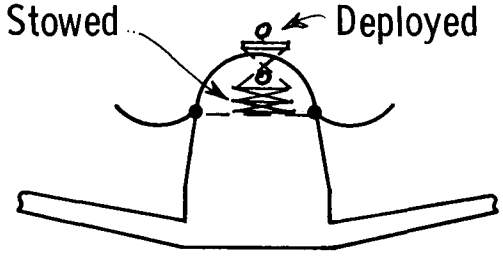

Fig. V-7 Concept F

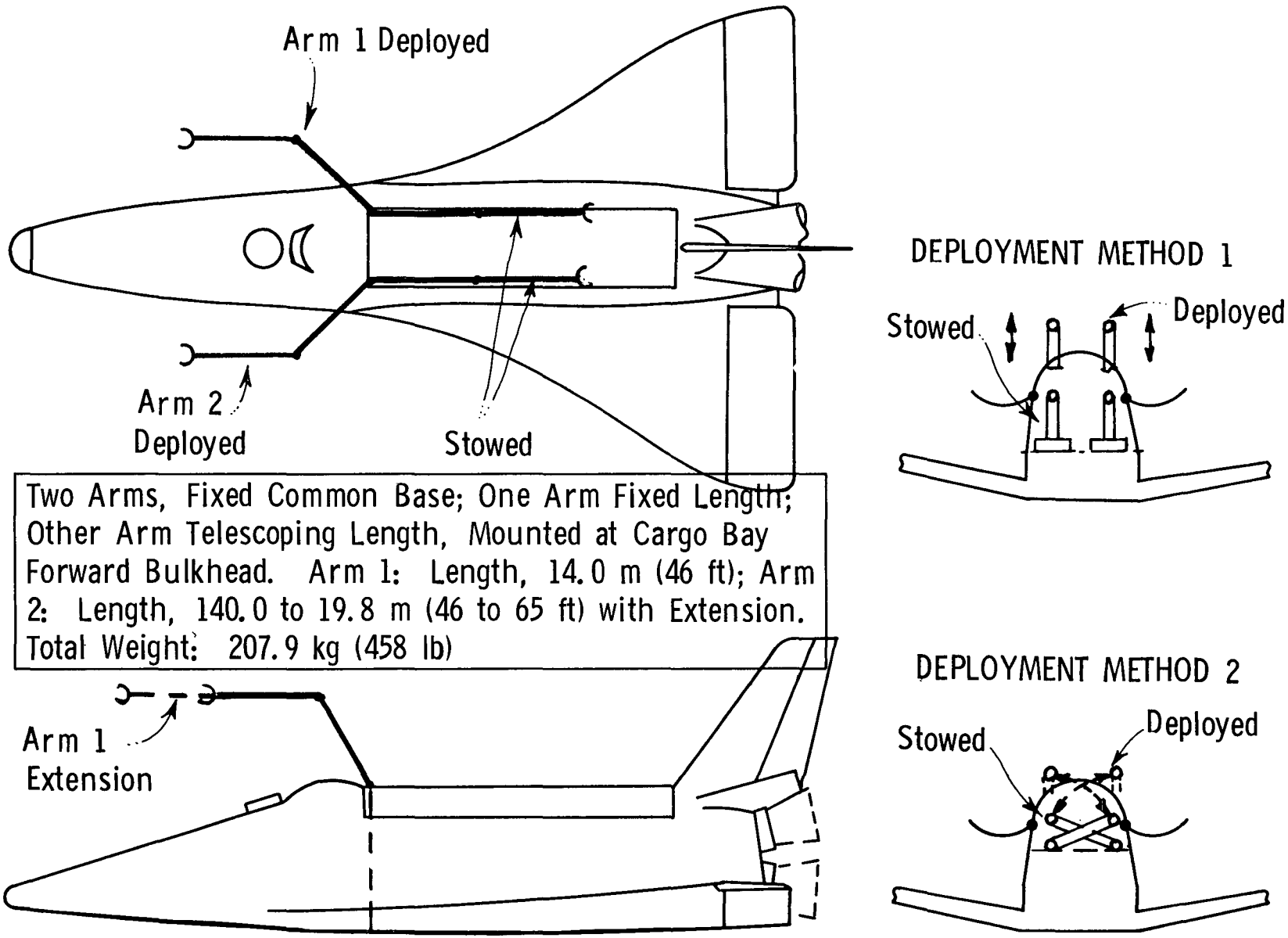

Fig. V-8 Concept G

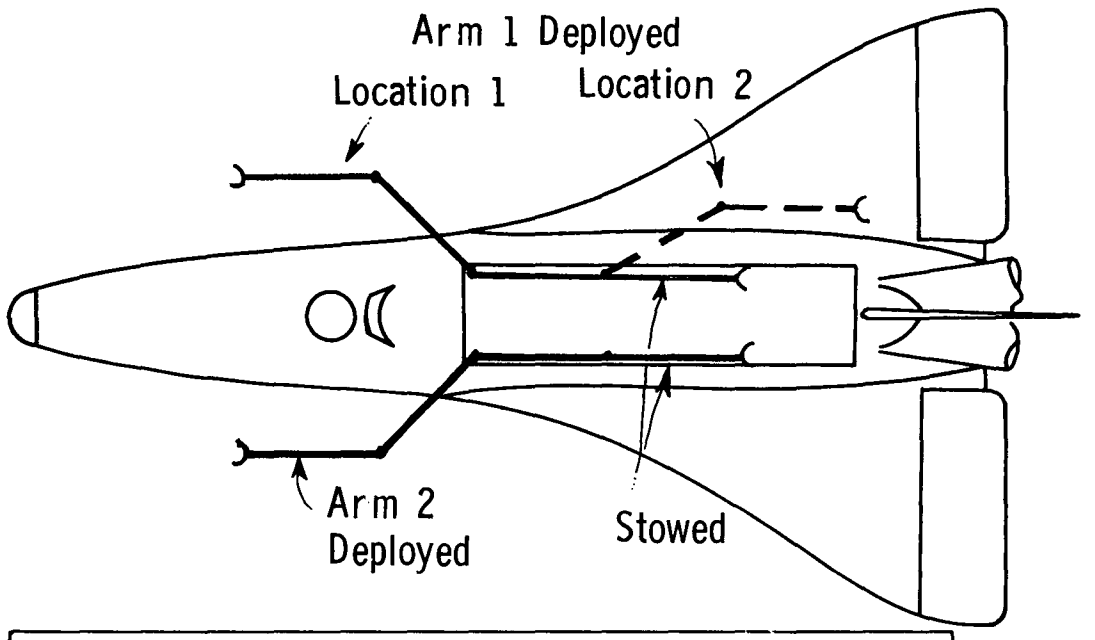

DEPLOYMENT METHOD 1

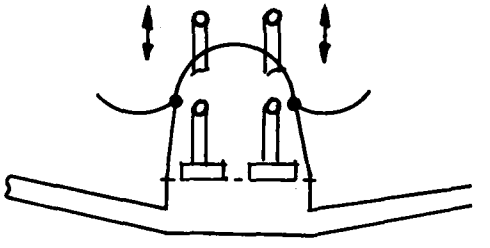

Two Arms, Fixed Length 14.0 m (46 ft); One Arm Fixed Base at Forward Bulkhead; Other Arm Moving Base with Primary Base at Forward Bulkhead. Total Weight: 240.2 kg (529 lb)

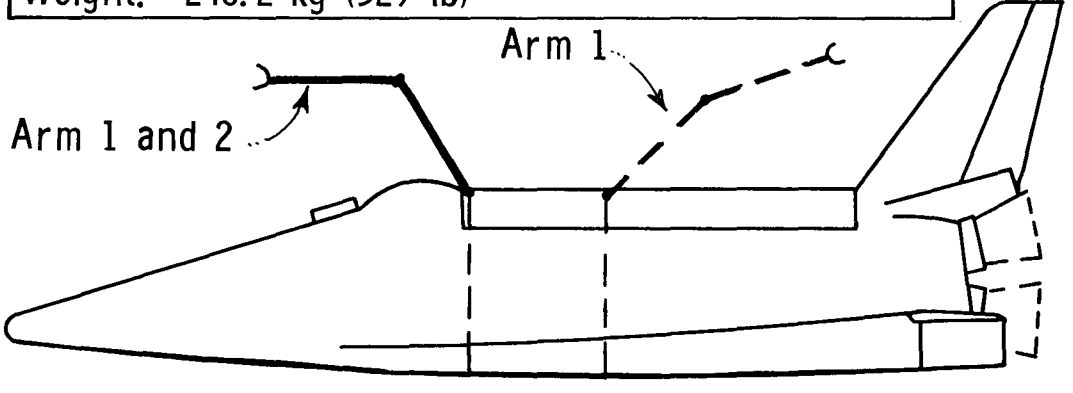

DEPLOYMENT METHOD 2

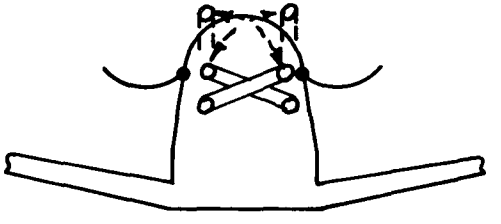

Fig V-9 Concept H

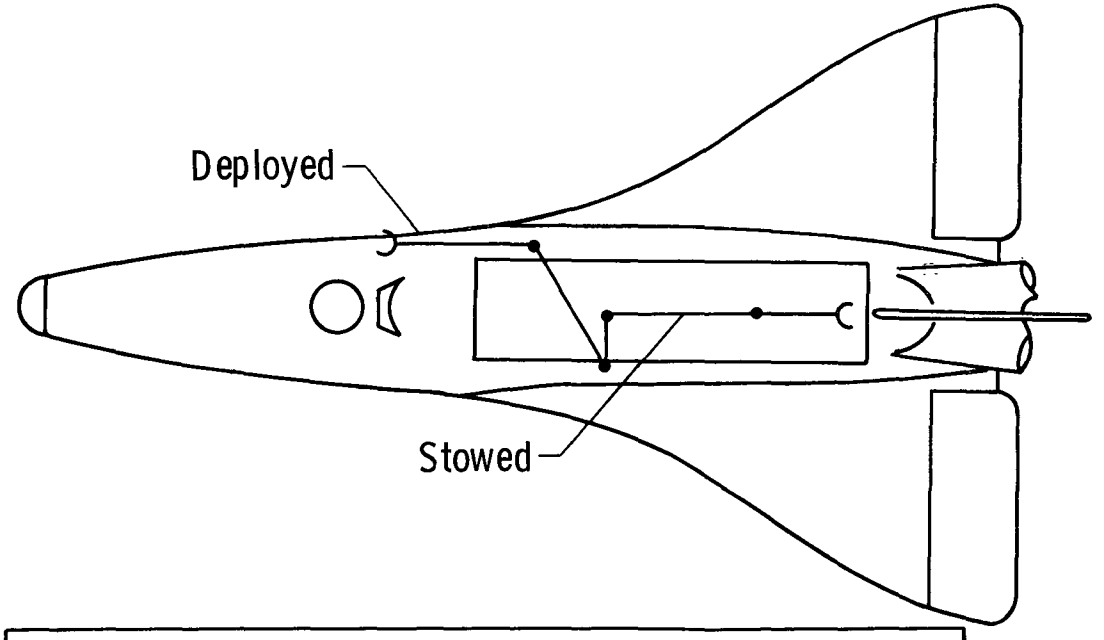

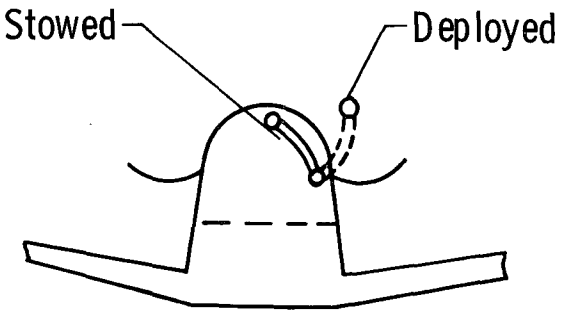

DEPLOYMENT METHOD 1

One Arm, Fixed 14.6 m (48 ft) Length, Fixed Base at 5.2 m (17 ft) Rearward from Forward Bulkhead.
Total Weight: 218.8 kg (482 ft)

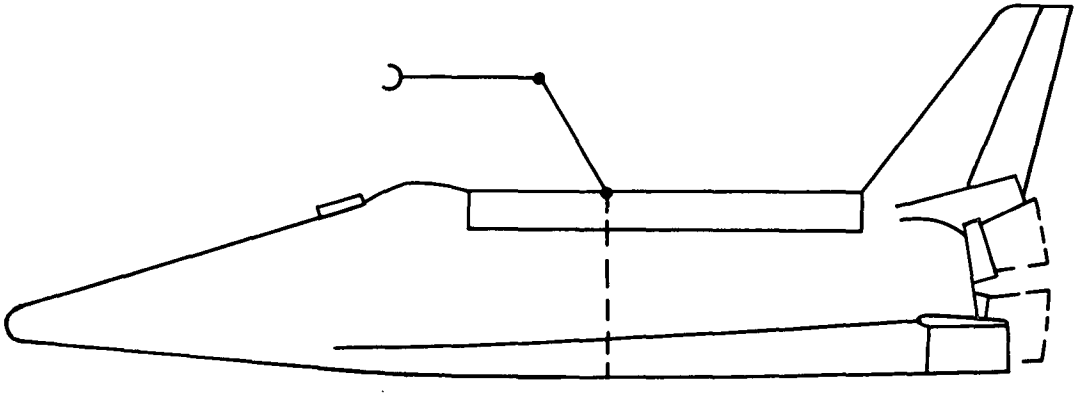

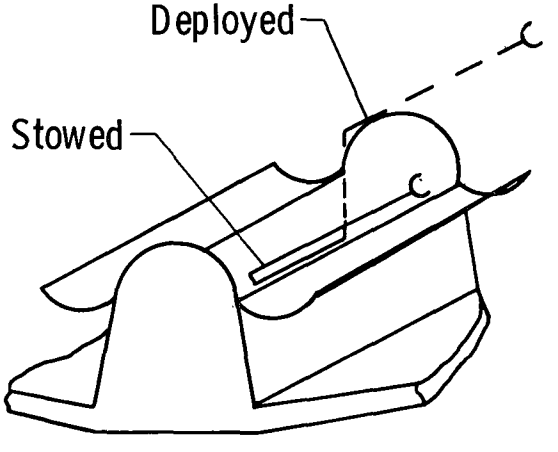

DEPLOYMENT METHOD 2

Fig. V-10 Concept I

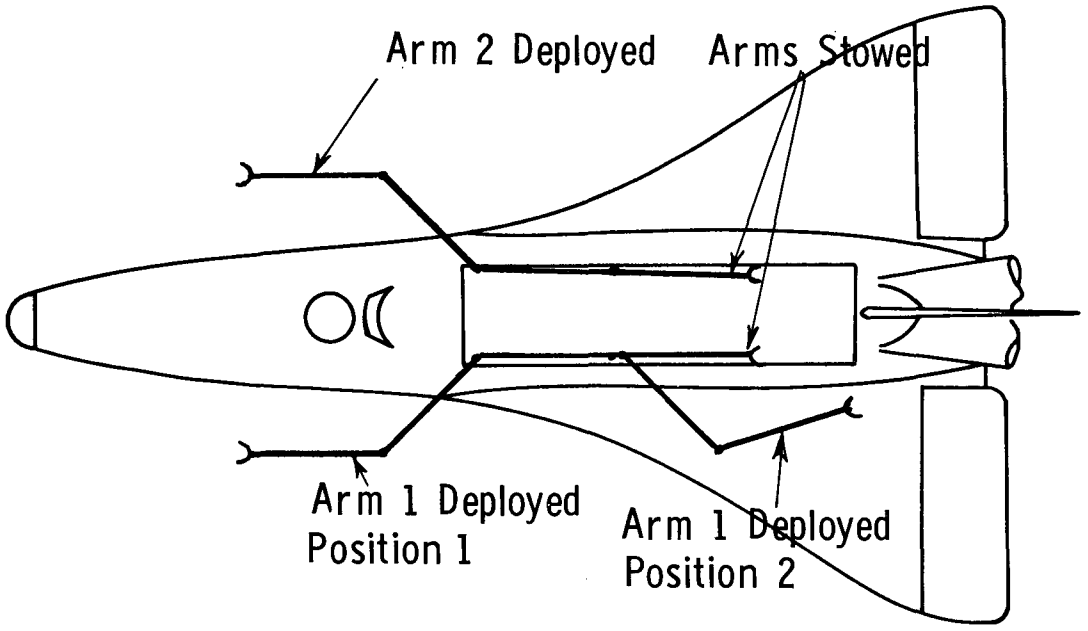

Two Arms, Fixed Length, One Arm Fixed Base; Other Arm Movable Base (self-locomotion) with Primary Position at Forward Bulkhead. Arm 1: Length 14.0 m (46 ft); Arm 2: Length 14.0 m (45 ft). Total Weight: 211.6 kg (466 lb)

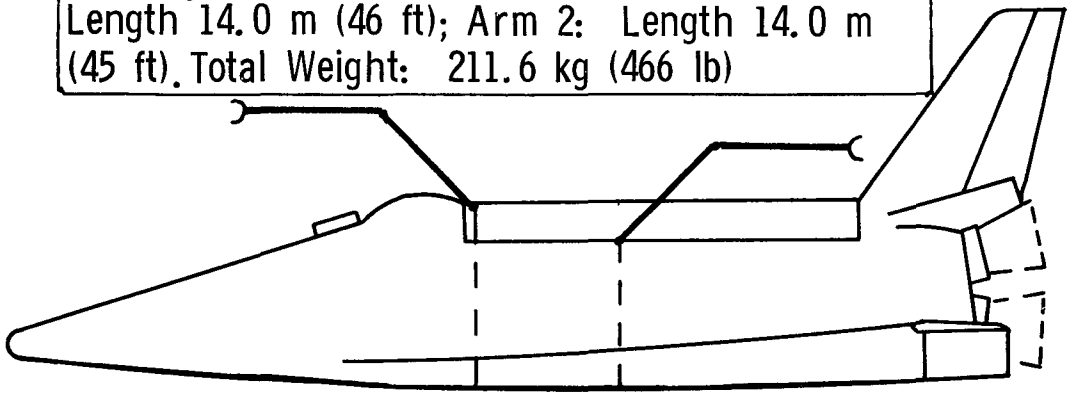

Note: Arm 1 Self-locomotion is done by a "boot-strapping" via an intermediate Shuttle surface-mounted receptacle.

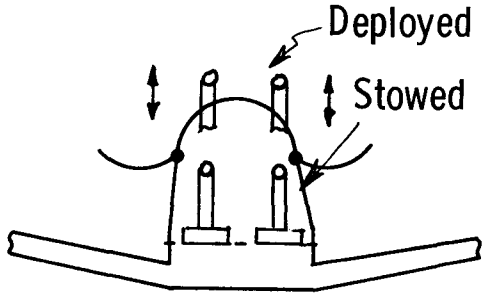

DEPLOYMENT METHOD 1

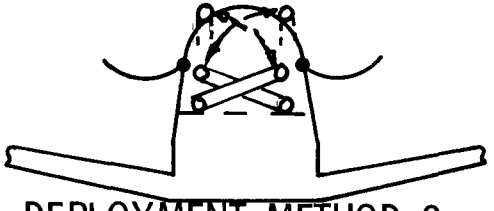

DEPLOYMENT METHOD 2

Fig V-11 Concept J

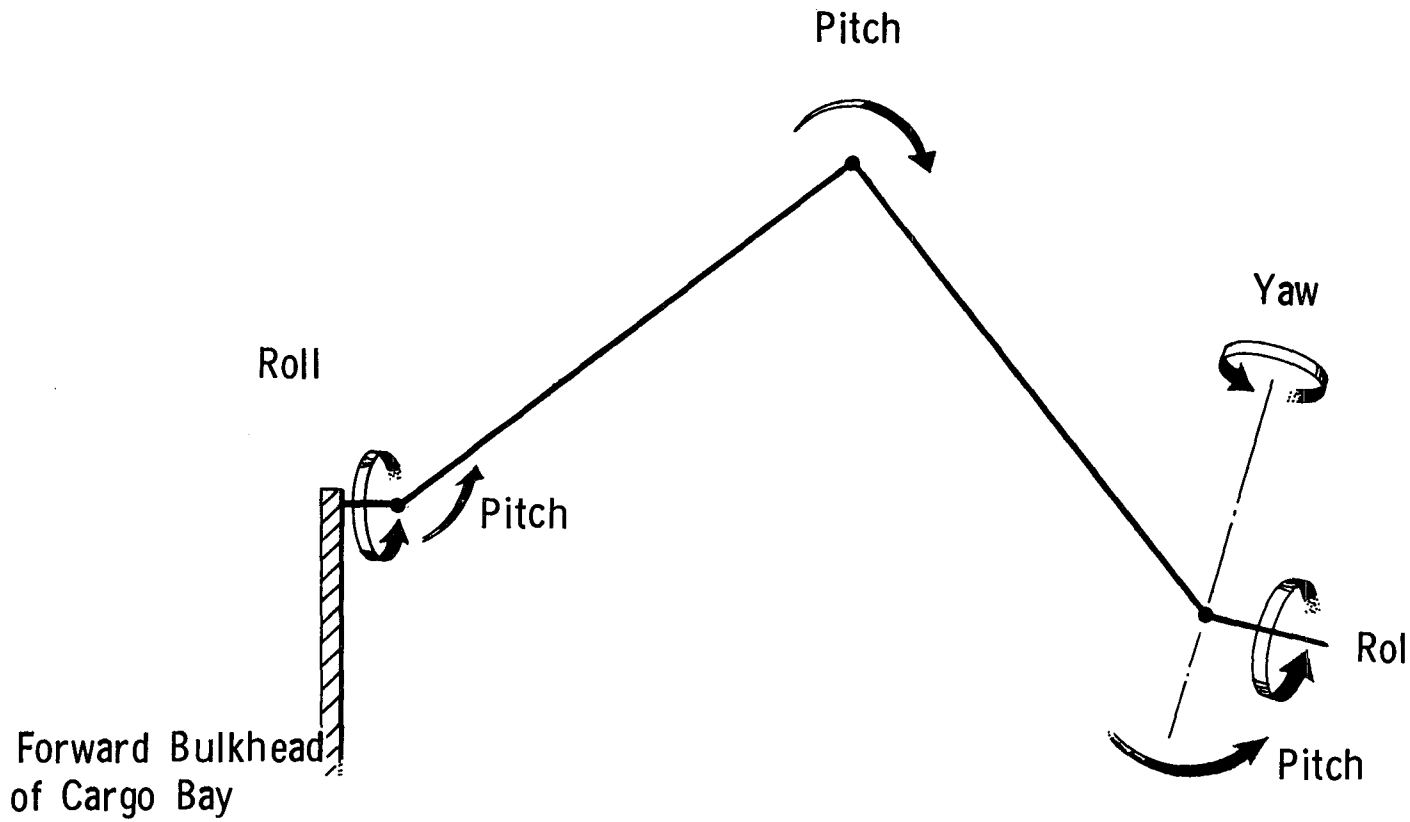

Fig. V-12 Typical Manipulator Degrees of Freedom

B. TELECOMMUNICATIONS SUBSYSTEM CONCEPTUAL DESIGN

The Telecommunications conceptual design for the RMS is shown in Fig. V-13. This conceptual design was used as an aid in concept selection. The ground rules used to develop the subsystem block diagram are given below. The selection of a concept will not be affected by these rules. Ground rules that would make the subsystem more complex for one concept would complicate all concepts, and vice versa.

Telecommunications Ground Rules For Concept Selection Purposes

1) Hard wire connections will be employed throughout telecommunication subsystems.
2) Stereo TV will not be employed.
3) TV docking pictures will not be retransmitted to Earth.
4) Color TV will not be employed.

The subsystem conceptual design is based on a system concept such as Concept A or I, i.e., a single arm with a fixed base using a minimum of components. All other concepts will require the same basic telecommunications subsystem except for different quantities of sensors and displays, as shown in Table V-1. A minimum of three cameras are proposed for concept selection purposes:

1) A panoramic camera mounted so as to achieve an overall view of the manipulator;
2) A terminal device camera to provide a closeup view of the operation of the terminal device and the object that it is to grasp;
3) A cargo camera to aid in handling cargo bay operations.

Each of these cameras will have the necessary controls required to obtain proper operations and assistance in viewing of the shuttle docking and cargo handling sequences.

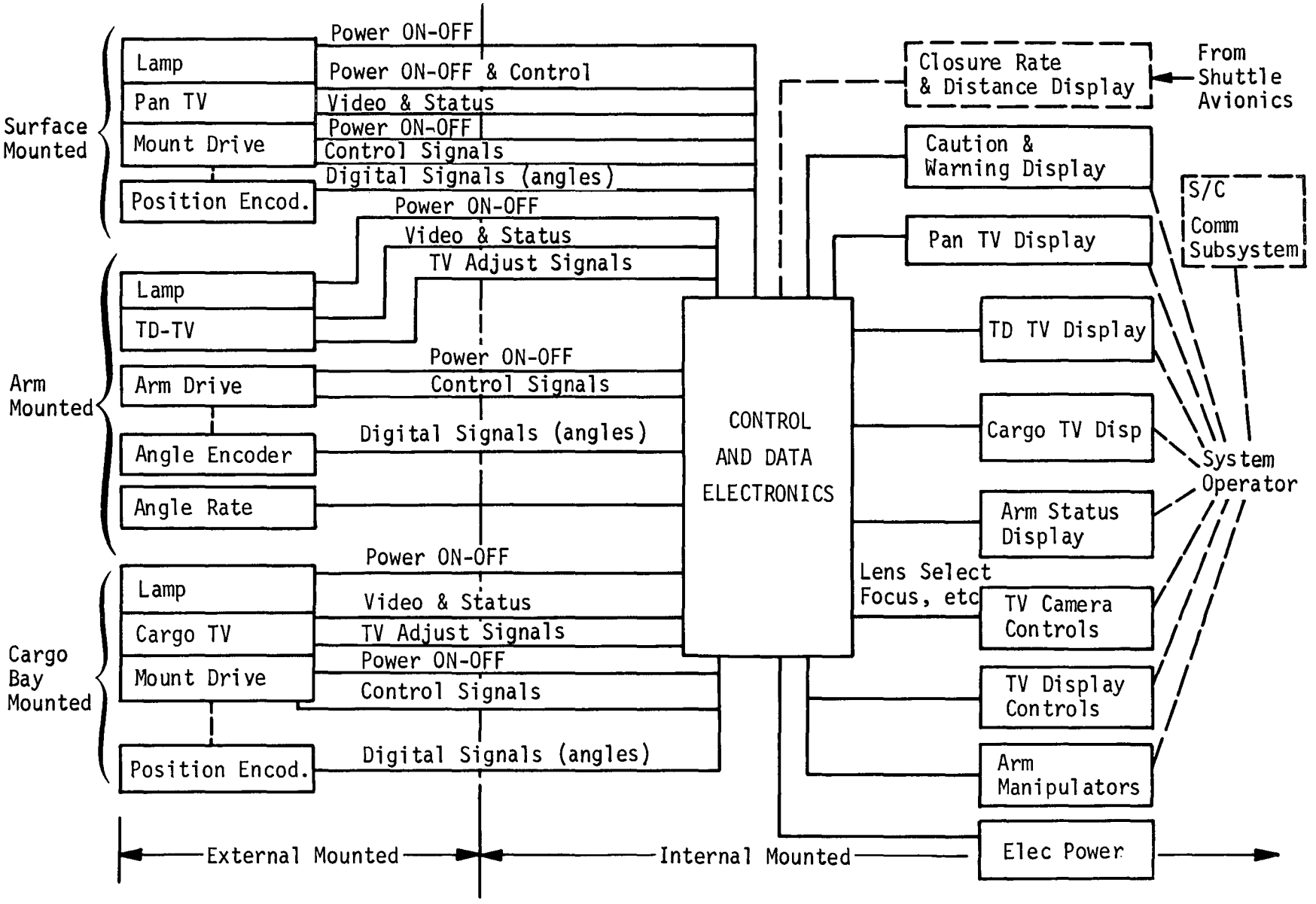

Fig. V-13 Telecommunications Conceptual Design

Table V-1 Component Quantities for Conceptual Design

MAJOR COMPONENT	TOTAL COMPONENTS REQUIRED CONCEPT									
	A	B	C	D	E	F	G	H	I	J
Pan TV Camera	1	1	1	1	1	1	1	1	1	1
Lamp	1	1	1	1	1	1	1	1	1	1
Mount Drive Motors	2	2	2	2	2	2	2	2	2	2
Position Encoders	2	2	2	2	2	2	2	2	2	2
Terminal Device TV	1	1	1	2	2	2	2	2	1	3
Lamp	1	1	1	2	2	2	2	2	1	3
Cargo TV	2	2	2	1	1	2	1	1	2	1
Lamp	2	2	2	1	1	2	1	1	2	1
Arm Drive Motors	7	8	8	14	14	7	15	15	7	14
Encoders	7	8	8	14	14	7	15	15	7	14
Rate Sensors	7	7	7	14	14	7	15	15	7	14
Console	1	1	1	1	1	1	1	1	1	1
Caution & Warning	1	1	1	1	1	1	1	1	1	1
Pan TV Display	1	1	1	1	1	1	1	1	1	1
Terminal Device TV Displ	1	1	1	2	2	1	2	2	1	2
Cargo TV Display	1	1	1	1	1	1	1	1	1	1
Arm Status Display	1	1	1	2	2	1	2	2	1	2
TV Camera Controls	1	1	1	2	2	1	2	2	1	2
TV Display Controls	1	1	1	2	2	1	2	2	1	2
Arm Manipulator	1	1	1	2	2	1	2	2	1	2
Electronics	1	1	1	1	1	1	1	1	1	1

The operator, stationed at a proposed display and control console in the Shuttle spacecraft, will be provided with three video displays--arm control display, caution and warning devices, arm manipulators--and other controls necessary to initiate, operate, and terminate the entire operation.

The telecommunications subsystem will include signal conditioning, encoded read-out, motor control, decoding, and computational circuits normally required in a system of this type.

Table V-2 describes the major system components.

Voice communications will be provided over the main Shuttle-to-ground station link.

Table V-2 Component Characteristics for Conceptual Design

COMPONENTS	ESTIMATED WEIGHT, kg (lb)	ESTIMATED POWER REQUIRED, (w)
Pan TV Camera	2.27 (5)	7
TV Lamp	0.91 (2)	250
Mount	1.36 (3)	--
Motor	0.23 (0.5)	2
Encoder	0.23 (0.5)	2
Terminal Device	2.27 (5)	7
Mount	1.36 (3)	--
Lamp	0.91 (2)	250
Cargo TV	2.27 (5)	7
Mount	1.36 (3)	--
Lamp	0.91 (2)	250
Cabling	10.90 (24)	--
Console	--	--
Caution Warning Electronics	2.27 (5)	10
Pan TV Display	2.72 (6)	8
Pan TV Display Electronics	1.82 (4)	10
Terminal Device TV Display	2.72 (6)	8
Terminal Device TV Display Electronics	1.82 (4)	10
TV Camera Controls	0.91 (2)	2
Arm Manipulator	0.91 (2)	4
Arm Manipulator Electronics	1.82 (4)	6
System Control Electronics	13.62 (30)	25

C. CONCEPT EVALUATION

For use in the evaluation of the concepts, Table V-3 was prepared to show the functions of each arm for the 2-arm or variable position or length concepts. The alternative concepts were designed with arm lengths such that the increased length capability was provided primarily for the 2270.0 kg (5000 lb) and 181.6 kg (400 lb) satellites. This can readily be seen in Table V-3.

Next, each concept was examined for weight analysis. This analysis was based on requirements for torques and velocities established in Chapter IV. Six items were included in the weight picture: beam, base, joints, extension mechanism, and stowage (or deployment) mechanism. The results of these estimates, shown in Fig. V-14, are striking. Calculating the average weight for all concepts we get 230.4 kg (512 lb). No concept varies more than 14% from the average which is well within the possible errors in the weight estimations. Therefore, the weight of the concepts was eliminated as a factor in concept selection.

Table V-4 is a compilation of the numerical data for each concept. A technology development status, Table V-5, was prepared for all major components involved in the ten concepts. This table shows that no components required an advance in the state-of-the-art.

To further aid in the evaluation of the concepts, a scale model (1:50) of a Shuttle Orbiter (less wings and tail) was used in conjunction with manipulator arms that were constructed to scale so that they could demonstrate each of the ten concepts. Scale payloads were also fabricated for this use. Figure V-15 shows the model of the Shuttle and manipulator arms.

Table V-3 Arm Functions

Configuration \ Functions *	Space Station		Space Station Module				29,545.6 kg (65,000 lb) Payload		2270.0 kg (5000 lb) Satellite		181.6 kg (400 lb) Satellite		Disable Shuttle	
	C	D	C	D	U	T	C	U	C	U	C	U	C	D
Concept B														
Length 1	X	X	X	X	X	X	X	X	X		X		X	X
Length 2									X	X	X	X		
Concept C														
Position 1	X	X	X	X	X	X	X	X	X		X		X	X
Position 2									X	X	X	X		
Concept E														
Arm 1	X	X	X	X	X	X	X	X	X		X		X	X
Arm 2									X	X	X	X		
Concept F														
Position 1	X	X	X	X	X	X	X	X	X		X		X	X
Position 2									X	X	X	X		
Concept G														
Length 1	X	X	X	X	X	X	X	X	X		X		X	X
Length 2									X	X	X	X		
Concept H														
Position 1	X	X	X	X	X	X	X	X	X		X		X	X
Position 2									X	X	X	X		
Concept J														
Position 1	X	X	X	X	X	X	X	X	X		X		X	X
Position 2									X	X	X	X		

* Function Codes: C = Capture; D = Dock; U = Unload & Deploy; T = Unload, Transfer & Dock

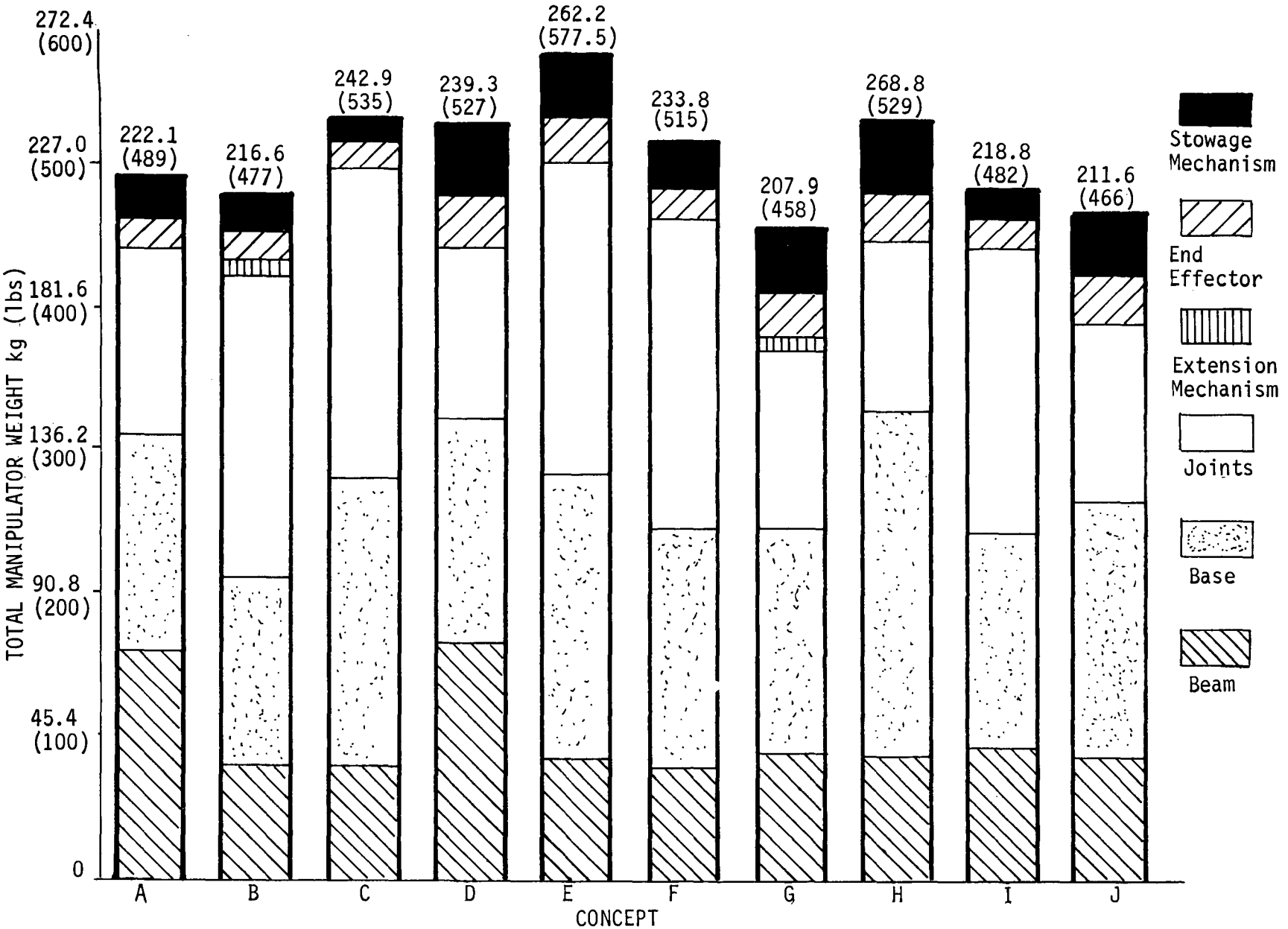

Fig. V-14 Manipulator Weight Distribution

Table V-4 Alternative Concepts Data

Parameter \ Concept	A	B	C	D	E	F	G	H	I	J
Number of Arms	1	1	1	2	2	1	2	2	1	2
Number of TV Cameras	4	4	4	4	4	4	4	4	4	4
Manipulator Weight, kg (lb)*	222 (489)	216.5 (477)	242.9 (535)	239.3 (527)	262.4 (578)	233.8 (515)	207.9 (458)	240.2 (529)	218.8 (482)	211.6 (466)
Arm 1 - Length, m (ft)	19.5 (64)	13.7 (45)	13.7 (65)	19.8 (45)	13.7 (45)	13.7 (45)	14 (46)	14 (46)	14.6 (48)	14 (46)
Base X - Location, m (in.)	27.5 (1082)	27.5 (1082)	27.5 (1082)	27.5 (1082)	27.5 (1082)	27.5 (1082)	27.5 (1082)	27.5 (1082)	32.4 (1277)	27.5 (1082)
Secondary Location, m (in.)			33 (1300)			33 (1300)				
Diameter, cm (in.)	30.5 (12)	30.5 (12)	30.5 (12)	30.5 (12)	30.5 (12)	30.5 (12)	30.5 (12)	30.5 (12)	30.5 (12)	30.5 (12)
Wall Thickness cm (in.)	0.25 (0.10)	0.15 (0.06)	0.25 (0.10)	0.25 (0.10)	0.15 (0.06)	0.15 (0.06)	0.15 (0.06)	0.15 (0.06)	0.2 (0.08)	0.15 (0.06)
Torque, N·m (ft-lb)	1525.5 (1125)	2034 (1500)	2034 (1500)	678 (500)	2034 (1500)	2034 (1500)	1000.7 (738)	1000.7 (738)	1661.1 (1225)	1000.7 (738)
Tip Force, N (lb)	200.2 (45)	342.5 (77)	342.5 (77)	80 (18)	342.5 (18)	342.5 (77)	164.6 (37)	164.6 (37)	262.4 (59)	164.6 (37)
Joint Accuracy (deg)	0.08	0.12	0.12	0.08	0.12	0.12	0.12	0.12	0.11	0.12
Arm 2 - Length, m (ft)	--	--	--	19.8	9.45	--	14.03	14.03	--	14.03
Base X Location m (in.)	--	--	--	27.5 (1082)	46.8 (1843)	--	27.5 (1082)	27.5 (1082)	--	27.5 (1082)
Secondary Location, m (in.)	--	--	--			--		33 (1300)	--	33 (1300)
Wall Thickness, cm (in.)	--	--	--							
Diameter, cm (in.)	--	--	--	30.5 (12)	5.7 (2.25)	--	30.5 (12)	30.5 (12)	--	30.5 (12)
Wall Thickness, cm (in.)	--	--	--	0.25 (0.15)	0.07 (0.03)	--	0.15 (0.06)	0.15 (0.06)	--	0.15 (0.06)
Torque, N·m (ft-lb)	--	--	--	678 (500)	5.42 (4)	--	1000.7 (738)	1000.7 (738)	--	1000.7 (738)
Tip Force, N (lb)	--	--	--	80 (18)	0.8 (0.18)	--	164.6 (37)	164.6 (37)	--	164.6 (37)
Joint Accuracy (deg)	--	--	--	0.08	0.17	--	0.08	0.08	--	0.08
Extension-Length, m (ft)	--	5.8 (19)	--	--	--	--	5.8 (19)	--	--	--
Diameter, cm (in.)	--	4.06 (1.6)	--	--	--	--	4.06 (1.6)	--	--	--
Wall Thickness, cm (in.)	--	0.08 (0.03)	--	--	--	--	0.08 (0.03)	--	--	--
Torque, N·m (ft-lb)	--	13.6 (10)	--	--	--	--	13.6 (10)	--	--	--
Tip Force, N (lb)	--	0.71 (0.16)	--	--	--	--	0.71 (0.16)	--	--	--

*Baseline Arm Material; Boron Epoxy, Baseline Degrees of Freedom; 7 per Arm + Extensions

Table V-5 Technology Development (Advance the State-of-the-Art)

MAJOR CONCEPT DEPENDENT COMPONENTS		TECHNOLOGY DEVELOPMENT REQUIRED		
		YES		
COMPONENT	PRIMARY CHARACTERISTIC	NO	MINOR	MAJOR
Harmonic Drives	200:1 max reduction	X		
Tachometer Generator	Speed Accuracy	X		
Potentiometer	Position Accuracy Space Environment	X		
DC Servomotor	High Torque Space Environment	X		
Bearings	Accuracy radial, axial	X		
Force Sensors	Torque, Pressure	X		
Arm Structure	High Strength Modulus	X		
Wiring	Weight, flexing	X		
Brakes	Electro dynamic mechanical deceleration control	X		
Gearing	Reduction, loads	X		
Panoranic Lamp and TV Mount	2 DOF	X		
Cargo Lamp & TV Mounting	Wide Field of View	X		
Encoders	14 Bit Accuracy	X		
Arm Status Display	Man-Machine Op	X		
Electrical Power	Power	X		
Electronics	Control	X		

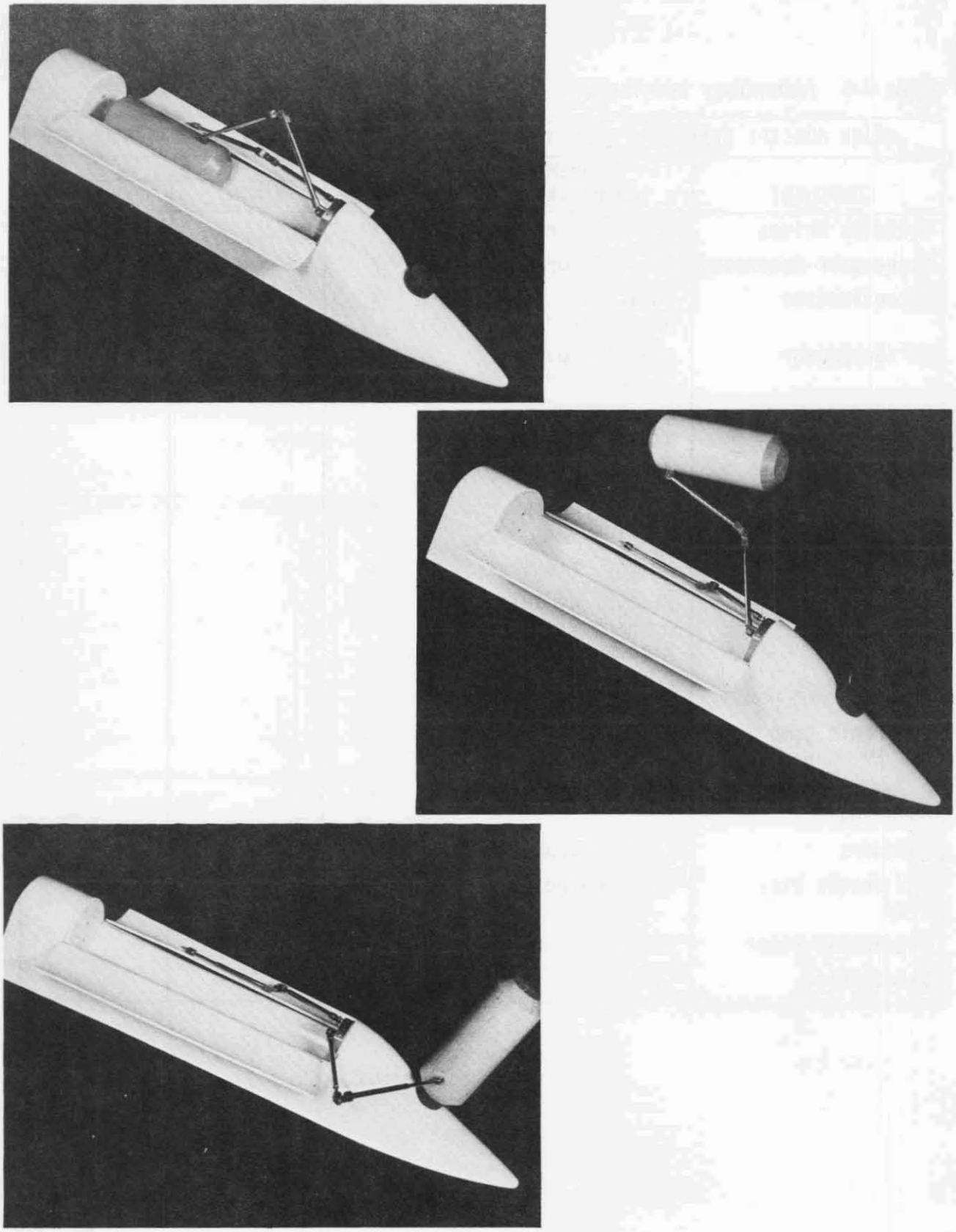

Fig. V-15 Scale Model of Shuttle and Manipulator Arms

D. CONCEPT RANKING AND SELECTION

In ranking the concepts the advantages and disadvantages of each were compiled as shown in Table V-6. The table reflects our approach to the ranking. The ideal concept has the least design complexity, interface problems, development cost, the best dynamic control, the most versatility, and the most redundancy, etc. A numerical approach to the ranking was carried out. The parameters considered are shown in the Concept Scoring Form (Fig. V-16). Each parameter was compared with the others and a weighting established. The use of the weighting provided a means for the more important parameters to affect the results more than those less important parameters. For example, whether a concept has a high or low development risk affects the ranking more than whether or not a concept has the capability for self-maintenance. The scoring was carried out by six system and subsystem engineers with the weighting (5, 3, 1) factors shown, with a different set of weighting (1, 2, 3), and again with no weighting. All scoring methods yielded the same first-ranked concept: Concept A, one arm, fixed length, fixed base. The entire ranking, based on weighting (5, 3, 1) is shown in Table V-7.

Additional requirements were placed on the RMS; namely, that it be capable of the assembling two orbital payloads, for which two arms would be required. In addition, for all other tasks, only one arm would be used (either of the two arms). Relating to the concept ranking table, the selected concept became two of Concept A. This is not the same as the two-arm concept (D) since in that case the arms are used as a pair. In the selected concept, the two arms are identical, both fixed length, and both mounted at the cargo bay forward bulkhead. The arms are structurally and mechanically designed so that all tasks (except orbital assembly) can be performed using only one arm. Thus, the concept has the operational and control simplicity of the one-arm concept and 100% redundancy on all tasks but one, which is an improvement over the two-arm concepts. Figure V-17 depicts the selected concept.

Further analysis of the Shuttle Traffic Model (July 1971) showed that stowage of the 227.0 kg (500 lb), 0.61x1.22 m (2x4 ft) satellite did not constrain it to the very end of the cargo bay payload envelope, and that it could be moved to a position near the cargo bay doors. Thus, the 181.6 kg (400 lb) satellite no longer was a severe driving force on the arm length requirement. (The arm length is discussed in Chapter VII, Section A, Part 1.)

Table V-6 Concept Advantages and Disadvantages

Configuration	Advantages	Disadvantages
Concept A One arm, Fixed Length Fixed Base	Simple design. Minimum interface problems. High reliability. Low cost. Straight forward controls and displays. Stows and deploys easily.	Long arm length. No redundancy. Orthogonal viewing at end effector not feasible. Limited capability for secondary tasks such as maintenance and repair.
Concept B One arm, Telescoping length, Fixed Base	Short basic arm length. Minimum interface problems. Better dynamic control with task dependent arm length. Minimum stowage volume.	Complex telescoping mechanism. No redundancy. Orthogonal viewing at end effector not feasible. Limited capability for secondary tasks. Additional displays required.
Concept C One arm, Fixed Length Moving Base	Short arm length. Better dynamic control with task dependent base location. High reliability.	Increased interface problems. Complex base mechanism. No redundancy. Requires additional controls and displays. Limited capability for secondary tasks.
Concept D Two arms, Fixed Length, Fixed Common Base	Good dynamic control. Redundancy for single arm failure for all non-docking tasks. Good capability for secondary tasks. Loads shared between arms.	Increased interface problems. Complex control for coordinated motion. Requires additional sensors/displays. Panoramic view more likely to be obstructed by arms. Long arm length. More complex collision avoidance.
Concept E Two arms, Fixed length, Fixed separate Bases	Short arm lengths. Provides limited redundancy for non-docking tasks. Better dynamic control with task dependent arm designs. Good capability for secondary tasks.	Increased interface problems. Separate controls/displays for each arm. High cost for development of two (2) different arms.
Concept F One arm, Fixed Length, Two Base Locations	Short arm length. Good dynamic control with task dependent base location. Minimum stowage volume.	Complex interface problems. Complex control problem to move base location. No redundancy. Limited capability for secondary tasks.
Concept G Two arms, One fixed length, One telescoping Fixed Base	Good dynamic control. Redundancy for single arm failure for most cargo handling tasks. Good capability for secondary tasks. Loads shared between arms. Basic arm length short.	Complex telescoping mechanism. Additional sensors/displays required. Complex control for coordinated motion. More complex collision avoidance.
Concept H Two arms, Fixed length, One fixed Base One Moving Base	Good dynamic control. Redundancy for single arm failure for most cargo handling tasks. Good capability for secondary tasks. Loads shared between arms. Arm length short.	Increased interface problems. Complex base mechanism. Additional controls/displays required. Complex control for coordinated motion. More complex collision avoidance.
Concept I One arm, Fixed length, Fixed Base	Simple design. High reliability. Low cost. Straight forward controls and displays. Shortest total arm length to perform all tasks with fixed base, non-extendible arm.	No redundancy. Limited capability for secondary tasks. Non-symmetrical loads on shuttle.
Concept J Two arms, Fixed length One fixed base One multiple base	Good dynamic control. Redundancy for single arm failure for most cargo handling tasks. Arm length short. Good capability for secondary tasks. Loads shared between arms.	Increased interface problems. Complex control problem to move base location. Complex control for coordinated motion. Additional controls/displays required. More complex collision avoidance.

Concept / Parameter	weighting	A	B	C	D	E	F	G	H	I	J
Cost	5										
Development Risk	5										
Shuttle Interface	5										
Weight	5										
Crew Work Load	5										
Engineering Development	5										
Probability of No Failure	3		Typical Raw Scoring								
Mechanical Complexity	3	1	3	7	2	5	9	6	8	4	10
Secondary Task Cap.(Main. & Repair Task)	3										
Fail Operational Capability	3										
Direct Viewing Potential	1										
Stowage Volume	1										
Arm Length	1										
Crew Training	1										
Control Complexity (Computer Augmentation)	1										
Self-Maintenance Capability	1										
Telecommunications Complexity	1										
Displays	1										
Orthogonal Viewing*	1										
Collision Avoidance	1										

* Capability of viewing end effector at right angle during task performance.

Fig. V-16 Concept Scoring Form

Table V-7 Alternative Concepts Ranked

RANK	CONCEPT	SCORE	DESCRIPTION
1	A	216	One arm, fixed length, fixed base at cargo bay forward bulkhead.
2	I	227	One arm, fixed length, fixed base at 17 feet rearward from forward bulkhead.
3	D	254	Two arms, fixed length, fixed common base at cargo bay forward bulkhead.
4	B	272	One arm, telescoping length, fixed base at cargo bay forward bulkhead.
5	G	290	Two arms, fixed common base; one arm fixed length; other arm telescoping length, mounted at cargo bay forward bulkhead.
6	C	304	One arm, fixed length, moving base with primary position at cargo bay forward bulkhead.
7	H	325	Two arms, fixed length; one arm fixed base at forward bulkhead; other arm moving base with primary base at forward bulkhead.
8	E	354	Two arms, fixed length, fixed separate bases; one arm at cargo bay forward bulkhead; other arm at near bulkhead.
9	J	401	Two arms, fixed length; one arm fixed base; other arm movable base (self-locomotion) with primary position at forward bulkhead.
10	F	414	One arm, fixed length, movable base (self-locomotion) with primary base at cargo bay forward bulkhead.

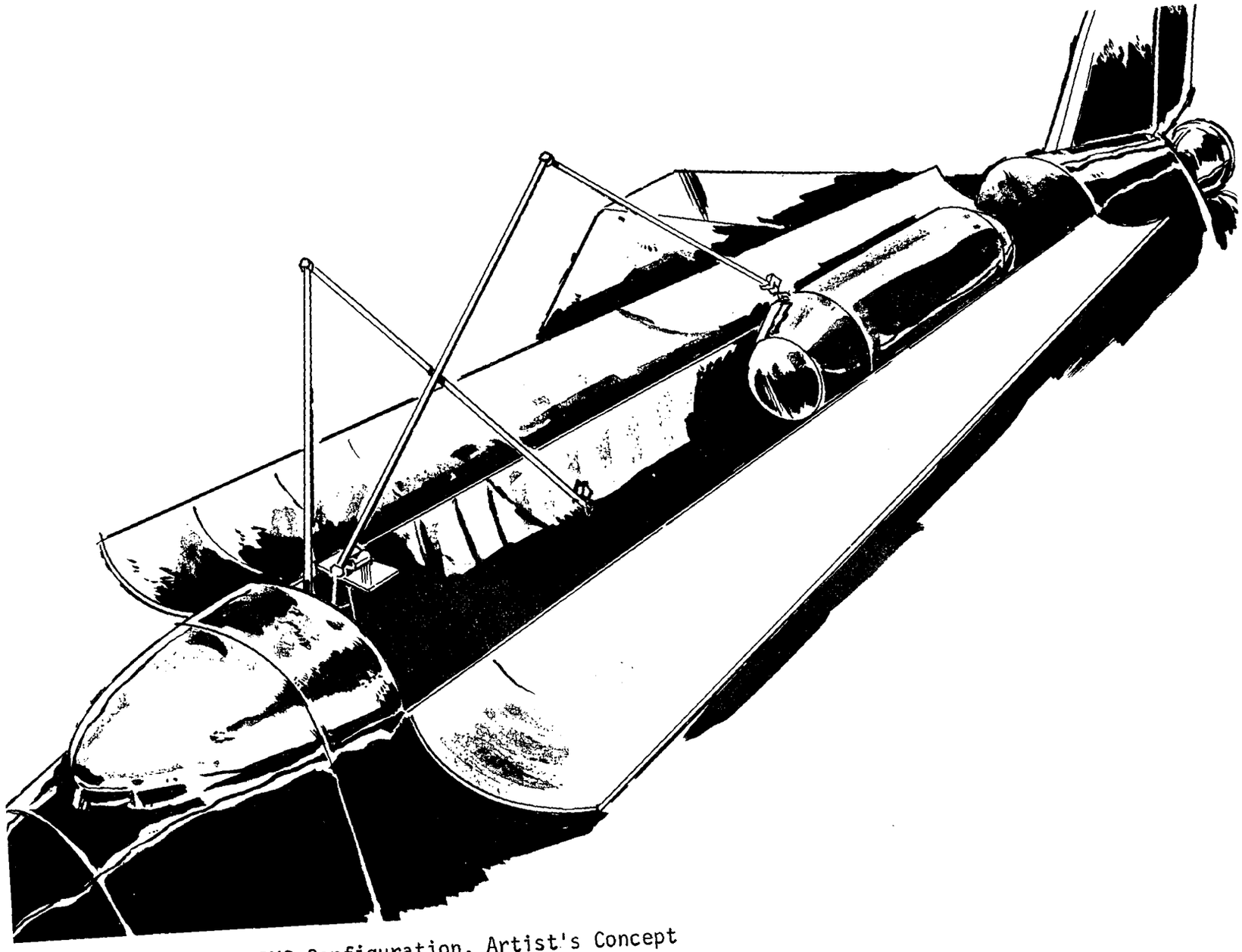

Fig. V-17 Selected RMS Configuration, Artist's Concept

A change in emphasis was made from docking to cargo handling. The concept selected for further analysis was one whose strength and torque capabilities were determined by the cargo handling tasks. The Shuttle reaction control system thrusters would be used to help reduce the relative velocities between the Shuttle and the Space Station (or other orbital payloads) after the RMS arm had been mechanically linked with the Space Station.

The stowage volume requirement was changed to approximately 8 inches diameter per arm so as to be more compatible with current Orbiter design concepts. In addition, aluminum was set as a design guideline material for the arms.

Lastly, the weight requirement was relaxed to 910 to 1135 kg (2000 to 2500 lb) for both arms and their deployment mechanism.

VI. MAN-IN-THE-LOOP SIMULATIONS

This section presents a detailed description of the simulation studies conducted on the controllability of long manipulator arms, using the MMC Space Operations Simulator. The text presented here is abstracted from an MMC research report titled *Manipulator Arm Control Technology Investigation* R-71-48664-004. The simulator configuration and equations explained in Sections A and B, which were set up and derived from the research study, were also used to obtain the contract data presented in Appendix A of this report. The results and conclusions (and task time summary data) are based on both the research and contract data. Two simulations were performed: one simulating a manipulator arm with a TV camera mounted on the terminal device; the other using an actual manipulator arm with a TV camera mounted at the manipulator arm base. A control station with a TV monitor and a control input device was assembled from which several operators remotely controlled the arms. The specific task was to maneuver a probe into a receptacle of a space station module mockup.

The following parameters were varied during the simulations: control input devices (hand controller, switch box, master arm); control axes (base and camera); control mode (position, rate, acceleration); camera control (hand, foot); and control characteristics.

NOMENCLATURE

cg	Center of gravity
DOF	Degrees of freedom
EAI	Electronic Associates Industries
MMC	Martin Marietta Corporation
SOS	Space Operations Simulator
TV	Television
WRT	With respect to
D	Symbol for transformation, identified by subscripts

L	Length of segment arm
$\overline{L}$	Vector locating distance to point defined by subscripts
$\overline{L}_{cg}$	Vector locating manipulator base from Shuttle cg
$\overline{L}_T$	Vector locating manipulator tip from Shuttle cg
r	Defined by Equation [5]
$\dot{r}$	Defined by Equation [8]
R	Defined by Equation [6]
$\dot{R}$	Defined by Equation [9]
S	LaPlace operator
x, y, z	Base, inertial, or simulator axes
x_c, y_c, z_c	SOS translational commands
$\dot{x}_H, \dot{y}_H, \dot{z}_H$	Control device output rates
x_I, y_I, z_I	Inertial coordinate distances defined by Equation [12]
x_T, y_T, z_T	Inertial coordinate distances from probe to target
x_o, y_o, z_o	Initial relative distance of Space Station to Shuttle
$\dot{x}_o, \dot{y}_o, \dot{z}_o$	Constant relative velocities of Shuttle and Space Station
x_3, y_3, z_3	Coordinate distance to manipulator wrist from base, components of $\overline{L}_3$
$\overline{l}_x$	Unit vector in x direction

ϕ_1, θ_1, θ_2, θ_3, ψ_1, ψ_3	Manipulator arm joint angles, defined by subscripts
$\dot{\phi}_1$ $\dot{\theta}_1$ $\dot{\theta}_2$	Manipulator arm joint angular rates, defined by subscripts
θ_c, ψ_c	TV camera angles
ϕ_s, θ_s, ψ_s	Relative attitude angles between Shuttle and Space Station
ϕ_o, θ_o, ψ_o	SOS attitude head command angles
ϕ_{30}	Initial desired wrist angle when θ_1 and θ_2 are zero
ω	Natural frequency of second order system
Sθ	Abbreviation for sine θ
Cθ	Abbreviation for cosine θ

INTRODUCTION

Spatial use of manipulator arms requires solution of a number of new operational and control problems. The arm itself must be much longer than any previously designed because of the variety of anticipated tasks and distances through which it may be required to operate. Possible lengths range from 40 to 65 feet. Full utilization of a manipulator arm in space requires that it perform tasks employing moving targets, a requirement not usually existing for ground-based tasks. Because of the possible large separation distances between operator and terminal device in space applications, direct viewing may not be always possible as it usually is on earth. Considering these problems, a simulation plan was developed to investigate control techniques using remote viewing, and to study various tradeoff parameters and command technique characteristics.

A. SIMULATION PLAN

Manipulator arm control problems were studied using the MMC Space Operations Simulator (SOS) supported by EAI 231R computers and a simplified control station mockup. The SOS has three rotational degress of freedom obtained by an attitude head, and 3 translational degrees of freedom obtained by moving carriages. All 6 degrees of freedom are controlled by position servo drive systems and computer generated commands. The control station mockup, shown in Fig. VI-1, consisted of a TV monitor and a chair from which the command input device was operated. This illustration shows operation with the 3-axis rotational handcontroller. The headset was used to communicate with the technician operating the SOS and computers.

The hardware configuration in the SOS and the analog computer program were dependent on specific simulation objectives. Two separate configurations and computer programs, identified by Phase 1 and Phase 2, were used in the simulation studies.

Phase 1 - This configuration, shown in Fig. VI-2, consisted of a scaled mockup of a docking port module of the space station, which was mounted to a stationary frame, and a TV camera and terminal device mounted to the attitude head of the SOS carriage. The real situation that this configuration represents is shown in Fig. VI-3. The simulated manipulator arm consisted of two main segments and a terminal device with the following characteristics:

Segment Length: 9.5 m (31 ft)

2 DOF at the shoulder: roll and pitch

1 DOF at the elbow: pitch

2 DOF at the wrist: pitch and yaw

The TV camera was mounted on the terminal device, part of which was visible in the TV field-of-view (Fig. VI-1).

For Phase 1, the manipulator arm was mathematically modeled in the computer according to the equations given in Section B. Inputs from the control device were used to calculate desired translational motion (in x, y or z direction) of the manipulator wrist. The computer then calculated how the manipulator arm shoulder and elbow joints must rotate to give the desired translational wrist motion, including effects of joint servo lags.

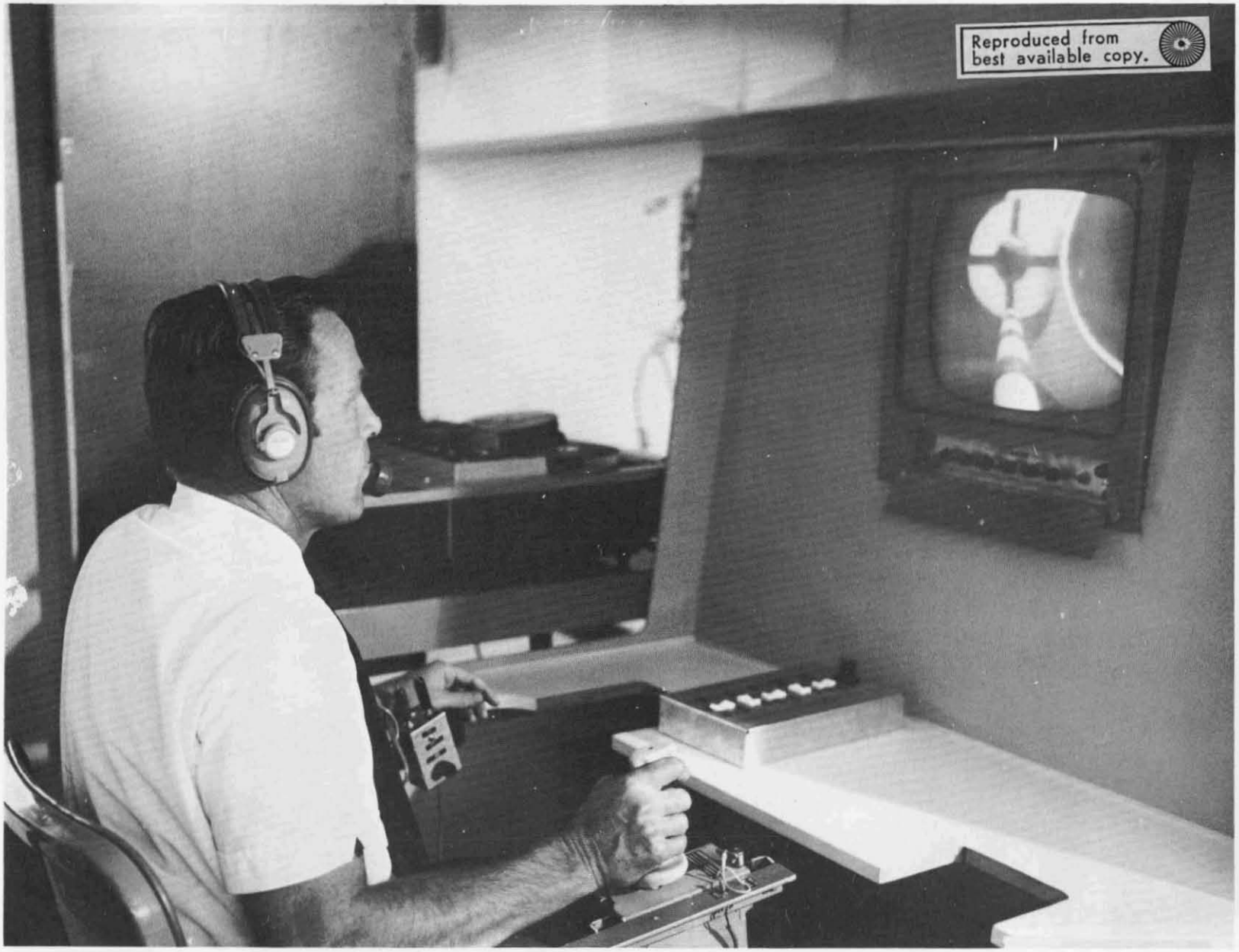

Fig. VI-1 Phase 1, Control Station

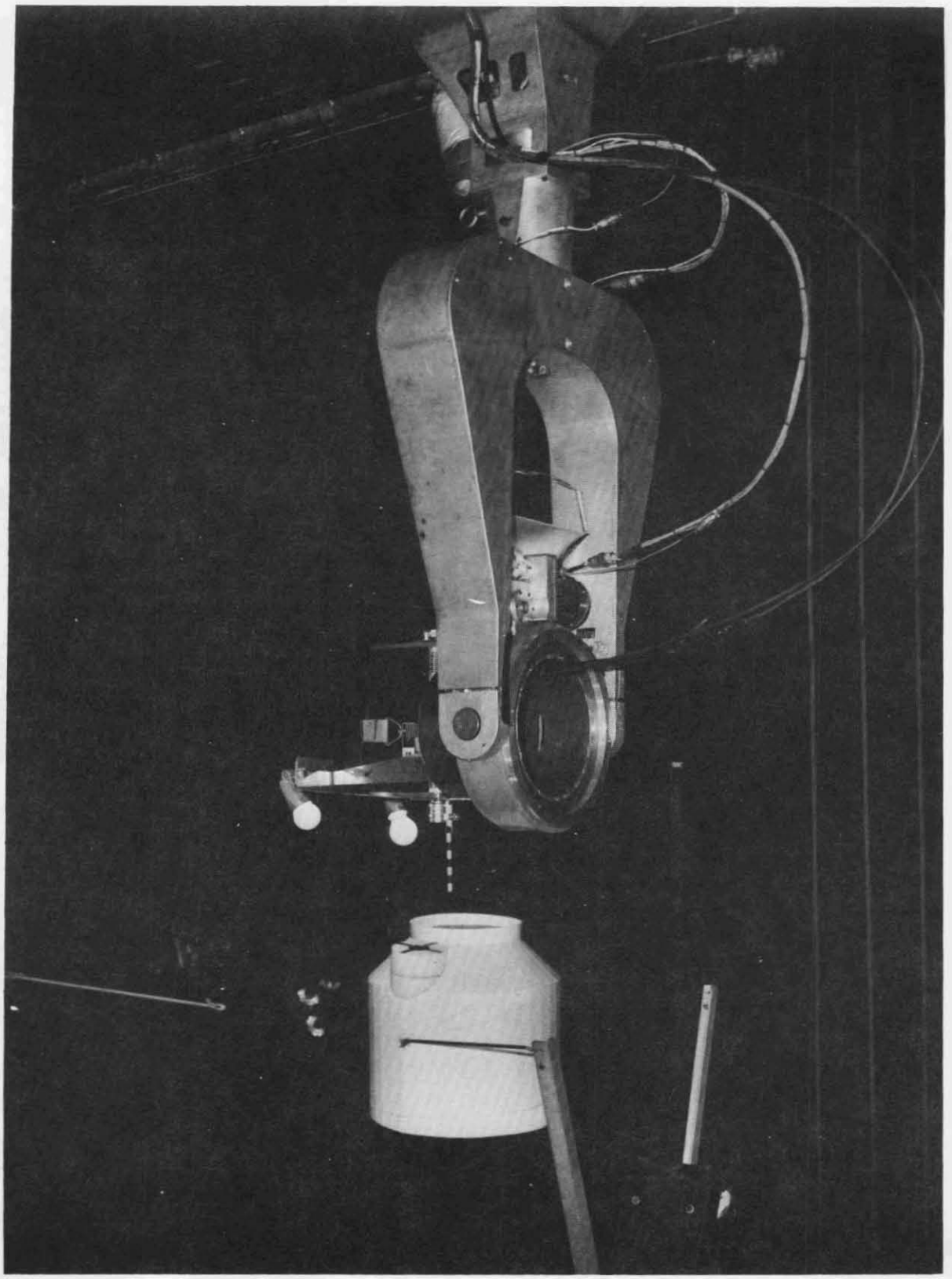

Fig. VI-2 Phase 1, SOS Configuration

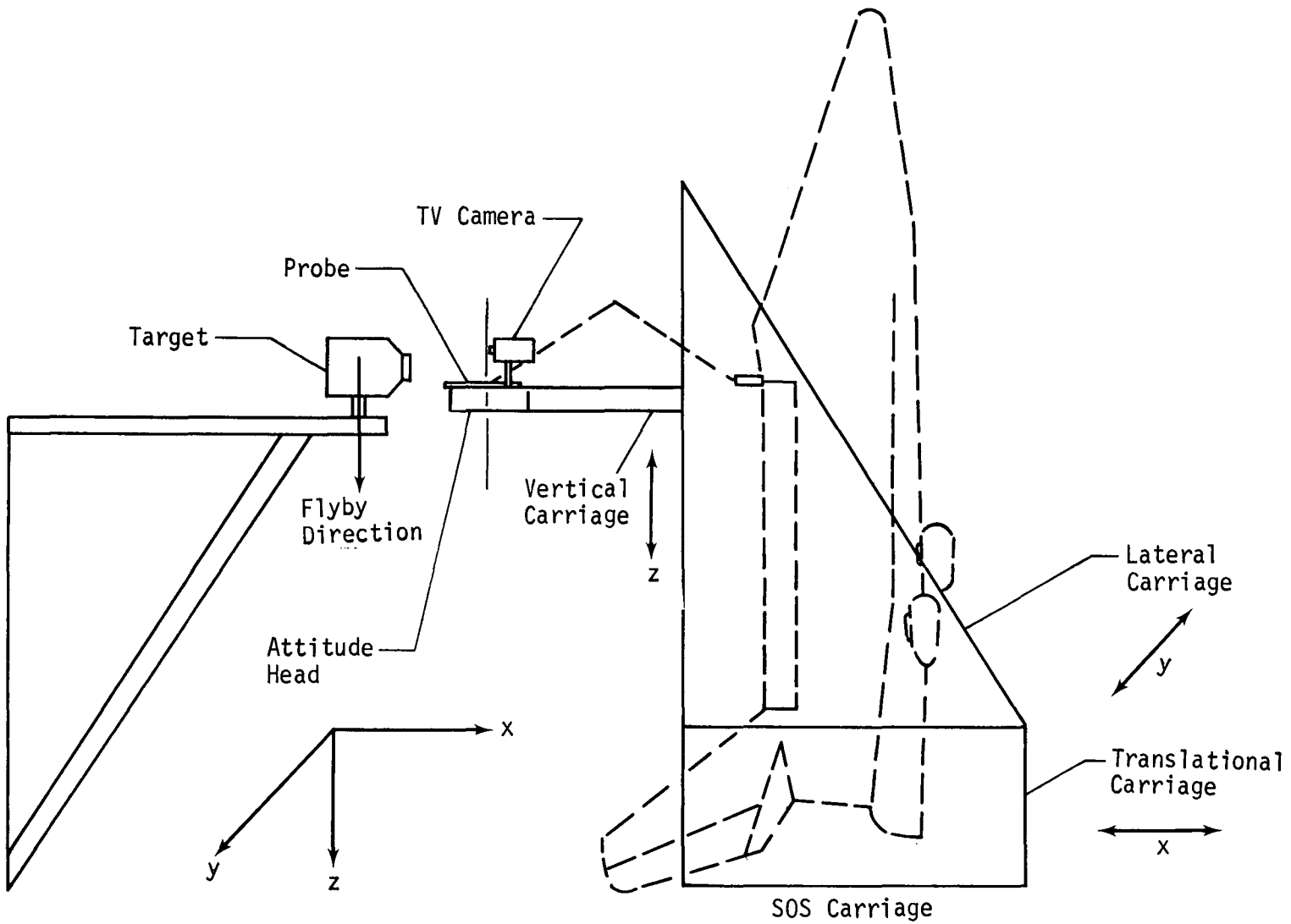

Fig. VI-3 Phase 1, Space Configuration

Translational wrist position was then recalculated, added to the relative motion between Shuttle and Space Station module, and the resultant was applied to the 3 translational degrees of freedom of the SOS carriage. The SOS attitude head rotational commands were obtained by a combination of 3 degrees of relative rotational rates between the Shuttle and Space Station, the 2 degrees of terminal device or wrist joint rotation, and the shoulder and elbow arm angles. The simulated wrist joint was operated as a function of manual input commands (from hand or foot) and arm shoulder and elbow joint angles. The wrist motion calculated as a function of joint angles was such that the terminal device (and TV camera) did not rotate inertially as the arm was moved around. Its inertial rotation then was a function of only manual input commands.

The specific task required of the operator in Phase 1 was to maneuver the probe into the receptacle of the docking port mockup. The same task was required for the various parameter variations and initial conditions mentioned later. Successful task completion occurred when the probe made contact with the receptacle; contact of the probe at any other point on the target was considered a failure. No postcontact dynamics were simulated and the probe and target were designed so that no damage occurred when contact was actually made. No manipulator arm structural vibration effects were included in the simulations.

The primary objectives of Phase 1 were to study the controllability and the difficulty of close-in maneuvering of a manipulator arm with a TV camera mounted on the terminal device.

Phase 2 - The Phase 2 configuration is shown in Fig. VI-4 and consisted of the same scaled module mounted this time to the SOS attitude head, and actual scaled manipulator arms mounted to the support structure. The situation that this configuration represents is shown in Fig. VI-5. The manipulator arms shown in Fig. VI-4 are scaled versions of space arms having two main segments each with the following characteristics:

Segment length: 9.5 m (31 ft)

2 DOF at the shoulder: yaw and pitch

1 DOF at the elbow - pitch

No mechanized wrist

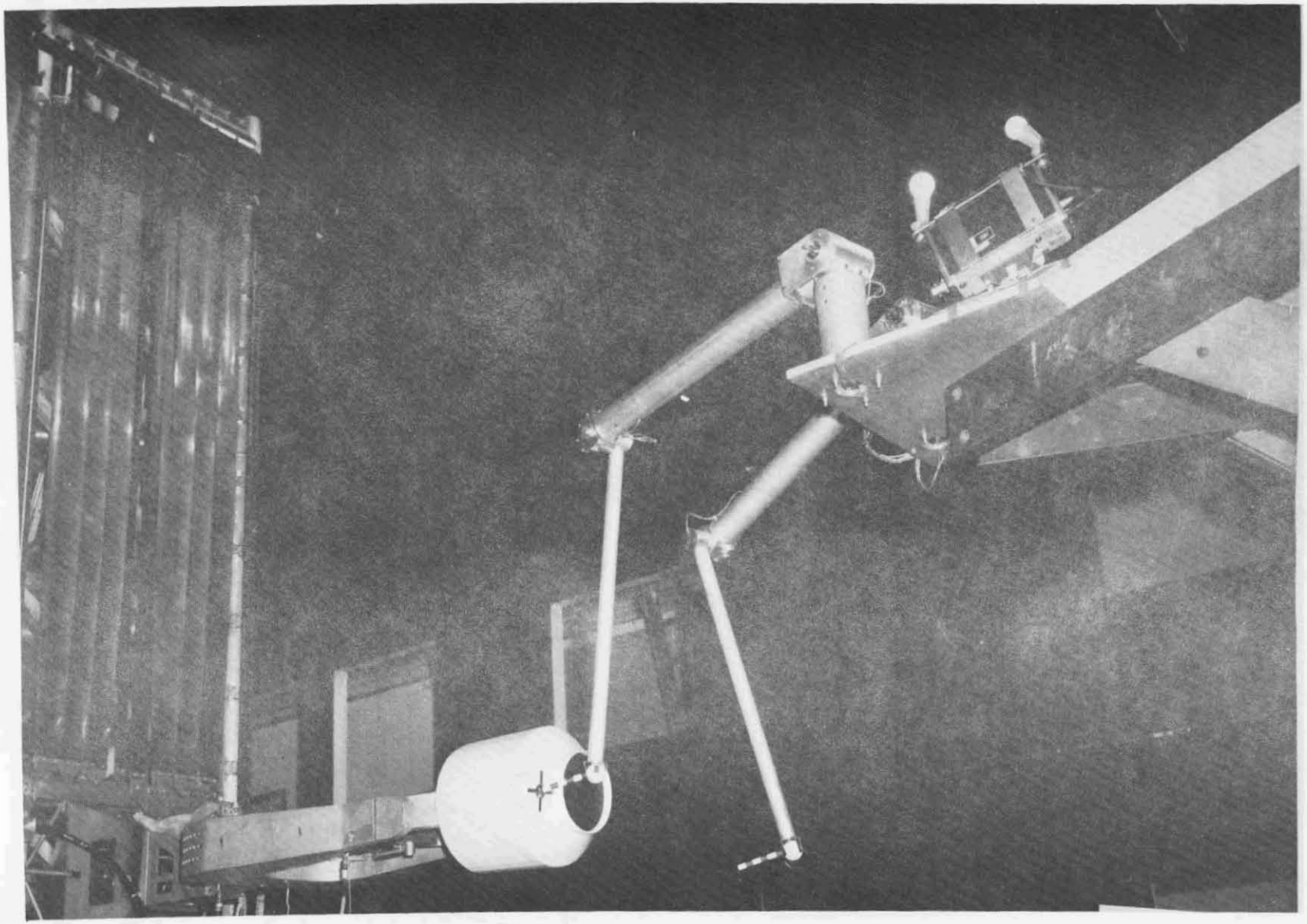

Fig. VI-4 Phase 2, SOS Configuration

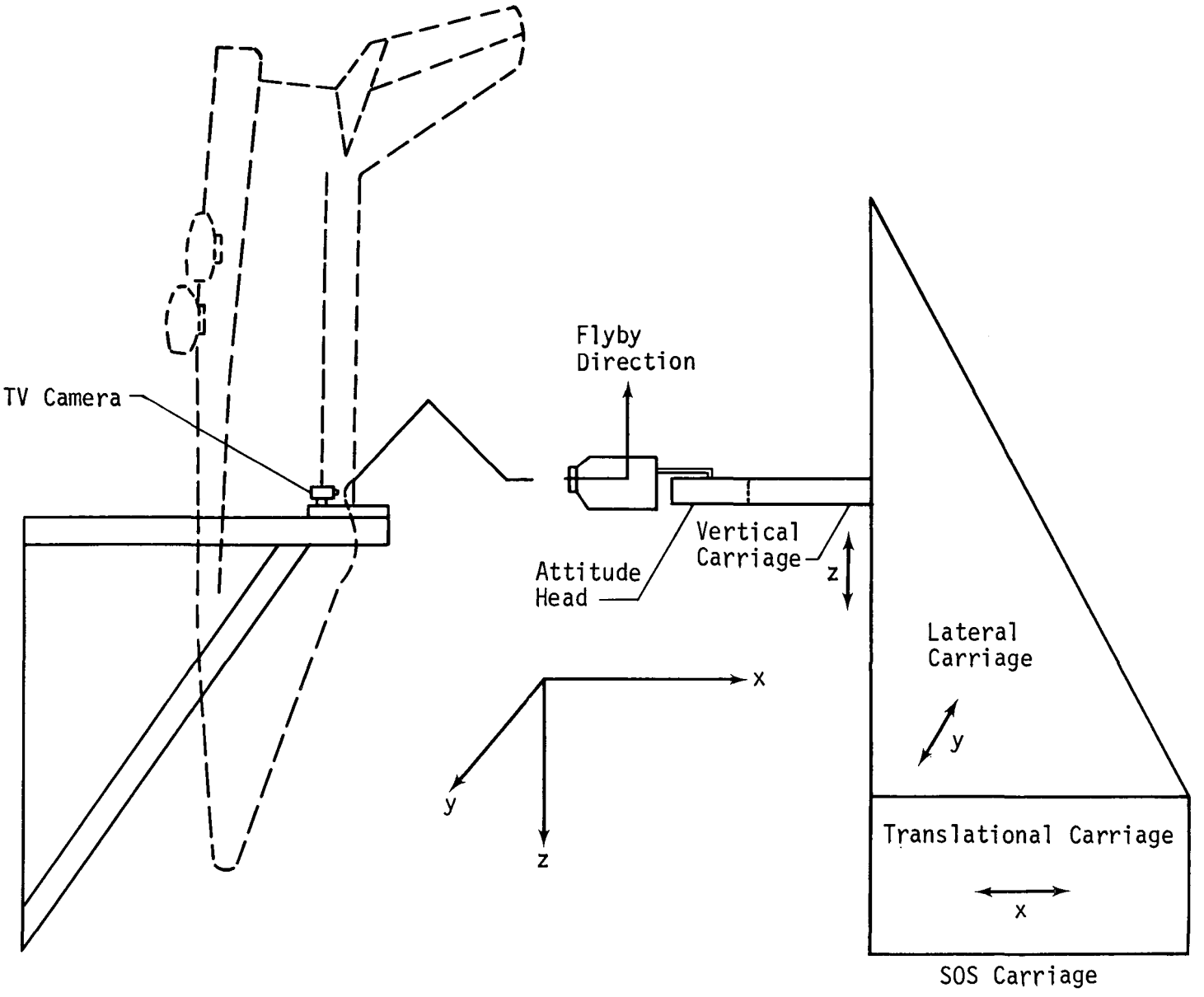

Fig. VI-5 Phase 2, Space Configuration

The TV camera in Phase 2 was mounted at the base of the arms, giving more of a view of the arm and module mockup. The TV view at the control station is shown in Fig. VI-6. The Phase 2 computer equations consisted of those required to calculate arm joint motions to give desired x, y, z translational motions of the wrist (similar to Phase 1). The results were applied directly to the position servo systems driving each manipulator joint. Since the wrist joint was not mechanized, the probe was fixed in a given position. The TV camera was mounted on its own pan-tilt head and was operated from the foot controller at the operator's console. The module mockup, mounted to the attitude head, was driven relative to the arms at scaled relative velocities and rotational rates between the Shuttle and Space Station.

The Phase 2 task required of the operator was identical to the task in Phase 1, including the task success/failure criteria. The primary objectives of Phase 2 were to study the controllability and difficulty of close-in maneuvering of a manipulator arm with a TV camera mounted at the base of the arm.

Parameter Variations

The various hardware or computer functions that were varied during the simulations are listed and explained in the following paragraphs. The Results section identifies and discusses the parameter choice generally preferred among operators.

1) Command Technique (control input device)

a) Handcontroller (joystick) - A three-axis Apollo Block I, proportional, rotational handcontroller, shown being used in Fig. VI-1 and VI-6, was one device used to obtain input commands to operate the manipulator arm. The correspondence between handcontroller motion and arm motion was variable according to the operator's choice and most commonly was as follows: handcontroller pitch - x, roll - y, and yaw - z. The handcontroller was also used to control individual joint motion according to the following: handcontroller yaw - shoulder yaw, handcontroller pitch - shoulder pitch, handcontroller roll - elbow pitch. The handcontroller axis system was assumed parallel to the operator axis system which is +x forward, +y to the right, and +z down.

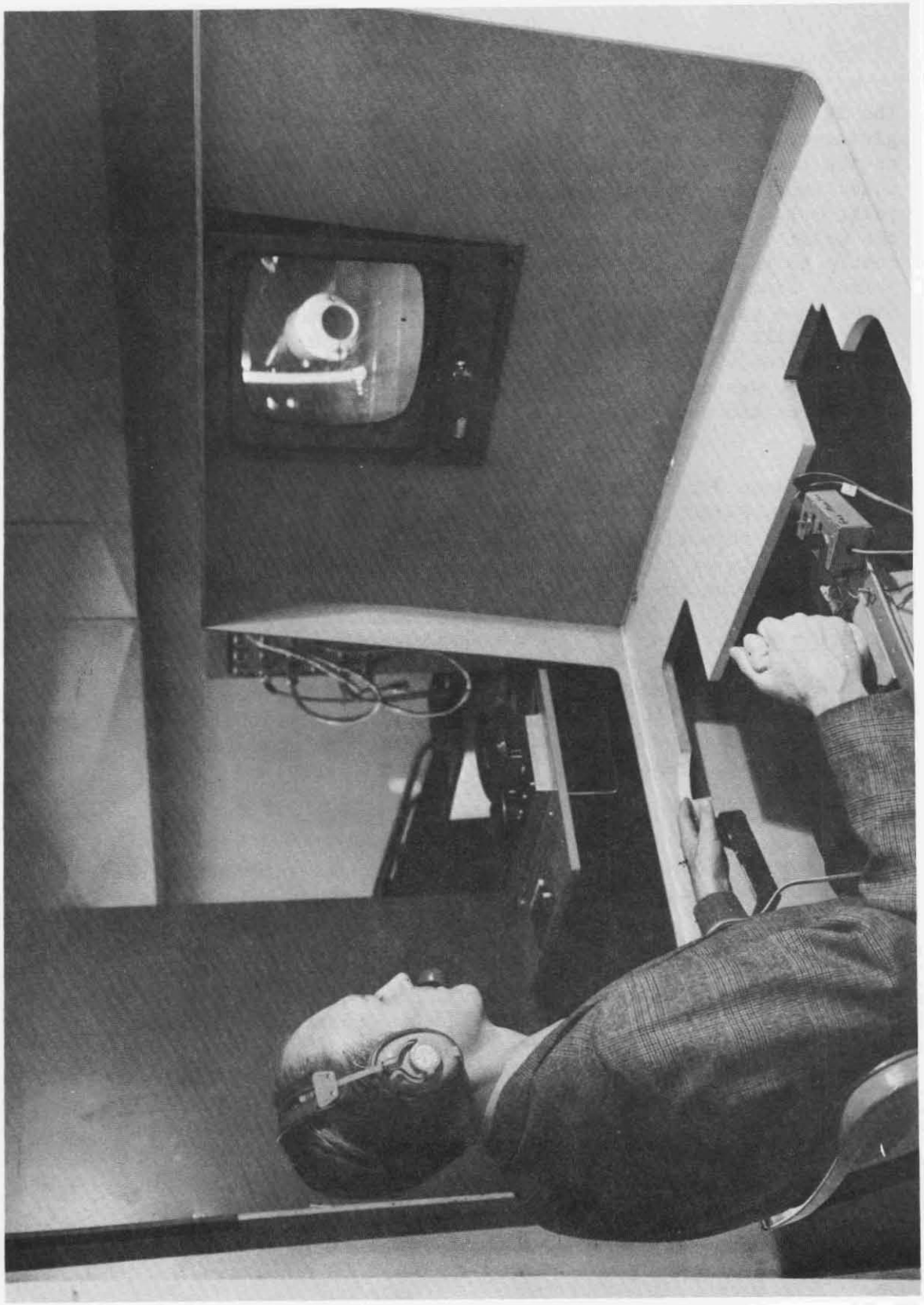

Fig. VI-6 Phase 2, Control Station

b) Switch Control Box - A switch box, shown in Fig. VI-1 and sketched in Fig. VI-7, was a second device for obtaining input commands. Switch boxes of this type have been used extensively in the past for manipulator control in Earth-oriented industrial tasks. The switches were momentary contact rocker arm type that give a constant output when activated. The rate potentiometer allowed varying magnitudes of the input command, if desired.

c) Master Arm - A third device for obtaining command imputs was a geometrically similar control, or "master" arm, shown in Fig. VI-8. In this case the manipulator arm, designated as a slave, is driven by commands taken directly from the potentiometers at the joints of the master. This resulted in a one-to-one angular rotation of the master and slave, but gave a 3.5-to-1 ratio of translational motion since the slave segment lengths are 1.1 m (3.5 ft), and the master 0.3 m (1 ft). No computers were required for manipulator control in this mode of operation.

2) Control Axes

a) Manipulator Base - Two axis systems into which control inputs can be resolved were investigated. The first, the manipulator base axes, is the axis system fixed at the base of the manipulator arms.

b) Camera Axes - The second axes system investigated was defined as camera axes, i.e., an axis system that remains fixed in the TV camera. Thus, for example, an input command calling for x motion would produce wrist translational motion in the direction in which the camera was pointing, i.e., the same direction in which the operator is looking. This axis system can, therefore, also be called display axes, or pilot axes.

3) Control Mode

a) Position - The position control mode is one in which the manipulator arm position is controlled with an input from the control device. The master arm was the only control device used for this mode. In a proportional handcontroller the amount of manipulator arm travel for a given amount of handcontroller travel (i.e., sensitivity), was not sufficient for a meaningful task.

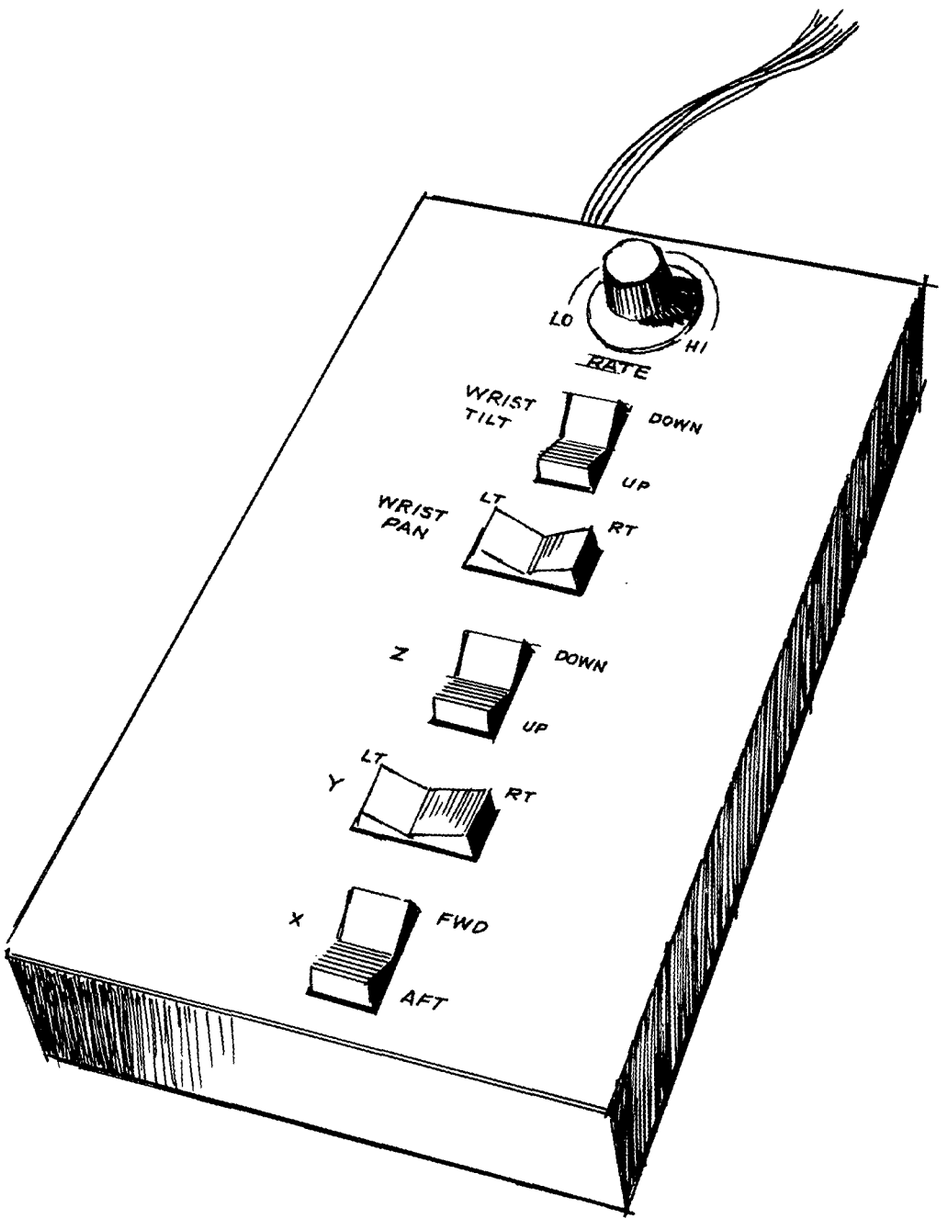

Fig. VI-7 Switch Box

Fig. VI-8 Geometrically Similar ("Master") Controller

b) Rate - The rate control mode is one in which the manipulator arm velocity is controlled with an input from the control device. The commanded velocity magnitude was varied according to handcontroller deflection or position of the RATE potentiometer on the switch box.

c) Acceleration - The acceleration control mode is one in which the manipulator arm acceleration is controlled with an input from the control device. The commanded acceleration magnitude was varied according to handcontroller deflection or the position of the RATE switch on the switch box.

4) Control Characteristics - The relationship between control device output and actual manipulator arm motion constitutes the control characteristics. One characteristic variable by computer control was the total system gain, i.e., maximum velocity or acceleration of the arm for a given control input level. The system gains were varied during the simulations and the optimum values were assessed. For the master-slave configuration, gains were not variable; however, maximum velocities and accelerations were limited by the servo system design for each of the manipulator arm joints. Maximum velocity and acceleration inputs from the handcontroller and switchbox were limited by the computer to levels anticipated as the RMS design values. These were well below the capability of the arm servos. For the handcontroller, a linear control characteristic (single slope) and a nonlinear control (double slope) characteristic were programmed and used as candidate control systems for both velocity and acceleration modes. Since the switches in the switch box were not the proportional type, the nonlinear control could not be implemented.

Another control characteristic investigated was termed Rate Bias and was implemented by an ON-OFF switch mounted near the hand controller. This switch, when activated, adds a constant velocity bias to the manipulator wrist in the direction of maximum relative velocity between the Shuttle and Space Station. The magnitude of the velocity bias is sufficient to cancel the maximum relative velocity. The purpose of the switch is to essentially remove one degree of freedom from necessary pilot control, thus reducing task difficulty. Impementation of rate bias is discussed in Chapter VII, Section E.

5) Wrist Control

a) Hand - Manual control of the wrist joint (and therefore probe and camera orientation) in pan (yaw) and tilt (pitch) was implemented, when using the handcontroller, by depressing with the forefinger a small momentary contact switch mounted directly on the control handle. When the switch was depressed, the handcontroller was converted from manipulator arm translational control to wrist rotational control where a pitch motion of the handcontroller produced probe (and camera) tilt, and a yaw rotation produced probe (and camera) pan. A handcontroller roll rotation remained in control of arm motion. When using the switch box, the probe orientation was controlled by special pan and tilt rocker arm switches provided on the box.

b) Foot - A special two-axis foot controller, sketched in Fig. VI-9, was constructed for wrist control. Up and down motion of the foot produced probe (and camera) tilt, and left-right motion produced pan.

Simulation Conditions

Although the basic simulation task remained the same for all runs, namely to maneuver the manipulator arm probe into the target receptacle, the initial conditions varied according to the setup. While initial checking and testing of each setup was being conducted, initial positions of the probe relative to the receptacle, and initial velocity directions were varied. When adequate conditions were established, they were used for all data runs for a particular setup. These conditions and the magnitude of the initial velocities, which remained the same for all simulations, are shown in Table VI-1. The values given in Table VI-1 are all scaled values (except, of course, for angles and angular rates which remain the same), scaled down from full size by a factor of approximately nine. The mechanical manipulator arms used in Phase 2 are 1.07 m (3.5 ft) long per segment, representing a total full-scale size of approximately 19 m (62 ft). By consistent scaling of the arms, Space Station module mockup, positions, and velocities, the TV monitor view and all motions are the same as if viewing the full-size space system. The only exception to this is with the master-slave configuration whose operation results in a 3.5-to-1 relationship between slave and master motion, instead of a 31-to-1 ratio. Of necessity, this fact must be factored into any conclusions based on comparisons of this control technique versus other techniques.

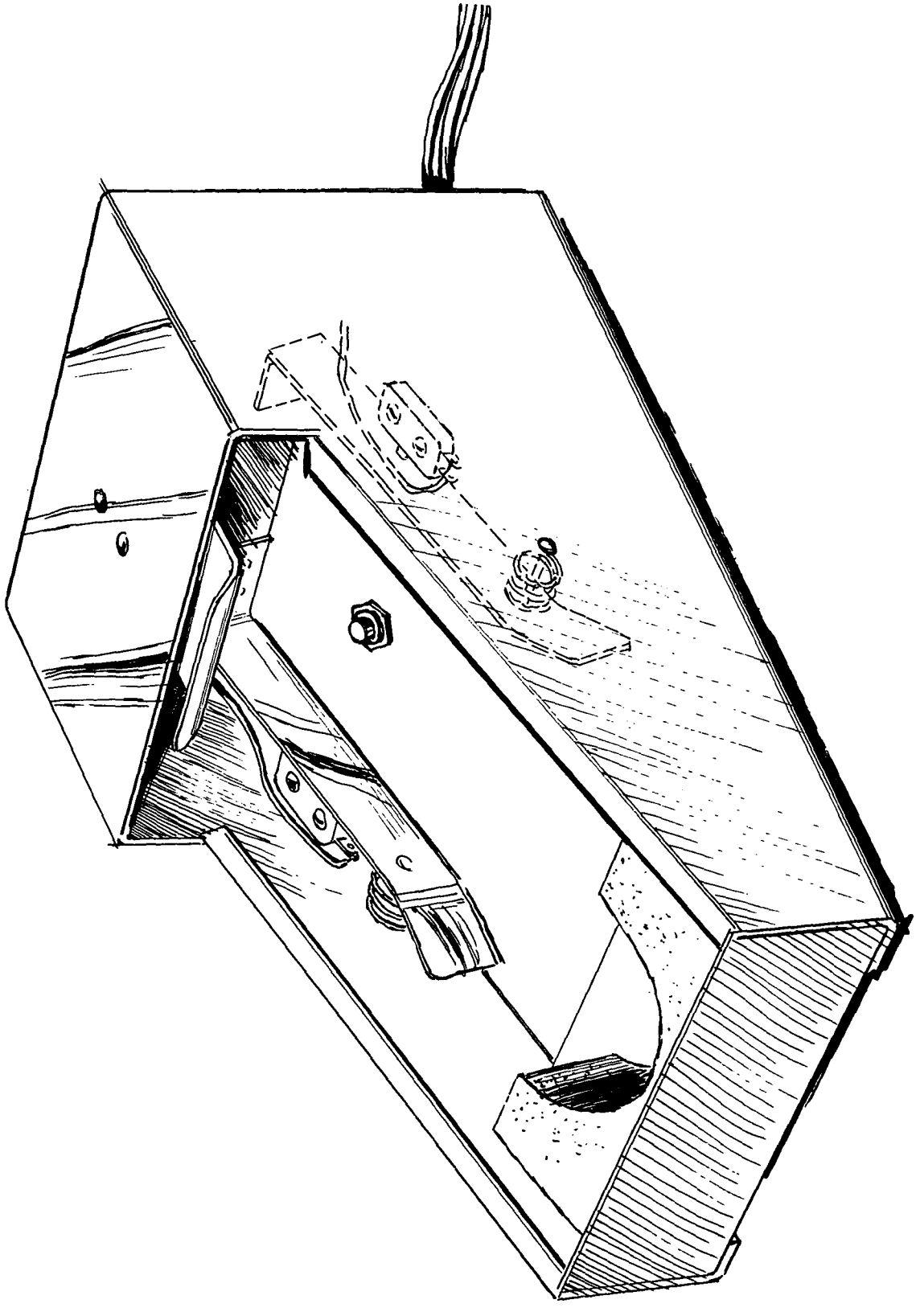

Fig. VI-9 Foot Controller

Table VI-1 Simulation Initial Conditions (Scaled)

Parameter	Phase 1 Value	Phase 2 Value
Position* - x	+0.18 m (+0.6 ft)	+0.7 m (+2.3 ft)
Position - y	0	+0.52 m (+1.7 ft)
Position - z	+0.12 m (+0.4 ft)	+1.07 m (+3.5 ft)
Velocity* - $\dot{x}$	+0.005 m/sec (+0.017 ft/sec)	-0.005 m/sec (-0.017 ft/sec)
Velocity - $\dot{y}$	+0.005 m/sec (+0.017 ft/sec)	+0.005 m/sec (+0.017 ft/sec)
Velocity - $\dot{z}$	-0.0137 m/sec (-0.045 ft/sec)	+0.0137 m/sec (+0.045 ft/sec)
Rotational Rates	0.1 deg/sec	0.1 deg/sec
Limit Cycle Angle Limits	±3°	±3°

*Positions and velocities are given in a coordinate system parallel to the one shown in Fig. VI-11.

The docking port module mockup used in the simulation is a scaled replica of the presently configured Space Station docking port with docking receptacles added. A sketch and scaled dimensions of the mockup are shown in Fig. VI-10.

Recorded Data

The following data was recorded on strip-chart recorders for a permanent record and postsimulation data analysis. Data was taken on all test runs for various operators (pilots) as the simulation parameters were varied. Sample results are shown in Appendix A.

1) Manipulator Arm Angles
2) Wrist Position Relative to Base
3) Wrist Position Relative to Target
4) Camera Attitude
5) Relative Shuttle - Space Station Attitude
6) Hand Controller Outputs

For master-slave operation, only the manipulator arm angles were recorded.

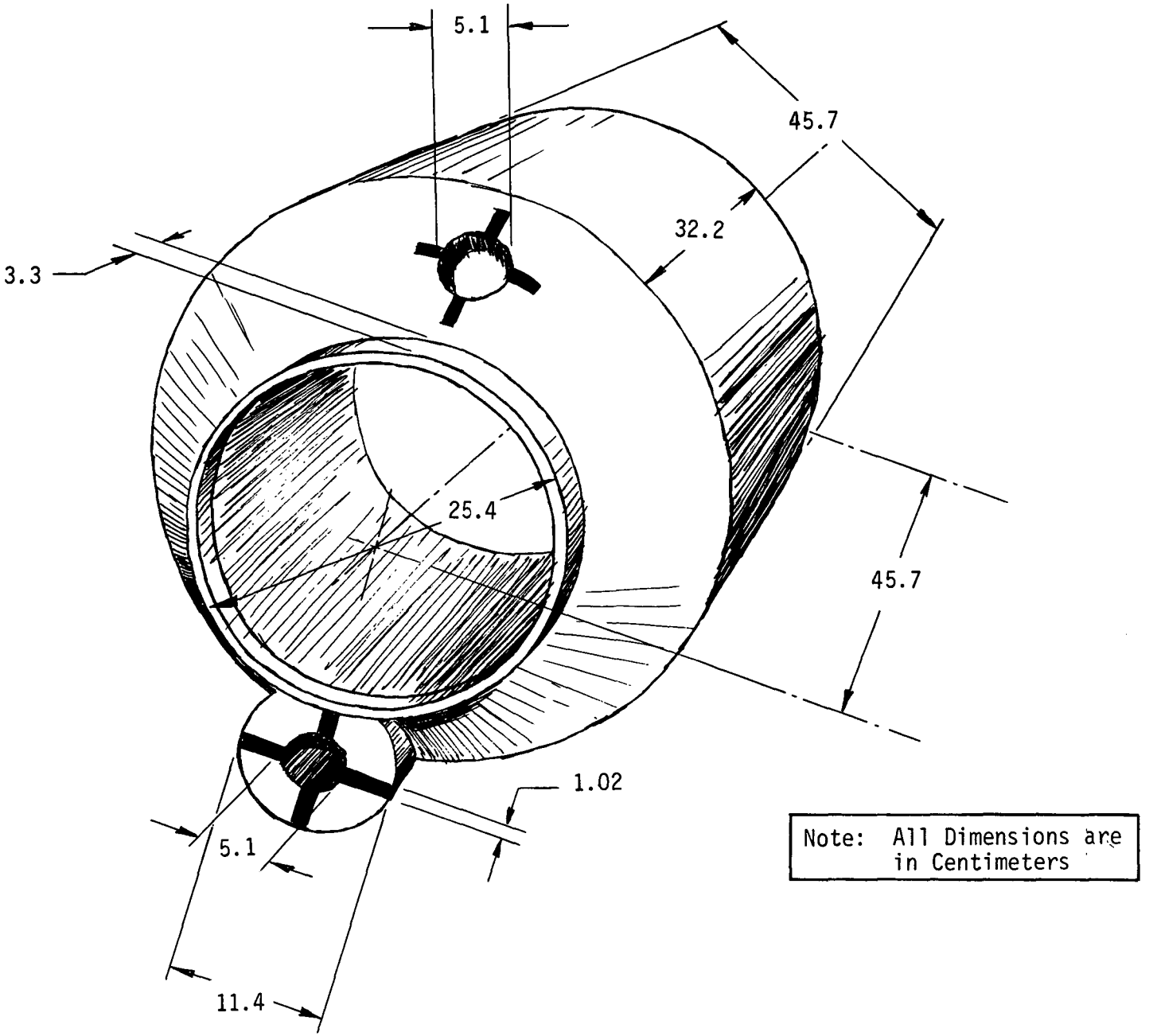

Fig. VI-10 Space Station Module Mockup

To aid in recording specific parameters and conditions being simulated, and any pertinent pilot comments, the data sheets shown in Tables VI-2 and VI-3 were developed.

Table VI-2 Simulation Parameter Matrix

	Command Techniques		Control Axes		Control Mode				Cam. Control		Initial Conditions					
Run #	Hand Cont	Switch Box	Base	Camera	Pos	Rate	Acc	Gain	Hand	Foot	x	y	z	$\dot{x}$	$\dot{y}$	$\dot{z}$

Table VI-3 Data Sheet

Run #3	Success/Failure	Parameter Choice	Comments

B. SIMULATION EQUATIONS

This section presents a derivation of the required equations of motion involved in the simulation of manipulator arm operation. The specific equations used depend on the exact configuration simulated, and thus two separate derivations are required, one for Phase 1 and another for Phase 2. See Nomenclature for definition of terms.

Phase 1 Equations

The following diagram defines the Phase 1 configuration and nomenclature used in deriving the equations.

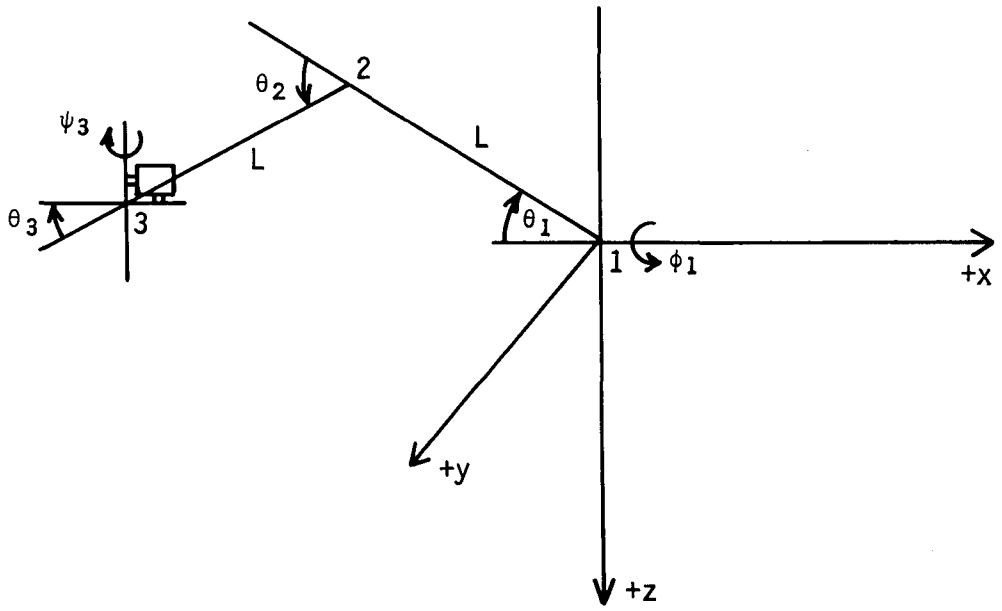

Fig. VI-11 Phase I Configuration and Nomenclature

Conditions:

Joint 1 has 2 DOF, Sequence: Roll, ϕ_1; Pitch, θ_1

Joint 2 has 1 DOF, Pitch, θ_2

Joint 3 has 2 DOF, Sequence: Pitch, θ_3, Yaw ψ_3

Simulator attitude head Sequence: Roll, ϕ_o; Pitch, θ_o; yaw, ψ_o.

Zero angles are defined when arm is coincident with -x axis.

It is desired to find expressions for the translational and rotational commands to drive the simulator in a manner which correctly simulates the problem.

Translational Commands

The wrist position relative to the axis origin is given by:

$$ {}_1\bar{L}_{31} = {}_1\bar{L}_{32} + {}_1\bar{L}_{21} \qquad \text{[VI-1]} $$

where

${}_1\bar{L}_{31}$ locates joint 3 WRT 1 in base axes

${}_1\bar{L}_{32}$ locates joint 3 WRT 2 in base axes

${}_1\bar{L}_{21}$ locates joint 2 WRT 1 in base axes

Then

$$ {}_1L_{31} = D_{21}\, D_{32}\, {}_3\bar{L}_{23} + D_{21}\, {}_2\bar{L}_{21} \qquad \text{[VI-2]} $$

where the Euler angle transformations D are defined according to previously mentioned sequences as:

$$ D_{32} = \begin{bmatrix} C\theta_2 & 0 & S\theta_2 \\ 0 & 1 & 0 \\ -S\theta_2 & 0 & C\theta_2 \end{bmatrix} $$

$$D_{21} = \begin{bmatrix} C\theta_1 & 0 & S\theta_1 \\ S\phi_1 S\theta_1 & C\phi_1 & -S\phi_1 C\theta_1 \\ -C\phi_1 S\theta_1 & S\phi_1 & C\phi_1 C\theta_1 \end{bmatrix}$$

By definition of the axes at each joint,

$$_3\bar{L}_{23} = {}_2\bar{L}_{21} = -L\,\bar{I}_x$$

and the wrist joint position relative to the base can be written as:

$$\begin{aligned} x_3 &= -L\,[C\theta_1 + C(\theta_1 + \theta_2)] \\ y_3 &= -LS\phi_1\,[S\theta_1 + S(\theta_1 + \theta_2)] \\ z_3 &= LC\phi_1\,[S\theta_1 + S(\theta_1 + \theta_2)] \end{aligned} \qquad \text{[VI-3]}$$

These equations can readily be solved for each of the three angles as a function of the wrist position, x_3, y_3, z_3, giving

$$\begin{aligned} \phi_1 &= \text{Cos}^{-1}\,\frac{z_3}{r} \\ \theta_1 &= \text{Cos}^{-1}\,\frac{x_3}{R} - \frac{\theta_2}{2} \\ \theta_2 &= 2\,\text{Cos}^{-1}\,\frac{R}{2L} \end{aligned} \qquad \text{[VI-4]}$$

where by definition,

$$r = \sqrt{y_3^2 + z_3^2} \qquad \text{[VI-5]}$$

$$R = \sqrt{x_3^2 + r^2} \qquad \text{[VI-6]}$$

Equations [VI-4] are most easily implemented on an analog computer in the rate form which bypasses the inverse functions. Taking derivatives of Equations [VI-4] gives:

$$\dot{\phi}_1 = \frac{y_3\dot{z}_3 - z_3\dot{y}_3}{r^2}$$

$$\dot{\theta}_1 = \frac{\dot{r}x_3 - x_3\dot{r}}{R^2} - \frac{\dot{\theta}_2}{2} \qquad \text{[VI-7]}$$

$$\dot{\theta}_2 = \frac{-2\dot{R}}{\sqrt{4L^2 - R^2}}$$

where

$$\dot{r} = \frac{y_3\dot{y}_3 + z_3\dot{z}_3}{r} \qquad \text{[VI-8]}$$

$$\dot{R} = \frac{x_3\dot{x}_3 + r\dot{r}}{R} \qquad \text{[VI-9]}$$

To simulate lag characteristics of the servos of a long manipulator arm, the following transfer function was applied to the angles:

$$\frac{\omega_n^2}{S^2 + 2\omega_n S + \omega_n^2} \qquad \text{[VI-10]}$$

The simulator translational commands also include motion due to Shuttle limit cycle rotation and translations. Thus,

$$\bar{L}_T = \bar{L}_{cg} + \bar{L}_3 \qquad \text{[VI-11]}$$

where

$\bar{L}_{cg}$ = distance from Shuttle cg to manipulator base

$\bar{L}_T$ = distance from Shuttle cg to manipulator wrist.

Assuming small angles for the Shuttle limit cycle excursion (±3°), in inertial or simulator coordinates $\bar{L}_T$ becomes

$$x_I = x_T - \psi_S y_T + \theta_S z_T$$

$$y_I = y_T + \psi_S x_T - \phi_S z_T \qquad \text{[VI-12]}$$

$$z_I = z_T - \theta_S x_T + \phi_S y_T$$

where

Subscript I refers to inertial coordinates

Subscript S refers to spacecraft attitude angles

The simulator translational commands can then be written as:

$$x_C = x_o + \int \dot{x}_o dt + x_I$$

$$y_C = y_o + \int \dot{y}_o dt + y_I \qquad \text{[VI-13]}$$

$$z_C = z_o + \int \dot{z}_o dt + z_I$$

where

x_o, y_o, z_o are initial relative positions of the Shuttle and Space Station,

$\dot{x}_o$, $\dot{y}_o$, $\dot{z}_o$ are constant relative velocities between the Shuttle and Space Station.

An information flow diagram showing how the above equations fit together to obtain the translational commands is shown in Fig. VI-12.

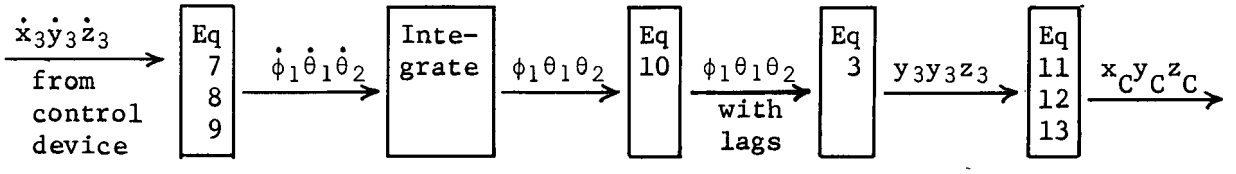

Fig. VI-12 Translational Commands Block Diagram, Phase 1

Rotational Commands

The SOS attitude angles are a function of manipulator arm angles, camera pan and tilt angles, and Shuttle attitude angles. If the wrist joint angles (or camera pan and tilt angles) are not controlled as a function of manipulator arm joint angles, the camera orientation will continually change as the wrist joint translates. This is a very undesirable effect, particularly when operating in camera axes, since continuous manual wrist joint control is required to keep the camera pointed toward the target. The effect, however, is easily removed by automatic wrist joint control according to the equation:

$$\theta_3 = -\theta_1 - \theta_2 + \theta_{30} \qquad \text{[VI-14]}$$

where θ_{30} is the initial desired wrist angle when θ_1 and θ_2 are zero. In the Phase 1 simulations, θ_{30} was assumed zero, i.e., the camera was initially pointing out the -x axis.

Defining an axis system, 4, fixed in the TV camera, the SOS attitude head angles can be found by equating the matrices:

$$D_{41} = D_{21}\, D_{32}\, D_{43} \qquad \text{[VI-15]}$$

where D_{41} is the transformation matrix using the SOS attitude head angles ϕ_o, θ_o, ψ_o:

$$D_{41} = \begin{bmatrix} C\theta_o C\psi_o & -C\theta_o S\psi_o & S\theta_o \\ C\phi_o S\psi_o + S\phi_o S\theta_o C\psi_o & C\phi_o C\psi_o - S\phi_o S\theta_o S\psi_o & -S\phi_o C\theta_o \\ S\phi_o S\psi_o - C\phi_o S\theta_o C\psi_o & S\phi_o C\psi_o + C\phi_o S\theta_o S\psi_o & C\phi_o C\theta_o \end{bmatrix} \qquad \text{[VI-16]}$$

Equation [15] gives

$$\begin{aligned} \phi_o &= \phi_1 \\ \theta_o &= \theta_1 + \theta_2 + \theta_3 \\ \psi_o &= \psi_3 \end{aligned} \qquad \text{[VI-17]}$$

The simple results are an outcome of the same gimbal sequences for the manipulator arm (roll, pitch, pitch, pitch, yaw) and the SOS attitude head (roll, pitch, yaw). As a first approximation, the

relative Shuttle attitude angles, ϕ_S, θ_S, ψ_S, defining the attitude limit cycle, can be summed directly to Equations [VI-17]. Using the results of Equation [VI-14], Equation [VI-17] can now be written as:

$$\phi_o = \phi_1 + \phi_S$$

$$\theta_o = \theta_3 + \theta_S \qquad \text{[VI-18]}$$

$$\psi_o = \psi_3 + \psi_S$$

where θ_3 and ψ_3 are the commanded wrist joint angles. The same system lag characteristics of Equation [VI-10] are also applied to θ_3 and ψ_3. To effect control in camera axes, it is necessary to transform the command signals from camera axes to inertial (or simulator axes) using the transformation D_{41} in Equation [VI-16]. When operating in the acceleration control mode, the control device outputs are first integrated before being transformed (or before going into Equation [VI-7], [VI-8], [VI-9] if not in camera axes).

Phase 2 Equations

Figure VI-13 defines the Phase 2 configuration and nomenclature used in deriving the equations:

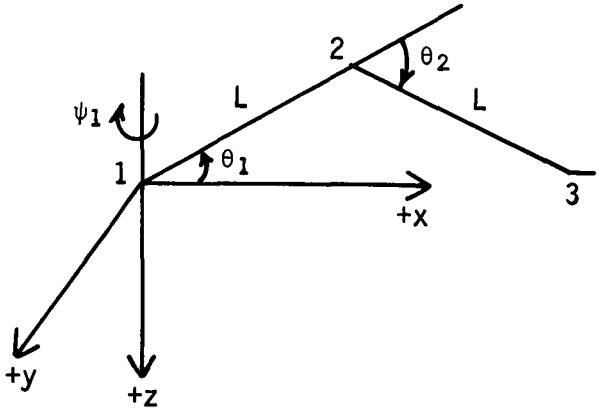

Fig. VI-13 Phase 2, Configuration and Nomenclature

Conditions:

Joint 1 has 2 DOF, Sequence: Yaw, ψ_1, Pitch, θ_1

Joint 2 has 1 DOF, Pitch, θ_2

Joint 3 is not mechanized.

Zero angles are defined when arm is coincident with +x axis.

For Phase 2, the SOS translational and rotational commands are very simple in that they reflect only the relative velocities between the Space Station and Shuttle. The equations to drive the manipulator arm angles are similar to those in Phase 1, but are different because of the varied gimbal sequence at the shoulder joint. First finding the wrist joint position, using the same approach as in Phase 1,

$$ {}_1\bar{L}_{31} = {}_1\bar{L}_{32} + {}_1\bar{L}_{21} \qquad \text{[VI-19]} $$

or

$$ {}_1\bar{L}_{31} = D_{21}\, D_{32}\, {}_3\bar{L}_{32} + D_{21}\, {}_2\bar{L}_{21} $$

where

$$ D_{32} = \begin{bmatrix} C\theta_2 & 0 & S\theta_2 \\ 0 & 1 & 0 \\ -S\theta_2 & 0 & C\theta_2 \end{bmatrix} $$

$$ D_{21} = \begin{bmatrix} C\psi_1 C\theta_1 & -S\psi_1 & C\psi_1 S\theta_1 \\ S\psi_1 C\theta_1 & C\psi_1 & S\psi_1 S\theta_1 \\ -S\theta_1 & 0 & C\theta_1 \end{bmatrix} $$

By definition of the axes at each joint,

$$ {}_3\bar{L}_{32} = {}_2\bar{L}_{21} = L\, \bar{1}_x $$

and the wrist joint position relative to the base becomes

$$x_3 = LC\psi_1\ [C\theta_1 + C(\theta_1 + \theta_2)]$$

$$y_3 = LS\psi_1\ [C\theta_1 + C(\theta_1 + \theta_2)] \qquad \text{[VI-20]}$$

$$z_3 = -L\ [S\theta_1 + S(\theta_1 + \theta_2)]$$

Solving these equations for the joint angles gives,

$$\psi_1 = \text{Cos}^{-1}\ \frac{x_3}{r}$$

$$\theta_1 = \text{Cos}^{-1}\ \frac{r}{R} - \frac{\theta_2}{2} \qquad \text{[VI-21]}$$

$$\theta_2 = 2\ \text{Cos}^{-1}\ \frac{R}{2L}$$

where

$$r = \sqrt{x_3^2 + y_3^2}$$

$$R = \sqrt{r^2 + z_3^2}$$

As before, taking the derivatives of Equations [VI-21] gives,

$$\dot{\psi}_1 = \frac{x_3\dot{y}_3 - y_3\dot{x}_3}{r^2}$$

$$\dot{\theta}_1 = \frac{\dot{r}z_3 - z_3\dot{r}}{R^2} - \frac{\dot{\theta}_2}{2} \qquad \text{[VI-22]}$$

$$\dot{\theta}_2 = \frac{-2\dot{R}}{\sqrt{4L^2 - R^2}}$$

where

$$\dot{r} = \frac{x_3\dot{x}_3 + y_3\dot{y}_3}{r} \qquad \text{[VI-23]}$$

$$\dot{R} = \frac{r\dot{r} + z_3\dot{z}_3}{R}$$

The angles calculated in Equations [VI-22] were integrated and sent directly to the position servos at the manipulator arm joints. An information flow diagram for Phase 2 simulator operation is shown in Fig. VI-14.

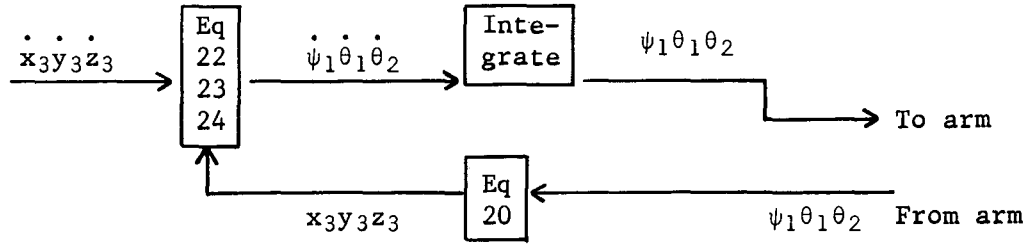

Fig. VI-14 Block Diagram for Arm Angle Commands, Phase 2

For camera axes control, it was necessary to calculate camera angles by integrating the rate commands coming from the foot controller going to the pan-tilt head of the TV camera. With the angles known, the control device outputs were transformed by a yaw-pitch sequence transformation. As before, in the acceleration control mode, the control device outputs are first integrated before being transformed (or before going into Equations [VI-22], [VI-23], [VI-24], if not in camera axes).

C. SIMULATION RESULTS AND DISCUSSION

Considerable information was learned about the controllability of manipulator arms during the initial set up and checkout period of the simulation, before any data was recorded. Of concern during this period was setting up a problem that was truly representative of a spatial capture task. An important objective was a control method that required a minimum of training time for the pilot. The following discussion mentions some of the important controllability factors discovered during Phase I initial set up.

As originally conceived, the Phase 1 task of maneuvering the probe into the target receptacle with a TV camera on the terminal device proved to be very difficult. Investigation into the reasons behind the difficulties revealed several factors that were individually studied, and corrections were made to improve performance.

One of the most important factors contributing to task difficulty were the time lags that were incorporated in the computer to simulate the joint drive servo system response characteristics of a spatial manipulator arm. These lags resulted in a time delay between an input command from the input control device and the resulting motion of the manipulator arm. The time lags were varied from 0 to approximately 5 seconds and it was concluded that a time constant of one second is about the maximum that can be tolerated without losing controllability. Undoubtedly, the joint servo system time lag or system response characteristics must be an important consideration in the design of the RMS. A second factor that added to task difficulty was the original mechanization of the TV camera control axes where the wrist joint did not rotate as a function of arm joint angles. This caused the camera and thus the control axes to continually change as translational motion was commanded. As explained in the Section B, *Simulation Equations*, the program was changed so that the TV camera rotated (in pitch and yaw) only as a function of commanded inputs from either the hand or foot controller. As a result, controllability was improved considerably. The use of base axes control in Phase 1 also proved extremely difficult because the operator could not retain the direction correspondence between a certain input command and the resulting motion direction (which continually changed as the task progressed). The same problem existed for individual joint motion control, which proved even more difficult than base axes control.

Another problem that accounted for some of the difficulty was an arbitrary angular velocity limit placed on the joint rotational rates. Based on a desired tip velocity of 0.46 m/sec (1.5 ft/sec) the joint angular limits were set at 3 deg/sec. Under certain arm configurations, the maximum velocities were being limited by the angular rate limitations to something less than 0.46 m/sec when this velocity was commanded. When the limits were raised to 6 deg/sec, there appeared to be no further problem. Another solution would be to design a gimbal ordering so that these troublesome arm configurations are eliminated or minimized.

With the above improvements made in the arm controllability, operators were still finding the task difficult to accomplish within the time limits established without considerable practice. The time limiation resulted from the desire to avoid operating near a singularity point, which for Phase 1 arm configuration was at the time the probe was on or near the x axis. It was also required that the probe be maneuvered to the left and the

TV camera rotated (wrist joint yaw), either intermittently or simultaneously, to the right approximately 45 deg to align the probe with the receptacle. These maneuvers consumed most of the allotted time and little time was left for insertion of the probe into the receptacle. To overcome this problem, the initial conditions were changed so that the initial angular misalignment was only a few degrees. This reduced task time to less than half of that previously used.

To summarize the above discussion, Phase 1 simulation data was recorded for the following conditions: servo system lag time constant, 1 second; "independent" camera control, i.e., inertial rotational control only by hand or foot commands; camera control axis; no individual joint control; a 6 deg/sec limit on joint angle rotation; and parallel (but offset) initial alignment of probe and receptacle axes, meaning that TV camera pan and tilt was possible but not required for task completion.

Phase 1 Results

Sample results from the Phase 1 simulations are presented in Appendix A. A task time summary, along with success/failure data, is given in Table VI-4. The task time includes the total time from start of the run until the probe was inserted in the receptacle. Most of the failures recorded in Table VI-4 were due to probe contact with the mockup, while the remaining failures were caused by complete loss of control when operating in the acceleration control mode. A total of five operators were used, A, B, and C were nonpilot operators and D and E were pilot operators. Task times are divided into only the four categories shown, as other factors affected times only slightly.

Phase 2 Results

Sample results for the Phase 2 simulations are also presented in Appendix A. Due to the Phase 2 arm configuration and gimbal sequence (the probe did not approach a singularity point), run times of up to 200 seconds were possible. In the Phase 2 task, operators were allowed to maneuver the probe into the receptacle several times if possible until the target was out of reach. The task times shown in Table VI-5, and also in the task time summary, Table VI-6, correspond to the time from start until the probe was inserted into the receptacle the first time. The failures noted in Table VI-5 occurred when the operator could not insert the probe into the receptacle during the total 200-second run time.

Table VI-4 Summary of Task Time Data, Phase 1

Operator	Hand-Controller Rate	Hand-Controller Acceleration	Switch Box Rate	Switch Box Acceleration
A				
Successes	3	0	1	--
Failures	3	3	2	--
Success Ratio, %	50	0	33	--
Average Time, sec	34	--	42	--
B				
Successes	6	2	1	0
Failures	1	3	1	2
Success Ratio, %	86	40	50	0
Average Time, sec	41	32	35	--
C				
Successes	5	0	3	--
Failure	1	4	0	--
Success Ratio, %	83	0	100	--
Average Time, sec	33	--	42	--
D				
Successes	9	5	1	2
Failure	5	1	1	0
Success Ratio, %	64	83	50	100
Average Time, sec	29	34	27	35
E				
Successes	5	3	4	2
Failure	0	3	0	1
Success Ratio, %	100	50	100	67
Average Time, sec	18	44	32	58

Table VI-5 Summary of Task Time Data, Phase 2

Handcontroller and Switch Box

Operator	Hand-Controller Rate	Hand-Controller Acceleration	Switch-Box Rate	Switch Box Acceleration
A	49	71	--	--
B	83	90	51	88
C	57	170	52	--
D	53	74	--	--
E	88	57	59	65

Master Arm

Operator	Average Task Time, sec
F	17
G	23
H	16
I	17
J	29
K	43
L	22
M	13

Table VI-6 Summary of Average Task Times

	Phase 1				Phase 2				
	Hand Controller		Switch Box		Hand Controller		Switch Box		Master Arm
	Rate	Acc	Rate	Acc	Rate	Acc	Rate	Acc	Position
Total Average Time, sec	31	37	36	46	66	92	54	76	22

The failures occurred only when operating in the acceleration control mode. Contrary to Phase 1 failure criteria, in Phase 2 the run was not terminated if contact was made between probe and mockup somewhere other than at the target receptacle, as usually occurred several times during the run. This was because less emphasis was placed on actual probe insertion because of the increased difficulty of seeing the probe and target (TV camera was farther away than in Phase 1) and judging depth perception. Also, normally final contact would be made using the terminal device TV rather than the base camera.

For hand controller and switch box operation, the same operators were used in Phase 2 as in Phase 1. For the Phase 2 master arm data, all new operators, identified by F thru M, were used. Operators A thru E also operated the master-slave configuration and their comments are factored into the conclusions. New operators were used for recording data in order to obtain task times unbiased by any "learning," resulting from the other Phase 1 and 2 operations. A summary of Phase 2 task times data for the four categories shown is presented in Table VI-5. A summary of average task times for both Phases is presented in Table VI-6.

Parameter Variation Discussion

1) Command Technique

All of the control input devices have their own advantages and disadvantages, and a final choice as to which device is best must depend on the specific task or tasks to be performed. For the task investigated in these simulations, it was generally agreed that the master-slave configuration provided the best and easiest control over the other two choices. Comparing task time data in Table VI-5, the task could usually be accomplished in less time with the master arm, and the operators agreed that very little training time was required, and more precise control of maneuvers was possible. These conclusions must be qualified however in several areas: 1) the master-slave configuration did not limit maximum probe velocities (except by maximum servo slew rate), and 2) probe control maneuvering used a 3.5-to-1 translational motion ratio (or sensitivity). The first area probably accounts for part of the reduced task time. Concerning the second area, a 3.5-to-1 sensitivity ratio would not exist in space (where a

18-to-1 ratio is more likely), *unless* the control system was specifically designed to effect this ratio. The simulation showed that the 3.5-to-1 ratio is about the maximum possible to retain the sensitivity required to perform the capture task. For even more precise control, the ratio would have to be reduced, possibly to 1-to-1.

Although the operators preferred using the master arm over the hand controller, the hand controller was certainly not an objectionable control device. After a short training time, the operators were at ease with the hand controller and could definitely perform the task adequately. Direction correspondence between controller deflection and arm motion varied some between operators, depending on past flight experience. Most operators also thought that the particular controller used in the simulation (Apollo Block I) was too "stiff" and hard to control for a manipulator arm application.

As the task time data shows, the switch box also proved to be an adequate control technique. The switch box was least preferred, however, as far more concentration and training time were required to operate the arm and accomplish the task. It was necessary, for example, to remove attention from the TV monitor to the switch box occasionally to find the appropriate switch to activate. Lack of proportional control was also a handicap.

2) Control Axes

As mentioned previously, base axis control in Phase I proved extremely difficult. In Phase 2, the problem was much less pronounced primarily because, with a wider field of view, the operator had more clues as to base axes orientation. As a result, base axes control was adequate; however, camera axes were found to be more natural and were unanimously preferred.

3) Control Mode

The control mode tradeoff was between the rate and the acceleration input commands. The task time data clearly shows that the acceleration mode takes significantly longer to accomplish the task, and also the success ratio is generally less.

Part of this extra time, however, must be attributed to the nature of the acceleration control where a "wait-and-see" attitude must be adopted to determine the extent of the velocity change input after it is commanded. Generally, the nonpilot oprators did poorly using the acceleration mode, although considerable improvement came with practice, and they definitely preferred the rate mode. The pilot operators, on the other hand, preferred the acceleration mode, even though it took longer and they failed more often. Their preference was due in part to familiarity with acceleration systems (e.g., thruster controlled maneuvering units) and in part to the fact that the hand controller was physically much easier to use in the acceleration mode. Since the acceleration mode allows rate matching of target and probe, the control handle does not need to be continually held in a deflected position as is required in the rate mode. This fact may have been less significant with a less "stiff" hand controller. Most operators agreed, however, that the rate mode would appear to provide more precise terminal control for stabilized or slow moving targets. Also, the servo lag times appeared more bothersome in the acceleration mode than in the rate mode. Considering all of the above factors, it is concluded that rate command implementation would probably be best for a hand controller.

4) Control Characteristics

For the proportional hand controller input device, the control characteristics shown in Fig. VI-15 were implemented on the computer. The first control tried was the nonlinear characteristic (a) which consisted of the straight line segments for both plus and minus. During operation it was concluded that there was no particular advantage to the nonlinear characteristic as operators were continually commanding maximum velocity (i.e., using full throw). Thus, the simpler single slope was implemented, and was generally preferred. Both characteristics required the deadband around zero so that no controller null bias would effect a command.

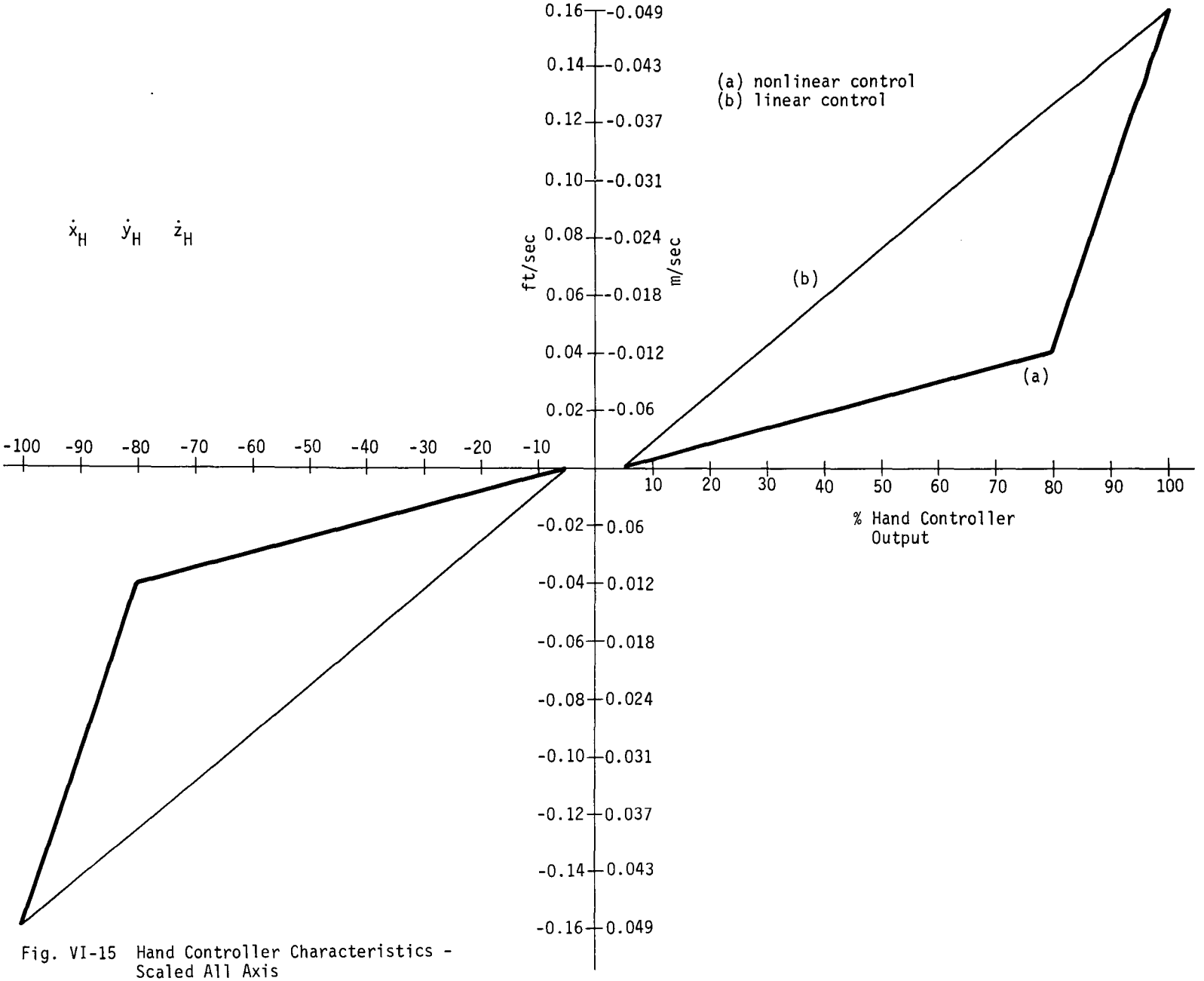

Fig. VI-15 Hand Controller Characteristics - Scaled All Axis

It was agreed among operators that the maximum probe velocity of approximately 3.5 times the relative Shuttle - Space Station closing velocity appeared to be optimum for the captive task. A faster rate, however, would speed up the initial positioning time, and therefore cut the total task time. Some increase in maximum velocity could probably be tolerated without affecting the terminal captive maneuver significantly. The maximum probe acceleration of approximately 0.012 m/sec^2 (0.04 ft/sec^2), scaled, was used during the simulations, and it was generally agreed that the value was somewhat slow. An acceleration of approximately 0.024 m/sec^2 (0.08 ft/sec^2), scaled, would be about optimum.

The use of the Rate Bias switch, which automatically added a constant velocity to the probe to match the maximum relative velocity, accomplished its intended purpose. The operators agreed that the task became somewhat easier when the Rate Bias was used. This result should be used whenever it is possible to obtain velocity information about a moving target.

5) Wrist Control

The manual wrist control, implemented in Phase 1 by depressing a switch on the control handle, did not prove satisfactory because of the momentary loss of probe velocity control. The foot-controller, however, was entirely satisfactory and could usually be operated simultaneously with probe control. A wrist (or camera pan-tilt) rate of 4 degree/sec was adequate for Phase 1 and a rate of 10 deg/sec was adequate for the Phase 2 camera. The latter rate is convenient for quick camera motion through relatively large angles but would be too fast for the terminal device mounted camera. Automatic base camera tracking of the terminal device, although not attempted in the simulations, would be relatively easy to implement and would relieve the operator of this task.

D. CONCLUSIONS AND RECOMMENDATIONS

The simulations discussed in this chapter have shown the feasibility of controlling manipulator arms for initial docking of the Shuttle to the Space Station, and the results can certainly be extrapolated to cover many other tasks with either moving or stationary targets. Depending on the extent of automatic control, space manipulator arm control will probably

require the full concentration of one operator. It is, therefore, not recommended that the operator be given any other task to be performed simultaneously, including active operation of a second arm. (Although two manipulator arms were constructed for the simulations, only one was active at a time.)

Independent of the input control device or control mode, the number of failures indicated that the task was still relatively difficult to accomplish. It was very difficult if not impossible to very closely match positions and velocities of the probe and receptacle at the same time. It was difficult enough to insert the 1.27 cm (0.5 in.) probe anywhere in the 5 cm (2 in.) receptacle without trying to insert it in the center of the receptacle. Final velocities at insertion ranged from near zero (not in all axes at once, however) to at least maximum relative Shuttle - Space Station velocities (say 0.015 m/sec, scaled). Phase 1 simulations also showed that it was very difficult to judge angular relationships between the probe and receptacle.

Contact of the probe with another part of the mockup other than the receptacle was considered a failure in these simulations, as would generally be the case for actual space operations. This implies that the terminal device and/or the capture interface should be designed to allow for some misalignment at contact. Self alignment features in the mating devices and force-feedback in the RMS design would relieve some of the difficulties associated with capture of the moving target. If all of these factors are accounted for in the design of a probe-receptacle (or other type of capture interface) and in the design of the manipulator arms, the problem might become inconsequential.

Another significant factor contributing to probe contact failure was the use of mono-TV viewing and the resultant lack of depth perception. Even though the operator's ability to judge probe-target distance improved significantly and rapidly with practice (primarily using object relative sizes for cues), it always remained somewhat of a problem. The general opinion of operators was that the mono-TV was "adequate" and could be successfully used for the simulated task, but that TV with depth perception would be a definite improvement. Being able to better judge depth perception would undoubtedly reduce the number of probe contact failures. Force reflection might allow mono-TV to be used without depth perception being a problem.

The Phase 1 and 2 simulations showed the need for at least two TV cameras in space applications of manipulator arms. The base TV camera used in Phase 2 is required for a wide field of view of the area the arms will be working in, and a general orientation of the operator to arm positions and possible interferences. It would be used for gross positioning of the arm near a target area. The base TV camera, however, cannot be used for precise terminal control, even with zoom capability, because too often the terminal device is in the line-of-sight between operator and target. It is, therefore, necessary to mount a TV camera on the terminal device for assurance of a clear target view during terminal maneuvering.

A summary of the conclusions reached in Section D follows.

1) The master-slave operating configuration was preferred over the hand controller or switch box. The master arm gave better control, faster operation, and took practically no learning time. This is partially attributable to the faster response and high sensitivity that was used for the master controller.

2) For hand-controller operation, the rate control mode and the use of TV camera control axes are recommended. Rate Bias is also recommended if information is available to implement it.

3) TV camera attitude control by foot is adequate.

4) The terminal device TV camera inertial attitude should be independent of manipulator arm motion.

5) Manipulator arm servo system time constants (lags) should not be greater than 1 second.

6) For the recommended control techniques and the capture task, task times should average from 0.5 to 1 minute.

VII. SELECTED CONCEPT REQUIREMENTS ANALYSIS

With man-in-the-loop simulations conducted, the stage is set for a pointed analysis of those detail requirements that are key to the preliminary design of the RMS. Requirements are established for 14 system parameters: arm length, velocity, torque, positional accuracy, rate accuracy, degrees of freedom, gimbal ordering, control method, reach envelope, angular travel, command and data link, tracking and ranging, deployment, and ground testing. The results of these analyses form the framework for the overall system configuration described in Chapter VIII, Section A.

A. ARM LENGTH

The reach requirements were updated to include the typical Shuttle payloads shown in Fig. VII-1. These payloads are derived from the NASA July 1971 Shuttle traffic model. The three grasping points, numbered 1, 2, and 3, are shown on the figure. With an unobstructed reach, point 3 requires the longest arm length. This length is 14 m (45.7 ft) for an arm offset 3.05 m (10 ft) from the Shuttle centerline. With the obstructed reach indicated in the figure, point 2 is the driving factor, requiring a 16.8-m (55 ft) arm, with the payload moved 2.9 m (9.5 ft) toward the rear of the cargo bay.

Because it was unrealistic to increase the arm length for this small payload, the possibility of raising the cargo was investigated. The Shuttle Orbiter specifications state that the payload can be moved from cargo centerline in the Z direction to create a maximum moment of 27,200 N-m (20,000 ft-lb). This means that the 328-kg (720 lb) payload can be raised 8.5 m (27.8 ft) and the 864 kg (1900 lb) payload can be raised 3.2 m (10.5 ft). This places the cargo at (or above) the top of the cargo bay, and thus, both cargos can be raised to allow an unobstructed reach distance. Point 3 set the longest reach requirement of 14 m (45.7 ft), which is also sufficient for any of the docking and module transfer tasks as determined in Chapter IV. The total arm length is set at 14.3 m (47 ft) to reach point 3 with the additional 0.3 m (1.3 ft) [over the 14 m (45.7 ft) reach requirement] added for precontact maneuvering and to allow positioning of the terminal device interface on the payload.

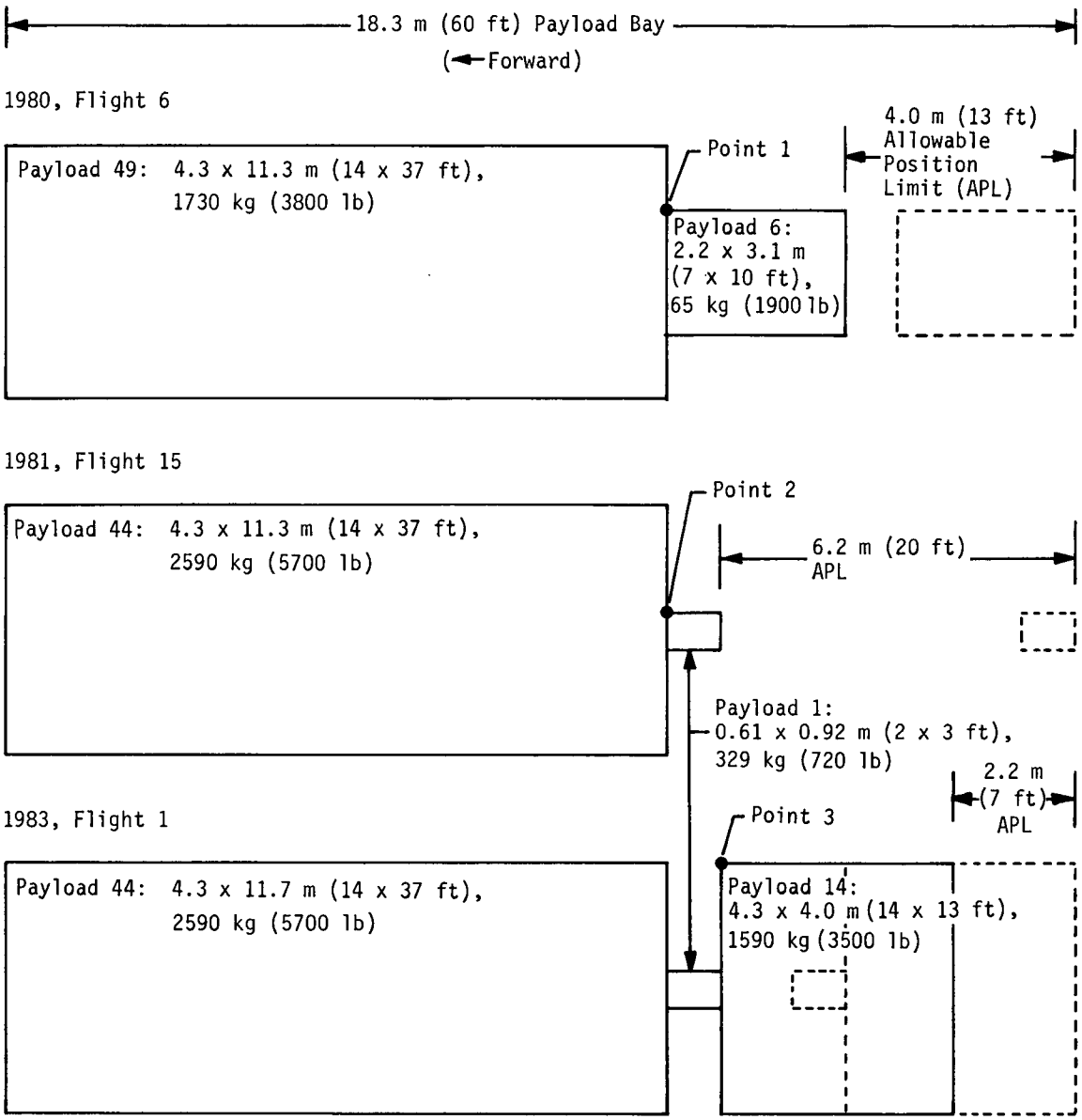

Fig. VII-1 Typical Shuttle Payloads

The linkage from wrist joint to the center of grasp of the terminal device was set to 0.9 m (3 ft) to allow for TV camera mounting and terminal device roll joint, as well as additional reach-around capability.

B. JOINT ACCURACY

In this section the relationship between the joint angles and the position of the wrist point is determined for a two-segment, typical three-degree-of-freedom arm. This relationship is then used to determine the positional and rate accuracy requirements necessary to maintain the wrist point position and velocity within particular limits. It is found that, for a segment length of 7.16 m (23.5 ft), a positional accuracy (of the wrist point) of ±5.08 cm (±2 in.) requires a joint accuracy of $\pm 1.97 \times 10^{-3}$ rad (±0.113 deg), and a velocity accuracy of ±0.015 m/sec (0.05 ft/sec) requires a joint rate accuracy of $\pm 5.82 \times 10^{-4}$ rad/sec (±0.033 deg/sec).

1. Joint Positional Accuracy

Given the three degree-of-freedom arm shown in Fig. VII-2, an answer is sought to the following question: What joint accuracy is required to guarantee an accuracy of ± e in the position of E? The answer to the question is determined under the following assumptions:

1) Rotational error at each joint is the same and equal to $\Delta\theta$.

2) The order of rotation is θ_3, θ_2, θ_1.

If $\bar{r}$ denotes the position vector of E relative to θ (see Fig. VII-2), one can write

$$\bar{r} = L[\text{Cos } \theta_2 + \text{Cos}(\theta_2 + \theta_3)]\ \bar{\eta}_x + L \text{ Cos } \theta_1[\text{Sin } \theta_2 + \text{Sin}(\theta_2 + \theta_3)]\ \bar{\eta}_y + L \text{ Sin } \theta_1[\text{Sin } \theta_2 + \text{Sin}(\theta_2 + \theta_3)]\ \bar{\eta}_z. \qquad [\text{VII-1}]$$

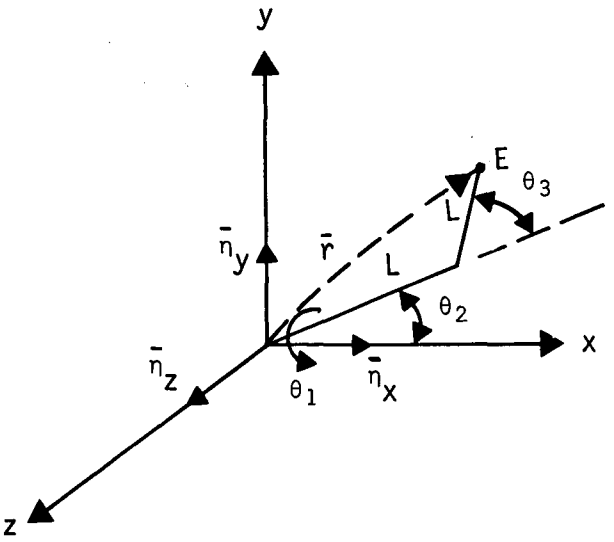

Fig. VII-2 Three-Degree-of-Freedom Arm

Now if θ_1, θ_2, and θ_3 are given small increments of amount $d\theta_1$, $d\theta_2$, and $d\theta_3$, respectively, one obtains for the corresponding change in $\bar{r}$

$$d\bar{r} = \frac{\partial \bar{r}}{\partial \theta_1} d\theta_1 + \frac{\partial \bar{r}}{\partial \theta_2} d\theta_2 + \frac{\partial \bar{r}}{\partial \theta_3} d\theta_3 \qquad \text{[VII-2]}$$

If $d\bar{r}$ is written as

$$d\bar{r} = dr_x \bar{\eta}_x + dr_y \bar{\eta}_y + dr_z \bar{\eta}_z \qquad \text{[VII-3]}$$

it follows from Eq [VII-1] thru [VII-3] that

$$dr_x = -L\Big\{[\text{Sin } \theta_2 + \text{Sin}(\theta_2 + \theta_3)]\, d\theta_2 + \text{Sin}(\theta_2 + \theta_3)\, d\theta_3\Big\} \qquad \text{[VII-4]}$$

$$\begin{aligned} dr_y = L\Big\{&-\text{Sin } \theta_1[\text{Sin } \theta_2 + \text{Sin}(\theta_2 + \theta_3)]\, d\theta_1 \\ &+ \text{Cos } \theta_1[\text{Cos } \theta_2 + \text{Cos}(\theta_2 + \theta_3)]\, d\theta_2 \\ &+ \text{Cos } \theta_1 \text{ Cos}(\theta_2 + \theta_3)\, d\theta_3\Big\} \end{aligned} \qquad \text{[VII-5]}$$

$$dr_z = L\{\text{Cos } \theta_1[\text{Sin } \theta_2 + \text{Sin}(\theta_2 + \theta_3)]\, d\theta_1$$

$$+ \text{Sin } \theta_1[\text{Cos } \theta_2 + \text{Cos}(\theta_2 + \theta_3)]\, d\theta_2$$

$$+ \text{Sin } \theta_1\, \text{Cos}(\theta_2 + \theta_3)\, d\theta_3\} \qquad \text{[VII-6]}$$

If one now assumes that

$$d\theta_1 = d\theta_2 = d\theta_3 = \Delta\theta \qquad \text{[VII-7]}$$

Equations [VII-4], [VII-5], and [VII-6] become

$$dr_x = -L[\text{Sin } \theta_2 + 2\ \text{Sin}(\theta_2 + \theta_3)]\ \Delta\theta \qquad \text{[VII-8]}$$

$$dr_y = L[\text{Cos}(\theta_1 + \theta_2 + \theta_3) + \text{Cos } \theta_1\ \text{Cos}(\theta_2 + \theta_3)$$

$$+ \text{Cos}(\theta_1 + \theta_2)]\ \Delta\theta \qquad \text{[VII-9]}$$

$$dr_z = L[\text{Sin}(\theta_1 + \theta_2 + \theta_3) + \text{Sin } \theta_1\ \text{Cos}(\theta_2 + \theta_3)$$

$$+ \text{Sin}(\theta_1 + \theta_2)]\ \Delta\theta \qquad \text{[VII-10]}$$

If the magnitude of $d\bar{r}$ is called dr, it follows from Eq [VII-8] thru [VII-10] that

$$dr = L\{5 + 4\ \text{Cos } \theta_3 + \text{Sin}(\theta_2 + \theta_3)\ [\text{Sin}(\theta_2 + \theta_3)$$

$$+ 2\ \text{Sin } \theta_2] + \text{Sin}^2\ \theta_2\}^{\frac{1}{2}}\ \Delta\theta \qquad \text{[VII-11]}$$

By inspection of Eq [VII-11], it is seen that dr will be greatest when

$$\theta_3 = 0 \text{ and } \theta_2 = \pi/2 \qquad \text{[VII-12]}$$

and when this is the case, dr becomes

$$dr = \sqrt{13}\ L\ \Delta\theta \qquad \text{[VII-14]}$$

Thus, assuming that dr must remain $\leq$e, the joint accuracy requirement is:

$$\Delta\theta \leq \frac{0.278\ e}{L} \qquad \text{[VII-15]}$$

Thus, to position the point E with a ±5.08 cm (2 in.) accuracy using an arm segment length of 7.16 m (23.5 ft) requires

$$\Delta\theta = \frac{0.278 \times 5.08 \times 10^{-2}}{7.16} = 1.97 \times 10^{-3} \text{ rad}$$

In other words, the joints must maintain an accuracy of ±0.113 deg.

2. Joint Rate Accuracy

To determine the corresponding rate accuracy requirement, one merely needs to differentiate the equations for positional accuracy. If it is assumed that the rate error at each joint is the same, it follows from Eq [VII-11] that

$$\frac{dr}{dt} = L\{5 + 4 \text{ Cos } \theta_3 + \text{Sin}(\theta_2 + \theta_3) \ [\text{Sin}(\theta_2 + \theta_3) + 2 \text{ Sin } \theta_2] + \text{Sin}^2 \ \theta_2\}^{\frac{1}{2}} \frac{d\theta}{dt} \qquad \text{[VII-16]}$$

and, as before, the above expression has a maximum at

$$\theta_3 = 0 \text{ and } \theta_2 = \pi/2 \qquad \text{[VII-17]}$$

with the corresponding maximum value of $\frac{dr}{dt}$ being

$$\frac{dr}{dt} = \sqrt{13} \ L \frac{d\theta}{dt} \qquad \text{[VII-18]}$$

Thus, if $\frac{dr}{dt}$ must remain $\leq \dot{e}$, the rate accuracy requirement is

$$\frac{d\theta}{dt} \leq \frac{0.278 \ \dot{e}}{L} \qquad \text{[VII-19]}$$

Hence, to maintain the point E within ±0.015 m/sec (0.05 ft/sec)* of some desired velocity [using an arm length of 7.16 m (23.5 ft)] necessitates a rate accuracy at the joints of

$$\frac{d\theta}{dt} \leq \frac{0.278 \times 0.015}{7.16} = 5.82 \times 10^{-4} \text{ rad/sec.}$$

*This velocity requirement is based on the Shuttle docking lateral velocity at contact.

C. DEGREES OF FREEDOM AND GIMBAL ORDERING

In this section, both the number of degrees of freedom and the order of joint rotations for the RMS are investigated. Both three- and four-degree-of-freedom arms (exclusive of the wrist and TD) are investigated. The selected configuration is a four-degree-of-freedom arm with a pitch-yaw sequence at the shoulder, and a roll-yaw sequence at the elbow. This, coupled with a three-degree-of-freedom wrist (yaw-pitch-roll) and one degree of freedom for the terminal device, results in an eight-degree-of-freedom arm.

1. Degrees of Freedom

The three-degree-of-freedom system, which is the simplest configuration from both a mechanical design and control standpoint, has several disadvantages (see Fig. VII-3).

First, with this system, the elbow position cannot be moved independent of the wrist position. For maneuvering in restricted quarters, such as reaching into the cargo bay, or docking modules to the space station, this can present interference problems.

Second, since the second and third rotations are normally about the same axis, both arm segments are always in a plane containing the first axis of rotation. This plane is defined by the line of the first axis of rotation and the first arm segment. (For a yaw-pitch-pitch configuration, as shown in Fig. VII-3, the arm would always be in a plane perpendicular to the Shuttle wings. The orientation of this plane is specified by the shoulder yaw angle.)

The third drawback of the three-degree-of-freedom system is that one degree of motion is lost when the wrist is positioned along the line of rotation of the first degree of freedom. With this condition, rotation of the first degree of freedom does not move the wrist. Thus, only two angles are available for movement of the wrist point, which is not sufficient to obtain three-degree-of-freedom motion. This condition can be shown by examination of the rate equations that define the wrist motion. For a yaw-pitch shoulder, the shoulder yaw rate is given as:

$$\dot{\psi} = \frac{\dot{x}y - \dot{y}x}{x^2 + y^2}$$

where x and y denote the wrist position in the respective axes. When the wrist is positioned on the z axis ($x = y = 0$), as shown in Fig. VII-4, this equation is indeterminate. Thus, motion of the shoulder yaw joint is undefined in this position.

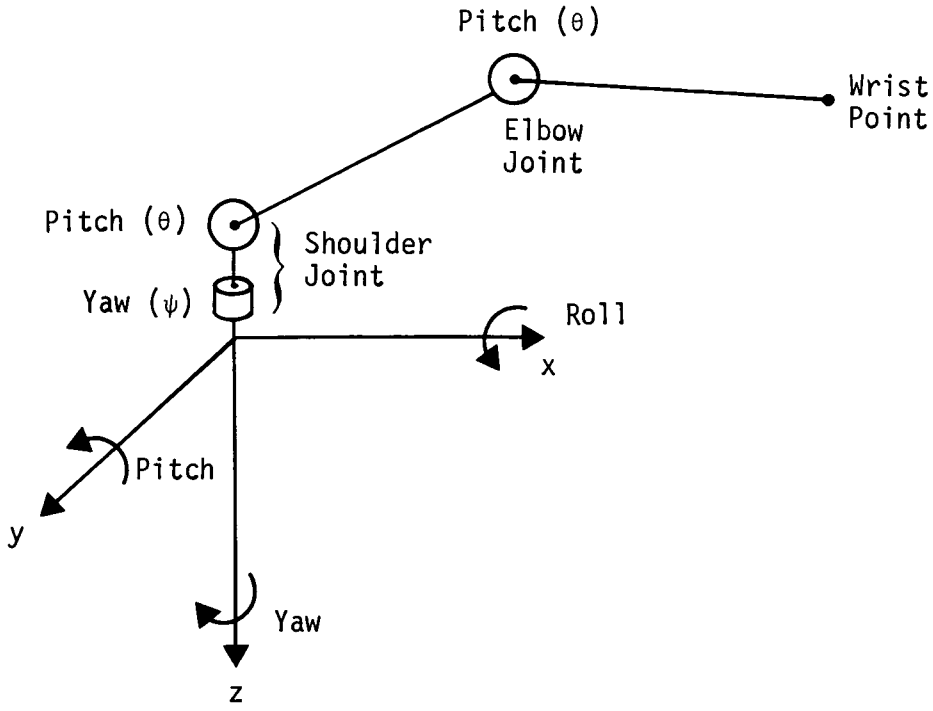

Fig. VII-3 Schematic of a Typical Three-Degree-of-Freedom System

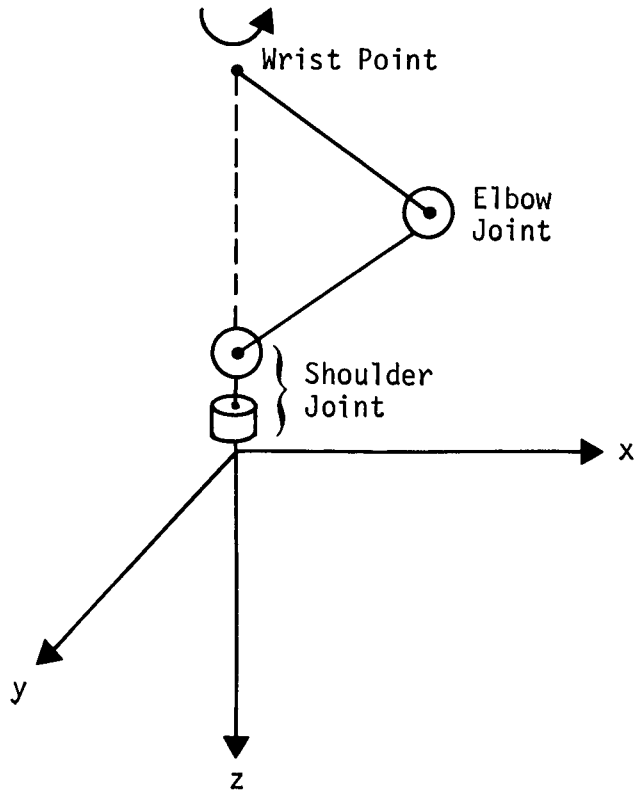

Fig. VII-4 Arm Configuration in a Motion Loss Position

The four-degree-of-freedom system, consisting of a two-degree-of-freedom shoulder and a two-degree-of-freedom elbow, overcomes all of these drawbacks, and was selected for the RMS preliminary design. This system is equivalent to a three-degree-of-freedom shoulder and a one-degree-of-freedom elbow system when the first elbow axis of rotation is along the axis of the first arm segment. This arrangement is similar to the arrangement of the human arm and is shown in Fig. VII-5.

With this system, the elbow position can be moved independent of the wrist position, thus aiding in maneuvering around obstacles and in restricted quarters. The arm motion is not restricted to any plane, but rather can be moved in any desired plane.

Three-degree-of-freedom motion of the wrist point is not lost in any position, except for the straightened position of the elbow, which applies to any joint configuration. This is essentially a four-gimbal system, with the fourth rotation used to overcome the problems associated with a degree-of-freedom loss condition.

Due to the fourth degree of rotation, there is not a unique set of joint angles for a given wrist position. Thus logic is required to determine which angles to drive to move the wrist in a desired direction. This can be simple logic, such as independent wrist and elbow control, wherein three angles are used to drive the wrist position, with the fourth angle being driven only when an elbow motion command is input. Complex computer-aided control could also be used, such as minimum energy paths, or automatic collision avoidance schemes.

2. Gimbal Ordering

After the number of joints had been determined, the next step was to determine the joint sequence best suited to accomplishment of the required tasks. By assigning two degrees of freedom to the shoulder and elbow, the matrix shown in Fig. VII-6 was obtained. Thirty-three of the 36 possible combinations were eliminated by examination of the resulting arm characteristics. For example, using a roll motion as the second elbow motion results in essentially a three-degree-of-freedom arm, since the elbow roll merely rotates the wrist without changing its position. Another factor considered was the location of the singular axis, since it was desirable to locate this axis in an area where little work would be performed, in order to reduce the control logic requirements. Using roll as the first shoulder rotation, this axis is located directly above and parallel to the cargo bay, and using a yaw first, the singular axis is above the Shuttle and perpendicular to the cargo bay. Since these are two prime working volumes for cargo handling and assembly tasks, a pitch motion was selected for the first shoulder rotation. This places the singular axis out to the side of the Shuttle in a volume where little work will be performed. As shown in the matrix, we are then left three possible combinations, any of which will accomplish the required tasks.

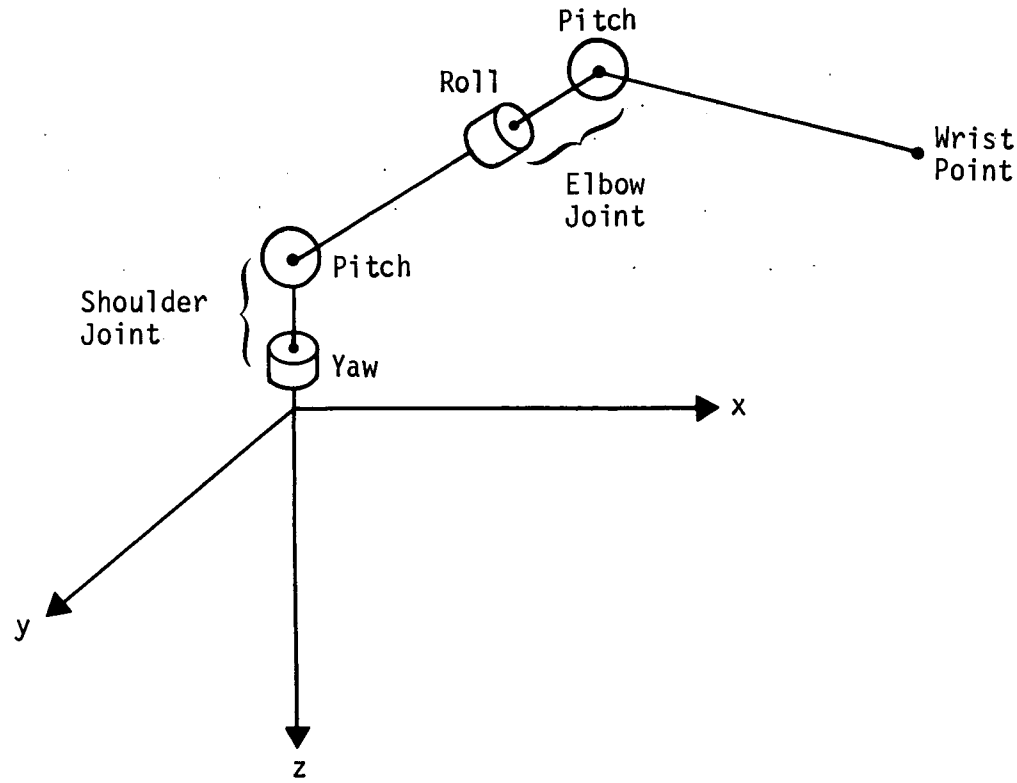

Fig. VII-5 Schematic of Typical Four-Degree-of-Freedom System

From the three choices that were left, the arrangement shown in Fig. VII-7 was selected for the preliminary design. This arrangement, which is similar to the human arm, consists of a pitch-yaw shoulder, a roll-yaw elbow, and a yaw-pitch-roll wrist joint for angular orientation of the terminal device. This configuration was chosen for two prime reasons. First, it uses only one yoke-type joint at the elbow, which results in a minimum size elbow joint, and second, the elbow roll joint can be used to orient the TV camera in the best location for stowage. The three-degree-of-freedom wrist shown allows angular orientation of the terminal device, and the TV location shown reduces the cable routing problems, since there is one less joint to route the TV cable around. The result is thus a 7-degree arm, with an eighth degree of freedom for a hand-type terminal device.

Elbow \ Shoulder	Pitch Yaw	Pitch Roll	Yaw Pitch	Yaw Roll	Roll Pitch	Roll Yaw
Pitch Yaw		■	▲	■	▲	●●
Pitch Roll	●	●	●	●	●	●
Yaw Pitch	▲	■	●●	■	●●	▲
Yaw Roll	●	●	●	●	●	●
Roll Pitch		▲	●●	▲	●●	●●
Roll Yaw		▲	●●	▲	●●	●●

● Elbow Roll Does Not Move Wrist Position
▲ No Significant Advantage for Two Identical Joints in Sequence
■ Upper Arm Can Move Only in One Plane
●● Places Singular Axis in Prime Working Volume

Fig. VII-6 Joint Sequence Alternatives

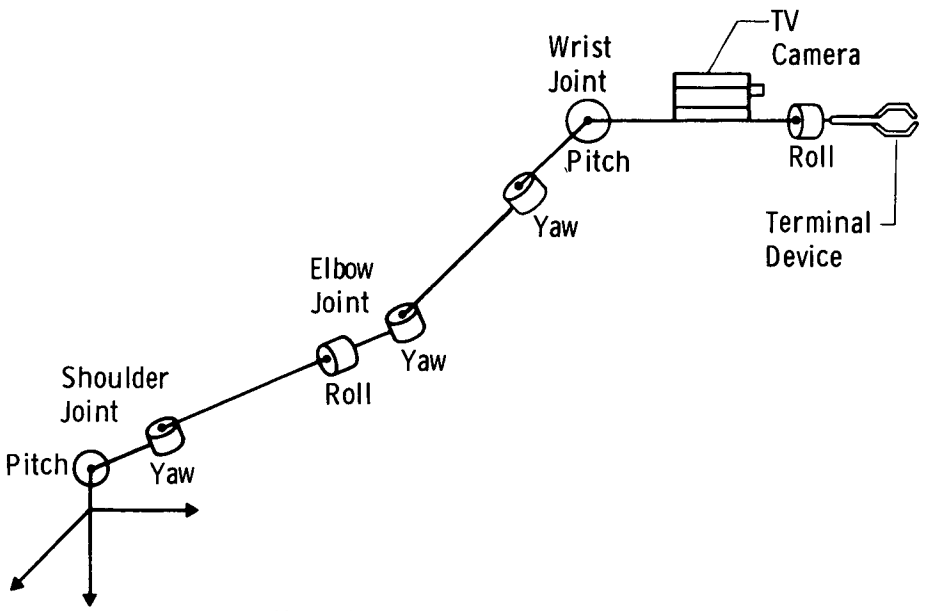

Fig. VII-7 Preferred Joint Sequence

D. VELOCITY AND TORQUE

In this section the RMS torque and velocity requirements are derived primarily from the cargo handling requirements, with an additional no-load velocity requirement based on the capture task for docking and payload retrieval operations. These requirements are analyzed and Table VII-1 summarizes joint velocities and torques.

Table VII-1 Joint Velocity and Torque Summary

Shoulder: (pitch, yaw)	No-Load Velocity	0.03 rad/sec
	Full-Load Velocity	0.0035 rad/sec
	Torque Capability	667 N-m (500 ft-lb)
Elbow: (roll, yaw)	No-Load Velocity	0.0565 rad/sec
	Full-Load Velocity	0.0066 rad/sec
	Torque Capability	474 N-m (350 ft-lb)
Wrist: (yaw, pitch, roll)	No-Load Velocity	0.174 rad/sec
	Full-Load Velocity	0.0265 rad/sec
	Torque Capability	202 N-m (150 ft-lb) (Yaw, Pitch)
		88 N-m (65 ft-lb) (Roll)

1. Velocity

Based on a precontact closing velocity of 0.122 m/sec (0.4 ft/sec) the no load linear wrist velocity has been set at 0.45 m/sec (1.5 ft/sec), which allows adequate margin for catchup and backoff maneuvers for capture tasks as verified in the simulations (Chapter VI). Based on a 14.3-m (47 ft) arm length (to wrist), this tip velocity results in shoulder joint no-load rotational rates of 0.03 rad/sec and elbow joint rates of 0.0565 rad/sec. The wrist joint no-load rates are a compromise between the low precontact payload rates (0.1 deg/sec) and the normal human response times. The selected value for the wrist joint rates is 0.174 rad/sec, which is more than adequate for capture purposes, and still is fast enough to be compatible with human control. So that maximum velocities at all joints can be reached in 2 sec, the no-load acceleration requirement becomes 0.015 rad/sec^2, for the shoulder, 0.028 rad/sec^2 for the elbow, and 0.087 rad/sec^2 for the wrist.

The loaded speed requirements are taken from the cargo handling timelines derived in Chapter IV. Using the worst-case condition (from a torque requirement standpoint) of deploying the 29,600-kg (65,000 lb) payload, the maximum full-load tip velocity is 0.052 m/sec (0.17 ft/sec). This results in a shoulder joint rate of 0.0035 rad/sec and a elbow rate of 0.0066 rad/sec under maximum loaded conditions. The wrist joint loaded rotational rate is specified at 0.0265 rad/sec to allow payload attitude orientation to be accomplished during cargo transfer or deployment operations. The velocity requirements for all of the joints under no-load and full-load conditions are summarized in Table VII-1.

2. Torque

Referring to Fig. IV-12 in Chapter IV, the maximum torque requirement is determined as approximately 176 N-m (130 ft-lb) at the shoulder for moving the 29,600-kg (65,000 lb) payload. Because it is necessary to have this torque at the maximum velocity of the payload, and because it is desirable to have higher torque for contingency operations, the stall torque requirement at the shoulder joint was established 667 N-m (500 ft-lb). Based on this shoulder torque, the elbow and wrist torques can be derived as shown in Fig. VII-8.

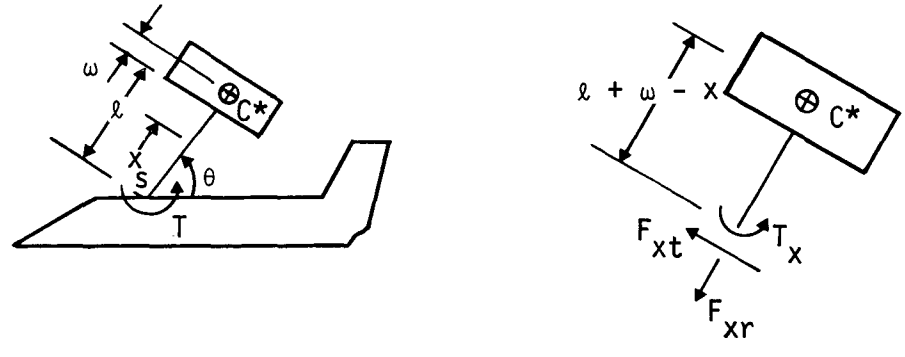

Fig. VII-8 Cargo Handling Free Body Diagram

When d = 0, Fig. IV-13 assumes the configuration shown above in Fig. VII-8. Because the Shuttle is fixed, one can write

$$T = I^{c/c*} + M_c(\ell + \omega)^2 \ddot{\theta} \qquad \text{[VII-20]}$$

where $I^{c/c*}$ and M_c have the same meaning as in Chapter IV Section C. Now, if a cut is made a distance x from s (see Fig. VII-8), the influence of the missing part of the arm can be replaced by the forces and torques shown. Because F_{xt} is the only force acting in the tangential direction one has from Newton's law

$$F_{xt} = M_c(\ell + \omega)\ddot{\theta} \qquad \text{[VII-21]}$$

and it follows that for a constant T, the shear force, F_{xt}, is constant and independent of x.

Applying the angular momentum principle about C*, the following is obtained

$$T_x = F_{xt}(\ell + \omega - \times) + I^{cc*}\ddot{\theta} \qquad \text{[VII-22]}$$

and substitution from Eq [VII-20] and [VII-21] into [VII-22] yields, after some simplification

$$T_x = T\left\{1 - \frac{M_c(\ell + \omega)\, x}{I^{c/c*} + M(\ell + \omega)^2}\right\} \qquad \text{[VII-23]}$$

which implies $T_x \leq T$ for any point on the arm.

Using Eq [VII-23], the torque required to hold the elbow and wrist position constant with 667 N-m (500 ft-lb) applied at the shoulder can be calculated. The results are 424 N-m (313 ft-lb) for the elbow and 171 N-m (126 ft-lb) for the wrist. Based on these calculations, the torque requirements are specified as 474 N-m (350 ft-lb) at the elbow joints and 202 N-m (150 ft-lb) at the wrist yaw and pitch joints. No additional margins are included in these torque requirements, since they are based on the 667 N-m (500 ft-lb) shoulder torque, which was specified to include the speed and contingency requirements. The wrist roll torque is based on a 180 deg rotation of the 29,600-kg (65,000 lb) cargo in 10 minutes, with the capability to stop in 15 deg of rotational motion. This calculation yields a torque requirement of 88 N-m (65 ft-lb) with speed and contingency allowances similar to those used for the shoulder. The resulting joint torque requirements are summarized in Table VII-1.

E. REACH ENVELOPE AND JOINT ANGULAR TRAVEL

In this section, the required joint angular travel limits and the resulting reach envelope are determined. The joint angular travel limits are derived from the reach requirements and the joint sequence of rotations determined in Section C. The analysis is based on wrist point reach and excludes additional reach produced by the wrist extension length of 0.9 m (3 ft). The result of this analysis is specification of the angular travel limits (Table VII-2), so that full volume coverage of the required work areas is obtained.

Table VII-2 Joint Angular Travel Limits

	Pitch	Yaw	Roll
Shoulder	±200°	±130°	NA
Elbow	NA	±155°	±200°
Wrist	±120°	±120°	±200°

1. Elbow Yaw

Considering first the elbow yaw motion, the travel limits can be determined from the requirement to reach into the forward area of the cargo bay, with the shoulder located in the same area of the cargo bay. This requires the arm to nearly fold over on itself, placing the wrist near the shoulder. With a 6.1-m (20 ft) separation distance between the shoulder joints, and with each arm capable of reaching within a 3.05-m (10 ft) radius of its shoulder, 100% coverage of the front of the cargo bay is achieved. This arrangement produces a ±155-deg elbow yaw rotational requirement. Each arm cannot reach a 3.05-m (10 ft) radius sphere near its own shoulder, but that area can be reached by the other arm. Figure VII-9 shows the area excluded by each arm and the 100% coverage.

2. Shoulder Yaw

Examining the shoulder yaw rotation, the angular travel limit is derived from the requirement to reach the other side of the cargo bay with either arm and from the requirement to reach within the 3.05-m (10 ft) sphere at the shoulder of the other arm. Based on the arm segment lengths of 7.2 m (23.5 ft) the shoulder yaw rotation limit is set at ±130 deg. This, coupled with the ±155-deg elbow and the four-degree-of-freedom arm (excluding

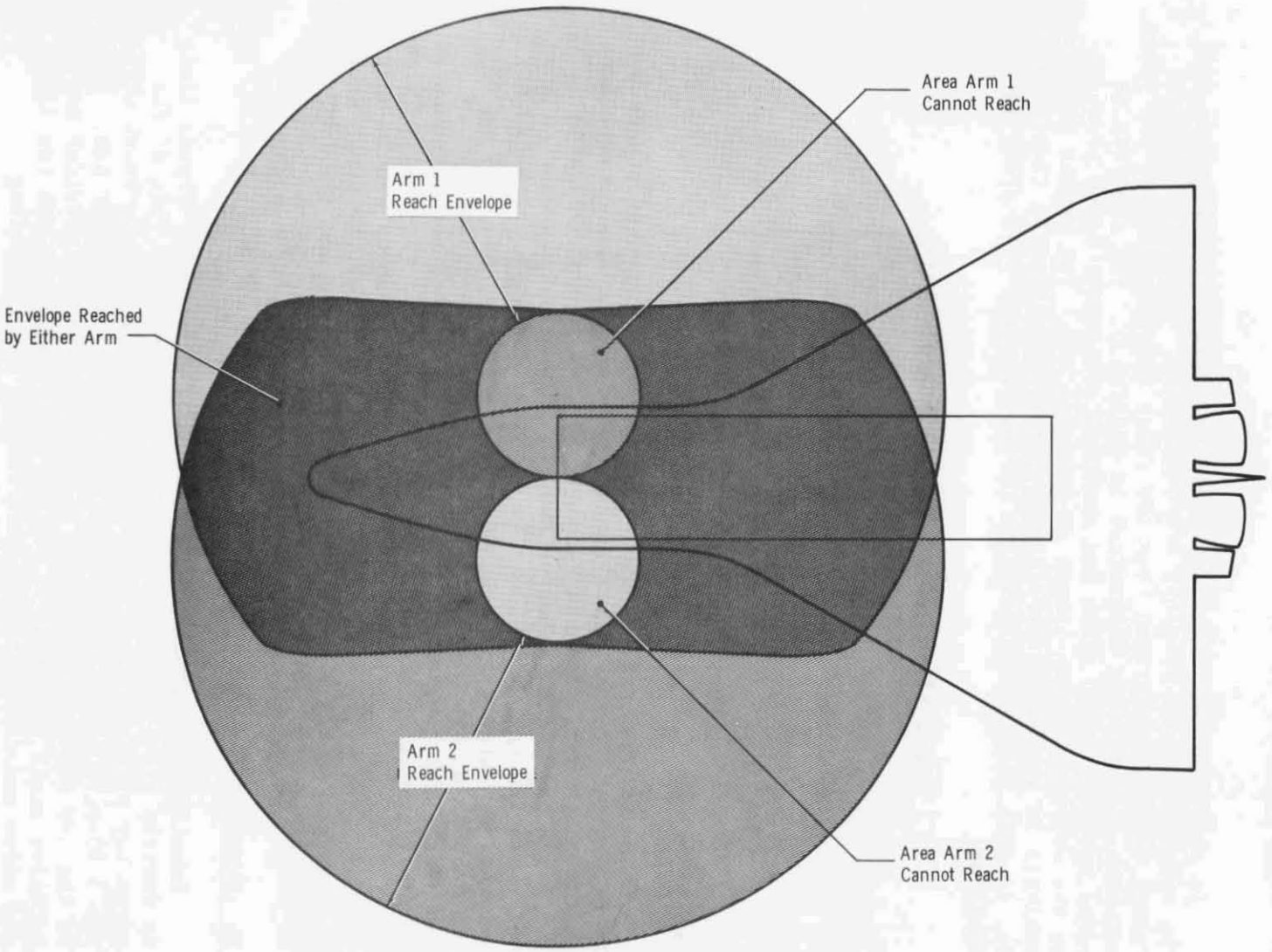

Fig. VII-9 Wrist Reach Envelope-Both Arms

the wrist joint and the terminal device), allows the wrist to be positioned along a line located 9.2 m (30 ft) from the shoulder and approximately parallel to the cargo bay door hinge line. This line is at the same height as the shoulder joint, and extends from the shoulder for approximately ±12.8 m (42 ft) in a longitudinal direction. Thus, full coverage of the cargo bay and the sphere at the shoulder of the other arm is achieved.

3. Other Joints

The wrist joint pitch and yaw rotation limits are based on the rotational payload handling requirements. Since cargo cannot be carried behind the wrist joint due to interference with the arm sections, these joint rotation limits are set at ±120 deg. This allows orientation of the cargo in any desired attitude, and prevents the wrist from folding back on the lower arm segment, which could cause damage to the arm structure or to the cargo.

Applying similar analyses to the remainder of the joints, the travel limits for all of the joints were determined and are shown as specified in Table VII-2. The approximate resulting wrist reach envelope is shown in Fig. VII-10. The additional reach capability resulting from the 0.9-m (3 ft) wrist extension is considered a "bonus."

F. CONTROL METHOD

In this section various control techniques for the RMS are discussed. These control alternatives range from unilateral joystick control, with and without computer augmentation, to various bilateral control systems, utilizing both master/slave and joystick controller configurations. The advantages and disadvantages of each system are discussed, and the number of possible alternatives is reduced to two; a mixed multimode bilateral master/slave system or a bilateral rate control system. Either system provides (1) the required sensitivity for fine manipulations and (2) gross movements of the large manipulator arm.

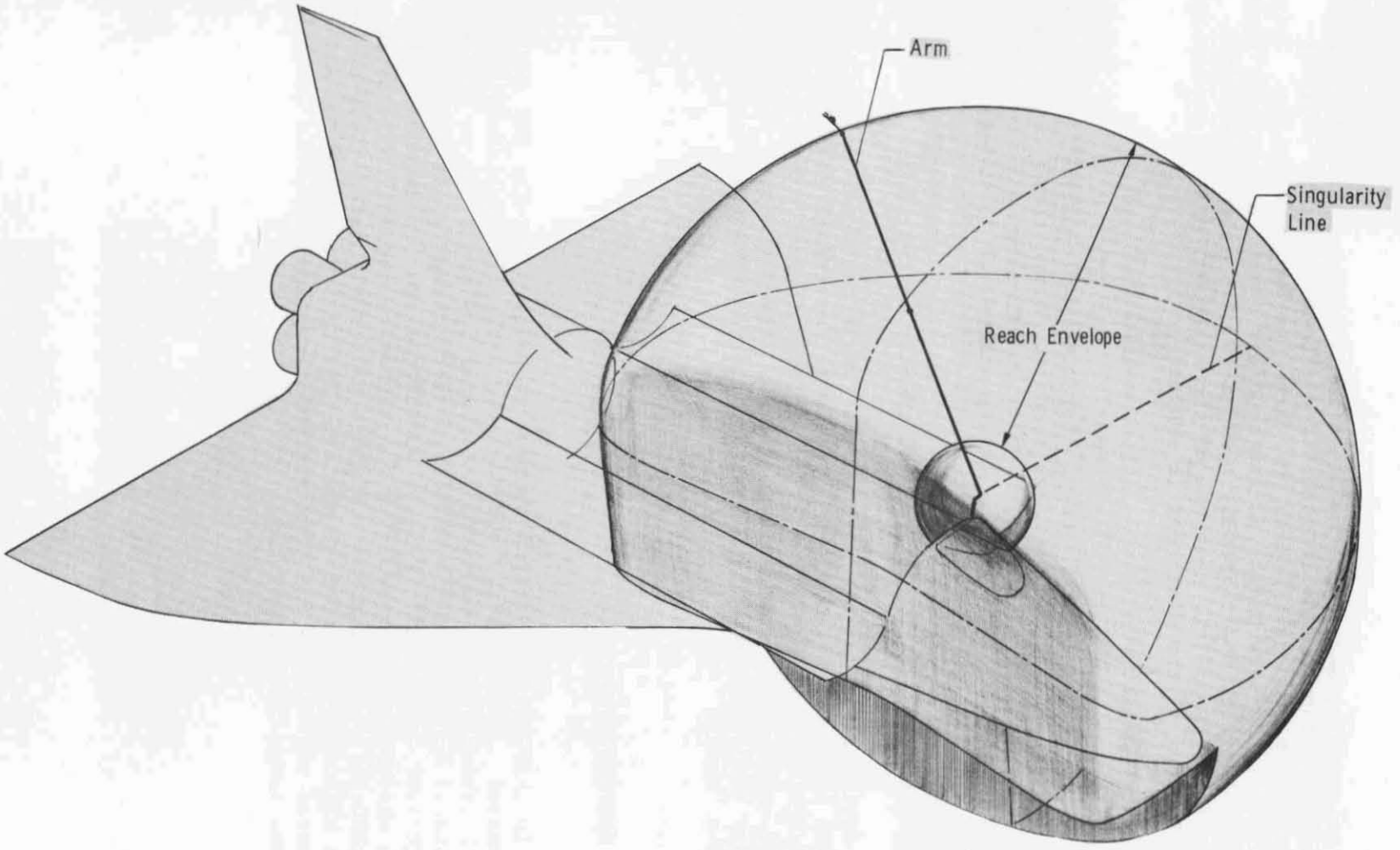

Fig. VII-10 Wrist Reach Envelope Using One Arm

1. Control Task Categories and Control Techniques

The tasks to be performed by the RMS can be broken down into five control categories, with each placing equal demands on the control subsystem. These categories are: (1) deploy arm; (2) capture; (3) decelerate mass; (4) transport mass; and (5) docking and close maneuvering.

Category 1 would normally be performed under computer control. Several deployment locations would be available to place the terminal device near the planned point of first contact for each particular task to be accomplished. Manual deployment would serve as a backup mode and for those operations not performed near an automatic deployment location. No restrictions are placed on the manual control mode for this category, since the operation is not seriously time or force limited.

Category 2 comes in two varieties: capture with finite relative velocity, and capture with zero relative velocity. It is clear that the second is easier and will be satisfied by any control mode capable of accomplishing the first. The constraint imposed is a time limit for accomplishing the task. With a 0.12 m/sec (0.4 ft/sec) relative velocity and a 14.3-m (47 ft) long arm on a flyby mode, approximately 12.2 m (40 ft) is available for capture and decceleration. Assigning 6.1 m (20 ft) to capture, 50 sec is available to accomplish this task.

Category 3 (decceleration) also comes in two varieties. The Shuttle reaction control system can be used for decceleration, with precise position and rate information supplied by the arm sensors, or the arm itself can be used for decceleration. This would normally be accomplished automatically, using computer control.

Category 4 (transport) should also be accomplished using computerized automatic control. The main problem is programming the computer to choose a good trajectory from the many possible trajectories without using very large amounts of memory and time. This might be solved by providing a model to be used for preprogramming the trajectory and monitoring the execution of the transport program. Alternatively a reasonable number of proprogrammed trajectories could be stored. However, this requires manually moving the object to an available initial position before execution of the preprogrammed trajectory.

Category 5 (docking, close maneuvering) is very similar to capture by the terminal device except for the magnitude of permissible velocities and accelerations. However, no severe limit in real time exists. It should, therefore, be possible to accomplish tasks in this category by the control mode chosen for category 2.

Candidate control schemes for this task are described in the following paragraphs.

Candidate 1, Rate or Acceleration Control - This is a simple control scheme but it requires large amounts of crew training. The main difficulty is one which is amply documented by human factors studies, namely the requirement to simultaneously control at least five degrees of freedom. It is assumed that the terminal device design takes care of one degree of freedom as well as grasping. Even with optimum display-control compatability this might be an obstacle.

Candidate 2, Rate or Acceleration Control with Automatic Tracking - With this method, the pilot matches end point velocities that are maintained using optical tracking devices and computer augmentation. This method still requires some, but much less training than Candidate 1. The main drawback is the control system complexity and the requirements for short-range tracking transducers (laser radars), which are extremely costly to develop.

Candidate 3, Rate or Acceleration Control with Rate Bias - This method is similar to Candidate 2 except that the matched velocity is maintained at a constant value rather than tracking the actual velocity. With the relative velocities remaining constant, a good match can be achieved. Required training is less than for Candidate 1 and more than Candidate 2.

Candidate 4, Position Control with Geometrically Similar Master - This requires less learning than for Candidates 1, 2, and 3, because it allows parallel control of all degrees of freedom, and is potentially also the fastest system. These conclusions are substantiated by results of the simulation program, reported in Chapter VI. However, since position control has only TV visual feedback, introduction of compliance (capability of backdriving the arm while Shuttle thrusters reduce ΔV) will aid final mechanical coupling of the terminal device. This can only be accomplished by bilateral force reflection on all degrees of freedom.

2. Control Scheme Analysis

The above analysis shows that two control modes must be chosen for actively working with the RMS. Deployment, acceleration, and transportation are operations ideally suited for computer control. The only options that remain to be decided relate to trajectory choice. The choice of the computer mode has little influence on the rest of the system.

For the manual control of the RMS a larger number of alternative modes exist. Furthermore, the choice influences requirements for the rest of the system to a larger extent. For instance, the required visual system must be much more elaborate for control modes 1, 2, and 3, than for 4. This is primarily because no other feedback path to the operator exists. The more elaborate visual systems influence telecommunications, lighting, and power requirements. Another problem with the control system candidates 1, 2, and 3 is the conflicting control inputs into the system that must be resolved when the system is being backdriven.

Candidate control scheme 4 has a serious difficulty. With a very maximum of 44.5 N (10 lb) tip force on the large arm, force reflection will be in a 1:1 ratio. However, there will be about a 1:18 [assuming a 0.76-m (2.5 ft) master arm] spatial scale factor. However, the first and second spatial derivatives (velocity and acceleration) require about a 1:1 or 1:2 ratio for natural low-training operation. Therefore, after relatively short excursions 0.61 m (2 ft of the large arm), geometrical similarity will be lost. Excursion requirements of large arm under this mode should never be very large, so that it seems possible that a solution may be found to this problem. Except for this, control scheme 4 seems to have the advantages of being the fastest, having natural collision reaction capability and the only system that could possibly allow one operator to handle both arms simultaneously, if this became a requirement.

To overcome some of the cited difficulties posed by control scheme 4 two additional candidate schemes are described.

Candidate 5, Hybrid Bilateral Master-Slave - This method employs a large 14.3-m (47 ft) long manipulator with five degrees of freedom for which, instead of a terminal device, a man-sized bilateral master-slave manipulator is used. The large arm need not be backdrivable and would be computer controlled, with the computer inserting bias velocity vectors on demand. The bias vector is derived by averaging the manual tracking trajectory of the dexterous arm.

For less complex computer requirements, the large arm could have a separate manual control to set its vector by small body motions of the operator. This would require a coordinate transformation operation within the computer. For computer control phases, (Categories 1, 3, and 4), redundant degrees of freedom can be frozen. The main advantage of this system is that no mode switching is necessary nor are compromises in arm design required as each arm can be designed to fit its control mode. The disadvantage of above system lies in the additional mechanical, control, and telecommunications complexity.

Candidate 6, Variable Ratio Mixed-Mode Bilateral Master-Salve - The basic difficulty with control scheme 4 is the disparity of the requirements for scale factors that are different for displacement and its first two derivatives. It has been established that sufficient no-load linear velocity capability must exist at the master controller to prevent the operator from pushing too hard and saturating force reflection. A 14.3-m (47 ft) long slave arm might typically be controlled by a master scaled down by a factor of 1:18. If a 1:1 ratio is maintained for all angular displacements and the maximum linear velocity of the slave is 0.46 m/sec (1.5 ft/sec), then the maximum master velocity becomes approximately 0.025 m/sec (1 in./sec). This slow velocity appears much more like an isometric control stick than a master-slave controller. Force reflection will likely be at least partially saturated, so that for initial approach, the system is in a mixed mode: bilateral master-slave wrist plus a high ratio (essentially rate control) for control of the wrist point x, y, and z. Close to the target, the angular slave-master displacement ratio is changed by the operator from 1:1 to about 1:18, [for a smaller 0.79 m (2.6 ft) master], resulting in a true bilateral master slave mode. This system allows gross movements of the slave to be accomplished easily, and also provides the necessary sensitivity for final alignment and capture.

Candidate 7, Bilateral Rate Control - One basic problem associated with all of the master/slave control systems is the requirement for additional space in the Shuttle cockpit to accommodate the master controller. To overcome this problem, a control system utilizing a six-degree-of-freedom (or two three-degree-of-freedom) bilateral joystick type handcontroller could be employed. This control system would operate in a normal rate command fashion with the additional feature of force feedback capability to allow the operator to feel the resisting forces and moments placed on the manipulator arm. The force feedback capability overcomes the problems associated with backdiving a unilateral rate control system, and also aids in attachment of the terminal device to the target. This system would employ multiple sensitivities for accomplishment of gross positioning as well as fine manipulations. The force-feedback capability could also be switched off for those tasks where it was not required. One problem associated with this system is that a force-feedback hand controller has not been developed.

At the present time, it appears that either control scheme 6 or 7 will be capable of accomplishing the required RMS tasks. Further analysis and simulations are required to determine which of these control systems should be used for the RMS final design.

G. TELECOMMUNICATIONS

The telecommunications subsystem provides the primary interfaces between the astronaut operator, the manipulator arms and the Shuttle. This subsystem must, therefore, have very high reliability. Hence, the tradeoff analyses are predicated on simplicity and reliability, except where an alternative method offers *significantly* better noise immunity, lower weight, or less power consumption. This section discusses those tradeoffs and analyses that have a major impact on the preliminary design of the telecommunications subsystem. It is possible to relay command and data information between the manipulator arm and the control and data electronics either by an RF link or by cables. This option is discussed and it is concluded that cable connections are preferable to an RF link. There is no requirement for auxiliary ranging or tracking and this equipment will not be included in the preliminary design. The relative merits of multiplexing arm data to reduce cable size versus direct simple cabling are discussed. The conclusion favors simple cabling. Computation of servo command signals and others may be performed either locally at the manipulator arm joints or remotely in the control and data electronics. It is determined that there is no advantage to local computation.

1. Hardline vs RF Transmission

The principal reason for considering both the hardline and the RF transmission methods of arm data transfer, or some variation of the two, is to investigate areas for optimizing the manipulator arm design by reducing the cabling complexity associated with the arm's component subsystems.

In the case of the hardline method, all data transfer between the arm's component subsystems such as angle and position encoders, joint and terminal device control, television and lighting control, etc, would be accomplished by hardwire connections to the Shuttle control station. This approach is obviously straightforward and results in a multiplicity of cabling. Time sharing, in certain cases, can help to reduce somewhat the amount of cabling at the expense of additional black boxes.

Another approach to the problem is the possible use of radio frequency transmission of manipulator arm data from the various component subsystems within, or associated with the arm to the central arm control station within the Shuttle. The obvious advantage of this approach, of course, is the elimination, or at least reduction of the wire runs installed in the arm, which reduces possible wire routing problems and cable flexing requirements.

Advantages and disadvantages are apparent with each method of data transfer. Only a few of the salient reasons are considered here to indicate, in a general way, the design aspects involved in selecting the final approach.

a. Data Flow - The flow of information associated with the control and monitoring of the manipulator arm will generally fall into one of two principal categories: command/control data and arm feedback data. Table VII-3 indicates the nature of the data within each of these categories. These data constitute the major flow of information from manipulator arm to the central arm control station and are the prime contributions to cabling bulk.

Table VII-3 Typical Data Function Transmitted

Category	Data Function
Command/Control Data	1) Arm Servomotors Shoulder Elbow Wrist Terminal Device 2) Electromagnetic Brakes Shoulder Elbow Wrist Terminal Device 3) Wrist TV Camera Control On/Off Iris Focus 4) Lighting Control (Wrist)
Arm Feedback Data	1) Position Data Shoulder Elbow Wrist Terminal Device 2) Velocity Data Shoulder Elbow Wrist 3) Wrist TV Camera Video

About 300 bits of arm-peculiar data are involved in the control and monitoring of a single arm that would have to be transmitted down (or from, in the case of an RF link) the arm.

b. Angle Encoder Data - The type of angle encoder data required from the various arm joints depends on the accuracy required of the joint. From Section C, the joint position accuracy is 1.97 mrad. From this, we get

$$\frac{2\pi}{1.97 \times 10^{-3}} = 3190 \text{ parts per revolution.}$$

Doubling, to allow the detection to be greater than joint accuracy required, the minimum angle sensor must resolve at least 1 part in 6380, indicating a shaft encoder of 13 bits for θ_{ST}. (θ_{ST} = shoulder, translational motion).

In a similar manner, for a rotational position accuracy of the terminal device of ±0.1 deg and the arm fully extended with the motion being effected by the shoulder, the required angle resolution is

$$\frac{360}{0.1} = 3600 \text{ parts per revolution.}$$

This indicates a shaft encoder of 12 bits for θ_{SR} (θ_{SR} = shoulder, rotational motion). If this resolution is doubled, where additional margin is desired, a shaft encoder of 13 bits is required.

c. Data Interface Estimate - Exclusive of the TV video data, an estimate of the digital data required for a single, seven-degree-of-freedom arm may be obtained from Table VII-4. For simplicity, a 13-bit angle encoder is assumed for each joint. The indicated TV data are for status and power only; the TV video bandwidth will be estimated later.

Table VII-4 Slave Arm Control and Monitoring Data

Shoulder	Elbow	Wrist	Terminal Device
2 DOF	2 DOF	3 DOF	1 DOF
θ_S (13 bits)	θ_ε (13 bits)	θ_W (13 bits)	Control (5 bits)
ψ_S (13 bits)	ϕ_ε (13 bits)	ψ_W (13 bits)	Position (5 bits)
Motor (θ_S) (13 bits)	Motor (ψ_ε) (13 bits)	ϕ_W (13 bits)	Brake (1 bit)
Motor (ψ_S) (13 bits)	Motor (ϕ_ε) (13 bits)	Motor (θ_W) (13 bits)	
ω (θ_S) (5 bits)	ω (ψ_ε) (5 bits)	Motor (ψ_W) (13 bits)	Lamp Power (2 bits)
ω (ψ_S) (5 bits)	ω (ϕ_ε) (5 bits)	Motor (ϕ_W) (13 bits)	
Brake (θ_S) (1 bit)	Brake (ψ_ε) (1 bit)	ω (θ_W) (5 bits)	TV Iris (3 bits)
Brake (ψ_S) (1 bit)	Brake (ϕ_ε) (1 bit)	ω (ψ_W) (5 bits)	TV Focus (4 bits)
		ω (ϕ_W) (5 bits)	TV Power (1 bit)
		Brake (θ_W) (1 bit)	
		Brake (ψ_W) (1 bit)	
		Brake (ϕ_W) (1 bit)	

The data frame for the control and monitoring of the manipulator arm is summarized in Table VII-5. Eight servo channels will be used for the seven manipulator arm joints and the terminal device. Each of these servo channels will also include velocity and position feedback channels. Sampling rates on the order of 25 to 50 samples/sec appear to be adequate.

For a sampling rate of 50 samples/sec, a data rate of 50 x 310 = 15.5 k bits/sec would be employed; and, one frame of data would be transmitted in

$$t_f = \frac{1}{15.5 \times 10^{-3}} \times 310 = 20 \text{ msec.}$$

Table VII-5 Data Frame Estimate

Function	Total Bits
Synchronization Word	16
TV & Lamp Control	10
Shoulder Pitch (θ_S)	32
Shoulder Yaw (ψ_S)	32
Elbow Roll (ϕ_ε)	32
Elbow Yaw (ψ_ε)	32
Wrist Yaw (ψ_W)	32
Wrist Pitch (θ_W)	32
Wrist Roll (ϕ_W)	32
Terminal Device	11
Spares	49
TOTAL	310

With a clock rate of 15.5 kHz, a control and sensing bandwidth for the arm would be 7.75 kHz.

An estimate of the maximum sampling frame time is obtained from the maximum joint translational and rotational rates as follows:

Translational Rate (Maximum) 0.457 m/sec (1.5 ft/sec)

Arm Length 14.5 m (47 ft)

Joint rate is $\frac{0.457}{14.5} = 0.032$ rad/sec

$$\frac{\theta}{\dot{\theta}} = \frac{1.97 \text{ mrad}}{0.032 \text{ rad/sec}} = 61 \text{ msec max Frame Time.}$$

Rotational Rate (Maximum), 1.0 deg/sec

Rotational Position Accuracy, 0.05 deg

$$\frac{\theta}{\dot{\theta}} = \frac{0.05}{1} = 50 \text{ msec max Frame Time.}$$

Thus, the choice of a 20 msec frame time appears adequate.

d. Terminal Device TV Camera - To obtain an estimate of the bandwidth requirements for the terminal device TV, the precontact dynamics of the Shuttle and the closing target (another Shuttle or satellite) must be considered. As a worst case it is assumed, therefore, that the terminal device TV could be used for viewing the closing target, together with the base TV camera, prior to contact. It is further assumed that the resolution will be 2.54 cm (1 in.) at 7.7 m (25 ft) for the terminal device TV camera.

Precontact Conditions - The Shuttle docking closure rates and misalignments are as follows: forward velocity, 0.122 m/sec (0.4 ft/sec); centerline miss distance, 15.2 cm (6 in.); angular rate 0.1 deg/sec; and angular error ±3.0 deg.

Closing Rates - Based on a 2.54 cm (1 in.) resolution at 7.7 m (25 ft) the minimum angle at the sensor is $2.54/(7.7 \times 100) = 3.33$ mrad; and, the expansion rate is approximately 0.06 mrad/sec. Thus, an estimate of the sampling rate is $\theta/\dot{\theta} = 3.33/0.06 = 55.5$ msec. For a 30° field of view and a 3.33 mrad resolution the number of TV lines would be $6.28/(6 \times 3.33 \times 10^{-3}) = 315$ lines. No magnification due to the TV optics (zoom lens) has been included.

Rotational Rates - The rotational position accuracy of the arm-mounted TV camera is ±0.05 deg. Based on a precontact angular rate of 0.1 deg/sec, an estimate of the sampling rate is $\theta/\dot{\theta}$ = 0.05/0.1 = 500 msec. Thus, a frame rate of 1/0.5 = 2 frames/sec, would suffice.

TV Video Bandwidth - From the preceding discussion concerning frame rates, the maximum requirement is for a frame rate of 18 frames/sec. Thus the selection of the standard 30 frames/sec rate--which simplifies interfacing requirements--will be adequate and give normal motion rendition.

e. RF Transmission - For an RF transmission system, the maximum range would be on the order of 15.3 m (50 ft) (slightly longer than length of arm extended) and the frequency would be approximately 400 MHz (λ = 0.75 m) based on allocated frequencies between space stations. The RF bandwidth is assumed to be the sum of the 4.5 MHz video sideband and the 1.5 MHz vestigial sideband or 6 MHz.

f. Free-Space Attenuation - The free-space path attenuation is given by

$$a = 10 \log \left(\frac{P_t}{P_r} \right)$$

and

$$\frac{P_r}{P_t} = \frac{A_r A_t}{d^2 \lambda^2}$$

where

A_r = effective area of receiving antenna

A_t = effective area of transmitting antenna

d = distance between antennas

λ = wavelength (0.75 m)

Note: This is valid provided $d >> 2\ a^2/\lambda$ where a is the largest line in dimension of either antenna; i.e., for a half wave dipole,

$a = \lambda/2$ or 0.375 m

$$\therefore 2\ a^2/\lambda = 2 \times \frac{\lambda^2}{4} \times \frac{1}{\lambda} = \frac{\lambda}{2} = 0.375 \text{ m}$$

$d = 50$ ft $= 15.2$ m

$A = 0.13\ \lambda^2$ (half wavelength dipole)

$= 0.13 \times 0.75 \times 0.75 = 0.0731$

$$\frac{P_r}{P_t} = \frac{0.13\ \lambda^2 \times 0.13\ \lambda^2}{15.2 \times 15.2 \times \lambda^2} = \frac{9.51 \times 10^{-3}}{231} = 4.12 \times 10^{-5}$$

$$\frac{P_t}{P_r} = 2.43 \times 10^4$$

$$\therefore a = 10 \log 2.43 \times 10^4$$

$$a = 43.9 \text{ db}$$

g. Required Transmitter Power - The required arm-mounted transmitter power can be obtained from the video link margin calculations outlined in Table VII-6.

Table VII-6 RF Link Margin Calculations

Transmitter Power (Pw)	+10 log P	dbw
Free-Space Attenuation		-43.9 db
Shuttle Receiver Antenna Gain		-3.0 db
Arm-Mounted Transmitter Antenna Gain		-3.0 db
Polarization Mismatch Loss		-3.0 db
RF Obscuration Loss		-3.0 db
Signal Power Available at Shuttle Receiver	10 log P	-55.9 dbw
Kt (T = 104°K)		-208.4 db
NF		+5.0 db
Receiver Bandwidth (6 MHz)		+67.8 db
S/N Required		+13.0 db
Margin		+9.0 db
Signal Power Required at Shuttle Receiver		-113.6 dbw
10 log P - 55.9 = -113.6		
10 log P = -113.6 + 55.9		
10 log P = -57.7		
$P = 1.7 \times 10^{-6} = 1.7$ μw		

h. RF Link Considerations - The possible use of an RF link to provide the media for the transfer of data between the manipulating arm activators and sensors invites a variety of approaches. The bandwidth variations between the types of data transmitted becomes a basic consideration. Other areas of concern involve the types of data, the extent of multiplexing, antenna and black box locations and, of course, cabling within the arm is never entirely eliminated because power must be supplied to all of the arm-mounted components and a backup safety system must be incorporated so that the arm can be either discarded or safely stowed should the RF link fail. In addition, with an RF link located at the wrist, all control and feedback data for the elbow and shoulders must still reach their destinations by cable from the wrist. Table VII-7 gives some examples of the numbers of RF links possible.

Table VII-7 Examples of RF Link Combinations

RF Links	General Functions
One Link	Used for reception and transmission of all data.
Two Links	One used for reception and transmission of all data except video; one used for reception of video data.
Two Links	One used for reception of all data including video; one used for transmission of all command data.
Three Links	One used for reception of only narrow bandwidth data; one used for reception of wideband data (TV video); and, one used for transmission of all command data.

Since the TV video data generally requires a much larger bandwidth, it is sometimes desirable to use a separate RF link for this information and a more narrow bandwidth RF link for the other data. Figure VII-11, however, indicates an arm-installed system in which all commands are sent over one link and all-arm-to-Shuttle data sent over another link. In this case 20 samples of general data (310 bits per frame) are transmitted every second together with eight TV frames of data. Commands can be sent continuously.

The ultimate choice of an RF link system would involve a review of a number of factors, such as system complexity, number of boxes required, suitable antenna locations, continuous or time-shared control and monitoring, etc. The investigation would compare those systems that use separate RF links for command, force feedback and telemetry, and video data respectively to those systems that multiplex and transmit all data over a single RF link.

Susceptibility to electromagnetic interference and the ability to prevent autogenous jamming of other onboard systems is also a major consideration.

A functional flow diagram in which a two-link system is used (command data transmitted over a separate link) is shown in Fig. VII-12. In this case, four antennas are used in a single arm configuration. Two are mounted on the arm and two are mounted on the Shuttle. The use of a second arm will increase the complexity. The subsystems shown dotted in Fig. VII-12 refer to the RF transmission link subsystem.

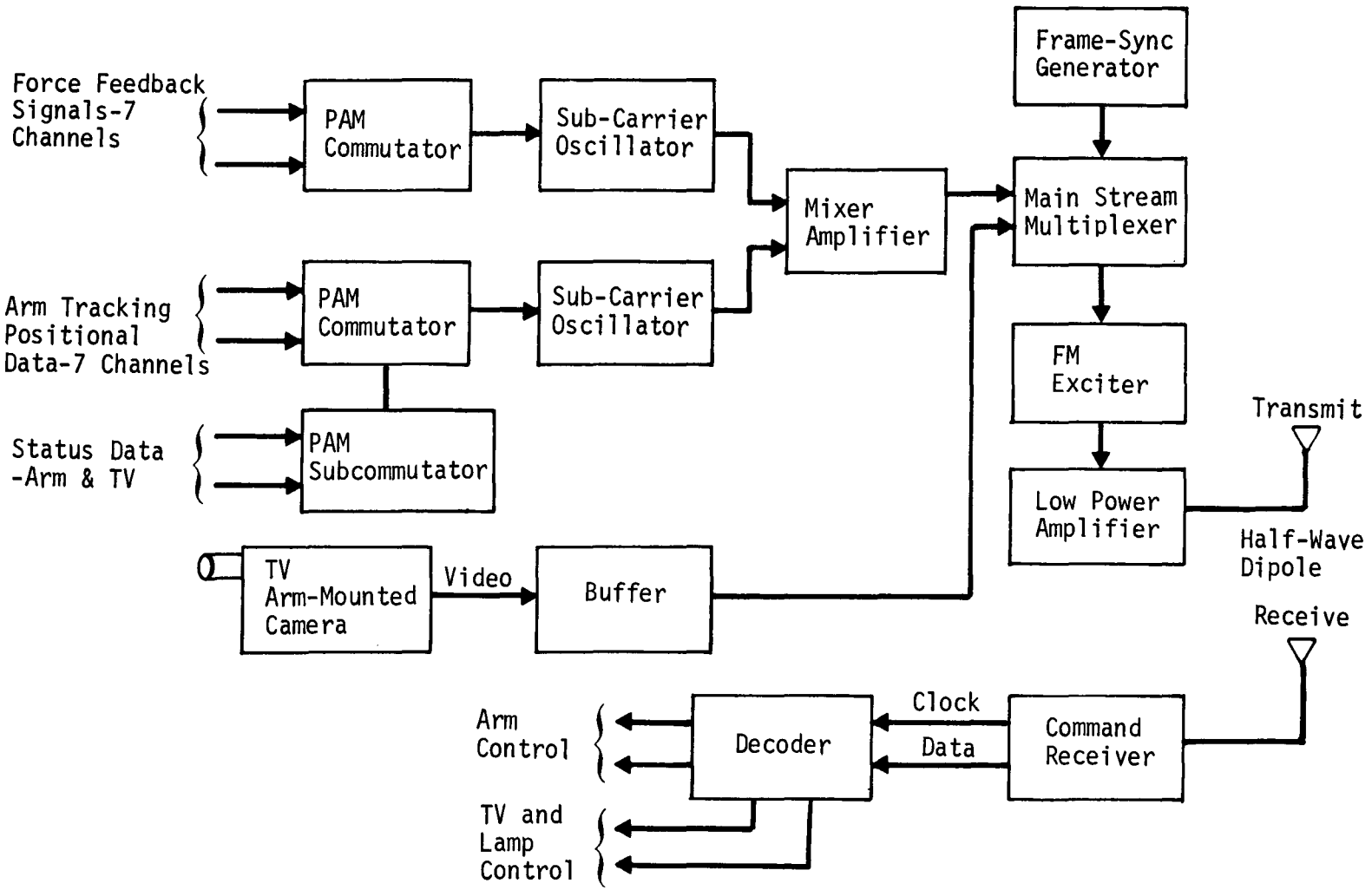

Fig. VII-11 Arm-to-Shuttle RF Link System Functional Flow Diagram

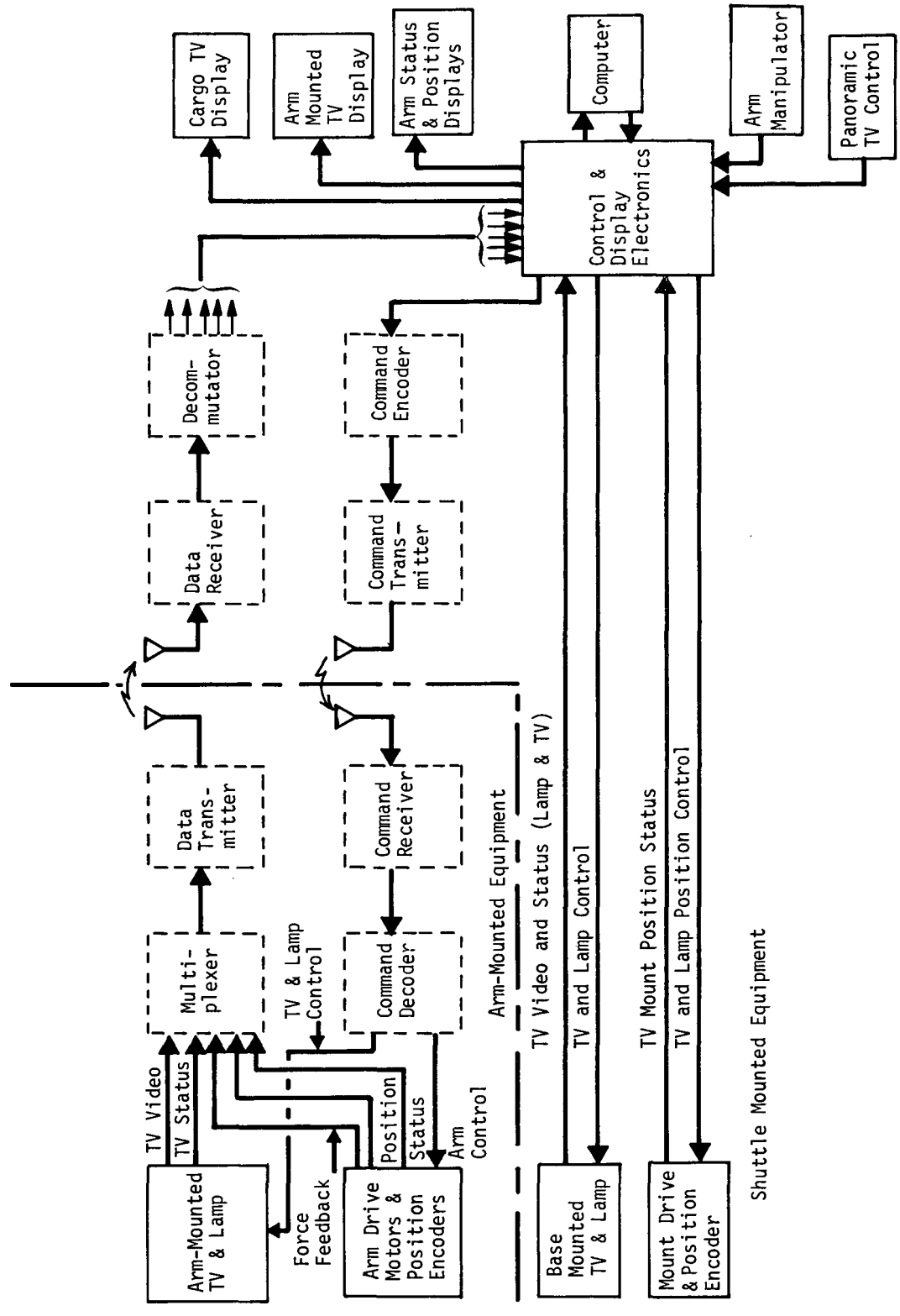

Fig. VII-12 RF Transmission System Functional Flow

i. Conclusions and Recommendations - The apparent advantage usually cited for the consideration of RF links in the transmission of manipulating arm data is that a multiplexing of cables within the arm can be avoided, and hence a more simple arm design achieved. This line of reasoning continues by showing that, while no arm design can avoid a certain number of cables; i.e., power for the joint and end-effector motors, television and lamps, the use of an RF link would somehow minimize the total number of cables required. To a certain extent, this reasoning is valid. However, to effect a suitable RF transmission network, whether a single or a multichannel link, a certain amount of multiplexing must be provided. However, this approach (using multiplexed data) is equally applicable for the hardwire system. Thus, in the case of a hardwire design, it is extremely unlikely that an attempt would be made to run large matrix bundles down the arm to the Shuttle's control and display processing subsystems. Generally, some form of multiplexing configuration would probably form the basis of the hardwire design.

If this reasoning is followed, then the only advantage regarding the cable reduction effected by the RF links would be the elimination of a command data cable, a TV video cable, and a narrow bandwidth feedback data cable. In fact, if the multiplexing is sufficiently sophisticated, all that is saved is a single cable; i.e., the actual RF link.

In addition to the installation problems associated with additional antennas and the location constraints within the arm for the transmitter and receiver subsystems, the power requirements for the manipulating arm are increased somewhat. Also, a backup control system should be considered for use with an RF transmission link. Such a system would provide a means of either releasing or stowing the arms automatically should it become necessary to abandon the docking or cargo handling operation due to an RF network failure. This backup system would further add to the complexity of the system. The need to hardwire from the arm-mounted transceiver to the other joints further reduces the savings in complexity over the hardwire case.

It appears, therefore, that any advantages in the use of an RF transmission link are far outweighed by the increase in complexity and attendant decrease in reliability. In accordance with the objective of maximum simplicity and dependability, the manipulation arms will be hardwired in this preliminary design.

With the decision to employ hardwire cabling as opposed to RF command and data link, the analysis will be directed specifically at hardwire. RF-related topics such as transmission range, bandwidth compression, near-field effects, antenna pattern obscuration, signal overloading, and EMC which are no longer applicable will not be discussed.

2. Tracking and Ranging Requirements - Navigation and guidance systems in conjunction with pilot viewing planned for the Shuttle are sufficient to rendezvous and maneuver to a position where the manipulator arms may then move to make contact with the target. Feedback from the arms through the Shuttle computer and avionics to the reaction control system will be used to accomplish closure after arm contact. No intermediate systems are necessary. Thus there are no tracking and ranging requirements for the Shuttle RMS.

3. Multiplexing vs Simple Cable

The question of reducing cabling complexity using multiplexing techniques has been discussed in the preceding subsection as part of the RF transmission/hardwire tradeoff. Multiplexing is judged in this subsection by its impact on subsystem complexity, serviceability, weight, and reliability, as opposed to a multiplicity of cabling. If the servo systems for the slave arms are analog (i.e., analog servomotor drive signals, position potentiometers, and tachometers for velocity outputs), the cabling problem is reduced significantly by eliminating the requirements for transmitting parallel data bits, each requiring a separate wire. Servo amplifiers will thus be hardwired with or without multiplexing. Because the TV camera video signal requires a high bandwidth, it will employ a single RG174B/U 75 ohm cable of its own in all cases.

a. Analysis of Potential Multiplexing Configurations - This discussion will deal with the location and number of multiplexing units rather than with the type of coding used. For purposes of this analysis the following four configurations will be studied: multiplexing unit located at wrist; multiplexing unit located at elbow; three multiplexing units located at wrist, elbow, and shoulder; and hardwire only (no multiplexing).

Each signal function that must be transmitted either by direct cable or encoded is detailed in Table VII-8. The functions are labeled in the Column A. Column B gives the wire size necessary. Column C is the number of wires in the cable for that particular function. All cables are presumed to be twisted shielded pair or twisted shielded triad for best noise and EMI protection. Columns D thru G give the starting and termination points of each cable, as shown in the chart immediately below the table. For example, T-E indicates that the cable runs from the terminal device to the elbow joint. The total length of each type of cable needed for each configuration is determined from the tabulated information. The weight for each cable type is then added to find the cable bundle weight for the four configurations. Table VII-9 summarizes these calculations.

Maximum bundle diameter is determined by analyzing the number of each type cable between each pair of joints and between the shoulder joint and control and data electronics (C&DE). For all configurations the largest diameter bundle occurs between the shoulder joint and the C&DE. This location also receives least flexing. But using this bundle as the worst case, the all-hardwire configuration has 45 cables in this area. The overall bundle diameter is approximately 2.5 cm (1 in.) exclusive of any protective covering. This size is not great enough to be considered a disadvantage. Many of the data wires are greatly oversized due to a reluctance to space-qualify high-strength alloy conductors. If this material is qualified, it is expected that the bundle size can be further reduced.

b. Noise Considerations - Considerable advantage in signal-to-noise ratio (S/N) is obtainable with certain multiplexing techniques such as PCM. However, these methods require signal conversion (analog to digital) and add to the complexity. The signals employed in the RMS are all of a high-level nature (no microvolt signals) and of reasonably low impedance. In addition, each signal is routed within its own shield as a pair or triad for containing or protecting from electromagnetic radiation. The noise immunity, even in a straight hardwire configuration, can be expected to be more than adequate.

Table VII-8 Arm Cabling Requirements

A	B	C	D	E	F	G
				Cable Run*		
Signal Item	Wire Size	Wires in Shield	With 1 Multiplexer at Wrist	With 1 Multiplexer at Elbow	With 3 Multiplexers at Wrist, Elbow, and Shoulder	All Hardwire
Terminal Device						
Servomotor 1	20	2	T-C	T-C	T-C	T-C
Servomotor 2	20	2	T-C	T-C	T-C	T-C
Brake Release (or command)	22	2	T-W	T-E	T-W	T-C
28 VDC Power	22	2	T-W	T-W	T-W	X
Position	22	3	T-W	T-E	T-W	T-C
Wrist Visual Sensing Group						
Video	75 ohm	coax	W-C	W-C	W-C	W-C
Iris	22	2	X	W-E	X	W-C
Focus	22	2	X	W-E	X	W-C
On/Off	22	2	X	W-E	X	W-C
Illumination	20	2	W-C	W-C	W-C	W-C
Wrist Joints						
Pitch Servomotor 1	20	2	W-C	W-C	W-C	W-C
Pitch Servomotor 2	20	2	W-C	W-C	W-C	W-C
Yaw Servomotor 1	20	2	W-C	W-C	W-C	W-C
Yaw Servomotor 2	20	2	W-C	W-C	W-C	W-C
Roll Servomotor 1	20	2	W-C	W-C	W-C	W-C
Roll Servomotor 2	20	2	W-C	W-C	W-C	W-C
Pitch Brake Release (or command)	22	2	X	W-E	X	W-C
Yaw Brake Release (or command)	22	2	X	W-E	X	W-C
Roll Brake Release (or command)	22	2	X	W-E	X	W-C
Pitch Position	22	3	X	W-E	X	W-C
Yaw Position	22	3	X	W-E	X	W-C
Roll Position	22	3	X	W-E	X	W-C
Pitch Velocity	22	2	X	W-E	X	W-C
Yaw Velocity	22	2	X	W-E	X	W-C
Roll Velocity	22	2	X	W-E	X	W-C
+28 VDC Power	22	2	W-E	W-E	W-E	X
±15 VDC Power	22	2	W-E	W-E	W-E	X
+5 VDC Power	22	2	W-E	W-E	W-E	X
Decoder Input	22	2	W-C	X	W-C	X
Encoder Output	22	2	W-C	X	W-C	X

*Length of cable from chart below:

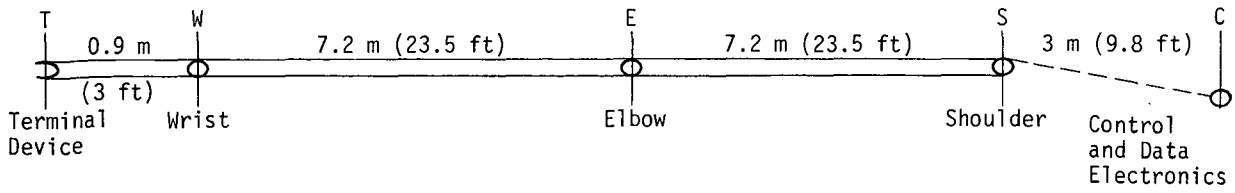

Table VII-8 (concl)

A	B	C	D	E	F	G
				Cable Run*		
Signal Item	Wire Size	Wires in Shield	With 1 Multiplexer at Wrist	With 1 Multiplexer at Elbow	With 3 Multiplexers at Wrist, Elbow, and Shoulder	All Hardwire
Elbow Joints						
Yaw Servomotor 1	20	2	E-C	E-C	E-C	E-C
Yaw Servomotor 2	20	2	E-C	E-C	E-C	E-C
Roll Servomotor 1	20	2	E-C	E-C	E-C	E-C
Roll Servomotor 2	20	2	E-C	E-C	E-C	E-C
Yaw Brake Release (or command)	22	2	W-E	X	X	E-C
Roll Brake Release (or command)	22	2	W-E	X	X	E-C
Yaw Position	22	3	W-E	X	X	E-C
Roll Position	22	3	W-E	X	X	E-C
Yaw Velocity	22	2	W-E	X	X	E-C
Roll Velocity	22	2	W-E	X	X	E-C
+28 VDC Power	22	2	E-S	E-S	E-S	X
±15 VDC Power	22	2	E-S	E-S	E-S	X
+5 VDC Power	22	2	E-S	E-S	E-S	X
Decoder Input	22	2	X	E-C	E-C	X
Encoder Output	22	2	X	E-C	E-C	X
Shoulder Joints						
Pitch Servomotor 1	20	2	S-C	S-C	S-C	S-C
Pitch Servomotor 2	20	2	S-C	S-C	S-C	S-C
Yaw Servomotor 1	20	2	S-C	S-C	S-C	S-C
Yaw Servomotor 2	20	2	S-C	S-C	S-C	S-C
Pitch Brake Release (or command)	22	2	W-S	E-S	X	S-C
Yaw Brake Release (or command)	22	2	W-S	E-S	X	S-C
Pitch Position	22	3	W-S	E-S	X	S-C
Yaw Position	22	3	W-S	E-S	X	S-C
Pitch Velocity	22	2	W-S	E-S	X	S-C
Yaw Velocity	22	2	W-S	E-S	X	S-C
+28 VDC Power	22	2	S-C	S-C	S-C	X
±15 VDC Power	22	2	S-C	S-C	S-C	X
+5 VDC Power	22	2	S-C	S-C	S-C	X
Decoder Input	22	2	X	X	S-C	X
Encoder Output	22	2	X	X	S-C	X

*Length of cable from chart on page VII-37.

Table VII-9 Manipulator Arm Cable Weights

Cable Type	Weight, kg/m (lb/ft)	1 Multiplexer at Wrist		1 Multiplexer at Elbow		3 Multiplexers at Wrist, Elbow, & Shoulder		Simple Cable	
		Length, m (ft)	Weight, kg (lb)	Length, m (ft)	Weight, kg (lb)	Length, m (ft)	Weight, kg (lb)	Length, m (ft)	Weight, kg (lb)
20-2	0.0214 (0.0143)	211 (692)	4.52 (10.0)	211 (692)	4.52 (10.0)	211 (692)	4.52 (10.0)	211 (692)	4.52 (10.0)
22-2	0.0162 (0.0108)	175 (573)	2.84 (6.2)	175 (573)	2.84 (6.2)	115 (377)	1.86 (4.1)	231 (757)	3.74 (8.25)
22-3	0.0220 (0.0147)	44 (144)	0.97 (2.1)	44 (144)	0.97 (2.1)	1 (3.3)	0.02 (0.04)	107 (351)	2.36 (5.2)
RG 174 B/U	0.0092 (0.0061)	17 (56)	0.16 (0.35)	17 (56)	0.16 (0.35)	17 (56)	0.16 (0.35)	17 (56)	0.16 (0.35)
Bundle Total Weight, kg (lb)			8.49 (18.7)		8.49 (18.7)		6.56 (14.5)		10.78 (23.6)
Bundle with Protective Jacket Total Weight, kg (lb)			11.1 (24.4)		11.1 (24.4)		8.5 (18.7)		14.0 (30.8)

c. Conclusions - From the above analysis the following conclusions can be drawn:

There is no significant savings in weight of multiplexing over simple cabling. Weight of the black boxes is likely to exceed the differential.

There is no significant saving in cable size with multiplexing.

The increase in signal-to-noise ratio does not justify the added complexity in multiplexing.

The manipulator arms are not in themselves complex enough to require multiplexing. For the present preliminary design with an all-analog servo system, multiplexing appears to offer no advantage, but only to complicate the data transfer. In keeping with the objectives of simplicity and reliability, it is recommended that simple cabling be employed without multiplexing. Further discussion of multiplexing techniques is not applicable.

4. Arm-Based vs Shuttle-Based Computation

Concerning signals used by the slave arm, it is possible that computations performed locally could reduce error, phase shift, and noise problems associated with remote (Shuttle-based) computation. A typical candidate would be digital-to-analog conversion of a shaft encoder output (if system was digital) and summing the resultant with a servo command to produce an error signal at the servoamplifier input. Rate feedback could be added in the same way. However, the present preliminary design assumes an all-analog servo loop with servoamplifiers located on the Shuttle rather than on the arm. This requirement makes any computation of servo parameters locally unnecessary and undesirable. There are no other signals that would profit from local computation. On the contrary, it would tend to complicate the system and compromise reliability.

H. DEPLOYMENT METHOD

Several deployment alternatives were reviewed. They are shown on Fig. VII-13, Concepts 1 thru 5. Many subalternatives and more complex arrangements can be depicted. However, with a goal of simplicity in design and other criteria listed, Concept 5 was selected. Some of these criteria are as follows in favor of Concept 5:

1) Easily meets a reasonable stowed position.
2) Deploys to a 6.1 m (20 ft) spread, clear of the top of the Shuttle, to provide adequate reach envelope (see Section E) and cargo clearance.
3) Can be made structurally adequate.
4) Has features amenable to ejection device if necessary in an abort.
5) Minimizes actuator mechanism envelope requirements between cargo and cargo bay forward bulkhead.
6) Relatively light weight.

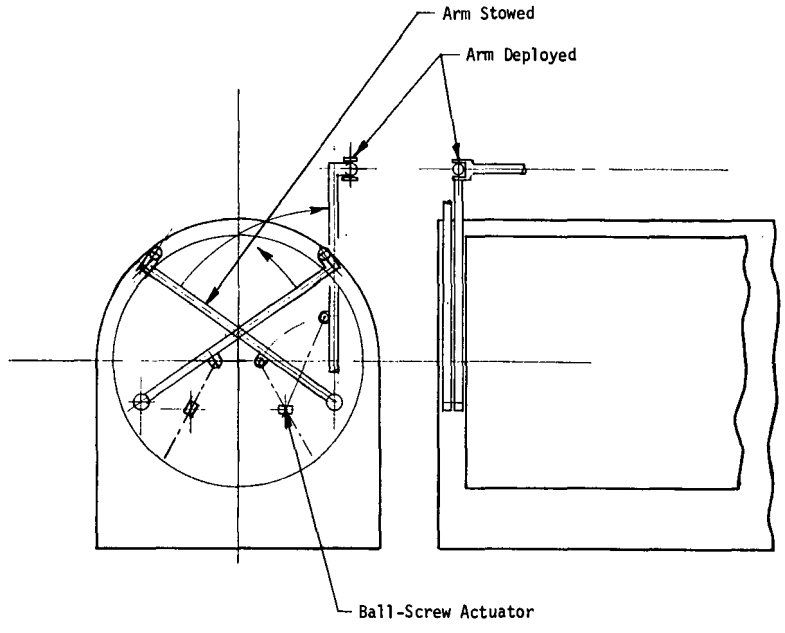

Concept 1

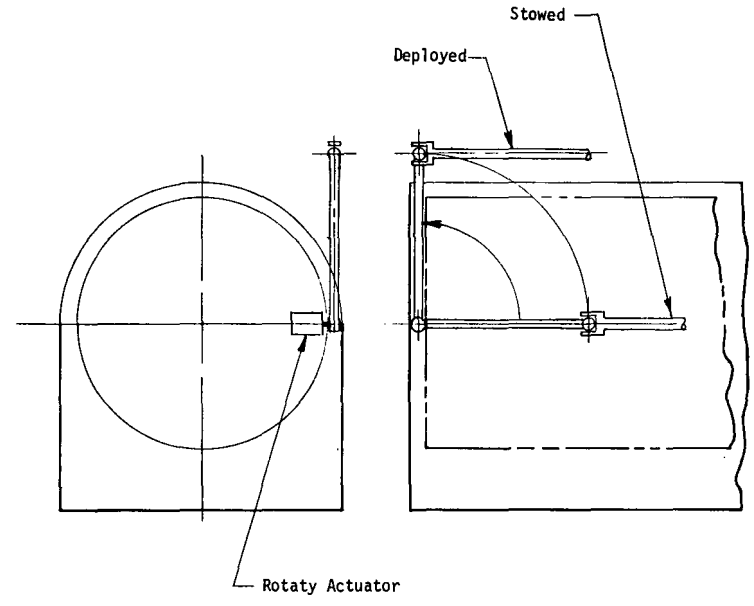

Concept 2

Fig. VII-13 Deployment Alternatives

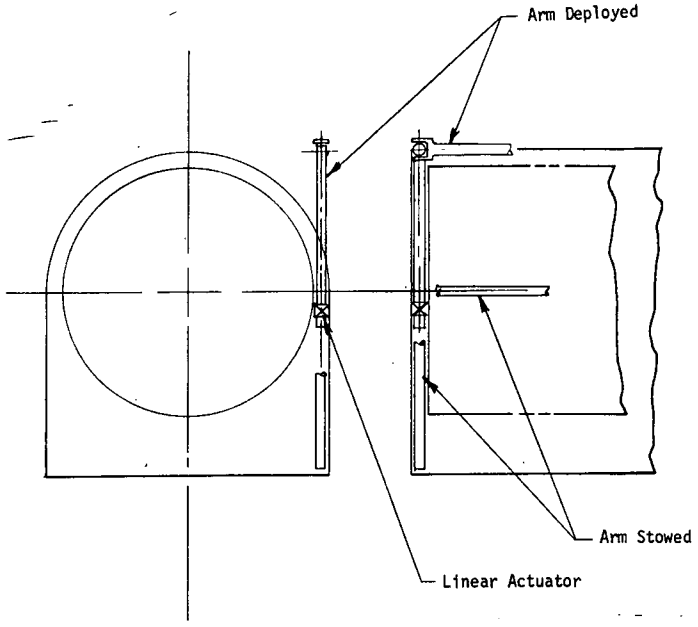

Concept 3

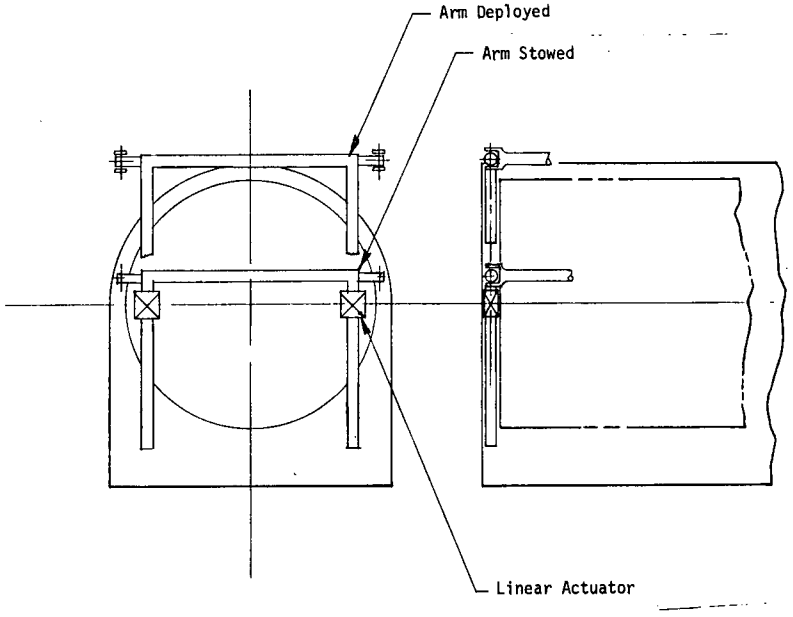

Concept 4

Fig. VII-13 (cont)

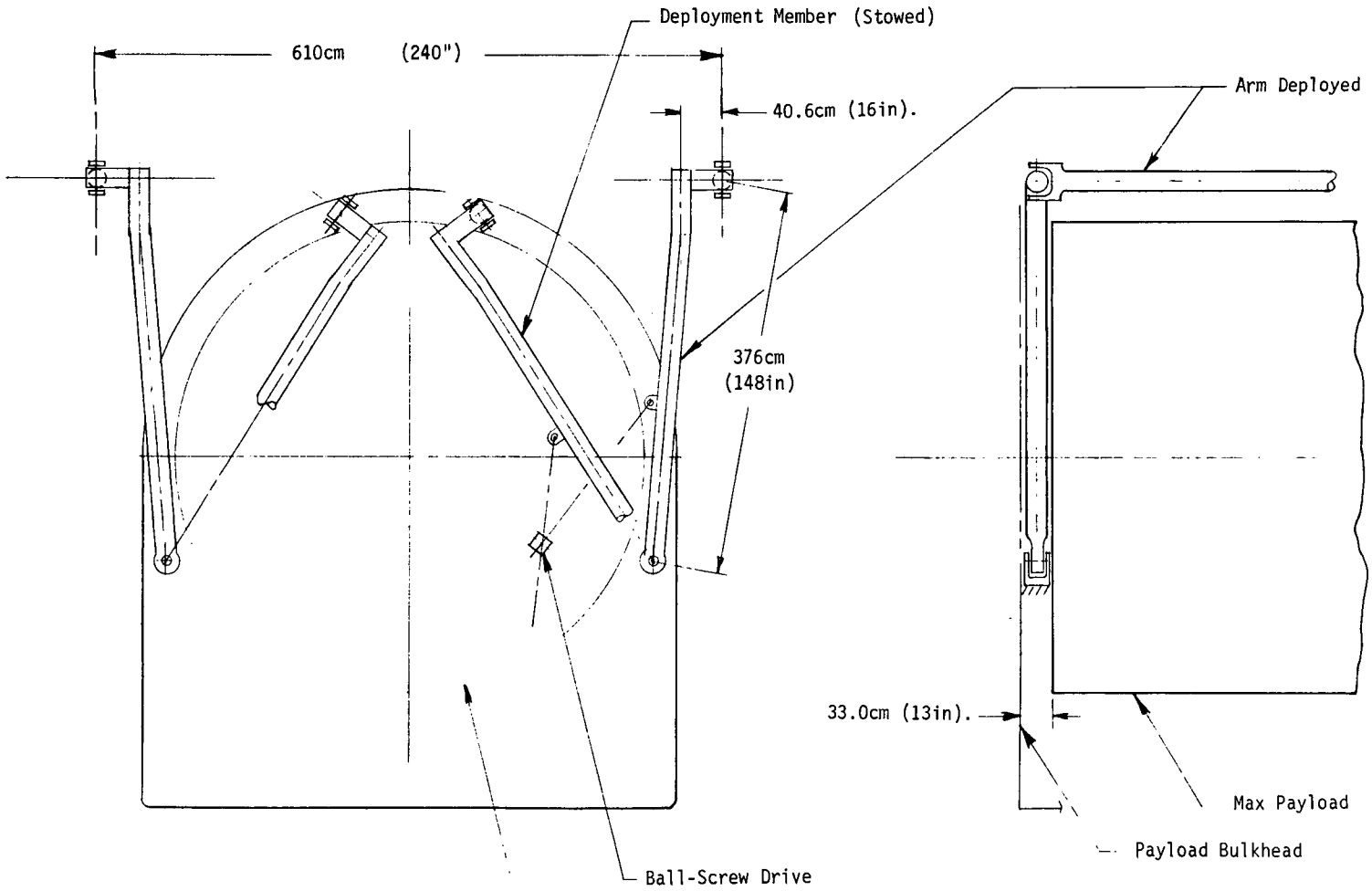

Fig. VII-13 (concl)

Details of the actuation mechanism for deployment can be varied. Although not included in this preliminary design, the mechanism selected is a screw jack device (with locks, stops, etc) as shown on the Concept 5 sketch. Here either the nut may be driven on a fixed ball screw or the screw may be driven on a fixed nut. The former is preferable from the standpoint of drive motor with wiring, fixed to the bulkhead.

Another drive scheme for the same deployment concept has a rotary actuator (hydraulic or electric motor driven) placed in the hinge pivot of the 376 cm (148 in.) deployment member. Torques are not high and a very small gear head motor could power the motion. If necessary a locking, hinged strut could be added as a truss member, similar to the jack screw. Many other devices such as cable drives, etc, could be considered; however, they are probably not necessary unless one of the above suggested schemes develops envelope problems.

I. GROUND TESTING

This section discusses the various alternatives available for ground testing of the RMS. The tests considered range from simple electrical tests to full motion tests. The disadvantages of designing the RMS to have full motion capability in a 1-g environment are presented, and an alternative technique for full motion testing using a booster actuator is presented.

1. Electrical Tests

The simplest checkout is continuity testing. This assures that all electrical components are electrically functional, but gives no indication of the state of the mechanical components. Torque can also be applied and measured at the torque motors without movement of the manipulator arm, but again this does not provide for checkout of the mechanical components. The primary accomplishment of the electrical checks is to provide a test of the telecommunications subsystem, and its interfaces with the other subsystems.

2. Motion Checks

If one considers the possibility of checking out the mechanical operation of the RMS on the launch pad, this seems only worthwhile if each degree of freedom can be moved through its entire range. Limited motion checks provide a little more than electrical checks. However, it is not necessary to check more than one motion at a time. An external load is also not required.

Examination of the beam stresses and deflection of a typical arm shows that it is safe to hold the arm out horizontally under its own weight. Deflections are higher than those encountered in space, but the stress limit of the arm is not approached.

Assuming a lower arm weight of 113 kg (250 lb) the torque required at the elbow to hold the lower arm fully horizontal is approximately 10 times the elbow torque required for cargo handling. With the 474 N-m (350 ft-lb) required elbow torque for the space applications, the lower arm can only be moved approximately 6° from an initial vertical position. If the torque capability of that joint were increased, a larger harmonic drive would be required; and if it is desired to have the same top speed in space as before a larger motor is required. The back drive friction would increase 4 to 5 times at the tip of the arm and the equivalent mass at the load cg increases accordingly, which results in degraded system performance and sensitivity.

To achieve full motion of the shoulder in a 1-g environment, a larger harmonic drive and motor are again required. The overall result on the arm design is a high weight penalty [estimated at 228 kg (500 lb) per arm], higher friction or back drive forces, and very badly deteriorated sensitivity. Therefore, this approach is not recommended.

3. Booster Actuator for Ground Checkout

To achieve full motion ground testing without significantly affecting the space design and performance, an alternative technique using a booster actuator is presented. The only place where one might conveniently place a booster actuator is on the first motion, which is a pitch motion with respect to the Shuttle. This also requires a large harmonic drive, but since neither top speed, inertia, or gear ratio are important for the checkout, a smaller motor will suffice. The booster actuator would be attached only for the checkout procedure and removed before launch. Thus the weight penalty does not apply to the flight hardware, and the performance characteristics for space tasks are not affected.

The test procedure would then be as follows: the pitch motion with booster actuator does not only move the arm through its entire range in this motion, but positions it so that the other motions can be checked out. For instance, yaw is checked out with the entire arm in the horizontal plane, upper arm roll with the entire arm vertically up, while for elbow motion, the pitch motion has to reposition itself in 12° increments so that the lower arm is never more than 6° from the vertical or, alternatively, a simple program could accomplish the same in synchronous fashion. Thus, full motion checkout of the RMS on the ground could be accomplished without any major effect on the design for space use. The only requirement is interface capability with a ground-mounted booster actuator for use during the checkout operations.

VIII. PRELIMINARY DESIGN AND ANALYSIS

A. SYSTEM DESCRIPTION

This section is divided into four major headings: (1) General Characteristics, (2) Physical Characteristics, (3) Performance Characteristics, and (4) Utility.

1. General Characteristics

The RMS consists of two identical manipulator arms mounted near the forward bulkhead of the Shuttle Orbiter cargo bay, as illustrated in Fig. VIII-1. Since the two arms are identical, the actual design effort is limited to only one arm. The arm is designed so that only one arm is required to accomplish all tasks associated with capture, docking, or cargo handling operations. Thus, the RMS is redundant, in that if one arm fails, the other arm can be used to accomplish all the required tasks except orbital assembly. In addition, each joint uses two motors, so that if one motor fails, the joint can still be moved with full speed and torque capabilities. In the event of a frozen joint failure, the arm possesses an explosive bolt device, so that the arm can be jettisoned to allow the cargo bay doors to be closed for reentry.

Viewing for manipulator operations will be provided by direct viewing from the Shuttle cockpit, supplemented by TV cameras each with two attached floodlights. One camera is mounted near the terminal device of each arm to provide close-up viewing. Another TV camera is mounted at the base between the two arms for more general viewing. This camera automatically tracks the terminal device. A third TV camera is mounted at the rear of the cargo bay for overall viewing. Two additional sets of floodlights are mounted in the cargo bay. All TV signals, as well as all control and actuator signals, will be transmitted via a hardwire system. The TV and control signals will be transmitted and processed in analog form, with A/D and D/A converters used for input-output interfaces with the Shuttle digital computer, which will perform the necessary computational tasks. The joint angular position and angular velocity are measured with a potentiometer and tachometer, respectively, at each joint. Motors and gear reducers form the actuators for the articulation of each joint.

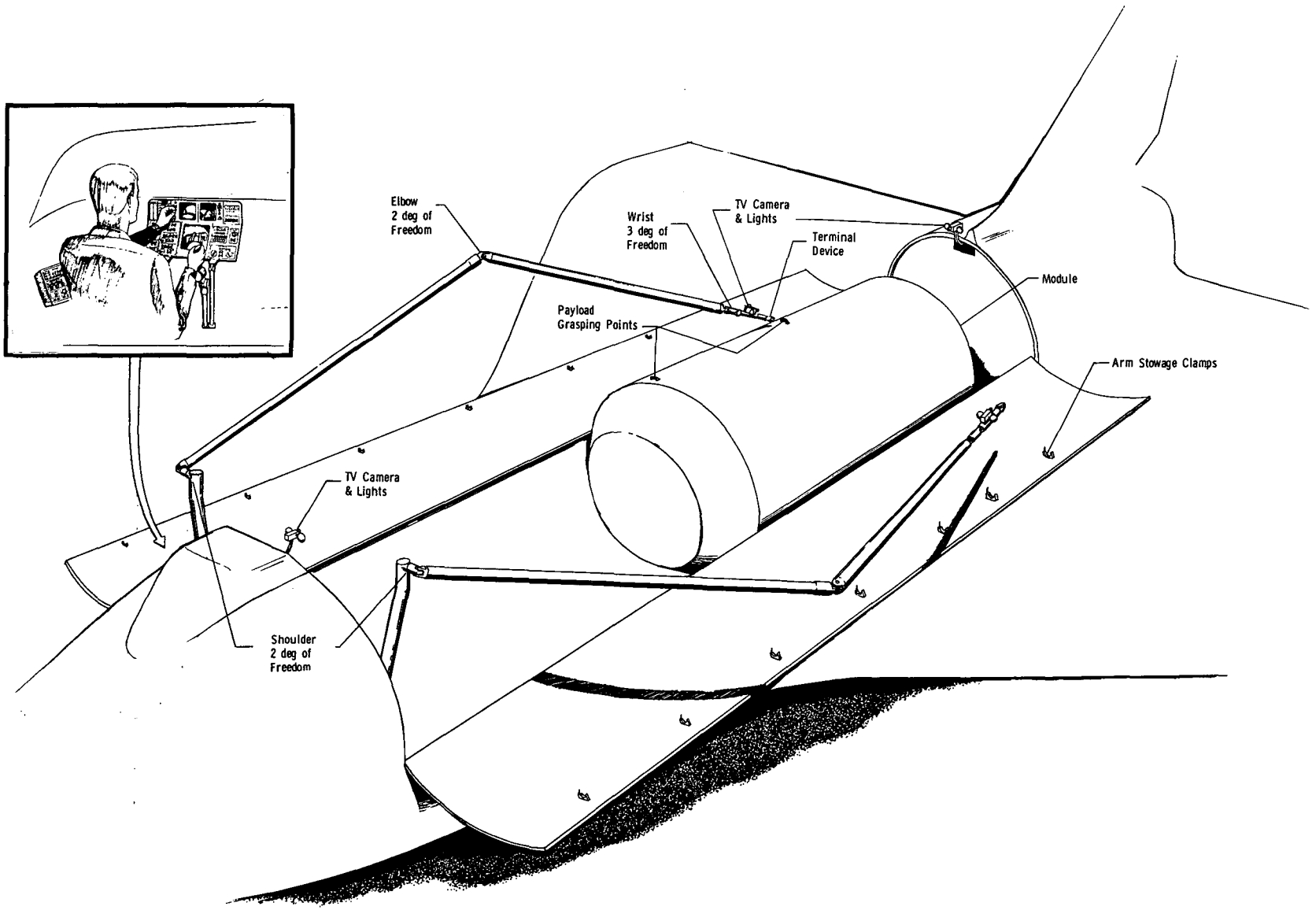

Fig. VIII-1 Remote Manipulator System

The RMS is controlled by a single crewman from a control and display station in the Shuttle crew quarters area. The controls and display station contains three TV monitors, two controllers, and all necessary activating, checkout, operating, and monitoring controls and displays. Figure VIII-2 is the block diagram representation of the RMS.

2. Physical Characteristics

The overall length of each arm from the shoulder to the wrist is 14.3 m (47 ft) with an additional 0.9 m (3.0 ft) from the wrist to the terminal device. The shoulder-to-elbow segment is 7.15 m (23.5 ft) and is equal to the elbow-to-wrist segment. The arm diameter is such that the arm can be stowed in an approximately 20.3 cm (8 in.) diameter volume along the length of the cargo bay. The arm is mounted to a deployment mechanism that raises the arm out of the cargo bay and places the shoulder joints at a separation distance of 6.1 m (20 ft). The total weight of both arms and their deployment mechanisms is less than 1135 kg (2500 lb); the arm beam material is aluminum. The total RMS weight including both arms, deployment mechanisms, control console, Shuttle surface mounted TV, and control and data electronics is 1263.6 kg (2783 lb). If Lockalloy were used in place of aluminum for the beam material, the total RMS weight would be 619.3 kg (1364 lb).

Each arm is comprised of a two degree of freedom shoulder with a pitch-yaw rotational sequence, a two degree of freedom elbow with a roll-yaw sequence, and a three degree of freedom wrist with a yaw-pitch-roll sequence. In addition, each arm is equipped with a hand type terminal device* with one degree of freedom. The joint travel limits, which are ±200 and ±130 degrees for the shoulder pitch and yaw, ±200 and ±155 degrees for the elbow roll and yaw, ±120 degrees for the wrist yaw and pitch, and ±200 degrees for the wrist roll, are such that full coverage of the working area is obtained.

The arm is designed for a maximum tip force of 44.5 N (10 lb), which results in shoulder torques of 667 N-m (500 ft-lb), elbow torques of 474 N-m (350 ft-lb), and wrist yaw and pitch torques of 202 N-m (150 ft-lb). The wrist roll torque is 88 N-m (65 ft-lb). The arm is designed for a maximum of 0.0254 m (1 in.) tip deflection with the maximum applied tip force of 44.5 N (10 lb).

*Terminal device is candidate concept.

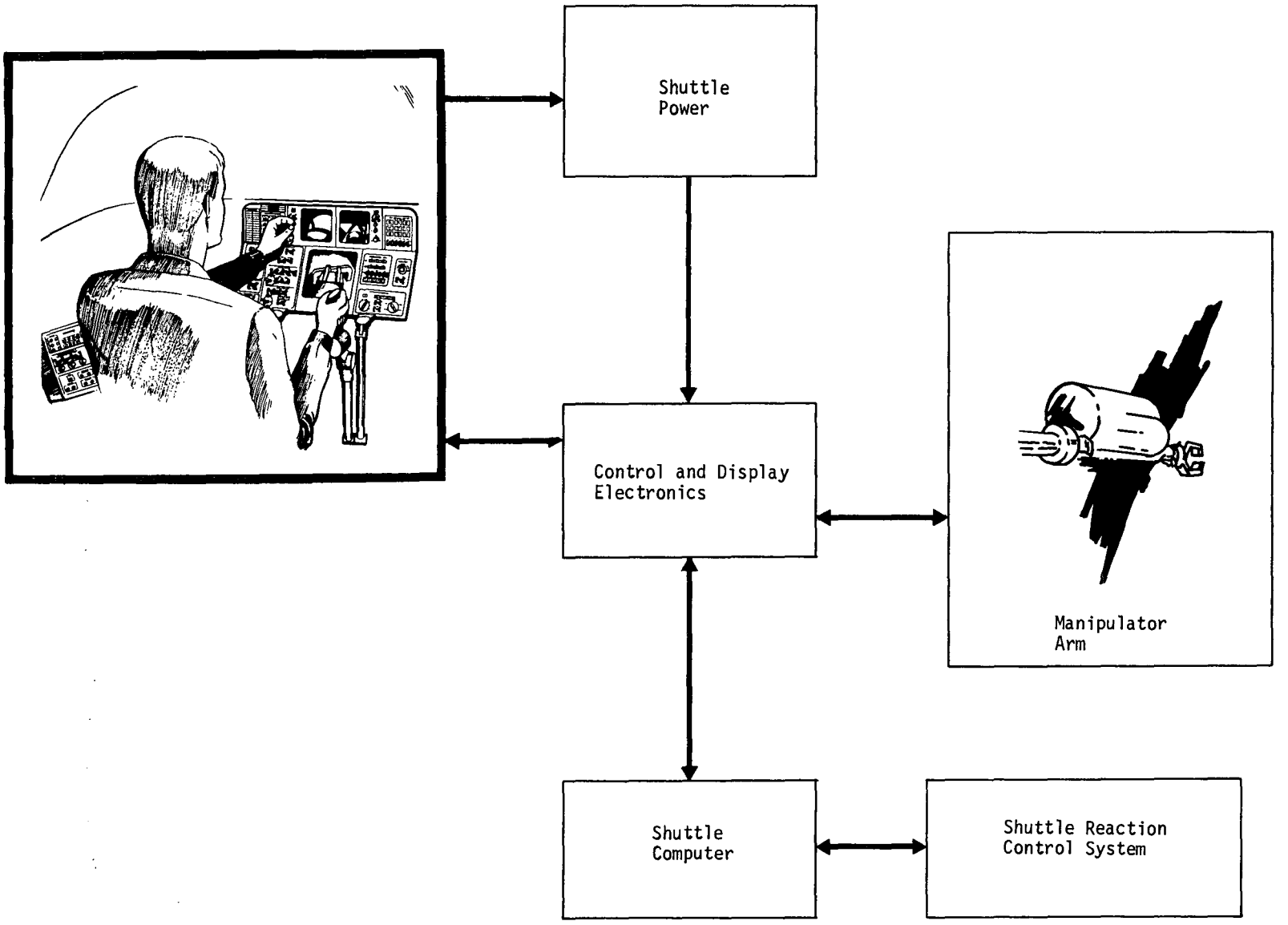

Fig. VIII-2 RMS Block Diagram

3. Performance Characteristics

The RMS control system incorporates force feedback to allow the operator to feel the contact forces and moments. The input controller consists of either a geometrically similar master controller, a six degree of freedom handcontroller, or two three degree of freedom handcontrollers. For analysis purposes, the master arm controller was assumed, since it presents somewhat higher requirements from the standpoint of crew cabin volume and control logic. The control system has four basic modes of operation: (1) manual control with low sensitivity for positioning the arm in the general vicinity of the desired area; (2) manual control with high sensitivity for fine manipulations; (3) computer augmentation for indexing and coordinate transformation requirements; and (4) computer programmed automatic control for predetermined tasks such as arm deployment and cargo transfer. The RMS is designed to be controlled by a single crewman.

Thus, the control system provides the necessary control sensitivity for fine manipulation tasks, and also provides reduced sensitivity for gross movements of the manipulator arm. The joint velocities are such that a no-load tip speed of 0.455 m/sec (1.5 ft/sec) and a full load tip speed of 0.053 m/sec (0.174 ft/ft/sec) can be attained. The joint acceleration levels allow the arm to be stopped in 0.455 m (1.5 ft) under no load, and in 4.57 m (14 ft) under full load, with an initial velocity equal to the appropriate maximum speed capability of the arm. The joint positional accuracy is ±0.03 deg/second. These accuracies allow a tip positional error of ±0.051 m (2 in.) and a tip velocity error of ±0.0152 m/sec (0.05 ft/sec) to be maintained, excluding the tip deflection and vibrational characteristics.

4. Utility

For the docking operation, the arm is used to capture the orbital payload. After capture the arm does not initially apply the necessary forces and moments to slow the initial relative velocities between the Shuttle and the Space Station or other orbital payloads. Instead, the arm acts as a sensor to provide control inputs to the Shuttle RCS thrusters. This can either be accomplished in a manual mode wherein the relative positions and velocities are displayed to the Shuttle pilot, or an automatic system can be employed with the arm sensors feeding directly through the RCS logic and controlling the thrusters.

After the initial velocity has been reduced to an acceptable level for arm control, [0.03 m/sec (0.1 ft/sec)], the arm can be used to supply the forces and moments to complete the docking maneuver, or the arm can provide control inputs to the RCS thrusters to perform the docking. The docking maneuver will be performed

in a flyby manner rather than a head-on approach, so that in the event of a "redesignate and fly-around" maneuver the two vehicles will not be on a collision course.

Assembly operations can be performed by utilizing both arms (one at a time) of the RMS system. The reach envelope of each arm provides enough overlap so that no difficulty will be encountered during assembly operations.

For the problem of cargo transfer to the Space Station from a station-keeping mode rather than from a docking configuration, no unsurmountable obstacles are found. In stationkeeping close to the Space Station (so that the arm can move the cargo from the Shuttle to the Space Station docking port), a high workload is placed on the Shuttle pilot, but it is not an impossible task. The stationkeeping task can be made much simpler or even completely automatic by capturing the Space Station with one arm of the RMS and using it as a sensor in a manner similar to that used for the Shuttle docking task. This reduces the workload and leaves the other arm free for cargo transfer. An important factor that could present a problem is the fact that with a large cargo attached to the arm, the RCS thruster firings place high torque loads on the joints. This could lead to undesirable and uncontrolled motion of the cargo. But this problem may be overcome with the bilateral force feedback compliant control system. With this system, the arm can be backdriven, and over a given distance the operator can manually compensate for the RCS torques (since he will feel them) by controlling the arm position; or similar to the docking technique, the computer can control both the docking, the Shuttle RCS, and the control inputs to the arm. Thus, cargo transfer can be accomplished from a stationkeeping mode as well as from a docked mode.

Many tasks other than those which are specific RMS requirements can be accomplished. Satellite retrieval and maintenance can be accomplished using one arm for retrieval and holding of the satellite, while the other arm is used to perform the maintenance tasks. With special terminal device (TD) designs, spinning satellites can be captured and despun, and if the TD has several degrees of freedom with fine control, repair or assembly of delicate components can be accomplished. Other tasks which can be accomplished include visual inspection of the Shuttle or Space Station exterior using the TD camera, orbital photography, self-maintenance wherein one arm performs maintenance operations on the other arm, and a wide variety of other orbital operations.

B. CONTROL

This section presents the preliminary design of a master/slave force reflecting servosystem. This system was selected for analysis purposes since it places somewhat higher logic requirements on the control system to accomplish the indexing and coordinate transformations necessary to allow full volume motion coverage of the large manipulator arm using a small master controller. Special attention is given to (1) design and analysis of the servo control for the shoulder joint, (2) computer augmentation for the master/slave system when the two arms are operating in a nondirect angle tracking mode, and (3) discussion and examples of the coordinate transformations needed for operation in different coordinate axis systems.

A position-position force reflecting system is selected for analysis of the shoulder joint, and is analyzed from the transfer function matrix view point. The conditions on the system gains are given for the master-slave operation to meet the required performance criteria. It is shown that the gains must change as the arms are transferred from a 1:1 to an 18:1 angle tracking mode. The servosystem was programmed on an analog computer and runs were made simulating the response of the shoulder joint for a representative set of system gains, with input torques applied at both the master and the slave. It is shown that the servosystem investigated has a damping ratio of $\delta = 0.68$ and a damped natural frequency of $\omega_d = 0.88$ rad/sec.

The computer augmentation needed for the master-slave system is discussed and a block diagram is presented illustrating the manner in which the computer will interact with the servo control. The functions performed by the computer include coordinate transformations, adjustment of the system gains, position indexing for full volume motion coverage, and the provision of control commands for preprogrammed operations.

SYMBOLS AND SUBSCRIPTS

θ = Pitch (rotation about reference y axis)

ϕ = Roll (rotation about reference x axis)

ψ = Yaw (rotation about reference z axis)

S = Sine

C = Cosine

T = Torque

s = Shoulder, slave

ε = Elbow

w = Wrist

m = Master

R = Reference axis

c = Command axis

q = Position Gain Between Master and Slave

where:

$_{k}[\ ]_{ij}$

i - Denotes joint location (i.e., shoulder, elbow, wrist)

j - Axis location (i.e., reference or command)

k - System Location (i.e., master or slave)

DEFINITIONS AND ACRONYMS

DOF	Degrees of Freedom
M/S	Master/Slave
Adaptive	Capable of making decisions based on past experience
Anthropomorphic	Actuators or controls resembling human body segments in terms of degrees of freedom and how they are articulated
Backlash	The movement a joint goes through before responding to a command
Bilateral	Force reflecting, two way, forces and motions at either master or slave act as control inputs
Closed Loop	Feedback is present (visual not included)
Cross Coupling	When motion in one direction causes motion in another
Degree of Freedom	A dimension of motion in a Teleoperator (i.e., shoulder rotation, wrist rotation, etc)
General Purpose Manipulator	A man-controlled device with seven or more independent motions
Indexing	The ability of a Teleoperator to change relative orientation between Master and Slave

Inertia Forces	A measure of the difficulty of accelerating and decelerating the manipulator arms
Master/Slave	A Teleoperator in which forces and torques are proportionally reproduced from controls (master) to the actuators (slave)
Open Loop	No feedback of any kind (other than visual)
Panel Control	Usually synonymous with unilateral systems, input commands originate from switches, potentiometers, joy stick, etc.
Preprogrammed	Commands are prerecorded
Reliability	The probability that the system will operate at some level of performance for a stipulated length of time
Special Purpose Manipulator	Limited motion manipulator with less than six degrees of freedom at the terminal device
Supervisory Control	Use of computers at the operator end to aid decision making and at the actuator end for adaptive control and application of subroutines
Time Delay	Command and feedback delay due to: (1) separation distance; (2) transmission lines; (3) human reaction; (4) system lags
Unilateral	One way control (inputs at master only)

1. Modes of Operation

The master-slave servosystem will have the following four basic modes of operation.

1) Manual control in the 1:1 angle tracking mode. For positioning the slave arm to a general location or in the transferring of an object over a sizable distance in the slave's work volume, it is desired that the joint angles transcribed by the master and slave be equal.

2) Manual control in the 18:1 angle tracking mode. When delicate maneuvers are to be performed with the slave, it is desired that an 18:1 angle tracking mode be initiated. In this mode of operation, angles transcribed at the joints of the master are 18 times as large as the corresponding transcribed angles on the slave.

3) Positional and coordinate indexing. It is desired that the system have positional indexing capabilities so that the restricted volume of operation for the master arm does not hinder full volume operation of the slave arm. Likewise coordinate indexing is required so that transformations of the control signals can be made when the master and slave arms are operating in different coordinate systems. The need to operate in different coordinate systems arises in three situations:

   a) Close in target approach is viewed from the terminal device camera; therefore the slave must operate in the terminal device coordinate system;

   b) Manipulator positioning and cargo handling is viewed from the slave arm base camera; therefore the slave must operate in the base camera coordinate system;

   c) Preprogrammed control routines for the slave manipulator assume a Shuttle coordinate axis; therefore the slave must operate in a Shuttle based coordinate system.

4) Computer preprogrammed control. For the various predetermined tasks that the slave arm must perform, such as deployment, docking and cargo placement or retrieval, the control routine for the slave servosystem need not be supplied by the man but can be computer-directed.

2. Servosystem Design

a. General - In the preliminary design of a force-reflecting remote manipulating system (RMS) where the slave arm is in the order of 25 times larger than the master arm, a single joint (the shoulder) is investigated. Although the torques encountered at the shoulder of the slave are considerably larger than the torques developed at the other joints, the design of the shoulder bilateral servosystem is representative of the design for the remaining joints of the RMS.

The RMS considered in the following design of the shoulder joint bilateral system consists of a 0.61 m (2 ft) master arm and a 15.25 m (50 ft) slave arm. Since the maximum slave tip force is 44.5 N (10 lb) and this is a comfortable operating range for manual control of the master, a 1:1 force reflection ratio is selected. This implies that a 44.5 N (10 lb) force applied to the

master results in the same 44.5 N (10 lb) tip force at the slave, and vice versa. Thus, the maximum torque on the output shaft of the slave is 679 N-m (500 ft-lb) and the maximum torque on the master output shaft is 27.2 N-m (20 ft-lb). When the maximum tip force of 44.5 N (10 lb) is applied at either the master or the slave, the steady-state angular velocity of the shoulder joint of either member of the RMS is not to exceed 0.03 rad/sec. Figure VIII-3 depicts the shoulder joint analyzed and its performance criteria as previously described.

Force-reflecting or bilateral servosystems have been extensively analyzed by Arzbaecher (Ref 1) and constructed in the Prototype phase by Flatau (Ref 2) and commercially produced by Central Research Laboratory, under the direction of Goertz (Ref 3) of the Argonne National Laboratory.

A force-reflecting system can be constructed by connecting two positional servomechanisms so that the overall system is bilateral. The two most widely investigated methods of realizing a bilateral system, the position-position and the position-force type configurations, are discussed briefly in the following paragraphs.

A position-position force reflecting system, shown in Fig. VIII-4, is constructed from two positional servomechanisms, each of which is driven by the error signal between the master and slave angular displacement. Thus, when an input torque is applied to the master servo of such a magnitude to overcome static friction, a change in the master position occurs and therefore an error signal is developed between master and slave. The error signal actuates the slave servo, which moves in the same direction as the master, in an attempt to null the position error signal. A similar mode of behavior develops when a disturbance torque is applied to the slave. Under this condition, a position error signal is developed which activates the master servo, and a torque, proportional to the disturbance torque, is developed which enables the master to "track" the slave. Thus, the system of Fig. VIII-4 is a positional tracking, force reflecting servosystem.

The position-force, force reflecting system, shown in Fig. VIII-5, differs from the position-position type configuration in that the master servo is no longer driven by a position error signal, but is activated by a signal directly proportional to the torque developed at the slave. Therefore, when the master receives an input torque of sufficient size to overcome the system static friction, the master undergoes a position change, a positional

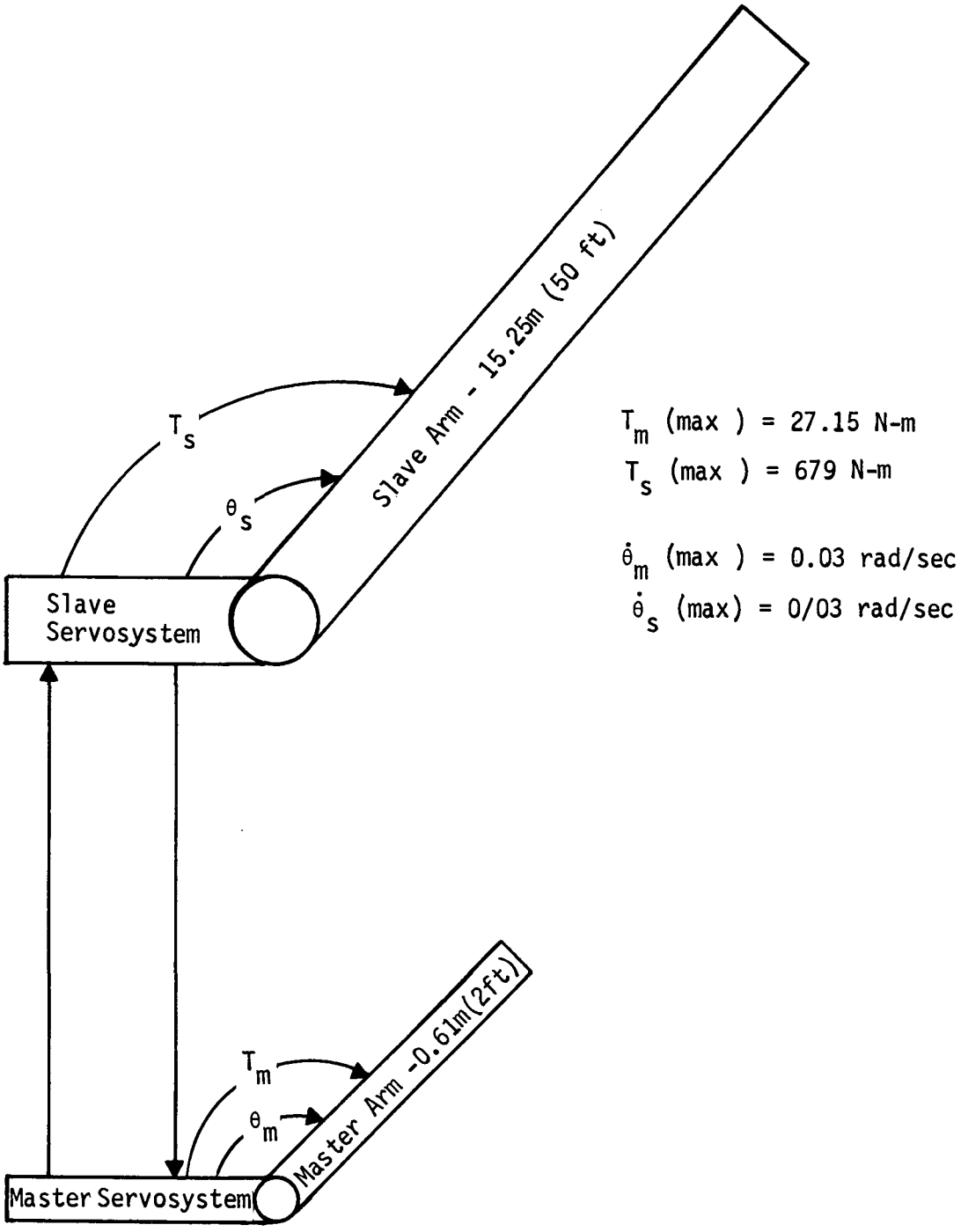

Fig. VIII-3 Master-Slave Shoulder Joint

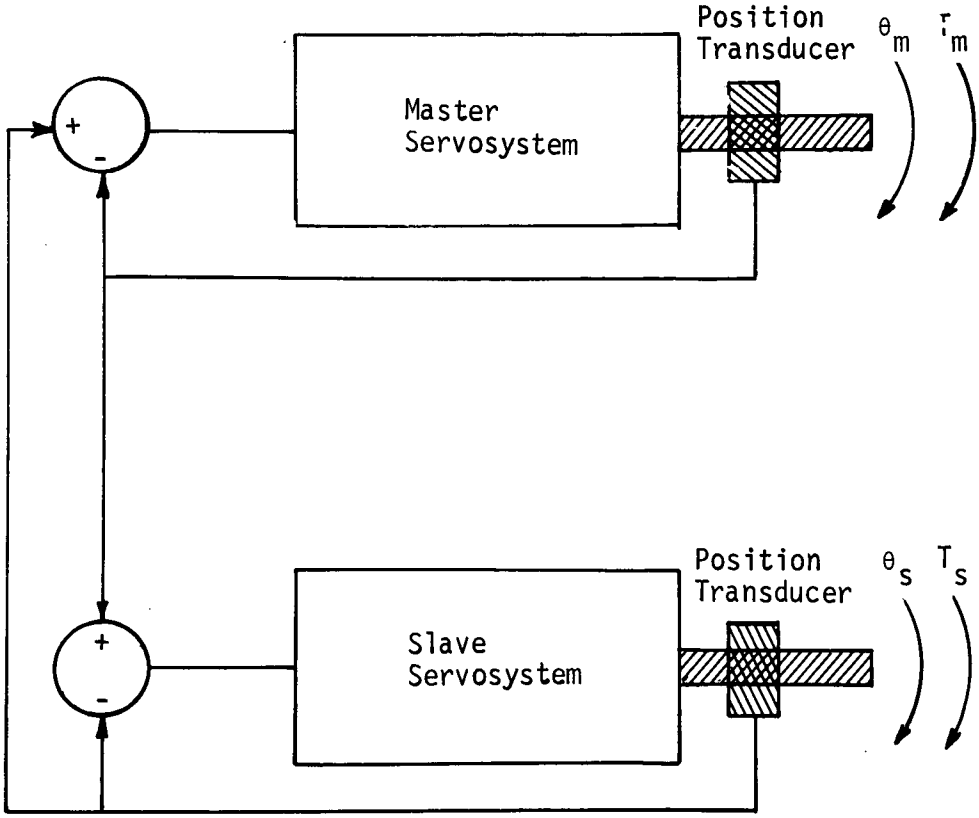

T_m = Torque on Master Output Shaft

T_s = Torque on Slave Output Shaft

θ_m = Master Angular Displacement

θ_s = Slave Angular Displacement

Fig. VIII-4 Position-Position, Force Reflecting Servosystem

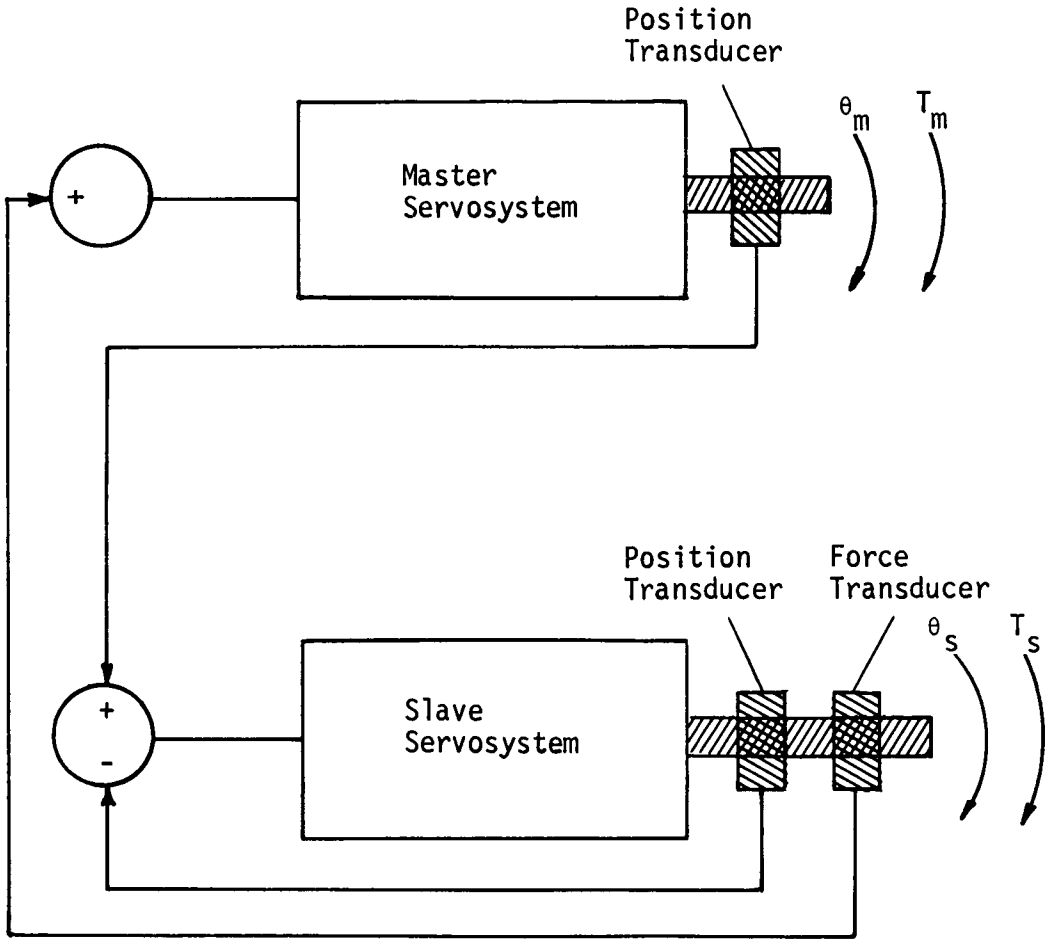

T_m = Torque on Master Output Shaft

T_s = Torque on Slave Output Shaft

θ_m = Master Angular Displacement

θ_s = Slave Angular Displacement

Fig. VIII-5 Position-Force, Force Reflecting Servosystem

error signal develops, and the slave attempts to follow the master. When a disturbance torque is applied to the slave, it is fed directly to the master which, if the torque is large enough to overcome static friction, undergoes a position change. A positional error signal is thus developed and the slave servo is activated to follow the master. Therefore, the system of Fig. VIII-5 is a positional tracking, force-reflecting servosystem.

b. Shoulder Joint Analysis - The position-position type force-reflecting system of Fig. VIII-4 was selected to be used for the analysis of the bilateral RMS shoulder joint. This selection was made primarily for two reasons. First, the position-position type system needs no force transducer, which is desirable since force transducers are inherently unstable, nonlinear, and difficult to calibrate. Secondly, if no force transducer is needed, the number of components and internal communication links of the RMS is reduced.

Figure VIII-6 shows the block diagram of the bilateral servosystem analyzed for the shoulder joint. Tachometric feedback is included in the master and slave servo loops as a means of stabilizing the system.

The gains, inertias, torques, and angles of Fig. VIII-6 are defined as follows.

T_m = Input torque on the master servo shaft

T_1 = Torque generated by the master servomotor

T_s = Disturbance torque on the slave servo shaft

T_2 = Torque generated by the slave servomotor

J_1 = Moment of inertia of master servo motor and gear train

J_2 = Moment of inertia of slave servo motor and gear train

θ_m = Angular displacement of master arm

θ_s = Angular displacement of slave arm

K_1 = Total gain of master servo; comprised of amplifier gain, gear train gain, and motor characteristics

K_4 = Total gain of slave servo; comprised of amplifier gain, gear train gain, and motor characteristics

K_2 = Back EMF coefficient of master servo plus gain of feedback tachometer

K_5 = Back EMF coefficient of slave servo plus gain of feedback tachometer

K_3 = Position feedback gain for master

K_6 = Position feedback gain for slave

τ_1 = Electrical time constant of master servo

τ_2 = Electrical time constant of slave servo.

It is necessary to determine the gains of the system shown in Fig. VIII-6, so that the required performance parameters are met. This is done by first deriving the transfer function matrix between the two inputs $\left(T_m \text{ and } T_s\right)$ and the two outputs $\left(\dot{\theta}_m \text{ and } \dot{\theta}_s\right)$, and then by relating the various performance criteria to the members of this matrix.

The above-mentioned transfer function matrix is easily derived by state variable methods, or simply by writing the various loop equations and solving for the appropriate terms, and is given by

$$\begin{bmatrix} \dot{\theta}_m \\ \dot{\theta}_s \end{bmatrix} = \begin{bmatrix} \frac{S(S^2J_1J_2^2 + SK_4K_5J_1J_2 + K_4K_6J_1J_2)}{D} & \frac{SK_1J_1J_2}{D} \\ \frac{SK_4J_1J_2}{D} & \frac{S(S^2J_1^2J_2 + SK_1K_2J_1J_2 + K_1K_3J_1J_2)}{D} \end{bmatrix} \begin{bmatrix} T_m \\ T_s \end{bmatrix} \qquad [B\text{-}1]$$

where the denominator term D is given by

$$D = S^4(J_1^2J_2^2) + S^3(K_1K_2J_1J_2^2 + K_4K_5J_1^2J_2) + S^2(K_1K_3J_1J_2^2 + K_1K_2K_4K_5J_1J_2 + K_4K_6J_1^2J_2) + S(K_1K_3K_4K_5J_1J_2 + K_1K_2K_4K_6J_1J_2) + (K_1K_3K_4K_6J_1J_2 - K_1K_4J_1J_2). \qquad [B\text{-}2]$$

The above transfer function matrix was derived under the assumption that the electrical time constants of the master and slave servos are negligibly small.

When a step input torque, T_m, occurs on the master, it is desired that the system velocities $\left(\dot{\theta}_m \text{ and } \dot{\theta}_s\right)$ rise to a constant steady-state value and remain there until the torque is removed or an opposing disturbance torque, T_s, is encountered. A similar

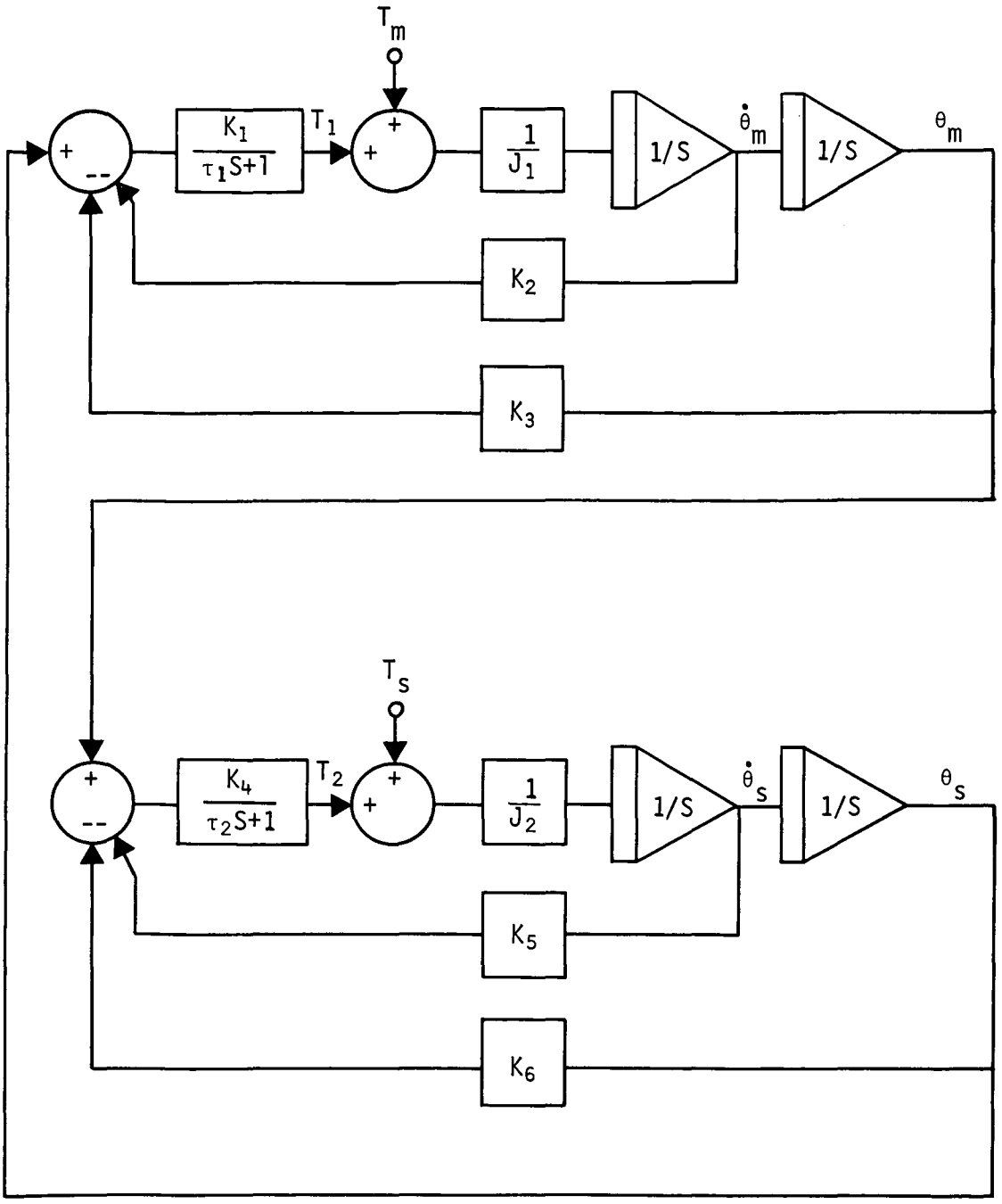

Fig. VIII-6 Master-Slave Position-Position Force-Reflecting Servosystem for a Single Joint, Block Diagram

operation is required when the disturbance torque, T_s, is a step input. Due to the zero at the origin in each element of the above matrix equation, this mode of operation will not occur unless each of these zeros is cancelled by a pole at the origin from the denominator polynomial D. For D to have a root at the origin, its last term must be made equal to zero, that is,

$$K_1K_3K_4K_6J_1J_2 - K_1K_4J_1J_2 = 0 \qquad [B-3]$$

or

$$K_3K_6 = 1. \qquad [B-4]$$

Therefore, the product of the positional feedback gains (K_3 and K_6) must equal 1 for the system to behave in the desired manner. Under this condition, D has one root at the origin and must have its remaining three roots in the left-half plane if the system is to be stable and exhibit the required behavior. Performing a Routh stability test on D reveals that for its non-zero roots to have negative real parts, a sufficient condition is for all the gains K_i of Fig. VIII-6 to be greater than zero. Thus,

$$K_i > 0 \quad i = 1, 2, \ldots 6 \qquad [B-5]$$

is the second condition that the gains of the system must satisfy.

As stated earlier, a one newton tip force at the master is desired to be reflected as a one newton tip force at the slave. Considering the lengths of the master and slave arms, this condition manifests itself as a 0.61 N-m (0.45 ft-lb) torque at the master servo output shaft being reflected to the slave servo output shaft as a 15.25 N-m (11.25 ft-lb) torque. Thus, if a one newton force is applied at the tip of the master and a minus one newton force is applied at the tip of the slave, it is desired that the system remain at rest. In other words, if $T_m(t) = 0.61\mu(t)$ and $T_s(t) = 15.25\mu(t)$, where $\mu(t)$ is the unit step, the steady-state velocities $\left(\dot{\theta}_m \text{ and } \dot{\theta}_s\right)$ are required to be zero. If Z_{11} is the (1,1) element, Z_{12} the (1,2) element, Z_{21} the (2,1) element, and Z_{22} the (2,2) element of matrix Equation [B-1], then $\dot{\theta}_m$ and $\dot{\theta}_s$ are given by

$$\begin{bmatrix} \dot{\theta}_m \\ \dot{\theta}_s \end{bmatrix} = \begin{bmatrix} Z_{11} & Z_{12} \\ Z_{21} & Z_{22} \end{bmatrix} \begin{bmatrix} T_m \\ T_s \end{bmatrix} \qquad [B-6]$$

If $T_m(t) = 0.61\mu(t)$ and $T_s(t) = -15.25\mu(t)$, the Laplace transforms of these two torques are $T_m(S) = \frac{0.61}{S}$ and $T_s(S) = \frac{-15.25}{S}$.

Substituting these values into Equation [B-6] yields

$$\begin{bmatrix} \dot{\theta}_m \\ \dot{\theta}_s \end{bmatrix} = \begin{bmatrix} \frac{Z_{11}}{S} & \frac{Z_{12}}{S} \\ \frac{Z_{21}}{S} & \frac{Z_{22}}{S} \end{bmatrix} \begin{bmatrix} 0.61 \\ -15.25 \end{bmatrix} \qquad [B-7]$$

Using the final value theorem and setting $\dot{\theta}_m$ (steady state) and $\dot{\theta}_s$ (steady state) equal to zero as required gives

$$\dot{\theta}_m \text{ (steady state)} = \lim_{S\to 0} S\dot{\theta}_m = \lim_{S\to 0} [0.61Z_{11} - 15.25Z_{12}] = 0$$

$$\dot{\theta}_s \text{ (steady state)} = \lim_{S\to 0} S\dot{\theta}_s = \lim_{S\to 0} [0.61Z_{21} - 15.25Z_{22}] = 0. \qquad [B-8]$$

Under the condition $K_3K_6 = 1$, substituting for the Z_{ij} from Equation [B-1], and letting S approach the limit zero, Equation [B-8] becomes

$$\begin{aligned} &1)\quad 0.61K_4K_6 - 15.25K_1 = 0 \\ &2)\quad 0.61K_4 - 15.25K_1K_3 = 0 \end{aligned} \qquad [B-9]$$

Since K_3K_6 is taken equal to 1, equations 1) and 2) of [B-9] are equal and given by

$$K_4 = 25\ K_1K_3. \qquad [B-10]$$

The above equation represents the third constraint on the K_i of Fig. VIII-6.

As mentioned previously, when a 44.48 newton (10 lb) tip force is applied at either the master or slave, the maximum value of $\dot{\theta}_m$ and $\dot{\theta}_s$ is not to exceed 0.03 rad/sec. Thus, if $T_m(S) = \frac{(0.61)(44.48)}{S} = \frac{27.15}{S}$ and $T_D(S) = 0$, the steady-state value of

$\dot{\theta}_m$ and $\dot{\theta}_s$ must equal 0.03 rad/sec. Mathematically, this is stated as

$$1)\quad \dot{\theta}_m \text{ (steady state)} = \lim_{S\to 0} S\dot{\theta}_m = \lim_{S\to 0} (27.15Z_{11}) = 0.03$$

$$2)\quad \dot{\theta}_s \text{ (steady state)} = \lim_{S\to 0} S\dot{\theta}_s = \lim_{S\to 0} (27.15Z_{21}) = 0.03. \qquad [B\text{-}11]$$

Substituting for Z_{11} and Z_{21} from Equation [B-1], letting S approach the limit zero and setting $K_3K_6 = 1$, Equation [B-11] becomes

$$1)\quad 27.15K_6 = 0.03(K_1K_3K_5 + K_1K_2K_6)$$

$$2)\quad 27.15 = 0.03(K_1K_3K_5 + K_1K_2K_6). \qquad [B\text{-}12]$$

Obviously K_6 must equal 1, and therefore $K_3 = 1$, for 1) and 2) of [B-12] to be simultaneously satisfied. With $K_3 = K_6 = 1$, 1) and 2) of [B-12] are equal and given by

$$905 = K_1(K_2 + K_5). \qquad [B\text{-}13]$$

Recapitulating, if the bilateral servosystem of Fig. VIII-6 is to meet the performance requirements as set forth previously, the following conditions must be met:

$$1)\quad K_3 = 1$$

$$2)\quad K_6 = 1$$

$$3)\quad K_i > 0 \qquad i = 1, 2, 3, 4 \qquad [B\text{-}14]$$

$$4)\quad K_4 = 25K_1$$

$$5)\quad 905 = K_1(K_2 + K_5).$$

Now that the conditions on the gains, K_i, have been set forth for the system of Fig. VIII-6 to meet the required performance criteria, it is desired to select a representative set of gains for the master-slave bilateral system being considered.

Inland Motor Company torque motors have been selected for the master-slave servos, with an Inland T-1352 being used for the master arm and an Inland T-1342 used for the slave arm. Considering the master arm first, the total gain of the master servo, K_1, is calculated as follows. K_1 is defined by the equation

$$K_1 = \frac{K_{T1}}{R_{T1}} \left(K_{S1}\right), \qquad [B-15]$$

where K_{T1} is the torque sensitivity of the master servo, R_{T1} is the total resistance of master servo and power amplifier, and K_{S1} is the master servo static sensitivity. The master servo static sensitivity, K_{S1}, is defined as the product of the gain of the master servo gear train and the gain of the master servo amplifier. If the master and slave angular displacements $\left(\theta_m \text{ and } \theta_s\right)$ are required to have a steady-state error of no larger than 4.6×10^{-4} radians, and if the static friction of the servo motor and gear train is no more than 25% of the stall torque of master servo, then K_{S1} is calculated to be

$$K_{S1} = 1.70 \times 10^5. \qquad [B-16]$$

For the Inland T-1352*, $K_{T1} = 0.0746$ and $R_{T1} = 19$, therefore K_1 is given as

$$K_1 = 680. \qquad [B-17]$$

From Equation [B-14], K_4 is

$$K_4 = 25K_1 = 17{,}000. \qquad [B-18]$$

Also, from Equation [B-14], $K_2 + K_5$ is denoted by

$$K_2 + K_5 = \frac{905}{K_1} = 1.33. \qquad [B-19]$$

If K_2 is arbitrarily selected to equal twice the value of K_5, Equation [19] reveals that

$$\begin{aligned} &1)\ K_2 = 0.88 \\ &2)\ K_5 = 0.45. \end{aligned} \qquad [B-20]$$

*See Motor selection discussion, Section D.

Summarizing, for the selected torque motors, the values of K_i for the bilateral system of Fig. VIII-6 to respond in the required manner are:

1) $K_1 = 680$

2) $K_2 = 0.88$

3) $K_3 = 1$ [B-21]

4) $K_4 = 17{,}000$

5) $K_5 = 0.45$

6) $K_6 = 1.$

Under these conditions and approximating J_1 as 13.6 kg-m^2 and J_2 as 17,000 kg-m^2 (These inertia values are pessimistic in that they represent a "worse case" situation, and in reality could be as much as 15 times as small.), the transfer function matrix of the force-reflecting system of Fig. VIII-6 becomes

$$\begin{bmatrix} \dot{\theta}_m \\ \dot{\theta}_s \end{bmatrix} = \begin{bmatrix} \dfrac{(7.36)(10^{-2})(s^2 + 0.4s + 1)}{D^1} & \dfrac{(2.94)(10^{-3})}{D^1} \\ \dfrac{(7.36)(10^{-2})}{D^1} & \dfrac{(5.89)(10^{-5})(s^2 + 44s + 50)}{D^1} \end{bmatrix} \begin{bmatrix} T_m \\ T_s \end{bmatrix} \quad [B-22]$$

where

$$D^1 = (s + 42.88)(s^2 + 1.62s + 1.43). \quad [B-23]$$

From Equation [B-23], it is clear that the dominant poles of the system of Fig. VIII-6, under the conditions

1) $K_1 = 680$

2) $K_2 = 0.88$

3) $K_3 = 1$

4) $K_4 = 17{,}000$

5) $K_5 = 0.45$ [B-24]

6) $K_6 = 1$

7) $J_1 = 13.6$

8) $J_2 = 17{,}000$

9) $\tau_1 \approx 0$

10) $\tau_2 \approx 0$,

are

$$s_{1,2} = -0.81 \pm j\ 0.88. \qquad \text{[B-25]}$$

Also, from Equation [B-23] it is seen that the damping ratio, δ, and the damped natural frequency, ω_d, of the system are

1) $\delta = 0.68$

2) $\omega_d = 0.88$ rad/sec. [B-26]

c. Analog Computer Simulation - In order to verify the analysis of the previous sections, analog computer runs simulating the system of Fig. VIII-6, under the conditions of Equation [B-24], are presented. The values monitored on these runs are T_m, T_s, T_1 T_2, $\dot{\theta}_m$, $\dot{\theta}_s$, θ_m, and θ_s. The inputs T_m and T_s on each of the runs are step functions representative of the maximum torques expected to be encountered in actual operation $T_m(\text{max}) = 27.15$ N-m (20 ft-lb) and $T_s(\text{max}) = 679$ N-m (500 ft-lb). Figure VIII-7 shows the analog program, with appropriate scale factors, used for the three runs. Figure VIII-8 shows the first run with $T_m = 27.15\ \mu(t)$ and $T_s = 0$. Noted are the facts that in the steady state condition, the net torques on the master and slave output shafts are zero, and the arm velocities $\left(\dot{\theta}_m \text{ and } \dot{\theta}_s\right)$ are constant and equal to 0.03 rad/second. Figure VIII-9 shows the second run with $T_m = 0$ and $T_s = 679\ \mu(t)$. Under these inputs, the system clearly behaves in the same fashion as in run number 1. Figure VIII-10 shows the third run with $T_m = 27.15\ \mu(t)$ and $T_s = 679\ \mu(t-10)$. Noted in this run is how maximum torques applied on the master and slave in opposite directions have the ability to drive the system velocities to

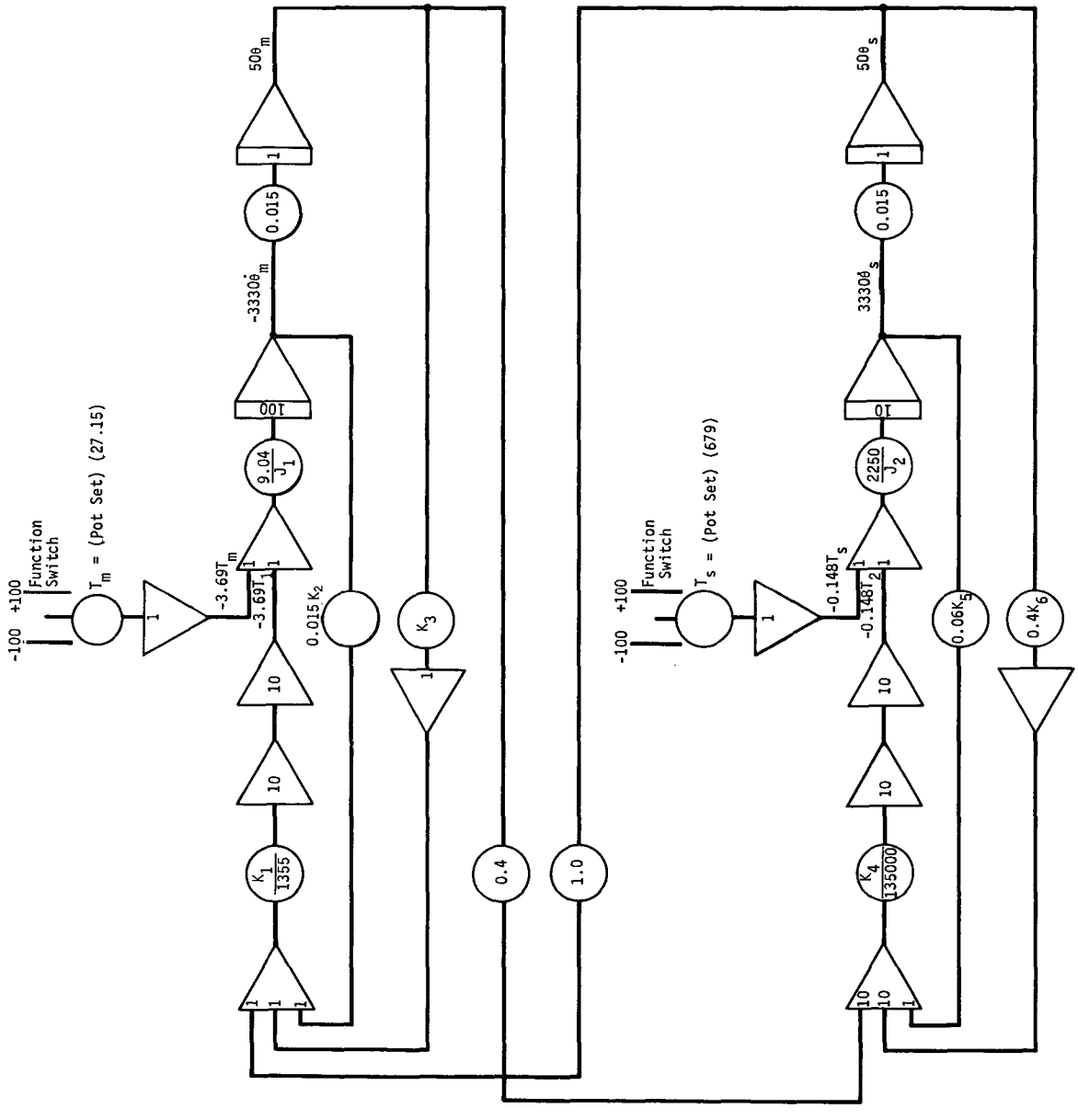

Fig. VIII-7 Analog Program of Force-Reflecting System

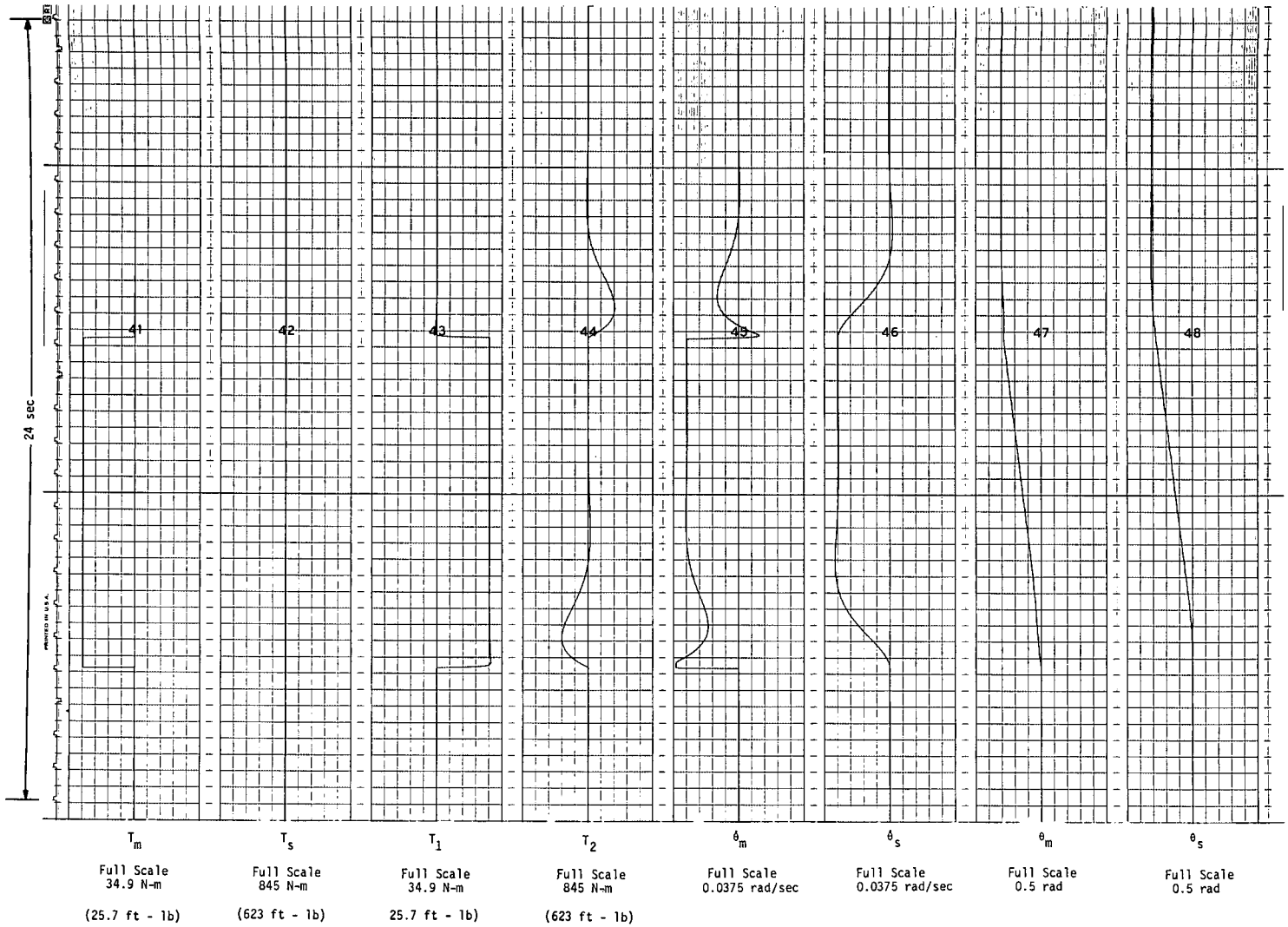

Fig. VIII-8 Analog Run of Force-Reflecting System with Only a Master Arm Input

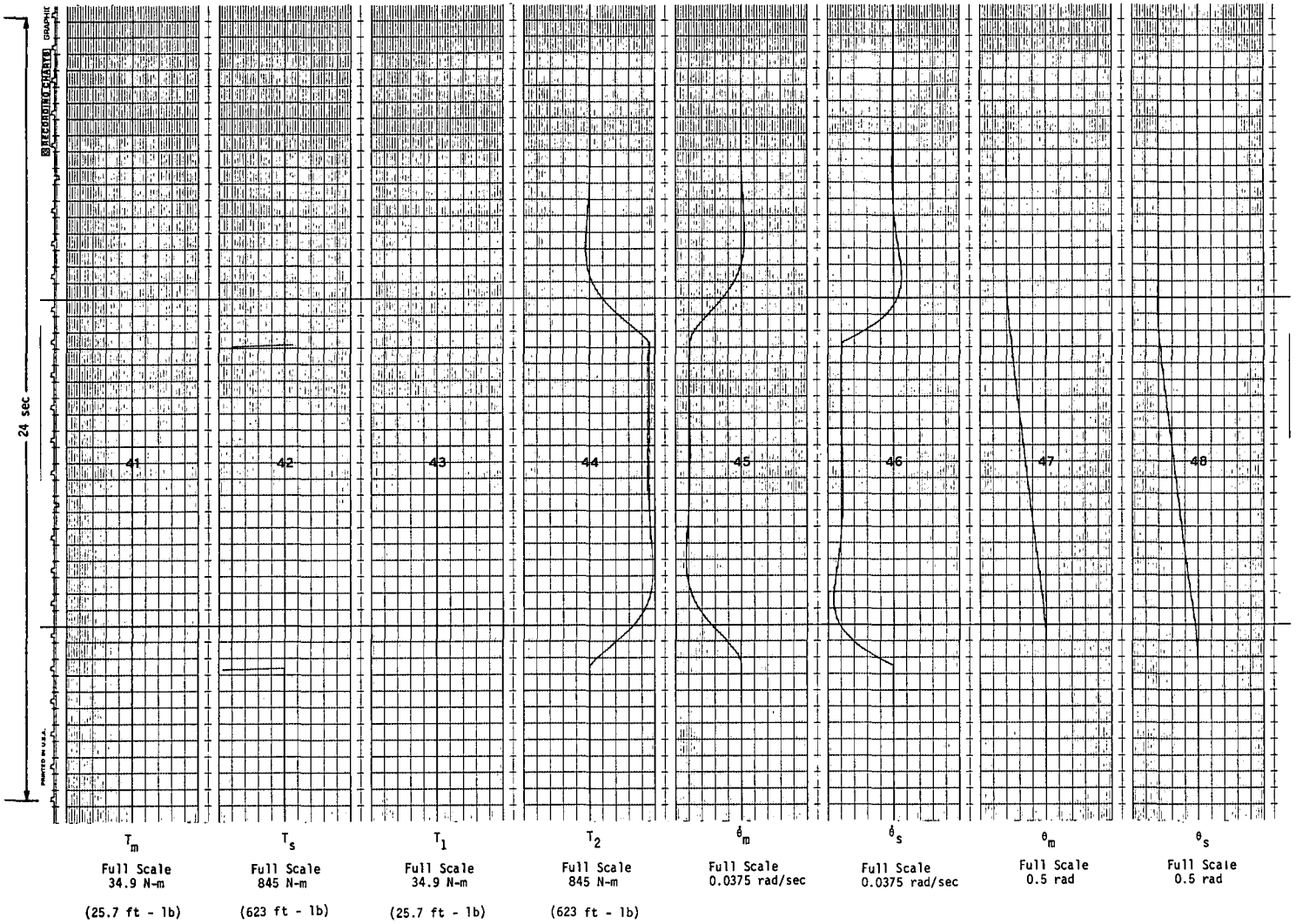

Fig. VIII-9 Analog Run of Force-Reflecting System with Only a Slave Arm Input

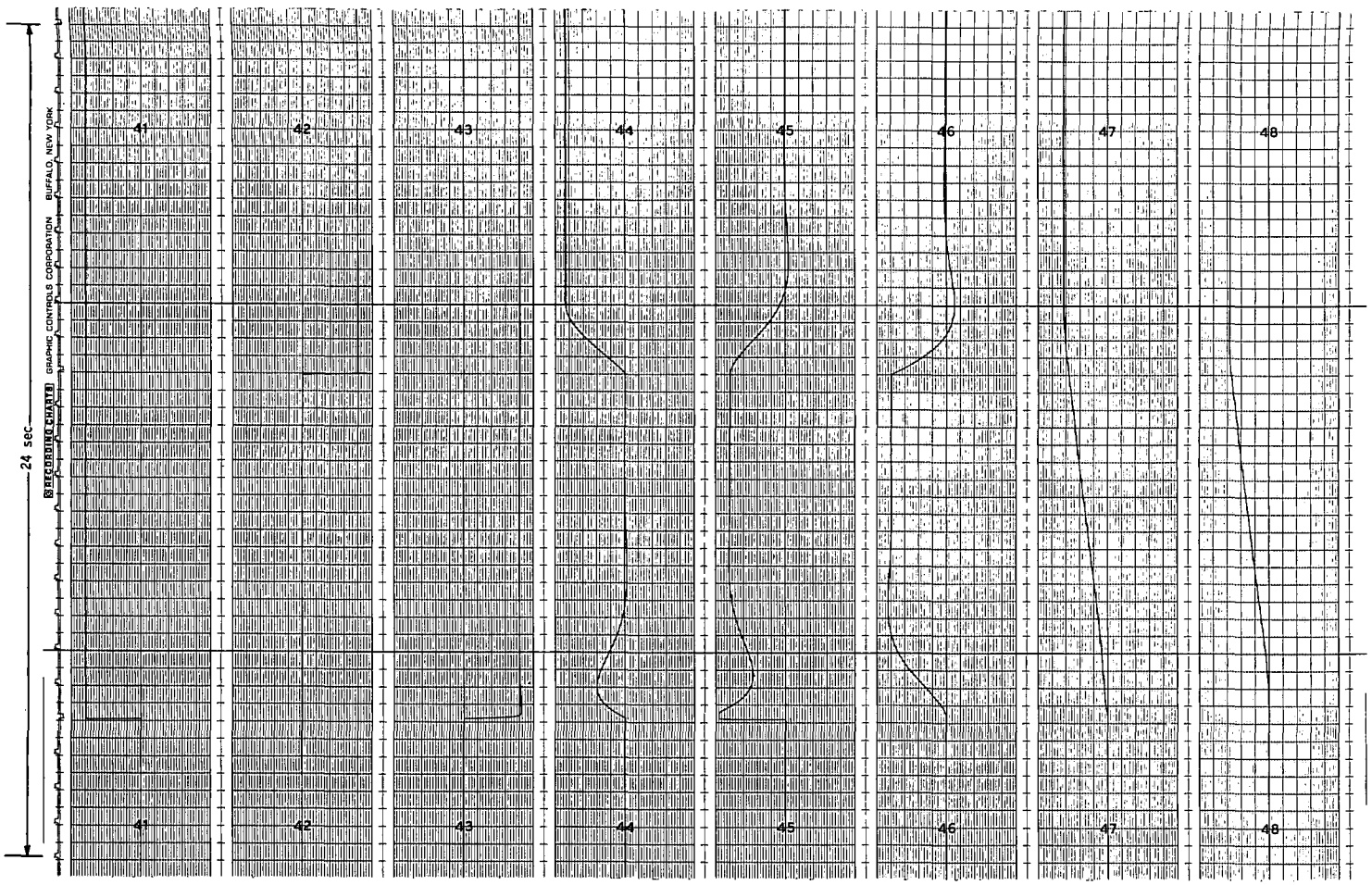

Fig. VIII-10 Analog Run of Force-Reflecting System with a Master Arm and a Slave Arm Input

zero, with the system angular displacements $(\theta_m$ and $\theta_s)$ remaining constant at the values that occurred when the maximum opposing torque was applied.

In conclusion, the analog runs of Fig. VIII-8 thru VIII-10 verify the validity of the analysis which was performed.

d. Variable Gain Requirements - When the master-slave bilateral system of Fig. VIII-6 is used for manipulating intricate objects, it is desired that the angular displacements of the master and slave are in an 18:1 ratio. That is, if the master joint undergoes an angular displacement of 18 radians, the slave joint is displaced by only 1 radian. If in the 18:1 mode of operation the performance criteria are to remain the same, the conditions that the K_i of Fig. VIII-6 must meet, as stated by Equation [B-15], change as described below.

To achieve an 18:1 mode of operation, K_3 and K_6 must become

$$1)\quad K_3 = \frac{1}{18}$$

$$2)\quad K_6 = 18. \qquad [B\text{-}27]$$

As stated by Equation [B-4], the product of K_3 and K_6 must equal 1, which is the case as seen in Equation [B-27]. To achieve equal force reflection from the tip of the master to the tip of the slave, and vice versa, Equation [B-9] showed that the requirement on K_4 is

$$K_4 = 25K_1K_3 \qquad [B\text{-}28]$$

For $K_3 = \frac{1}{18}$, this requirement reduces to

$$K_4 = 1.39K_1 \qquad [B\text{-}29]$$

If a maximum input torque on either the master or the slave is to produce maximum system velocities, in the 18:1 mode, these velocities are

$$1)\quad \dot{\theta}_m(\max) = 0.03 \text{ rad/sec}$$

$$2)\quad \dot{\theta}_s(\max) = \frac{0.03}{18} \text{ rad/sec}. \qquad [B\text{-}30]$$

Under the above conditions, Equation [B-12] becomes

$$1)\quad 27.16K_6 = 0.03(K_1K_3K_5 + K_1K_2K_6)$$

$$2)\quad 27.16 = \frac{0.03}{18}(K_1K_3K_5 + K_1K_2K_6) \qquad [B\text{-}31]$$

Substituting [B-27] into [B-31], the two equations above become equal and are given by

$$16{,}290 = K_1\left(\frac{K_5}{18} + 18K_2\right). \qquad [B\text{-}32]$$

In summary, if the master-slave bilateral servosystem under consideration is to be transformed from a 1:1 to an 18:1 angle tracking mode, the conditions that the system gains must satisfy are changed from those given by Equation [B-14] to:

$$1)\quad K_3 = \frac{1}{18}$$

$$2)\quad K_6 = 18$$

$$3)\quad K_i > 0 \qquad i = 1, 2, 3, 4 \qquad [B\text{-}33]$$

$$4)\quad K_4 = 1.39K_1$$

$$5)\quad 16{,}290 = K_1\left(\frac{K_5}{18} + 18K_2\right).$$

e. Automatic Mode Operations - When the RMS is operated in an automatic mode with the computer supplying input commands, the master is disconnected and the slave operates as a single position servo. Figure VIII-11 shows the block diagram of the slave arm servo system in the automatic mode. For the slave arm to respond in a reasonable manner to the computer inputs, it is desired that its servosystem have a damping ratio of 1. This results in a fast response system and also a system that experiences no overshoot for position input commands. Thus, K_5 must be altered as described below for the slave servosystem to have unity damping in an automatic mode of operation.

From Fig. VIII-11, the transfer function, Z, between the input supplied by the computer and the output θ_S, with $K_4 = J_2 = 17{,}000$, is

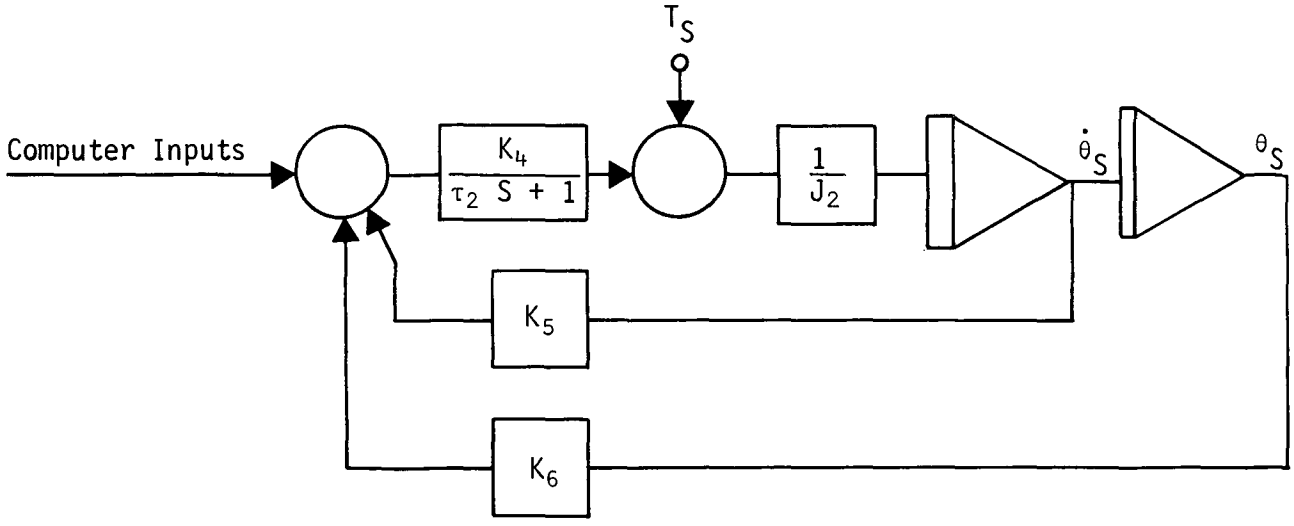

Figure VIII-11 Slave Servosystem in the Automatic Mode, Block Diagram

$$Z = \frac{1}{S^2 + K_5 S + K_6} \qquad [B-34]$$

The damping ratio is seen to be

$$\delta = \frac{K_5}{2\sqrt{K_6}} \qquad [B-35]$$

If before switching to the automatic mode the system was operating in the 1:1 angle tracking mode, then $K_6 = 1$ and the required value of K_5 for unity damping is

$$K_5 = 2\delta\sqrt{K_6} = 2. \qquad [B-36]$$

If the 18:1 angle tracking mode was in use before switching to the automatic mode, then $K_6 = 18$ and the required value of K_5 for unity damping is

$$K_5 = 2\delta\sqrt{K_6} = 8.5. \qquad [B-37]$$

Summarizing, in the automatic mode of operation, it is required that the slave servosystem have unity damping. To achieve this, K_5 must be set equal to 2, if $K_6 = 1$, and equal to 8.5, if $K_6 = 18$.

3. Computer Augmentation

The RMS is composed of two major components: the master, which is the point of input command; and the slave, which is the working end of the system. The master has seven degrees of freedom: two at the shoulder; pitch, yaw sequence, one at the elbow; yaw and four at the wrist; yaw, pitch, roll, terminal device sequence. The slave has eight degrees of freedom: two at the shoulder; pitch, yaw sequence, two at the elbow; roll, yaw sequence and four at the wrist; yaw, pitch, roll, terminal device. Each degree of freedom, will be force reflecting. In addition, all of the rotational degrees of freedom will operate without force reflection for automatic positioning of the terminal device and slave position indexing.

The control system for the RMS is depicted by a signal flow diagram, Fig. VIII-12. It is composed of five primary subsystems with two secondary inputs. Each subsystem has the following operational characteristics:

Master Arm - The master arm will act as either the input or output of the control system. It will provide joint positions and rates to the electronics assembly and will accept torque signals from the electronics.

Slave Arm - The slave arm will act as either the input or output of the control system when operating in the force reflecting mode, or as the output in the position mode. It will provide joint positions and rates to the control electronics, and accept torque command from the electronics.

Master Signal Conditioning and Control Electronics - This system will accept signals from signal sources and condition them for interface compatability. It also contains the servosystem electronics (e.g., power amplifiers. signal logic, gain control, etc), and provides torque signals to the master arm.

Slave Signal Conditioning and Control Electronics - Similar to above.

Computer - In order to provide coordinated motion control, the computer will perform any needed coordinate transformations. These transformations will ensure that motions in the master reference coordinate system will be transformed into coordinated motions in the selected slave reference coordinate axis. The computer will also perform any calculations necessary for RMS operation.

a. Axis Location and Joint Rotations - The slave reference axis system will be located at three positions: (1) at the television camera mounted on the terminal device with the origin at the geometric center of the camera. (The positive x-axis along the line of sight, the z-axis parallel to the line connecting the camera geometric center to the camera attachment centerline on the terminal device and positive toward that centerline connection, and the positive y-axis will complete the right handed system.); (2) at the television located at the base of the RMS, with the origin located at the pan tilt rotation point, with coordinate definitions similar to (1); and (3) at the base of the terminal device with the origin located at the RMS attachment point and parallel to the Shuttle reference axis system. The axis systems located at the two television cameras will be used for manual control and will require coordinate transformations, while the axis system fixed to the Shuttle will be the reference axis for the automatic control modes, and for operations in the direct viewing mode.

FOLDOUT FRAME 1

FOLDOUT FRAME 2

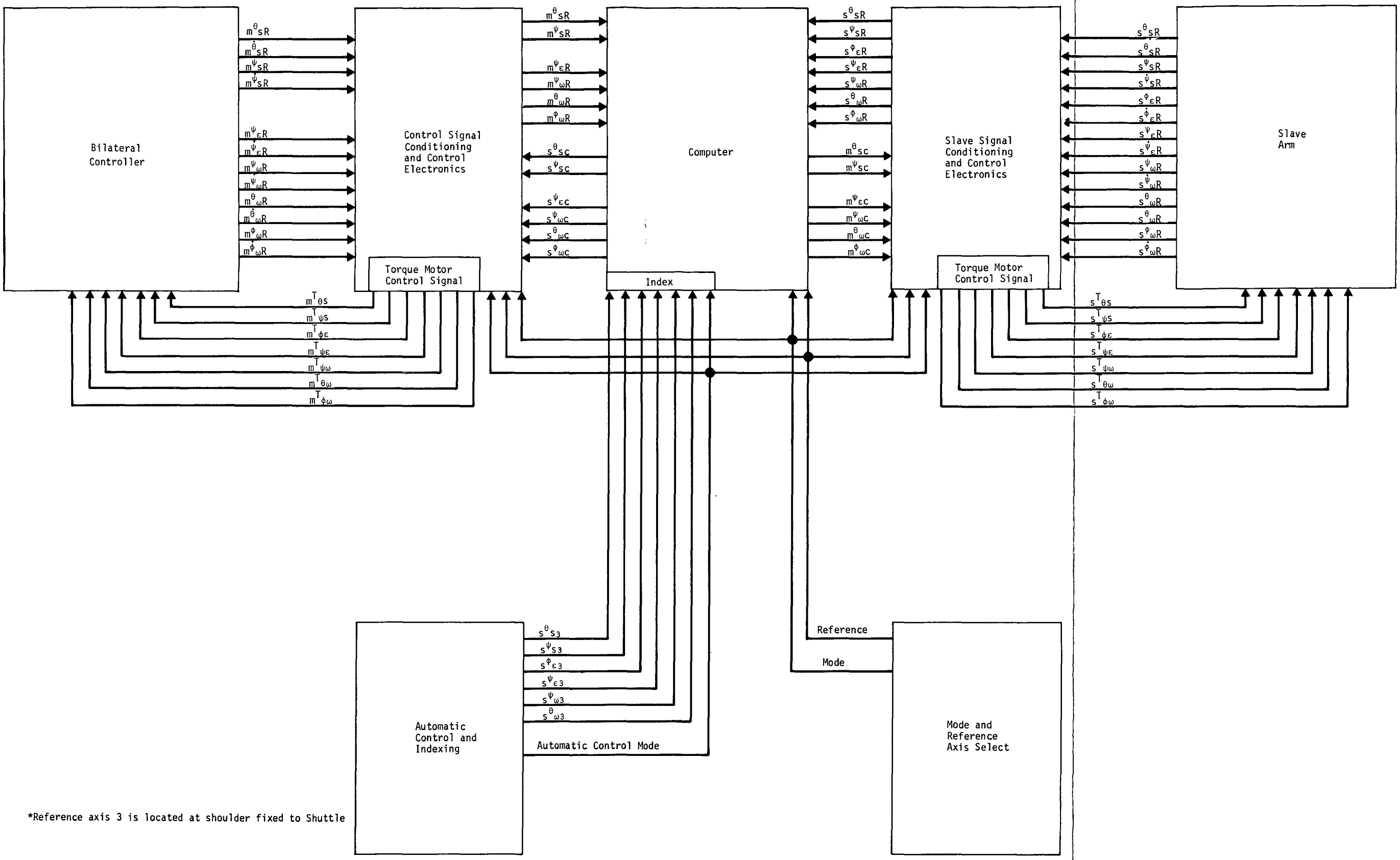

*Reference axis 3 is located at shoulder fixed to Shuttle

Fig. VIII-12 Control System Signal Flow Diagram

VIII-33 and VIII-34

Another source of coordinate rotations arises from slave position indexing. Each joint rotational degree of freedom, with the exception of wrist roll, can be indexed, which accounts for six additional coordinate transformations. Finally, when a control mode is selected that does not permit 1:1 master-slave joint rotations, a coordinate transformation similar to the first three indexing transformation will be needed.

b. Coordinate Transformation Matrices - One method of obtaining a transformation matrix between two orthogonal sets of coordinate systems is by rotating the reference system successively about each of its own axis so that after three rotations the reference system is parallel to a second specified axis system. This method generates conventional Euler angles defined as follows:

ψ (yaw) - a positive rotation about the reference z axis

θ (pitch) - a positive rotation about the reference y axis

ϕ (roll) - a positive rotation about the reference x axis

Transformations from the second system into the reference system for a single rotation about an axis are defined as:

$$D(\psi) = \begin{bmatrix} C\psi & -S\psi & 0 \\ S\psi & C\psi & 0 \\ 0 & 0 & 1 \end{bmatrix} \qquad [B-38]$$

$$D(\theta) = \begin{bmatrix} C\theta & 0 & S\theta \\ 0 & 1 & 0 \\ -S\theta & 0 & C\theta \end{bmatrix} \qquad [B-39]$$

$$D(\phi) = \begin{bmatrix} 1 & 0 & 0 \\ 0 & C\phi & -S\phi \\ 0 & S\phi & C\phi \end{bmatrix} \qquad [B-40]$$

Equivalent transformations from the reference system into the second system are denoted by $D^{-1}(\psi)$, $D^{-1}(\theta)$, and $D^{-1}(\phi)$ and can be obtained (since these matrices are orthogonal) from,

$$\begin{aligned} D^{-1}(\psi) &= D^{T}(\psi) = D(-\psi) \\ D^{-1}(\theta) &= D^{T}(\theta) = D(-\theta) \\ D^{-1}(\phi) &= D^{T}(\phi) = D(-\phi) \end{aligned} \qquad [B-41]$$

where $^{-1}$ denotes the inverse and T denotes the transpose.

Since the final orientation of the reference system depends on the sequence of rotations, it is necessary to specify and maintain a specific sequence. Assume the rotational sequence, when going from the reference to the second system, is α_1, α_2, α_3. Vectors in the reference system are then transformed into the second system by

$$\overline{2^r} = \left[D^{-1}(\alpha_3)\ D^{-1}(\alpha_2)\ D^{-1}(\alpha_1)\right]\overline{R^r} \qquad [B-42]$$

Also, transforming from the second system into the reference the sequence must be $-\alpha_3$, $-\alpha_2$, $-\alpha_1$, giving

$$\overline{R^r} = \left[D^{-1}(-\alpha_1)\ D^{-1}(-\alpha_2)\ D^{-1}(-\alpha_3)\right]\overline{2^r} \qquad [B-43]$$

or

$$\overline{R^r} = \left[D(\alpha_1)\ D(\alpha_2)\ D(\alpha_3)\right]\overline{2^r} \qquad [B-44]$$

Using these coordinate transformations, the wrist location of either the master or the slave relative to a reference coordinate axis system can be determined as a function of the joint angles. This calculation is required when the master and slave are not operating in geometrically similar configurations.

Referring to Fig. VIII-13, the position of the wrist in the reference axes, denoted $_0\overline{R}$, is given by:

$$\overline{{}_0R} = \overline{{}_0r_1} + \overline{{}_0r_2} \qquad [B-45]$$

and the position of the wrist in the upper arm coordinate system, denoted $\overline{{}_1r_2}$, is given by:

$$\overline{{}_1r_2} = \overline{{}_1\ell_1} + \overline{{}_1\ell_2}. \qquad [B-46$$

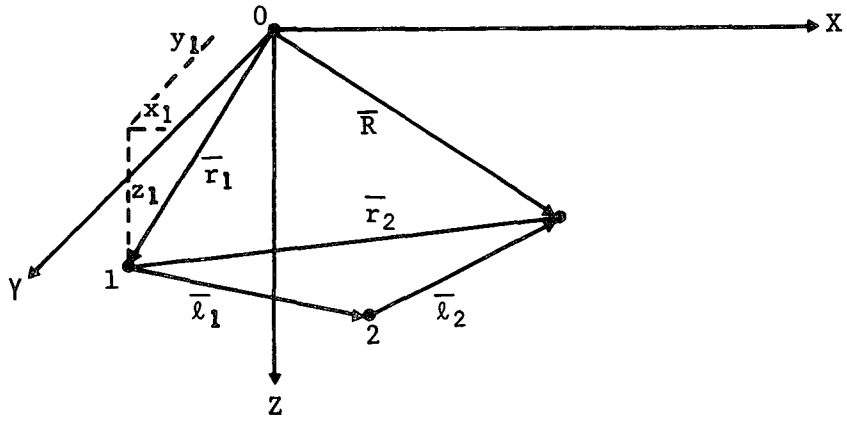

Fig. VIII-13 Arm Geometry and Reference Axes

This equation can be expressed in terms of the individual arm length vectors in their respective coordinate systems as:

$$ {}_1\bar{r}_2 = {}_1\bar{\ell}_1 + D_{21}\ {}_2\bar{\ell}_2 \qquad [B\text{-}47] $$

where D_{21} is the elbow yaw transformation matrix.

Equation [B-47] can be expanded as:

$$ \begin{bmatrix} {}_1X_2 \\ {}_1Y_2 \\ {}_1Z_2 \end{bmatrix} = \begin{bmatrix} L_1 + L_2\ C\ \psi_\varepsilon \\ L_2\ S\ \psi_\varepsilon \\ 0 \end{bmatrix} \qquad [B\text{-}48] $$

where S and C denote the sine and cosine functions.

Considering the elbow roll as a shoulder motion, the wrist position can be transformed into the reference coordinate system using the shoulder pitch-yaw-roll transformation matrix, which yields:

$$\begin{bmatrix} {}_0X_2 \\ {}_0Y_2 \\ {}_0Z_2 \end{bmatrix} = \begin{bmatrix} \left(C\theta_s C\psi_s\right) & \left(S\theta_s S\phi_\varepsilon - C\theta_s S\psi_s C\phi_\varepsilon\right) & \left(C\theta_s S\psi_s S\phi_\varepsilon + S\theta_s C\phi_\varepsilon\right) \\ \left(S\psi_s\right) & \left(C\psi_s C\phi_\varepsilon\right) & \left(-C\psi_s S\phi_\varepsilon\right) \\ \left(-S\theta_s C\psi_s\right) & \left(S\theta_s S\psi_s C\phi_\varepsilon + C\theta_s S\phi_\varepsilon\right) & \left(C\theta_s C\phi_\varepsilon - S\theta_s S\psi_s S\phi_\varepsilon\right) \end{bmatrix} \begin{bmatrix} L_1 + L_2 C\psi_\varepsilon \\ L_2 S\psi_\varepsilon \\ 0 \end{bmatrix} \quad [B\text{-}49]$$

Expanding matrix Equation [B-49] with $L_1 = L_2 = L$, and adding the position of the shoulder relative to the reference axis system origin, denoted ${}_1\bar{r}_0$, the following result is obtained:

$$\begin{bmatrix} {}_0X \\ {}_0Y \\ {}_0Z \end{bmatrix} = \begin{bmatrix} {}_0X_1 + \left(C\theta_s C\psi_s C\psi_\varepsilon + S\theta_s S\phi_\varepsilon S\psi_\varepsilon - C\theta_s S\psi_s C\phi_s S\psi_\varepsilon\right) L \\ {}_0Y_1 + \left(S\psi_s + S\psi_s C\psi_\varepsilon + C\psi_s C\phi_\varepsilon S\psi_\varepsilon\right) L \\ {}_0Z_1 + \left(-S\theta_s C\psi_s C\psi_\varepsilon + S\theta_s S\psi_s C\phi_\varepsilon S\psi_\varepsilon + C\theta_s S\phi_\varepsilon S\psi_\varepsilon\right) L \end{bmatrix} \quad [B\text{-}50]$$

Equation [B-50] defines the position of the wrist in the reference axes coordinate system and provides for a position offset of the reference origin with respect to the shoulder joint.

c. Slave Positioning Transformations - As an example of the transformations required for slave positioning, assume that the reference axis system is initially aligned with the upper and lower arm axis systems. Assuming that the slave can be indexed in any of the first six rotational degrees of freedom, the relationship between the reference axis system and the indexed command axis system is given by:

$$\begin{bmatrix} X \\ Y \\ Z \end{bmatrix}_R = \begin{bmatrix} \\ A \\ \\ \end{bmatrix} \begin{bmatrix} X \\ Y \\ Z \end{bmatrix}_C \quad [B\text{-}51]$$

Since $(X, Y, Z)_R$ and A are known, the equation of interest is:

$$\begin{bmatrix} X \\ Y \\ Z \end{bmatrix}_C = \begin{bmatrix} \\ A \\ \\ \end{bmatrix}^{-1} \begin{bmatrix} X \\ Y \\ Z \end{bmatrix}_R \quad [B\text{-}52]$$

Since the transformation matrices are orthogonal, the inverse matrix A^{-1}, is given as:

$$[A]^{-1} = D\left[\theta_{\omega}\right]^{-1} D\left[\psi_{\omega}\right]^{-1} D\left[\psi_{\varepsilon}\right]^{-1} D\left[\phi_{\varepsilon}\right]^{-1} D\left[\psi_{s}\right]^{-1} D\left[\theta_{s}\right]^{-1} \qquad [B-53]$$

and the terms of the individual inverse matrices are:

$$D(\phi)^{-1} = D(-\phi) = \begin{bmatrix} 1 & 0 & 0 \\ 0 & C\phi & S\phi \\ 0 & -S\phi & C\phi \end{bmatrix}$$

$$D(\psi)^{-1} = D(-\psi) = \begin{bmatrix} C\psi & S\psi & 0 \\ -S\psi & C\psi & 0 \\ 0 & 0 & 1 \end{bmatrix} \qquad [B-54]$$

$$D[\theta]^{-1} = D(-\theta) = \begin{bmatrix} C\theta & 0 & -S\theta \\ 0 & 1 & 0 \\ S\theta & 0 & C\theta \end{bmatrix}$$

Equation [B-53], which relates the indexed command position to the reference axes, can thus be expanded using Equation [B-54] or it can be programmed directly in the matrix form. The choice of the form of equation to use (expanded or matrix) is dependent on the computer computational speed, and the required cycle time for RMS operations.

A transformation will also be required when the reference axis system is rotated with respect to the shoulder fixed axis system. The final form of the command equation is then:

$$\begin{bmatrix} X \\ Y \\ Z \end{bmatrix}_C = \begin{bmatrix} B \end{bmatrix} \begin{bmatrix} X \\ Y \\ Z \end{bmatrix}_R \qquad [B-55]$$

where the B matrix is the total transformation matrix resulting from all of the axis rotations.

d. Computer Functions - The computer will perform the following operations or sequence of operations. Given

$$m^{\theta}s,\ m^{\psi}s,\ m^{\psi}\varepsilon \qquad [B-56]$$

calculate, using Equation [B-50], for the master

$$ {}_{m}\begin{bmatrix} X \\ Y \\ Z \end{bmatrix}_{R} - {}_{m}\begin{bmatrix} {}_{0}X_{1} \\ {}_{0}Y_{1} \\ {}_{0}Z_{1} \end{bmatrix} = {}_{m}\begin{bmatrix} \Delta X \\ \Delta Y \\ \Delta Z \end{bmatrix}_{R} \qquad [B\text{-}57] $$

and

$$ {}_{S}\begin{bmatrix} \Delta X \\ \Delta Y \\ \Delta Z \end{bmatrix} = q\begin{bmatrix} L_s \\ \overline{L_m} \end{bmatrix} {}_{m}\begin{bmatrix} \Delta X \\ \Delta Y \\ \Delta Z \end{bmatrix}_{R} = \left\{ {}_{S}\begin{bmatrix} X \\ Y \\ Z \end{bmatrix}_{R} - {}_{S}\begin{bmatrix} {}_{0}X_{1} \\ {}_{0}Y_{1} \\ {}_{0}Z_{1} \end{bmatrix} \right\} q\left(\frac{L_s}{L_m}\right) \qquad [B\text{-}58] $$

Then, using Equation [B-55]

$$ {}_{S}\begin{bmatrix} \Delta X \\ \Delta Y \\ \Delta Z \end{bmatrix}_{C} = q\left(\frac{L_s}{L_m}\right)[B] \; {}_{S}\begin{bmatrix} \Delta X \\ \Delta Y \\ \Delta Z \end{bmatrix}_{R} \qquad [B\text{-}59] $$

Now, using Equation [B-50] for the slave

$$ q\left(\frac{L_s}{L_m}\right)[B] \; {}_{S}\begin{bmatrix} \Delta X \\ \Delta Y \\ \Delta Z \end{bmatrix}_{R} = L_s \begin{bmatrix} \left(C\theta_s C\psi_s C\psi_\varepsilon + S\theta_s S\phi_\varepsilon S\psi_\varepsilon - C\theta_s S\psi_s C\phi_s S\psi_\varepsilon\right) \\ \left(S\psi_s + S\psi_s C\psi_\varepsilon + C\psi_s C\phi_\varepsilon S\psi_\varepsilon\right) \\ \left(-S\theta_s C\psi_s C\psi_\varepsilon + S\theta_s S\psi_s C\phi_\varepsilon S\psi_\varepsilon + C\theta_s S\phi_\varepsilon S\psi_\varepsilon\right) \end{bmatrix} \qquad [B\text{-}60] $$

Realizing that L_s, L_m, [B], ΔX, ΔY, ΔZ are known, solve for:

$$ {}_{S}\begin{bmatrix} \theta_s \\ \psi_s \\ \psi_\varepsilon \end{bmatrix}_{C} = \left[F\left({}_{s}X_{R},\ {}_{s}Y_{R},\ {}_{s}Z_{R}\right) \right] \qquad [B\text{-}61] $$

The RMS computer must perform at least ten basic types of signal transformation. It is estimated that each of these transformations will require 500 words of computer memory. An additional 1000 words are reserved for as yet unforseen needs, resulting in an estimate of 6000 words of memory for the RMS computational functions.

C. STRUCTURES

In this chapter, it is shown that by proper distribution of the structural material of the arms important weight savings are possible, within the deflection and size constraints imposed on the manipulator arms. An optimizing procedure is developed to distribute the mass and stiffness among the sections of the arm to minimize the total weight for a 2.54 cm (1 in.) tip deflection under the design loading conditions, and with a constraint of 20.32 cm (8 in.) maximum diameter placed on the arm from shoulder to wrist. The conclusion is reached that considerable latitude is possible in the distribution of material without changing the total structural weight much from a nominal value of 453.5 kg (1000 lb). Because of the relatively heavy structure required to keep the tip deflection down to 2.54 cm (1.0 in.) stresses are negligibly low. A brief analysis is made comparing the baseline material, aluminum, to Lockalloy and boron epoxy. The results show a 70% decrease in weight if Lockalloy were used for the beam material. Frequencies associated with several of the more important possible modes of vibration are calculated under simplifying assumptions to permit preliminary comparison to control system or other disburbances.

1. Assumptions, Approximations, and Constraints

Each manipulator arm is assumed to be a chain or cascade of simple (Ref 6) cantilever beams or torque tubes, each rigidly connected to adjacent members by the joints (see Fig. VIII-14). The deflection, slope, and twist at the outer (nearest the load) end of each member contributes to the deflection of the member next outboard and hence to the total deflection at the load.

For analysis purposes each side of each joint is assumed to have identical bending and torsional stiffnesses to the member to which it is attached. Each member therefore extends effectively to the centerline of its bounding joints.

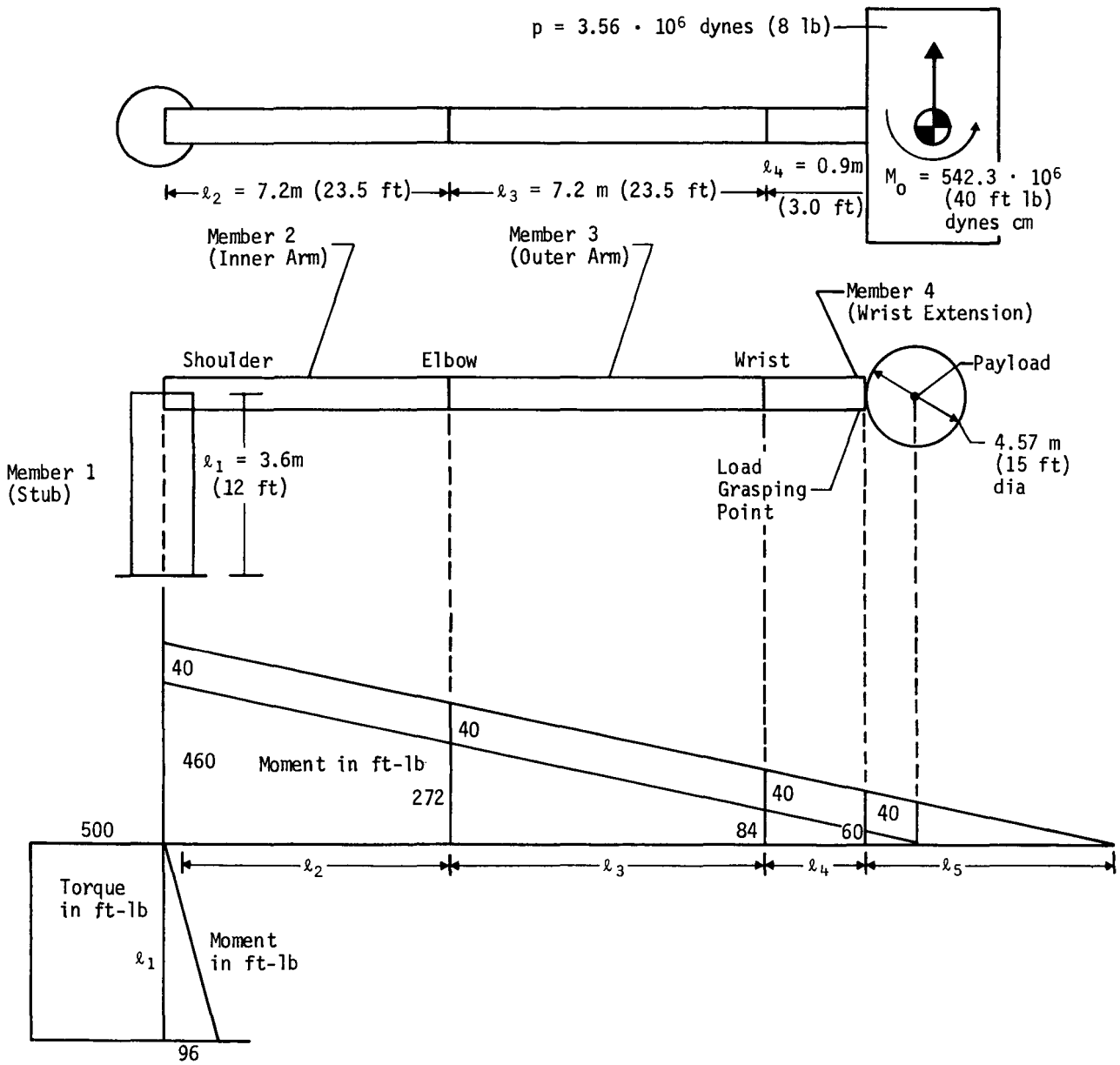

Fig. VIII-14 Loading Conditions

Loads are considered to act perpendicular to the line connecting the extremes of the moving arms, i.e., the end of the 3.66 m (12 ft) deployment member (or stub) section and the load grasping point. Only deflections in the direction of the load are considered. Under these assumptions maximum deflection for a given load occurs when the inner and outer arms are colinear. No beam-column effects are considered because of the small permissible deflections, the relatively low capability of the outermost joint, and the small loads considered.

Aluminum is the baseline material, with a density of 2.80 gm/cc (0.101 lb/in.^{3}), a Young's modulus of 0.738×10^{12} dynes/cm^2 (10.7×10^6 psi) and a modulus of rigidity $G = 0.276 \times 10^{12}$ dynes/cm^2 (4.0×10^6 psi). No alloy or heat treatment is specified because of the low strength requirement.

Since both the bending and torsional stiffnesses of the tubes considered depend directly on the tube wall thickness and on the cube of the mean radius, while the weight depends on the thickness and the first power of the mean radius, it is obvious that the stiffest tube for a given weight is the one with the largest mean radius and the minimum thickness. Under the given constraints of 30.5 cm (12 in.) diameter for member 1, 20.3 cm (8 in.) diameter for members 2 and 3, and 10.2 cm (4 in.) diameter for member 4, the stiffness of each member is approximately proportional to its weight. A tip deflection of 2.54 cm (1 in.) was set as a requirement.

The usual expression for the deflection δ_1 of a simple end-loaded cantilever beam may be found in many handbooks. $\delta_1 = \frac{P\ell^3}{3EI_1}$, where ℓ is the length, P the load, and I_1 the constant section stiffness. It may be shown also that if the beam is tapered from I_2 at the root to zero at the tip, the deflection

$$\delta_2 = \frac{P\ell^3}{2EI_2}$$

Holding the deflection constant

$$\frac{P\ell^3}{3EI_1} = \frac{P\ell^3}{2EI_2} \rightarrow I_2 = \frac{3}{2} I_1$$

If as discussed above, stiffness is proportional to weight

$$W_1 = KI_1\ell \text{ and } W_2 = K \frac{I_2}{2} \ell = K \frac{3I_1}{4} \ell = \frac{3}{4} W_1$$

This says that by tapering a beam, about 25% of its weight can be eliminated. This suggests that even in more realistic cases considerable weight can be saved by proper distribution. An optimization procedure is developed to investigate this possibility.

2. Structural Sizing and Deflection Analysis

It is required that the handling arm not deflect more than 2.54 cm (1 in.) at the terminal device (hand) under the design loads. The loading condition upon which the joint designs were based is shown in Fig. VIII-14.

The sidewards application of the load produces both twisting and bending of the 365.8 cm (12 ft) stub section (member 1). The deflection δ_1 of the top due to bending and the rotation θ_1 due to twisting both contribute to the deflection δ_4 at the terminal device. The slope due to bending does not. Proceeding outward toward the payload, the location and orientation of the inward end of each section are fixed by the accumulated slopes and deflections due to loads and moments on the preceding sections. It is necessary to proceed in this incremental fashion because the stiffnesses of the various sections are not the same.

It is convenient to replace the end moment due to rotational acceleration of the payload by application of the end load at a fictitious distance ℓ_5 from the load grasping point

$$\ell_5 = \frac{100 \text{ ft/lb}}{8 \text{ lb}} = 381 \text{ cm } (12.5 \text{ ft})$$

Another possibly critical condition in which the joint 2 was bent 90 deg so that side application of the load produced both bending and twisting in members 1 and 2 was also considered. This turned out to be less critical than the conditions shown, and was not considered further.

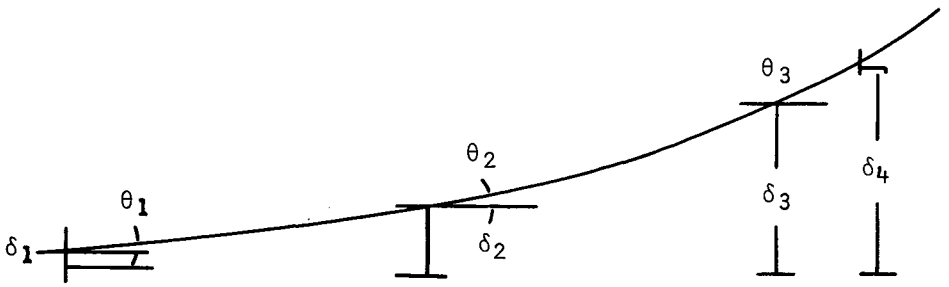

$$\theta_1 = \frac{T_1 \ell_1}{GJ_1} = \frac{T_1 \ell_1}{2EI_1} 2(1 + \nu) = \frac{1.33\ T_1 \ell_1}{EI_1}$$

$$\delta_1 = \frac{P\ell_1^3}{3EI_1}$$

$$\theta_2 = \frac{M_2 \ell_2}{EI_2} + \frac{P\ell_2^2}{2EI_2} + \theta_1$$

$$\delta_2 = \frac{M_2 \ell_2^2}{2EI_2} + \frac{P\ell_2^3}{3EI_2} + \theta_1 \ell_2 + \delta_1$$

$$\theta_3 = \frac{M_3 \ell_3}{EI_3} + \frac{P\ell_3^2}{2EI_3} + \theta_2$$

$$\delta_3 = \frac{M_3 \ell_3^2}{2EI_3} + \frac{P\ell_3^3}{3EI_3} + \theta_2 \ell_3 + \delta_2$$

$$\delta_4 = \frac{M_4 \ell_4^2}{2EI_4} + \frac{P\ell_4^3}{3EI_4} + \theta_3 \ell_4 + \delta_3$$

$$T_1 = P(\ell_2 + \ell_3 + \ell_4 + \ell_5)$$

$$M_2 = P(\ell_3 + \ell_4 + \ell_5)$$

$$M_3 = P(\ell_4 + \ell_5)$$

$$M_4 = P\ell_5$$

$P = 3.56 \times 10^6$ dynes (8 lb)

$\ell_1 = 365.8$ cm (144 in.)

$\ell_2 = 716.3$ cm (282 in.)

$\ell_3 = 716.3$ cm (282 in.)

$\ell_4 = 91.4$ cm (36 in.)

$\ell_5 = 381.0$ cm (150 in.)

Making the indicated substitutions in the cascade equation for δ_4.

$$\delta_4 = \frac{P}{3E}\left[\frac{\ell_4^3 + 3/2\ \ell_4^2\ \ell_5}{I_4} + \frac{(3/2)\ell_3(\ell_3 + 2\ell_4)\ell_5 + \ell_3(\ell_3^2 + 3\ell_3\ell_4 + 3\ell_4^2)}{I_3}\right.$$

$$+ \frac{(3/2)\ell_2(\ell_2 + 2\ell_3 + 2\ell_4)\ell_5 + \ell_2^2(\ell_2 + 2\ell_3 + 2\ell_4) + 3\ell_2(\ell_3 + \ell_4)^2}{I_2}$$

$$\left. + \frac{4\ell_1(\ell_2 + \ell_3 + \ell_4 + \ell_5)(\ell_2 + \ell_3 + \ell_4) + \ell_1^3}{I_1}\right]$$

$$\delta_4 = \frac{A}{I_4} + \frac{B}{I_3} + \frac{C}{I_2} + \frac{D}{I_1} \qquad \delta_4 \text{ in inches} \qquad [C\text{-}1]$$

$A = 0.084300$ in.^{5}

$B = 13.601$ in.^{5}

$C = 60.334$ in.^{5}

$D = 65.342$ in.^{5}

Similarly, the total weight may be expressed as the sum of contributions from the individual sections.

$$W_1 = 2\pi r_1 t_1 \ell_1 \rho$$

$$W_2 = 2\pi r_2 t_2 \ell_2 \rho \quad \text{etc}$$

$$W_T = W_1 + W_2 + W_3 + W_4$$

$$= 2\pi\rho[r_1 t_1 \ell_1 + r_2 t_2 \ell_2 + r_3 t_3 \ell_3 + r_4 t_4 \ell_4]$$

and since $I_1 \approx \pi r_1^3 t_1$ etc

$$W_T = 2\rho\left[\frac{\ell_1}{r_1^2} I_1 + \frac{\ell_2}{r_2^2} I_2 + \frac{\ell_3}{r_3^2} I_3 + \frac{\ell_4}{r_4^2} I_4\right]$$

Where r is the mean radius of a tube and is approximately equal to the outside radius R for preliminary estimates.

$r_1 = 15.25$ cm (6 in.)

$r_2 = 10.16$ cm (4 in.)

$r_3 = 10.16$ cm (4 in.)

$r_4 = 5.08$ cm (2 in.)

$\rho = 2.80$ gm/cc (0.101 lb/in.^{3})

Substitution of the appropriate values gives

$$W_T = LI_4 + MI_3 + NI_2 + QI_1 \qquad [C\text{-}2]$$

where

$$L = 1.818 \text{ lb in.}^{-4}$$

$$M = 3.560250 \text{ lb in.}^{-4}$$

$$N = 3.560250 \text{ lb in.}^{-4}$$

$$Q = 0.808 \text{ lb in.}^{-4}$$

Equation [C-1] may be written (since δ_4 is required to be 1.0 in.)

$$I_1 = \frac{AI_1}{I_4} + \frac{BI_1}{I_3} + \frac{CI_1}{I_2} + D$$

$$= \frac{A}{X_4} + \frac{B}{X_3} + \frac{C}{X_2} + D$$

where

$$X_i = \frac{I_i}{I_1}$$

and Eq [C-2] may be written

$$W_T = I_1[LX_4 + MX_3 + NX_2 + Q]$$

$$= \left[\frac{A}{X_4} + \frac{B}{X_3} + \frac{C}{X_2} + D\right] [LX_4 + MX_3 + NX_2 + Q]$$

The total weight of the arm (less joint mechanisms) is expressed here as a function of three variables which are the ratios of the stiffnesses of the member cross sections. It is desired to minimize the total weight with respect to these variables, under the constraint that the tip deflection always be 2.54 cm (1 in.).

$$\frac{\partial W_T}{\partial X_4} = 0 = \left[\frac{A}{X_4} + \frac{B}{X_3} + \frac{C}{X_2} + D\right] L - [LX_4 + MX_3 + NX_2 + Q] \frac{A}{X_4^2}$$

$$\frac{\partial W_T}{\partial X_3} = 0 = \left[\frac{A}{X_4} + \frac{B}{X_3} + \frac{C}{X_2} + D\right] M - [LX_4 + MX_3 + NX_2 + Q] \frac{B}{X_3^2}$$

$$\frac{L}{M} = \frac{A}{B}\left(\frac{X_3}{X_4}\right)^2$$

Similarly

$$\frac{L}{N} = \frac{A}{C}\left(\frac{X_2}{X_4}\right)^2$$

$$\frac{M}{N} = \frac{B}{C}\left(\frac{X_2}{X_3}\right)^2$$

It is immediately apparent that these equations are not independent, that is, any one may be derived from the other two. Hence only two are useful.

$$X_4 = X_2\left(\frac{AN}{CL}\right)^{\frac{1}{2}} = 0.052309\ X_2 \rightarrow I_4 = 0.052309\ I_2$$

$$X_3 = X_2\left(\frac{BN}{CM}\right)^{\frac{1}{2}} = 0.474793\ X_2 \rightarrow I_3 = 0.474793\ I_2$$

Substituting these into the modified Eq [C-1]

$$I_1 = \frac{A}{X_2}\left(\frac{CL}{AN}\right)^{\frac{1}{2}} + \frac{B}{X_2}\left(\frac{CM}{BN}\right)^{\frac{1}{2}} + \frac{C}{X_2} + D$$

$$I_1 - D = \frac{I_1}{I_2}\left[A\left(\frac{CL}{AN}\right)^{\frac{1}{2}} + B\left(\frac{CM}{BN}\right)^{\frac{1}{2}} + C\right]$$

$$I_2 = \frac{I_1}{I_1 - D}\left[A\left(\frac{CL}{AN}\right)^{\frac{1}{2}} + B\left(\frac{CM}{BN}\right)^{\frac{1}{2}} + C\right]$$

$$I_2 = \frac{90.591\ I_1}{I_1 - 65.342} \qquad I \text{ in inches}^4 \qquad [C\text{-}3]$$

$$I_3 = 0.474793\ I_2 \qquad [C\text{-}4]$$

$$I_4 = 0.052309\ I_2 \qquad [C\text{-}5]$$

There are three equations in the four unknowns I_1, I_2, I_3, I_4. If a value of I_1 is chosen arbitrarily, values of I_2, I_3 and I_4 result, which assure the lightest arm for a 2.54-cm (1 in.) tip deflection, for the chosen value of I_1. These values also define the structural weight of the arm according to Eq [C-2]. It remains then to select a number of values of I_1 and calculate the resulting weight. The optimum configuration is the quartet of values of I_1, I_2, I_3, I_4 which gives the lightest weight for a 2.54-cm (1 in.) tip deflection, and the tube radii specified above. Table VIII-1 shows some results of this procedure with I_1 from 8325 cm^4 (200 $in.^4$) to 12,487 cm^4 (300 $in.^4$).

Table VIII-1 Variation of I_1

Equation:	[C-3]	[C-4]	[C-5]	[C-1]	[C-2]
I_1 cm^4 ($in.^4$)	I_2	I_3	I_4	δ_4 cm (in.)	W_T kg (lb)
8,325 (200)	5598 (134.5)	2660 (63.9)	291 (7.0)	2.54 (1.00)	400 (881)
9,573 (230)	5265 (126.5)	2502 (60.1)	275 (6.6)	2.54 (1.00)	391 (862)
10,406 (250)	5103 (122.6)	2422 (58.2)	266 (6.4)	2.54 (1.00)	389 (857)
12,487 (300)	4820 (115.8)	2289 (55.0)	254 (6.1)	2.54 (1.00)	391 (862)

It is apparent that a fairly broad range of values of I_1 exists over which the total structural weight changes only slightly. Tables VIII-2 and VIII-3 summarize the properties of the arm sections over this range. The minimum weight clearly lies between I_1 = 9573 cm^4 (230 $in.^4$) and I_1 = 12,487 cm^4 (300 $in.^4$). The tables show these two cases in detail.

Table VIII-2 Case 1, I_1 = 9573 cm^4 (230 $in.^4$)

Member	1	2	3	4	Total
ℓ, cm (in.)	366 (144)	716 (282)	716 (282)	91.9 (36)	
R, cm (in.)	15.24 (6)	10.16 (4)	10.16 (4)	5.08 (2)	
I, cm^4 ($in.^4$)	9573 (230)	5265 (126.5)	2502 (60.1)	275 (6.6)	
t, cm (in.)	0.94 (0.37)	2.24 (0.88)	0.86 (0.34)	0.86 (0.34)	
r, cm (in.)	14.77 (5.815)	9.04 (3.56)	9.73 (3.83)	4.65 (1.83)	
A, cm^2 ($in.^2$)	87.23 (13.52)	127.0 (19.68)	52.8 (8.18)	25.2 (3.91)	
$\bar{r}$, cm (in.)	10.48 (4.125)	6.44 (2.535)	6.88 (2.710)	3.30 (1.299	
W, kg (lb)	89.3 (197)	254.4 (561)	105.2 (232)	6.3 (14)	455.3 (1004)
M, dyne cm (in. lb)	6.78×10^9 (6000)	6.78×10^9 (6000)	4.23×10^9 (3744)	1.68×10^9 (1488)	
σ, $dyne/cm^2$ (psi)	10.8×10^6 (157)	13.1×10^6 (190)	17.2×10^6 (249)	31.1×10^6 (451)	

Table VIII-3 Case 2, I_1 = 12,487 cm^4 (300 $in.^4$)

Member	1	2	3	4	Total
I, cm^4 ($in.^4$)	12,487 (300)	4820 (115.8)	2289 (55.0)	254 (6.1)	
t, cm (in.)	1.27 (0.50)	1.98 (0.78)	0.79 (0.31)	0.79 (0.31)	
r, cm (in.)	14.60 (5.75)	9.17 (3.61)	9.77 (3.845)	4.69 (1.845)	
A, cm^2 ($in.^2$)	116.5 (18.06)	114.1 (17.69)	48.3 (7.49)	23.2 (3.59)	
$\bar{r}$, cm (in.)	10.35 (4.076)	6.50 (2.559)	6.88 (2.710)	3.31 (1.304)	
W, kg (lb)	118 (261)	229 (505)	97 (214)	6 (13)	450 (993)
M, dyne cm (in. lb)	6.78×10^9 (6000)	6.78×10^9 (6000)	4.23×10^9 (3744)	1.68×10^9 (1488)	
σ, $dyne/cm^2$ (psi)	8.3×10^6 (120)	14.3×10^6 (207)	18.8×10^6 (272)	33.6×10^6 (488)	

Because Case 2 has slightly less total weight it is the selected beam design.

The terminology for Tables VIII-2 and VIII-3 is as follows:

$I = \frac{\pi}{4}\left(R^4 - r_i^4\right)$; r_i = inside radius; R = outside radius

$t = R - r_i$ = wall thickness

$r = \frac{R + r_i}{2}$ = mean wall radius

$A = 2\pi rt$ = cross sectional area

$\overline{r} = \sqrt{I/A}$ = radius of gyration

$\sigma = \frac{MR}{I}$ = maximum wall stress

$W = 0.101\ A\ell$ = weight

ℓ = length

M = bending moment

It will be noticed that the weights in Table VIII-1 are different from those in Tables VIII-2 and VIII-3. This is because the latter have been calculated exactly rather than approximately. Simplifying approximations were used in the optimization procedure.

For purposes of comparison, Eq [C-1] may be solved assuming that I is constant throughout the structure. When this value is substituted in Eq [C-2] a weight of 612 kg (1360 lb) results. Exact calculation of the weight gives 661.5 kg (1470 lb) as against approximately 454 kg (1000 lb) for the optimized arm.

The calculated stresses in the tube walls are so low that no further consideration is given to strength. This leaves only stiffness and weight, i.e., Young's modulus and density as material parameters.

The ratio E/ρ tends not to vary much among the common structural materials such as steel, aluminum, and magnesium. However, there are some materials that offer significant improvements in this ratio. Some values for comparison purposes are:

Aluminum

$$E/\rho = \frac{0.738 \cdot 10^{12} \text{ dynes/cm}^2}{2.80 \text{ gm/cm}^3} = 0.263 \cdot 10^{12} \frac{\text{dyne cm}}{\text{gm}} \quad (106 \cdot 10^6 \text{ in.})$$

Lockalloy

$$E/\rho = \frac{1.931 \cdot 10^{12} \text{ dynes/cm}^2}{2.094 \text{ gm/cm}^3} = 0.922 \cdot 10^{12} \frac{\text{dyne cm}}{\text{gm}} \quad (370 \cdot 10^6 \text{ in.})$$

Boron epoxy

$$E/\rho = \frac{1.241 \cdot 10^{12} \text{ dynes/cm}^2}{1.551 \text{ gm/cm}^3} = 0.800 \cdot 10^{12} \frac{\text{dyne cm}}{\text{gm}} \quad (321 \cdot 10^6 \text{ in.})$$

It is apparent that the weight can be reduced by a factor of $0.922/0.263 = 3.5$ by use of Lockalloy material.

Weight is also related to the tube radius as shown in Eq [C-2], which shows that the weight decreases approximately as the square of the tube radius increases.

3. Vibrational Modes

a. Beam - The arm is designed to deflect 2.54 cm (1 in.) under a side load of 3.7 kg (8 lb) applied at the fictitious point 381 cm (12.5 ft) past the end of the terminal device so it has a spring constant of 1.5 kg/cm (8 lb/in.). The payload considered weighs 29,480 kg (65,000 lb). Hence the frequency of the payload vibrating on the extended arm is

$$f = \frac{1}{2\pi}\sqrt{\frac{K}{W/g}} = \frac{1}{2\pi}\sqrt{\frac{8 \times 386}{65{,}000}} = 0.0347 \text{ Hz.}$$

The arm may also vibrate as a cantilever beam with no payload attached. Since the beam is bent and has both variable mass and stiffness some approximations are required to permit an analytic solution. From Timoshenko (Ref 6), Equation (116)

$$p^2 = \frac{k^4 EIg}{A\rho}$$

from which

$$f = \frac{k^2}{2\pi}\sqrt{\frac{EIg}{A\rho}} = \frac{k^2 \bar{r}}{2\pi}\sqrt{\frac{Eg}{\rho}} = 32.2\ \bar{r}\ k^2\ 10^3 \doteq 0.0837\ k^2 \cdot 10^6 \text{ Hz}$$

where k comes from the successive roots of the eigenfunction pertaining to the particular end conditions of the beam and defines the frequencies associated with different mode shapes. E and ρ are the Young's modulus and density of the material and g is the acceleration of gravity.

To evaluate k for any particular case, it is necessary to define the end conditions and length of the beam which approximate the actual structure. It is also necessary to define a beam of constant properties that approximate the actual varying beam.

The table of beam properties (Table VIII-3) shows that while I and A change from member 2 to member 3, the ratio I/A, or more specifically, the radius of gyration, $\bar{r}$ changes only slightly. It is assumed that $\bar{r}$ = 6.6 cm (2.6 in.) for all frequency calculations.

In cantilever bending the whole arm is involved and the full length of the arm, 18.90 m (744 in.) is used.

From Timoshenko (Ref 6), page 338, the first three eigenvalues for a cantilever beam with no payload are:

$$k_1 \ell = 1.875, \quad k_1 = \frac{1.875}{744} = 0.00252, \quad f_1 = 0.53 \text{ Hz}$$

$$k_2 \ell = 9.694, \quad k_2 = \frac{9.694}{744} = 0.006309, \quad f_2 = 2.23 \text{ Hz}$$

$$k_3 \ell = 7.855, \quad k_3 = \frac{7.855}{744} = 0.010588, \quad f_3 = 9.39 \text{ Hz}$$

Note that the presence of a concentrated mass of mechanism at each joint will tend to lower these frequencies, while the fact that the base of the beam is in fact stiffer than assumed will tend to raise them. Thus, these errors tend to compensate, and are neglected.

There are also possible modes of the arm in the presence of a very large payload, such as the Space Station which have frequencies so high that the payload cannot respond to them and hence appears fixed. The arm then vibrates between stationary ends that may be either fixed or hinged. It is assumed that if the long part of the arm vibrates in the plane containing both the stub (member 1) and the rest of the arm, at least one end of the long part will be able to rotate (bending member 1) and it will have an effective length of 15.24 m (600 in.) and hinged ends. From Timoshenko (Ref 6), page 331, the Shuttle-to-Space Station case becomes

$k_1 \ell = \pi, \quad k_1 = \frac{\pi}{600} = 0.005236, \quad f_1 = 2.29$ Hz

$k_2 \ell = 2\pi, \quad k_2 = \frac{2\pi}{600} = 0.010472, \quad f_2 = 9.18$ Hz

$k_3 \ell = 3\pi, \quad k_3 = \frac{3\pi}{600} = 0.015708, \quad f_3 = 20.7$ Hz

If the long part of the arm vibrates perpendicularly to the plane containing both stub and long part, the whole arm will bend with an effective length of 18.9 m (744 in.) and built-in ends.

From Timoshenko (Ref 6), page 338

$k_1 \ell = 4.730, \quad k_1 = \frac{4.730}{744} = 0.006358, \quad f_1 = 3.39$ Hz

$k_2 \ell = 7.853, \quad k_2 = \frac{7.853}{744} = 0.010555, \quad f_2 = 9.32$ Hz

$k_3 \ell = 10.996, \quad k_3 = \frac{10.996}{744} = 0.014207, \quad f_3 = 16.9$ Hz

The two sets of reasonable assumptions give frequency predictions which agree within a few Hertz. They are probably accurate enough for preliminary work but should be checked by a computer dynamic analysis before final design.

b. Control System - From the analysis of the control system servo design in Section A it was determined that

Damped natural frequency, f = 0.127 Hz

Damping ratio = 0.68

c. Shuttle Orbiter - From Phase B McDonnell Douglas Orbiter design the approximate orbiter bending modes are:

Full-fuel lateral bending modes

$f_1 = 3.0$ Hz

$f_2 = 6.9$ Hz

No-fuel lateral bending modes

$f_1 = 4.2$ Hz

$f_2 = 22.6$ Hz

d. Vibration Environment - By comparing the control system damped natural frequency of 0.127 Hz with the no load f_1 fundamental bending mode of the beam, 0.53 Hz, it can be seen that they are only a factor of 4 apart. Therefore, it is conceivable that the control system in conjunction with the human operator might excite the arm. However, the control system is damped so that there is only one overshoot and one small undershoot associated with a step command; consequently, energy could only be added over a very short time period. This means the generated arm oscillation would have very small or almost no amplitude over and above those modes excited by the step input. All other arm bending mode frequencies are well out of range of the control system and therefore present no conflict. A potential conflict does exist between the manipulator arm and the Shuttle vehicle. Both the f_2 bending mode of the unloaded arm and the f_1 bending mode of the Space Station loaded arm (2.23 Hz and 2.29 Hz, respectively), are nearly equal to the Shuttle full-fuel lateral bending mode f_1 (3.0 Hz). Because these vibration modes are very close it is theoretically possible for either the Shuttle to excite the arm or vice versa. In practice it would be difficult to imagine the very small energy input due to the arm having any major effect on the Shuttle structure. However, it is very possible that the Shuttle vibration will excite the arm vibration modes. When the Shuttle phase plane autopilot is activated, the Shuttle vibration modes will be set into motion, which, in turn, could add energy to the manipulator arm at the frequency, and possibly set the arm into resonant oscillation. One solution to this problem would be to change the structural characteristics of the arm so that its associated vibration modes would not coincide with the Shuttle or control system. However, the wide range of payloads handled by the manipulator arm produces a correspondingly wide range of vibration modes. Elimination of all possible interreacting modes would be very difficult. A second, better solution would be to automatically damp the generated oscillation either actively using the arm control system and joint articulation, or by a passive damping technique.

Due to the many presently unknown factors of this vibrational mode problem, its complete analysis is not carried out here and the preliminary design of the RMS does not include any special damping techniques.

D. MECHANICAL

The manipulator arm joints were analyzed for strength and component selection to fulfill the requirements of torque, speed, and acceleration. Deployment was studied for stowed volume, conceptual configurations, and methods to position the manipulator arm in an optimal operational position. The selected deployment technique as described in Chapter VII, Section H is illustrated in Fig. VIII-15. Joints were designed to provide reliable, safe operation with a minimum of ground maintenance for multiple launch usage and seven-day Shuttle missions. Nitrogen pressurized joints were incorporated for reliability and improved heat transfer. Each joint is designed to contain 2 DC torque motors, a brake, tachometer generator, gearing and harmonic drive, potentiometer, limit switches, bearings, shafts, etc to produce required outputs. Full-scale preliminary mechanical design drawings of the arm joints were made. Photo reduced versions of these joints are presented in Appendix B.

A candidate concept for terminal device is described.

1. General

A schematic depicting one of the two arms required is shown in Fig. VIII-16, which illustrates the arrangement of the joints, deployment member, terminal device, joint motion limits, design torques and arm tip force, and lengths. Schematically it shows yoke and roll joints. In all cases, with the exception of the wrist pitch joint, the drive mechanisms are contained in the housing adjacent to each joint, in the direction toward the base structure. The potentiometer and tachometer are for measuring articulation angle and angular rates respectively. A fail safe brake is also incorporated in each joint.

The mechanical design and analysis consisted of identifying the criteria affecting the preliminary design; analyzing the given velocity, acceleration, and load requirements for their affect on component design and function; selecting arrangements and schemes for emplacement within the envelope (to allow for reasonable assembly and test); selecting commercially available components which either have been or could readily be qualified for space use; and preparing preliminary design of the manipulator arm, which is compatible with other aspects of the system, i.e., controls, force feedback, master slave relationship, telecommunications, etc.

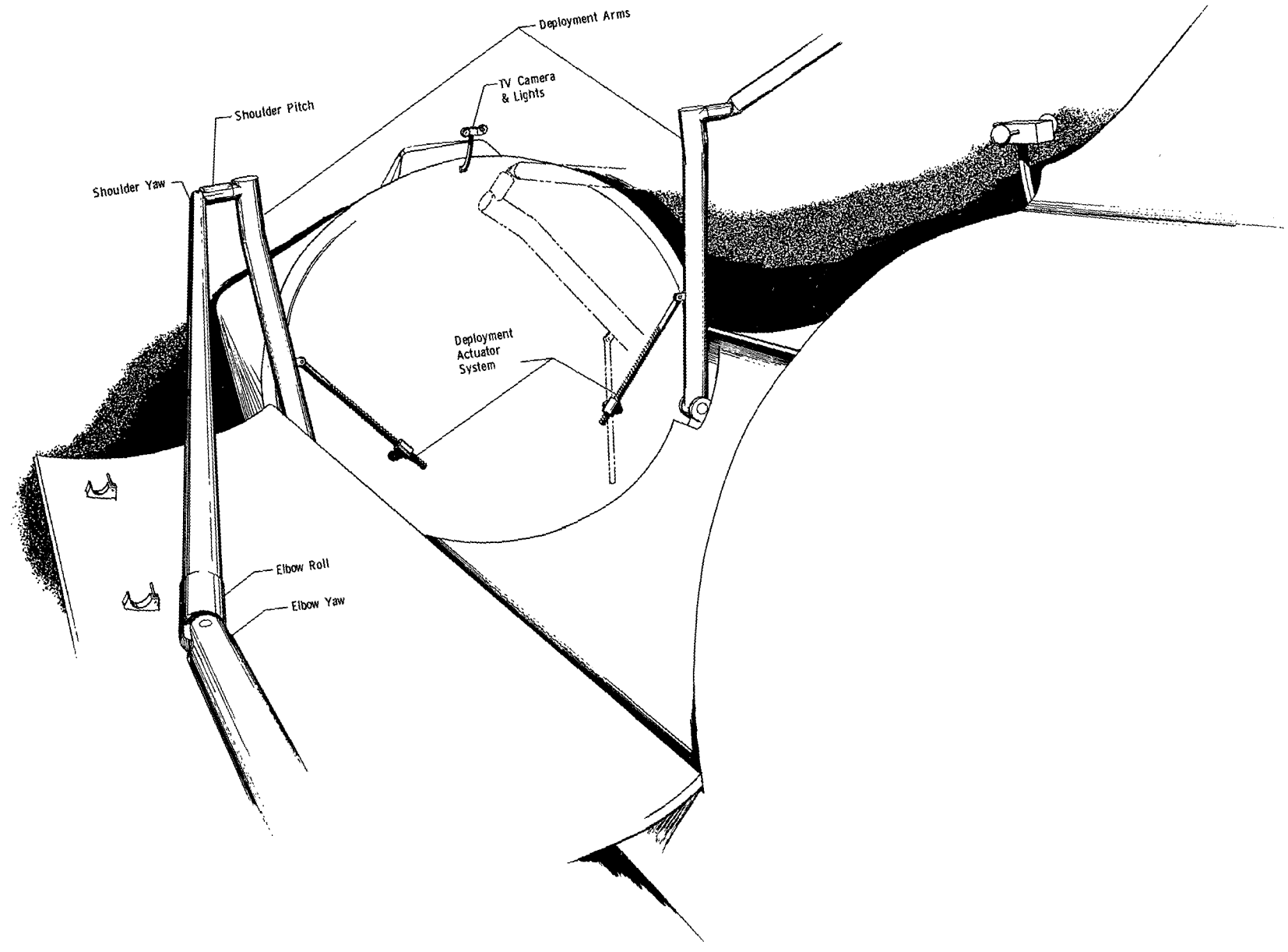

Fig. VIII-15 Remote Manipulator System Selected Deployment Concept

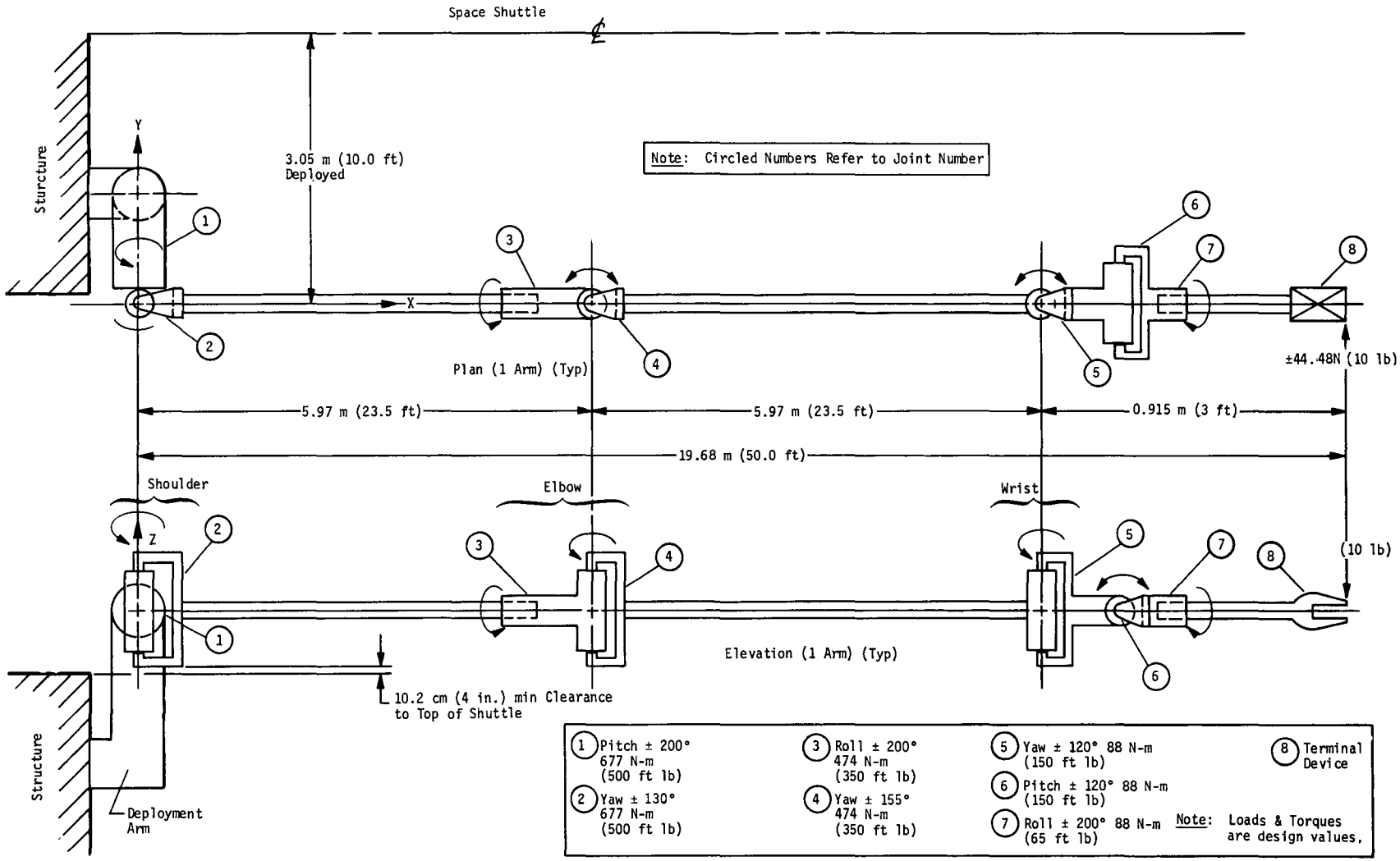

FIg. VIII-16 Schematic of Manipulator Arms (2 Required) Seven Degrees of Freedom (Plus Deployment & Terminal Device)

Extensive use has been made of design and assembly techniques learned from the construction of two three-degree-of-freedom manipulators used in simulations (Chapter VI), from experience gained on Viking, Skylab, and Shuttle programs, and from vendors who have supplied space hardware.

A fundamental philosophy has been to strive for simplicity, and straightforward, uncomplicated designs. To this end we have purposely shied away from hermetically sealed units, brushless motors, delicate planetary systems, bevel gearing, and avoided components that would have difficulty passing space qualification testing. Further discussion on the general design approach follows a discussion on motors, which is probably the most critical component.

Use of brushless and brush-type DC torque motors were considered. Many DC brush-type motors have been used successfully for long periods directly in the space environment, close to 1×10^{-11} torr (vapor pressure of some brush lubricants). Vendors supplying such motors are Inland Motor Corp., Magnetic Technology Div., and Clifton Division of Litton Industries. Ball Brothers Inc. of Boulder have coatings that probably will be adequate for our designs for bearings, brushes, etc. N_2 environment should further increase their reliability.

The general design approach is as follows:

1) Wherever joint motion will allow ($\lesssim \pm 155°$ rotation) use yoke-type joints for double shear and bearing support. (Also provides common arm axis.)

2) Keep bearings spread as far as possible to minimize arm deflection at tip and minimize bearing loads.

3) Use similar designs to those where we or others have experience, rather than design something new.

4) Be somewhat conservative in analysis and selection, in anticipation of more detailed analysis and additions.

5) Provide dual motors for redundancy capability.

6) Provide fail-safe brakes to prevent inertia forces from continuing arm movement in event of loss of power.

7) Minimize backlash effect of gearing on arm slop (or deflection). This can be accomplished by very precision gearing, etc, minimal number of gears, use of harmonic drives where possible, emplacement of any spur gearing on motor output/harmonic drive input.

8) Provide for putting motors, tachometer generators, brakes, gearing, support bearings (as many as possible) into a dry nitrogen (N_2) "can" at 5 psig, with a single output shaft having a 1 to 2 rms surface finish, riding in 2 Viton shaft O-ring seals (accepting a minimal leakage). The output shaft will be on the output side of the Harmonic Drive. The reason for this approach is twofold: The gas can will help, if necessary (not proven yet), for heat transfer from the motor, and the gas pressure can help lubrication reliability with low vapor pressure lubricants. It would be very difficult to add the cans later; it will be very easy to delete their pressurized use if proven unnecessary later.

9) Carefully consider order of assembly of components. Often overlooked is the requirement for removal of motor field magnet "keepers" after the armature is installed in place. (Also applies to tachometer generators.)

10) Design motor sizes capable of meeting two loaded conditions consisting of (a) full maximum load [29,450 kg (65,000 lb)] cargo, its velocity, and acceleration, and (b) the arm "unloaded" condition with its own inertias, velocity, and acceleration requirements. Both of these design conditions must be fulfilled without use of a variable gear box.

11) Select brakes compatible with motor torques but not sufficiently large to fracture shafts.

12) Bearings should be the highest precision available in every case. Every effort will be made to use ball bearings exclusively. Bearing loads will be very small compared to capabilities, particularly when adequate spacing is used. Standard and very thin ball bearings may be used. Consideration must be given to entire temperature operating range. For space use all will be cleaned and coated with space-qualified lubricants [such as Vackote types, Bar Temp (The Barden Corp) retainers, etc].

2. Requirements for Arm/Joint Design

This subsection summarizes major criteria extracted from overall systems requirements, from other Shuttle sources, and adds some assumptions used as guidelines for the preliminary design.

Fig. VIII-16 shows the degrees of freedom, angular travel, and torque design requirements for each joint.

Table VIII-4 presents the joint angular velocity requirements and the calculated angular accelerations.

Additional requirements are listed below.

1) Arm Stowage: 20.3 cm (8 in.) dia envelope. Latches (with verification) on cargo bay (underside) doors to support for launch and reentry. Deployment to be automatic.

2) Safety: Fail-safe/explosive bolt/release system in base of deployment arm. Fail-safe brakes to be supplied at each degree of freedom mechanism to lock up in event of power failure.

3) Manipulator arms and deployment device weight: Not to exceed 1135 kg (2500 lb).

4) There will be no specific hydrocarbon contamination elimination requirement.

5) Some outgassing will be permissible, however, every effort will be made to minimize this.

6) Space environment pressure: 6.7×10^{-9} mb mean.

7) Ground testing using GSE will be required. This applies to both prior to installation and installed in Shuttle.

Table VIII-4 Joint Velocities and Accelerations

	Shoulder		Elbow		Wrist		
	(1) Pitch	(2) Yaw	(3) Roll	(4) Yaw	(5) Yaw	(6) Pitch	(7) Roll
Arm No Load							
ω (rad/sec)	0.03 0.457 m/sec (1.5 ft/sec tip)	0.03 0.457 m/sec (1.5 ft/sec tip)	0.0565 0.457 m/sec (1.5 ft/sec tip)	0.0565 0.457 m/sec (1.5 ft/sec tip)	0.174	0.174	0.174
α (rad/sec^2)	0.015	0.015	0.0283	0.0283	0.087	0.087	0.087
Arm Loaded 29,450 kg (65,000 lb)							
ω (rad/sec)	0.0035 0.0534 m/sec (0.175 ft/sec tip)	0.0035 0.0534 m/sec (0.175 ft/sec tip)	0.0066 0.0534 m/sec (0.175 ft/sec tip)	0.0066 0.0534 m/sec (0.175 ft/sec tip)	0.0265	0.0265	0.0265
α (rad/sec^2)	8.87×10^{-4}	8.87×10^{-4}	1.725×10^{-4}	1.725×10^{-4}	0.232×10^{-3}	0.232×10^{-3}	0.385×10^{-3}

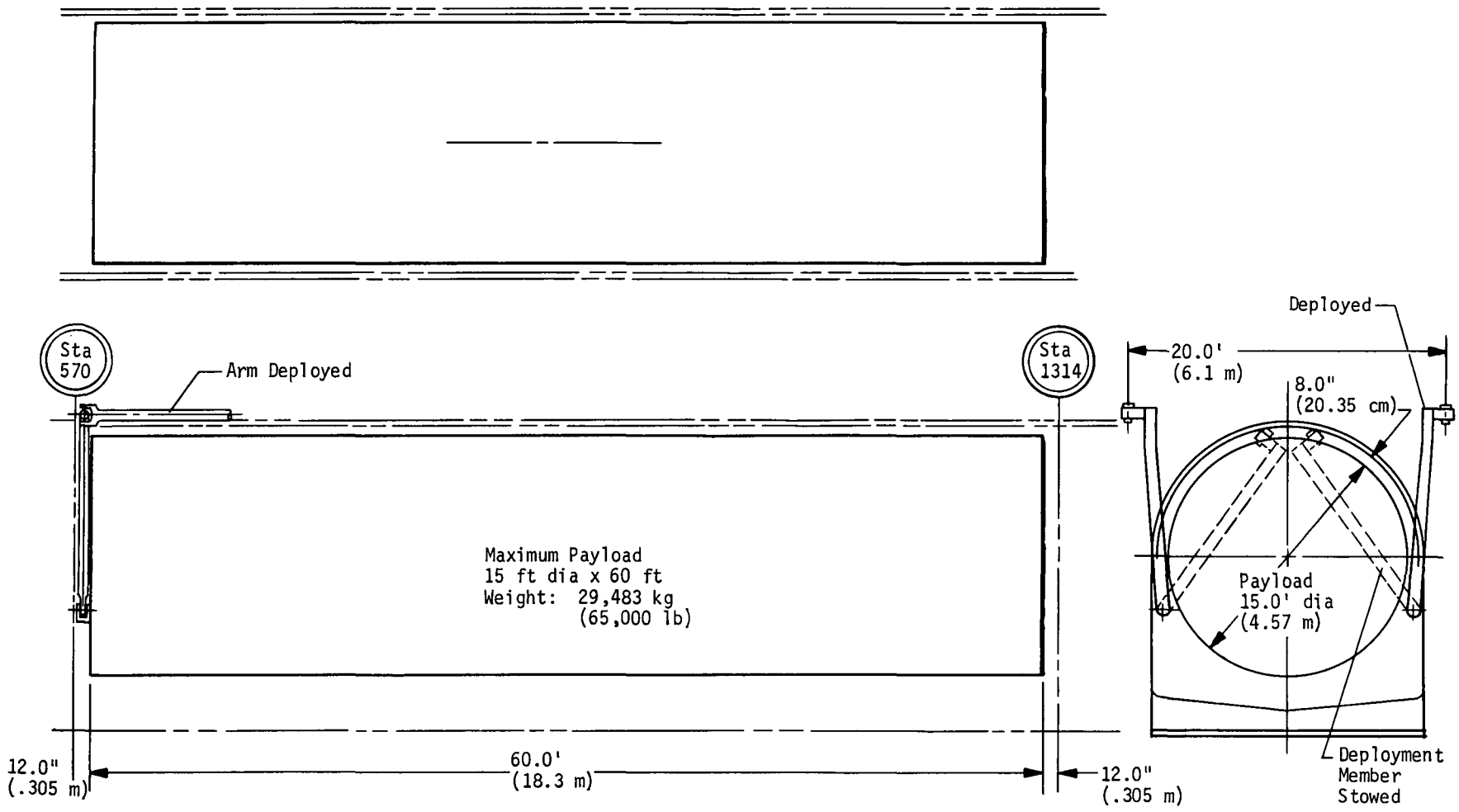

Fig. VIII-17 Payload Bay Envelope

3. Component and Joint Design Summary

Table VIII-5 presents a summary of the major joint components in the preliminary design. The selection of these components, gear ratios, etc, was made after performing a preliminary design analysis to assure conformity with the systems criteria. These components are not space-qualified. However, consideration has been given to this aspect in their selection to allow adequate envelope and functional relationship between components.

Sizing of the harmonic drives (HD) is probably the most critical item from the view point of determination of envelope size (diameter). The 4M* HDs force the diameter over the 20.3 cm (8 in.) diameter goal. Shoulder pitch envelope is 29.5 cm x 18.5 cm (11.6 in. x 7.3 in.) Shoulder yaw envelope is 23.1 cm x 19.8 cm (9.1 in. x 7.8 in.) The elbow roll will require a diameter of approximately 21.6 cm (8.5 in.) because it is rotary mechanism which allows the HD axial emplacement. The wrist HDs are significantly smaller and present no problem in envelope.

It is possible to replace the HDs in the envelope critical areas with multiple gear trains such as planetary systems; however, these create other undesirable problems of added inertia and backlash. Further, they tend to violate the major goal of simplicity. This line of reasoning could be extended to install the entire mechanism in perhaps a 10.2 cm (4 in.) diameter, but the mechanism would be very complicated and less reliable.

The selected motors are very small, less than 5.1 cm (2 in.) diameter, and offer commonality, insofar as practicable, from joint to joint. Motor wiring has not been specifically routed. However, from our experience there is no problem of providing access holes (which may be potted for space use) so the wire can be routed outside the joint. Also, a miniature tachometer generator is used in all joints. Conversion of these items for space use involves, primarily, cleaning, evacuating the proper brush material, and impregnating with low vapor pressure lubricant. Some conditioning is also done on the commutator.

*United Shoe Machinery Corporation.

Table VIII-5 Summary of Joint Components and Sizes

Column A Joint	Column B Type	Column C Motion	Column D Motor	Column E Approximate Gear Ratio	Column F Brake	Column G Potentiometer	Column H Limit Switches	Column I Tach Gen	Remarks
Shoulder 1) Pitch	Overhand Cantilever Outward from Shuttle	±200°	2 Inland* T-1342.	Gears - 6:1 + 4.7:1 HD - 200:1 (4M)† (Total Ratio - 5670:1)	Simplatrol Model PMB-43 (Simplatial Corp)	CIC Multiple Turn or Stack of 2 to Obtain ±200° (Computer Instrument Corp)	2 Herm Sealed Microswitches.	Mag Tech. 1500C-038 (Magnetic Technology Corp)	Put D, E, F, I in 5 psi N_2 Can Seal Output (2 rms) Shaft with 2 Viton Shaft Seals
2) Yaw	Yoke	±130°	Same as above	Same as 1)	Same as above	CIC 205 or Equiv (Only 240° Rqd)	Same as 1)	Same as 1)	Same as 1)
Elbow 3) Roll	Rotary	±200°	Same as above	Gears - 3.88:1 + 3.88:1 HD - 200:1 (4M) (Total Ratio: 3000:1)	Same as above	CIC Multiple Turn or Stack of 2 to Obtain ±200°. Wiper to Be Mounted On Output Shaft.	Same as 1)	Same as 1)	Same, Except Arrangement. Change to Roll/ Rotary Can.
4) Yaw	Yoke	±155°	Same as above	Same as 3)	Same as above	CIC 205 or Equivalent (Only 310° Rqd)	Same as 1)	Same as 1)	Same as 1)
Wrist 5) Yaw	Yoke	±120°	Same as above	Gears - 3:1 + 2.5:1 HD - 200:1 (2M) (Total Ratio - 1500:1)	Simplatral PMB 33 or Equiv	CIC 205 or Equivalent (Only 240° Rqd)	Same as 1)	Same as 1)	Same as 1)
6) Pitch	Yoke	±120°	Same	Same as 5)	Same as 5)	Same as 5)	Same as 1)	Same as 1)	Same as 1)
7) Roll	Rotary	±200°	2 Inland T-1352	Same as 5)	Same as 5)	Same as 3)	Same as 1)	Same as 1)	Same as Elbow Roll 3)

Note: 1. The joint number [1), 2), etc] are referenced to Fig. VIII-16.
2. All gear ratios may be changed (without changing overall ratio) to facilitate design layout fitting.

*Inland Motor Company
†United Shoe Machinery Corporation

Bearings will be ABEC 7 class precision if allowed by temperature extremes, and will be cleaned and lubricated for space use, using space lubricated retainers when run dry. This same approach will be used whether in the pressurized can or directly in the space environment. In all preliminary analyses bearing loads are sufficiently low to allow very small sizes for even the largest load-carrying members. Motions (velocities) are all very low, comparatively speaking, to what we normally deal with in rotary devices, except for the motor shaft bearings and those for the brake. Dust covers can be added for earth prelaunch and return stay times.

The potentiometers selected have infinite resolution, are capable of $\sim 350°$ readout per element, and are very smooth and precise. Identical pots with the exception of bearing treatment have been used in other comparable space applications. Variations, using clean dry bearings or vacuum coated bearings, have been applied successfully. The resistance element was unchanged. For extremely low temperatures heaters may be required. Further analysis would be desirable in terms of optimizing (reducing) pot sizes. There is a direct correlation with the control electronics. On the elbow roll joint a larger-than-normal shaft through the pot is assumed, with attachment of the wipers to that large diameter shaft output from the HD. This allows the most direct and simple assembly.

The only place hermetically sealing is proposed is for the microswitches as limit switches. Limit switches will be used as a safety back-up in the event of position potentiometers failure. Limit switches would permit automatic detection of overtravel of the joint and determine which end of motion overtravel occurs, to allow automatic reversal or stopping as required.

There will also be mechanical stops in the pitch and yaw joints. These motions are automatically limited, because yoke-type joints exist.

Selection of DC torque motors depends on a number of factors: maximum shaft power required, size, voltage (we try to stay with 24-28 vdc), maximum continuous power and torque at stall, stall torque, no load speed, overload voltage parameters (reel-type motors have quite varied characteristics and power capabilities), etc. In addition, a workable relationship between speed input and arm output must be established. For preliminary designs the motors must meet two design conditions: the fully loaded arm condition [29,600 kg (65,000 lb) cargo], and the arm unloaded condition with its higher velocity. Another factor is an attempt to keep speed reducers below 5000 or 6000:1 where possible. Motor commonality is also desirable.

Motor sizing calculations included the effects of reflected inertia due to all power train components as well as the effects of friction. For the fully loaded arm, the motors also meet the shaft power requirement which was calculated for each joint. Gear train efficiency was taken to be 75%. Motor torque losses were taken to be 7.2×10^5 dyne cm (10 in. oz)/joint.

The maximum power capability of the motor cannot be used because two design conditions must be met. An example of multiple design conditions is as follows:

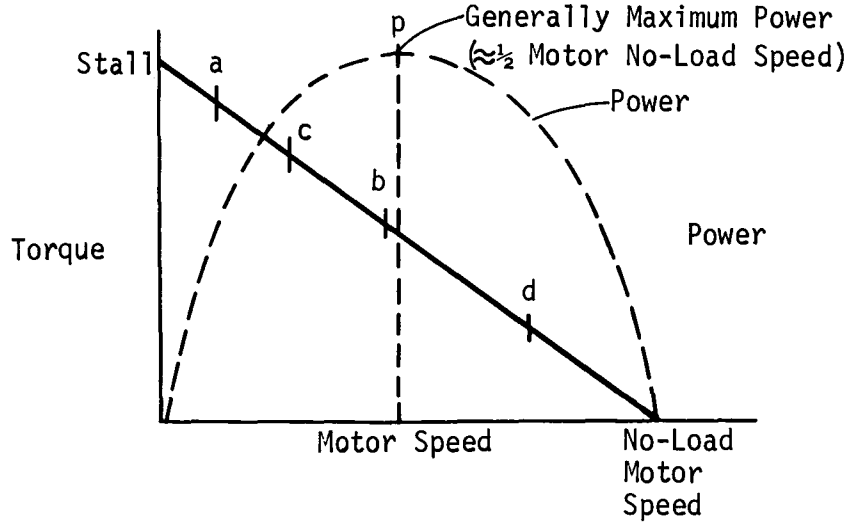

where we let

a represent loaded 29,600 kg (65,000 lb) cargo requirement
b represent unloaded arm requirement
} at gear ratio x and motor z

or

c represent loaded 29,600-kg (65,000 lb) cargo requirement
d represent unloaded arm requirement
} at gear raio y and motor z

The above simply states that there are two criteria points (i.e., a, b) which must be satisfied by the motor/gearing design. Each has a different speed requirement (no-loaded arm and loaded arm),

and operational duration. Selection of p to match a or c does not guarantee that b or d can fall on the torque curve. Optimization of gearing and motor sizes are desirable. In our preliminary analysis we have only selected a motor/gear combination which is correct but not optimized.

A variable speed transmission cannot be used here effectively to enable motor operation at peak power. The resultant motor selection and corresponding gearing is conservative.

Harmonic drives for speed reduction offer some advantages, such as small inertias, minimal backlash, and convenient sizing and weights. These must be coupled with some additional spur gear reducers for proper overall speed reduction. For preliminary designs we propose to use HD catalog data of commercially available parts. As space design evolves some material changes, and possibly minor design changes, can be expected.

Generally, sizing for preliminary design is then directly from catalog torque capabilities for various model numbers. All are conservative selections.

Table VIII-6 and VIII-7 show the performance data and dimensions for the selected motors.

Table VIII-6 Performance Data and Dimensions for Inland T-1342 Motors

Peak Torque at Stall	0.935 N-m (0.210 lb ft)
Continuous Watt at Stall	$6 \times 10^7 \frac{\text{dyne cm}}{\text{sec}}$ (6.0 watts)
No Load Speed	340 rad/sec
Full Load Speed	170 rad/sec
Friction	7.04×10^{-3} N-m (5.20×10^{-3} lb ft)
Rotor Inertia	1.125×10^{-5} N-m (8.3×10^{-6} lb ft sec^2)
Maximum Shaft Power	$26 \times 10^7 \frac{\text{dyne cm}}{\text{sec}}$ (26 watts)
Maximum Power Rate	$7050 \frac{\text{N m}}{\text{sec}^2}$ (5208 lb ft/sec^2)
Dimensions	4.9 cm (1.93 in.) O.D.
	1.575 cm (0.62 in.) I.D.
	2.135 cm (0.84 in.) Thick
Weight	0.215 kg (7.6 oz)

Table VIII-7 Performance Data and Dimensions for Inland T-1352 Motors

Peak Torque at Stall	0.466 N (0.104 lb ft)
Continuous Watts at Stall	$5.1 \times 10^7 \frac{\text{dyne cm}}{\text{sec}}$ (5.1 watts)
No Load Speed	400 rad/sec
Full Load Speed	200 rad/sec
Friction	7.04×10^{-3} N m (5.2×10^{-3} lb ft)
Rotor Inertia	0.57×10^{-5} N m sec^2 (4.2×10^{-6} lb ft sec^2)
Maximum Shaft Power	$14 \times 10^7 \frac{\text{dyne cm}}{\text{sec}}$ (14 watts)
Maximum Power Rate	$3240 \frac{\text{N m}}{\text{sec}^2}$ (2396 lb ft/sec^2)
Dimensions	4.9 cm (1.93 in.) O.D.
	1.575 cm (0.62 in.) I.D.
	1.27 cm (0.50 in.) Thickness
Weight	0.1215 kg (4.3 oz)

The shaft sizes required were calculated for each joint based on SAE 4340 with 200,000 psi yield. Shaft diameters (with a safety factor of 2) are 1.90 cm (0.75 in.), 1.52 cm (0.597 in.), and 1.14 cm (0.450 in.) for the shoulder, elbow, and wrist joints. Shaft torsional deflections will be critical and may require considerably larger output shaft diameters.

4. Dry Nitrogen Supply System

A leakage rate of 5 cc/minute is assumed for each joint degree of freedom pressurized can pressurized at 5 psia. This leakage rate is an average maximum estimate from various other applications where 14.7 psi ambient has been used and should be a very conservative estimate. It considers both a static and dynamic (negligible) shaft. In all probability the leakage can be reduced to 2 cc/minute or less with use of multiple O-ring Viton shaft seals on a 1 to 2 rms shaft finish, or even less if a magnetic fluid seal (capable of 10^{-13} torr and micro torque drag) currently under development can be applied.

For preliminary design the following schematic illustrates the N_2 system:

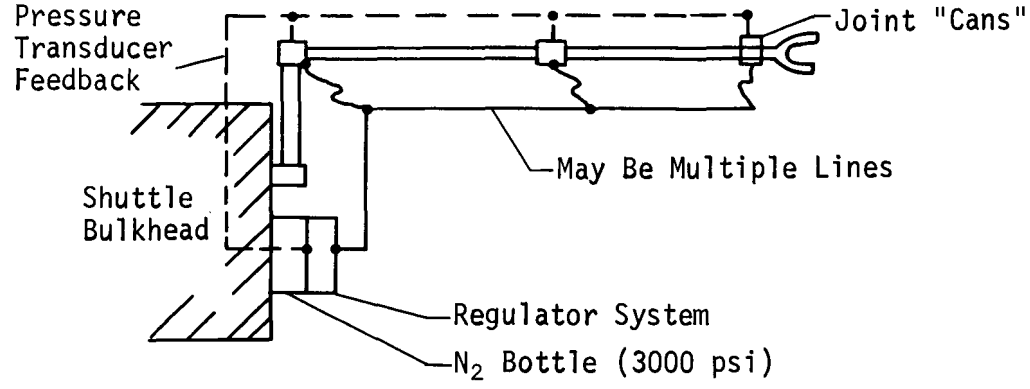

With two arms and seven-degrees-of-freedom/arm plus terminal device (excluding deployment mechanism) the maximum leakage rate would be 2 x 8 x 5 = 80 cc/minute. Calculations show the total leak per pressurized can for a 7-day period is 58.5 gm (0.129 lb) N_2. The total leakage for all joints for 7 days converted to volume is 388 cm^3 (23.7 $in.^3$). This requirement can be met with a pressurized sphere approximately 8.9 cm (3.5 in.) diameter at 3000 psi.

5. Terminal Device - Candidate Design

Torque capabilities of the wrist joint produce a requirement of approximately 174 N-m (128 ft-lb) torque in pitch and yaw for a terminal device (TD).

This requirement formed the main forcing function for the preliminary design of a terminal device. A 5.1 cm (2 in.) square bar was taken as a baseline grasping hard point and a "hand" concept formed TD baseline approach. The design concept is shown in the engineering drawing Fig. VIII-18 with an artists concept shown in Fig. VIII-19.

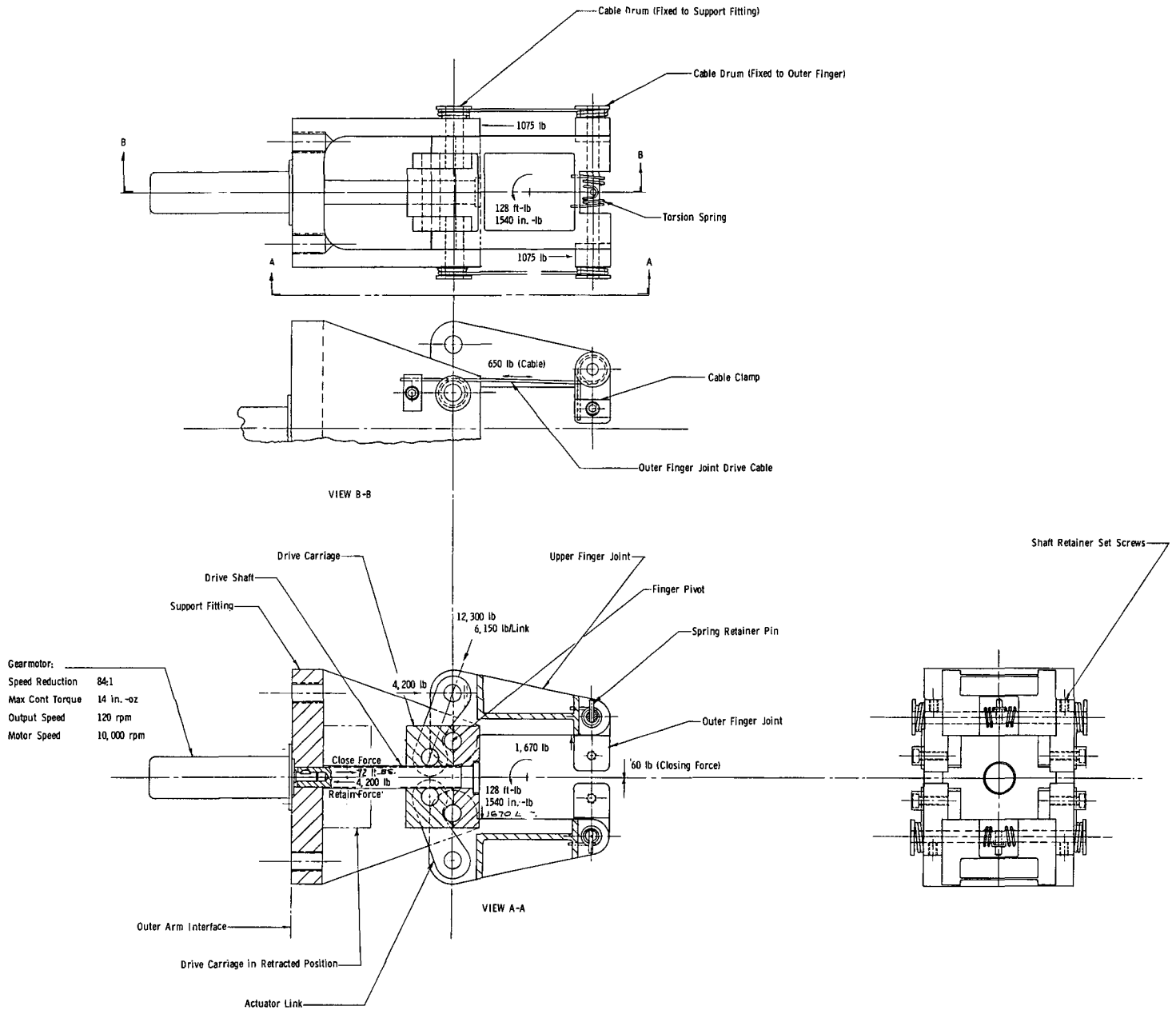

Fig. VIII-18 Terminal Device (Candidate Configuration)

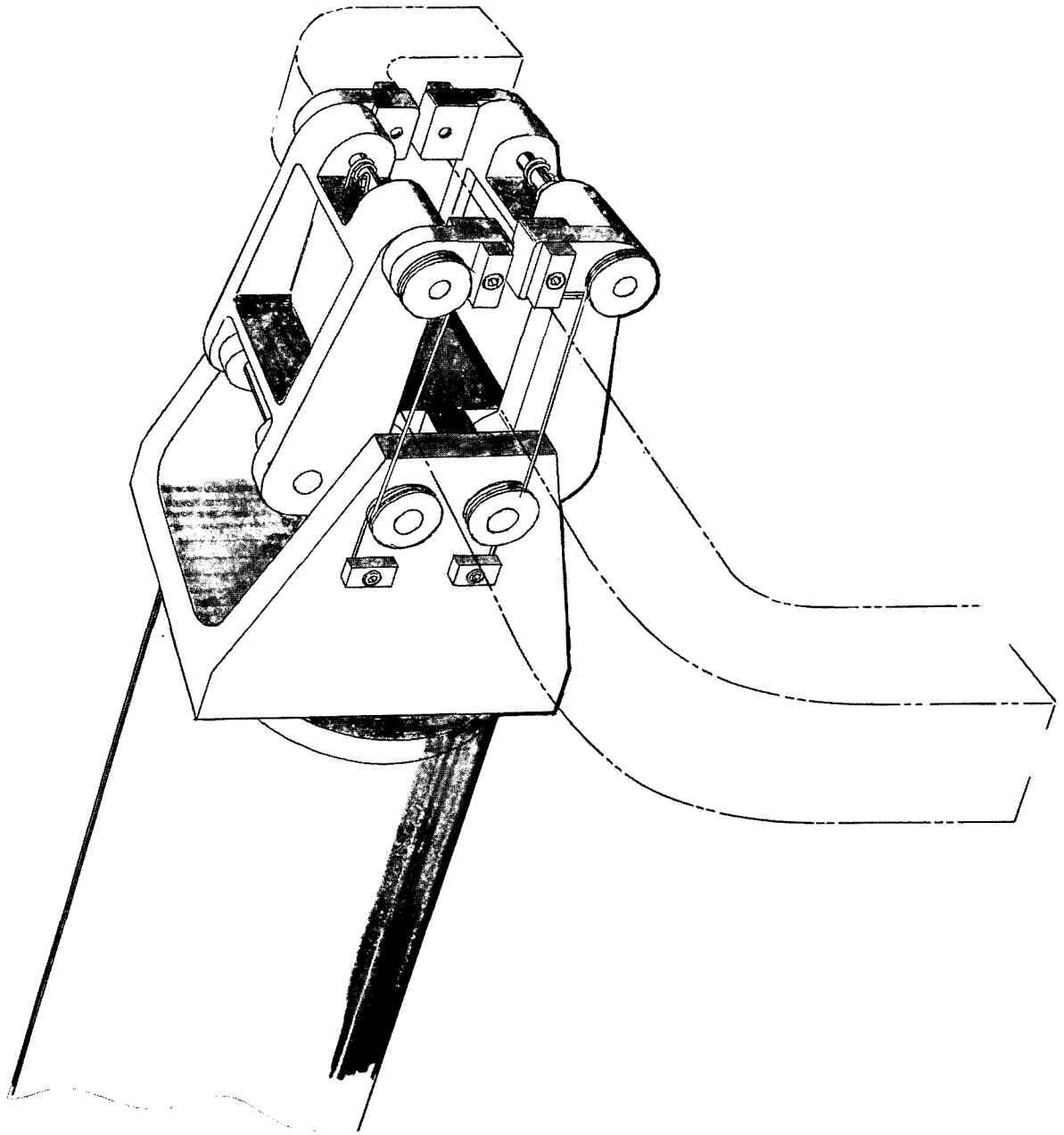

Fig. VIII-19 Candidate Terminal Device

The device operates this way. The gear motor transmits torque to the threaded drive shaft which moves the threaded drive carriage back. When the drive carriage moves back, the actuator links attached to the drive carriage move back and actuate the upper and lower finger joints around the finger pivot joint. This motion continues until the drive carriage touches the support fitting and stops. At this point the upper and lower finger joints have rotated 90°. The outer finger joints also move 90° simultaneously in conjunction with the upper and lower finger joints. This is accomplished as the outer finger drive cable unwinds from the cable drum fixed to the support fitting allowing the cable drum fixed to the outer finger to turn. The torsion spring located on the finger shaft supplies the force needed to rotate the finger. To close the hand onto the payload, the reverse of the above described motion is accomplished. The high torque loads are not imposed on the hand while it is being actuated. See Fig. VIII-18 for closing forces.

When the 174 N-m (128 ft-lb) is applied at the center of the closed hand as shown in Fig. VIII-18, the force reacted through the drive shaft thread is 18,900 N (4200 lb) well within the capability of the 1.27 cm (0.5 in.) 13 thread. A shear force of 53,750 N (11,500 lb) on the drive shaft screw at the front of the drive carriage is partially reacted by the load from the lower finger link.

Once the hand is closed on the payload and the motor stopped, the loading conditions imposed by the payload during acceleration and deceleration will not be reflected to the motor. These loads will be reacted finally through the drive screw thread and linkage.

If the 174 N-m (128 ft-lb) force is applied in the payload yaw axis the upper and lower fingers on one side will be required to react the torque through the two cables provided. Each finger would see a force 2414.5 N (537 lb) resulting in a cable tensile load of 2925 N (650 lb).

$$\frac{650 \text{ lb}^*}{0.60 \text{ (Ratio Yield to tensile)}} = 7200 \text{ N (1600 lb) cable required}$$

A 0.32 cm (0.125 in.) diameter stainless cable will carry 7920 N (1760 lb).

*Includes 1.5 safety factor.

The motor speed selected for this design will result in a fingers closing time of about 11 sec. This time can be varied by changing the gear motor reduction or drive shaft thread. The closing force will vary accordingly.

An umbilical lanyard that can be snapped on before handling of the payload by the hand would be grasped by the hand to accomplish a hookup, then released. The design of the snap on lanyard can be designed to be released as well by the hand.

E. DYNAMICS

The plane motion of two rigid bodies connected by a two-segment arm is analyzed in this section. It is assumed that torque producing devices exist at each of the three arm joints.

The equations of motion are derived, and two of these are solved; the result is used to eliminate two of the variables from the problem. The remaining equations are then used to analyze two Shuttle tasks.

The first case deals with the Shuttle performing a cargo handling task. The equations of motion are used to arrive at expressions for the joint torques necessary for the task.

The second example involves the Shuttle, docking with an infinite Space Station. In this instance, the maximum relative velocity of the Shuttle, which does not exceed the torque capability of the joints, is determined. For a torque capability of 150, 350, and 500 ft-lb at the wrist, elbow, and shoulder joints respectively, the maximum flyby velocity is shown to be approximately 0.1 ft/sec.

1. System Description

The system to be studied consists of two rigid bodies, A and B, connected by a two-segment arm with three joints designated a, b, and c (see Fig. VIII-20). It is assumed the bodies are constrained to planar motions.

The point O designates the origin of an inertial reference frame, R, in which the orthogonal unit vectors, $\bar{R}_1$, $\bar{R}_2$, $\bar{R}_3$ are fixed.

The center of mass of A is called A* and is located relative to O by the position vector $\bar{P}$. Joint a is located relative to A* by the vector $\bar{r}_A$, and the positions of c relative to a, and that of b relative to c, are given by $\bar{L}_A$ and $\bar{L}_B$, respectively. The magnitude of $\bar{L}_A$ is L_A and that of $\bar{L}_B$ is L_B. The position of B* (the mass center of B) is located by $\bar{r}_B$ relative to joint b.

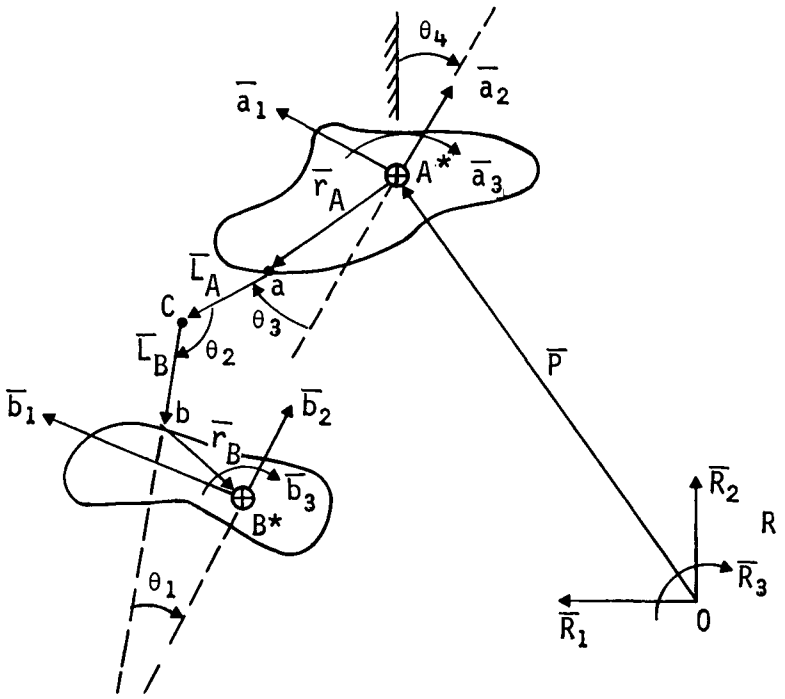

Fig. VIII-20 Two Bodies Connected by a Two-Segment Arm

The orthogonal unit vectors $\bar{a}_1$, $\bar{a}_2$ and $\bar{a}_3$ are fixed in A and $\bar{b}_1$, $\bar{b}_2$, and $\bar{b}_3$ are unit vectors fixed in B. The angle between $\bar{b}_2$ and $-\bar{L}_B$ is called θ_1, while θ_2 designates the angle between $\bar{L}_A$ and $\bar{L}_B$. Finally, the angle between $\bar{L}_B$ and $-\bar{a}_2$ is θ_3 and the rotation of $\bar{a}_2$ relative to $\bar{R}_2$ is called θ_4 and is considered positive as shown in Fig. VIII-20.

The mass of A is m_A and its moment of inertia about A* in the $\bar{a}_3$ direction is I_A. The mass of B is m_B and its moment of inertia is I_B.

Torques of magnitudes T_a, T_b. and T_c are assumed to act at the three joints, as shown in Fig. VIII-21.

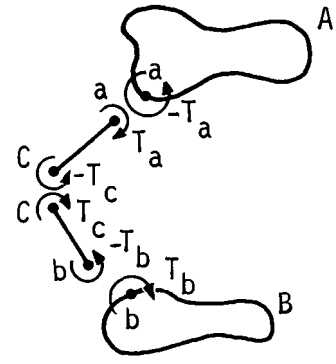

Fig. VIII-21 Torque Distribution

The following scalar quantities are used in the analysis of the system:

$$x_i = \bar{P} \cdot \bar{R}_i, \; i = 1, 2 \qquad [E\text{-}1]$$

$$r_{Ai} = \bar{r}_A \cdot \bar{a}_i, \; i = 1, 2 \qquad [E\text{-}2]$$

$$r_{Bi} = \bar{r}_B \cdot \bar{b}_i, \; i = 1, 2 \qquad [E\text{-}3]$$

2. Equations of Motion

The system described above constitutes a holonomic system with six degrees of freedom, and the equations of motion may be obtained by employing Lagrange's equations.

$$\frac{d}{dt}\left(\frac{\partial K}{\partial \dot{q}_r}\right) - \frac{\partial K}{\partial q_r} = Q_r \quad (r = 1, 2, \ldots, 6) \qquad [E\text{-}4]$$

where K is the kinetic energy of the system, q_r is a generalized coordinate, $\dot{q}_r$ is the first time derivative of q_r, and Q_r is the generalized active force associated with the coordinate q_r.

The kinetic energy of the system is

$$K = \tfrac{1}{2} m_A \left(\dot{x}_1^2 + \dot{x}_2^2\right) + \tfrac{1}{2} m_B \left(\bar{V}^{A*} \cdot \bar{V}^{A*}\right) + \tfrac{1}{2} I_A \dot{\theta}_4^2 + \tfrac{1}{2} I_B \left(\dot{\theta}_1 + \dot{\theta}_2 + \dot{\theta}_3 + \dot{\theta}_4\right)^2 \qquad [E\text{-}5]$$

where $\bar{V}^{A*}$ denotes the velocity of A* in R and can be written

$$\bar{V}^{A*} = \left\{ \dot{\phi}_1 \left(r_{B1} \sin \phi_1 + r_{B1} \cos \phi_1 \right) - L_B \dot{\phi}_2 \cos \phi_2 + L_A \dot{\phi}_3 \cos \phi_3 \right.$$
$$\left. - \dot{\phi}_4 \left(r_{A1} \sin \phi_4 + r_{A2} \cos \phi_4 \right) + \dot{x}_1 \right\} \bar{R}_1$$
$$+ \left\{ -\dot{\phi}_1 \left(r_{B1} \cos \phi_1 - r_{B2} \sin \phi_1 \right) - L_B \dot{\phi}_2 \sin \phi_2 \right.$$
$$\left. + L_A \dot{\phi}_3 \sin \phi_3 + \dot{\phi}_4 \left(r_{A1} \cos \phi_4 - r_{A2} \sin \phi_4 \right) + \dot{x}_2 \right\} \bar{R}_2 \qquad [E-6]$$

where

$$\phi_1 = \theta_1 + \theta_2 + \theta_3 + \theta_4 \qquad [E-7]$$

$$\phi_2 = \theta_2 + \theta_3 + \theta_4 \qquad [E-8]$$

$$\phi_3 = \theta_3 + \theta_4 \qquad [E-9]$$

$$\phi_4 = \theta_4 \qquad [E-10]$$

Inspection of Equations [E-5] and [E-6] suggests the following choices for the generalized coordinates

$$q_i = x_i \quad (i = 1, 2) \qquad [E-11]$$

$$q_i = \phi_{i-2} \quad (i = 3, 4, 5, 6) \qquad [E-12]$$

When Equations [E-11] and [E-12] are used for the q_i, the generalized active forces, Q_i, are given by

$$Q_i = 0 \quad (i = 1, 2) \qquad [E-13]$$

$$Q_3 = T_b \qquad [E-14]$$

$$Q_4 = T_c - T_b \qquad [E-15]$$

$$Q_5 = T_a - T_c \qquad [E-16]$$

$$Q_6 = -T_a \qquad [E-17]$$

Substitution from Equations [E-5] - [E-17] into [E-4] results in the following equations of motion:

$$\frac{d}{dt}\left\{\left(m_A + m_B\right)\dot{x}_1 - m_B \frac{d}{dt}\left[g_6 + L_B \sin\phi_2 - L_A \sin\phi_3 - f_7\right]\right\} = 0 \qquad [E\text{-}18]$$

$$\frac{d}{dt}\left\{\left(m_A + m_B\right)\dot{x}_2 - m_B \frac{d}{dt}\left[f_6 - L_B \cos\phi_2 + L_A \cos\phi_3 + g_7\right]\right\} = 0 \qquad [E\text{-}19]$$

$$\left[I_A + m_B\left(r_{A1}^2 + r_{A2}^2\right)\right]\ddot{\phi}_4 + m_B\left[\ddot{\phi}_1 f_3 + \ddot{\phi}_2 f_4 + \ddot{\phi}_3 f_5 + \ddot{x}_1 g_7 + \ddot{x}_2 f_7 - \dot{\phi}_1^2 g_3 - \dot{\phi}_2^2 g_4 + \phi_3^2 g_5\right] = -T_A \qquad [E\text{-}20]$$

$$m_B\left[\ddot{\phi}_1 L_A f_2 - \ddot{\phi}_2 L_A L_B \cos(\phi_2 - \phi_3) + L_A^2 \ddot{\phi}_3 + \ddot{\phi}_4 f_5 + \ddot{x}_1 L_A \cos\phi_3 + \ddot{x}_2 L_A \sin\phi_3 + \dot{\phi}_1^2 L_A g_2 + \dot{\phi}_2^2 L_A L_B \sin(\phi_2 - \phi_3) - \dot{\phi}_4^2 g_5\right] = T_a - T_c \qquad [E\text{-}21]$$

$$m_B\left[\ddot{\phi}_1 L_B f_1 + \ddot{\phi}_2 L_3^2 - \ddot{\phi}_3 L_A L_B \cos(\phi_2 - \phi_3) + \ddot{\phi}_4 f_4 - \ddot{x}_1 L_B \cos\phi_2 - \ddot{x}_2 L_B \sin\phi_2 - \dot{\phi}_1^2 L_B g_1 - \dot{\phi}_3^2 L_A L_B \sin(\phi_2 - \phi_3) + \dot{\phi}_4^2 g_4\right] = T_c - T_b \qquad [E\text{-}22]$$

$$\left[I_B + m_B\left(r_{B1}^2 + r_{B2}^2\right)\right]\ddot{\phi} + m_B\left[\ddot{\phi}_2 L_B f_1 + \ddot{\phi}_3 L_A f_2 + \ddot{\phi}_4 f_3 + \ddot{x}_1 f_6 - \ddot{x}_2 g_6 + \phi_2^2 L_B g_1 - \dot{\phi}_3^2 L_A g_2 + \dot{\phi}_3^2 g_3\right] = T_b \qquad [E\text{-}23]$$

where

$$f_1 = r_{B1} \sin(\phi_2 - \phi_1) - r_{B2} \cos(\phi_2 - \phi_1) \qquad [E\text{-}24]$$

$$g_1 = r_{B1} \cos(\phi_2 - \phi_1) + r_{B2} \sin(\phi_2 - \phi_1) \qquad [E\text{-}25]$$

$$f_2 = r_{B1} \sin(\phi_1 - \phi_3) + r_{B2} \cos(\phi_1 - \phi_3) \qquad [E\text{-}26]$$

$$g_2 = r_{B1} \cos(\phi_1 - \phi_3) - r_{B2} \sin(\phi_1 - \phi_3) \quad [E\text{-}27]$$

$$f_3 = r_{B1}\left[r_{A2} \sin(\phi_4 - \theta_1) - r_{A1} \cos(\phi_4 - \phi_1)\right] - r_{B2}\left[r_{A1} \sin(\phi_4 - \phi_1) + r_{A2} \cos(\phi_4 - \phi_1)\right] \quad [E\text{-}28]$$

$$g_3 = r_{B1}\left[r_{A2} \cos(\phi_4 - \phi_1) + r_{A1} \sin(\phi_4 - \phi_1)\right] - r_{B2}\left[r_{A1} \cos(\phi_4 - \phi_1) - r_{A2} \sin(\phi_4 - \phi_1)\right] \quad [E\text{-}29]$$

$$f_4 = L_B r_{A1} \sin(\phi_4 - \phi_2) + L_B r_{A2} \cos(\phi_4 - \phi_2) \quad [E\text{-}30]$$

$$g_4 = L_B r_{A1} \cos(\phi_4 - \phi_2) - L_B r_{A2} \sin(\phi_4 - \phi_2) \quad [E\text{-}31]$$

$$f_5 = L_B r_{A1} \sin(\phi_3 - \phi_4) - L_B r_{A2} \cos(\phi_3 - \phi_4) \quad [E\text{-}32]$$

$$g_5 = L_B r_{A1} \cos(\phi_3 - \phi_4) + L_B r_{A2} \sin(\phi_3 - \phi_4) \quad [E\text{-}33]$$

$$f_6 = r_{B1} \sin\phi_1 + r_{B2} \cos\phi_1 \quad [E\text{-}34]$$

$$g_6 = r_{B1} \cos\phi_1 - r_{B2} \sin\phi_1 \quad [E\text{-}35]$$

$$f_7 = r_{A1} \cos\phi_4 - r_{A2} \sin\phi_4 \quad [E\text{-}36]$$

$$g_7 = -r_{A1} \sin\phi_4 - r_{A2} \cos\phi_4 \quad [E\text{-}37]$$

Equations [E-18] and [E-19] can be integrated twice to give the position of A* in R:

$$x_1 = \frac{m_B}{m_A + m_B}\left[g_6 + L_B \sin\phi_2 - L_A \sin\phi_3 - f_7\right] + A_1 t + A_2 \quad [E\text{-}38]$$

$$x_2 = \frac{m_B}{m_A + m_B}\left[f_6 - L_B \cos\phi_2 + L_A \cos\phi_3 + g_7\right] + B_1 t + B_2 \quad [E\text{-}39]$$

where A_1, A_2, B_1, B_2 are constants of integration and can be expressed in terms of the initial conditions.

Equations [E-20] - [E-23] can be simplified by eliminating $\ddot{x}_1$ and $\ddot{x}_2$ using Equations [E-18] and [E-19]. The result is

$$\ddot{\phi}_1 f_3 + \ddot{\phi}_2 f_4 + \ddot{\phi}_3 f_4 + \ddot{\phi}_3 f_5 + \left[\frac{m_A + m_B}{m_A m_B} I_A + r_{A1}^2 + r_{A2}^2\right] \ddot{\phi}_4$$

$$- \dot{\phi}_1^2 g_3 - \dot{\phi}_2^2 g_4 + \dot{\phi}_3^2 g_5 = -T_a \left(\frac{m_A + m_B}{m_A m_B}\right) \qquad [E\text{-}40]$$

$$\ddot{\phi}_1 L_A f_2 - \ddot{\phi}_2 L_A L_B \cos(\phi_2 - \phi_3) + \ddot{\phi}_3 L_A^2 + \ddot{\phi}_4 f_5$$

$$+ \dot{\phi}_1^2 L_A g_2 + \dot{\phi}_2^2 L_A L_B \sin(\phi_2 - \phi_3) - \dot{\phi}_4^2 g_5$$

$$= \left(T_a - T_c\right) \left(\frac{m_A + m_B}{m_A m_B}\right) \qquad [E\text{-}41]$$

$$\ddot{\phi}_1 L_B f_1 + \ddot{\phi}_2 L_B^2 - \ddot{\phi}_3 L_A L_B \cos(\phi_2 - \phi_3) + \ddot{\phi}_4 f_4$$

$$- \dot{\phi}_1^2 L_B g_1 - \dot{\phi}_3^2 L_A L_B \sin(\phi_2 - \phi_3) + \dot{\phi}_4^2 g_4$$

$$= \left(T_c - T_b\right) \left(\frac{m_A + m_B}{m_A m_B}\right) \qquad [E\text{-}42]$$

$$\ddot{\phi}_1 \left[\frac{m_A + m_B}{m_A m_B} I_B + r_{B1}^2 + r_{B2}^2\right] + \ddot{\phi}_2 L_B f_1 + \ddot{\phi}_3 L_A f_2 + \ddot{\phi}_4 f_3$$

$$+ \dot{\phi}_2^2 L_B g_1 - \dot{\phi}_3^2 L_A g_2 + \dot{\phi}_4^2 g_3 = T_b \left(\frac{m_A + m_B}{m_A m_B}\right) \qquad [E\text{-}43]$$

Equations [E-40] thru [E-43] describe the relative motion of the two bodies, and once the ϕ_i are known, the joint angles can be determined from Equations [E-7] thru [E-10].

If the inertia properties of the system are known, one is left with four equations and seven unknowns: ϕ_1, . . . ϕ_4, T_a, T_b, and T_c. Thus, in order to obtain results, one can either specify the torques and solve for the motion (May require numerical integration with a computer.), or specify the motion and solve for the torques, or a combination of the two. In the following calculations, some special cases are treated to illustrate these techniques.

3. Cargo Handling

By assuming that body A takes on the properties of the Shuttle, and that the shuttle is fixed inertially so that $\bar{a}_i$ coincides with $\bar{R}_i$ (i = 1, 2); and further assuming that

$$r_{B1} = -d, \; r_{B2} = -w \qquad [E-44]$$

$$L_A = L_B = \ell/2 \qquad [E-45]$$

$$\theta_1 = 0, \; \theta_2 = \pi \qquad [E-46]$$

the system in Fig. VIII-20 assumes the appearance in Fig. VIII-22. Further, since A is inertially fixed,

$$\theta_4 = \phi_4 = 0 \qquad [E-47]$$

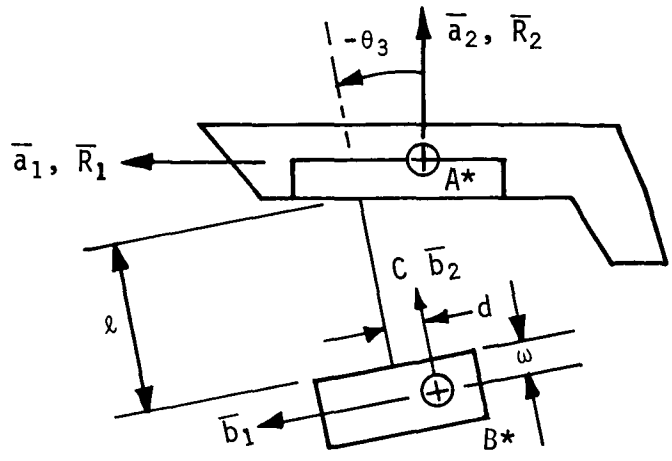

Fig. VIII-22 Cargo Handling Case

Substitution from [E-46] and [E-47] into [E-7] thru [E-10] yields

$$\phi_3 = \theta_3 \qquad [E-48]$$

$$\phi_2 = \pi + \theta_3 \qquad [E-49]$$

$$\phi_1 = \pi + \theta_3 \qquad [E-50]$$

And substitution from Equations [E-48]thru [E-50] into Equations [E-40]thru [E-43] and solving for T_a, T_c, T_b, one is left with

$$T_a = \ddot{\theta}_3 \left\{ I_B + M_B[(\ell + \omega)^2 + d^2] \right\} \qquad [E-51]$$

$$T_c = \ddot{\theta}_3 \left\{ I_B + M_B[(\ell/2 + \omega)(\ell + \omega) + d^2] \right\} - \ell d\, M_B\, \dot{\theta}_3^2 \qquad [E-52]$$

$$T_b = \ddot{\theta}_3 \left\{ I_B + M_B[d^2 + \omega^2 + \ell\omega] \right\} - 2\ell d\, M_B\, \dot{\theta}_3^2 \qquad [E-53]$$

Comparison of [E-51] with the torque expression in Chapter IV, Section C reveals that the above result agrees with the preliminary analysis, which serves as a check on [E-40] thru [E-43].

From [E-52] and [E-53], one can conclude that when a constant torque $\left(T_a\right)$ is applied at the shoulder joint, the torques required at the elbow and wrist $\left(T_c \text{ and } T_b, \text{ respectively}\right)$ to maintain those joint angles constant will be functions of time unless d = 0. If d is set equal to zero one has for the torques.

$$T_a = \left[I_B + M_B\, (\ell + \omega)^2 \right] \ddot{\theta}_3 \qquad [E-54]$$

$$T_c = \left[I_B + M_B\, (\ell + \omega)(\ell/2 + \omega) \right] \ddot{\theta}_3 \qquad [E-55]$$

$$T_b = \left[I_B + M_B\, \omega(\ell + \omega) \right] \ddot{\theta}_3 \qquad [E-56]$$

Solving Equation [E-54] for $\ddot{\theta}_3$ and substituting into Equations [E-55] and [E-56] results in

$$T_c = T_a \left\{ \frac{I_B + M_B\, (\ell + \omega)(\ell/2 + \omega)}{I_B + M_B\, (\ell + \omega)^2} \right\} \qquad [E-57]$$

$$T_b = T_a \left\{ \frac{I_B + M_B\, \omega(\ell + \omega)}{I_B + M_B\, (\ell + \omega)^2} \right\} \qquad [E-58]$$

which agree with the result obtained in Chapter VII, Section B for $x = \ell/2$ and $x = \ell$, respectively.

4. Flyby Docking

When the moment of inertia and mass of body A becomes infinite, and assuming body B has the inertia properties of the Shuttle, the system takes on the appearance shown in Fig. VIII-23. It has also been assumed that

$$\left.\begin{aligned} \theta_1 &= -\pi/6 \\ \theta_2 &= 4/3\pi \\ L_A &= L_B = L \end{aligned}\right\} \qquad \text{[E-59]}$$

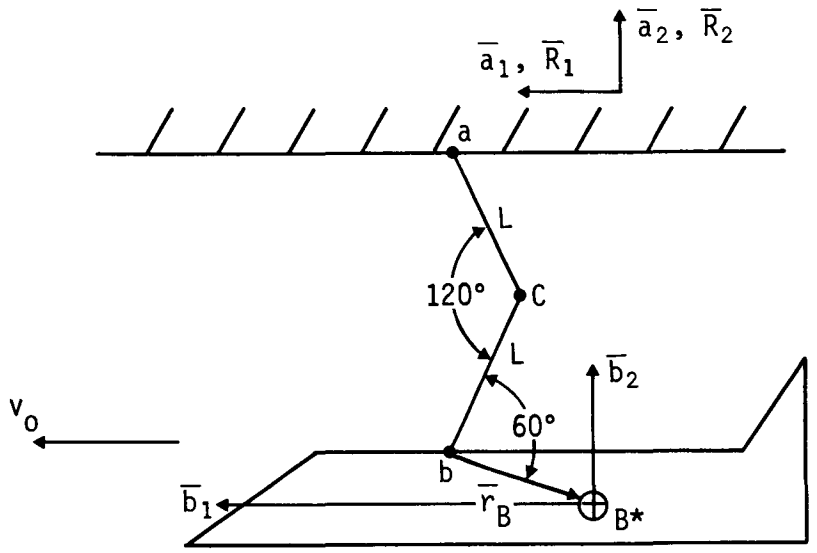

Fig. VIII-23 Flyby Docking

Given the configuration shown in Fig. VIII-23, the following question presents itself: If the maximum allowable torques at the joints are T_a, T_b, and T_c, what maximum tangential velocity, v_o, are these torques capable of arresting in an arc subtended by an angle of 1 radian? Equations [E-38]thru [E-43] will be used to obtain the answer to this question.

First, when m_B and I_B become infinite, Equations [E-38] thru [E-40] reduce to

$$x_1 = A_1 t + A_2 \qquad [E\text{-}60]$$

$$x_2 = B_1 t + B_2 \qquad [E\text{-}61]$$

$$\ddot{\phi}_4 = 0 \qquad [E\text{-}62]$$

which simply means that if body A is initially at rest in inertial space, it remains so. That is, if one assumes

$$x_1(0) = \dot{x}_1(0) = x_2(0) = \dot{x}_2(0) = \phi_4(0) = \dot{\phi}_4(0) = 0 \qquad [E\text{-}63]$$

then

$$x_1 = x_2 = \phi_4 = 0 \qquad [E\text{-}64]$$

Now, from Equations [E-7] thru [E-10] and [E-64], it follows that

$$\begin{aligned} \phi_3 &= \theta_3 \\ \phi_2 &= 4/3\pi + \theta_3 \\ \phi_1 &= 7/6\pi + \theta_3 \end{aligned} \qquad [E\text{-}65]$$

If Equation [E-65] is substituted into Equations [E-41] thru [E-43] and the result is used to solve for T_a, T_b, and T_c, one is left with

$$T_a = M_B \left[-2\sqrt{3}\, L r_{B2} + 3L^2 + \frac{I_B}{M_B} + r_{B1}^2 + r_{B2}^2 \right] \ddot{\theta}_3 \qquad [E\text{-}66]$$

$$T_b = M_B \left[\frac{I_B}{M_B} + r_{B1}^2 + r_{B2}^2 - \sqrt{3}\, L r_{B2} \right] \ddot{\theta}_3 + \sqrt{3}\, L r_{B1}\, M_B\, \dot{\theta}_3^2 \qquad [E\text{-}67]$$

$$T_c = M_B \left[\frac{I_B}{M_B} + r_{B1} + r_{B2} + \left(\frac{r_{B1}\, L - 3\sqrt{3}\, r_{B2}\, L + 3L^2}{2} \right) \right] \ddot{\theta}_3$$

$$- \frac{L}{2} M_B \left(r_{B2} - \sqrt{3}\, r_{B1} + \sqrt{3}\, L \right) \dot{\theta}_3^2 \qquad [E\text{-}68]$$

where Equations [E-59] and [E-65] have been used to express the f_i and g_i in terms of r_{B1}, r_{B2}, and L.

Assuming that T_a is a constant, two integrations of Equations [E-66] leave

$$\dot{\theta}_3 = \frac{T_a}{\alpha} t + \dot{\theta}_3(0) \qquad [E-69]$$

$$\Delta\theta_3 = \frac{T_a}{\alpha} \frac{t^2}{2} + \dot{\theta}_3(0)t \qquad [E-70]$$

where

$$\alpha = M_B \left[-2\sqrt{3}\, L r_{B2} + 3L^2 + \frac{I_B}{M_B} + r_{B1}^2 + r_{B2}^2 \right] \qquad [E-71]$$

As in the preliminary analysis in Chapter IV, Section C, Equation [E-69] can be solved for the time required for T_a to arrest the motion, i.e.,

$$t_f = \frac{-\alpha\dot{\theta}_3(0)}{T_a} \qquad [E-72]$$

and since

$$\dot{\theta}_3(0) = v_o/\sqrt{3}\, L \qquad [E-73]$$

[72] becomes

$$t_f = \frac{-\alpha v_o}{\sqrt{3}\, L\, T_a} \qquad [E-74]$$

Now, if Equation [E-74] is used for t in Equation [E-70], and $\Delta\theta$ is set equal to one radian, the following is obtained

$$1 = \frac{-\alpha v_o^2}{6L^2 T_a} \qquad [E-75]$$

from which

$$v_o = \left(\frac{-6L^2T_a}{\alpha}\right)^{\frac{1}{2}} \qquad [E-76]$$

It is noted here that T_a is negative since it must slow the rotation to a stop.

Now Equation [E-76] gives the maximum v_o that the shoulder joint is capable of stopping. To determine if the torque capabilities of the other two joints are exceeded by this v_o, one can substitute from Equations [E-66], [E-69] and [E-73] into [E-67] and [E-68] to express T_b and T_c in terms of v_o and the inertia properties of the system. To illustrate this, the following example is considered:

Let

$$T_a = -150 \text{ ft-lb}$$

$$|T_b| \text{ max} = 500 \text{ ft-lb}$$

$$|T_c| \text{ max} = 350 \text{ ft-lb}$$

$$L = 23.5 \text{ ft}$$

$$r_{B1} = -32.5 \text{ ft}$$

$$r_{B2} = -16.75 \text{ ft}$$

$$M_B = 10^4 \text{ slugs}$$

$$I_B = 15.1 \times 10^6 \text{ slug-ft}^2$$

When the above values are substituted into Equations [E-71] and [E-76], one obtains for v_o

$$v_o = 0.093 \text{ ft/sec} \approx 0.1 \text{ ft/sec} \qquad [E-77]$$

and substitution into Equations [E-67] and [E-68] leaves

$$T_b = -92 - 1.33 \times 10^7 \left(-2.6 \times 10^{-6}t + 2.27 \times 10^{-3}\right)^2 \text{ (ft-lb)} \quad [E-78]$$

$$T_c = -69 + 0.651 \times 10^7 \left(-2.6 \times 10^{-6}t + 2.27 \times 10^{-3}\right)^2 \text{ (ft-lb)} \quad [E-79]$$

Now the expression within the parentheses in Equations [E-78] and [E-79] is $\dot{\theta}_3$, which approaches zero as t approaches t_f. Therefore, the maximum torque requirements are

$$\left|T_b\right|_{t=0} = 155.5 \text{ ft-lb} \quad [E-80]$$

$$\left|T_c\right|_{t=t_f} = 69 \text{ ft-lb} \quad [E-81]$$

Thus, the torque capabilities of joints b and c are not reached in this case, and therefore the torque capability of joint a is the determining factor. If, on the other hand, the torque capability at either of joints b and c had been exceeded, one would use Equations [E-67] and [E-68] to express T_b and T_c in terms of v_o, determine the maximum values as in the case above, and then solve for v_o.

5. Cargo Stopping Distance

In addition to the nominal stopping distances from the maximum velocities of 4.6 m (15 ft) loaded, the stopping distance for the loaded arm was calculated using the full 667 nm (500 ft-lb) capability of the shoulder joint. Based on the maximum loaded velocity of 0.53 m/sec (0.17 ft/sec) for the unloading and deployment of the 29,600 kg (65,000 lb) payload, the stopping distance is 1.34 m (4.4 ft) when the full capability of the joint is utilized. This stopping distance could be further reduced under emergency conditions by applying the brakes which are incorporated into the joint designs.

F. CREW SYSTEMS AND MAN/MACHINE INTERFACE

A preliminary task/systems analysis was conducted for the activation and operational sequences of RMS use, as related to the Shuttle and Space Station. A detailed task analysis was performed for the capture/docking and cargo transfer tasks, since these tasks include most of the subfunctions of each of the other operational sequences. The required crew station volume was defined for the bilateral master/slave system, since the movement envelope of the masters dictates a larger volume than that required for the hand controller system. This additional volume is approximately 0.06 to 0.08 cubic meters (2-3 cub ft). A control console was designed to provide the controls and displays necessary to allow the RMS operator to perform the tasks defined in the prior analysis.

1. Control Station Layout

a. General

A NASA-MSC version of the Shuttle flight deck is shown in Fig. VIII-24. It is manned by two astronauts. During RMS operations the command pilot flies the Shuttle from a small auxiliary, rear facing control console, and the copilot becomes the RMS operator. The visual angles, shown in relation to the Shuttle payload, are 60° from side to side, 20° down, and 55° up. The basic volumes required, which are shown on the Fig. VIII-24, provide for a 95 percentile astronaut, the master controller movement envelope, and the control console.

This control station layout is designed around the two master RMS controllers. These controllers are the dominant feature of the station and take up the most volume when in operation. A neutral position was selected (shown in Fig. VIII-25) for each controller and a movement volume worked out from that. Two-dimensional mockups were made to determine the movement arc of each master segment. Since the master controller movement extends below the operator's waist he must be in a semistanding position. The movement of the master controllers is limited mechanically so they cannot extend beyond their operational reach. This will eliminate the possibility of contact with the instrument panel or other station equipment. The astronaut is restrained by a small seat with a waist strap. His shoulders are not restrained and he is free to lean forward to reach the control console switches. The control console is located 26 to 30 inches from the astronaut's eye when his back is vertical. The layout shown in Fig. VIII-26 depicts a 95 percentile man (worst case) volumewise. All toggle switches are guarded, and rotary switches and pushbuttons are recessed to prevent inadvertent activation.

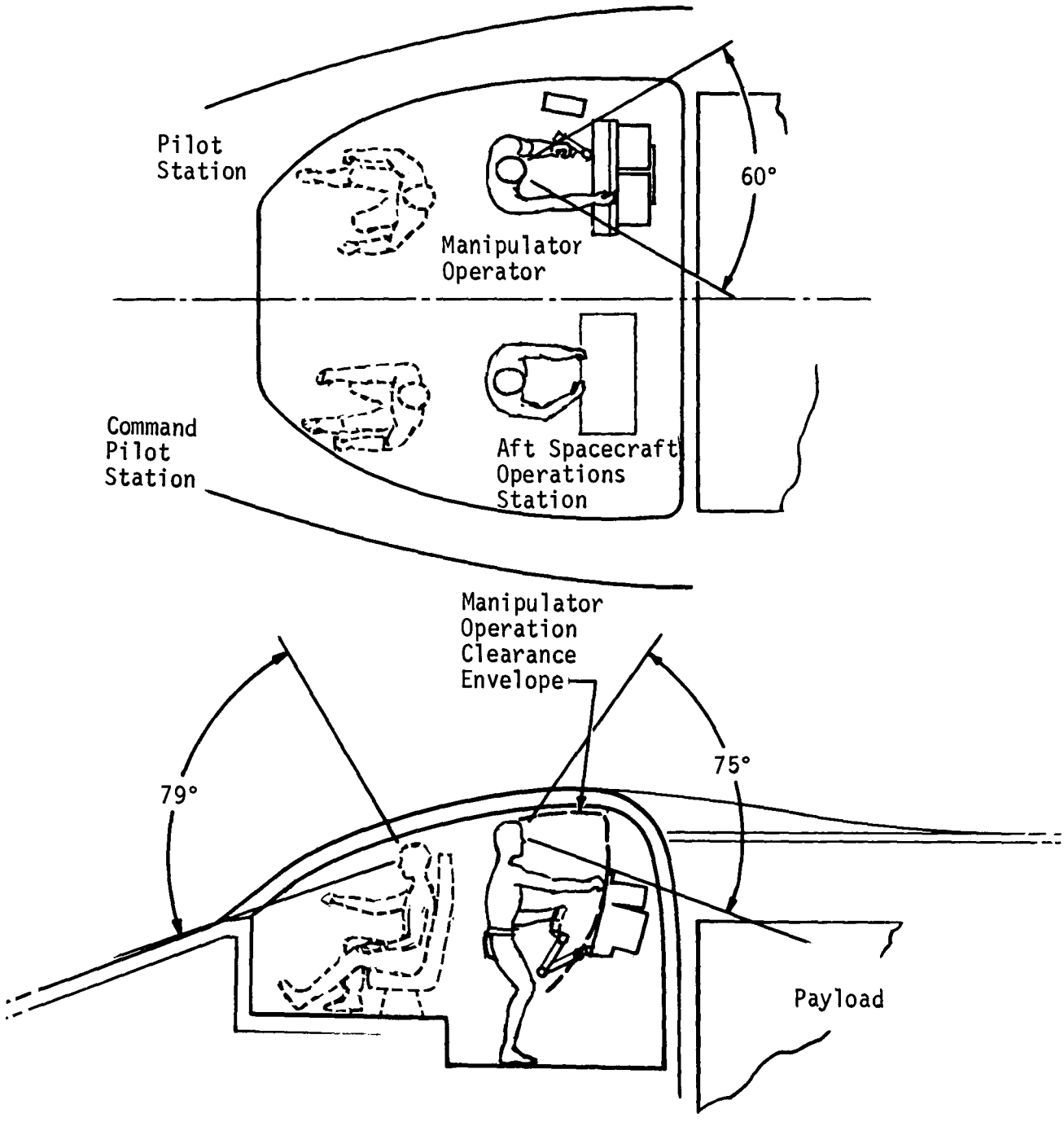

Fig. VIII-24 Shuttle Crew Station

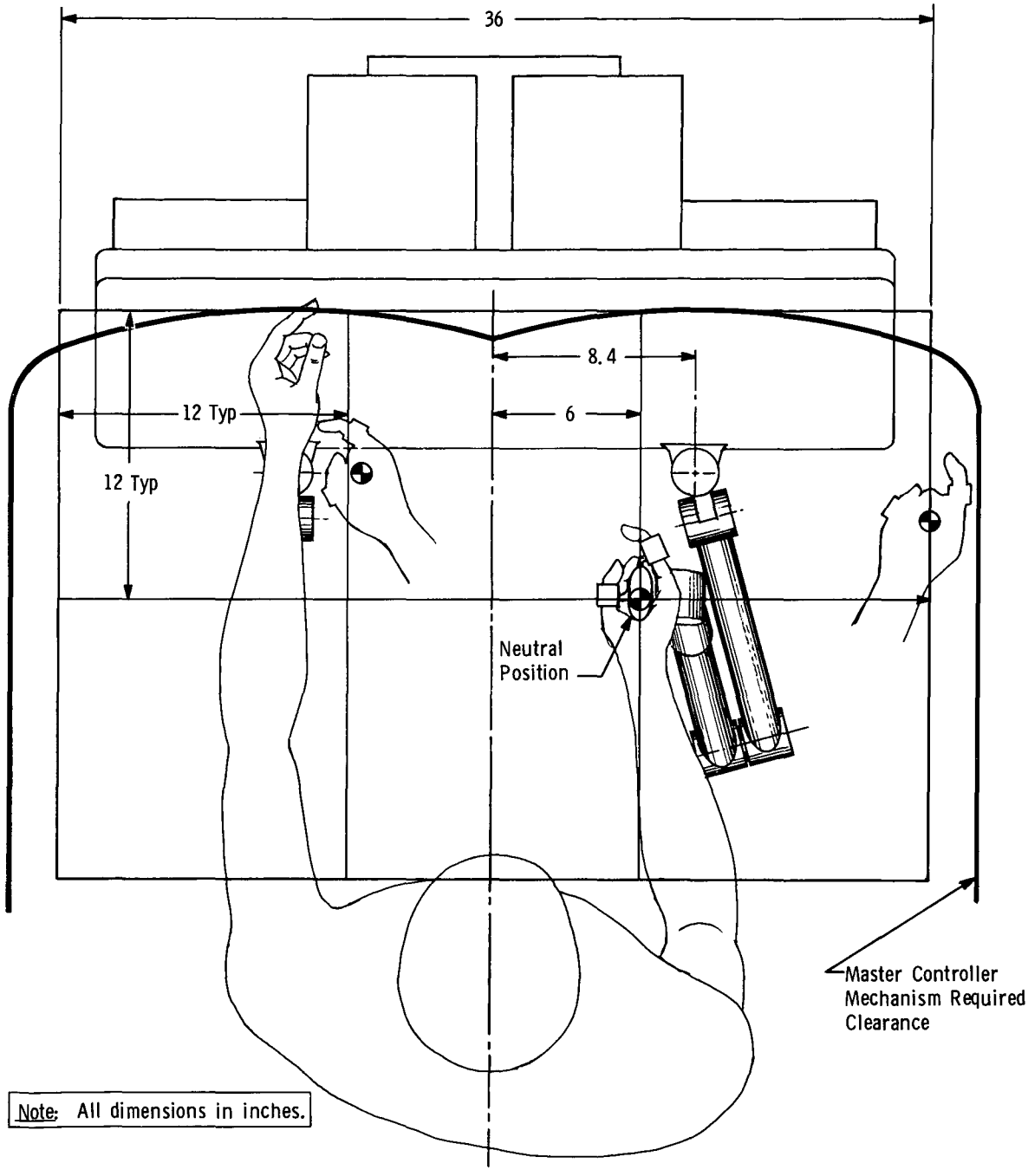

Fig. VIII-25 RMS Control Station, Neutral Position

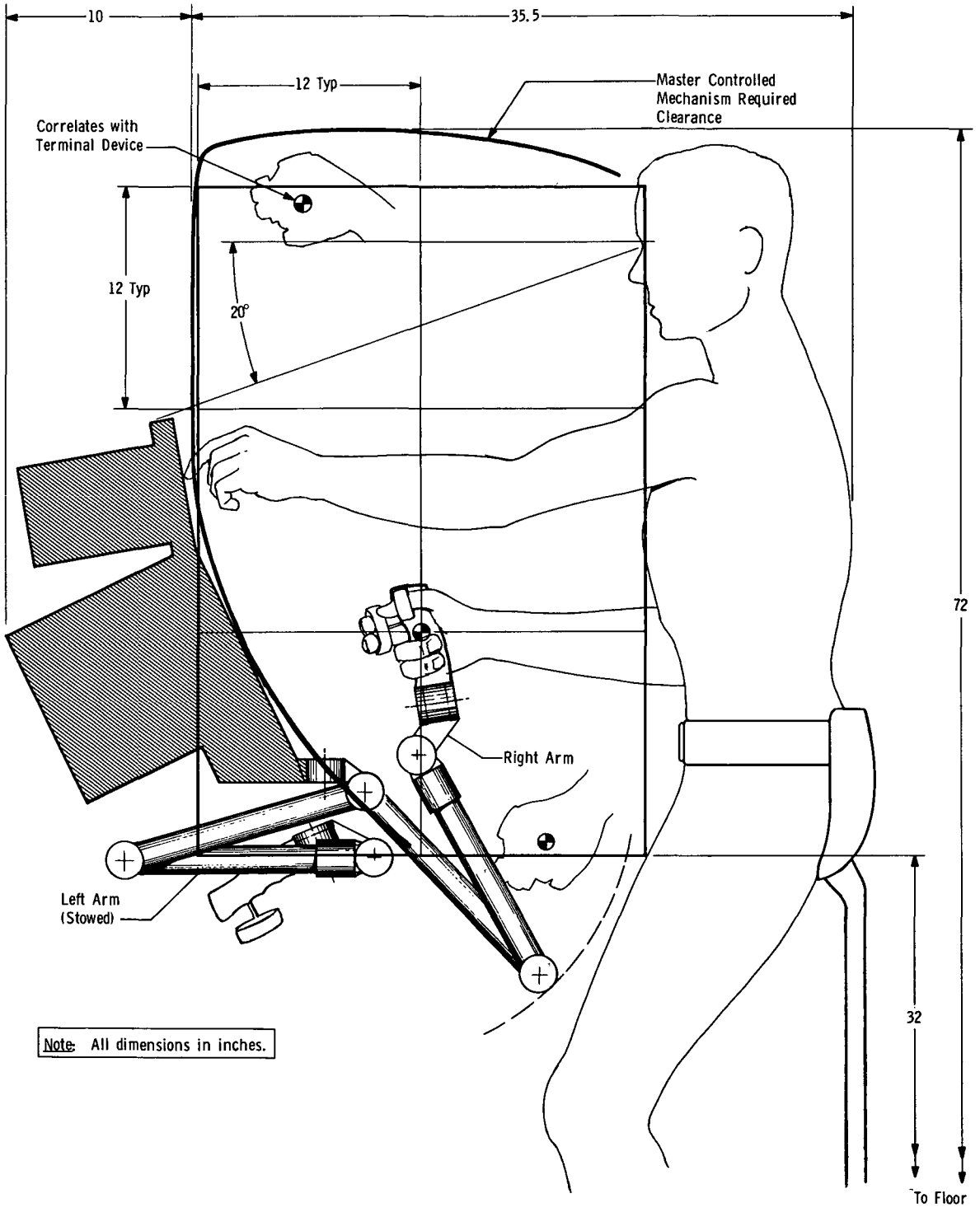

Fig. VIII-26 RMS Control Station, Volumetric Requirements, 95 Percentile Man

Operational, full-scale, three-dimensional mockups, further Human Engineering analysis, numerous simulations, and trade-offs with the selected Shuttle contractor must be made before a final RMS controller station can be configured. However, for the master-slave concept, this layout represents a starting point for determining the volume required in the Shuttle vehicle.

Each functional group of controls on the control panel (Fig. VIII-27) and subconsole (Fig. VIII-28) is discussed in the following paragraphs. Figure VIII-29 shows an artist's concept of the RMS control station.

b. TV Monitors

Three black and white, monoscopic, TV monitors are located to provide a 20° down visual sighting angle. The primary, 12-in. monitor normally displays signals from the terminal device TV cameras. There is no requirement for a TV system with resolution greater than the obtainable ETA standard 525 scan lines. Each monitor has standard ON/OFF, brightness, contrast, and test controls. In addition, any of the four TV cameras can be selected on any of the three TV monitors. This gives tridundant backup for the indirect visual mode. The controls are located on the outboard edge of each monitor to allow the screens to be placed as close together as possible; thereby, minimizing eye shift between monitors.

c. RMS Checkout

This control/display panel serves two functions. First, it evaluates the condition of the master-slave arm motors, tachometers and potentiometers, and their associated wiring. Second, it is used as a manual backup mode to the standard master-slave control.

The RMS checkout takes place before power is applied to either the slaves or masters. The right-hand rotary switch selects the slave or master to be evaluated. The left-hand rotary switch selects the joint or terminal device. The upper toggle switch selects the motor, tachometer, or potentiometer in each joint. Upon selecting the desired parameter to be evaluated, a predetermined voltage is applied and displayed on the digital readout. This is the voltage that has been sent to the system. Pressing the push-button displays the actual voltage the system accepts and returns. These voltages should match in each case. Application of these voltages will not move the joints since the brakes are locked when power is off.

These controls are also used to move each joint independently, if desired, in the event of a master or slave joint failure. The desired joint would be set up on the rotary switches and the lower toggle switch activated (±) to provide the desired direction of travel. Activation of this switch releases the selected joint brake and applies the same voltage used for checkout. In the event of a malfunctioning motor in one of the seven slave joints, power to the slave could be shut off, thereby, rigidizing the slave and individual joints could be moved to position the slave in a stowed or out of the way location.

d. Slave Arm "Jettison"

This capability is provided to jettison the slaves in the event of a partial or total slave arm failure that would not allow the arm(s) to be placed in a stowed position and the Shuttle bay doors to be closed. An explosive device will separate the slave's shoulder mechanism and allow the Shuttle to be flown away from them. These switches are locked toggle switches to prevent inadvertent activation.

e. Slave Arm Launch Locking Mechanisms

The exact location of the slave arms launch holddown mechanisms will be determined by examining the detail interfaces during the design phase of the Shuttle. However, for this preliminary design it has been assumed that they will be in the Shuttle cargo bay doors and consist of seven latching devices per arm. These latches must be unlocked and verified before the Shuttle cargo bay doors are opened. The two toggle switches activate all of the latching devices per arm. The indicator lights verify that they all achieved the desired position.

f. Slave Shoulder Deploy

The shoulders of both slave arms pivot out of their stowed position, in the forward end of the cargo bay, to the deployed position. These two toggle switches position the shoulders and the indicator lights are activated to verify their location.

g. Master Controller Power

A separate power control for the masters is provided to allow slave movement by automatic or manual means if desired or in the event of master controller failure. A master control reversal switch is provided with the standard ON/OFF switches. This three-position switch allows master (1) to control slave (2), or master (2) to control slave (1). The OFF position maintains the normal

FOLDOUT FRAME 1

FOLDOUT FRAME 2

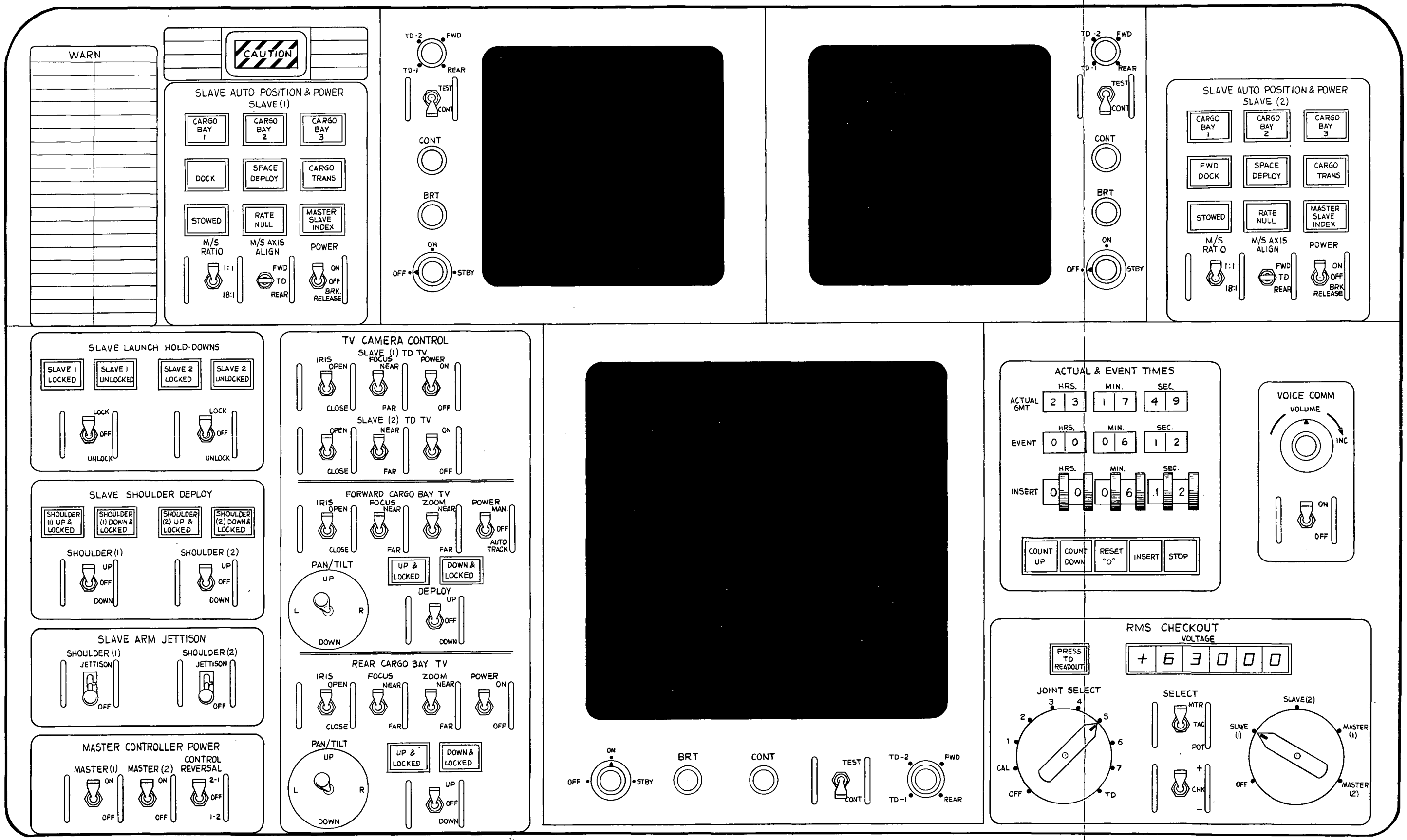

Fig. VIII-27 RMS Control Console

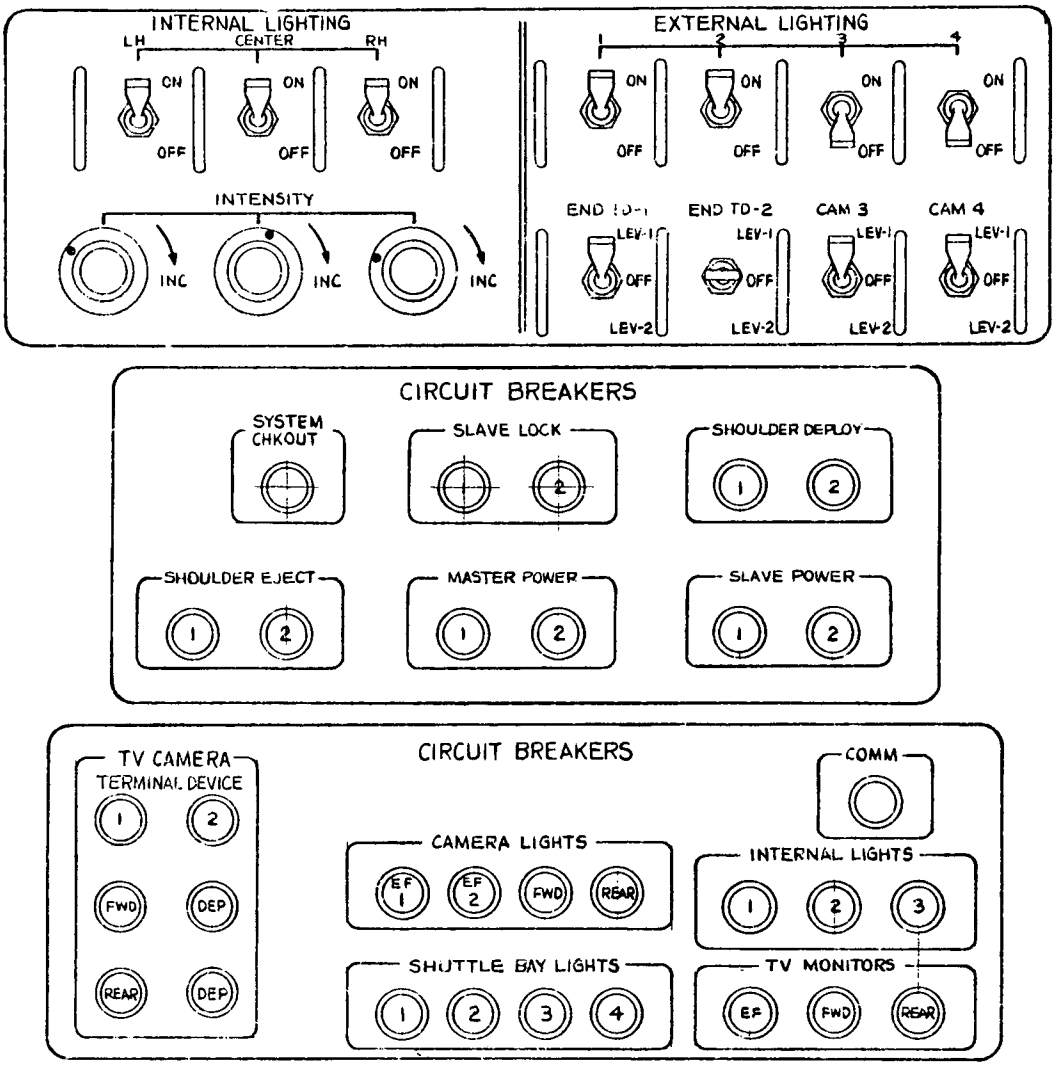

Fig. VIII-28 Subconsole

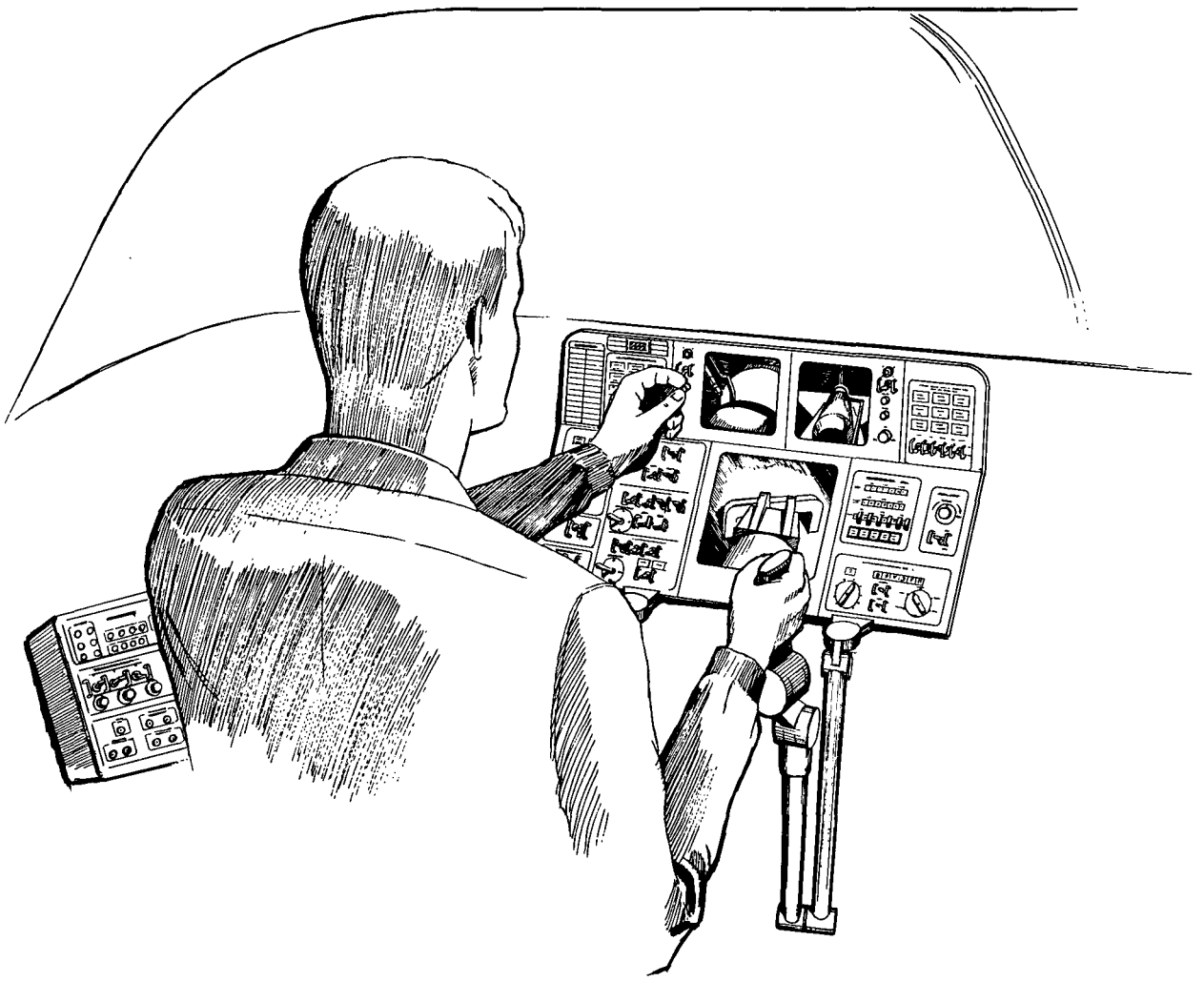

Fig. VIII-29 Artist's Concept of RMS Control Station

control mode. In a sense, this control reversal capability provides redundant master controllers and allows the astronaut to select right or left masters in accord with his optimum motor skills.

h. Slave Auto Position and Power

These two panels provide control for the automatic, computer controlled functions of the slave arms. Six pushbutton/lights are used to command the slave arm to various functions. These six are representative and will undoubtedly change as the RMS and Shuttle designs are formalized. These automatic modes will position the slaves from wherever they are to the selected location, while always keeping the arm positioned so it will not contact the Shuttle or the cargo.

Selecting any of the three (exact number to be determined) positions in the cargo bay will command the slave arm to within grasping distance (2 to 4 ft) of a cargo module attach point. Activation of the switch also activates the light, which stays on until the slave arm reaches its destination and its location is verified by the computer.

The "Forward Dock" command positions the slave arm in an optimum forward position for docking with either the Space Station or another Shuttle.

"Space Deploy" positions the slave up and away from the Shuttle for deployment of a subsatellite.

"Cargo Transfer" positions the Space Station modules from out of the cargo bay to within a predetermined distance from the Space Station.

The "Stowed" position will command the slave arms from wherever they are to the straight fore and aft location. With the shoulders deployed the slave arms will be parallel to but not over the cargo bay.

After the slave arm has been mechanically coupled to a Space Station or other orbital payload, the "Rate Null" switch is depressed, thereby allowing the computer to reduce the rate differences between the vehicles by sensing the angles and angular changes at the arm joints and applying optimum reaction control system braking power.

Activation of the "Master/Slave Indexing" switch commands the computer to position the master arm to a neutral position. This provides a standard starting point and when maximum master travel has been reached, provides a capability to "hold" movement of the slaves while indexing the masters for continued movement.

The two-position toggle switch "Master/Slave Ratio" selects the movement ratio between the master and slave. The ratio 18:1 means a 1 ft movement of the master commands a 1 ft movement at the slave terminal device. The ratio 1:1 moves the terminal device 18 ft/ft of master travel.

For most of the RMS tasks the slave arm wrist TV camera will be used for visual positioning cues. This means, for example, that a forward motion of the master will command a slave terminal device motion along the longitudinal axis of the TV camera. This movement disregards the actual position of the slave arm wrist and moves with respect to the picture presented in the monitor. The slave wrist TV for master positioning control is used only before the terminal device has grasped an object. At this time all that is presented in the monitor is the grasping point, thereby, eliminating spatial cues. After an object has been grasped it is necessary to monitor the slave/object movement using the base mounted TV. This means that the master/slave movement relationship is viewed from a different reference point and must be realigned with the axis of the TV camera used. "M/S Axis Alignment" selects the desired slave movement alignment with respect to the TV camera used for positioning control.

The "Power" switch is a three-position toggle. "ON" releases the individual joint brakes and enables power to be applied to all motors, potentiometers, and tachometers by movement commands from the master controller. The motors will hold their position until the commanded movement is made by the master, automatically or manually. "OFF" shuts off all power and engages the electromagnetic brakes. "Brake Release" applies a voltage to the brakes, from a separate power souce, and will allow one slave arm (limp) to be positioned by the other controlled slave arm.

i. Voice Communication

Internal Shuttle communication control is provided to the RMS controller. This consists of ON/OFF and volume control. A press-to-talk switch may be required depending on the Shuttle communication system. It was not included now, however, since the logical place to put it is on the master hand controller, which already has many functions. Activation of the power switch provides continuous communication with the Shuttle crew. All channel or frequency selecting will be done by the Shuttle pilot.

j. Internal and External Lighting

The exact number of lights required and their intensities for both internal (at the RMS controller station) and external (cargo bay) lighting was beyond the scope of this contract. A representative number are included on the subconsole for layout planning and overall sizing.

k. Actual and Event Times

This digital timer is slaved from the master timer system in the Shuttle. Actual GMT (Greenwich mean time) is continuously displayed on the top line. An "Event" time may be inserted using the thumb wheels on the "Insert" row and counted down, or the digits can be "Reset to 0" and an event can be "Counted up." The "Stop" switch stops the event timer.

ℓ. Master Caution and Warn Panel

The caution and warn lights are located in panels on the upper left corner of the control console. This location places them in a near optimum visual area that, if activated, will command an immediate response from the RMS controller. The caution light include monitors from those systems whose failure will cause a threat to life or mission success. The warn lights are activated in the case of system operating out of tolerance but not an immediate danger.

m. Circuit Breakers

All of the RMS circuit breakers are presently located in the subconsole. The exact number of breaker was estimated and not derived from an engineering evaluation.

2. RMS Operational Sequence

a. RMS Checkout

The RMS checkout sequence will be conducted before each major operational activation. The operation of each joint is checked first and then the interface between the master and slave is verified before the total system activation.

1) Unlock (slave arm) launch holddowns (assuming they are in the sequence). Switches activate and lights verify position of locks.

2) Open Shuttle doors.

3) Activate support subsystems, interior and exterior lights, TV, communications.

4) Perform static electrical checks on slaves (checks motor windings and wiring).

   a) Select CAL and verify number on digital readout

   b) Select master or slave to be checked

   c) Select number of joint to be checked

   d) Check motor, tachometer, and potentiometer

      i) As the number is selected the correct voltage or current appears on digital readout

      ii) When press to readout "pushbutton" is activated the actual voltage or current is shown and compared with the desired voltage or current.

5) Deploy (slave) shoulders to operational location.

6) Deploy cargo bay TV cameras 2 and 3.

7) Activate and check pan/tilt/zoom on TV cameras 2 and 3.

8) Manually unstow master arms from launch holddown.

9) Turn power on to slave 1.

10) Turn power on to master 1.

11) Position ratio select switch 9 on 1:1 ratio.

12) Conduct operational movement check of No. 1 master/slave, visually.

13) Place No. 1 master/slave in "hold" location (out of the way) and shut off power to both. Slave is ridigized by brakes, place master in stowed position.

14) Repeat Steps 9 thru 12 for master/slave No. 2.

15) Conduct operational task using desired master/slave.

b. Shuttle to Space Station Docking and Module Transfer

This sequential task was selected as a typical RMS activity. The description is of normal operating mode, i.e., using automatic modes when available. Total manual backup is provided for the capture, differential velocity nulling, and docking.

Master/Slave checkout complete and all required operations systems ON

1) RMS Controller

a) Depress "Forward Docking" button on automatic slave positioning panel. Computer control automatically positions slave and activates master to neutral position as shown in Fig. VIII-25. Position is verified by computer and switch light goes off. The RMS operator can verify the slave position since it is in his direct visual field.

b) Index master with slave.

c) Select desired Master/Slave movement ratio.

2) Shuttle Pilot (Uses direct vision and TV from 100 ft to docking)

a) Verify and hold coplanar orbit.

b) Establish and hold y/z translations, uses direct vision and terminal device TV with grid pattern.

c) Establish and hold pitch, roll, and yaw.

d) Determine closure distance [≈1.5 m (5 ft)] and slave reach envelope in x,y,z axes. Hold reach envelope conditions.

e) Stand by for abort.

3) RMS Controller (concurrent with pilot closure operation)

a) Monitor final closure using direct vision and terminal device-TV.

b) Reach for an grasp Space Station receptacle, verify terminal device engagement, and lock terminal device by exerting pincher force with fingers and thumb to overcome detent, thereby, locking terminal device.

c) Verify mechanical coupling.

d) Depress "Rate Null" automatic mode switch. (Sensors in RMS control Shuttle RCS to suppress velocity difference and then computer directs RCS to docking.) Shuttle pilot monitors attitudes, positions, and rates of vehicles by direct vision.

e) Monitor translation and docking.

4) Shuttle Pilot

Verify hard docking.

5) RMS Controller

a) Detach terminal devices and back off slave 0.6 to 1.2 m (2 to 4 ft) manually.

b) Reposition slave automatically to area 1 in cargo bay.

c) Select 1:1 master/slave ratio and terminal device TV axis alignment and index.

d) Manually reach to Space Station module (in cargo bay) attach point and grasp terminal device attach point.

e) Verify attachment.

6) Shuttle Pilot

Release module holddown fixtures and verify.

7) RMS Controller

a) Select forward cargo bay TV axis alignment and index master/slave.

b) Using forward TV as visual reference move module out of holddown fixture and clear of cargo bay.

c) Depress "cargo transfer" pushbutton and monitor slave/cargo movement.

d) Verify module location and index master slave.

e) Select 1:1 master/slave movement ratio.

f) Manually, insert module into docking port and verify hard dock.

g) Release terminal device and manually back off 0.6 to 1.2 m (2 to 4 ft).

h) Depress "stowed" automatic position.

i) Deactivate RMS.

G. TELECOMMUNICATIONS

This section discusses the preliminary design of a Shuttle RMS telecommunications subsystem.

The TV system is designed to meet requirements for field of view, depth of focus, resolution, motion rendition, dynamic range, sun protection and signal to noise ratio. It is determined that presently developed Apollo TV cameras are suitable with minor modifications. Lighting requirements are also discussed and it is recommended that lamps similar to the Apollo CSM docking floodlight be used. Geometry of the lighting placement is also discussed.

A basic functional block diagram of the telecommunications subsystem is developed and discussed. Each block is broken down further to show signal inputs and outputs.

The telecommunication signals are analyzed according to their routing, format, and expected interface with the mission operational timeline. Where appropriate, signal accuracies and error rates are discussed.

1. TV System

The telecommunications subsystem will include four television cameras: one TV camera located on each slave arm wrist just prior to the roll joint; one located at the forward end of the cargo bay, capable of auto-tracking a slave arm; and one camera at the rear of the cargo bay to assist in loading or unloading, to serve as a backup to the other three, or to provide wide angle entire scene coverage.

Excellent space-qualified TV cameras, such as those used on the Apollo program, are available and would hold down costs if they are acceptable. Therefore, the initial task in this section will be to examine the specifications of these cameras to determine their suitability to the RMS.

a. Picture Quality - Two aspects that have to do with picture quality have already been treated in Chapter VII Section G. The required resolution was 300 lines. The Apollo color camera has a specified resolution of 300 lines or greater, so it is acceptable in this area. The calculated minimum video frame rate was

20 frames/sec. The Apollo camera frame rate is 30 frames/sec--more than adequate for the task. The higher frame rate will produce nearly flicker-free, natural motion rendition to the operator--an advantage from the human factors standpoint. The higher bandwidth is not a problem in a direct wire-connected system.

A signal-to-noise ratio of 20 db is generally regarded as the minimum acceptable picture quality. The Apollo 15 LRV camera without color filters, has a S/N ratio of 35 db at 0.6 millilambert brightness--more than adequate.

The Apollo cameras have essentially infinite gray scale resolution. The total contrast range is determined by the dynamic range of the camera tube and electronics; for these cameras it is at least 1000 to 1. Best use of the dynamic range is made by switching the Automatic Level Control (ALC) to function either from the peak or brightest object in the field of view or from the average illumination in the scene. Additional contrast enhancement is possible by altering the video signal within the RMS control and data electronics.

The field of view is a somewhat arbitrary quality, depending upon the uses to which the camera is to be put: Does the task require closeups as well as wide-angle views, or is it all one or the other? It can be assumed that the wrist TV camera will be most involved with small movements occurring close to the lens. Thus, a fixed focal length should suffice. The lens must be a compromise between a number of factors. For example, the closer the object is to the lens, the lower the depth of field (or the distance range in which the object will remain in focus). Depth of field is inversely proportional to the focal length, however, so the wide angle lens will be more suitable than telephoto at near distances. A good choice for the wrist TV fixed focal length lens, taking into account these factors, is about 36 mm for a 30° field of view with the Apollo camera. This configuration will give a resolution of 2.5 cm (1 in.) at 7.6 m (25 ft). For the forward and rear cargo bay TV cameras, both telephoto and wide angle viewing will be required. The standard Apollo 15 LRV camera zoom lens, having a field of view of from 9 to 54° will be adequate in both applications.

b. TV Lighting Considerations - The problems associated with the visual environment in space are very different from those in the Earth's atmosphere. There exist extremes of contrast: very high levels of essentially collimated illumination that produce harsh shadows due to a lack of atmospheric diffusion. Lower levels of diffuse illumination are reflected from the Earth in near-Earth orbit and can be used to some advantage for Shuttle RMS television. However, it may not always be possible to orient the spacecraft to make use of earthlight, and auxiliary floodlighting becomes necessary to raise the minimum scene illumination. The Apollo cameras, modified to remove the color filters and motor will produce a picture having better than 30 db S/N with a scene illumination of approximately 2.5 m-c (0.25 ft-c). Thus, floodlighting must produce a minimum scene illumination of 2.5 m-c (0.25 ft-c).

1) Wrist TV Auxiliary Lighting - The wrist TV scene should be adequately illuminated at a distance of 7.6 m (25 ft). The Apollo docking floodlight, modified to a 48° 10% power beamwidth (from the present 24°), will give a scene illumination of 20 m-c (2 ft-c) at 7.6 m (25 ft). Using two such lamps to fill in shadows will double the luminous flux and produce 40 m-c (4 ft-c) illumination. This value is more than an order of magnitude above the minimum necessary and will help to reduce the contrast between brightest and dimmest objects in the scene. Where such high intensity is not needed the lamp power may be reduced to conserve power.

2) Forward Cargo Bay TV Camera - If the same floodlighting method is used as for the wrist TV group, the illumination at a distance of 15 m (50 ft) (maximum reach of arms) will be 10 m-c (1 ft-c). In the backup mode where the wrist TV is not functioning, the illumination on the target at 22.5 m (75 ft) will still be over 4 m-c (0.4 ft-c), which is more than adequate for a noise-free picture.

3) Rear Cargo Bay TV Camera - The rear cargo bay TV is used to ensure clearance of the RMS elbows and to give an overview of the entire operation. If the arms are extended as far forward as possible, the illumination level (assuming two 48° beamwidth floodlights) from these lights alone will be 2 m-c (0.2 ft-c), which is near the acceptable minimum. Lower light levels are acceptable but the S/N will decrease below 30 db.

4) Lighting Geometry - The forward and rear cargo bay TV cameras generally operate at distances of 10 m (33 ft) or more. Therefore, the preferred configuration is for the two lamps, one located on either side of the camera, moving with it in pan and tilt, to have their beam axes parallel to the camera axis.

For the wrist TV lighting it is desirable to fully illuminate the operation at a distance of 1 m (3 ft). Assume two lamps with 48° beamwidth located 0.3 m (1 ft) either side of the camera axis. Lamp axes are in the same plane as the camera axis but cross the camera axis at a distance of 3 m (10 ft). The angle with the camera axis is then

$$\theta_L = \arctan \frac{3}{0.3} = 84.3°.$$

The 10% power angle is $84.3° - \frac{48°}{2} = 60.3°$.

The point at which beam power from each source drops to 10% is

$d_m = 0.3 \tan 60.3 = 0.525$ m (1.7 ft) from the camera lens.

Thus the terminal device will be fully illuminated as will objects at a distance of 7.6 m (25 ft) for closing.

5) Automatic Light Level Control (ALC) - The dynamic range (ALC) of the TV camera must be considered when sunlight, either direct or specularly reflected, is in the same area where detail in the shadows is important. The dynamic range of Apollo cameras is 1000 to 1. Solar illuminance in Earth orbit is approximately 1.24×10^5 m-c (1.24×10^4 ft-c). Thus the object observed needs to receive $\frac{1.24 \times 10^5}{1000} = 124$ m-c (12.4 ft-c) in the shadow area. Assuming two 48°-beamwidth floodlights the distance between object and floodlights should not exceed 4.25 m (14 ft) for acceptable detail where sunlight and shadow are present.

The methods of ALC employed in the Apollo cameras have been proven in similar space conditions and will be applicable to this program.

6) Vidicon Protection - The silicon intensifier target (SIT) tube employed on Apollo 15 is not subject to burn even when pointed directly at the sun. This development is well suited to this program.

7) Cargo Bay Lighting - The cargo bay will necessarily have supplemental lighting capabilities to aid in cargo loading and unloading. Present Shuttle design calls for four wide-angle floodlights, independently controlled.

c. Apollo Camera Suitability - With only minor modifications the Apollo color cameras, in particular the newer types with a burn-free silicon target, are entirely suitable for all RMS visual sensing requirements. The modifications required are (1) removal of the color filter wheel and motor, (2) replacement of the zoom lens with a fixed focal length lens for the wrist TV cameras, and (3) addition of remote synchronization inputs.

2. Block Diagram

a. Design Overview - The recommended design of the telecommunications subsystem for the master/slave system analyzed in the previous sections is presented in Fig. VIII-30. This diagram is the integral result of analyses and tradeoffs performed earlier and is the basis of the discussion to follow. The telecommunications system for the bilateral rate control system would be very similar, with minor modifications in the crew station area to accommodate the bilateral handcontroller. Each section in Fig. VIII-30 is broken down and examined in greater detail in the input/output diagrams (Fig. VIII-31 through VIII-47).

1) Slave Arms - Each of the two slave arms consists of a terminal device, wrist sensing group, wrist joint, elbow joint, and shoulder joint. The terminal device and each joint is part of a closed loop servosystem including the slave servoamplifier group. A brake release command from the command group is necessary to activate any joint or the terminal device and feedback signals (position, velocity) are sent to the sensor data distribution unit. The wrist visual sensing group consists of a TV camera and associated illumination source. Iris and focus are controlled by signals from the TV camera controls. Illumination power is supplied through the illumination controls. Video output is sent directly to the TV monitor group in the crew station.

2) Control and Data Electronics (C&DE) - The C&DE section is primarily an interface between Crew Station, Cargo Bay, Slave arms and the Shuttle computer.

FOLDOUT FRAME 1

FOLDOUT FRAME 2

ARMS

CARGO BAY

CREW STATION

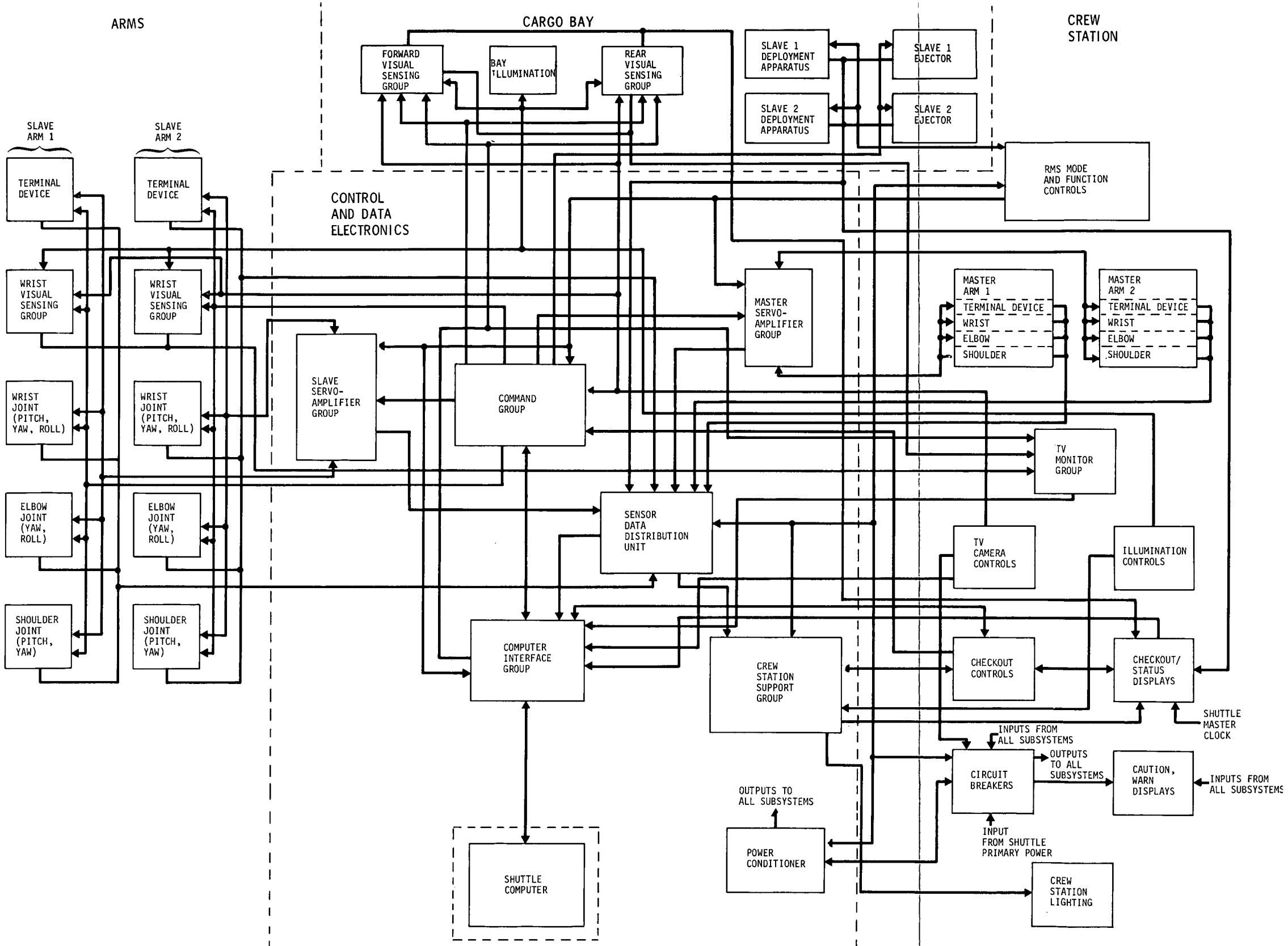

Fig. VIII-30 Telecommunications Subsystem Functional Block Diagram

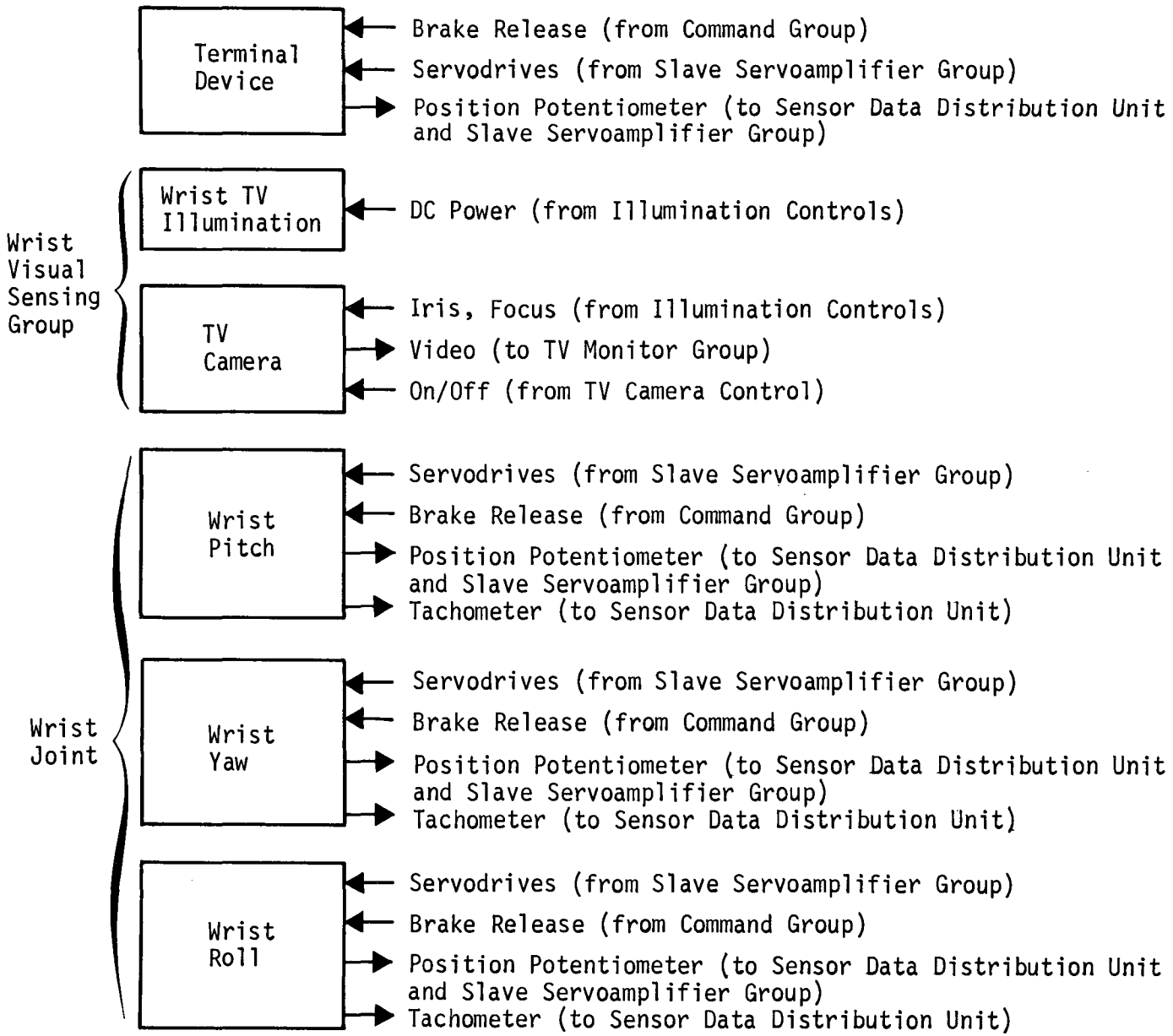

Fig. VIII-31 Slave Arm--Wrist Joint and Terminal Device

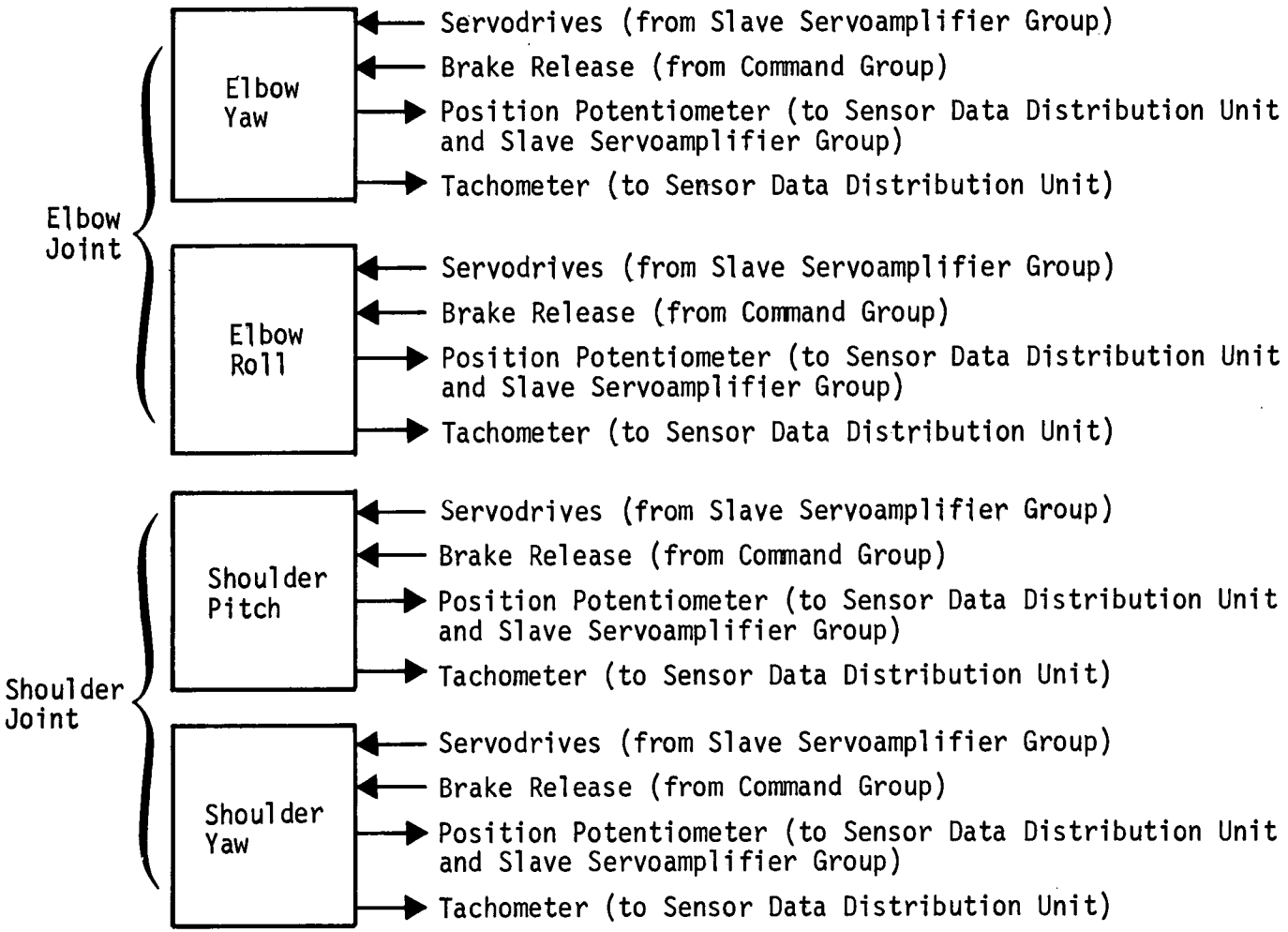

Fig. VIII-32 Slave Arm--Elbow Joint and Shoulder Joint

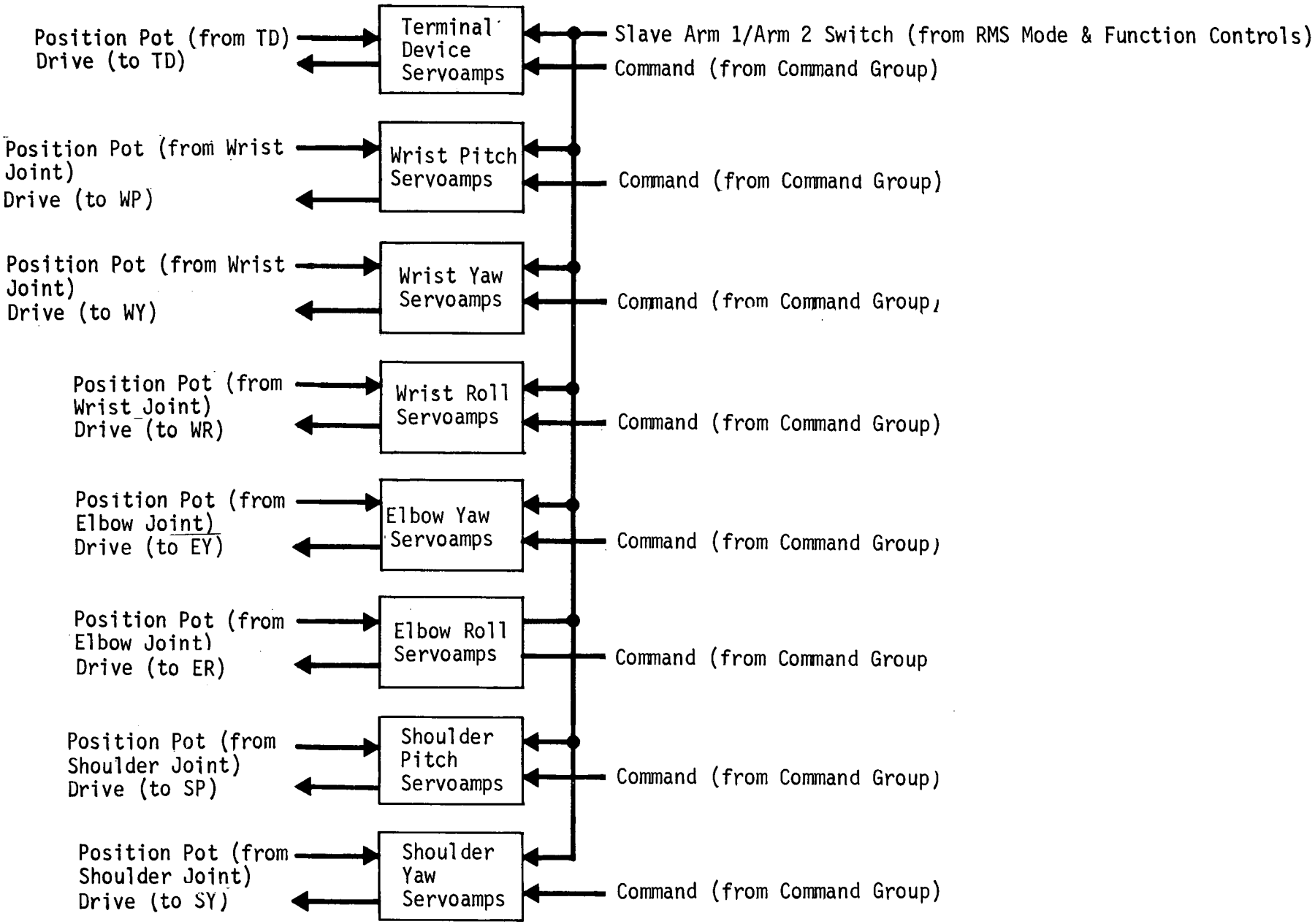

Fig. VIII-33 Control and Data Electronics--Slave Servoamplifier Group

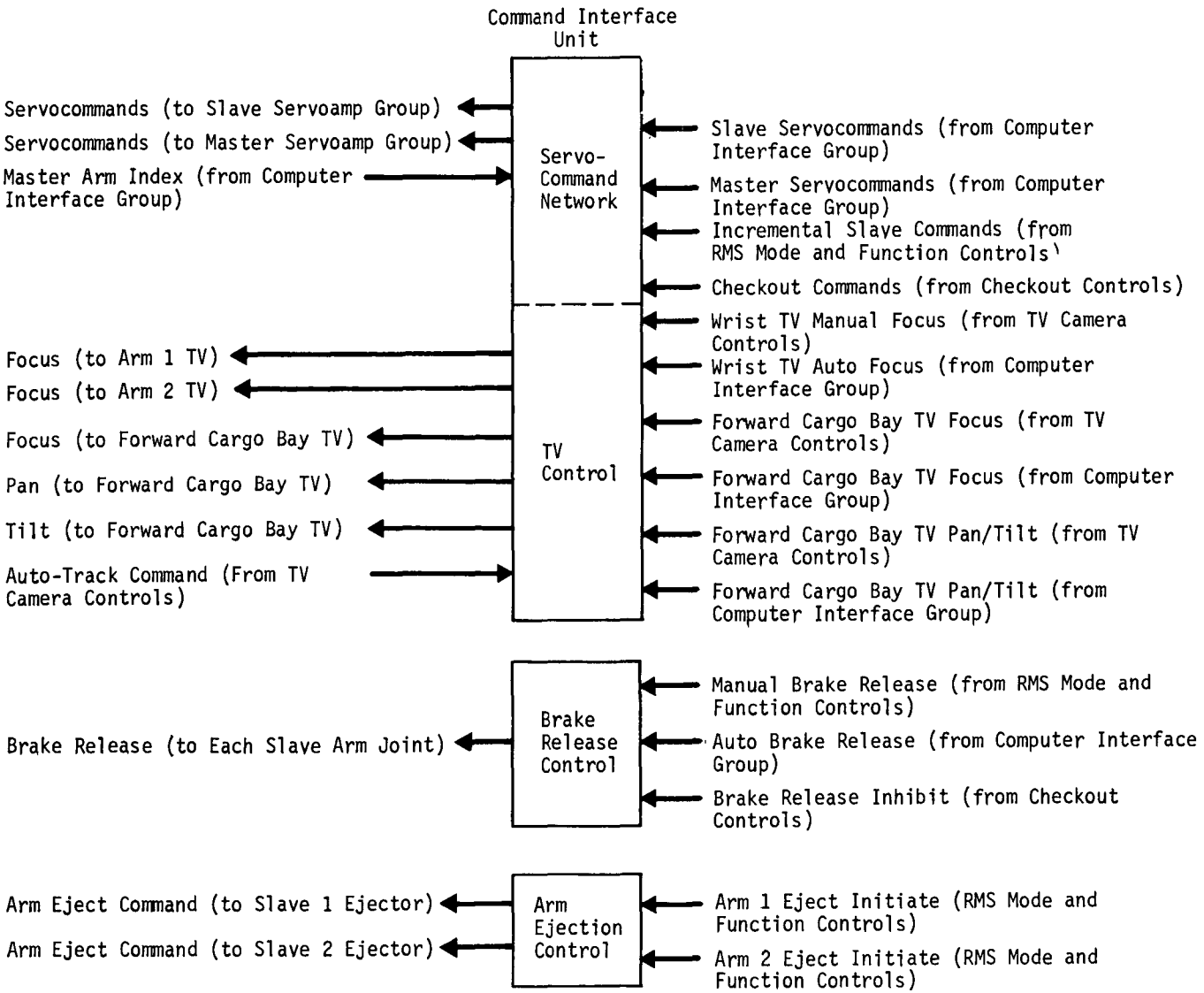

Fig. VIII-34 Control and Data Electronics--Command Group

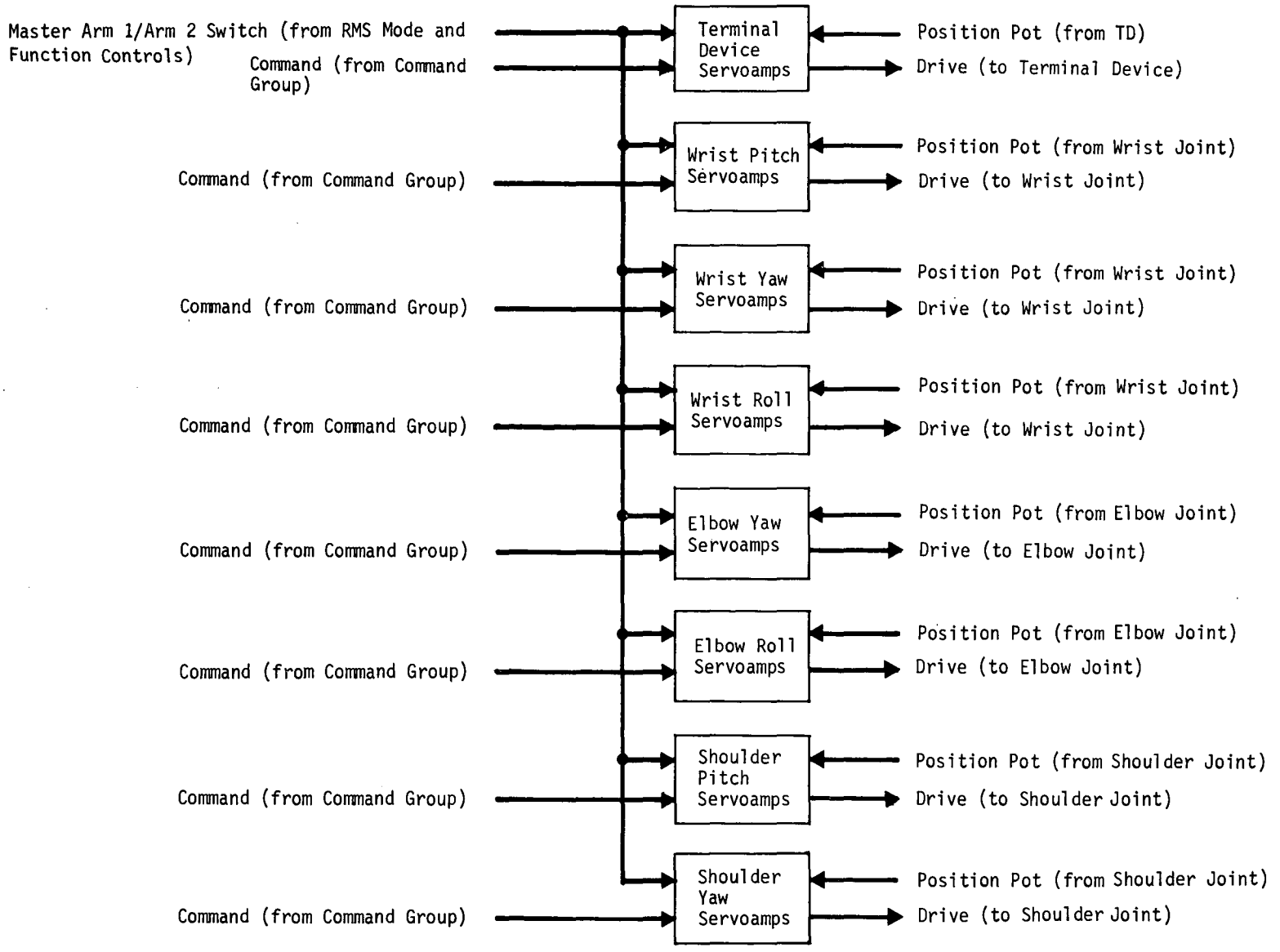

Fig. VIII-35 Control and Data Electronics--Master Servoamplifier Group

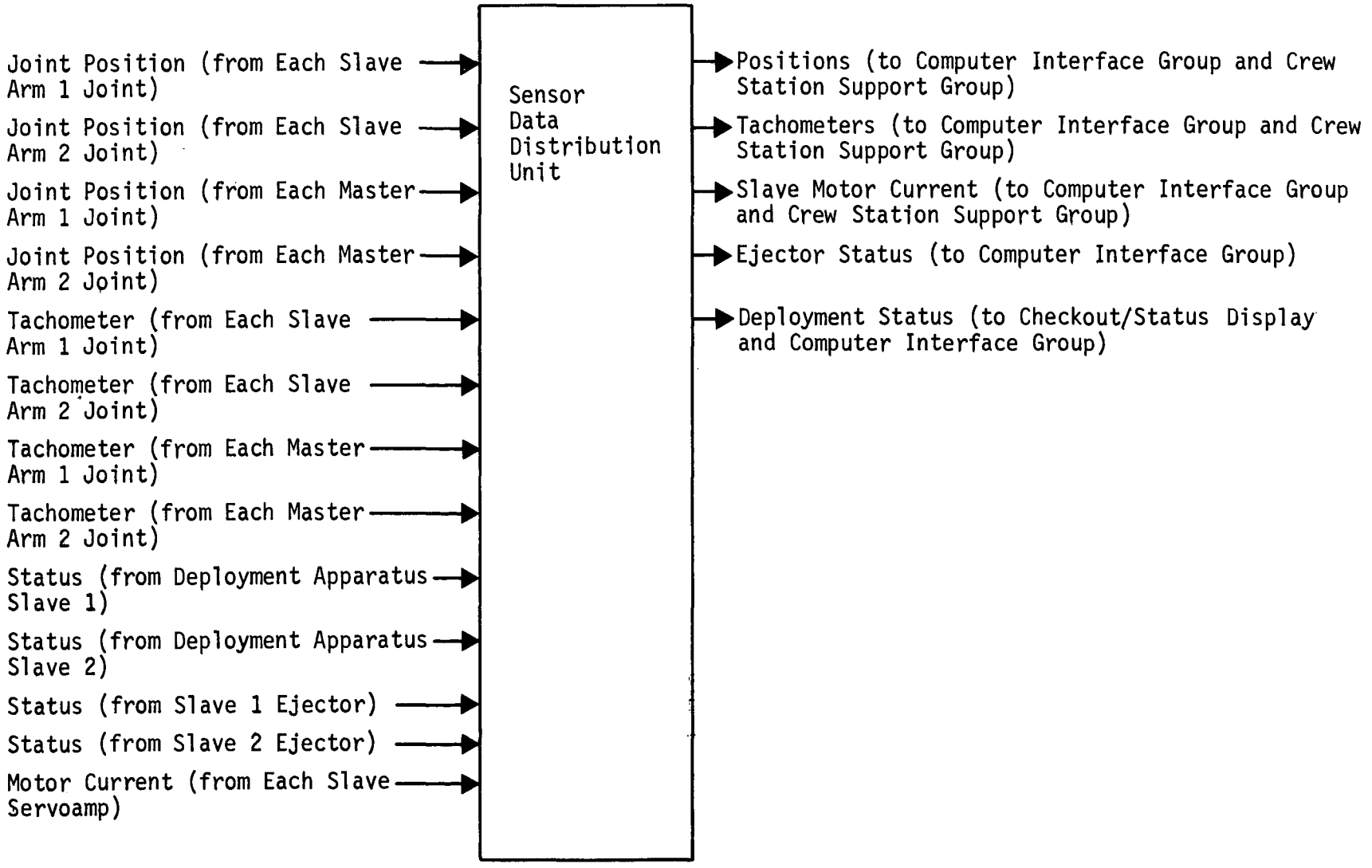

Fig. VIII-36 Control and Data Electronics--Sensor Data Distribution Unit

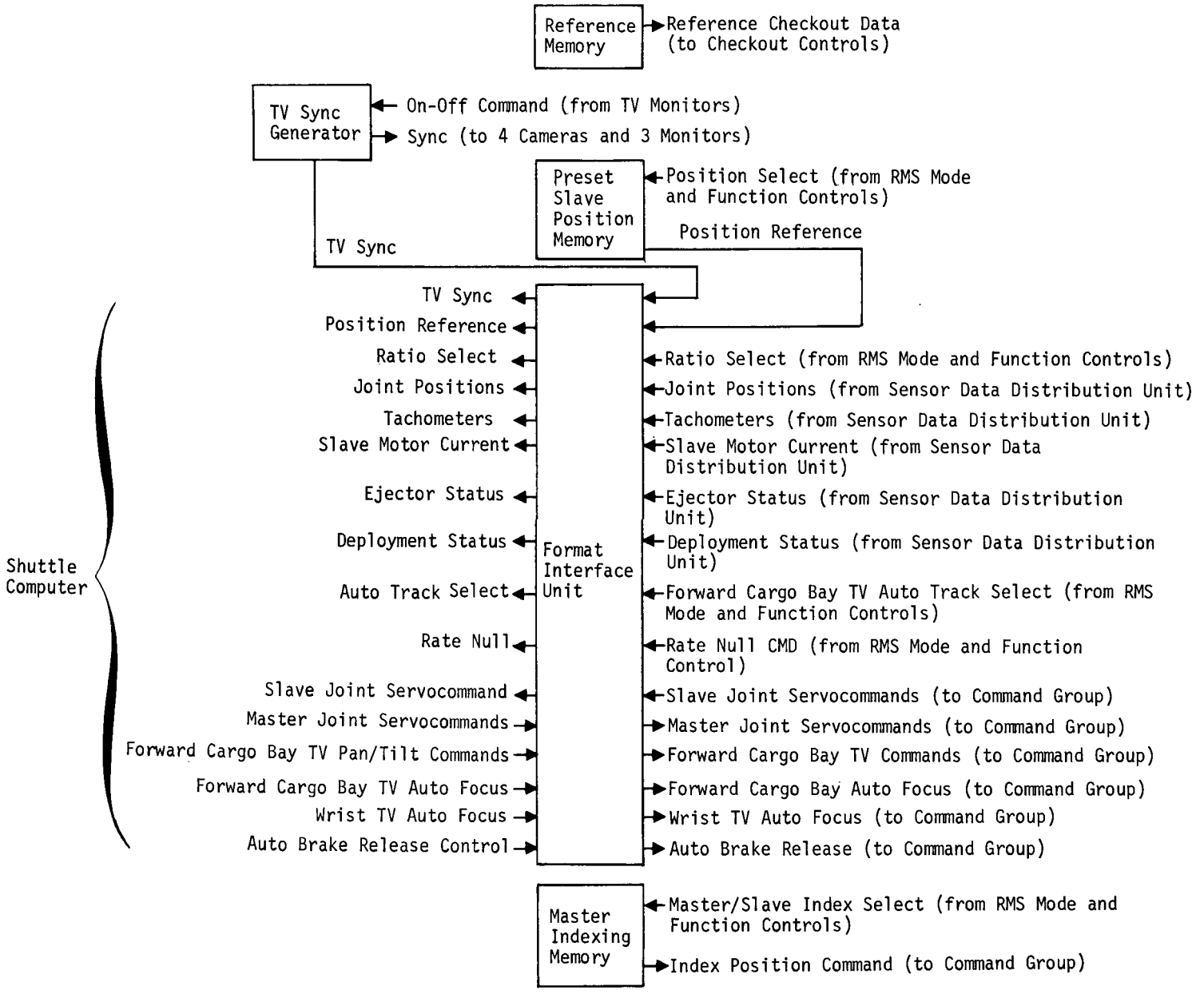

Fig. VIII-37 Control and Data Electronics--Computer Interface Group

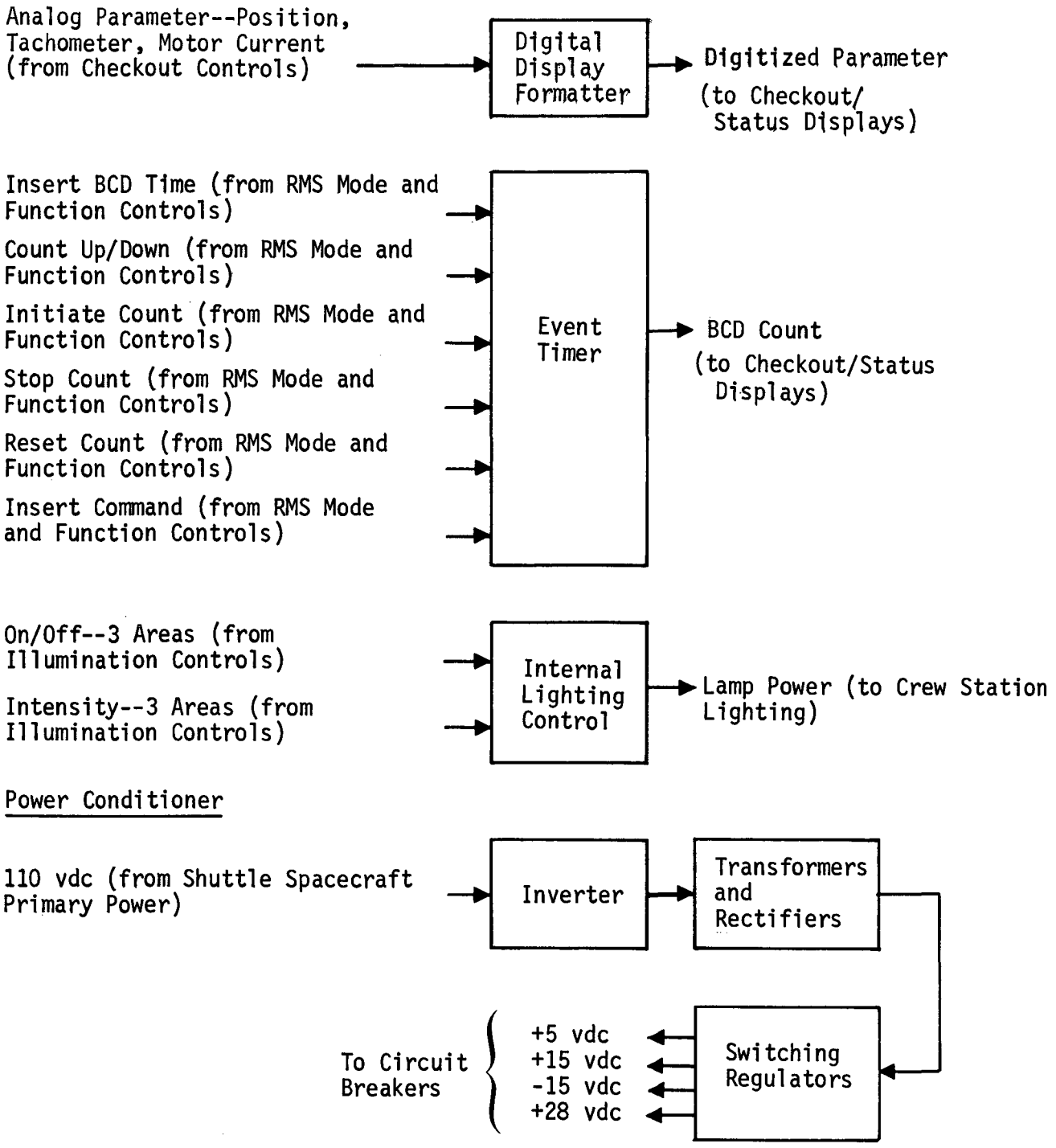

Fig. VIII-38 Control and Data Electronics--Crew Station Support Group and Power Conditioner

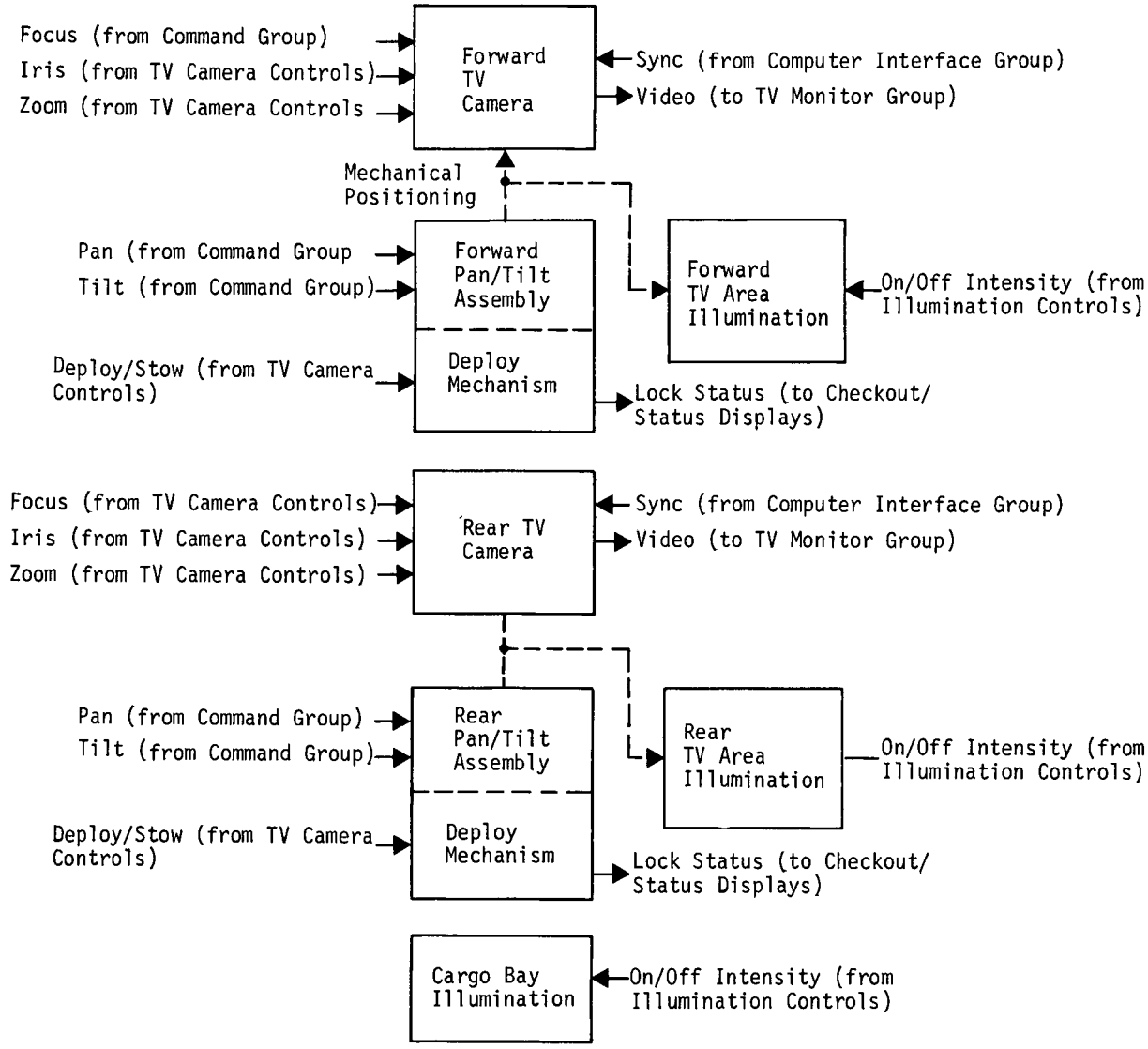

Fig. VIII-39 Cargo Bay

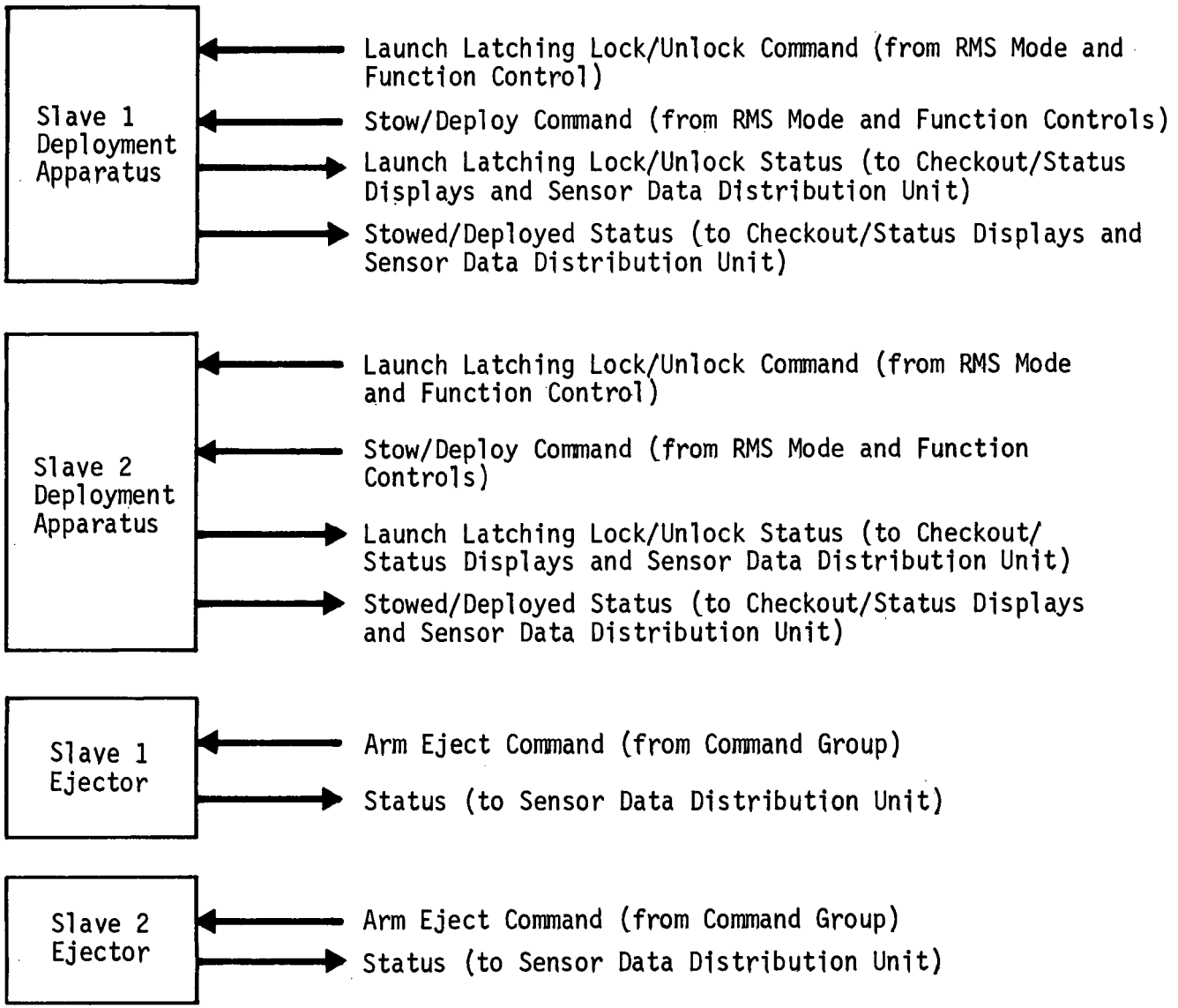

Fig. VIII-40 Cargo Bay

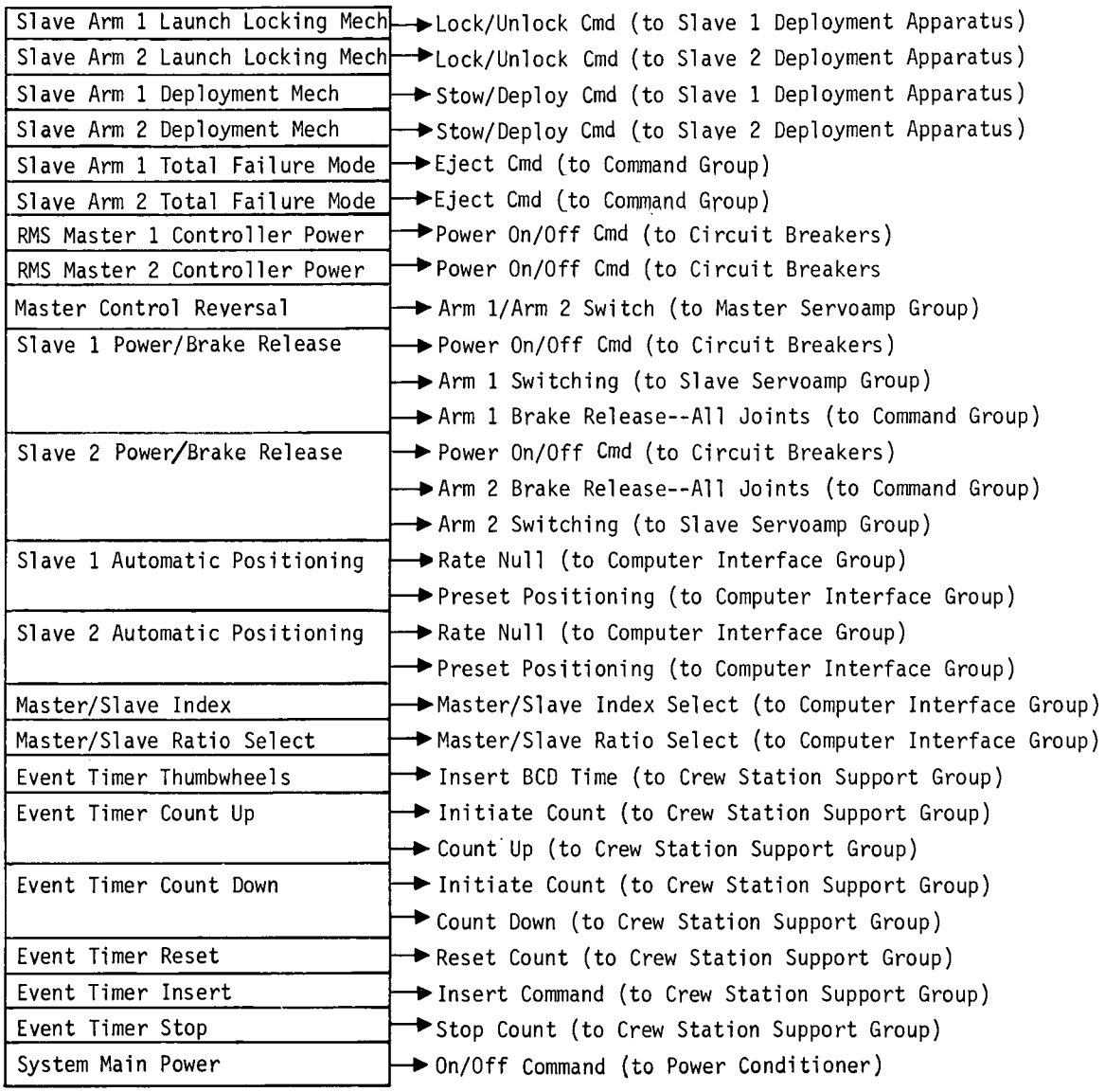

Fig. VIII-41 Crew Station--RMS Mode and Function Controls

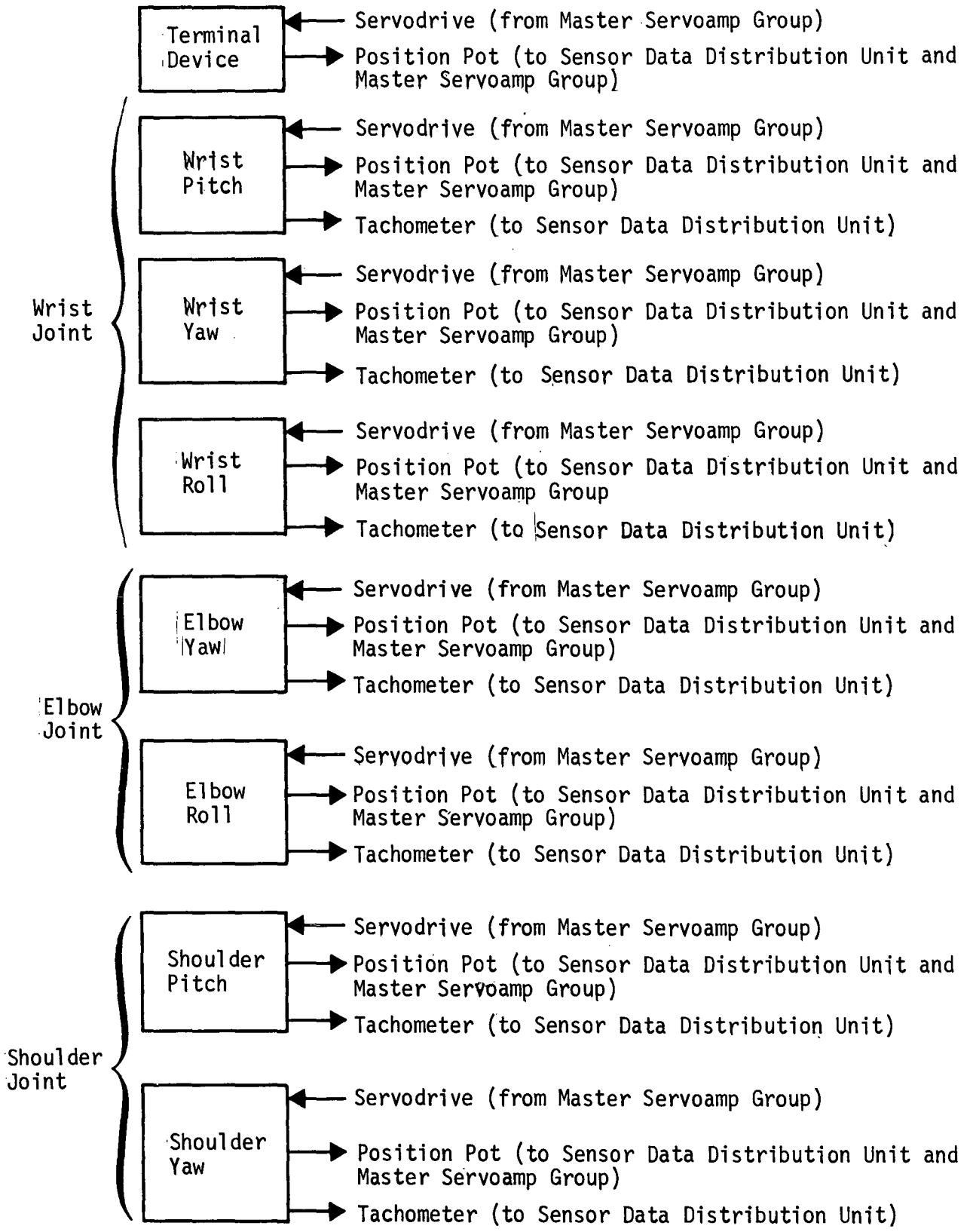

Fig. VIII-42 Crew Station--Master Arm

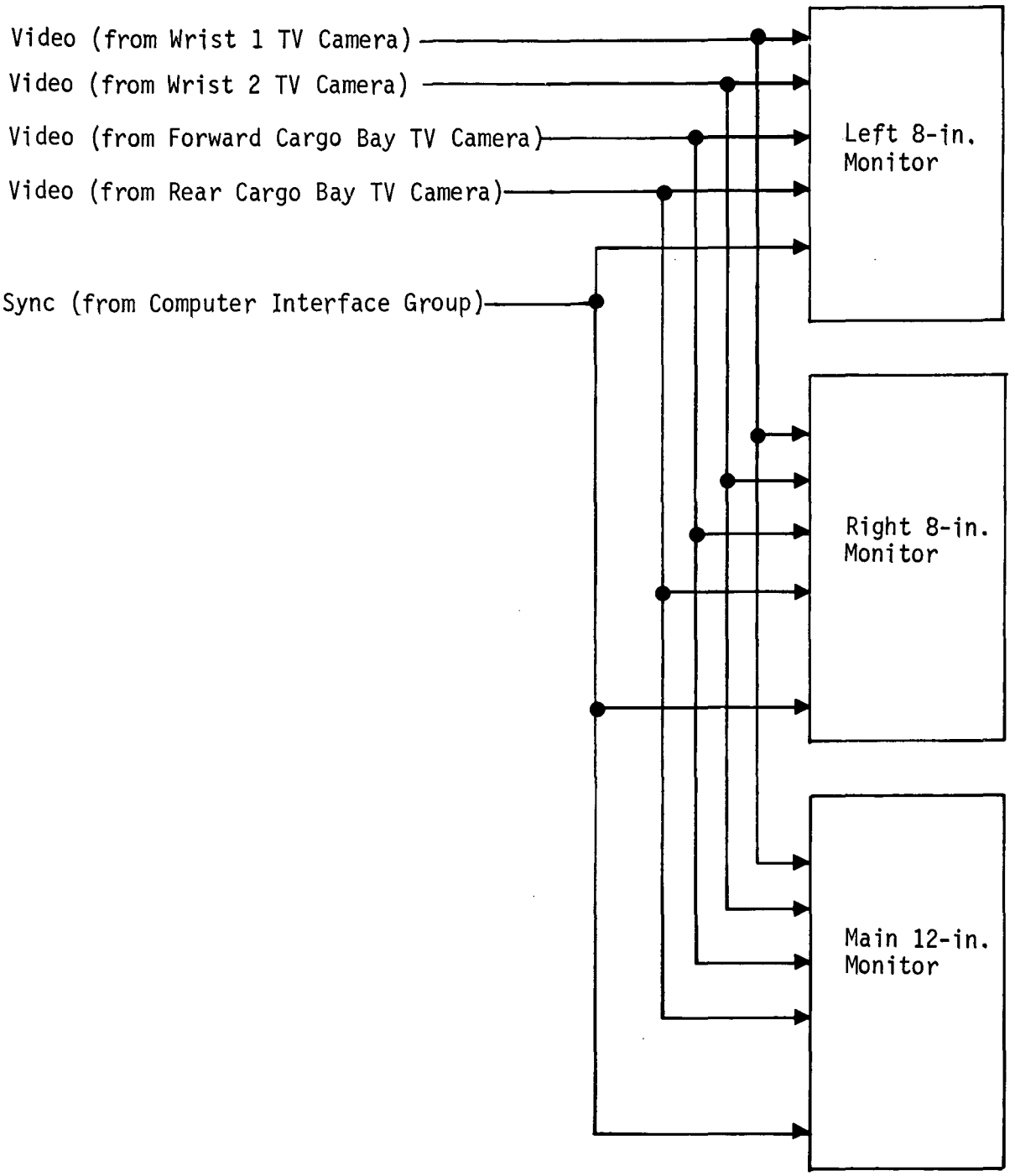

Fig. VIII-43 Crew Station--TV Monitor Group

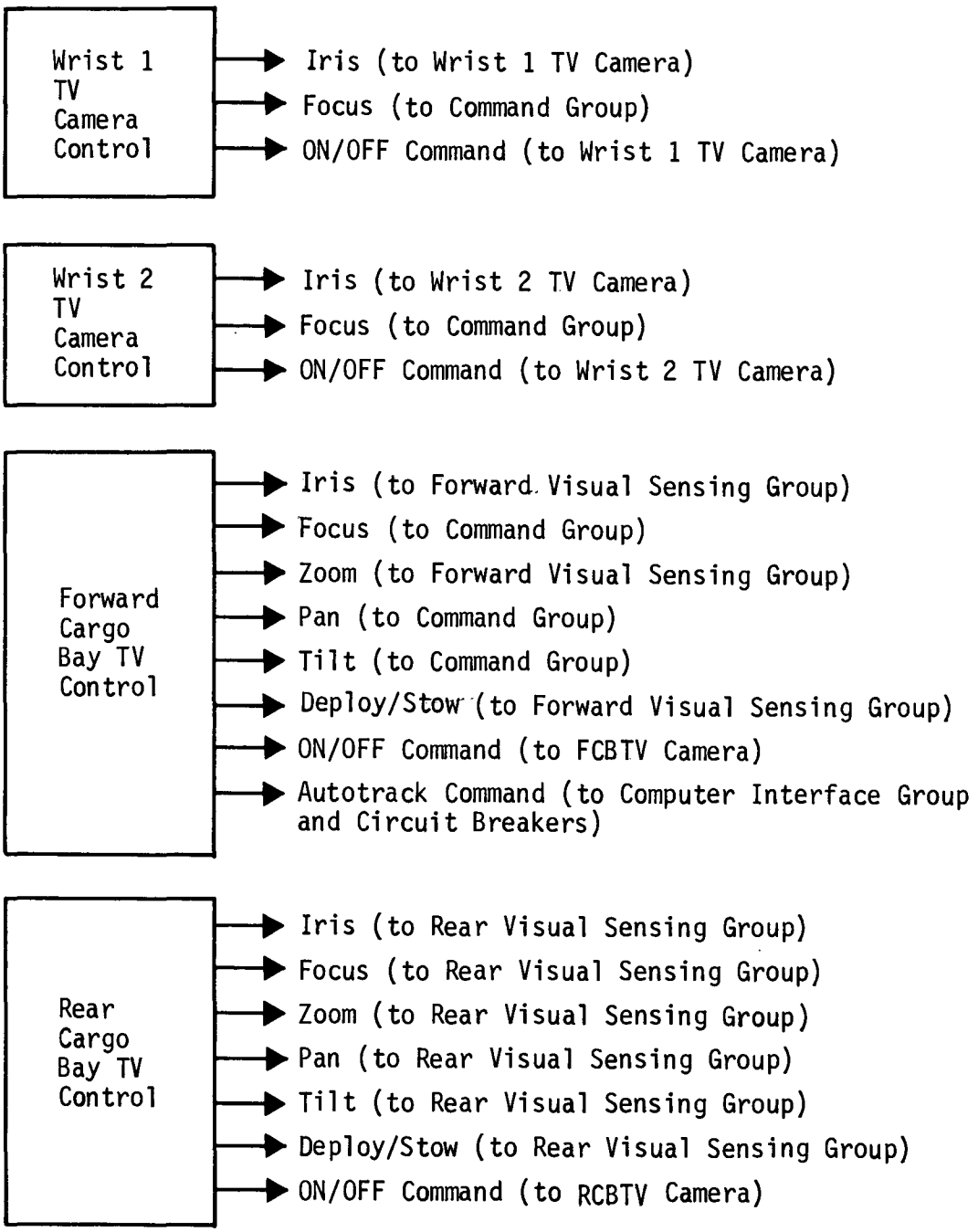

Fig. VIII-44 Crew Station--TV Camera Controls

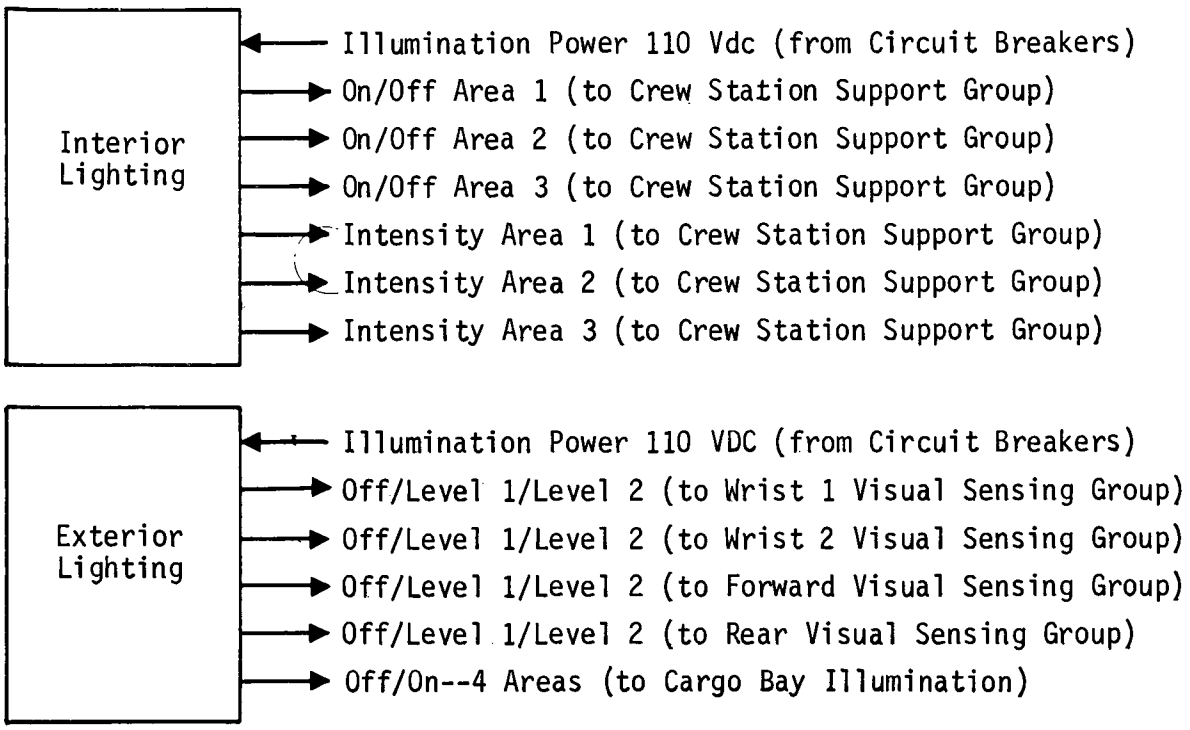

Crew Station Lighting

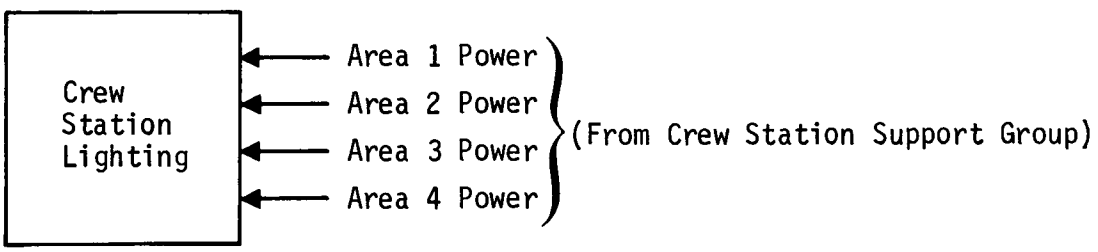

Fig. VIII-45 Crew Station--Illumination Controls and Lighting

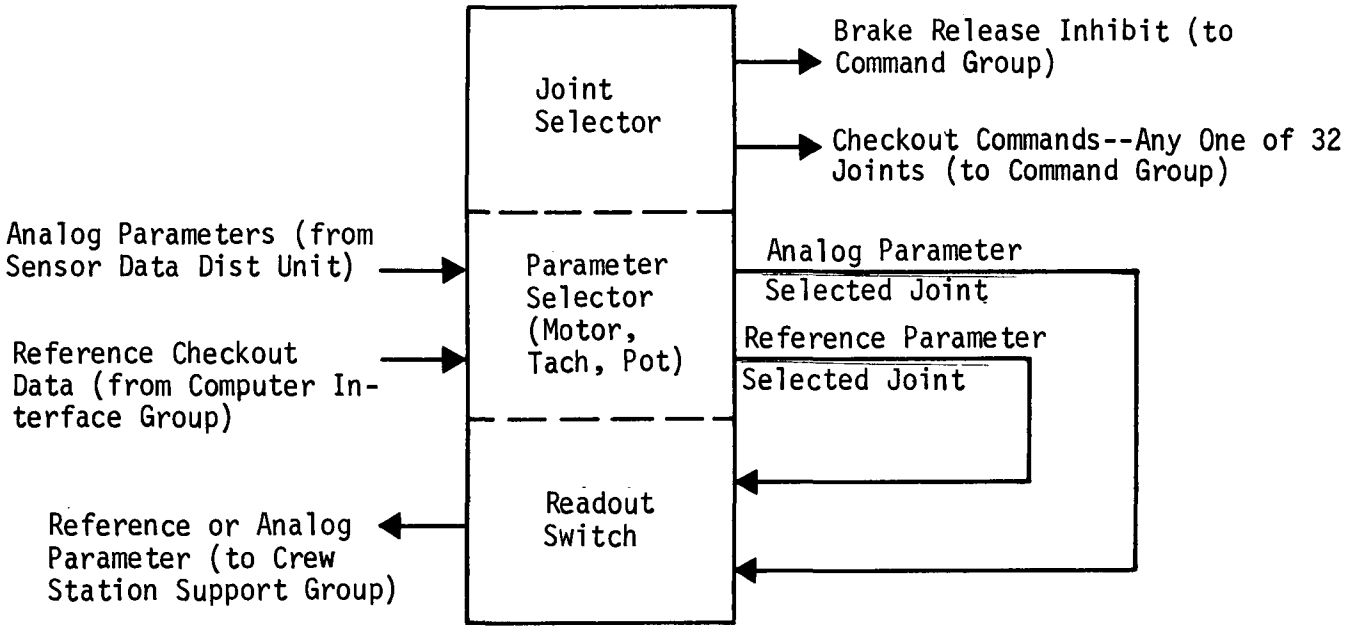

Fig. VIII-46 Crew Station--Checkout Controls

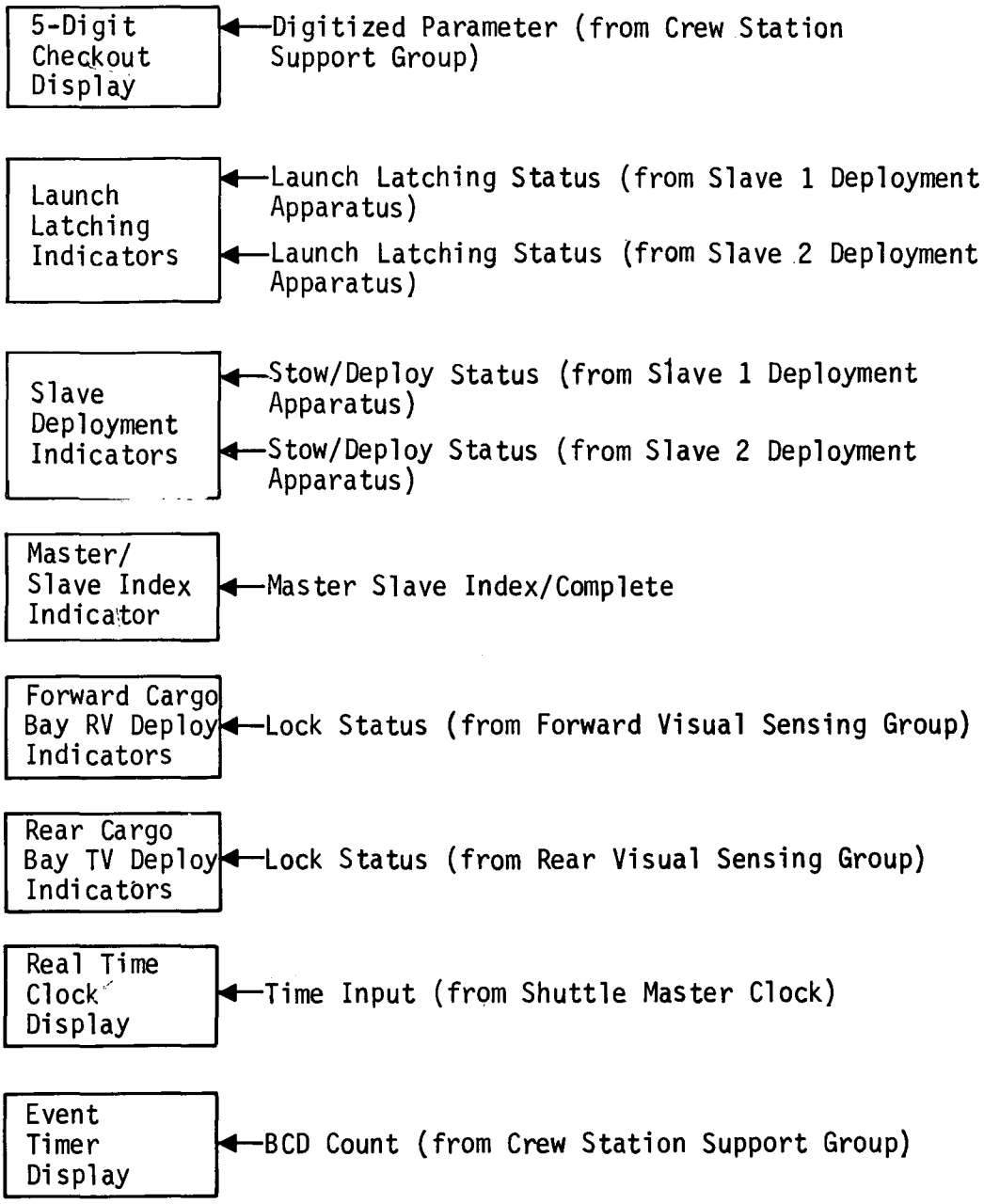

Fig. VIII-47 Crew Station--Checkout/Status Displays

The slave servoamplifier group drives the eight joints of one or the other slave arm. The command is derived from the command group.

The command group functions as a distribution center for slave and master servocommands, TV camera lens and positioning commands, and brake release commands. It functions under the direction of the operator either directly by the RMS mode and function, TV camera, or checkout controls, the master arms, or indirectly via the Shuttle computer.

The sensor data distribution unit determines the routing of the data signals. It receives position and velocity signals from the arms, status signals from the deployment and ejector mechanisms in the cargo bay and motor current signals from the servoamplifiers. Signal routing can be controlled by the operator or computer. The data can be displayed in the crew station and utilized by the Shuttle computer.

The computer interface group performs several functions. Primarily, it contains the format conversions necessary for compatibility between the Shuttle digital computer and the basically analog RMS control system. It also provides memory capability for preset slave arm positioning and for checkout of system functions and is capable of performing master/slave arm ratio changes.

The Crew Station Support Group comprises electronic circuitry associated with the crew station controls and displays: e.g., operator area lighting, event timer, formatter for the operator's digital checkout display.

The power conditioner utilizes the 120 vdc primary Shuttle spacecraft power and employs dc-dc conversion with efficient switching regulation to supply the RMS system components with their required operating voltages.

3) Cargo Bay - The cargo bay contains several items of RMS equipment: the mechanisms for deployment and ejection of the slave arms; illumination for the cargo area; and two television cameras located at opposite ends of the bay.

The slave deployment apparatus is physically connected to the shoulder of the slave arm and moves the arm out of the cargo bay into operating position or vice versa under command of the operator through the command group.

The slave ejector is an explosive device to discard a slave arm that has become a safety hazard due to malfunction or accident. This function is also operator controlled through the command group.

The bay illumination consists of four floodlights placed to generally illuminate the bay area and eliminate major shadow areas that could concern the operator.

The forward visual sensing group consists of a remotely positioned TV camera and associated illumination. This camera may be positioned manually by the operator or programmed to track the slave arm in use by the Shuttle computer through the computer interface group and command group. The rear visual sensing group is similar except it does not have the automatic tracking feature. Video output from each camera is routed to the crew station monitors.

4) Crew Station - The crew station is the point at which all operational man/machine interfaces occur.

Each master arm is capable of controlling either slave arm as selected by the RMS mode and function controls via the command group. Outputs from the master arms also go through the sensor data distribution unit and computer interface group for computer augmentation.

The RMS mode and function controls determine the operational RMS configuration for each mission, such as determining starting position for slave arms, indexing of master arms, master/slave ratio, arm deployment, etc. These controls function through the command group and with some inputs from the sensor data distribution unit.

The TV monitor group is essentially three self-contained monitors, each of which can display video information from any of the four TV cameras. Sync is obtained from a sync generator in the computer interface group.

The TV camera controls adjust iris and focus in the slave TV cameras and iris, focus, zoom, pan and tilt in the forward and rear cargo bay TV cameras.

The illumination controls are used to adjust lighting in the crew station, cargo bay and the lighting associated with each of the four TV cameras.

The checkout controls are used in static checkout of the system before operation. They may also be used to monitor certain functions during operation. These controls are normally used in conjunction with the checkout/status displays.

The circuit breakers provide for quick disconnect of power from a malfunctioning component or for conservation of power while a component is not in use.

Caution and warning displays indicate malfunctions throughout the RMS. Crew station lighting refers to illumination within the RMS operator's immediate area. A complete description of the controls, displays and their function can be found in Section F.

b. Input/Output Diagrams - The input/output diagrams show in detail the subblocks and interconnections between the major blocks in Fig. VIII-30. Each input and output is related to one or more blocks in the functional block diagram and is referred to in the titles (Fig. VIII-31 thru VIII-47).

3. Signal Requirements and Formats

a. Signal Breakdown - A detailed breakdown of the telecommunications signals is listed in Table VIII-8. The list corresponds to the preliminary design and is complete except for caution/warning signals and power supply connections that are not defined. The table gives each signal followed by its routing, the number of similar signals (rather than listing each joint's servosignal separately, for example), its format and additional information if defined, and finally its activity during various phases of a RMS mission.

b. Error and Signal Accuracies - Most of the signal paths in the telecommunications subsystem are on/off or pulsed (1-bit digital). In some cases a 2- or 3-bit word is used to define a numbered switch position or 3-level status. In addition, some analog signals--such as internal lighting--are arbitrarily adjusted to suit the operator. All of these signals are not critical as far as accuracy. If their levels are correct within about 10% no deviation in function will be detected.

On the other hand, the most critical parameters are those associated with the joint servoloops. As specified by earlier calculation in Chapter VII Section G, the overall accuracy must be 1 part in 3540 or 0.028%. Thus the sum of all errors in the

Table VIII-8 Telecommunications Subsystem Signal Breakdown

	From	To	No.	Signal Format	Signal Active During:*								
					Check-Out	Pre-Capture	Capture	Reduce Velocity	Near Dock	Position for Dock	Dock	Unload & Deploy	Module Handling
Slave Servomotor Drives	SSAG†	SJ†	16	A§ 0 to ±28 vdc	X	X	X					X	X
Slave Brake Release Signals	BRC	SJ	16	D +28 vdc		X	X	X	X	X	X	X	X
Slave Position Signals	SJ	SDDU/SSAG	16	A 0 to ±15 vdc	X	X	X	X	X	X	X	X	X
Slave Tachometer Signals	SJ	SDDU	14	A	X	X	X	X	X	X	X	X	X
Wrist Illumination Power	ELC	WTVI	2	D 3 Level	X	O	O	O	O	O	O	O	O
Wrist TV Camera Iris Commands	WTVCC	WTVC	2	A	X	O	O	O	O	O	O	O	O
Wrist TV Camera Focus Commands	WTVCC	WTVC	2	A	X	O	O	O	O	O	O	O	O
Wrist TV Video Signals	WTVC	TVMG	2	A	X	X	X	X	X	X	X	X	X
Wrist TV On/Off Commands	CB	WTVC	2	D +28 vdc Power	X								
Slave Arm 1/Arm 2 Switch	RMFC	SSAG	1	D 2 Bits	X	O				O		O	O
Slave Servocommands	SCN	SSAG	16	A	X	X	X					X	X
Master Arm Index Commands	MIM	SCN	14	A	X	O	O	O	O	O	O	O	O
Slave Servocommands	FIU	SCN	16	A	X	X	X					X	X
Master Servocommands	FIU	SCN	16	A	X	X	X					X	X
Incremental Slave Commands	RMFC	SCN	16	A	X	O						O	O
Checkout Commands	JS	SCN	16	A	X								
FCBTV Focus Command	TVC	FCBTV	1	A	X	O	O	O	O	O	O	O	O
FCBTV Pan Command	TVC	FCBTV	1	A	X	O	O	O	O	O	O	O	O
FCBTV Tilt Command	TVC	FCBTV	1	A	X	O	O	O	O	O	O	O	O
Auto Track Command	FCBTVC	TVC	1	D 1 Bit	X	O	O	O	O	O	O	O	O
Wrist TV Manual Focus Commands	WTVCC	TVC	2	A	X	O	O	O	O	O	O	O	O
Wrist TV Auto Focus Commands	FIU	TVC	2	A	X	O	O	O	O	O	O	O	O
FCBTV Manual Focus Command	FCBTVC	TVC	1	A	X	O	O	O	O	O	O	O	O
FCBTV Auto Focus Command	FIU	TVC	1	A	X	O	O	O	O	O	O	O	O
FCBTV Manual Pan Command	FCBTVC	TVC	1	A	X	O	O	O	O	O	O	O	O
FCBTV Auto Pan Command	FIU	TVC	1	A	X	O	O	O	O	O	O	O	O
FCBTV Manual Tilt Command	FCBTVC	TVC	1	A	X	O	O	O	O	O	O	O	O
FCBTV Auto Tilt Command	FIU	TVC	1	A	X	O	O	O	O	O	O	O	O
Manual Brake Release Commands	RMFC	BRC	16	D 1 Bit	X	O	O	O	O	O	O	O	O
Auto Brake Release Commands	FIU	BRC	16	D 1 Bit		X	X	X	X	X	X	X	X
Brake Release Inhibit Commands	JS	BRC	16	D 1 Bit	X								
Arm Eject Initiate Commands	RMFC	AEC	2	D 1 Bit		O						O	O
Arm Eject Commands	AEC	SE	2	D +28 vdc		O						O	O
Illumination Power (Interior)	CB	IL	1	D 110 vdc	X	X	X	X	X	X	X	X	X
Illumination Power (Exterior)	CB	EL	1	D 110 vdc	X	X	X	X	X	X	X	X	X
Master Arm 1/Arm 2 Switch	RMFC	MSAG	1	D 2 Bits	X	O				O	X	O	O
Master Servocommands	SCN	MSAG	16	A	X	X	X					X	X
Master Servomotor Drives	MSAG	MJ	16	A 0 to ±28 vdc	X	X	X			X	X	X	X
Master Position Signals	MJ	SDDU/MSAG	16	A 0 to ±15 vdc	X	X	X	X	X	X	X	X	X
Master Tachometer Signals	MJ	SDDU	14	A	X	X	X	X	X	X	X	X	X
Motor Current	MSAG	SUDU	16	A	X	X	X	X	X	X	X	X	X
Slave Arm Positions	SDDU	FIU/DDF	16	A	X	X	X	X	X	X	X	X	X
Master Arm Positions	SDDU	FIU/DDF	16	A	X	X	X	X	X	X	X	X	X
Slave Arm Tachometers	SDDU	FIU/DDF	14	A	X	X	X	X	X	X	X	X	X
Master Arm Tachometers	SDDU	FIU/DDF	14	A	X	X	X	X	X	X	X	X	X
Slave Motor Current Signals	SDDU	FIU/DDF	16	A	X	X	X	X	X	X	X	X	X
Time	SC	RTCD	1	D 6 BCD Digits	X	X	X	X	X	X	X	X	X
Deployment Status Signals	SDDU	SDI	2	D 2 Bits	X	X	X	X	X	X	X	X	X
Analog Parameter	PS	RS	1	A	X	O	O	O	O	O	O	O	O
Reference Checkout Data	RM	PS	48	A	X	O	O	O	O	O	O	O	O
TV Sync On/Off	TVMG	TVSG	1	D 1 Bit	X	O	O	O	O	O	O	O	O
Sync Signals	TVSG	FIU/WTVC TVMG/FCBTV /RCBTV	5	D NTSC Standard	O	O	O	O	O	O	O	O	O
Position Select	RMFC	PSPM	1	D 3 Bits	X	O				X		O	O
Position References	PSPM	FIU	6	A	X	O				X		O	O
Reference Parameter	PS	RS	1	A	X	O	O	O	O	O	O	O	O
Position References	FIU	SGPC	1	D	X	O				X		O	O
Ratio Select	FIU	SGPC	1	D	X	O			O	O	O	O	O
Slave Joint Positions	FIU	SGPC	16	D 13 Bits	X	X	X	X	X	X	X	X	X
Master Joint Positions	FIU	SGPC	16	D 13 Bits	X	X	X	X	X	X	X	X	X
Slave Tachometers	FIU	SGPC	14	D 13 Bits	X	X	X	X	X	X	X	X	X
Master Tachometers	FIU	SGPC	14	D 13 Bits	X	X	X	X	X	X	X	X	X
Slave Motor Currents	FIU	SGPC	16	D 13 Bits	X	X	X	X	X	X	X	X	X
Ejector Status	FIU	SGPC	1	D 1 Bit	X	X	X	X	X	X	X	X	X
Deployment Status	FIU	SGPC	1	D 2 Bits	X	X	X	X	X	X	X	X	X
Auto Track Select	FIU	SGPC	1	D 1 Bit	X	O	O	O	O	O	O	O	O

*X = Mandatory; O = Optional. †These acronyms are defined at the end of the table. §D = Digital, A = Analog.

Table VIII-8 (concl)

	From	To	No.	Signal Format	Signal Active During;*								
					Check-Out	Pre-Capture	Capture	Reduce Velocity	Near Dock	Position for Dock	Dock	Unload & Deploy	Module Handling
Rate Null Command	FIU†	SGPC†	1	D§ 1 Bit				X	X	X	X		
Slave Joint Servocommands	SGPC	FIU	16	D 13 Bits	X	X	X			X	X	X	X
Master Joint Servocommands	SGPC	FIU	16	D 13 Bits	X	X	X			X	X	X	X
FCBTV Pan Command	SGPC	FIU	1	D	X	O	O	O	O	O	O	O	O
FCBTV Tilt Command	SGPC	FIU	1	D	X	O	O	O	O	O	O	O	O
FCBTV Auto Focus	SGPC	FIU	1	D	X	O	O	O	O	O	O	O	O
Wrist TV Auto Focus	SGPC	FIU	1	D	X	O	O	O	O	O	O	O	O
Auto Brake Release Control	SGPC	FIU	16	D 1 Bit		X	X	X	X	X	X	X	X
FCBTV Auto Track Select	RMFC	FIU	1	D 1 Bit	X	O	O	O	O	O	O	O	O
Rate Null CMD	RMFC	FIU	1	D 1 Bit				X	X	X	X		
Master/Slave Index Complete	SGPC	FIU	1	D 1 Bit	X	O	O	O	O	O	O	O	O
Master/Slave Index Select	RMFC	MIM	1	D 2 Bits	X	O	O	O	O	O	O	O	O
Analog Parameter--Position, Tach, Current	PS	DDF	1	A	X	O	O	O	O	O	O	O	O
Digitized Parameter	DDF	FDCD	1	D 5 BCD Digits	X	O	O	O	O	O	O	O	O
Master/Slave Index Complete	FIU	MSII	1	D 1 Bit	X	O	O	O	O	O	O	O	O
Insert BCD Time	RMFC	ET	1	D 6 BCD Digits	X	O	O	O	O	O	O	O	O
Count Up/Count Down	RMFC	ET	1	D 1 Bit	X	O	O	O	O	O	O	O	O
Initiate Count	RMFC	ET	1	D 1 Bit	X	O	O	O	O	O	O	O	O
Stop Count	RMFC	ET	1	D 1 Bit	X	O	O	O	O	O	O	O	O
Reset Count	RMFC	ET	1	D 1 Bit	X	O	O	O	O	O	O	O	O
Insert Command	RMFC	ET	1	D 1 Bit	X	O	O	O	O	O	O	O	O
BCD Count	ET	ETD	1	D 6 BCD Digits	X	O	O	O	O	O	O	O	O
Internal Lighting On/Off	IL	ILC	3	D 1 Bit	O	O	O	O	O	O	O	O	O
Internal Lighting Intensity	IL	ILC	3	A	O	O	O	O	O	O	O	O	O
Lamp Power	ILC	CSL	3	A	O	O	O	O	O	O	O	O	O
FCBTV Iris Command	FCBTVC	FCBTV	1	A	X	O	O	O	O	O	O	O	O
FCBTV Zoom Command	FCBTVC	FCBTV	1	A	X	O	O	O	O	O	O	O	O
FCBTV Video	FCBTV	TVMG	1	A	X	X	X	X	X	X	X	X	X
FCBTV Deploy/Stow	FCBTVC	FCBTV	1	D 1 Bit	X								
FCBTV Lock Status	FCBTV	FCBTVDI	1	D 2 Bits	X	X	X	X	X	X	X	X	X
FCBTV Illumination On/Off/Intensity	EL	FCBTV	1	D 3 Level	X	O	O	O	O	O	O	O	O
RCBTV Focus	RCBTVC	RCBTV	1	A	X	O	O	O	O	O	O	O	O
RCBTV Iris	RCBTVC	RCBTV	1	A	X	O	O	O	O	O	O	O	O
RCBTV Zoom	RCBTVC	RCBTV	1	A	X	O	O	O	O	O	O	O	O
RCBTV Video	RCBTV	TVMG	1	A	X	X	X	X	X	X	X	X	X
RCBTV Deploy/Stow	RCBTVC	RCBTV	1	D 1 Bit	X								
RCBTV Lock Status	RCBTV	RCBTVDI	1	D 2 Bits	X	X	X	X	X	X	X	X	X
RCBTV Illumination On/Off/Intensity	EL	RCBTV	1	D 3 Level	X	O	O	O	O	O	O	O	O
Cargo Bay Lights On/Off	EL	CBI	4	D 110 vdc	O	O	O	O	O	O	O	O	O
Launch Latching Lock/Unlock CMD	RMFC	SDA	2	D 2 Bits	X								
Stow/Deploy CMD	RMFC	SDA	2	D 2 Bits	X								
Launch Latching Lock/Unlock Status	SDA	SDDU/LLI	2	D 2 Bits	X	X	X	X	X	X	X	X	X
Stowed/Deployed Status	SDA	SDDU/SDI	2	D 2 Bits	X	X	X	X	X	X	X	X	X
Arm Eject Status	SE	SDDU	2	D 2 Bits	X	X	X	X	X	X	X	X	X
RMS Master Controller Power On	RMFC	CB	2	D 1 Bit	X	X	X	X	X	X	X	X	X
Slave Power On	RMFC	CB	2	D 1 Bit	X	X	X	X	X	X	X	X	X
System Main Power On	RMFC	PC	1	D 110 vdc	X	X	X	X	X	X	X	X	X
Wrist TV On	WTVCC	CB	1	D 1 Bit	X	X	X	X	X	X	X	X	X
FCBTV On	FCBTVC	CB	1	D 1 Bit	X	X	X	X	X	X	X	X	X
RCBTV	RCBTVC	CB	1	D 1 Bit	X	X	X	X	X	X	X	X	X

AEC	Arm Ejection Control	ILC	Interior Lighting Control	RTCD	Real Time Clock Display
BRC	Brake Release Control	JS	Joint Selector	SC	Shuttle Clock
CB	Circuit Breakers	LLI	Launch Lock Indicator	SCN	Servo Command Network
CBI	Cargo Bay Illumination	MIM	Master Indexing Memory	SDA	Slave Deployment Apparatus
CSL	Crew Station Lighting	MJ	Master Joints	SDDU	Sensor Data Distribution Unit
DDF	Digital Display Formatter	MSAG	Master Servo Amplifier Group	SDI	Slave Deployment Indicators
EL	Exterior Lighting	MSII	Master Slave Indexing Indicator	SE	Slave Ejector
ELC	Exterior Lighting Control	PS	Parameter Selector	SGPC	Shuttle General Purpose Computer
ET	Event Timer	PSPM	Preset Slave Position Memory	SJ	Slave Joints
ETD	Event Timer Display	RCBTV	Rear Cargo Bay TV Camera	SSAG	Slave Servo Amplifier Group
FCBTV	Forward Cargo Bay TV Camera	RCBTVC	Rear Cargo Bay TV Control	TVC	TV Control (Command Interface Unit)
FCBTVC	Forward Cargo Bay TV Control	RCBTVDI	Rear Cargo Bay TV Deployment Indicator	TVMG	TV Monitor Group
FCBTVDI	Forward Cargo Bay TV Deployment Indicators	RM	Reference Memory	TVSG	TV Sync Generator
FDCD	5-Digit Checkout Display	RMFC	RMS Mode & Function Controls	WTVC	Wrist TV Camera
FIU	Format Interface Unit	RS	Readout Switch	WTVCC	Wrist TV Camera Control
IL	Interior Lighting			WTVI	Wrist TV Illumination

*X = Mandatory; O = Optional; †These acronyms are defined above. §D = Digital; A = Analog

loop--which includes the Shuttle computer--cannot exceed this figure. The tachometer is used only for rate damping and is a high resolution analog device. Used in this way its accuracy is not critical.

Positioning of the TV cameras to follow the action places certain requirements on the automatic positioning of the lenses and pan/tilt mechanism. Assuming that the minimum telephoto field of view of the Forward Cargo Bay TV camera is 9°, a misalignment of 10% (of the field of view) from the correct centering point would not be particularly noticeable to the operator. If this misalignment is taken as a maximum, the position error should not be greater than 10% of 9° or 0.9°. The total position accuracy is then

$$\frac{0.9^\circ}{360^\circ} = \frac{1}{400} = 0.0025 \text{ or } 0.25\%$$

Thus the pan and tilt mechanisms for the automatically positioned forward cargo bay TV camera should be within the stated accuracy.

Focus servosystems need be less accurate. Focus control signals with an accuracy of 1 part in 32 will be adequate.

Reference and analog parameters to be converted to digital and displayed on the checkout display need to be accurate to ±1 part in 10^5.

Error rate becomes significant only in the interface between the telecommunications subsystem and the Shuttle computer. The mechanical time constant of the servomotors is 0.02 sec. If the data frame time is 2 msec (or 0.10 x 20 msec), reasonably smooth operation can be expected to result. Assuming that data errors are random, one error per 100 frames in any variable would be imperceptible. Thus the maximum error rate is 5/sec/channel.

IX. FUTURE DEVELOPMENT PROGRAM

This chapter includes a typical development schedule, and a conceptual estimate for the resources to design, develop, and manufacture the RMS for the Shuttle Orbiter. Presented first are those activities normally associated with a program of this type.

A. PROGRAM ACTIVITIES

1. Program Management

The program management activities are defined as follows:

Project Management - Provide management of the activities required to develop, design, fabricate, test and deliver the subsystem.

Program Schedule - Implement and maintain a program event status log that reflects the statement of work functional tasks, internal schedules, and delivery schedules.

Cost/Schedule Control System - Conduct cost and scheduling planning and control in accordance with Martin Marietta Corporation current practices used on the launch vehicles project.

Configuration Management - Develop and prepare specifications that define the design requirements and product configuration baselines of the subsystem; develop and prepare implementation plans that define the methods of implementing the program; develop and prepare the interface documentation that defines the subsystem interface with the Space Shuttle orbiter; and provide the status and accounting configuration control system required to define and control the subsystem product configuration baseline.

Data Control - Implement a contract data control schedule, and status, selloff, and distribution system.

Liaison - Provide the necessary liaison required to interface with program participants. Attend technical interchange and interface meetings.

2. Engineering Management

Engineering management activities are defined as follows:

Payload Mission Requirements - Conduct analysis of Space Shuttle traffic model to determine payload mission requirements.

Trade Studies and Analysis - Conduct trade studies and analysis to develop subsystem approach and design requirements.

Subsystem Design Requirements - Develop subsystem baseline design requirements.

Design Reviews - Conduct design reviews with customer; Preliminary Design Reviews (PDRs) and Critical Design Reviews (CDRs), to develop subsystem product configuration baseline.

Control Requirements - Develop requirements and maintain EMC and mass property control of the subsystem.

Procedures Development - Develop and maintain all required procedures for the subsystem.

Engineering Program Integration - Provide the engineering integration of all elements of the program to provide an integrated subsystem.

3. Product Assurance

The product assurance activities are defined as follows:

Reliability - Develop and implement a reliability program to assure adequate reliability considerations throughout all aspects of the design, development, and production phases as necessary to meet Space Shuttle program reliability requirements. Implement a contractor-fabricated critical electronic piece parts traceability program.

Quality Assurance - Develop and implement a quality assurance program that complies with the requirements of MIL-Q-9858 throughout all phases of contract performance including design, development, fabrication, processing, assembly, inspection, test, checkout, packaging, and shipping of the subsystem.

System Safety - Develop and implement a system safety program in general accordance with the requirements of MIL-S-38130 that provides an integrated system safety program throughout all program phases.

4. Logistics and Maintenance

The logistics and maintenance activities are defined as follows:

Maintainability - Conduct maintainability activities to translate operations, support, engineering, and cost considerations into maintenance concepts for the subsystem.

Maintenance - Establish a maintenance program that supports installed subsystem maintenance requirements.

Support Parts - Establish a support parts supply program that identifies provisioning and control of consumable and nonconsumable support parts for the subsystem.

Training - Develop and implement a training program for contractor personnel for design, test, and fabrication operations, and customer personnel for operational and maintenance activities. Provide a 1-g training subsystem* to support operational training.

5. Airborne Subsystem Hardware/Software

The airborne subsystem hardware/software activities are defined as follows:

Development - Define and conduct a design development and verification testing program for the airborne subsystem, including associated software.

Design - Accomplish design for the airborne subsystem, including associated software, in accordance with the applicable Part I specification.

Qualification - Define and conduct a qualification test program to qualify the airborne hardware subsystem to the Space Shuttle program requirements.

Preproduction Test Hardware - Provide hardware (breadboards, prototype, test articles, instrumentation, and preproduction test articles) required to perform development, verification, and qualification testing.

*Resources estimate does not include a 1-g training subsystem (beyond the scope of this effort).

6. Ground Support Equipment (GSE)

The GSE activities are defined as follows:

Development - Conduct ground hardware test programs that may consist of reliability, design development, electromagnetic interference, design verification, and model tests.

Design - Accomplish design for the ground subsystem hardware in accordance with the requirements of the applicable Part I CEI specifications.

Preproduction Test Hardware - Provide breadboards, prototype test articles, special test equipment, and instrumentation required to perform ground development testing.

7. Airborne Subsystem Production

The airborne subsystem production activities are defined as follows:

Fabrication - Fabricate and deliver one flight subsystem to the requirements of the applicable Part II specifications (it is assumed that the orbiter will supply digital computer and power supply services to the subsystem.)

Acceptance - Conduct acceptance testing of the one flight subsystem in accordance with section 4 of the Part II specification; conduct a first article configuration inspection (FACI) on the first production flight subsystem to establish a subsystem product configuration baseline.

Environmental Acceptance Testing (EAT) - Define and conduct EAT on selected subsystem components.

Engineering Maintenance - Provide engineering maintenance associated with changes to the subsystem in-scope to the subsystem requirements.

Factory Tooling - Design, procure, fabricate, check out, install, and maintain necessary nondeliverable special tooling, i.e., jigs, fixtures, handling equipment, etc, to manufacture test code hardware and contractor-furnished airborne subsystems.

Special Test Equipment (Test Tools) - Provide nondeliverable special test equipment required to support airborne subsystem fabrication and acceptance activities at the contractors plant.

8. Ground Support Equipment (GSE) Production

The GSE production activities are defined as follows:

Fabrication - Fabricate two sets of GSE to the requirements of the applicable Part II specifications.

Acceptance - Conduct acceptance testing of the GSE in accordance with Section 4 of the Part II specifications.

Engineering Maintenance - Provide engineering maintenance associated with changes to the subsystem in-scope to the GSE requirements.

Factory Tooling - Design, procure, fabricate, check out, install, and maintain the necessary nondeliverable test tooling, i.e., jigs, fixtures, handling equipment, related manufacturing, etc, to manufacture test code hardware and contractor-furnished GSE.

Special Test Equipment - Provide nondeliverable special test equipment required to support GSE fabrication and acceptance activities at the contractors plant.

Note: Support of the subsystem at the orbiter contractor's plant and at the operational launch site is not included in resources estimate.

B. DEVELOPMENT SCHEDULE

Figure IX-1 is a typical development schedule. It includes delivery of one qualification unit and one flight unit; it does not include crew training hardware or postflight unit delivery support.

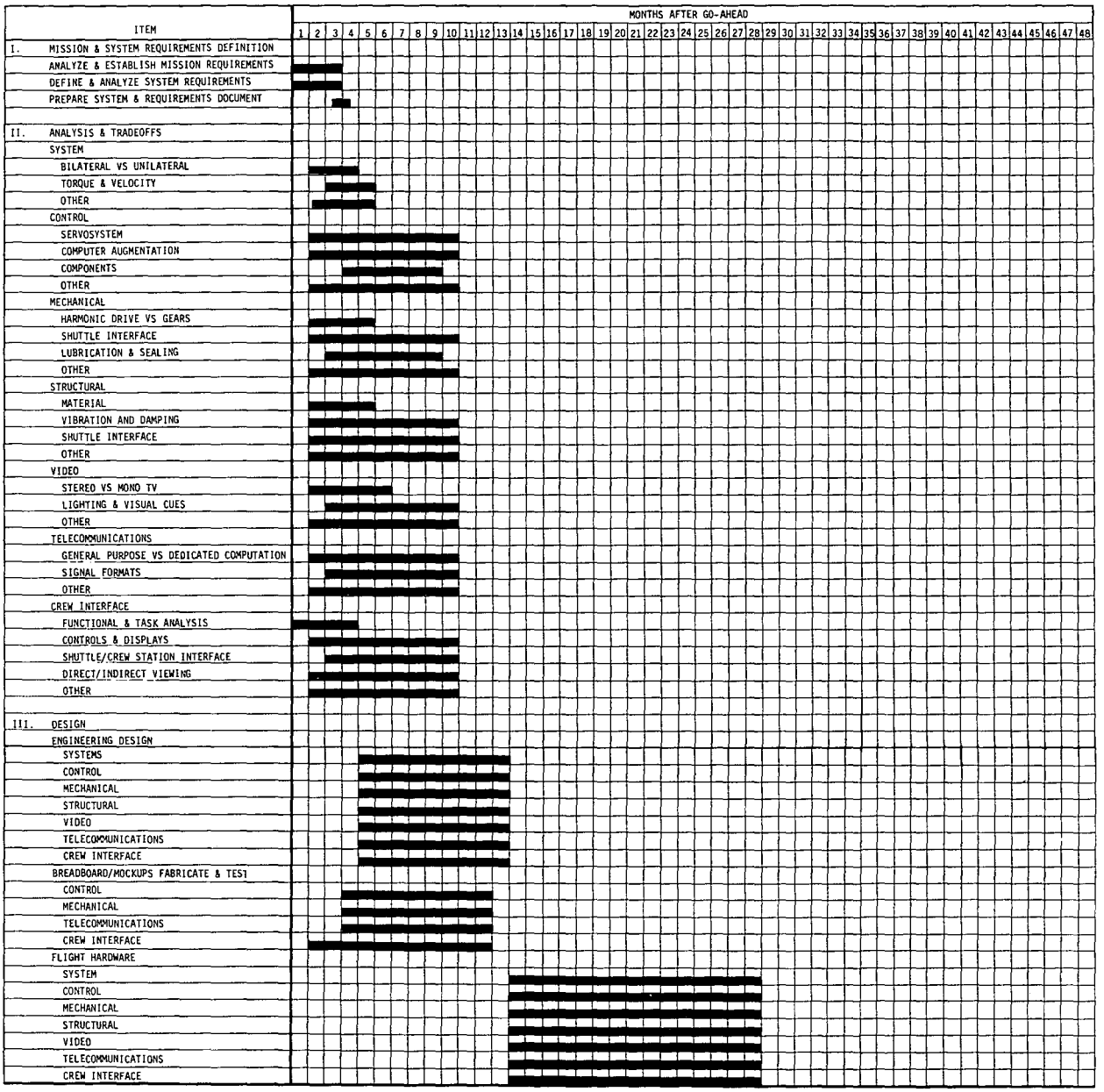

Fig. IX-1 Typical Development Schedule

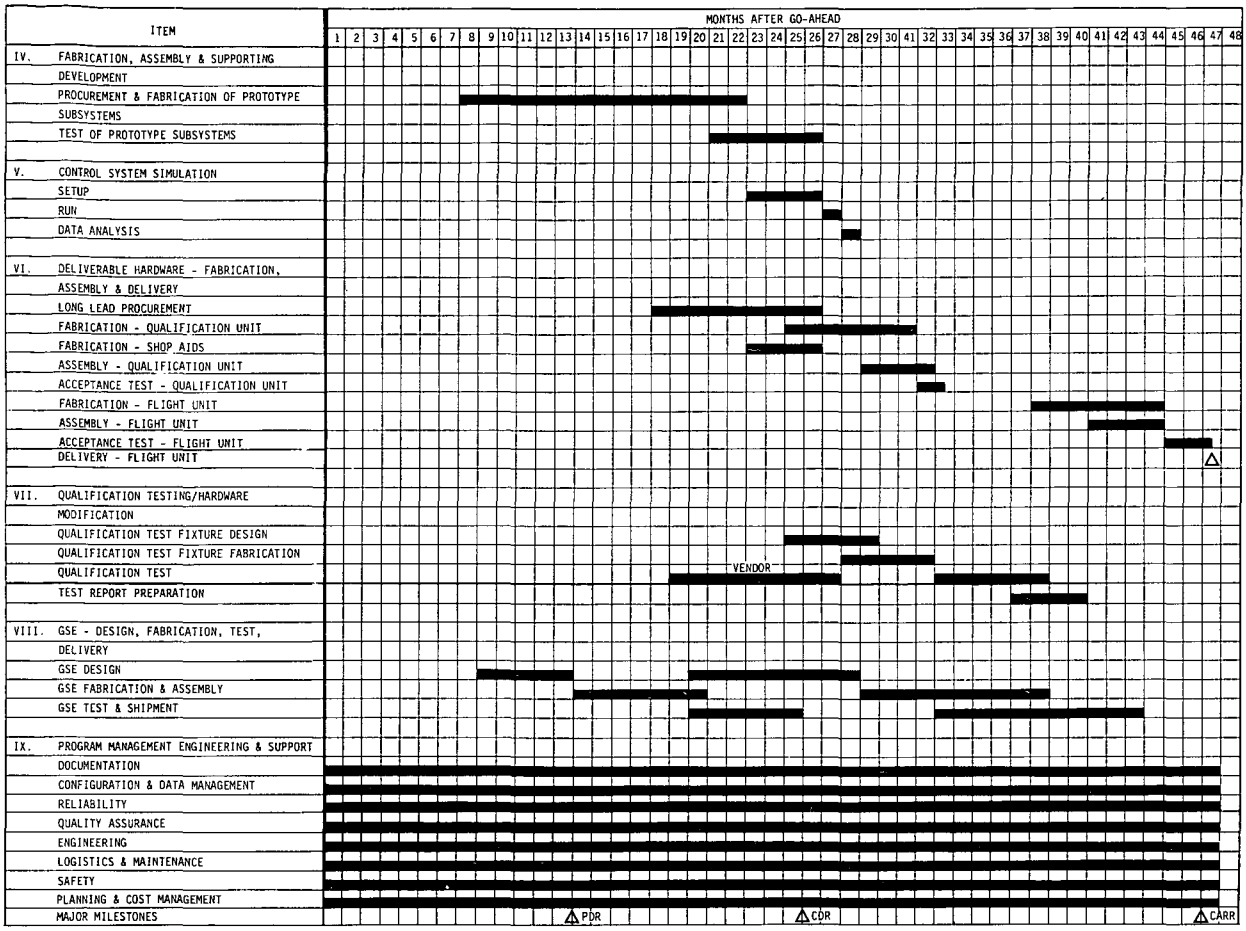

Fig. IX-1 (concl)

C. MAJOR RMS COMPONENTS

Table IX-1 lists the major RMS components.

Table IX-1 Major RMS Components

SUBSYSTEM	COMPONENT	QUANTITY
1. Mechanical & Structural		
A. Deployment	Rotary Actuator	2
	Solenoid	4
	Bearings	8
	Arm Tubing	7.2 m (24 ft)
	Explosive Bolt Separation System	2
B. Arm Retention	Latches & Linkages	12
	Drive Motors or Solenoids	12
	Limit Switches	12
	Position Sensors	12
	Explosive Bolt Separation System	2
C. Manipulator Arm*	Motors	28
	Harmonic Drives	14
	Spur Gears	56
	Brakes	14
	Housings	14
	Bearings	168
	Tach Generators	14
	Potentiometers	14
	Limit Switches	28
	Tubing	30.5 m (100 ft)
2. Telecommunications and Control	TV Camera	4
	TV Pan-Tilt Assembly	2
	Wrist Area Illumination System	2
	Digital Display Formetter	1
	Reference Memory	1
	Preset Slave Position Memory	1
	Power Conditioner	1
	TV Sync Generator	1
	Command Distribution Unit	1
	Sensor Data Distribution Unit	1
	Format Interface Unit	1
	Servo Power Amplifiers	26
	Cargo Bay Illumination System	1
	Cargo Bay Camera Deployment System	2
3. Crew System	Switches	52
	Digital Readouts	6
	Verification & Caution Lights	30
	12 in. TV Monitor	1
	8 in. TV Monitor	2
	Actual and Event Timer	1
	Controllers	2
	Circuit Breakers	32

*Terminal device(s) has been exluded from resources estimate.

D. RESOURCES ESTIMATE

Table IX-2 shows a breakdown of the estimates for manpower, material, computer, and travel for the RMS program. Estimate covers one qualification unit and one flight unit. Excluded from this estimate are a 1-g training unit, the terminal device(s), and postdelivery support.

Table IX-2 Estimated Resources

COST ELEMENTS	TASK 1		2		3		4		5		6		7		8		9		TOTAL	
	MM	$	MM	$	MM	$	MM	$	MM	$	MM	$	MM	$	MM	$	MM	$	MM	$
Engineering	24	0.076	303	1.093	553	2.098	102	0.382	26	0.253			12	0.060	80	0.376	180	0.786	1280	5.124
Tooling											81	0.300			15	0.057			96	0.357
Manufacturing											272	0.964	14	0.056	44	0.175			330	1.195
Quality											88	0.402	62	0.078	19	0.092	135	0.540	304	1.112
Test													48	0.254	16	0.085			64	0.339
Configuration & Data Management																	351	1.404	351	1.404
Safety																	45	0.180	45	0.180
Planning & Cost Management																	135	0.538	135	0.538
Material												5.241				0.110				5.351
Computer										0.145										0.145
Travel																		0.050		0.050
Total	24	0.076	303	1.093	553	2.098	102	0.382	26	0.398	441	6.907	136	0.448	174	0.895	846	3.498	2605	15.795* ±25%

Note: $ in millions

MM (man-months)

*Estimate covers one qualification unit and one flight unit. Excluded from this estimate are a 1-g unit, the terminal device(s) and postdelivery support.

X. CONCLUSIONS

This report satisfies the RMS study, design and development objectives (See Appendix B.). A preliminary design of a system for Shuttle docking and cargo handling has been completed. Analyses and design on the system and subsystem level show that no fundamental technical problems or restrictions exist; the RMS concept is feasible and practical. Our preliminarily designed RMS (1) can perform the required Shuttle tasks, (2) is compatible with the Shuttle Orbiter design, (3) has reasonable size and weight, and (4) has great operational flexibility and versatility (See Summary, Chapter II.). No technology development (advancement in the state-of-the-art) is required for future development.

A. SUMMARY OF SYSTEM SPECIFICATIONS

This section includes five tables: Table X-1, RMS Preliminary Design Characteristics Summary; Table X-2, Joint Preliminary Design Characteristics Summary; Table X-3, RMS Equipment Weight Estimate Summary; Table X-4, RMS Total Weight Summary; and Table X-5 RMS Electrical Power Estimate Summary.

1. Design Characteristics

Design characteristics are summarized in Table X-1 and X-2.

Table X-1 RMS Preliminary Design Characteristics Summary

1.	Arm Length	Upper, 7.16 (23.5 ft); Lower, 7.16 m (23.5 ft); Wrist Extension, 0.9 m (3 ft); Total, 15.25 m (50 ft)
2.	Deployment Mechanism	Diameter, 30.5 cm (12 in.), Wall thickness 1.27 cm (0.5 in.); Weight, 118 kg (261 lb)
3.	Upper Arm	Diameter 20.3 cm (8 in.); Wall Thickness, 2.0 cm (0.78 in.); Weight, 229 kg (505 lb)
4.	Lower Arm	Diameter, 20.3 cm (8 in.); Wall Thickness, 0.8 cm (0.31 in.); Weight, 97 kg (214 lb)
5.	Wrist Extension	Diameter, 10.1 cm (4 in.); Wall Thickness, 0.8 cm (0.31 in.); Weight, 6 kg (13 lb)
6.	Arm Stowage Volume	Diameter, 0.2 m (8 in.); length, 15.3 m (50 ft); Inside Cargo Bay
7.	Control and Display Panel Size	0.66 x 0.84 m (26 x 33 in.)
8.	Crew Operating Location	Shuttle Crew Cabin
9.	Deployment	At Forward Cargo Bay Bulkhead; Swing Out with 6.0 m (20 ft) Separation Distance
10.	Maximum Cargo Handling Capability	29,600 kg (65,000 lb)
11.	Baseline Structural Material	Aluminum
12.	Total Weight of RMS (Aluminum Arms)	1263.6 kg (2783 lb)
13.	Total Weight of RMS (Lockalloy Arms)	619.3 kg (1364 lb)
14.	Weight of Arms and Deployment Mechanisms	1135 kg (2500 lb)
15.	Degrees of Freedom	Shoulder - 2; Elbow - 2; Wrist - 3; TD - 1; Total - 8
16.	Gimbal Order	Shoulder - Pitch, Yaw; Elbow - Roll, Yaw; Wrist - Yaw, Pitch, Roll
17.	Joint Sensors	Angular Position; Angular Rate
18.	Tip Acceleration	No Load - Stop in 0.46 m (1.5 ft) from maximum velocity Full Load - Stop in 4.6 m (15 ft) from maximum velocity
19.	Tip Position Accuracy	±0.051 m (±2 in.)
20.	Full Load Tip Deflection	0.025 m (1 in.)
21.	Arm Natural Frequency (First Fundamental)	0.53 Hz (no-load); 0.035 Hz (Max Cargo Load); 2.3 Hz (Shuttle-to-Shuttle)
22.	Servo System	Bilateral Force-Reflecting
23.	Control Scheme	Variable Gain Control Augmented with Selected Pre-programmed Trajectories
24.	Command and Data Link	Hardwire, Analog
25.	Computation	Shuttle On-Board General Purpose Digital Computer
26.	Viewing	Direct Viewing Supplemented by Remote Control TV - 1 on each Wrist (before Roll Joint), 1 at Front of Cargo Bay, 1 at Rear of Cargo Bay
27.	External Lighting	Apollo Type, 2 per Camera

Table X-2 Joint Preliminary Design Characteristics

	Shoulder		Elbow		Wrist		
	Pitch	Yaw	Roll	Yaw	Yaw	Pitch	Roll
1. Angular Travel (deg)	±200	±130	±200	±155	±120	±120	±200
2. Torque, N-m (ft-lb)	667 (500)	667 (500)	474 (350)	474 (350)	202 (150)	202 (150)	88 (65)
3. No Load Velocity (rad/sec)	0.03	0.03	0.0565	0.0565	0.174	0.174	0.174
4. Full Load Velocity (rad/sec)	0.0035	0.0035	0.0066	0.0066	0.0265	0.0265	0.0265
5. Position Accuracy (deg)	±0.113	±0.113	±0.113	±0.113	±0.113	±0.113	±0.113
6. Rate Accuracy (deg/sec)	±0.033	±0.033	±0.033	±0.033	±0.033	±0.033	±0.033

2. Weight

Weight figures are summarized in Table X-3 and X-4.

Table X-3 RMS Equipment Weight Estimate Summary

RMS Equipment	Estimated Weight, kg (lb)	
Manipulator Arm (One) and Deployment Device		
Beams*		
Upper Arm	229.3	(505)
Lower Arm	97.2	(214)
Wrist Extension	5.9	(13)
Deployment Member	118.5	(261)
Joints		
Shoulder		
Pitch	13.2	(29)
Yaw	13.2	(29)
Elbow		
Roll	11.4	(25)
Yaw	12.2	(27)
Wrist		
Yaw	6.8	(15)
Pitch	6.8	(15)
Roll	6.4	(14)
Deployment Actuator	11.4	(25)
Terminal Device	4.5	(10)
Wrist TV and Lights	6.4	(14)
Cabling	7.3	(16)
Total	550.5	(1212)
Control Console (Masters Used for Maximum Weight)		
Two Master Arms		
Beams	2.7	(6)
Joints		
Shoulder	10.9	(24)
Elbow	10.9	(24)
Wrist	10.9	(24)
Three TV Displays	18.2	(40)
Control Switches	6.8	(15)
Mounting Face and Hardware	4.5	(10)
Total	64.9	(143)
Control and Data Electronics		
Servo System Electronics	4.5	(10)
Power Converter	7.7	(17)
Command and Data Interface	5.0	(11)
Total	17.2	(38)
Shuttle Surface Mounted Equipment		
TV		
Two Cameras and Lights	15.4	(34)
Two Pan and Tilt Mechanisms	10.0	(22)
Cabling	1.8	(4)
Fourteen Stowage Clamps	50.8	(112)
Nitrogen Supply System	2.7	(6)
Total	80.7	(178)

*Weight based on aluminum beams; 70% reduction in weight if Lockalloy is substituted for aluminum.

Table X-4 RMS Total Weight Summary

Quantity	RMS Equipment	Estimated Weight, kg (lb)
2	Manipulator Arm and Deployment Device	1101.0 (2424)
1	Control Console	64.9 (143)
1	Control and Data Electronics	17.2 (38)
1	Shuttle Surface Mounted Equipment	80.7 (178)
Total Weight of RMS		1263.8 (2783)*
*Total would become 619.3 kg (1364 lb) if Lockalloy substituted for aluminum for beams.		

3. Electrical Power

Electrical power estimates are summarized in Table X-5.

Table X-5 RMS Electrical Power Estimate Summary

Electrical Equipment	Average Power (watts)					
	Checkout	Precapture	Capture	Dock	Unload and Deploy	Module Unload Transfer and Dock
Slave Servo System	200	200	200	150	300	300
Master Servo System	100	100	100	50	100	100
Control and Data Electronics	55	55	55	55	55	55
Deployment Mechanisms	15	15	0	0	0	0
Ejector Mechanisms	0	0	0	0	0	0
TV System	32	40	40	30	40	40
Lighting System	1	164	164	164	410	328
Displays	5	3	3	3	3	3
Power Conditioner	80	80	80	60	100	100
Total Power per Task (watts)	488	657	642	512	1008	926
Operational Time (min)	10	5	3	10	10	10
Total Energy per Task (w-hr)	81.3	54.8	32.1	85.3	168.0	154.3

B. FURTHER ANALYSIS AND TRADEOFFS REQUIRED

The design areas listed below include those areas (1) examined in this preliminary design which require further detail analysis, and (2) those areas which were beyond the scope of this preliminary work, but which whould be examined before final design work.

1) Master-slave force feedback servo design and simulation; (Chapter VI; Chapter VIII, Section B);
2) Dynamics computer analysis, six degrees of freedom (including Orbital effects) (Chapter VIII, Section B);
3) Gimbal lock, reach envelope (Chapter VII, Section C,E);
4) Master arm design for limited space (Chapter VIII, Section F);
5) Arm structural material (Chapter VIII, Section C);
6) Vibration, damping, and deflection criteria (Chapter VIII, Section C);
7) Sun, shadows, glare and lighting (Chapter VIII, Section F,G);
8) Visual cues for two dimensional TV (Chapter VI, Chapter VI VIII, Section F);
9) Mono TV with force feedlock simulation (Chapter VI);
10) Functional task timeline analyses (Chapter VIII, Section F);
11) Terminal device requirements and design (Chapter VIII, Section D);
12) Launch pad test techniques (Chapter VII, Section I);
13) Collision avoidance methods (Chapter VIII, Section B);
14) Arms as sensors simulation (Chapter VIII, Section A);
15) Computer augmentation software (Chapter VIII, Section B);
16) Joystick vs articulated controller (master) (Chapter VI).

The design areas that follow should be worked as part of the final design.

1) Internal vs external arm stowage;
2) Thermal control;
3) Actuators and gear reducers;
4) Reliability improvement;
5) Joint and structural design tradeoff for small diameter areas;

6) Failure mode analysis;

7) Deployment mechanism tradeoff;

8) Arm eject methods for abort;

9) Wire flexing in space;

10) Direct vision and/or TV viewing tradeoff.

The following paragraphs include a brief description of selected design areas from the list presented on the previous page.

1. System

Several areas were not considered in depth in the preliminary design and should be considered for a final detailed design. These areas include the following: maintainability, environmental conditions, electromagnetic radiation, quality assurance, transportability, commonality, and interchangeability.

In addition, the interface, reliability, and training requirements and their effect on RMS system design should also be analized in detail along with launch pad test techniques.

2. Mechanical

In the mechanical subsystem, several items should be analyzed in more detail. These include a complete weight and performance tradeoff of the various arm deployment techniques, a complete analysis of the various electromechanical components used in the system (brakes, motors, tach generators, potentiometers, etc) to determine the applicability of existing space-qualified components, and an investigation of drive systems components (harmonic drives, gears, etc) for space-qualification. In addition, the bearing, lubrication, and sealing problems of the joints should be thoroughly investigated. The requirements analysis and design of terminal devices should be conducted. Preliminary work indicates a "tool box" concept is desirable. An internal vs external RMS stowage tradeoff should be made in coordination with Orbiter design as well as design of the master arms for the available space.

3. Structural

The structural analyses should include a complete and detailed computer programmed vibration mode analysis to determine the arm bending mode characteristics, and to investigate potential RMS/Shuttle vibration problems. A material weight, cost, performance tradeoff should also be performed to determine the optimum material for the RMS structural members.

4. Control and Dynamics

The complete six-degree-of-freedom equations of motion should be derived. These equations should include: structural vibration modes, Shuttle RCS characteristics, orbital effects, friction and motor characteristics, arm and payload inertia characteristics, dissipation functions, and arm servo control characteristics.

A total modal analysis of the arm should be performed and integrated into the force reflecting control system design. If the dynamic behavior of the system is incorporated in the control system design equations, they can be accounted for and possibly eliminated or made negligible. The computer function is one of the more important parts of the control system and the software should be studied in depth. The gimbal singularity should be thoroughly studied with possible techniques to eliminate it.

5. Crew Systems

The use of TV monitors for remote slave monitoring limits direct (through the window) viewing. The monitors and associated RMS controls are preferable directly in front of the operator, thereby blocking a portion of a possible direct view looking toward the Shuttle cargo bay. In addition, if large portions of the crew station are covered with glass intense sun glare could result unless shielding is provided.

6. Telecommunications

Cabling to the joints will require a high degree of flexing. Further study is necessary to determine the mechanical properties required for the cable compared to existing space-qualified cable.

There could be a considerable saving in power at the expense of some complexity if the TV lighting could be replaced by reflectors to direct diffuse sunlight into shadow areas. This is a potential area for sun sensors and computer control to direct the reflectors into the best position, and should be investigated.

7. Simulations

Full sized, 15.3 m (50 ft) arm RMS should be designed and constructed so that 1-g man-in-the-loop simulations can be conducted. It should include various force-feedback configurations. The required equations and operational logic should be included in the simulation. These simulations should include the complete six-degree-of-freedom equations of motion of the system. In addition, terminal device simulations under realistic conditions, using actual control and viewing systems should be conducted, as well as simulations of the automatic control modes, and collision avoidance techniques.

XI. REFERENCES

1. R. C. Arzbaecher: "Servomechanisms with Force Feedback". ANL-6157, Argonne National Laboratory, May, 1960.

2. C. R. Flatau: "Compact Servo Master-Slave Manipulator with Optimized Communication Links". Brookhaven National Laboratory.

3. R. Goertz, J. Grimson, C. Potts, D. Mingesz: "ANL Mark EVA Electric Master-Slave Manipulator". Proceeding of 14th Conference on Remote Systems Technology, 1966.

4. J. R. Tewell and C. H. Johnson: "EVA/IVA Simulation Dynamics". Martin Marietta Corporation, February, 1967.

5. F. J. Greeb: "Equations of Motion for Control of an Upper Extremity Splint Structure". Thesis, Denver University, May, 1970.

6. S. Timoshenko and D. H. Young: *Vibration Problems in Engineering*. D. Van Nostrand Company, Inc, New York, New York, Third Edition, January 1955.

APPENDIX A

SIMULATION DATA

This appendix presents the strip chart recorded data obtained during the Phase 1 and Phase 2 simulations. All pertinent identifying data appears on the figures. All data are for successful runs.

Hand Controller
Camera Control Axis
Rate Control Mode
Camera Control - None
Rate Bias - No

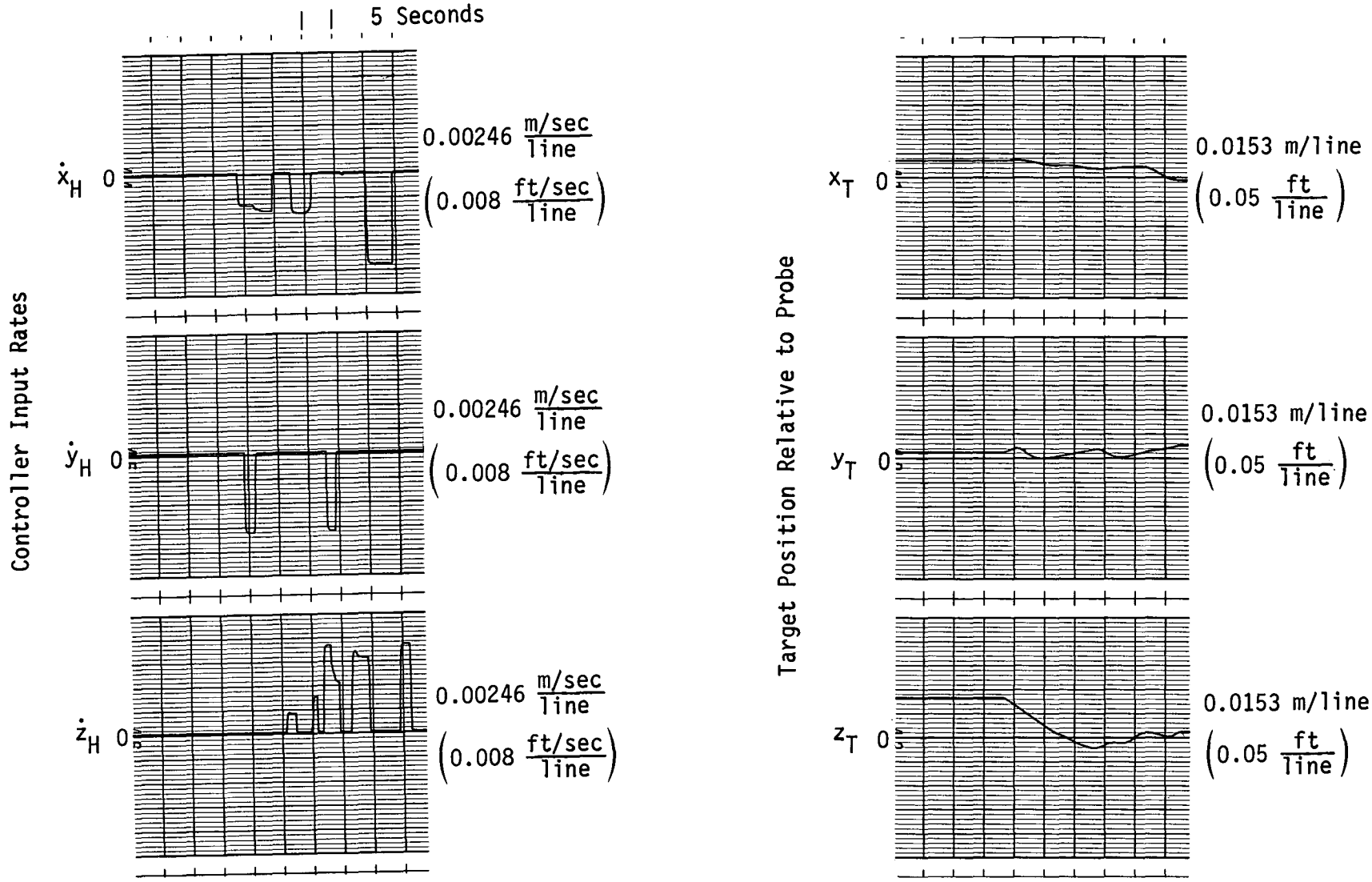

Fig. A-1 Strip Chart Recorded Data, Phase 1, Operator E, Run 1

Hand Controller
Camera Control Axis
Rate Control Mode
Camera Control - None
Rate Bias - No

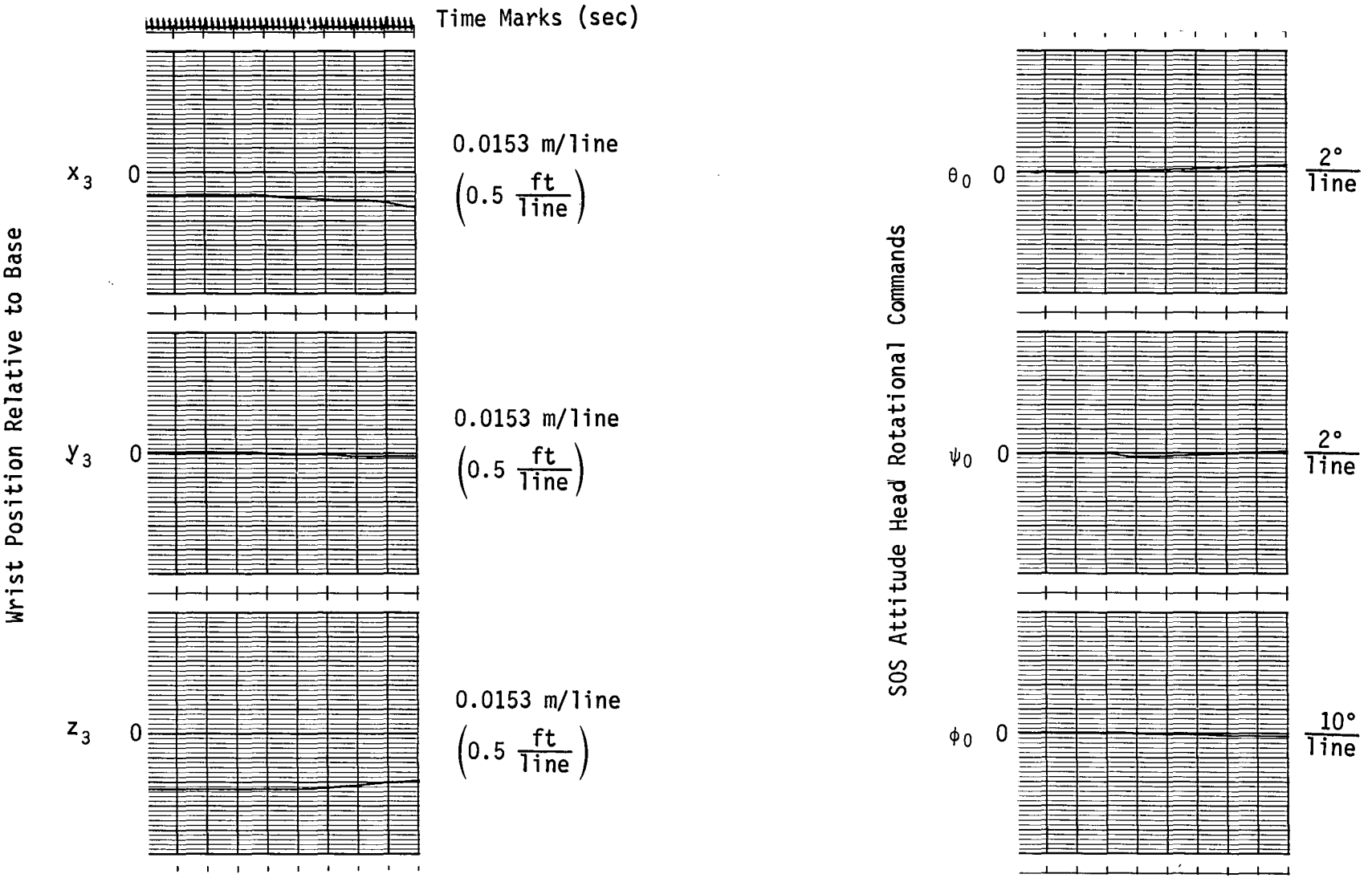

Fig. A-1 (cont)

Hand Controller
Camera Control Axis
Rate Control Mode
Camera Control - None
Rate Bias - No

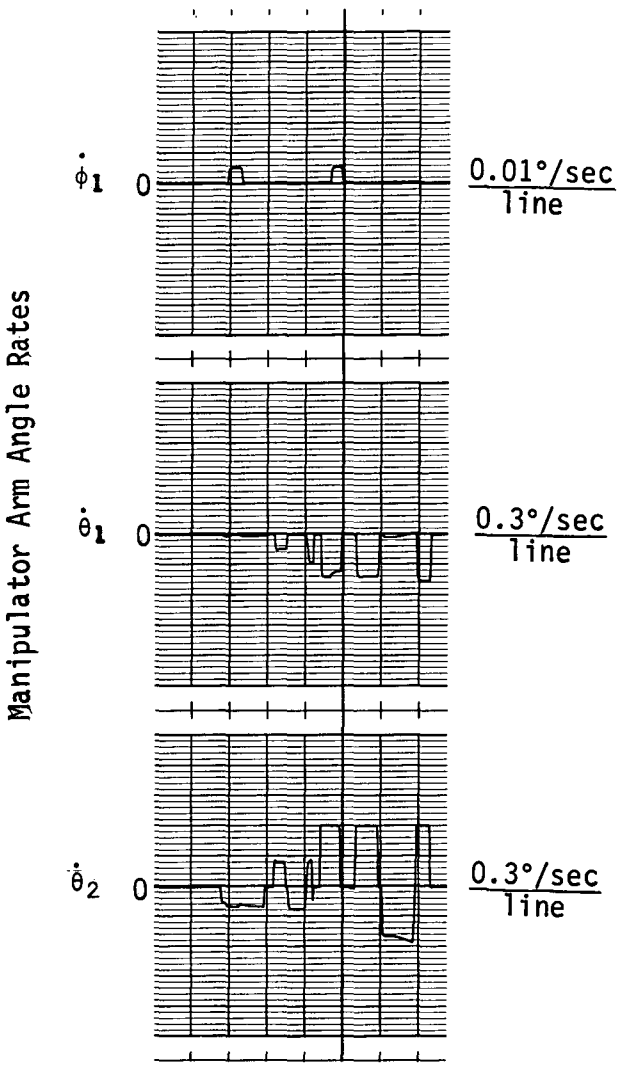

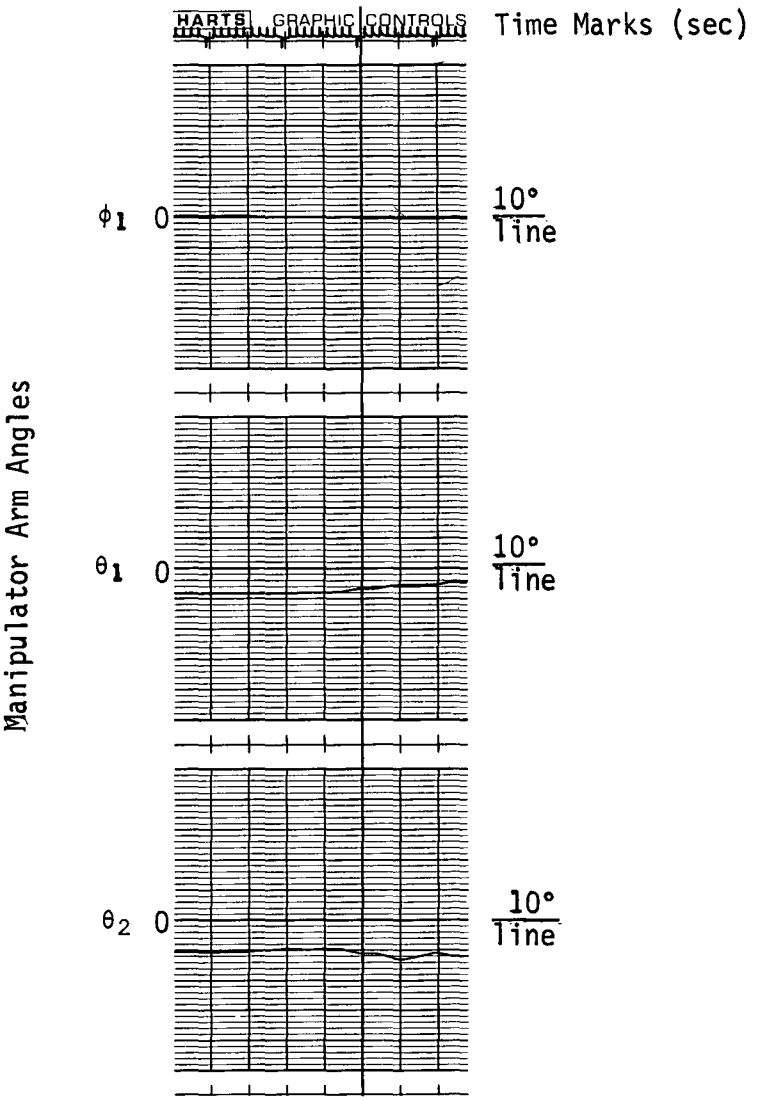

Fig. A-1 (concl)

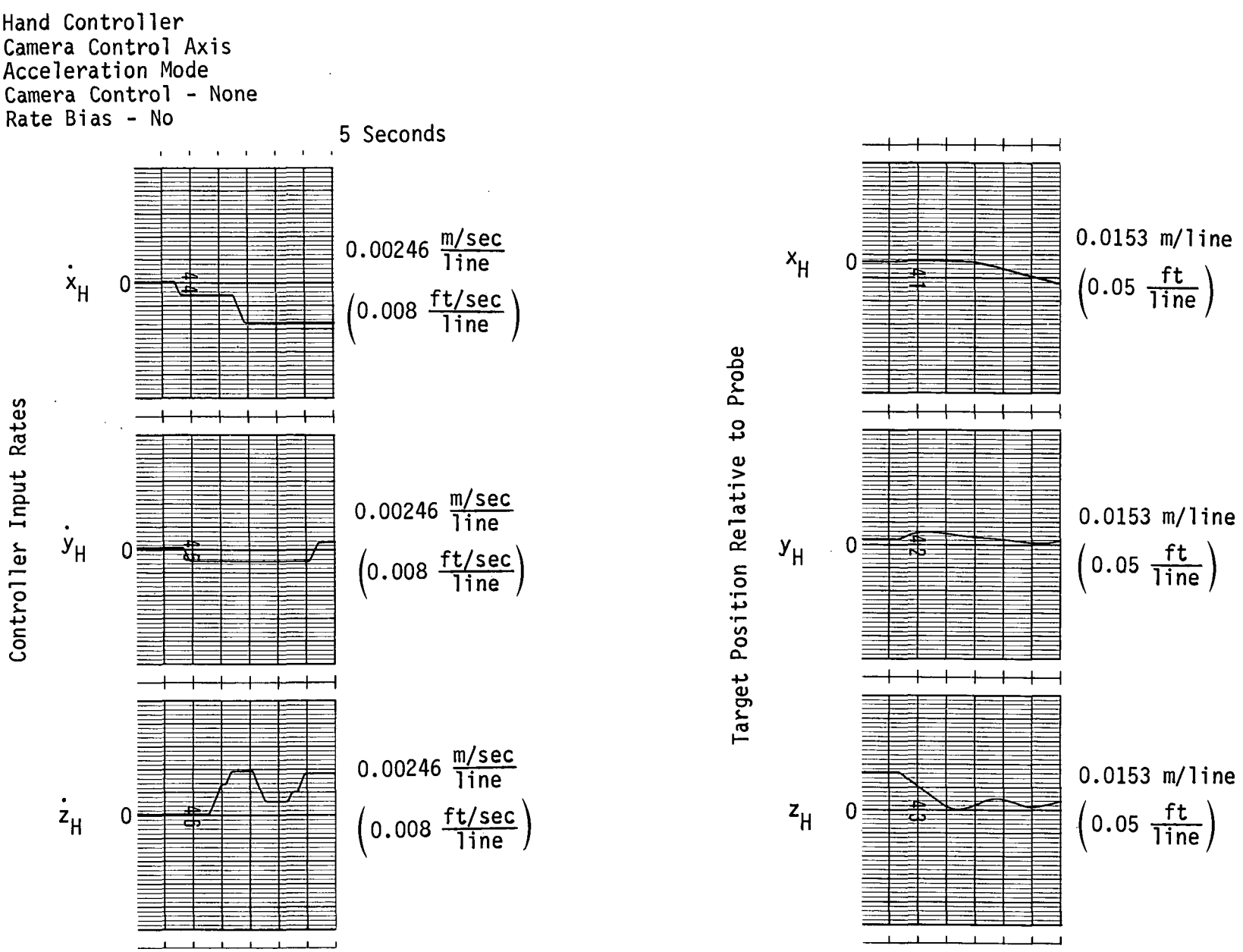

Fig. A-2 Strip Chart Recorded Data, Phase 1, Operator E, Run 6

Hand Controller
Camera Control Axis
Acceleration Mode
Camera Control - None
Rate Bias - No

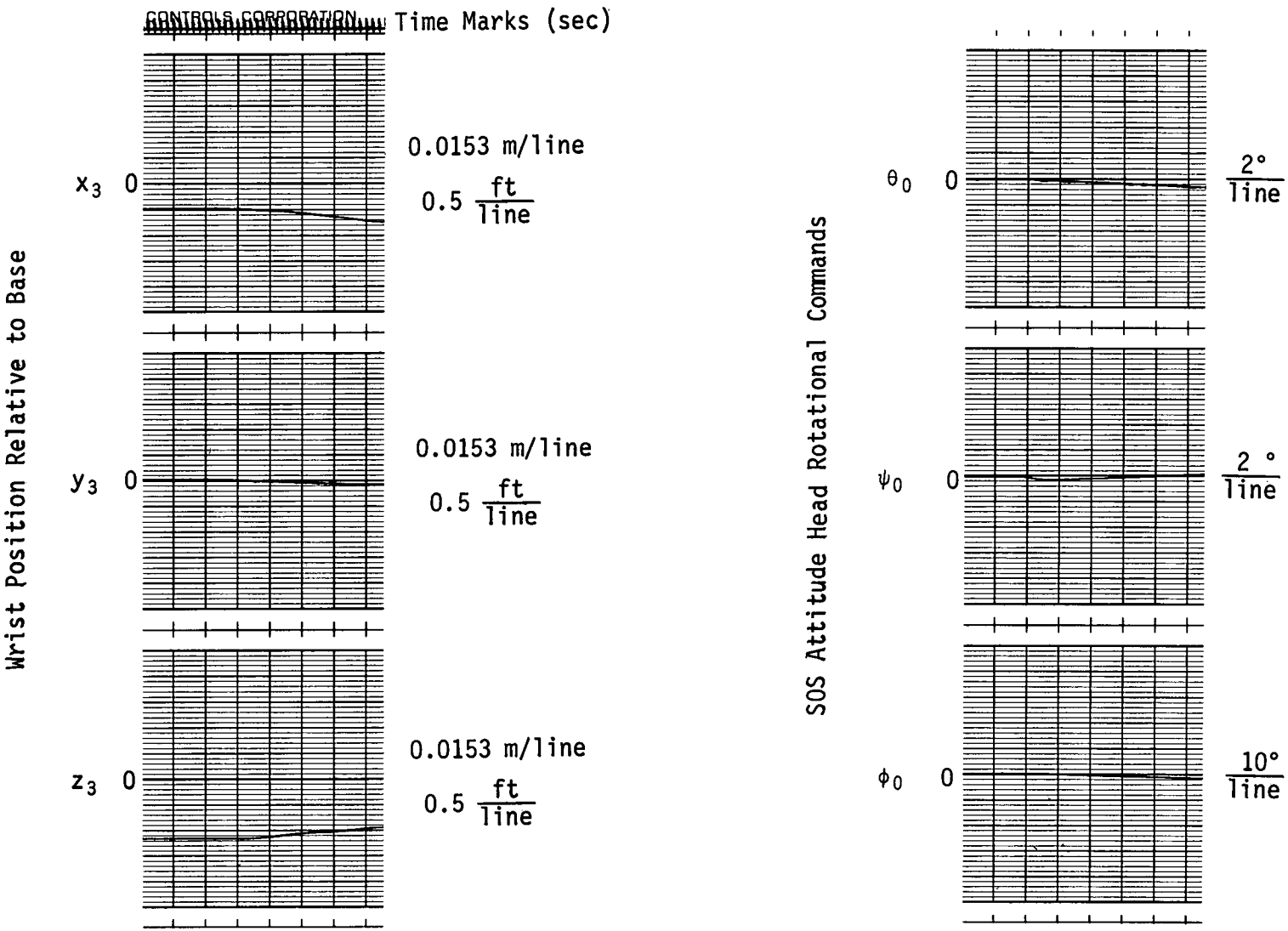

Fig. A-2 (cont)

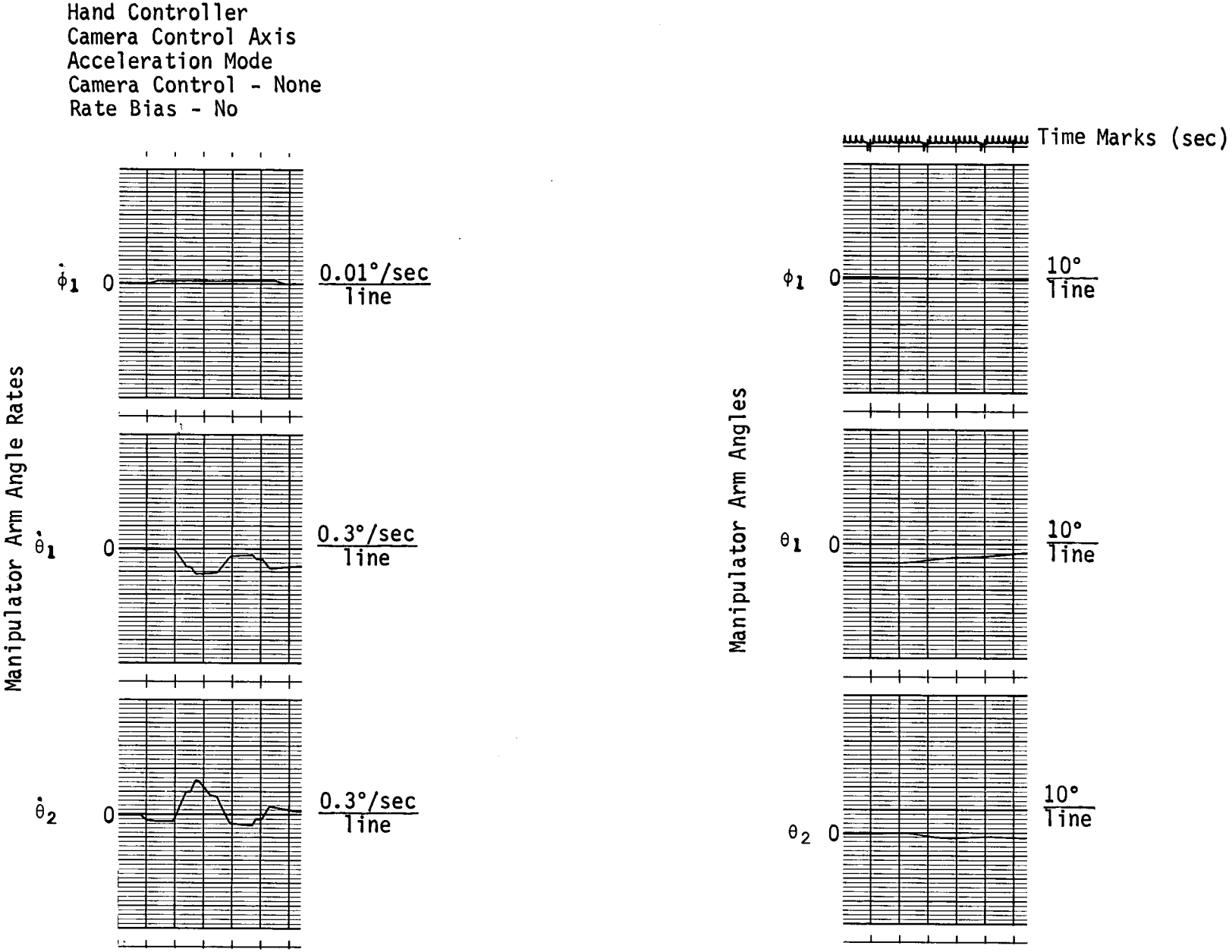
Hand Controller
Camera Control Axis
Acceleration Mode
Camera Control - None
Rate Bias - No
Manipulator Arm Angle Rates
$\dot{\phi}_1$ 0
0.01°/sec line
$\dot{\theta}_1$ 0
0.3°/sec line
$\dot{\theta}_2$ 0
0.3°/sec line
Time Marks (sec)
Manipulator Arm Angles
ϕ_1 0
10° line
θ_1 0
10° line
θ_2 0
10° line

Fig. A-2 (concl)

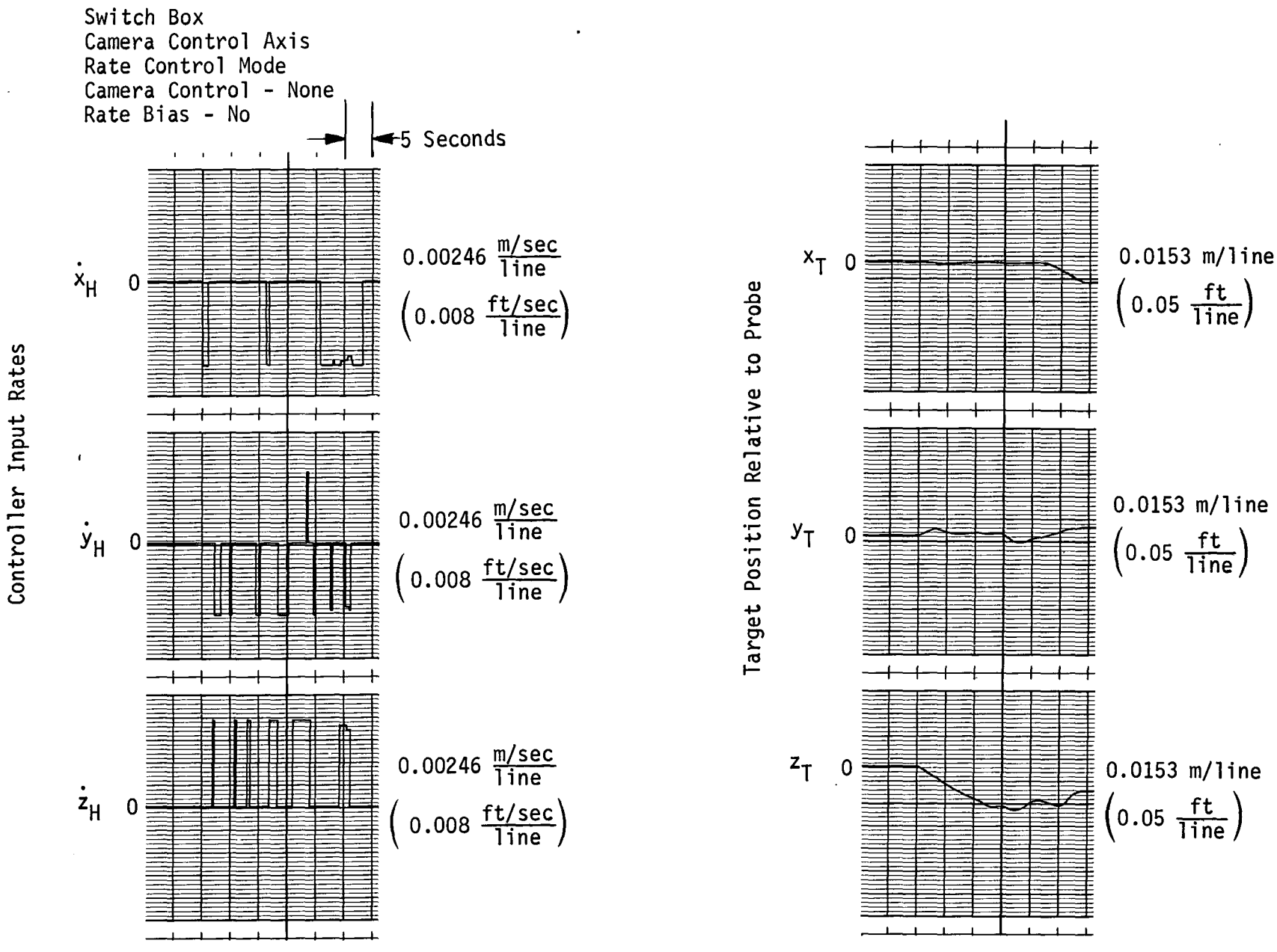

Fig. A-3 Strip Chart Recorded Data, Phase 1, Operator E, Run 12

Switch Box
Camera Control Axis
Rate Control Mode
Camera Control - None
Rate Bias - No

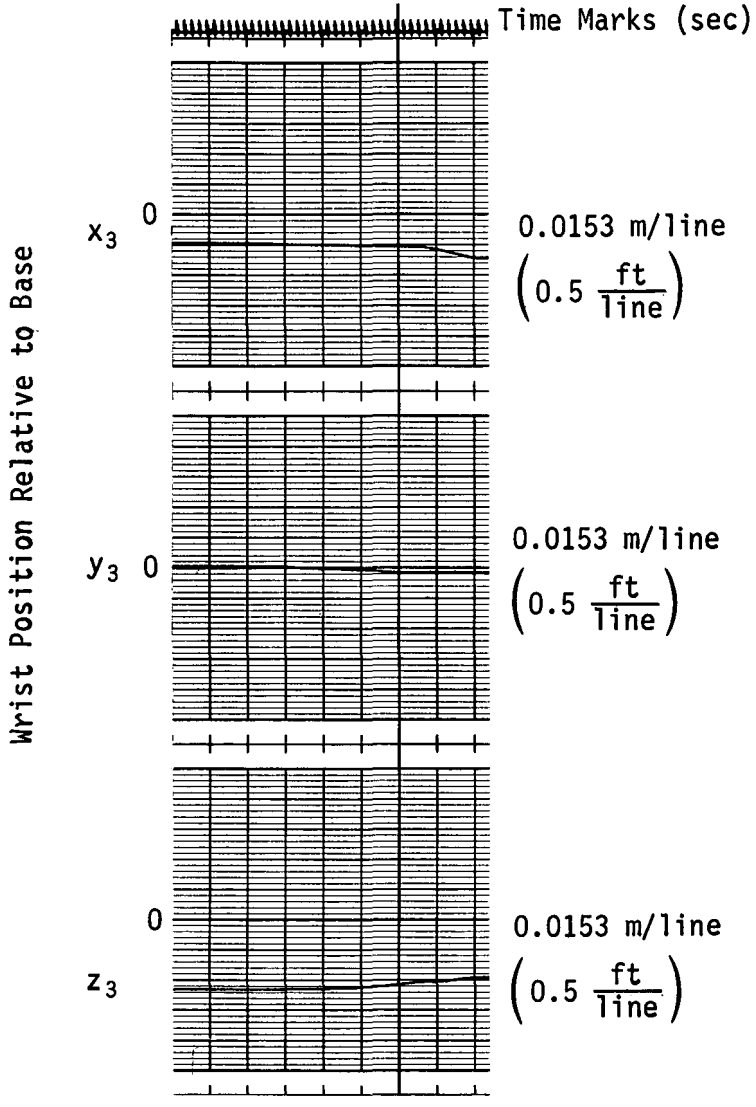

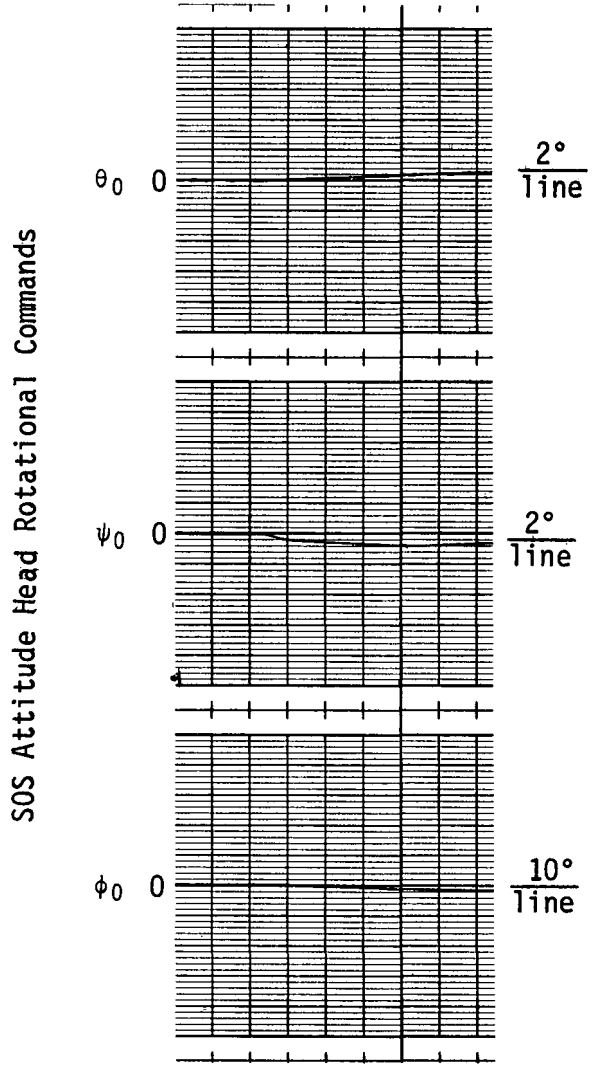

Fig. A-3 (cont)

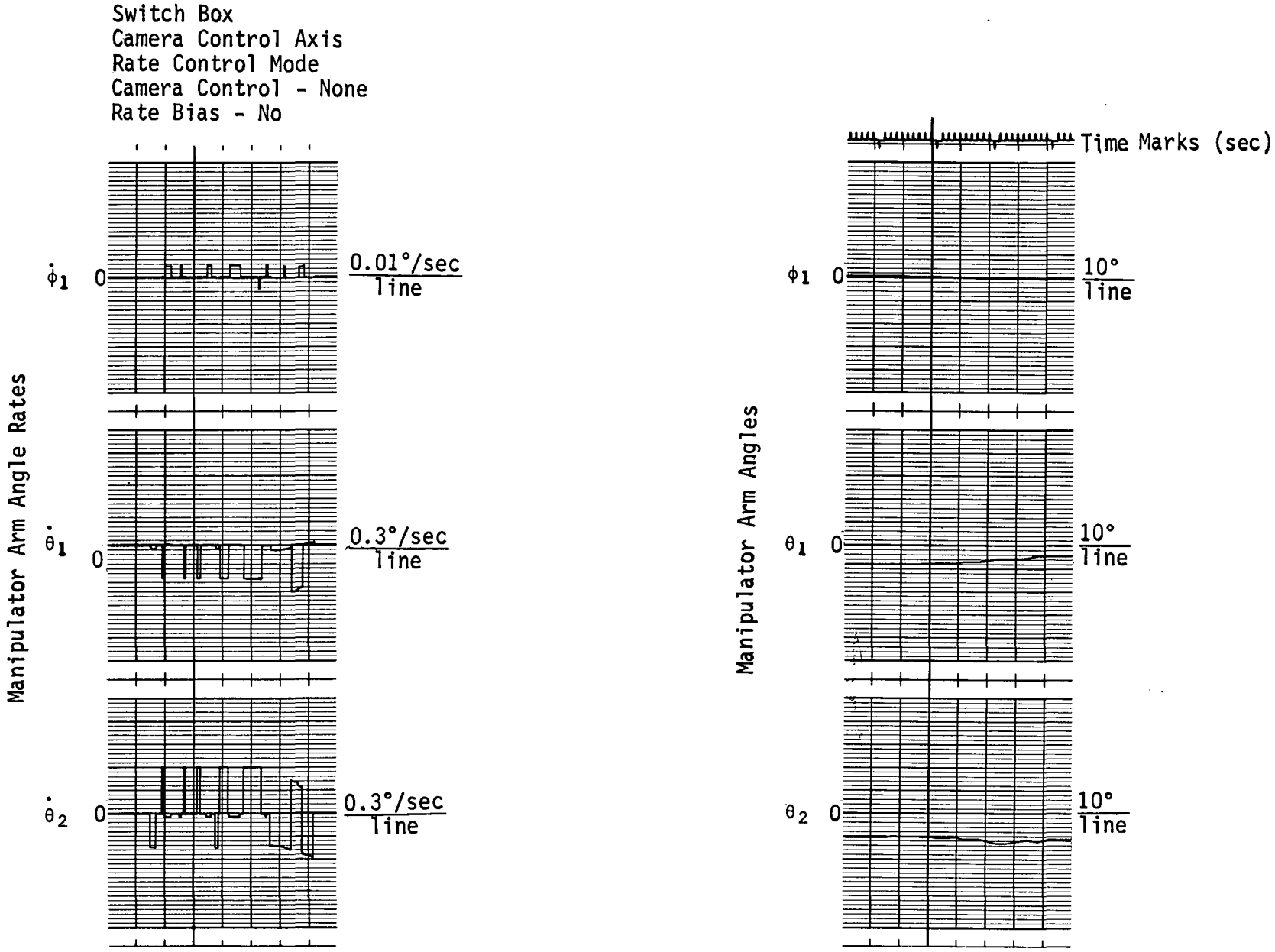
Switch Box
Camera Control Axis
Rate Control Mode
Camera Control - None
Rate Bias - No
Manipulator Arm Angle Rates
$\dot{\phi}_1$ 0
0.01°/sec line
$\dot{\theta}_1$ 0
0.3°/sec line
$\dot{\theta}_2$ 0
0.3°/sec line
Time Marks (sec)
Manipulator Arm Angles
ϕ_1 0
10° line
θ_1 0
10° line
θ_2 0
10° line

Fig. A-3 (concl)

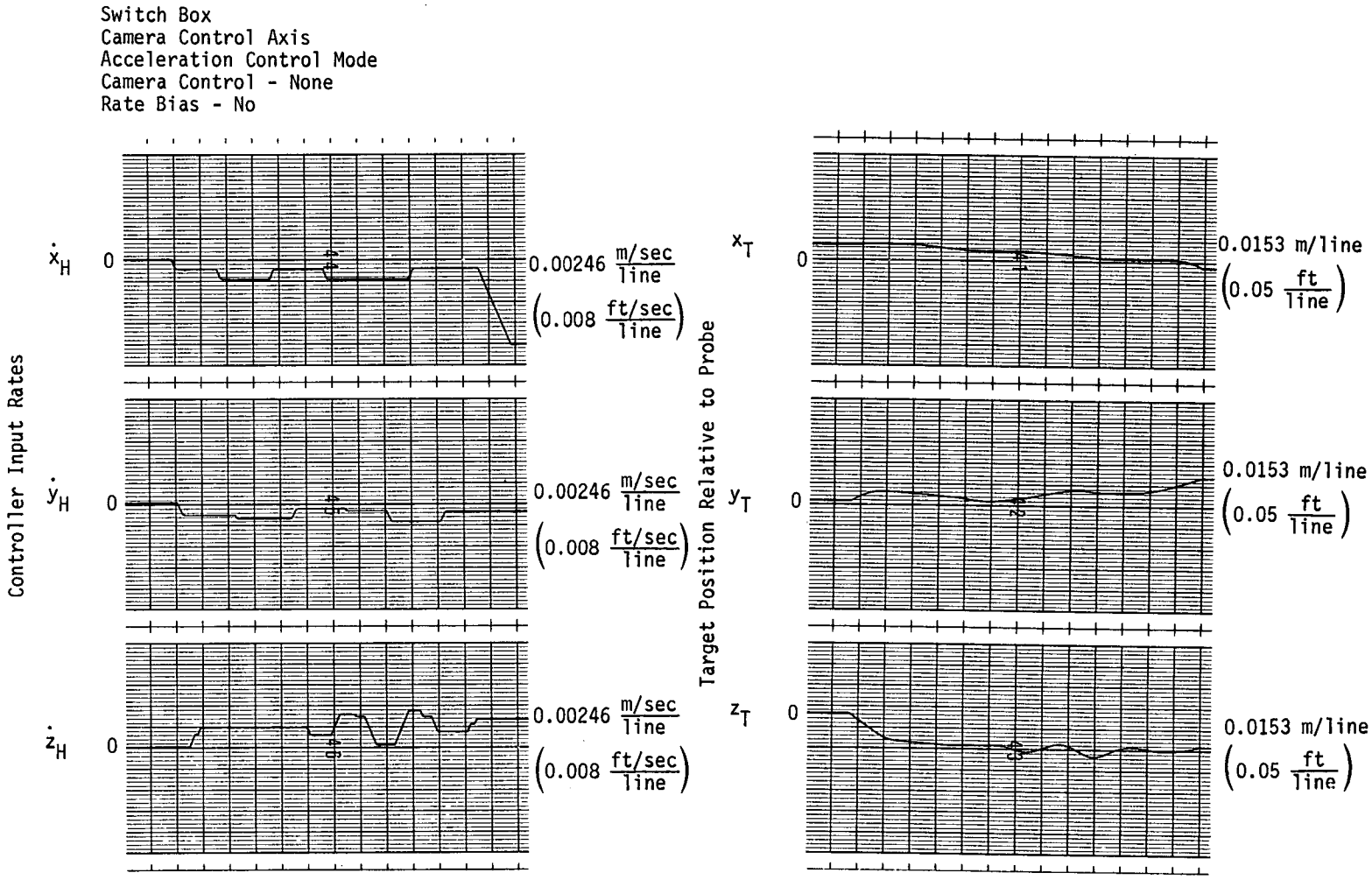

Fig. A-4 Strip Chart Recorded Data, Phase 1, Operator E, Run 18

Switch Box
Camera Control Axis
Acceleration Control Mode
Camera Control - None
Rate Bias - No

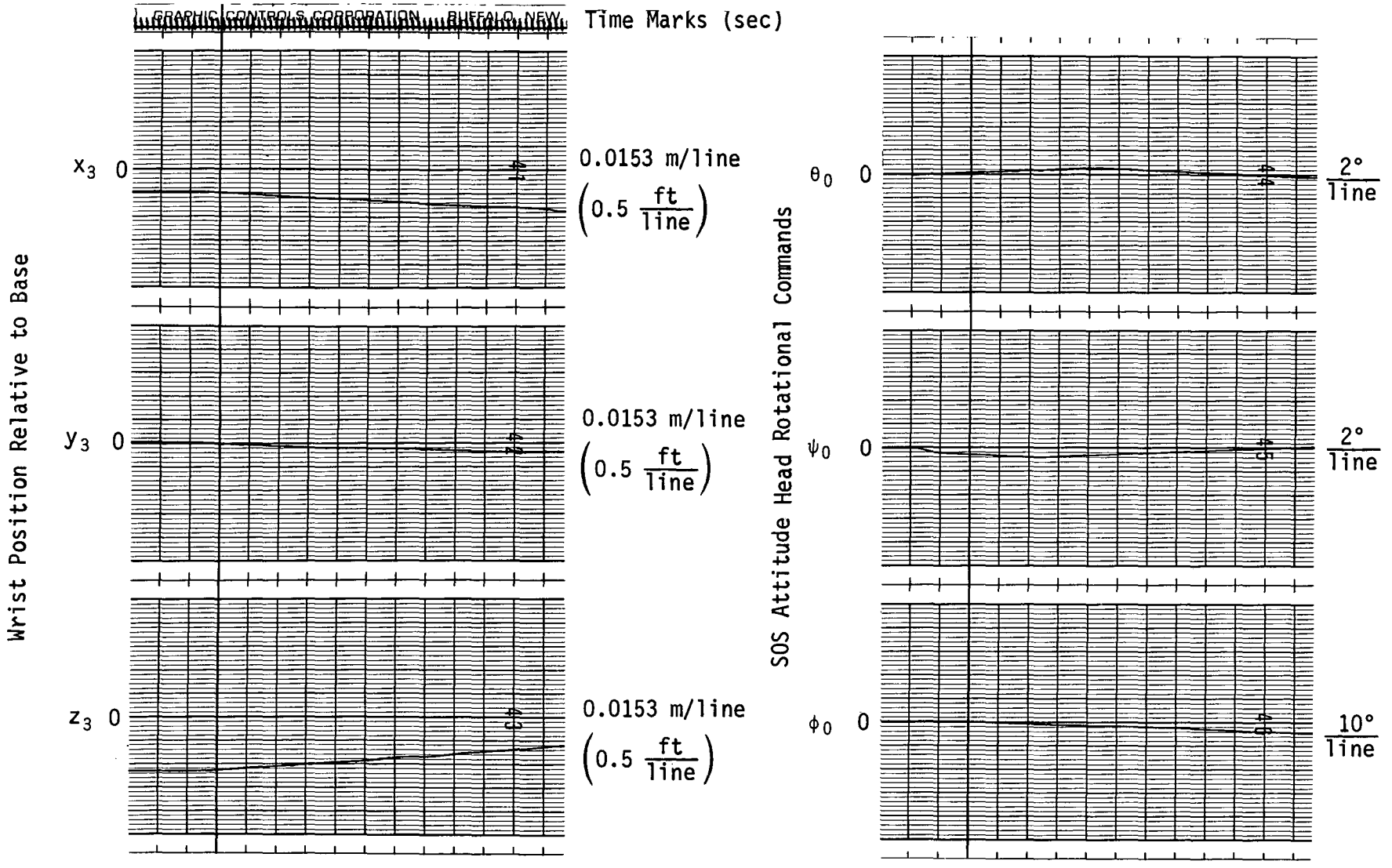

Fig. A-4 (cont)

Switch Box
Camera Control Axis
Acceleration Control Mode
Camera Control - None
Rate Bias - No

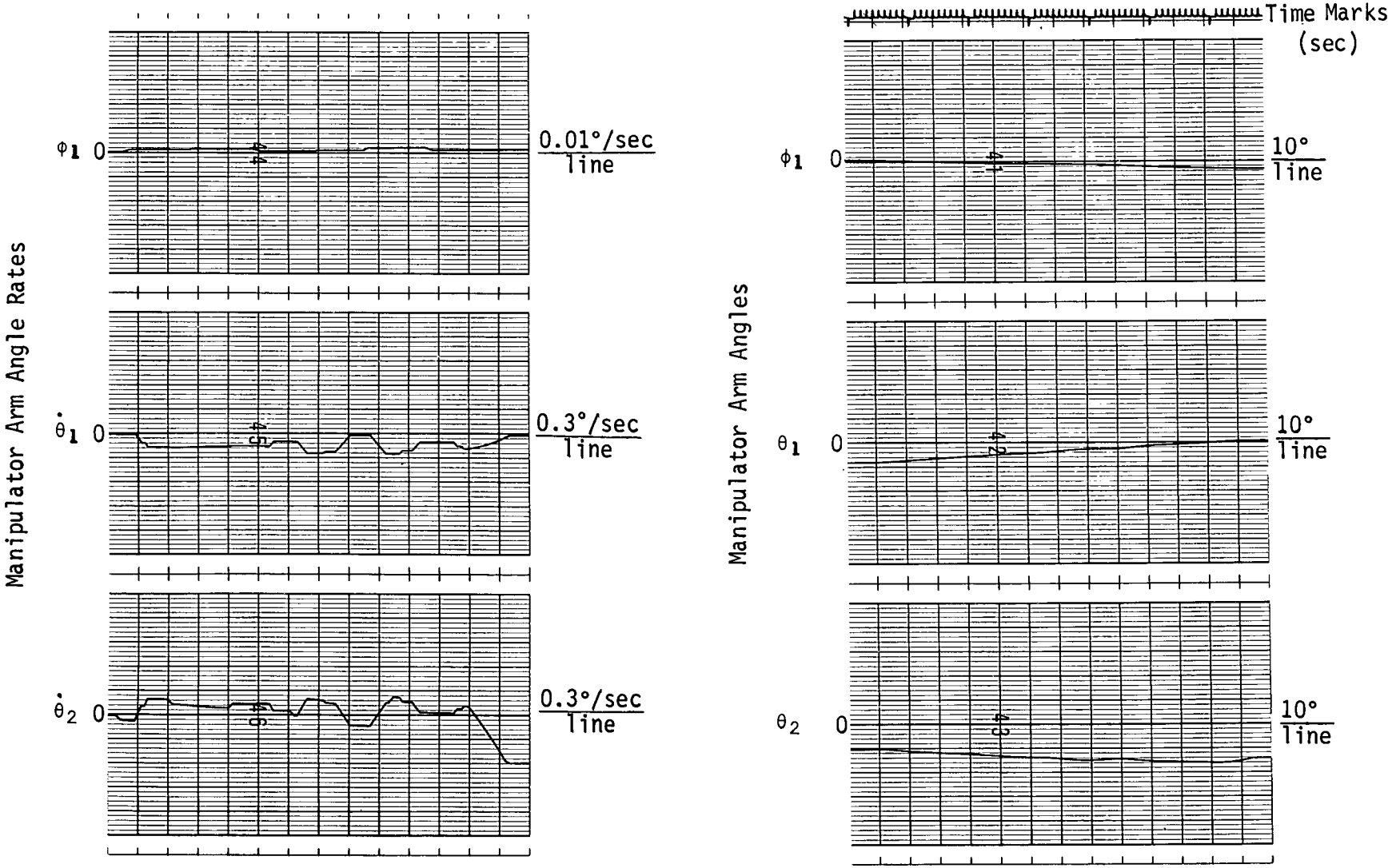

Fig. A-4 (concl)

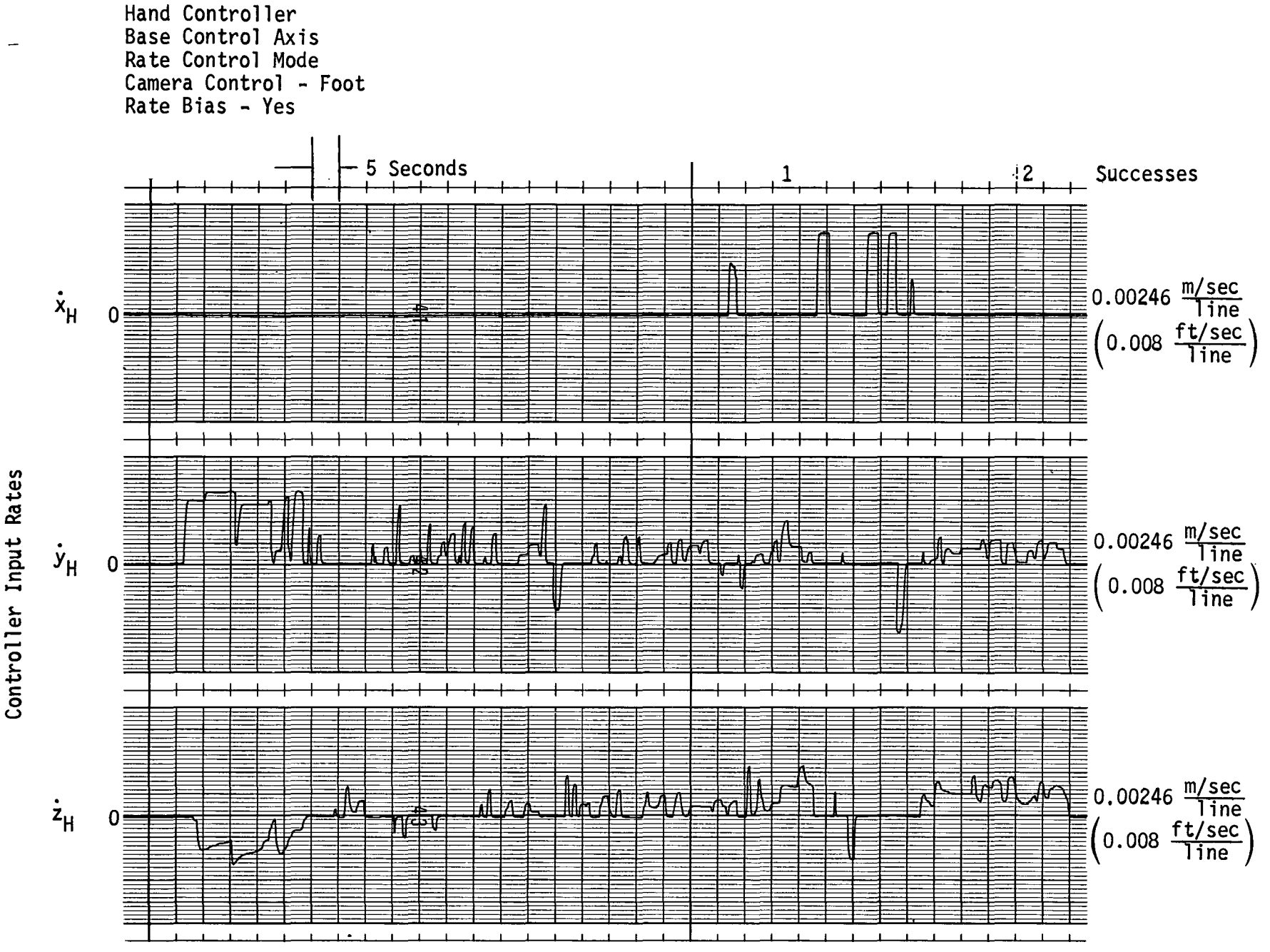

Fig. A-5 Strip Chart Recorded Data, Phase 2, Operator E, Run 1

Hand Controller
Base Control Axis
Rate Control Mode
Camera Control - Foot
Rate Bias - Yes

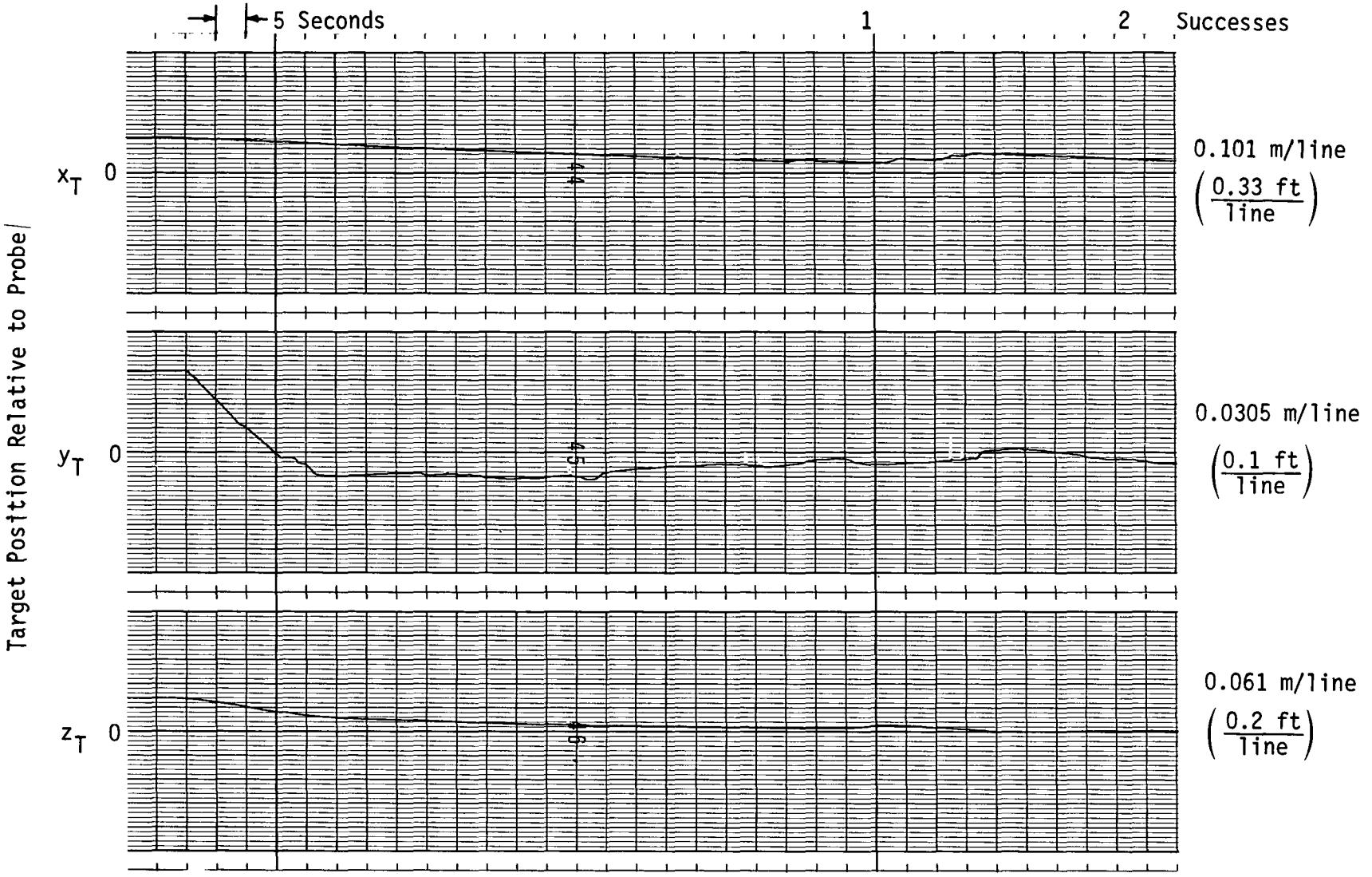

Fig. A-5 (cont)

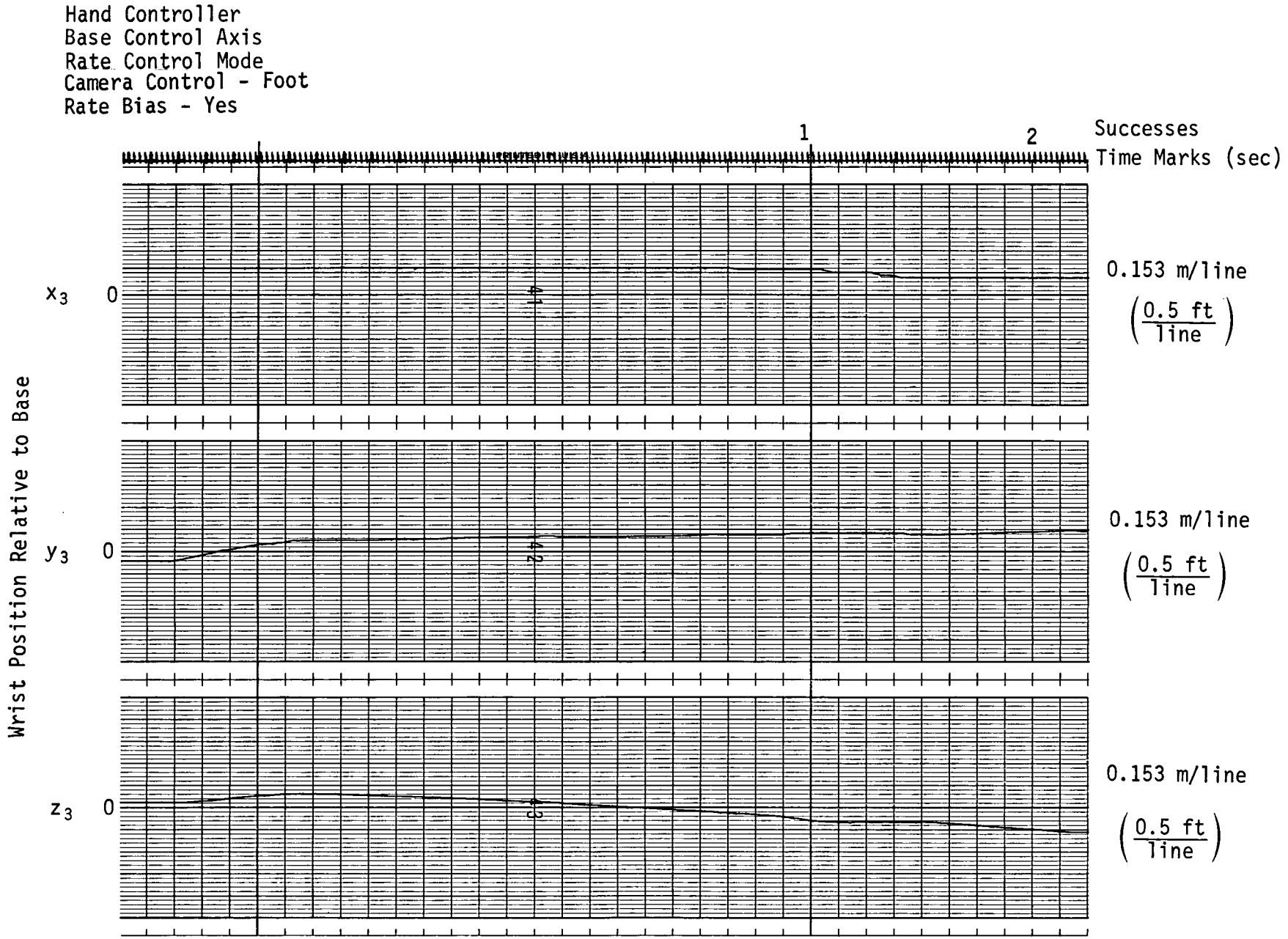
Hand Controller
Base Control Axis
Rate Control Mode
Camera Control - Foot
Rate Bias - Yes
1
2
Successes
Time Marks (sec)
Wrist Position Relative to Base
x_3 0
y_3 0
z_3 0
0.153 m/line
$\left(\frac{0.5 \text{ ft}}{\text{line}}\right)$
0.153 m/line
$\left(\frac{0.5 \text{ ft}}{\text{line}}\right)$
0.153 m/line
$\left(\frac{0.5 \text{ ft}}{\text{line}}\right)$

Fig. A-5 (cont)

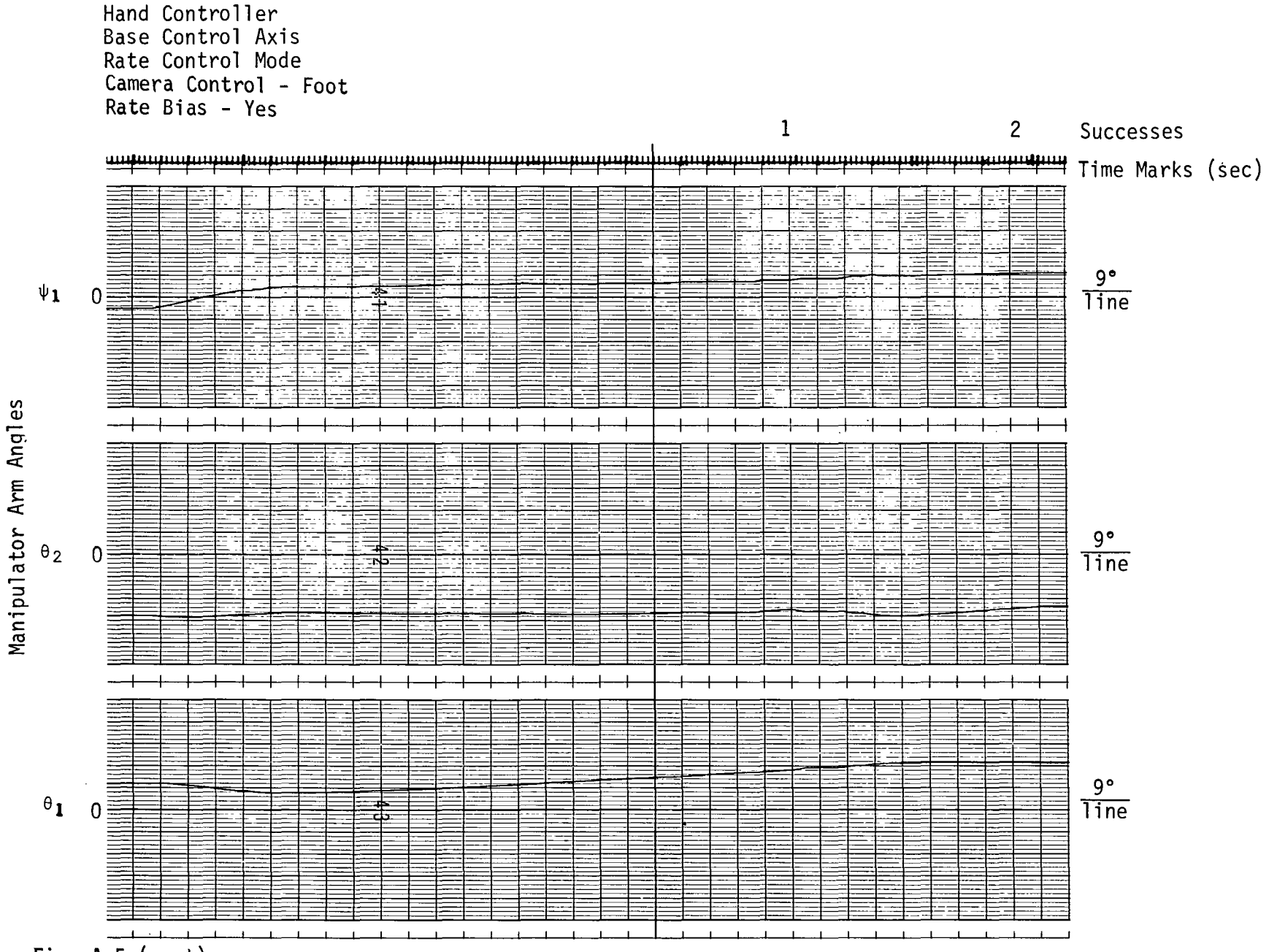
Hand Controller
Base Control Axis
Rate Control Mode
Camera Control - Foot
Rate Bias - Yes
1
2
Successes
Time Marks (sec)
Manipulator Arm Angles
ψ_1 0
θ_2 0
θ_1 0
9° / line
9° / line
9° / line

Fig. A-5 (cont)

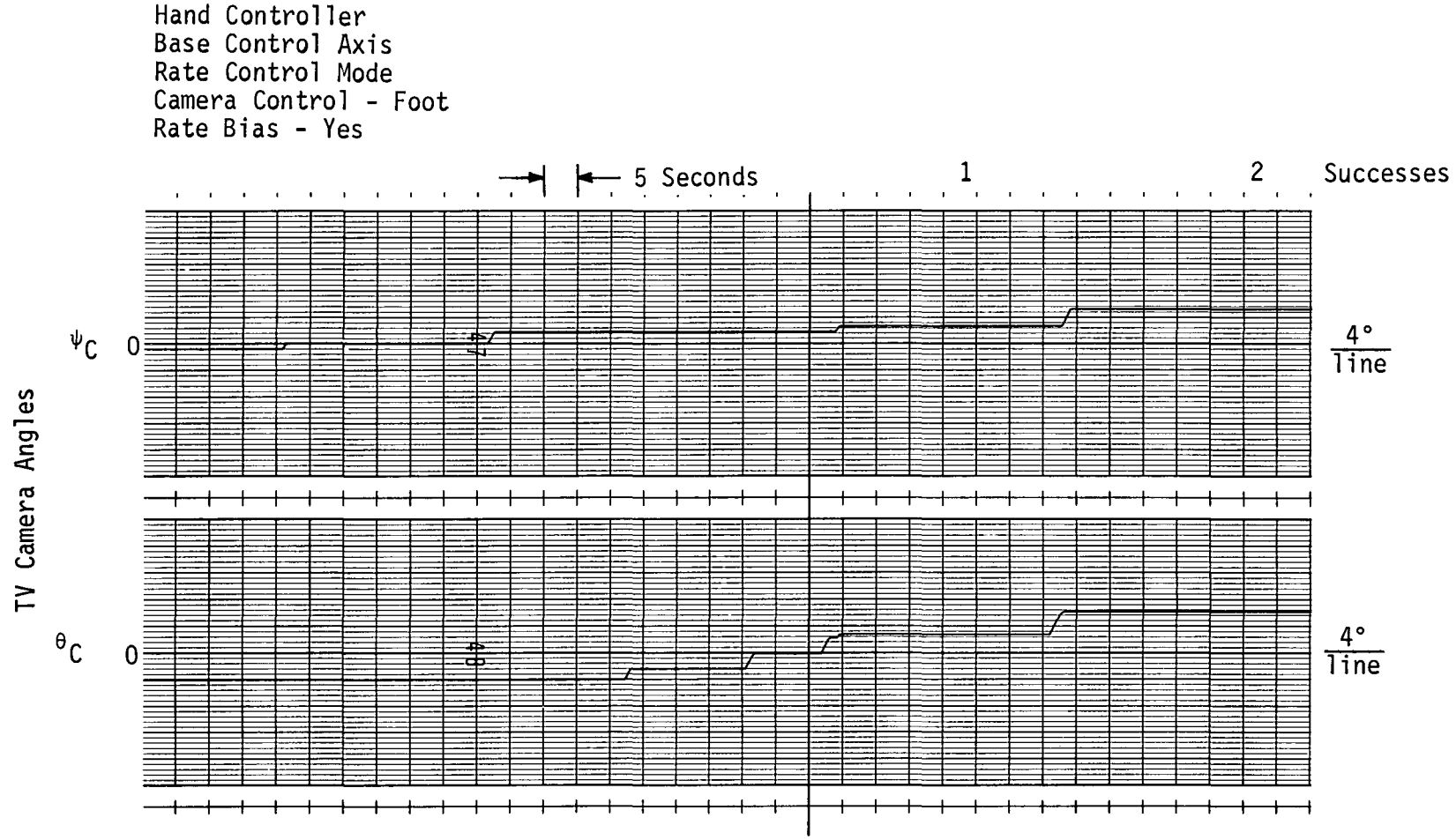
Hand Controller
Base Control Axis
Rate Control Mode
Camera Control - Foot
Rate Bias - Yes
5 Seconds
1
2
Successes
TV Camera Angles
ψ_C 0
θ_C 0
4° / line
4° / line

Fig. A-5 (concl)

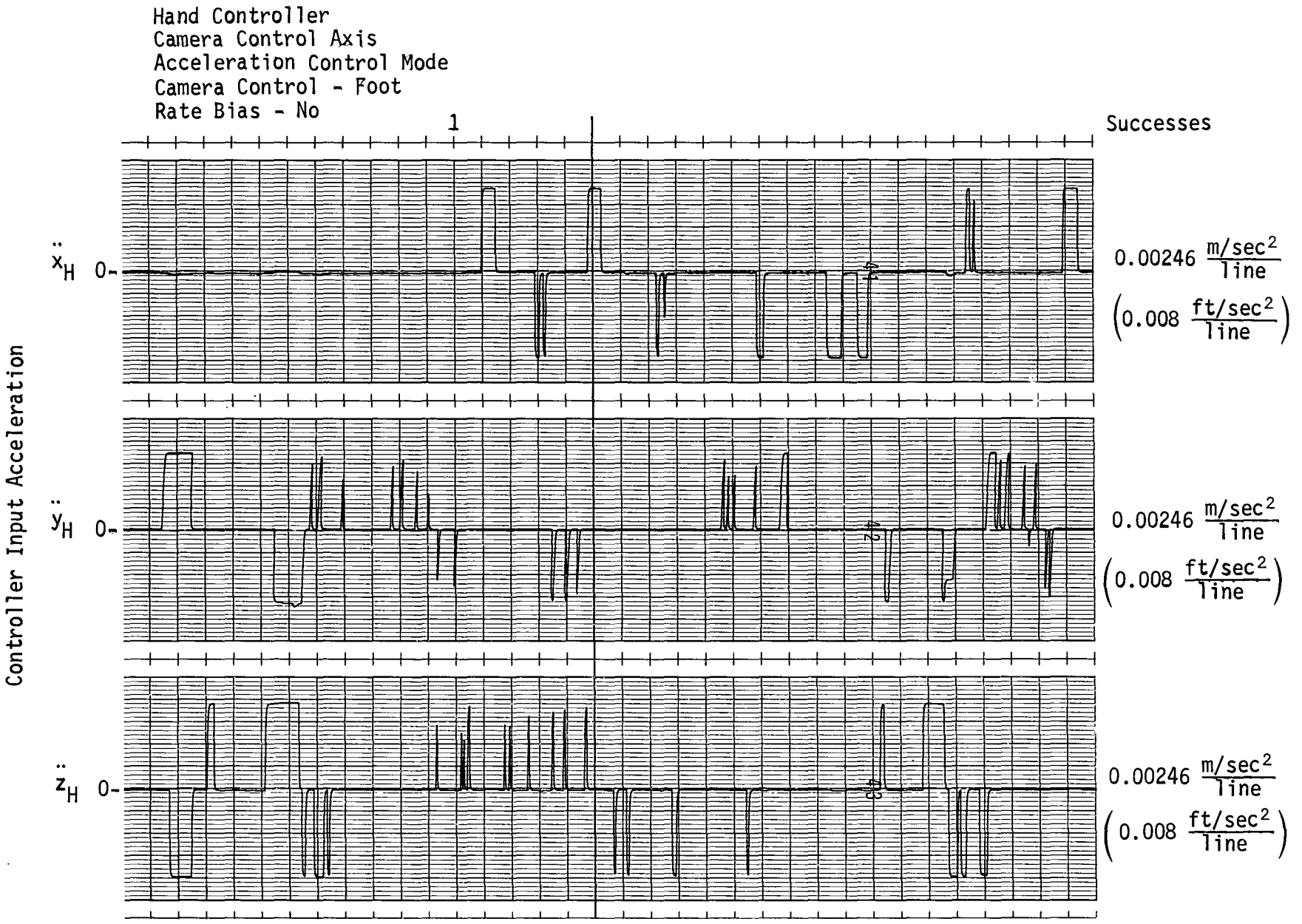

Fig. A-6 Strip Chart Recorded Data, Phase 2, Operator E, Run 6

Hand Controller
Camera Control Axis
Acceleration Control Mode
Camera Control - Foot
Rate Bias - No

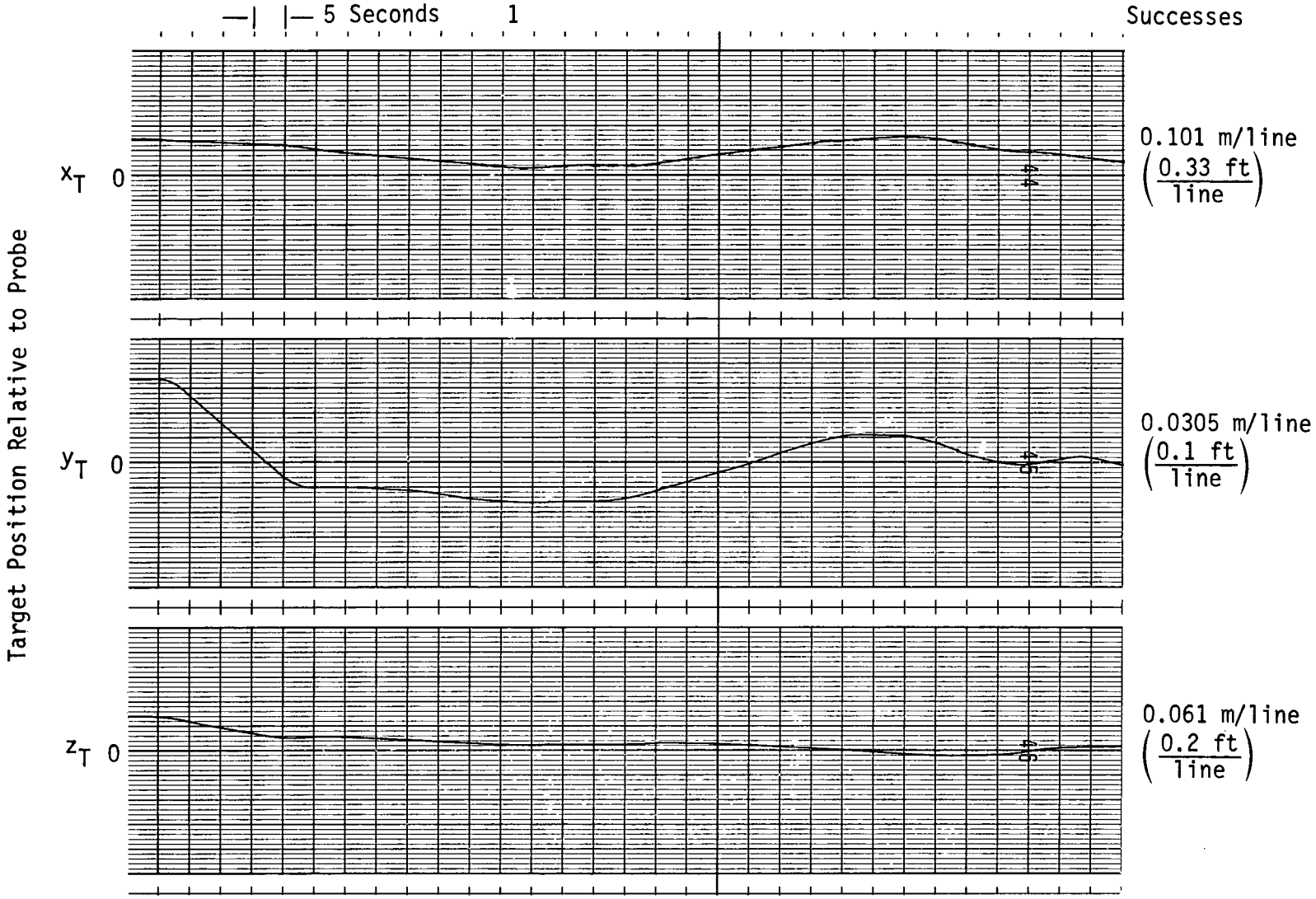

Figure A-6 (cont)

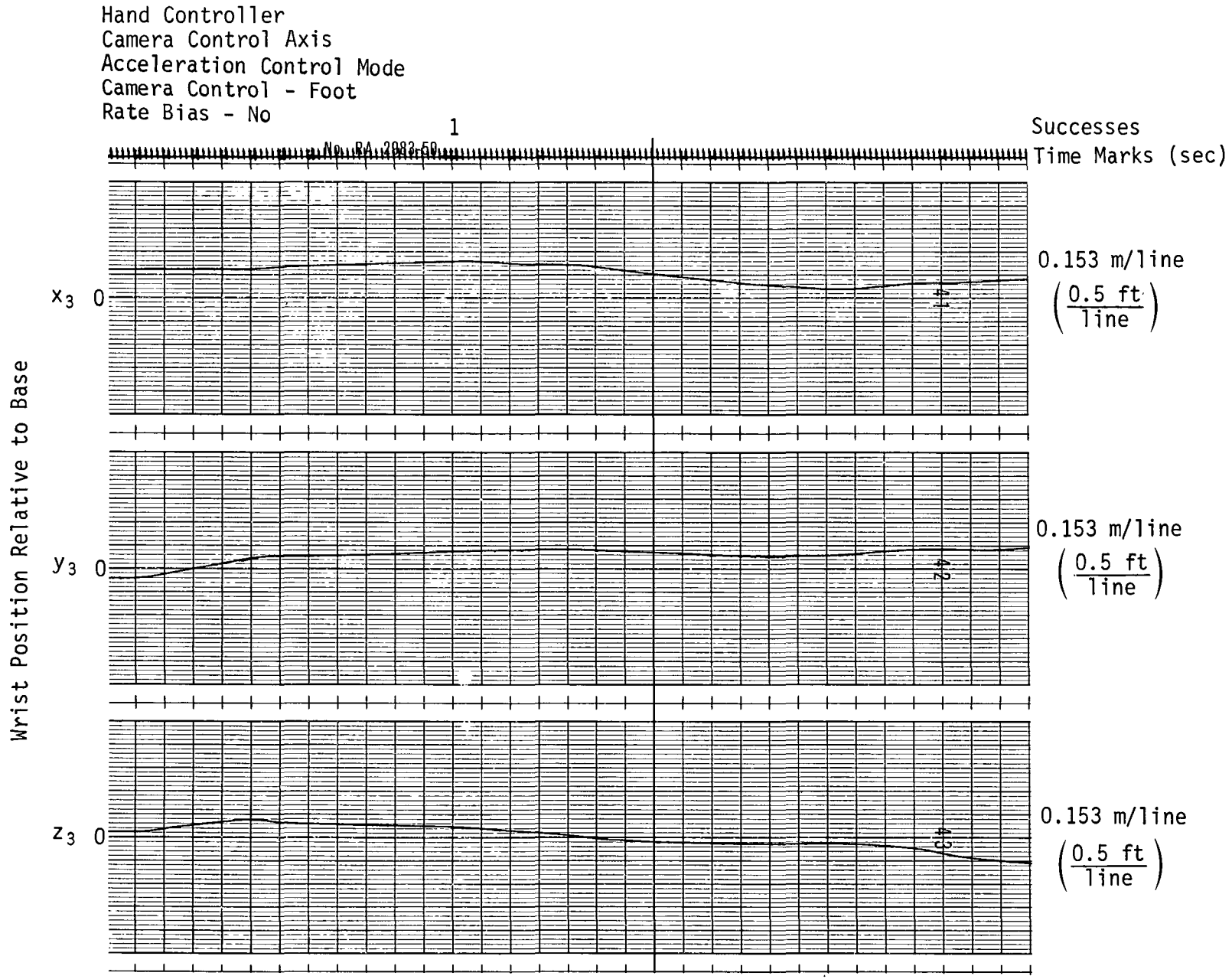
Hand Controller
Camera Control Axis
Acceleration Control Mode
Camera Control - Foot
Rate Bias - No
1
Successes
Time Marks (sec)
No. RA 2083-59
Wrist Position Relative to Base
x_3 0
y_3 0
z_3 0
0.153 m/line
$\left(\frac{0.5\ ft}{line}\right)$
0.153 m/line
$\left(\frac{0.5\ ft}{line}\right)$
0.153 m/line
$\left(\frac{0.5\ ft}{line}\right)$

Fig. A-6 (cont)

Hand Controller
Camera Control Axis
Acceleration Control Mode
Camera Control - Foot
Rate Bias - No

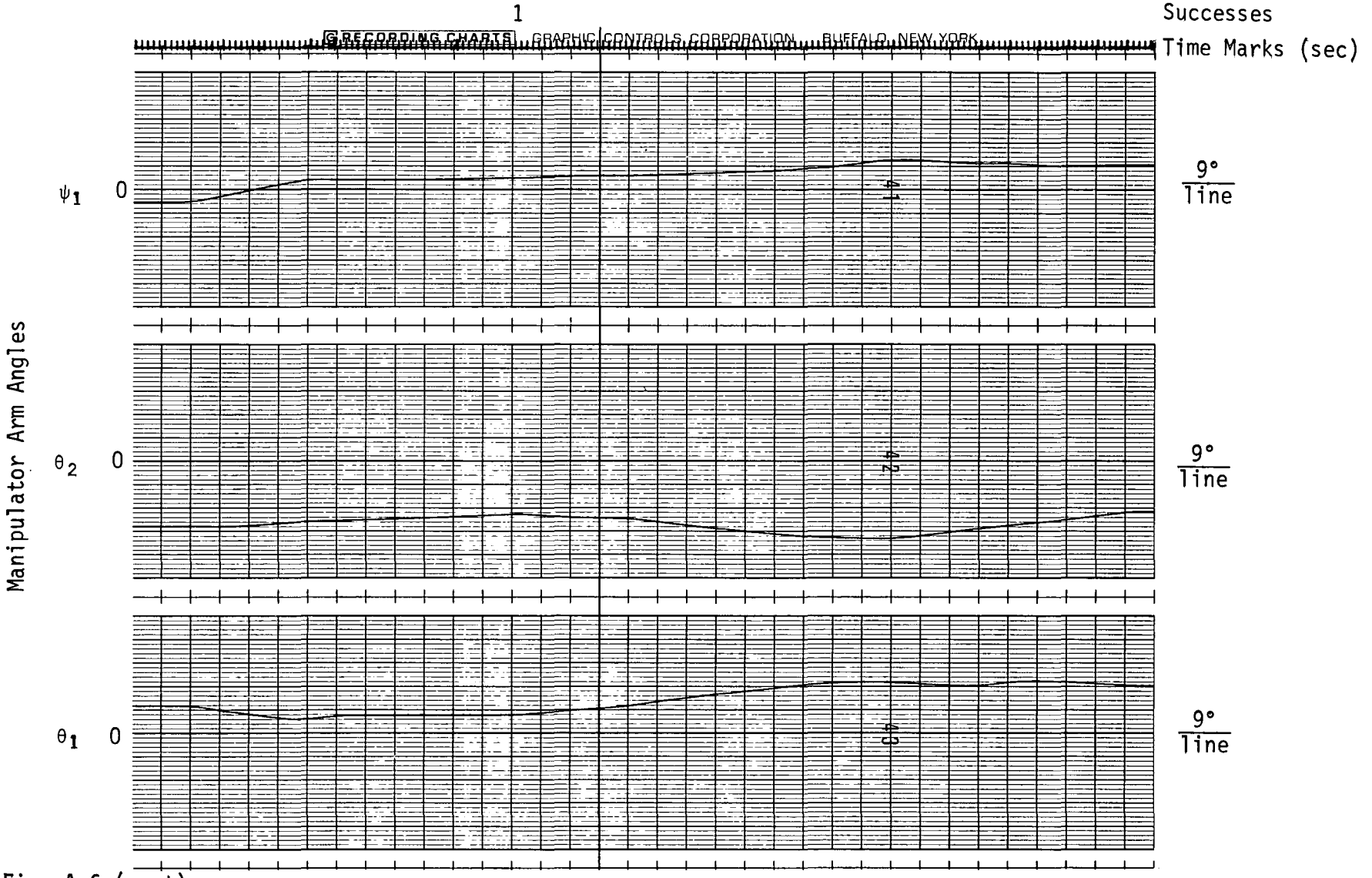

Fig. A-6 (cont)

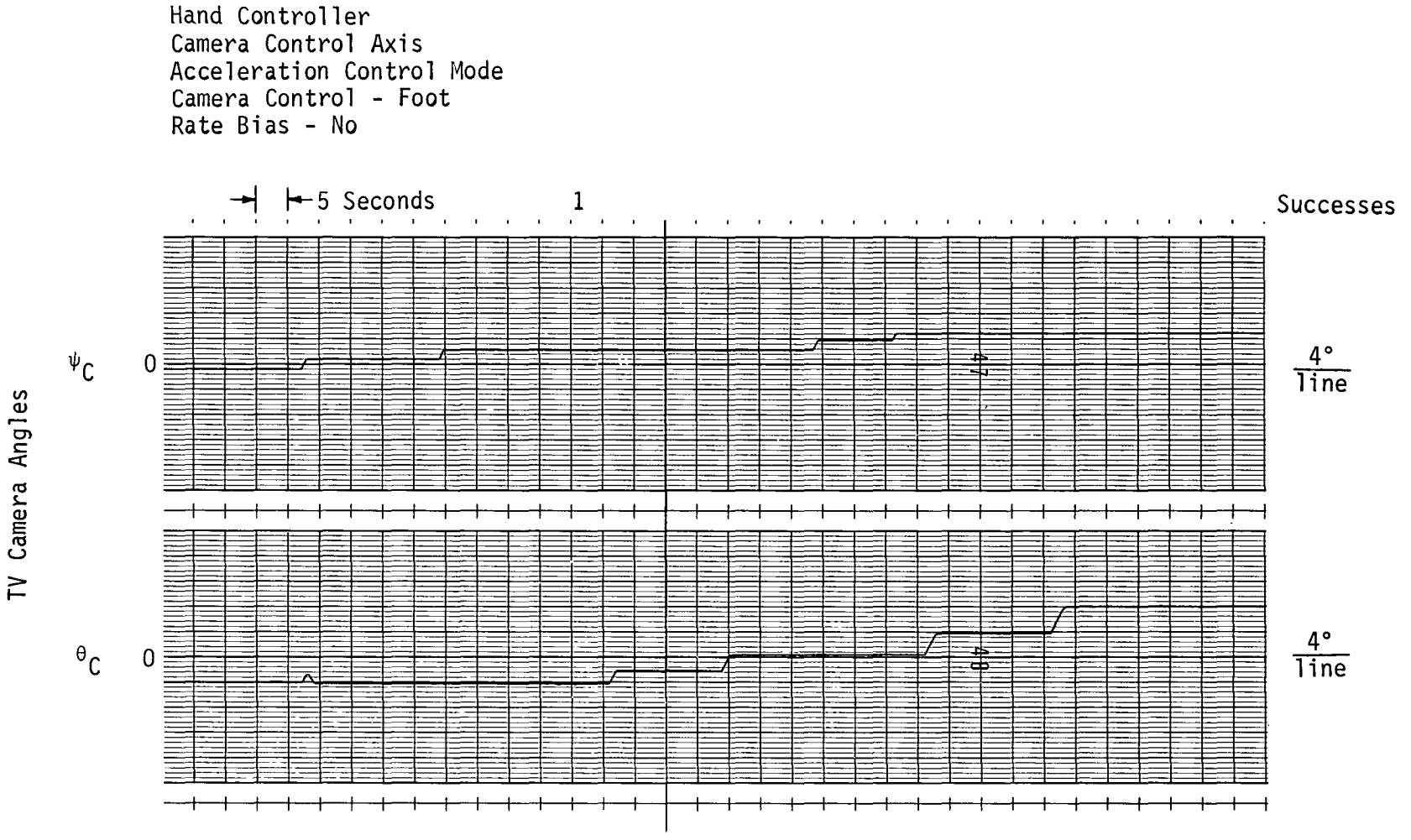
Hand Controller
Camera Control Axis
Acceleration Control Mode
Camera Control - Foot
Rate Bias - No
5 Seconds
1
Successes
TV Camera Angles
ψ_C
0
θ_C
0
4°
line
4°
line

Fig. A-6 (concl)

Switch Box
Camera Control Axis
Rate Control Mode
Camera Control - Foot
Rate Bias - No

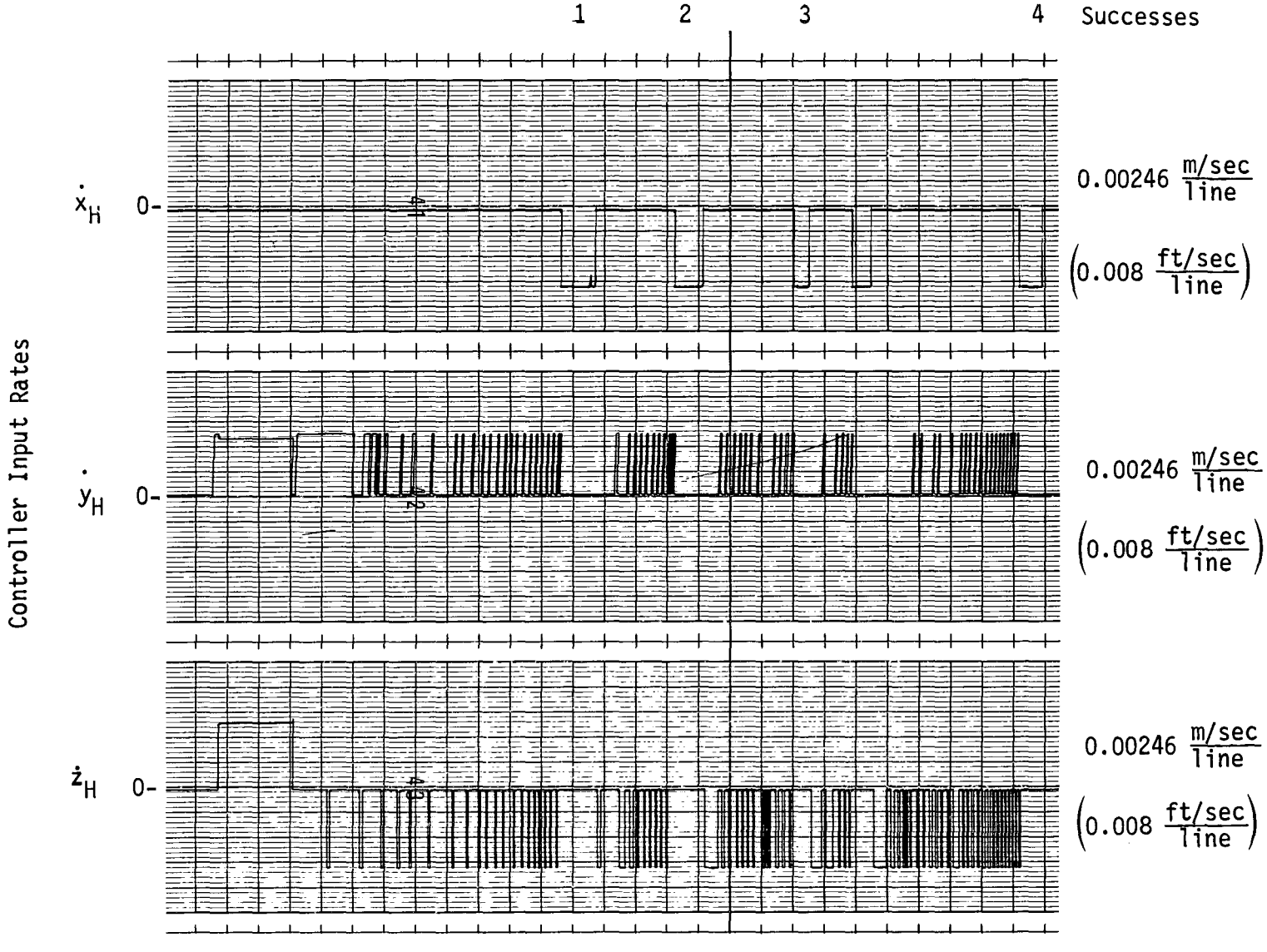

Fig. A-7 Strip Chart Recorded Data, Phase 2, Operator E, Run 7

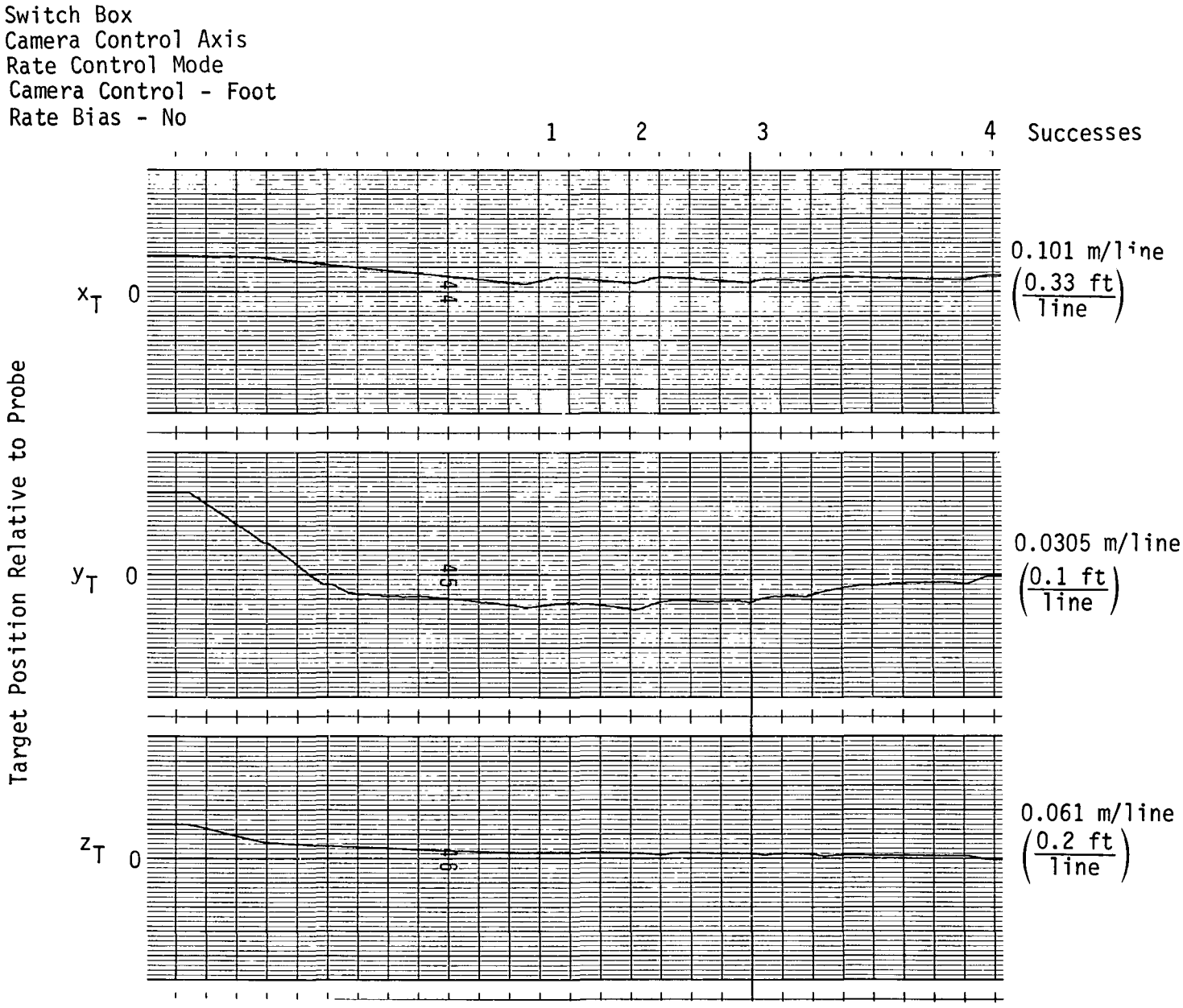

Figure A-7 (cont)

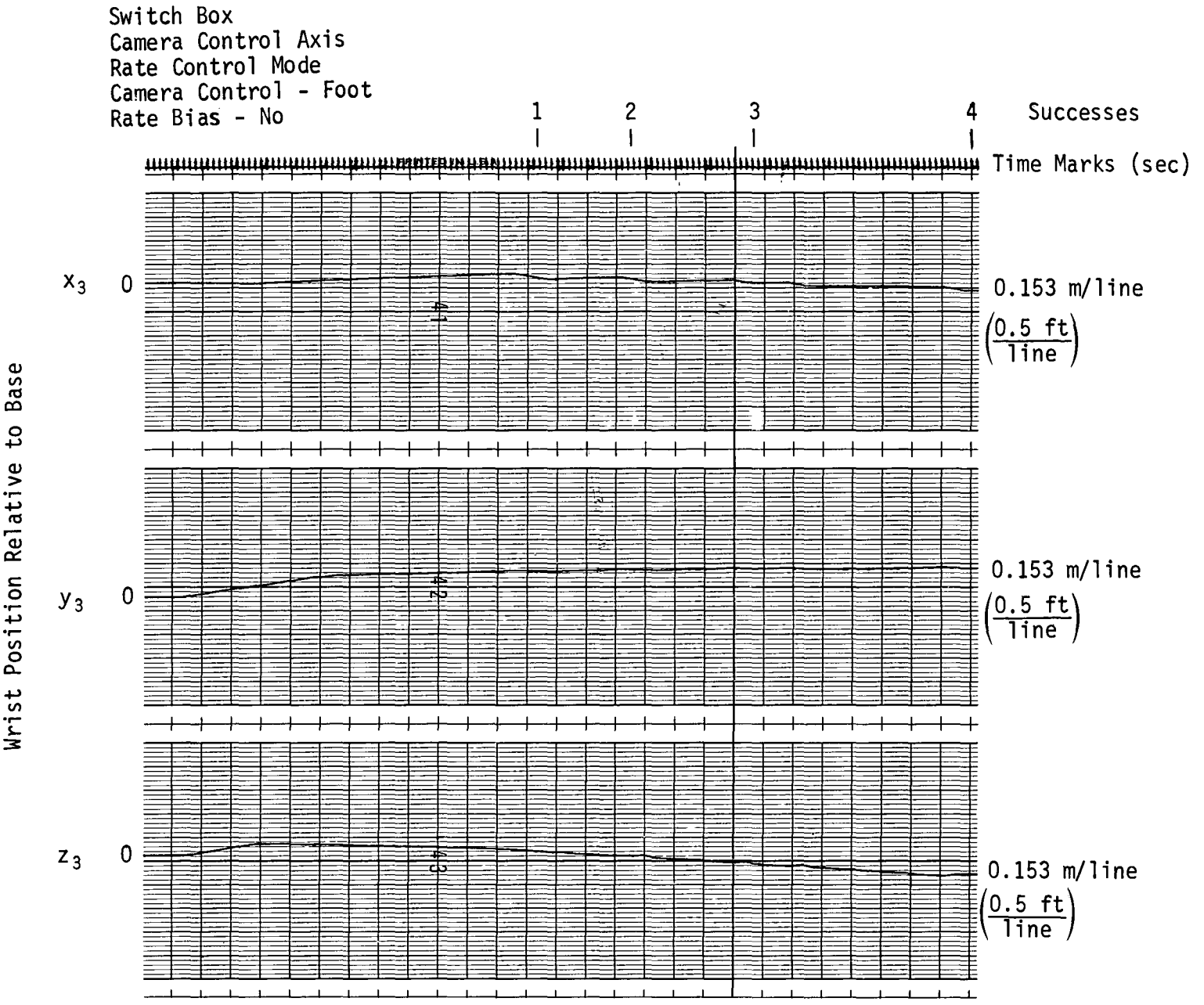
Switch Box
Camera Control Axis
Rate Control Mode
Camera Control - Foot
Rate Bias - No
1
2
3
4
Successes
Time Marks (sec)
x_3
0
0.153 m/line
(0.5 ft/line)
y_3
0
0.153 m/line
(0.5 ft/line)
z_3
0
0.153 m/line
(0.5 ft/line)
Wrist Position Relative to Base

Fig. A-7 (cont)

Switch Box
Camera Control Axis
Rate Control Mode
Camera Control - Foot
Rate Bias - No

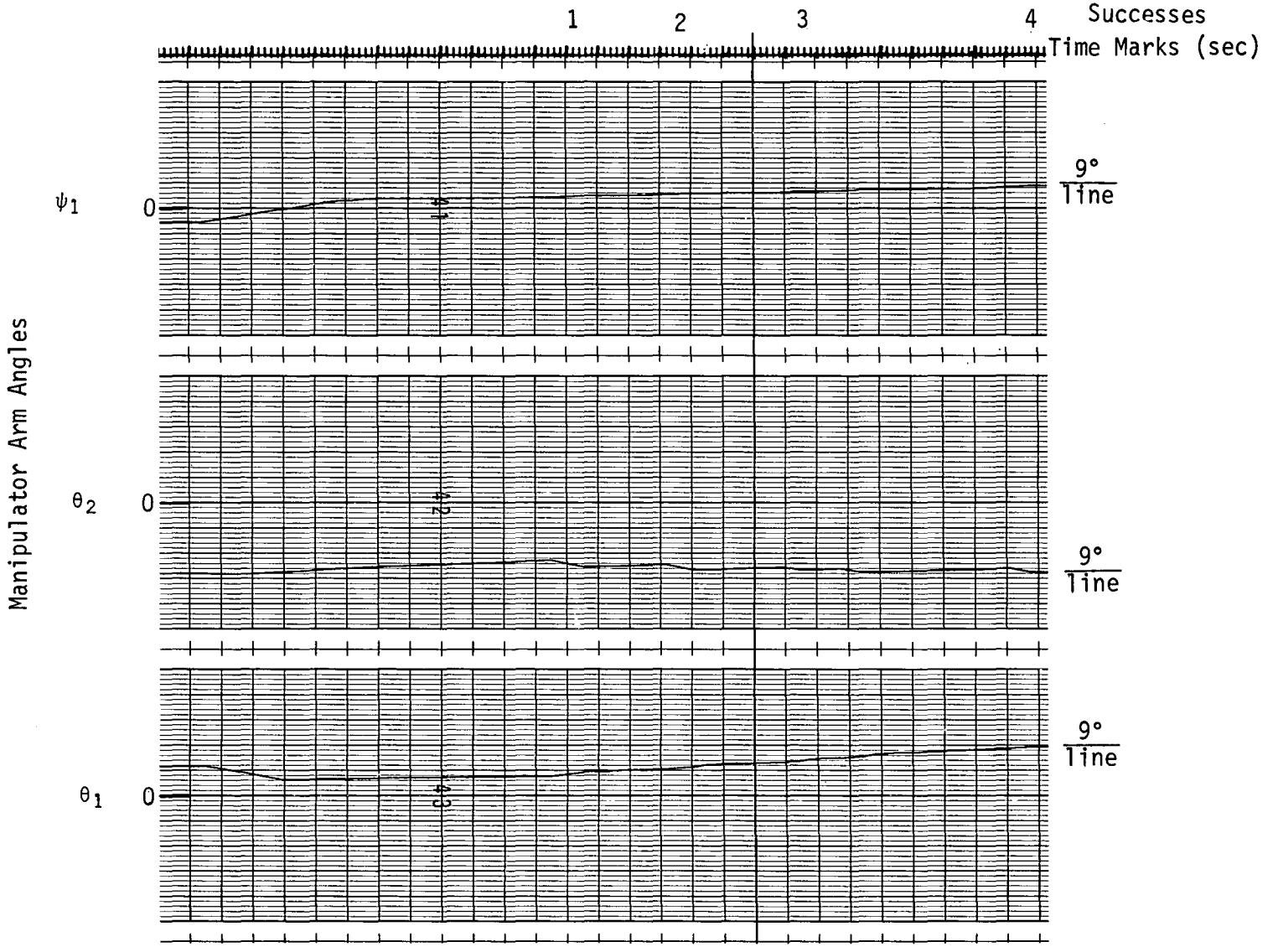

Fig. A-/ (cont)

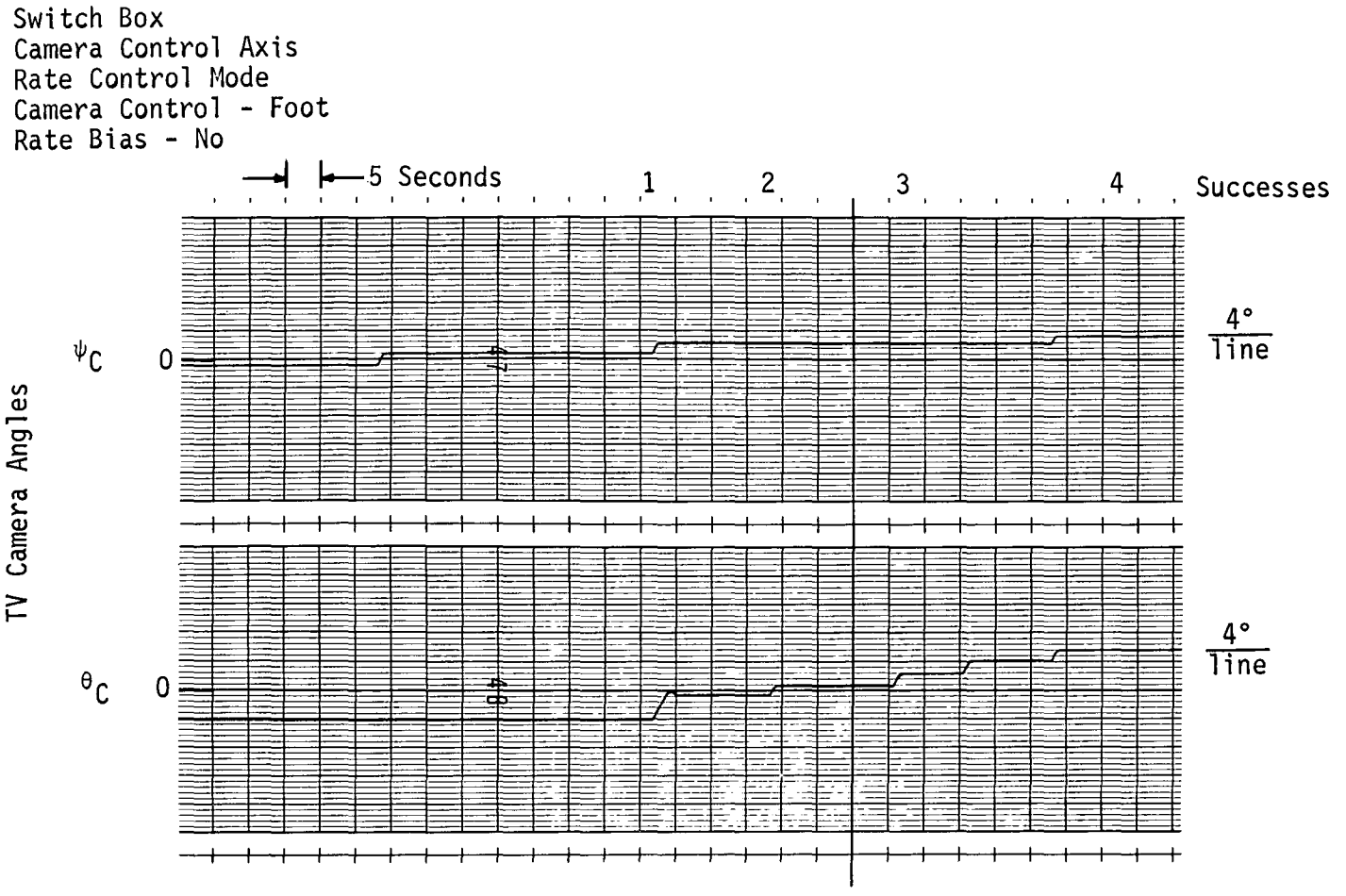
Switch Box
Camera Control Axis
Rate Control Mode
Camera Control - Foot
Rate Bias - No
5 Seconds
1
2
3
4
Successes
TV Camera Angles
ψ_C
0
θ_C
0
4° / line
4° / line

Fig. A-7 (concl)

Switch Box
Camera Control Axis
Acceleration Control Mode
Camera Control - Foot
Rate Bias - No

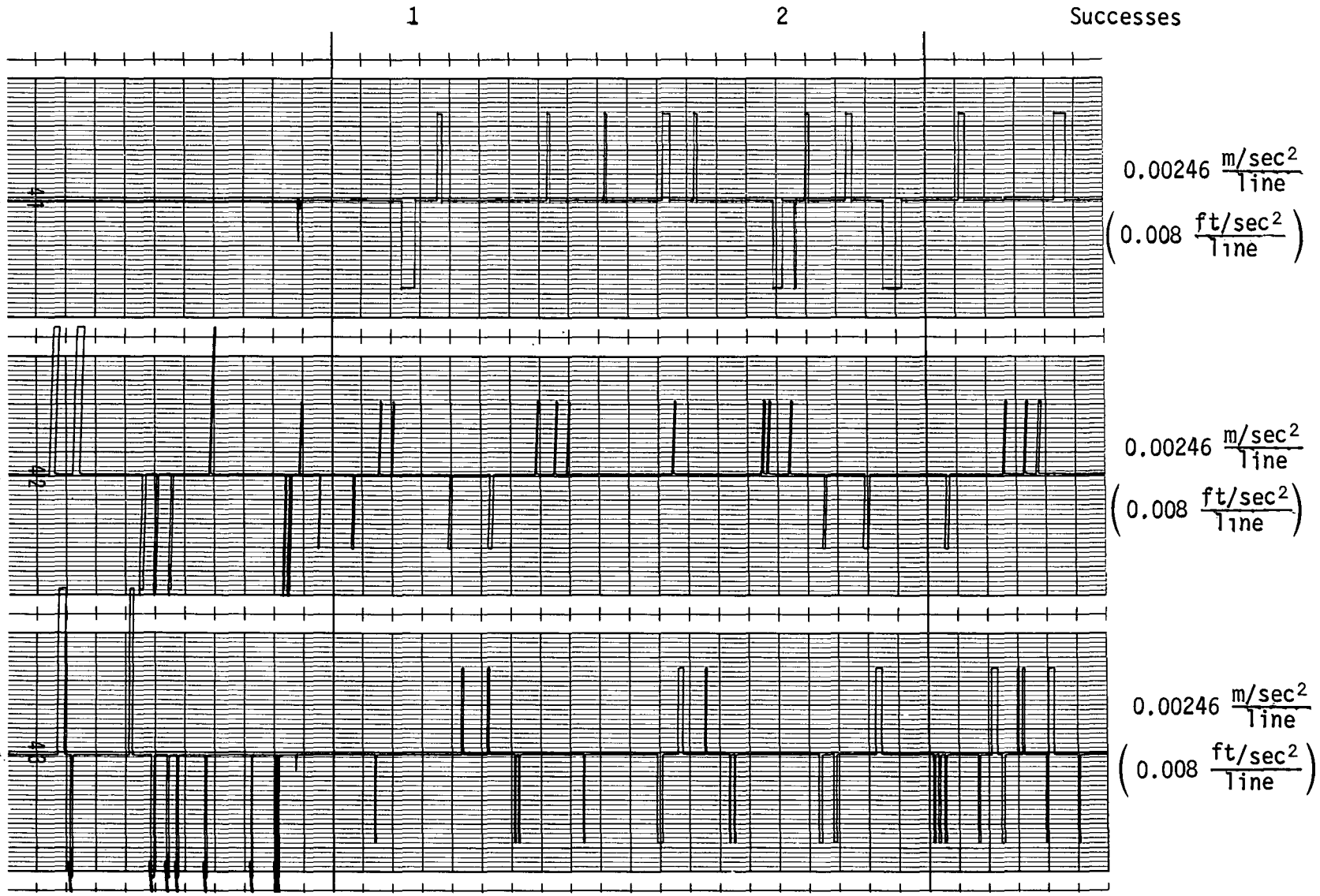

Fig. A-8 Strip Chart Recorded Data, Phase 2, Operator E, Run 8

Switch Box
Camera Control Axis
Acceleration Control Mode
Camera Control - Foot
Rate Bias - No

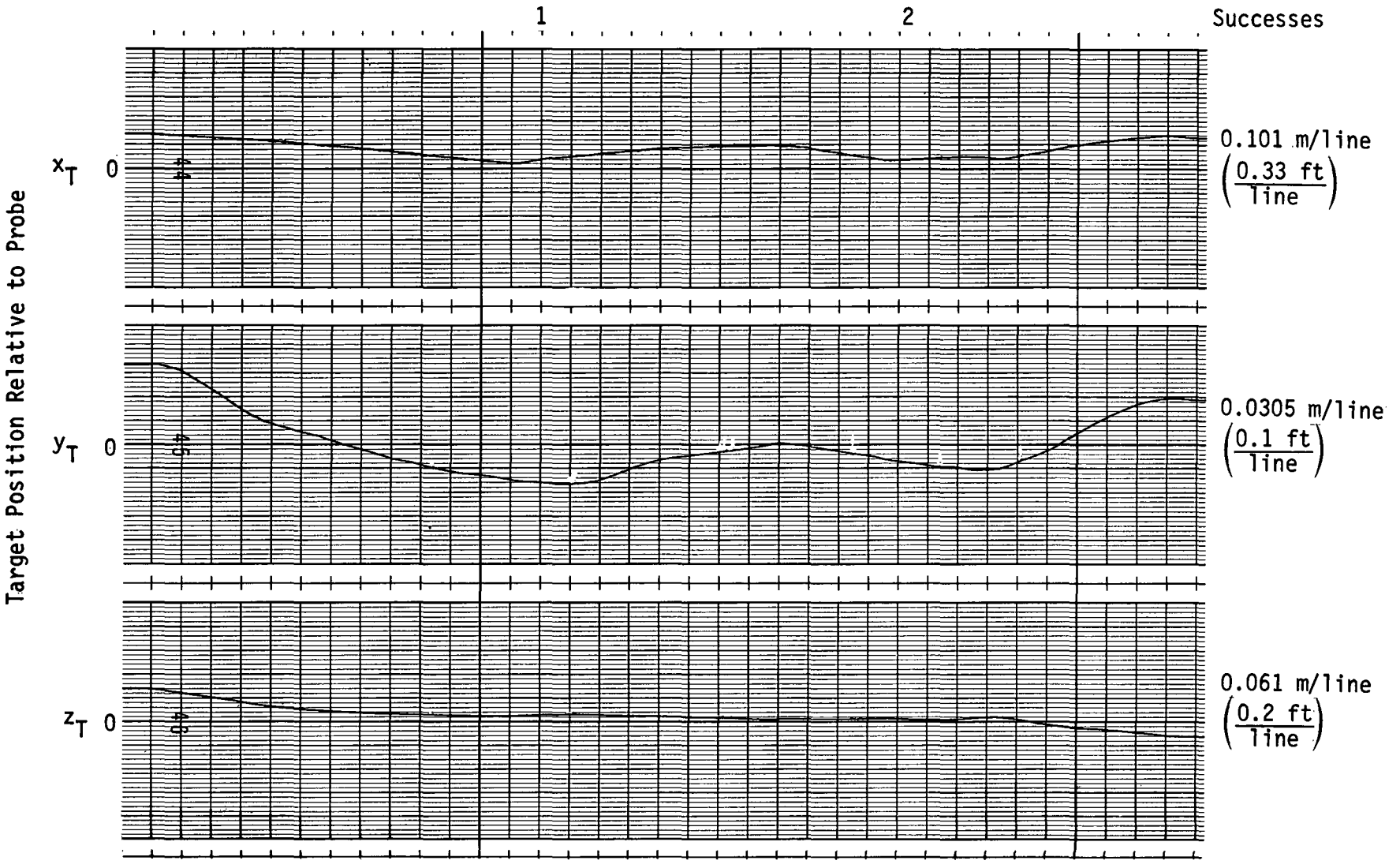

Figure A-8 (cont)

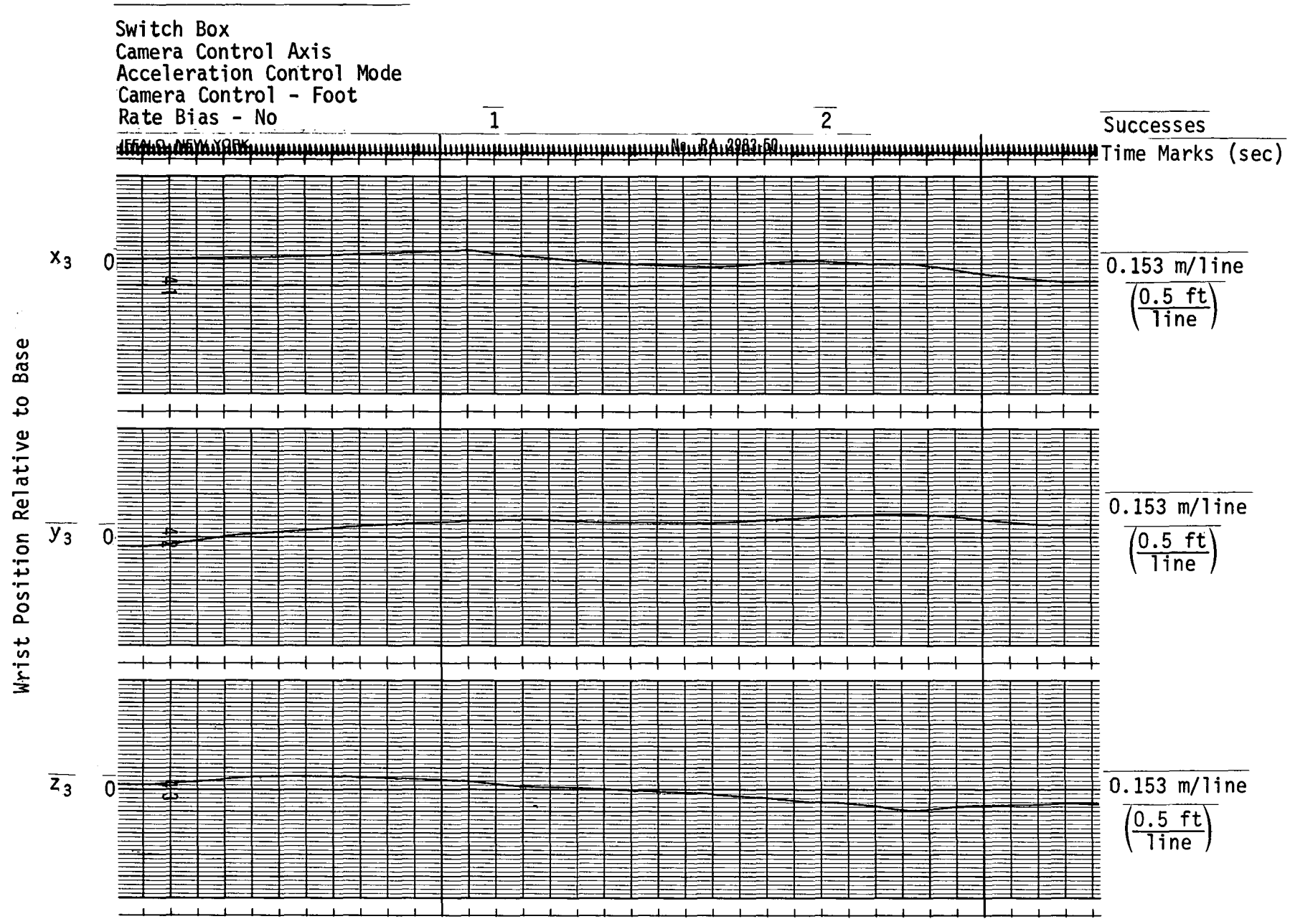
Switch Box
Camera Control Axis
Acceleration Control Mode
Camera Control - Foot
Rate Bias - No
1
2
Successes
Time Marks (sec)
Wrist Position Relative to Base
x_3
0
0.153 m/line
(0.5 ft / line)
y_3
0
0.153 m/line
(0.5 ft / line)
z_3
0
0.153 m/line
(0.5 ft / line)

Fig. A-8 (cont)

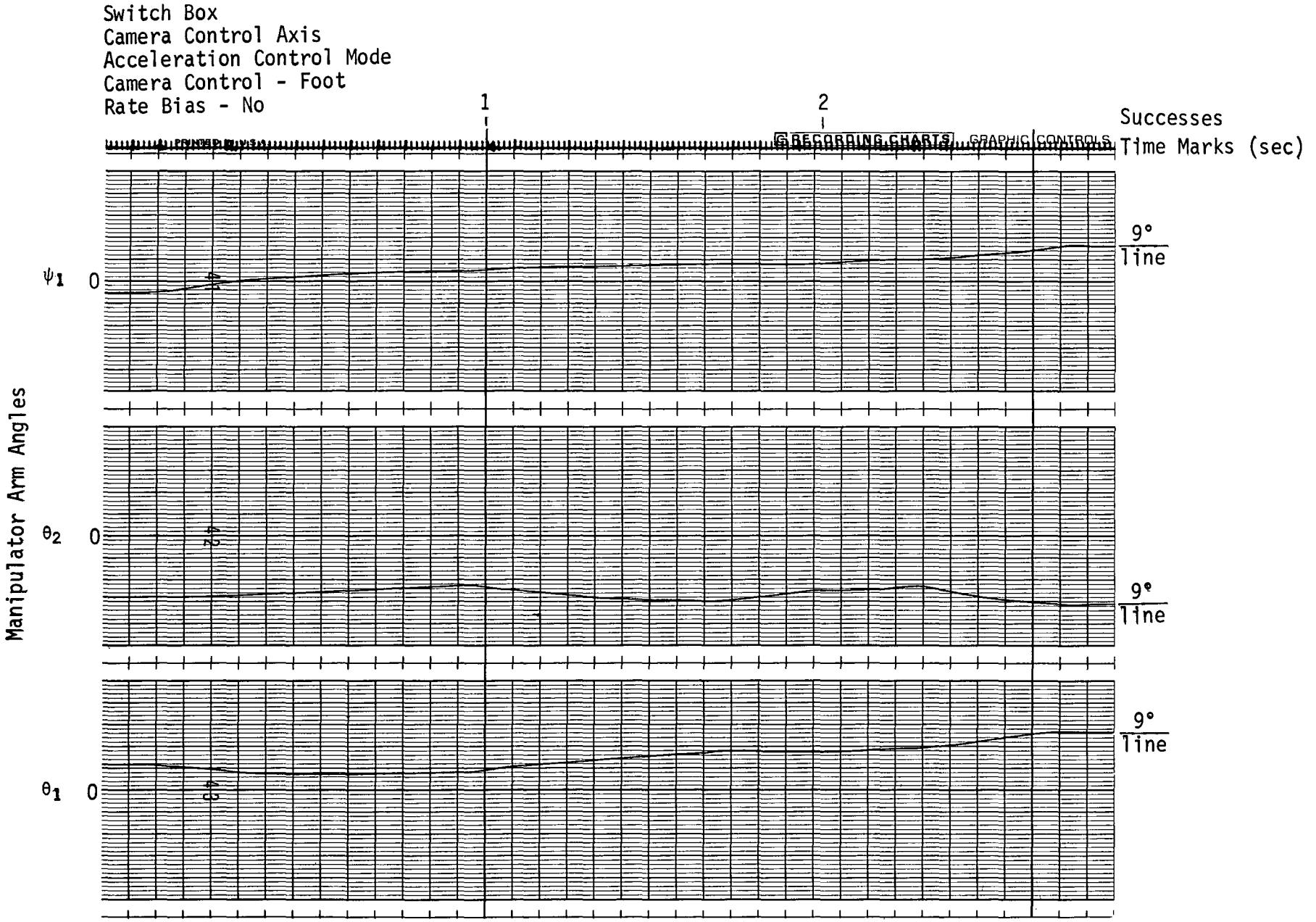
Switch Box
Camera Control Axis
Acceleration Control Mode
Camera Control - Foot
Rate Bias - No
1
2
Successes
Time Marks (sec)
RECORDING CHARTS
GRAPHIC CONTROLS
Manipulator Arm Angles
ψ_1 0
θ_2 0
θ_1 0
9° / line
9° / line
9° / line

Fig. A-8 (cont)

Switch Box
Camera Control Axis
Acceleration Control Mode
Camera Control - Foot
Rate Bias - No

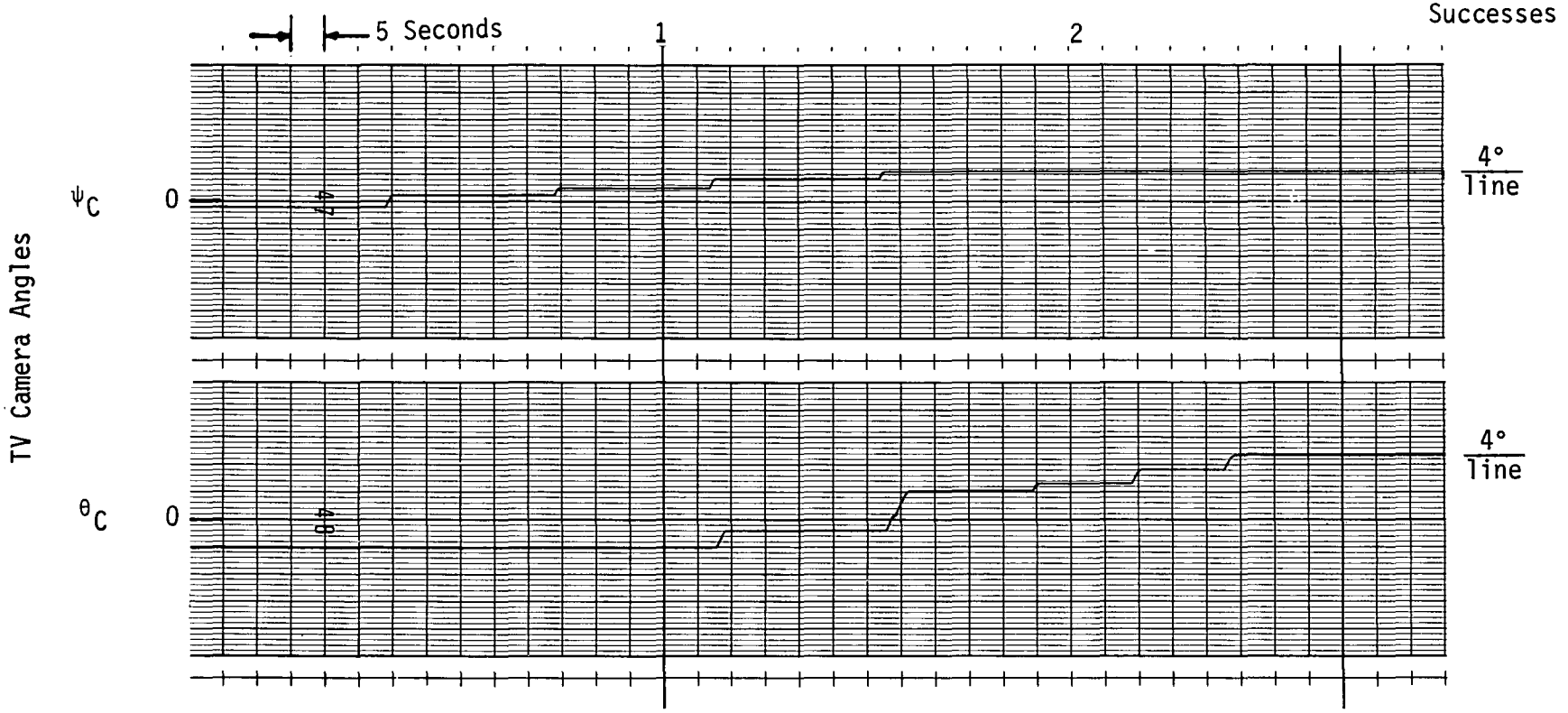

Fig. A-8 (concl)

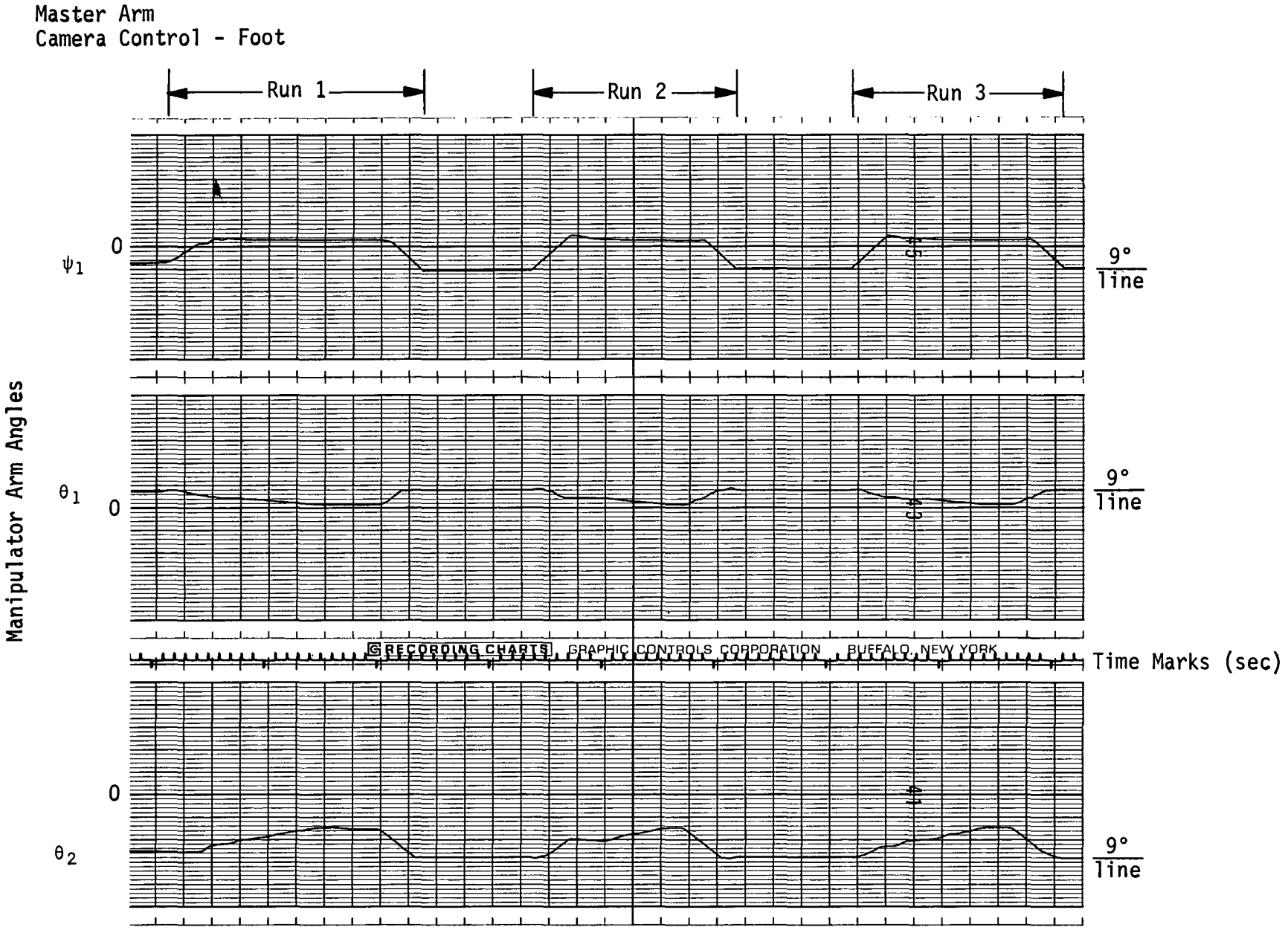

Fig. A-9 Strip Chart Recorded Data, Phase 2, Master Arm, Sample A

Master Arm
Camera Control - Foot

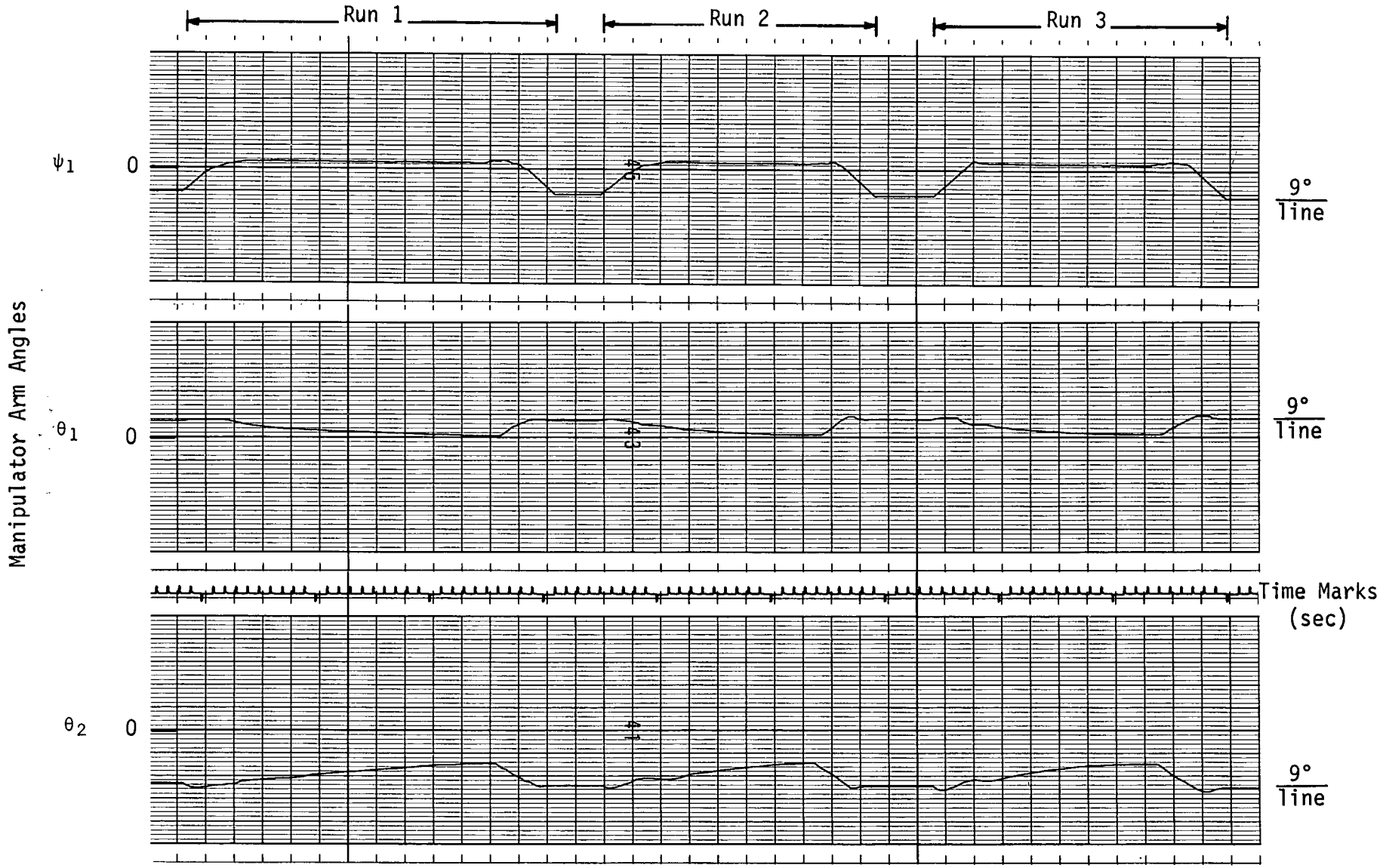

Fig. A-10 Strip Chart Recorded Data, Phase 2, Master Arm, Sample B

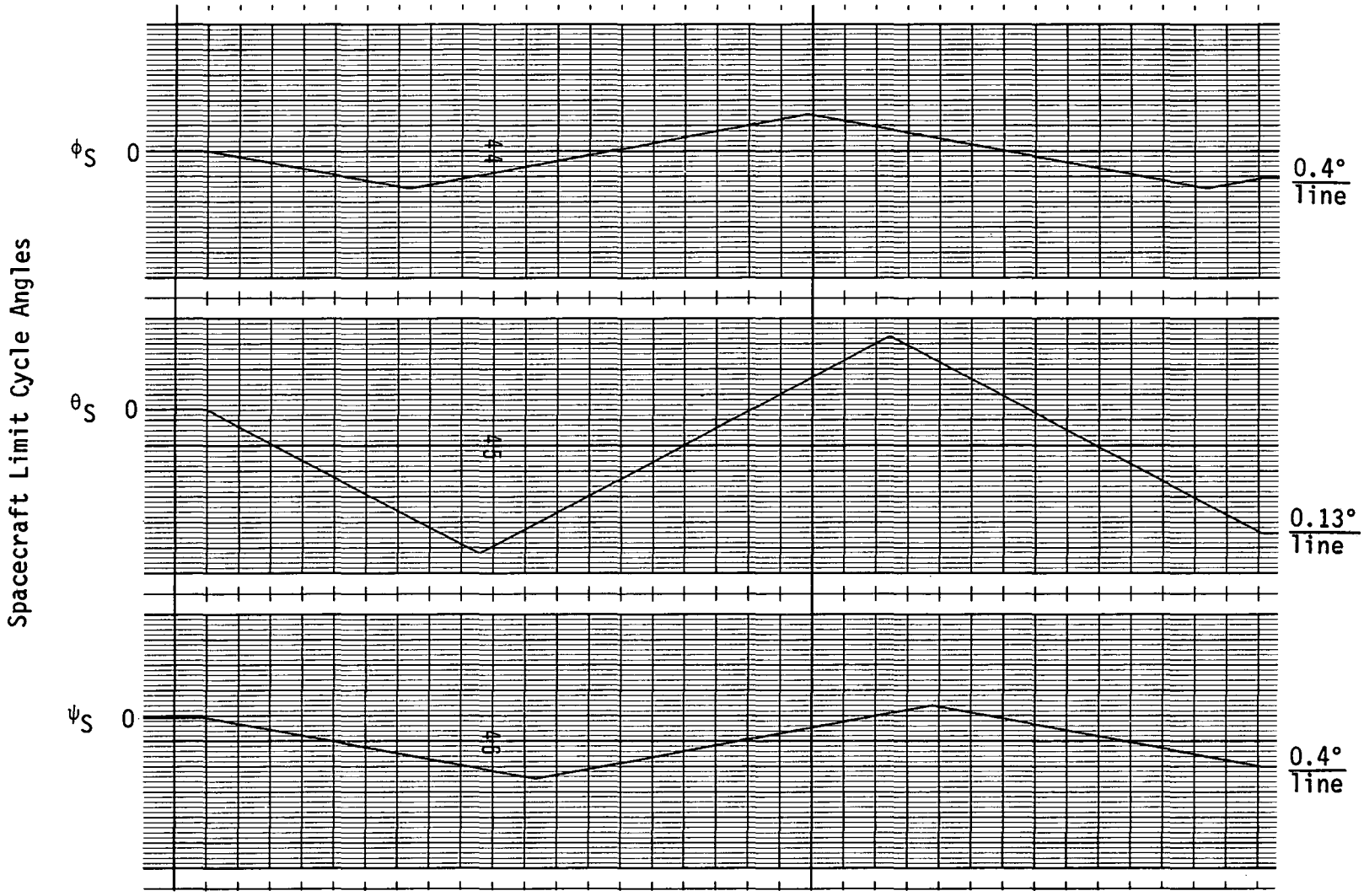

Fig. A-11 Strip Chart Recorded Data, Phase 2, All Runs

APPENDIX B

MECHANICAL JOINT DESIGN

This appendix presents photo-reductions of the drawings of each of the joints that were designed.

Page intentionally left blank

FOLDOUT FRAME 1

FOLDOUT FRAME 2

B-3

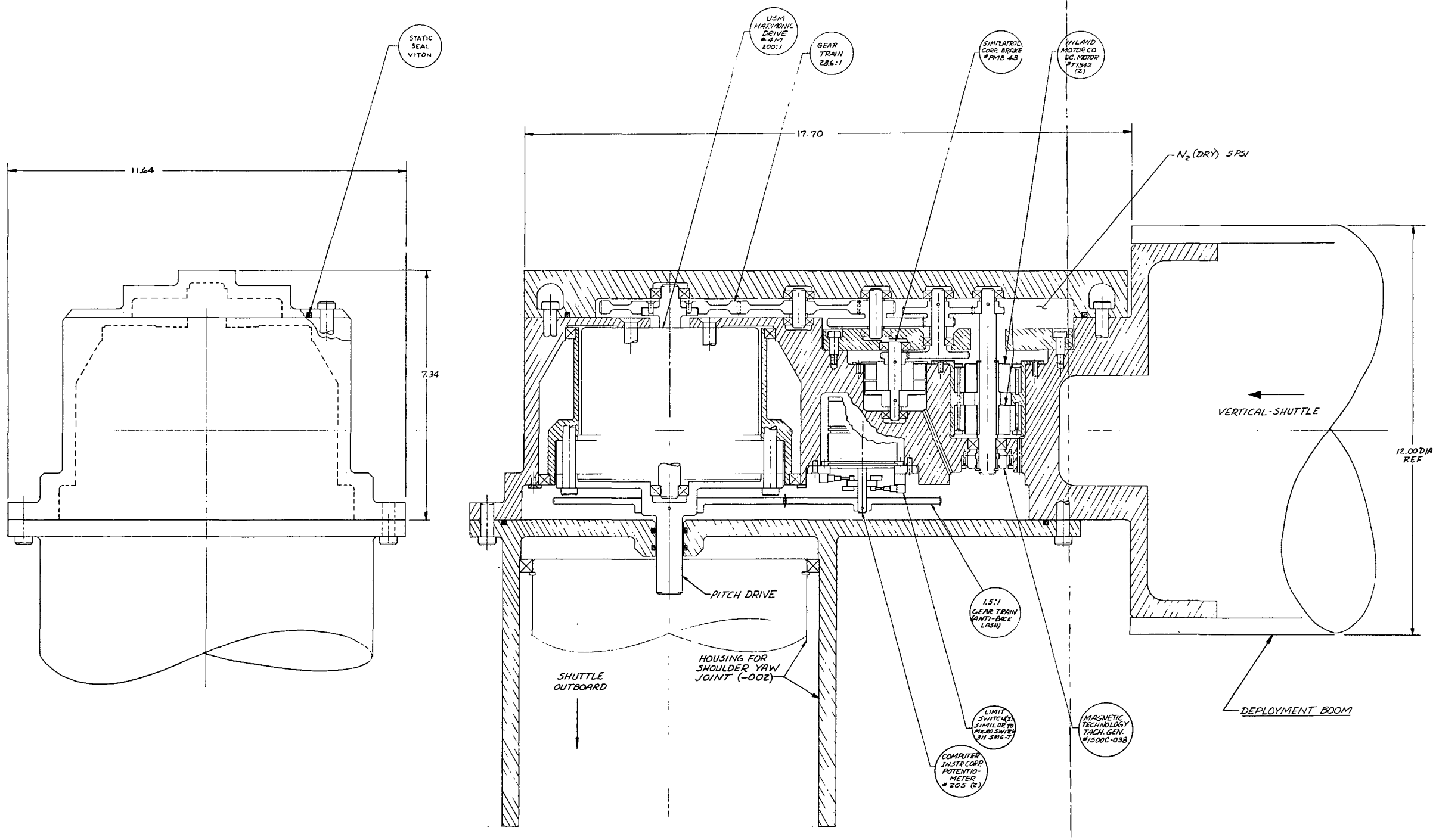

-001

PITCH JOINT ASSEMBLY SHOULDER

(MCR 71-319 FINAL REPORT)
PRELIMINARY DESIGN

C. DOUCETTE 1641 11/8/71

NAS 9-11932 NASA MSC

PITCH JOINT - SHOULDER, MANIPULATOR ARM - RMS

SRD 193210001

1/1 1 of 6

FOLDOUT FRAME 1

FOLDOUT FRAME 2

B-4

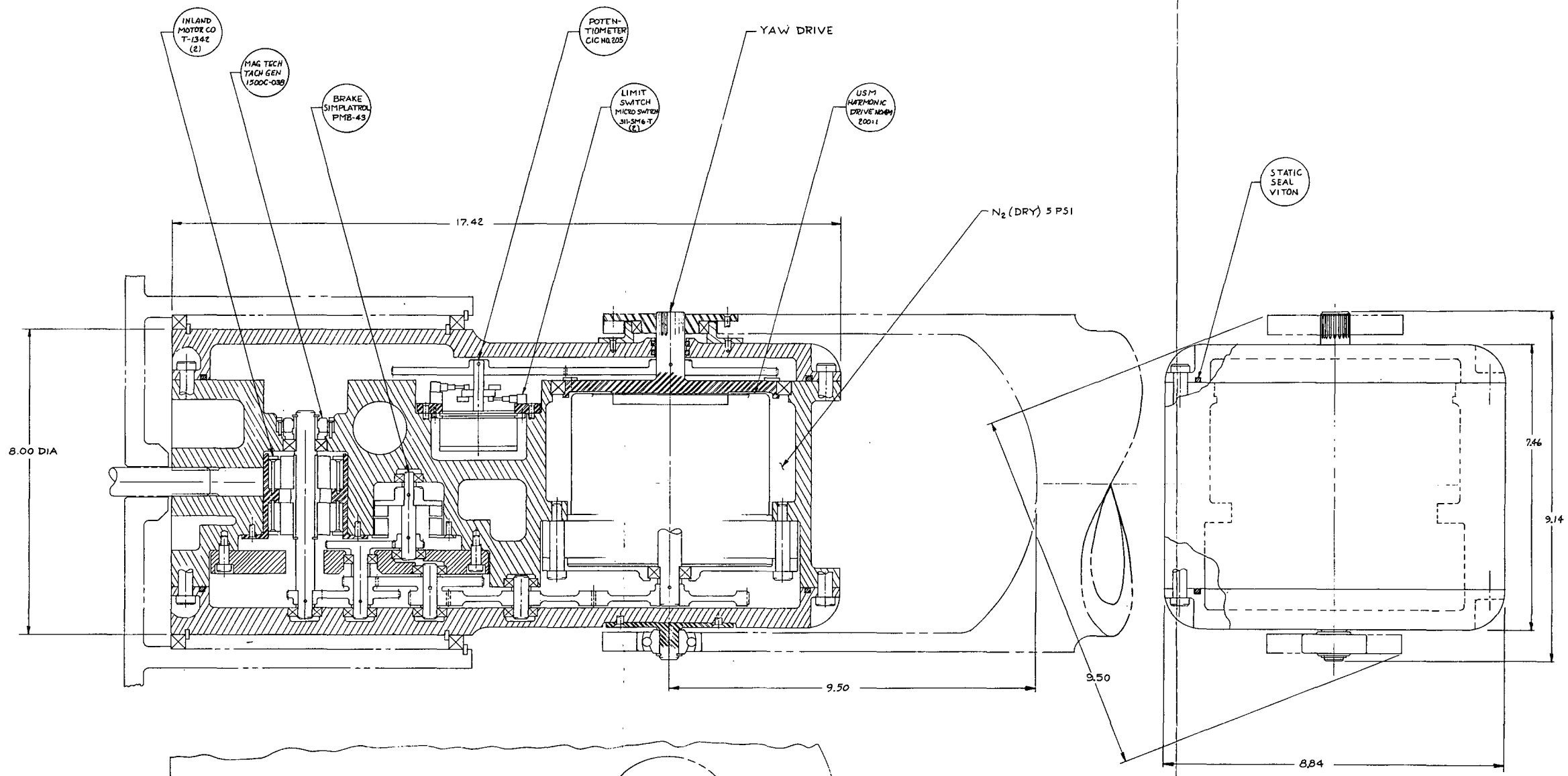

-002
YAW JOINT ASSY
SHOULDER

(MCR 71-319 FINAL REPORT)
PRELIMINARY DESIGN

C. DOUCETTE 1641 11/11/71

MARTIN MARIETTA CORPORATION
NAS 9-11932 NASA-MSC
YAW JOINT, SHOULDER - MANIPULATOR ARM, R M S

04236 SRD193210001

1/1 2 OF 6

FOLDOUT FRAME 1

FOLDOUT FRAME 2

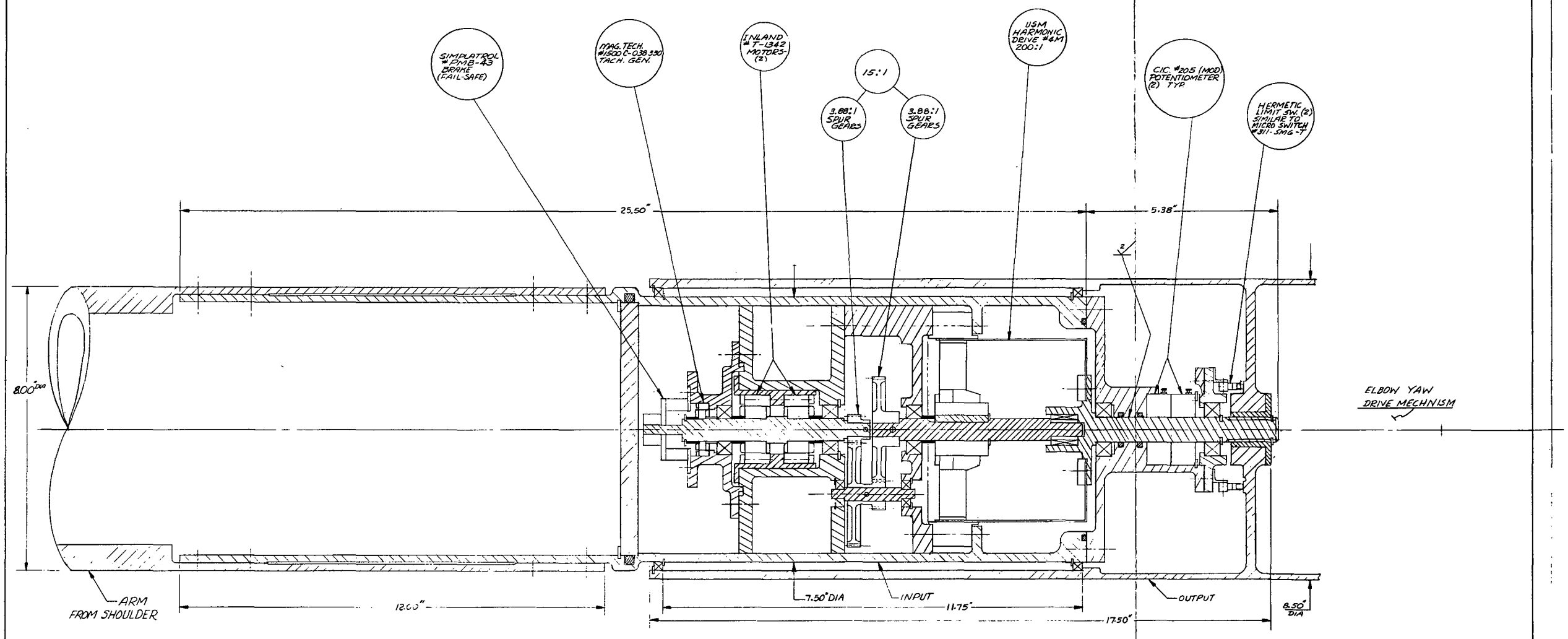

SCALE 1/1

(-003)

ELBOW-ROLL JOINT

(MCR 71-319 FINAL RPT)
PRELIMINARY DESIGN

CHIS BEAM 10-91 10/29/71

MARTIN MARIETTA CORPORATION

NAS 9-11932 (NASA-MSC)

ROLL JOINT - ELBOW MANIPULATOR ARM RMS

04235 SRD 1932/10001

V1 3 of 6

FOLDOUT FRAME 1

FOLDOUT FRAME 2

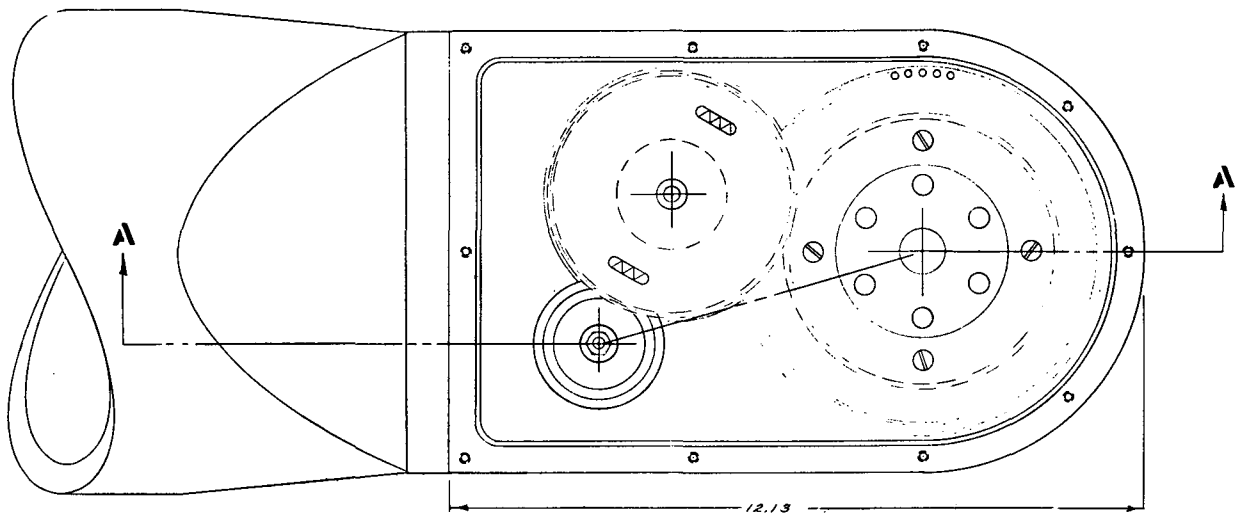

VIEW WITH TOP PLATE REMOVED

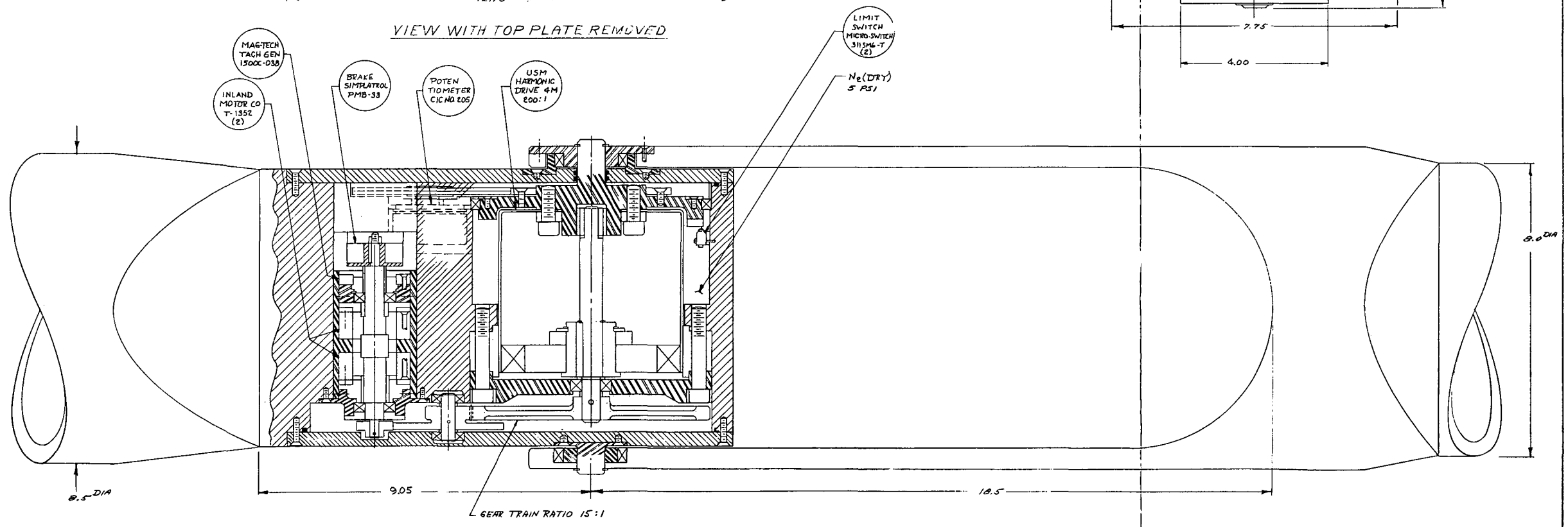

SECTION A A

-004

YAW ASSEMBLY
ELBOW

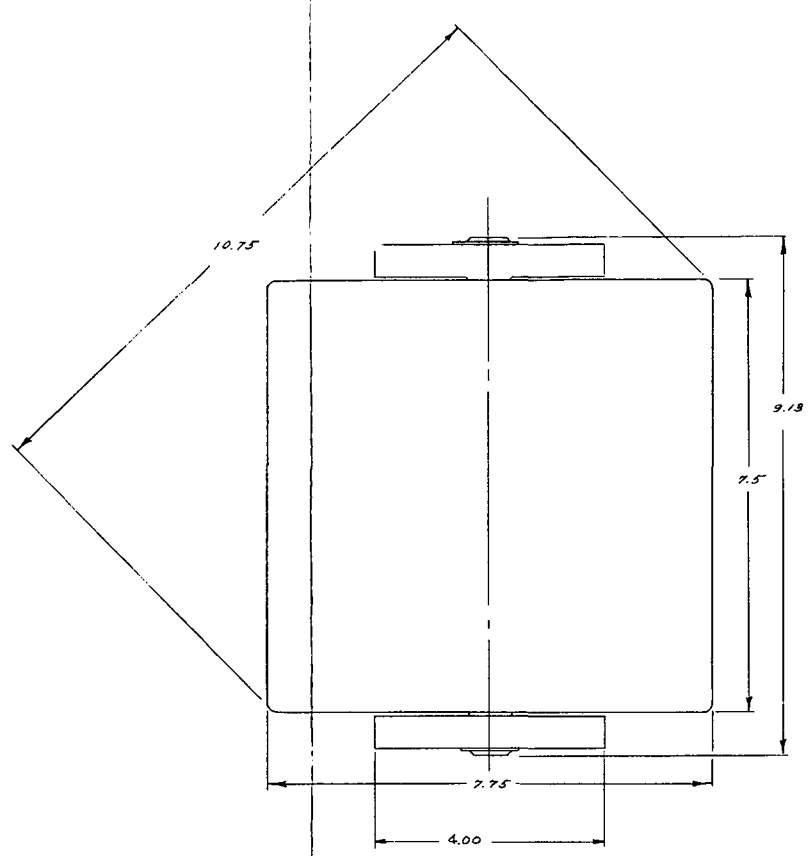

MCR 71-319 FINAL REPORT
PRELIMINARY DESIGN
P CORVELEYN 11/11/71
C DAIUTTA 11-11-71
MARTIN MARIETTA CORPORATION
NAS 9-11932 (NASA-MSC)

YAW
ELBOW ASSEMBLY
MANIPULATOR ARM

SIZE SRD193210001

1/1 4 OF 6

FOLDOUT FRAME 1

FOLDOUT FRAME 2

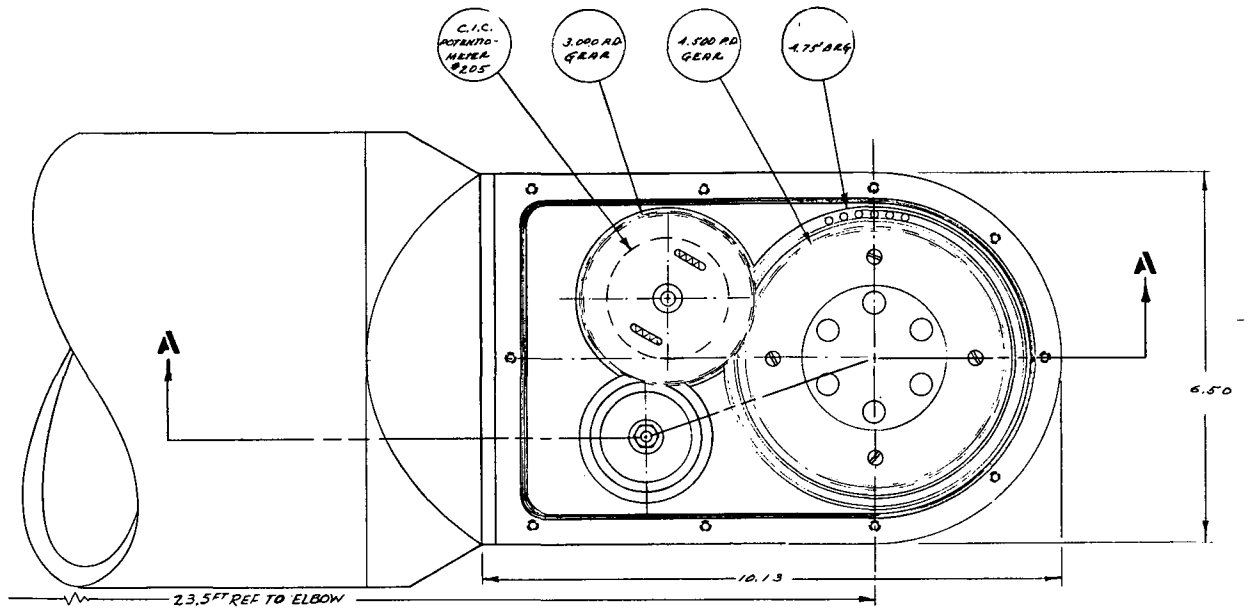

VIEW WITH TOP PLATE REMOVED

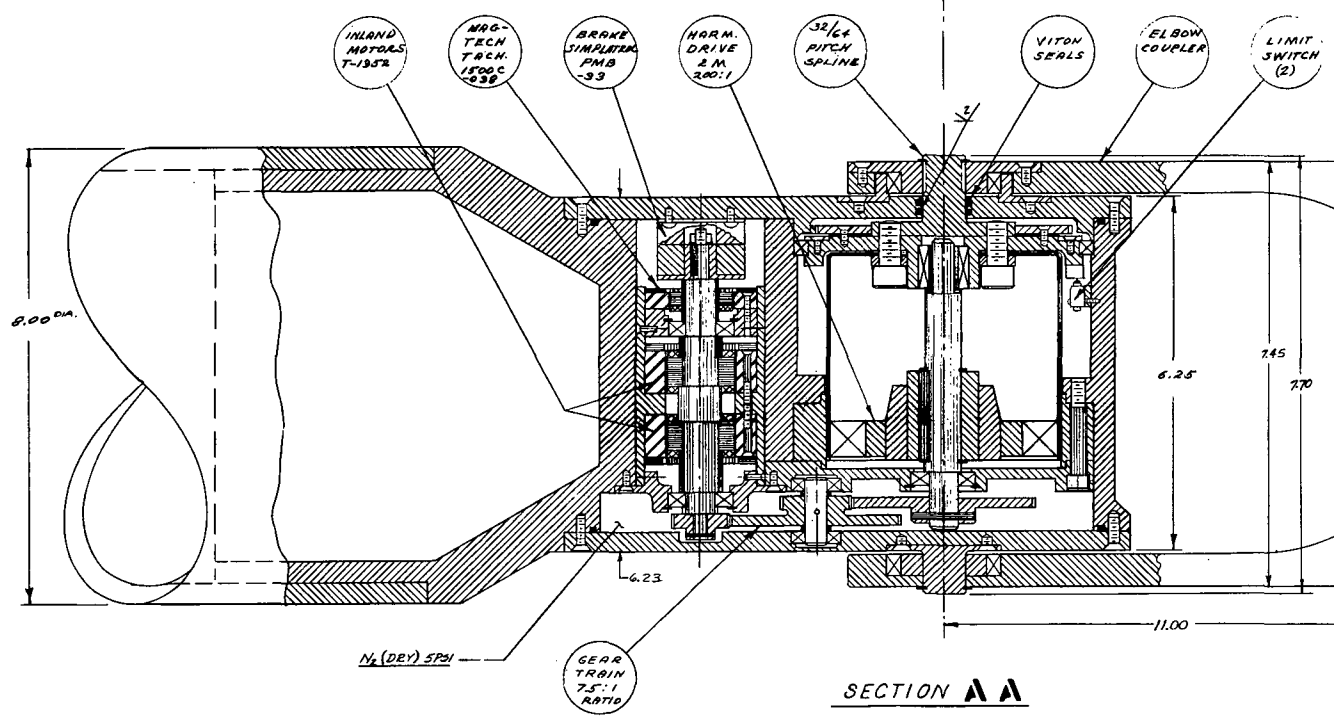

SECTION A A

-005
YAW ASSEMBLY-
WRIST

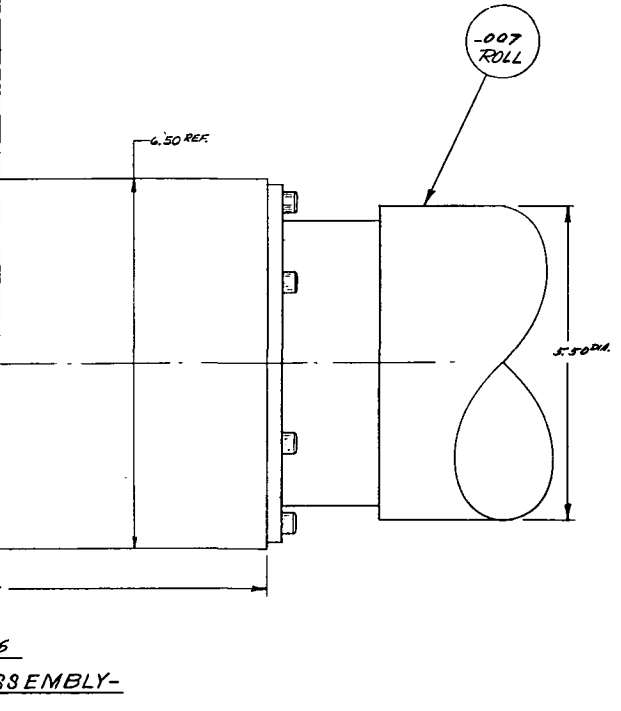

-006
PITCH ASSEMBLY-
WRIST

GENERAL NOTES

1-INTERNAL CONSTRUCTION OF BOTH PITCH AND YAW ASSEMBLIES ARE IDENTICAL

(MCR 71-319 FINAL REPORT)
PRELIMINARY DESIGN

MARTIN MARIETTA CORPORATION
NAS 9-11932 NASA-MSC

PITCH AND YAW WRIST ASSEMBLIES MANIPULATOR ARM

04236 SRD193210001

FOLDOUT FRAME 1

FOLDOUT FRAME 2

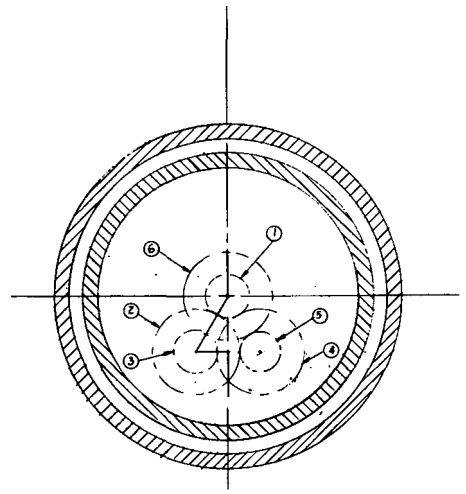

SECTION A A

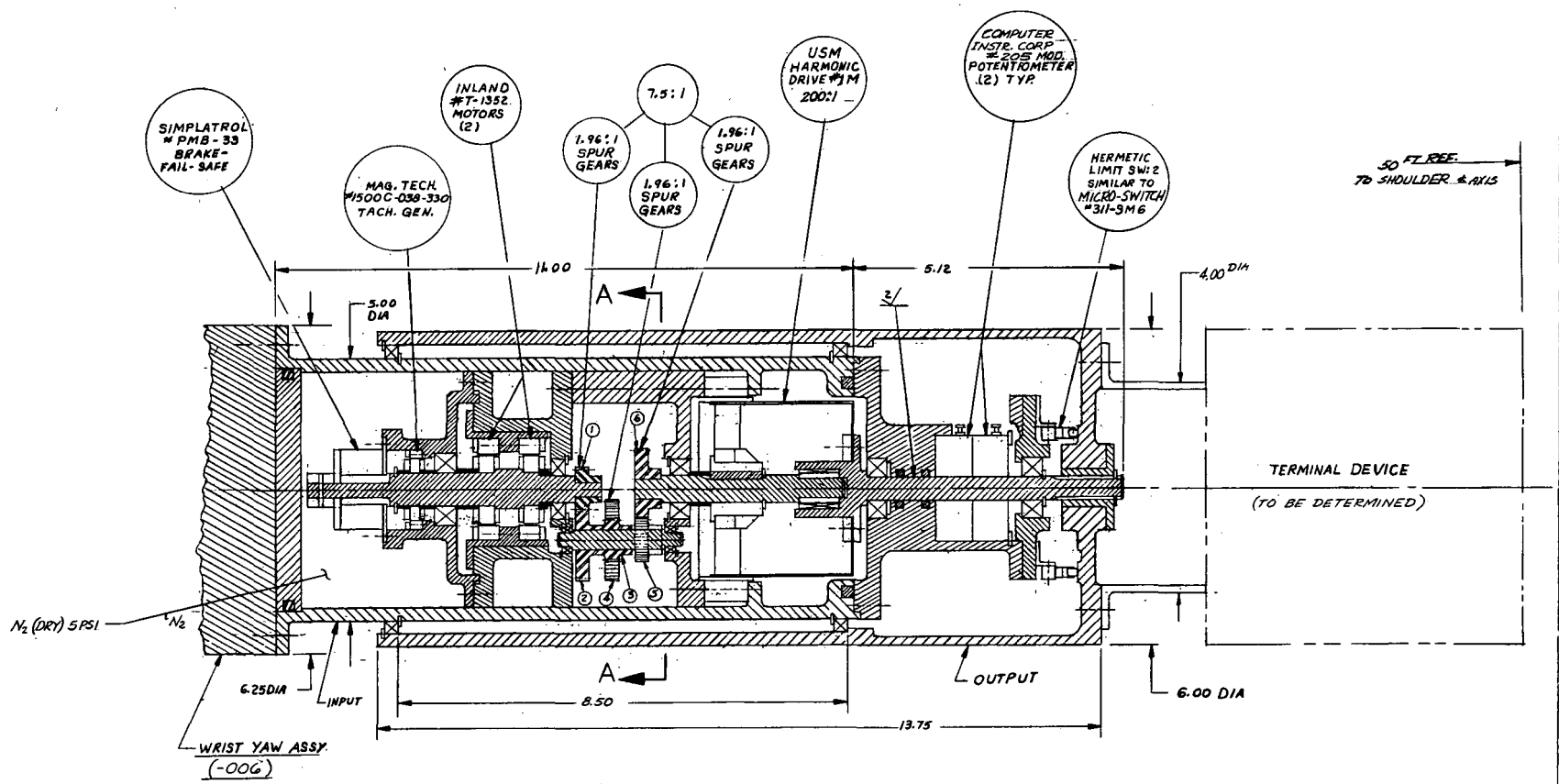

-007
ROLL JOINT ASSEMBLY-
WRIST

NOTE: SEE SRD 193210000 INSTALLATION-MANIPULATOR ARM (SH 1 OF 1)

(MCR 71-319 FINAL REPORT)
PRELIMINARY DESIGN

C. BEAM 1641 11-9-71

MARTIN MARIETTA CORPORATION
DENVER, COLORADO
NAS 9-11932, NASA-MSC

ROLL JOINT- WRIST
MANIPULATOR ARM
RMS

04236 SRD 193210001

1/1

APPENDIX C

STATEMENT OF WORK, TASK IDENTIFICATION

Chapter	Task No.
III. RMS Requirements	3.1.1, 3.2.1, 3.2.2
IV. Preliminary Requirements Analysis	3.1.1, 3.2.3, 3.3.2, 3.3.3, 3.3.4
V. Alternative Concepts, Evaluation & Selection	3.1.2, 3.1.1, 3.3.1, 3.3.5
VI. Man-in-the Loop Simulation	3.1.3, 3.10
VII. Selected Concept Requirements Analysis	3.1.3, 3.4.1, 3.5, 7.0
VIII. Preliminary Design & Analysis	3.4.2, 3.4.3, 3.4.4, 3.9, 3.11, 3.12, 7.0, 8.0
IX. Future Development Program	4.8